Ichnology and Sedimentology of deep-marine clastic systems, Middle Eocene, Ainsa - Jaca basin, Spanish Pyrenees

Thomas George Heard

2007

University College London,

University of London

Thesis submitted for examination for the award of Doctor of Philosophy

(Ph.D.)

ProQuest LLC
789 East Eisenhower Parkway
P.O. Box 1346
Ann Arbor, MI 48106-1346

Abstract

Despite considerable research into the characterisation of the architectural elements of submarine fans, few studies have attempted the full integration of ichnology and sedimentology. In this thesis, a quantitative analysis of trace fossils from the Early-Middle Eocene deep-marine clastic systems, Ainsa-Jaca basin, Spanish Pyrenees, shows that trace fossils are powerful discriminators of deep-marine fan and related environments.

Sixteen fan and related environments have been recognised in the Ainsa-Jaca basin, from upper-slope gully to distal basin-floor. In the more laterally confined and channel-dominated Ainsa basin, there is a trend of increasing bioturbation intensity and trace-fossil diversity away from channel-axis to off-axis environments. In the more unconfined and distal Jaca basin, there is a trend of increasing trace-fossil diversity and number of pre-depositional trace fossils including graphoglyptids from the channel-lobe transition to the fan-fringe. The trace-fossil assemblages of the Ainsa-Jaca basin are characteristic of a number of subichnofacies of the *Nereites* ichnofacies. In the distal Jaca basin, the *Paleodictyon* subichnofacies occurs in the lobe-fringe and fan-fringe, whereas the distal basin-floor has a trace-fossil assemblage typical of the *Paleodictyon* subichnofacies, but with a high proportion of post-depositional *fodinichnia*. Trace-fossil assemblages of proximal basin, axial, environments are characteristic of the *Ophiomorpha rudis* subichnofacies, whilst proximal off-axis environments, have a mixed *Paleodictyon-Ophiomorpha rudis* subichnofacies trace-fossil assemblage.

In core, a detailed ichnofabric study of the proximal Ainsa channel system shows a clear trend of increasing bioturbation intensity and trace-fossil diversity from channel axis to levee-overbank. Spectral analysis of bioturbation intensity in thin-bedded turbidites deposited in overbank and interfan environments from one of the wells (A6), suggests, for the first time from a siliciclastic turbidite succession at a tectonically active plate margin, a strong cyclicity interpreted to reflect the ~41 k.yr and ~112 k.yr. Milankovitch frequencies. It is, therefore, proposed that global climate change acted as the principal environmental driver in controlling changes in bottom-water conditions within the deep-marine Ainsa basin.

Table of contents

Chapter 4 - Sedimentological terminology, facies and facies associations

Chapter 6 – Ainsa basin: Proximal fan and related environments

Chapter 8 - Trace fossils in the subsurface

List of figures

List of tables

Acknowledgments

I wish to acknowledge the invaluable support of my supervisors, Prof. K.T. Pickering (UCL) and Dr A.D. Reynolds (BP). A special thanks must also be given to Prof A. Uchman (Jagiellonian University) for his support, and for giving me access to the Marian Ksiazkiewicz trace fossil collection at the Institute of geological sciences, Jagiellonian University (Krakow).

I also wish to thank my family for their support over the past few years, and those friends of mine who have helped me so much over the past few months and years.

Chapter 1

Introduction

1.1. Objectives

Despite considerable research into the characterisation of the architectural elements of submarine fans, very few studies on ancient submarine fans have attempted to fully integrate ichnology and sedimentology. There are, however, a number of detailed studies on trace-fossil assemblages in fan and related environments (e.g., Crimes 1977, Książkiewicz 1977, Crimes *et al.* 1981, Uchman 1995a, 1998, 1999, Tchoumatchenco & Uchman 1999, Orr 2001, Uchman *et al.* 2004), including a study focused on distal environments of the Ainsa-Jaca basin (Uchman 2001). None of these have attempted a systematic study of the full range of fan and related environments. The Middle Eocene Ainsa-Jaca basin, Spanish Pyrenees, with its well-defined deep-marine architectural elements in world-class outcrops, provides an excellent natural laboratory in which to integrate sedimentological and ichnological data to improve the understanding of the uses of trace fossils in deep-marine environments. It was on this basis that the original objectives of the Ph.D. thesis were based, including:

(1) The use of trace fossils at outcrop as diagnostic indicators of deep-marine environments, including a detailed study of the full range of fan and related environments in the Ainsa-Jaca basin, and the different trace-fossil assemblages / abundances that characterise each environment.
(2) A quantitative ichnological study and detailed ichnofabric analysis of a number of cores through the Ainsa turbidite system, with the aim of fully understanding the uses of trace fossils as diagnostic indicators of deep-marine clastic fan and related environments in the subsurface.
(3) To determine whether trace fossils can be used to infer a Milankovitch-type control in deep-marine siliciclastic turbidite successions.

The scope of the project was expanded following a study of the oldest turbidite systems in the Ainsa basin, including Fosado and Arro (Fig. 1.1C). The basis of the integrated

sedimentological and ichnological outcrop study was that the architectural elements in the basin were well-defined. However, the oldest turbidite systems of the Ainsa basin have received little attention by previous researchers and are poorly understood. A more detailed sedimentological study was therefore conducted. However, a complete study of these systems, including detailed geological mapping and structural analysis was beyond the scope of this project.

1.2. Study Area

The study area is located in the central and western sectors of the Eocene Tremp-Pamplona Basin, south-central Pyrenees. The eastern sector of the basin consists of fluvial and deltaic successions, whilst the central and western sectors, referred to as the Ainsa and Jaca basin respectively in this thesis, comprise deep-marine deposits collectively known as the Hecho Supergroup (Mutti *et al.* 1972) (Fig. 1.1A). The Hecho Supergroup may be considered as a turbidite complex *sensu* Mutti and Normark (1987).

1.2.1. Structural Overview

Collision of the Iberian and European plates created a two-sided orogen, with paired fold-and-thrust belts and foreland basins north and south of the Axial Zone riding on imbricate stacks of crystalline thrust sheets (Morris *et al.* 1998, Muñoz *et al.* 1992). In the central Pyrenees, maximum shortening occurred between 55 and 28 Ma (Burbank *et al.* 1992, Meigs & Burbank 1997). Verges *et al.* (1998) show that maximum rates of tectonic subsidence in the foreland basin coincided with the maximum rates of shortening and thrust front advance at ~41.5 Ma (Middle Lutetian), broadly contemporaneous with the accumulation of the deep-marine Ainsa basin sediments.

The Middle Eocene South Pyrenean foreland basin (that became a thrust-top or piggy-back basin during the Early Eocene) was filled mainly by non-marine / marginal marine deposits in the east, whilst further west fluvio-deltaic deposition passed into deep-marine systems (the Ainsa-Jaca basin) (Fig. 1.1A). Although the Ainsa-Jaca basin is believed to have been an essentially contiguous basin during deposition of the Mid Eocene deep-marine systems, the present geographic separation of the depositional components across the Boltaña anticline, and the fact that the more proximal (Ainsa)

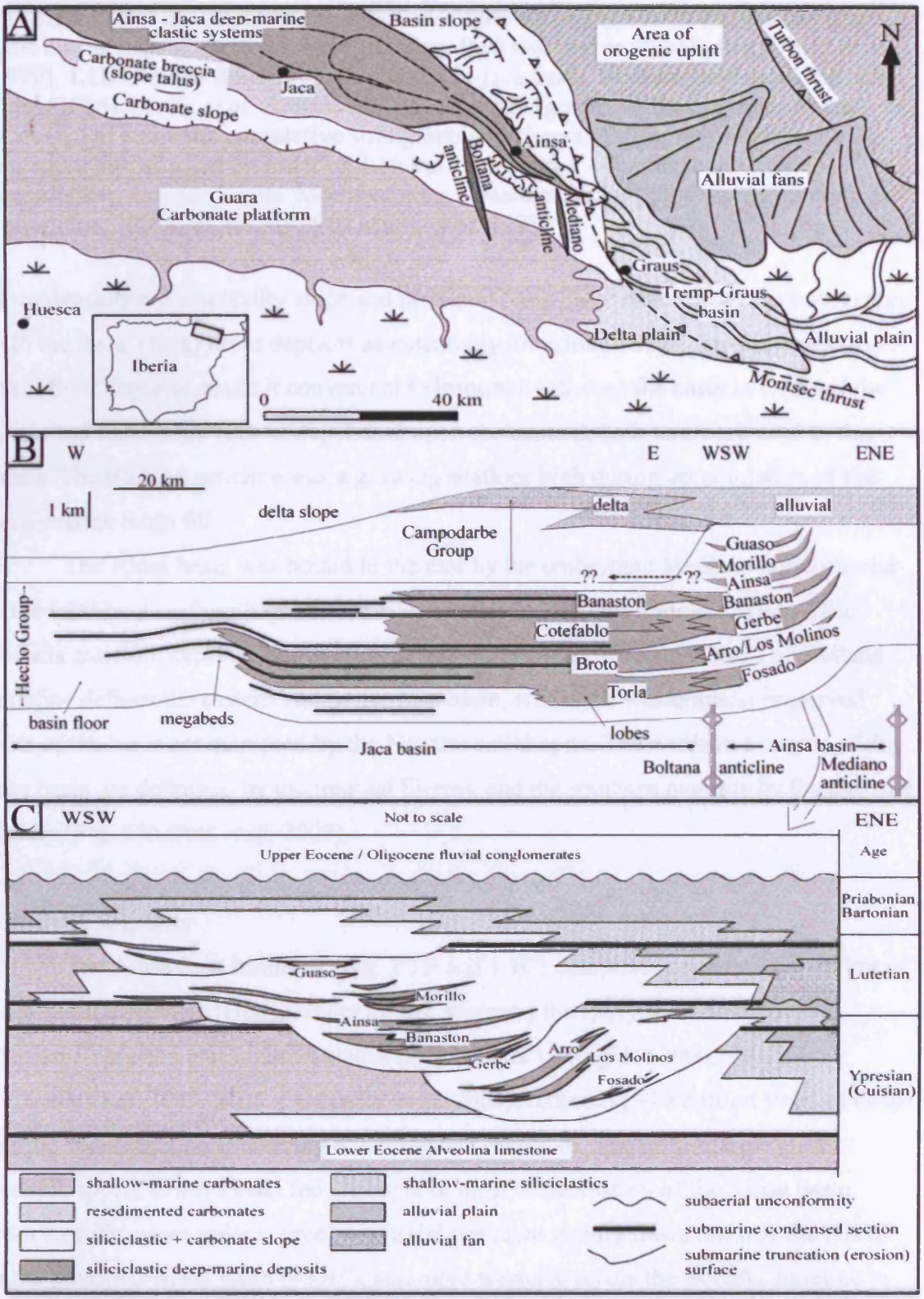
A
Ainsa - Jaca deep-marine clastic systems
Basin slope
Area of orogenic uplift
Turbon thrust
N
Carbonate breccia (slope talus)
Jaca
Carbonate slope
Ainsa
Boltana anticline
Mediano anticline
Alluvial fans
Guara Carbonate platform
Graus
Tremp-Graus basin
Huesca
Delta plain
Alluvial plain
Iberia
Montsec thrust
0
40 km
B
W
E
WSW
ENE
20 km
1 km
delta slope
delta
alluvial
Campodarbe Group
Guaso
Morillo
Ainsa
??
??
Banaston
Banaston
Gerbe
Cotefablo
Arro/Los Molinos
Hecho Group
Broto
Fosado
Torla
basin floor
megabeds
lobes
Jaca basin
Ainsa basin
Boltana anticline
Mediano anticline
C
WSW
Not to scale
ENE
Upper Eocene / Oligocene fluvial conglomerates
Age
Priabonian Bartonian
Lutetian
Guaso
Morillo
Ainsa
Banaston
Arro
Los Molinos
Gerbe
Fosado
Ypresian (Cuisian)
Lower Eocene Alveolina limestone
shallow-marine carbonates
resedimented carbonates
siliciclastic + carbonate slope
siliciclastic deep-marine deposits
shallow-marine siliciclastics
alluvial plain
alluvial fan
subaerial unconformity
submarine condensed section
submarine truncation (erosion) surface

Fig. 1.1A Palaeogeographic reconstructions of the Ainsa-Jaca basin and surrounding areas during deposition in the early Lutetian. Redrawn and modified after Dreyer *et al.* (1999). **1.1B** General stratigraphy of the Ainsa-Jaca basin. Redrawn and modified after Mutti (1985), Mutti, *et al.* (1985). **1.1C** General stratigraphy of the proximal Ainsa basin (not to scale, but cumulative stratigraphic thickness of deep-marine deposits ~4 km, and width of panel on order of 8-10 km). Numbers 1 - 4 indicate the four unconformity-bounded units. Modified after Fernandez, *et al.* (2004), and Pickering & Corregidor (2005a, b), (cf. fig. 5 of Mutti, *et al.* 1985).

basin deposits are essentially slope and proximal basin-floor channelised environments, with the distal (Jaca) basin deposits as essentially lobe, lobe-fringe, fan-fringe and distal basin floor deposits, make it convenient to informally discuss the basin in terms of the Ainsa and Jaca basin. Hence, depending upon the context, both terms are used in this thesis. The Boltaña anticline was a growing seafloor high during accumulation of the deep-marine basin fill.

The Ainsa basin was bound to the east by the embryonic Mediano anticline and to the west by a seafloor high, which later formed the Boltaña anticline. Today, the Boltaña anticline exposes mainly Eocene and older carbonate sequences. The Boltaña anticline defines the eastern end of the Jaca basin, whilst the westernmost preserved parts of the basin are disrupted by the Navarre salt diapirs. The northern margins of the Jaca basin are delimited by the internal Sierras, and the southern margins by the external Sierras (Fig. 1 in Oms *et al.* 2003).

1.2.2. Stratigraphy

The Ainsa-Jaca basin fill (Fig. 1.1B and 1.1C) comprises cumulatively ~4 km of deep-marine deposits (Hecho Supergroup), spanning the Early to Middle Eocene, Cuisian / Ypresian and Lutetian stages (Pickering & Corregidor 2000, 2005a, b, Remacha *et al.* 2003, 2005, Fernandez *et al.* 2004), recording ~10 million years of deep-marine sedimentation (Pickering & Corregidor 2005a, b). The deep-marine clastic systems appear to have been fed, throughout most of the history of the Ainsa basin, from a southeastern point source, with axial sediment gravity flows towards the NNW in the proximal Ainsa basin (~320°), and more westerly across the Boltaña anticline in the relatively distal Jaca basin (~270°) (Pickering & Corregidor 2005a, b) (Fig. 1.1A). The younger deep-marine systems in the Ainsa basin (Morillo and Guaso systems) were fed from a southern source between the growing Mediano and Boltaña anticlines. In the younger, upper Lutetian part of the deep-marine fill of the Ainsa-Jaca basin, west of the

Boltaña anticline in the Jaca basin, an additional northerly-derived sediment supply is recognised (Remacha *et al.* 2003).

The Eocene fill of the southern central Spanish Pyrenees foreland basin has been divided into a number of stratigraphic groups: Alveolina Limestone Group (Palaeocene to Lower Eocene); Figols (Lower Eocene); Castigaleu (Lower Eocene); Castisent (Lower Eocene); Santa Liestra (Lower to Middle Eocene); and Campodarbe (Middle Eocene) (Mutti *et al.* 1989, Mutti 1992).

1.2.2.1. Ainsa basin

The infill of the proximal Ainsa basin consists of two principal depositional units separated by an angular unvonformity (Fernandez *et al.* 2004) in which each succeeding unit is both structurally less deformed and shows a southwestward shift in depositional axis (Pickering & Corregidor 2005a, b) (Fig. 1.1C). These "tectono-stratigraphic units" are packaged into eight coarse clastic depositional complexes or systems, each of which is in the order of 100-700 m thick and contains 2-6 individual sand bodies from 30-100 m thick, separated by 10s m of mainly thin-bedded and very thin-bedded sandstones with subordinate marls. The depositional systems are separated vertically from other systems by several hundred metres of mainly marl deposits, aswell as thin-bedded and very thin-bedded sandstone turbidites. Although some sand bodies show an aggradational stacking pattern, overall each depositional system (e.g., Banastón, Ainsa) show a WSW, foreland-stepping pattern (Fig. 1.1C) (Pickering & Corregidor 2000, 2005a, b). The sediments within the basin have been deformed by both synsedimentary and post-depositional tectonics that affected the region during the growth of the Pyrenees. The bathymetry of the Ainsa basin suggests that water depths were at least several hundred metres, probably in the range 400-800 m (Pickering & Corregidor 2000, 2005a, b).

The eight coarse clastic depositional systems in the Ainsa basin (Fig. 1.1C), were deposited in a variety of depositional settings: (1) Fosado = slope channels; (2) Los Molinos = slope channels (this thesis); (3) Arro = canyon-base-of-slope channel system

(this thesis); (4) Gerbe = canyon-erosional submarine channel system (Clark & Pickering 1996); (5) Banastón = base-of-slope and proximal basin-floor channel system (Bayliss & Pickering, in prep.), but previously interpreted as a canyon system (Clark & Pickering 1996); (6) Ainsa = lower slope erosional channels and proximal basin-floor

channelised fan system (Pickering & Corregidor 2000, 2005a, b); (7) Morillo = canyon-base-of-slope erosional channel system (Clark & Pickering 1996, Bayliss, pers. comm. 2006), and (8) Guaso = "prodeltaic clastic ramp" (Pickering & Corregidor 2005a, b, Sutcliffe & Pickering, in review).

The older turbidite systems in the Ainsa basin have been correlated with four principal systems in the Jaca basin, namely the Fosado-Torla, Arro-Broto, Gerbe-Cotefablo, and Banaston-Fiscal systems (Mutti *et al.* 1985) (Fig. 1.1B). In each system, the first name denotes the main outcrop area of the channelised deposits in the Ainsa basin, and the second name the main outcrop area of the depositional lobes in the Jaca basin (Mutti *et al.* 1985).

1.2.2.2. Jaca basin

The Jaca basin comprises several vertically-stacked major sandy turbidite systems (Fig. 1.1B), which, from oldest to youngest are the: (1) Torla; (2) Broto; (3) Cotefablo; (4) Banastón, and (5) Jaca systems. The Torla and Broto systems represent the first major sand-rich depositional systems in the Jaca basin (Remacha *et al.* 2003). However, Mutti *et al.* (1988), and Remacha *et al.* (1998) recognise two older heterolithic turbidite systems in the Jaca basin, the Figols and Castigaleu "systems" (shown as Ypresian or Cuisian in age). As these latter two turbidite systems are poorly exposed, and slightly older than the sandy systems in the Ainsa basin, they shall not be discussed further in this thesis. A distinctive feature of the Hecho Supergroup in the Jaca basin is the occurrence of nine thick resedimented carbonate mega-beds (up to 250 m thick) interbedded with the siliciclastic turbidites (Labaume *et al.* 1987; Payros *et al.* 1999). These mega-beds extend for considerable distances along the Jaca basin and provide useful marker beds throughout the basin.

In the youngest (upper) parts of the Hecho Supergroup, in the Jaca basin, a new northerly, partly channelised, sediment source is recognised as supplying, at least part of, the coarse clastic systems to the Jaca turbidite system (Remacha & Picart 1991, Remacha *et al.* 1995, 2003, their fig. 13). This new sediment provenance has been interpreted as occurring at a time when the Ainsa and Jaca basins temporarily became separated (detached) by the growth of the Boltaña anticline, with sediment supply in the thrust-top Ainsa basin still coming from a southerly source (Remacha *et al.* 2003).

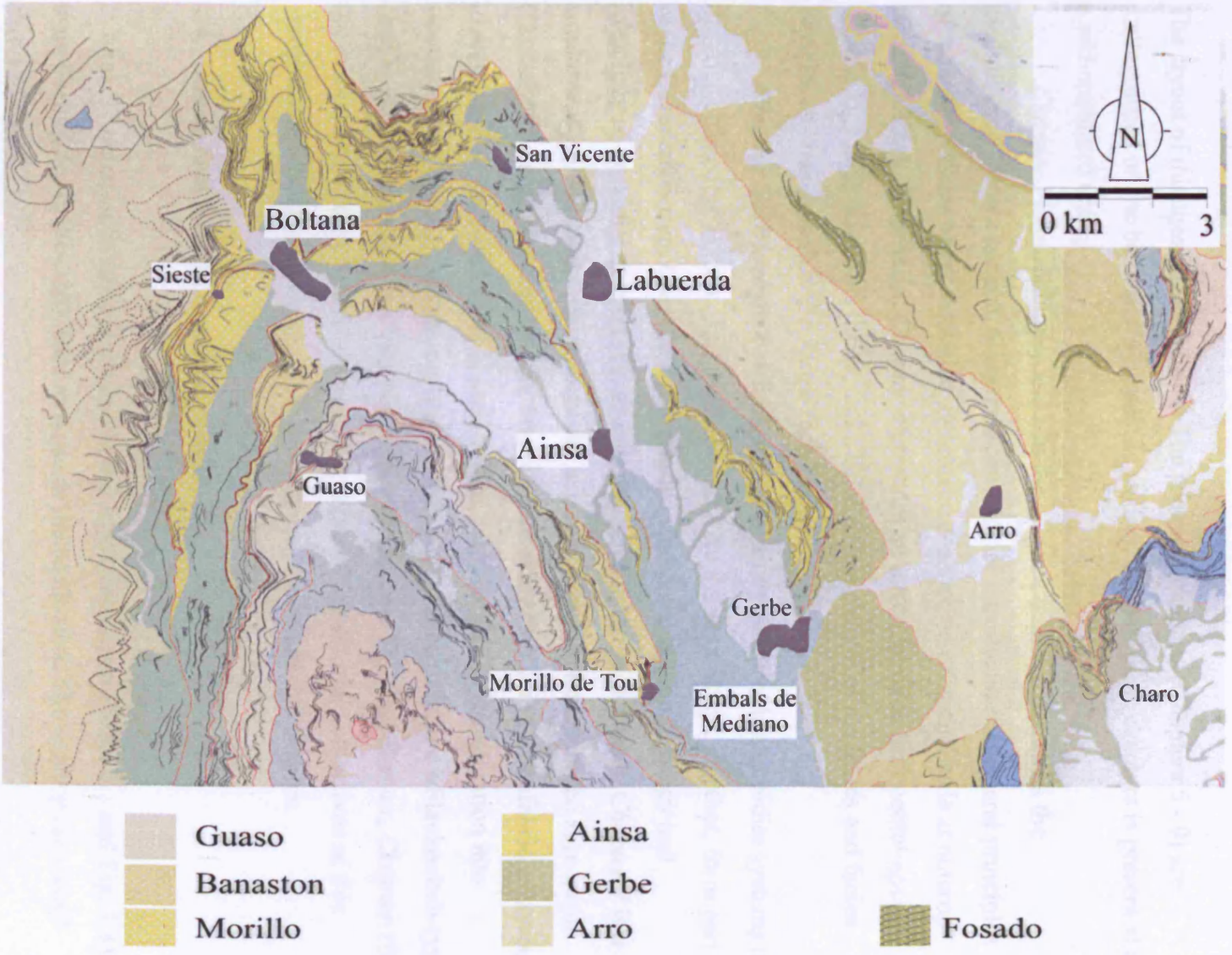

Fig. 1.2. Geological map of the Ainsa basin, redrawn after Remacha *et al.* (2003)

1.3. Thesis Layout

The layout of this thesis is as follows. The principal chapters (Chapters 5 - 9) are distinguished on the basis of their specific studies. Each of these chapters is presented as a self-contained unit.

Chapter 1 is introductory and sets the scene. *Chapter 2* describes the methodology of the research. *Chapter 3* provides an introduction to general principles of ichnology followed by a detailed systematic description of trace fossils at outcrop from the Ainsa –Jaca basin. *Chapter 4* provides an introduction to sedimentological terminology adopted in this thesis, and a detailed description of the facies and facies associations recognised in the Ainsa-Jaca basin.

Chapter 5 is based on a sedimentological study of the oldest turbidite systems in the Ainsa basin, the Fosado, Los Molinos and Arro systems which, together, form part of the Castisent Group. *Chapter 6* is a detailed study of the sedimentology and ichnology of proximal fan and related environments in the Ainsa basin. *Chapter 7* is a similar study based on the more distal fan and related environments in the Jaca basin. *Chapter 8* is a sedimentological and ichnological study (including ichnofabric analysis) of 6 cores from the Ainsa I and II sand bodies. *Chapter 9* is an investigation into whether bioturbation intensity and ichnofabrics can be used to infer a Milankovitch-type control in deep-marine siliciclastic turbidite successions. The final chapter, *Chapter 10*, is a summation of the overall conclusions in light of the aims and objectives of this study. Some ideas for future work are presented at the end of this chapter.

1.4. Ainsa-Jaca basin: Outcrops studied

In total, 37 outcrops have been studied in the Ainsa-Jaca basin (Table 1.1 and Fig. 1.3) from Formigales in the south-east, to Anso in the north-west. The outcrops are listed above (Table 1.1).

Loc.	Environment	Locality Description
1	Channel axis, Fosado system	South of Fosado village
2	Channel axis, Los Molinos system	Tozal de Sans, south of Los Molins
3	Channel axis, Los Molinos system	Bco. Picalbe
4	Channel margin and slope, Los Molinos system	Bco. Sierra
5	Arro system	Bco. Sierra
6	Arro system	Road section parallel to Bco. Sierra
7	Channel off-axis, Arro system	Old road section parallel to Rio Nata
8	Channel off-axis, Arro system	Santa Catalina, northeast of Bojetar farm
9	Canyon fill, Gerbe I sandbody	Tozal de Charo, north of Charo village
10	Canyon fill, Charo-1 Canyon	Tozal de Charo, north of Charo village
11	Channel axis, Gerbe I sandbody	Road section (N260) between Arro and Gerbe
12	Upper slope gully	Road section north of Formigales village
13	Overbank, Banaston system	Bco. os Biñés
14	Channel off-axis, Banaston III sand body	Bco. Pinar, north of San Vicente
15	Channel axis, Ainsa I fan	Bco. Buchosa, Ainsa quarry
16	Channel off-axis, Ainsa I fan	Road section (A138) south of Ainsa
17	Channel margin, Ainsa I fan	Track above Bco. Forcaz, next to electric tower
18	Outermost channel-to-levee-overbank	Road section (A138) opposite Pena Montenesa hotel
19	Channel axis , Ainsa I fan	Bco. Royo
20	Channel margin, Ainsa II System	Bco. Forcaz
21	Proximal interfan	Bco. Forcaz
22	Channel margin, Morillo system	Bco. Cotón, north of Morillo de tou
23	Channel axis, Morillo system	Rio Sieste
24	"Prodeltaic clastic ramp" sand bodies, Guaso system	Rio Ena, southeast of Guaso
25	"Prodeltaic clastic ramp" thin-bedded sandstones at top of Guaso	Rio Ena, southeast of Guaso
26	Slope gully, Guaso system	Rio Ena, southwest of Latorrecilla
27	Basin slope, Guaso system	Rio Ena, southwest of Latorrecilla
28	Channel-lobe transition, Broto system	Road section between Sarvise and Fanlo
29	Lobe, Broto system	Road section east of Sarvise
30	Lobe, Broto system	Road section north of Aragues del Puerto
31	Lobe fringe, Cotefablo system	Road section (N260) west of Cotefablo tunnel
32	Fan fringe, Cotefablo system	Road section northeast of Jasa
33	Fan fringe, Cotefablo system	Urdues village
34	Fan fringe, Cotefablo system	Road section southwest of Urdues
35	Fan fringe, Cotefablo system	Road section (A176) at Puerto d' Anso
36	Distal basin floor, Cotefablo system.	Road section between Hecho and Siresa
37	Distal basin floor, Cotefablo system.	Road section (A176) west of Anso

Table 1.1. Studied outcrops including depositional environment and locality description

Fig. 1.3. Location map for the studied sections. The name of each numbered locality is documented within Table 1.1.

Chapter 2

Methods

2.1. Introduction

Various analytical methods were employed during the course of this study. These were used to facilitate sedimentological and ichnological analysis at core and outcrop. Where the results are presented in the thesis it should be assumed that the techniques and methods applied were consistent.

2.2. Outcrop Analysis

2.2.1. Sedimentology

Representative outcrops of typical fan and related environments were identified on the basis of general field observations, as well as previously published work (e.g., Clark & Pickering 1996, Mutti *et al.* 1985, 1988, Pickering & Corregidor 2005a, b, Remacha & Fernández 2003, Remacha *et al.* 2003, 2005). Detailed bed-by-bed sedimentary logs were constructed for each section. In some cases, several sedimentary logs have been completed in the same area and correlated in order to understand lateral thickness changes of individual beds and units and thus enabling a more accurate palaeoenvironmental interpretation.

2.2.2. Trace fossil analysis at outcrop

Trace fossils were analysed on well-exposed bedding planes and this data was then integrated with the sedimentary logs. Trace fossils were analysed on ~25% of all bedding planes logged, with 1,614 bedding planes studied in total. Ichnological observations were focused on the type and abundance of bioturbation on the base and top of beds. On each bedding plane, individual trace fossils were identified and the percentage of the trace-fossil assemblage characterised by each trace fossil was estimated. Average bioturbation (intensity) on each bedding plane was measured quantitatively using a 10 cm x 10 cm grid placed at random on the bedding plane, with the percentage of bioturbation measured as the number of 1-cm squares containing bioturbation. This differs from previous methods for measuring average bioturbation on

bedding planes such as that of Miller and Smail (1997), which is based on semi-quantitative bioturbation indices. However, because both methods are based on percentages of bioturbation, the bioturbation indices of Miller and Smail (1997) can be applied to the average bioturbation recorded in the current paper. A total of 95 ichnospecies from 49 ichnogenera were identified in this study.

Trace fossils were analysed in vertical section in fine-grained intervals between sandstones. Suitable intervals were polished using a specialist sandpaper attachment on an electric drill. Observations were based on the methodology outlined in section 2.3.2.

2.3. Core Analysis

2.3.1. Core Preparation - The Ainsa Project

The Ainsa Project (Phase I, 1997-1999, and ongoing research) is an integrated outcrop-subsurface study of the Ainsa turbidite system. Eight wells were drilled as part of a consortia-based research study at University College London. The wells were drilled at 400-500 m spacing, to subsurface depths *c.* 250 m each, with about 97% core recovery. As the core is tightly cemented by carbonate cement, it was unnecessary to line the core. A standard suite of wireline logs was run in each hole (calliper, gamma, spectral gamma, sonic, neutron, density). The core was cut into archive and working halves, and the archive part then polished and photographed. A detailed bed-by-bed sedimentary log was then constructed for each core (Pickering & Corregidor 2000). Three sets of core are housed at UCL, with the remaining cores stored in Norway with the FORCE Deep-Water Clastics Workgroup. These cores were studied from high-resolution digital images.

Semi-quantitative micropalaeontological and palynological analyses were carried out by Robertson Research International to constrain the age, and provide a sequence stratigraphic framework. Three further quantitative micropalaeontological / palynological studies aimed at establishing robust correlations of channel and levee-overbank sediments between wells and outcrop have also been made (e.g., Jones *et al.* 2005).

2.3.2. Trace fossil analysis

Ichnological measurements were obtained at 10-cm intervals in the core, as bioturbation intensity, type and abundance of individual ichnotaxa. When working with core material housed at UCL, the surface of the core was wetted to improve measurements. Digital images of the core were enhanced by modifying the brightness and contrast on a specialist program. A 10 x 6 cm grid was placed on the core, and the bioturbation intensity quantitatively measured by recording the number of 1-cm squares containing bioturbation. This was then recalculated into a percentage value.

Bioturbation intensity was also measured using the semi-quantitative ichnofabric index (*ii*) schemes of Droser and Bottjer (1986, 1991) based on the degree of biogenic disruption of primary fabric (Fig. 2.1). Indices range from *ii* = 1 for non-bioturbated sediment, to *ii* = 6 which reflects total homogenisation. For totally homogenised sediments, a secondary index was used to describe discrete trace fossils emplaced on a background of homogenised sediment (*ii* = 2/6 to *ii* = 4/6). MTCs were assigned a value of zero. The abundance of individual ichnotaxa was recorded as the number of separate burrows or burrow networks for each trace fossil identified, as well as counting the number of 1-cm squares containing bioturbation by particular ichnotaxa. In general,

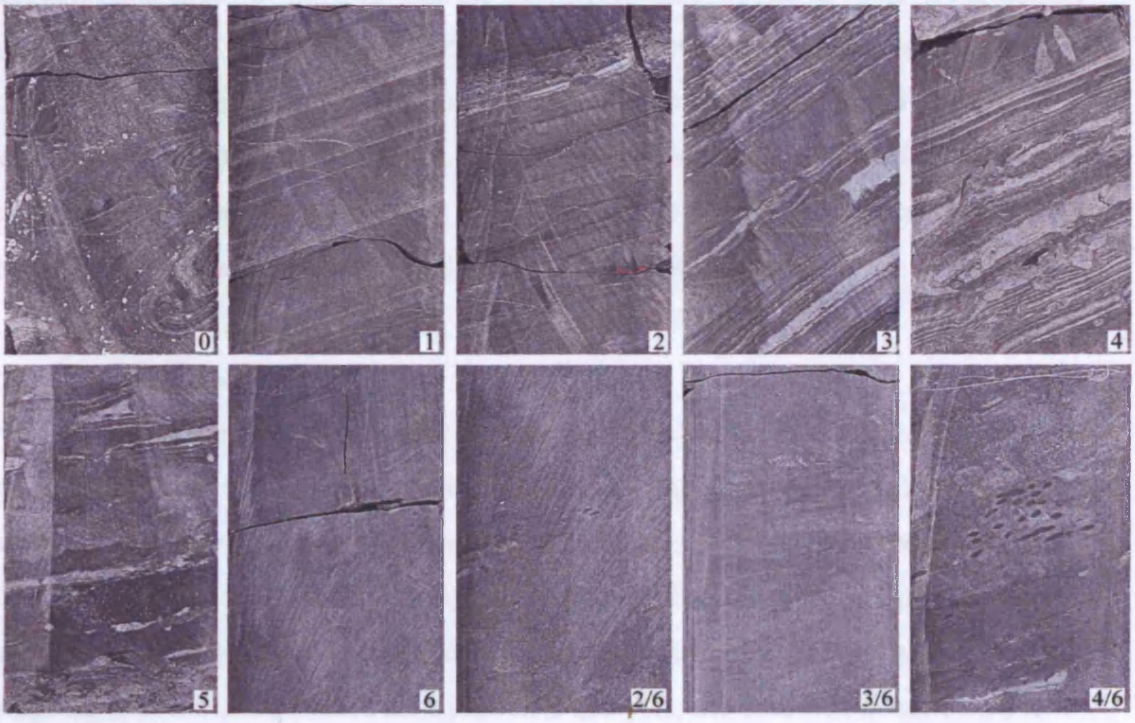

Fig. 2.1. Examples of ichnofabric indices in core (See text for details).

trace fossils were identified in vertical cross-sections, and defined at the ichnogenus level, as described by Häntzschel (1975). A detailed description of trace fossils in core can be found in section 8.2. This quantitative and semi-quantitative data was then used to establish a number of ichnofabrics, based on the sediments texture created by bioturbation (see section 8.3).

2.4. Well A6 Core

2.4.1. Trace fossil analysis

The same method described in section 2.3.2 was applied to ichnological analysis of Well A6 Core.

2.4.2. Geochemistry

200 samples were collected from the working half of core A6 at 1 m intervals, and analysed for total organic carbon (TOC) and total carbon (TC) content using a Leco CS-200 Carbon and Sulphur Analyser (University College London). Samples were not collected from the Mass-Transport Complexes (MTCs) (*sensu* Pickering & Corregidor 2005a, b). For TOC analyses, between 0.35-0.4 g of sample was weighed in a sterilised standard Leco crucible and treated with 10% hydrochloric acid, to remove carbonate, and then washed with distilled water. The samples were then dried, covered in iron chip accelerator and the residual C was measured using the Leco Analyser. Total C was determined using 0.35-0.45 g of sample weighed in a sterilised standard Leco crucible and covered in iron chip accelerator. Total inorganic carbon was calculated from TOC and TC contents, and then converted to % $CaCO_3$ by multiplication.

2.4.3. Spectral analysis

Spectral analysis was conducted on the intensity of bioturbation. Analysis was not undertaken on the gamma-ray data, as the entire A6 core is essentially silty and sandy mudstones without candidate pelagic / hemipelagic intervals where significant differences in U, Th or K values would be expected. This approach is supported by the fact that the TOC values do not indicate significant variations, at least within the sampling interval used. Before using spectral analysis, the data was conditioned to remove MTCs (sediment slides and debris flow deposits), as these represent geologically instantaneous events approximately two orders of magnitude thicker than the typical laminated turbiditic sediments in the core. This then gave a modified depth

scale in the core. AnalySeries 2.0 (Paillard *et al.* 1996) was used to depth shift the original sample depths to provide equally spaced data points. A 15-point moving average was used to smooth out high-frequency noise, and the Blackman-Tukey spectral analysis method was applied to the data.

Chapter 3

General principles of ichnology
and
systematic description of trace fossils at outcrop

3.1 Introduction

Ichnology is the study of biogenic sedimentary structures formed as a result of the life activity of an individual organism (or a monospecific group of organisms) that modifies the substrate. In general, two types of biogenic sedimentary structures can be distinguished, trace fossils and biodeformational structures (Schäfer 1956). Trace fossils have a definite shape and sharp outlines, allowing classification. Biodeformational structures lack a sharp outline and are not characterised by a distinct shape, but destroy formerly existing structures (Wetzel 1983). The field of ichnology can be considered as both palaeontological and sedimentological, underlining the importance of the discipline in bridging the gap between two of the main subdivisions in sedimentary geology.

3.2 Trace-fossil nomenclature

The history of the nomenclature and taxonomy of invertebrate trace fossils has been a complex and controversial practice since it started in the first half of the 19th Century, which is in part responsible for many nomenclatural and taxonomic problems, which exist today (see Bromley 1996 for discussion). It was not until the second half of the 20th Century that a workable taxonomic framework was produced (e.g., Häntzschel 1975, Książkiewicz 1977). However, imprecisely defined ichnotaxa are still the weak point of ichnology.

The two fundamental ranks of ichnotaxa are the ichnogenus and ichnospecies (abbreviated as igen. and isp. respectively in this thesis). Classification above the ichnogeneric level of trace fossils typical in turbidite systems is generally based on a system developed by Książkiewicz (1977) and later modified by Uchman (1995a, 1998). This simple, informal, non-interpretative classification of turbidite trace fossils

was based solely on morphological criteria. Ten morphological groups were established, namely: (1) circular and elliptical; (2) simple; (3) branched; (4) rosetted; (5) spreite; (6) winding; (7) spiral; (8) meandering; (9) branched winding and meandering; and (10) nets. This classification was adapted by Uchman (1995a, 1998) so that simple and branched structures were united in one group. This modified scheme is used in this thesis.

3.3. Toponomy

The toponomic classification of trace fossils describes both the mode of occurrence and the mechanical-sedimentological processes of alteration and preservation of a trace (Pemberton *et al.* 2001). Toponomic classification schemes have been devised by a number of authors including Seilacher (1964a, 1964b), Simpson (1957), Martinsson (1965, 1970), and Chamberlain (1971).

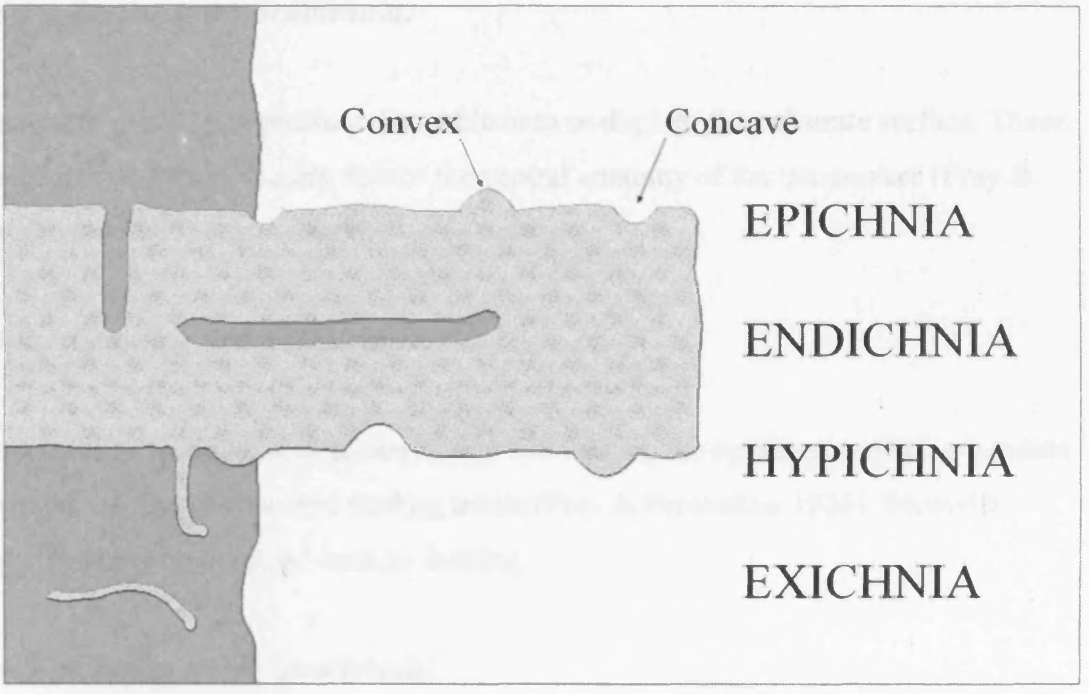

Fig. 3.1. Stratinomic classification of trace fossils in relation to the casting medium (turbidite sandstone) (redrawn after Martinsson 1965).

The classification scheme most widely adopted by ichnologists, including the current author, is that of Martinsson (1965, 1970). Biogenic structures on the lower surface of the casting medium are termed hypichnia, whilst corresponding structures on

the upper surface are called epichnia. Structures within the casting medium are termed endichnia, and those mostly outside the medium, exichnia. Exichnia and endichnia are by definition full relief (contained within the host sediment) whilst hypichnia and epichnia are semirelief (occur at lithological interfaces).

3.4. Ethological Classifications

The classification of trace fossils according to behavioural patterns was devised by Seilacher (1964a). Originally, Seilacher (1964a) recognised five ethological groups, however, this classification scheme has been expanded by a number of authors (e.g., Ekdale 1985, Frey *et al.* 1987, Bromley 1996) and now comprises eleven compartments. A complicating factor in the ethological classification of trace fossils is that not all traces are fully understood (e.g., *Zoophycos*).

3.4.1. *Resting traces (**cubichnia**)*

Structures made by organisms that settle onto or dig into the substrate surface. These traces in many cases closely mirror the ventral anatomy of the tracemaker (Frey & Pemberton 1985) e.g., *Lockeia.*

3.4.2. *Crawling traces (**repichnia**)*

Structures reflecting directed locomotion and lacking the systematic probing patterns characteristic of grazing and feeding traces (Frey & Pemberton 1985). Secondary activities may be involved such as feeding.

3.4.3. *Grazing traces (**pascichnia**)*

Where a trackway or locomotion trace clearly indicates exploitation of a particular region of the substrate for food, such as meandering or spiral traces (Ekdale 1985, Bromley 1996). Grazing traces commonly follow surfaces parallel with the sea floor and generally reflect very efficient coverage of space (Bromley 1996). Examples include *Phycosiphon* and *Nereites.*

3.4.4. *Feeding traces* ***(fodinichnia)***

Characterised by a combination of deposit feeding and dwelling. The structure has a degree of permanence but its morphology reflects exploitation of the substrate for food, e.g. *Thalassinoides* (Bromley 1996).

3.4.5. *Dwelling traces* ***(domichnia)***

Permanent or semi permanent domiciles. Mostly for the hemisessile suspension feeders, or, in some cases, carnivores (Pemberton *et al.* 2001). The burrow walls may be strengthened and most dwelling structures are later passively filled with sediments (Frey & Pemberton 1985). A common example of a dwelling trace is *Ophiomorpha.*

3.4.6. *Traps and gardening traces* ***(agrichnia)***

Regularly patterned burrows in which the activities of permanent dwelling and feeding are combined. Non-foraging graphoglyptids are examples of *agrichnia* (Ekdale *et al.* 1984, Ekdale 1985). Sulphide pumps such as *Chondrites* have also been interpreted to be *agrichnia* (Bromley 1996).

3.4.7. *Predation traces* ***(praedichnia)***

Traces resulting from predation typically are common in hard substrates as round drill holes in shells and as shell damage by predators (Ekdale 1985). Soft substrate disturbance due to predation is not easily recognisable in the fossil record.

3.4.8. *Equilibrium traces* ***(equilibrichnia)***

Traces representing the response of organisms to aggrading or degrading substrates as organisms attempt to maintain functional equilibrium in a dynamic sedimentological environment (Frey & Pemberton 1985). An example is that of *Diplocraterion.*

3.4.9. *Escape traces (**fugichnia**)*

Panic escape by organisms due to sudden burial by a package of sediment such as a turbidite.

3.4.10. *Edifices constructed above substrate (**aedifichnia**)*

Structures built of sediment more or less cemented by the architect, e.g. termite colonies (Bromley 1996).

3.4.11. *Structures made for breeding purposes (**calichnia**)*

Structures made exclusively for raising larvae or juveniles (Bromley 1996).

3.5. Colonisation of event beds - Opportunistic and equilibrium ecology

The colonisation of event beds such as turbidity currents by trace-making organisms is characterised by two population strategies; opportunistic ("r-selected") and equilibrium ("K-selected") strategies. Opportunistic ("r-selected") species include those organisms, which exhibit high reproduction rates, rapid growth rates, broad environmental tolerances and generalised feeding habits (Pianka 1970). In contrast, equilibrium ("K-selected") species are those, which are rather slow to colonise new environments, but are adaptively superior over the long run to the more rapidly colonising opportunists (Pianka 1970).

R-selected opportunistic taxa are pioneers and will bioturbate a deposit fairly rapidly to exploit whatever the sediment has to offer and then move on to another site. Recognition of r-selected taxa in the fossil record is palaeoecologically important, because opportunists are not resource-limited (Ekdale 1985). Consequently, they prosper in physically controlled environments where ecological conditions fluctuate wildly and commonly become inhospitable to most life as a consequence of factors such as oxygen depletion, highly variable salinity or very uneven sediment accumulation rates (Ekdale 1985, Bromley 1996).

K-selected equilibrium species generally exhibit lower reproductive and growth rates than r-selected taxa, and their environmental tolerances are much narrower (Ekdale

1985, Bromley 1996). They tend to be stenobathic, stenohaline and stenothermic in the marine realm and are rather specialised feeders, which have adapted to occupy specialised niches in stable, predictable and largely unchanging environments. Typically they are members of high-diversity, persistent, climax communities in which individual species abundances and population densities generally are low (Ekdale 1985). Structures formed by K-selected taxa are exemplified by complex, ornate burrow systems that reflect long-term occupation or highly specialised feeding behaviour (Bromley 1996).

3.6. Pre- and Post-depositional trace fossils

Trace fossils on the soles of turbidites represent two suites, a pre-depositional suite, those structures uncovered by shock erosion and immediately cast by turbidite fallout, and a post-depositional suite, those which have resulted from colonisation from the top of the bed (Kern 1980, Goldring 1999, Taylor *et al.* 2003). In turbidite sequences, producers of post-depositional trace fossils generally follow an r-selected opportunistic strategy in colonising the sea floor, related to the pioneer stage during colonisation of newly deposited sediments. In contrast, pre-depositional forms of trace fossils generally represent a K-selected equilibrium strategy connected with long intervals of time between deposition of turbidites (Uchman 1995a).

3.7. Ichnofacies

Particular assemblages of trace fossils tend to be characteristic of given environmental regimes, which are recurrent through time and space, wherever the requisite set of environmental conditions occur (Frey & Seilacher 1980). The description of environmentally related and contemporaneous trace-fossil assemblages in a modern environment is termed an 'ichnocoenose'. The preserved record of the original ichnocoenose is an ichnofacies (Pemberton *et al.* 2001). Ichnofacies all have the two important components of biological input and taphonomic loss, the relative importance of which, vary considerably in different ichnofacies (Bromley 1996).

The archetypal ichnofacies concept was originally developed by Seilacher (1964a 1967). Initially, Seilacher (1967) established six ichnofacies, named after characteristic ichnogenera. More recently, there has been a proliferation of ichnofacies

(see Bromley 1996, Pemberton *et al.* 2001, McIlroy, 2004). Only those ichnofabrics observed in the Ainsa-Jaca basin are described in detail below. The ichnofacies concept was based on the premise that the main control on trace-fossil assemblages was bathymetry. However, the basic controlling factors are not that of water depth or distance from the shore, but rather, such innate dynamic controlling factors such as substrate consistency, food supply, hydrodynamic energy, rates of deposition, salinity and oxygen levels and toxic substances (Frey *et al.* 1990, Pemberton *et al.* 1992, Pemberton *et al.* 2001).

3.7.1. Marine Softground Ichnofacies

3.7.1.1. *Psilonichnus* ichnofacies

This ichnofacies is associated with supralittoral/upper littoral, moderate to low-energy marine and/or aeolian conditions typical of beach to backshore to dune environments (Pemberton *et al.* 2001).

3.7.1.2. *Skolithos* ichnofacies

The *Skolithos* ichnofacies represents lower littoral to infralittoral, moderate to high-energy conditions; slightly muddy to clean, well-sorted, shifting sediments, which are subject to abrupt erosion or deposition (Frey & Pemberton 1985, Pemberton *et al.* 2001). It is indicative of relatively high levels of wave or current energy (Pemberton *et al.* 1992) and generally corresponds to the beach foreshore and shoreface (Frey & Pemberton 1985). Upper tiers which are generally characterised by a high diversity and intensity bioturbation in modern communities are rarely preserved resulting in a low diversity, low intensity trace-fossil assemblage. Ichnotaxa are commonly orientated vertically and are associated with organisms that were slow suspension feeders, which seeked security by burrowing deeply and remaining stationary for long periods of time (Bromley 1996, Pemberton *et al.* 2001). Trace fossils representative of the Skolithos ichnofacies include *Skolithos, Diplocraterion, Monocraterion,* and certain forms of *Arenicolites* and *Ophiomorpha* (Frey & Pemberton 1985).

3.7.1.3. *Cruziana* ichnofacies

This ichnofacies is usually associated with infralittoral/shallow circalittoral marine substrates in the region between wavebase and storm wavebase (Frey & Pemberton 1985, Pemberton *et al.* 2001). Typically it is associated with a moderate to relatively low energy environment in which the preservation potential of upper tiers is high (Bromley 1996, Pemberton *et al.* 2001). Consequently, it is characterised by a high diversity, high intensity trace-fossil assemblage with a high proportion of biodeformational structures and horizontally orientated burrows. Characteristic trace fossils include *Cruziana, Dimorphichnus, Teichichnus, Rosselia, Phycodes, Rusophycus, Asteriacites,* parallel-sided forms of *Rhizocorallium,* as well as certain forms of *Scolicia, Arenicolites, Ophiomorpha* and *Thalassinoides* (Frey & Pemberton 1985).

3.7.1.4. *Zoophycos* ichnofacies

This ichnofacies is characterised as circalittoral to bathyal, quiet-water conditions, or protected epeiric sites, more or less deficient in oxygen; offshore sites are below storm wavebase to fairly deep water, in areas free of turbidity flows or significant bottom currents (Frey & Pemberton 1985, Pemberton *et al.* 2001). Sediments of this ichnofacies usually exhibit total bioturbation due to the quiet accumulation of mud that allows climax communities to develop (Bromley 1996). This ichnofacies is characterised by a low diversity trace-fossil assemblage dominated by grazing traces and shallow feeding structures (Frey & Pemberton 1985). Horizontally to gently inclined spreiten structures are commonly present (Pemberton *et al.* 2001).

3.7.1.5. *Nereites* ichnofaces

This ichnofacies is characteristic of bathyal/abyssal, low-energy, oxygenated marine environments subject to periodic turbidity flows (Pemberton *et al.* 2001). According to Pemberton *et al.* (2001), the *Nereites* ichnofacies is restricted to turbidite sequences, whilst sediments beyond the influence of turbidites do not exhibit a well-preserved record of specific ichnocoenoses due to the dominance of biodeformational structures rather than discrete traces. It is characterised by ornate and complicated ichnotaxa,

pascichnia and agrichnia. Grapholglyptids are common and are preserved by slight erosion and sudden burial as semirelief casts on the sole of the overlying turbidite (Bromley 1996).

The *Nereites* ichnofacies has been divided into a number of subichnofacies; the *Ophiomorpha rudis, Nereites* and *Paleodictyon* subichnofacies. The *Ophiomorpha rudis* subichnofacies occurs in thick-bedded sandstones typical of proximal axial environments in the submarine fan (Uchman 2001). This is typified by trace fossils such as *Ophiomorpha rudis, Ophiomorpha annulata* and *Scolicia strozzii.* Seilacher (1974) proposed the *Paleodictyon* subichnofacies and the *Nereites* subichnofacies within the *Nereites* ichnofacies, which tend to occur in sandier and muddier parts of turbidite systems, respectively. The *Nereites* subichnofacies is dominated by post-depositional back-filled burrow systems made by sediment feeders (e.g., *Nereites*, *Phycosiphon*, *Zoophycos*) whilst the *Paleodictyon* subichnofacies is characterised by an abundance of open tunnels preserved on the soles of turbidites (e.g., *Paleodictyon*).

3.7.2. Hardground Ichnofacies

3.7.2.1. Glossifungites ichnofacies

This ichnofacies develops in firm but unlithified substrates; i.e. dewatered muds, formed as a result of burial and exhumation by later erosion (Pemberton *et al.* 2001). This may be related to coastal erosion in shallow-water environments, or from submarine channels cutting through previously deposited sediments (Pemberton *et al.* 2001). Glossifungites associations consist of a mixture of burrows and borings (Pemberton *et al.* 2001). Burrows generally consist of permanent vertical to steeply inclined domiciles, which generally exhibit no evidence of burrow wall reinforcement but may exhibit scratched surfaces (Uchman *et al.* 2000, Pemberton *et al.* 2001). Most trace fossils are suspension feeders. Characteristic trace fossils include *Rhizocorallium, Diplocraterion, Gastrochaenolites, Thalassinoides* and *Spongeliomorpha* (Pemberton *et al.* 2001).

3.7.2.2. Trypanites ichnofacies

This ichnofacies characterises fully lithified marine substrates such as hardgrounds, reefs, rocky coasts, beachrock, unconformities, and other kinds of omission surfaces (Pemberton *et al.* 2001).

3.7.2.3. Teredolites ichnofacies

This is characteristic of borings in mostly marine or marginal marine xylic (woody) substrates (Pemberton *et al.* 2001).

3.8. Ichnofabrics

The component of a sediments texture and internal structure created by the action of organisms is known as its ichnofabric (Ekdale & Bromley 1983). Both the production and preservation of ichnofabrics are functions of the local physical and biological environment (Droser & Bottjer 1989). Consequently, palaeoenvironmental interpretation is enhanced through the integrated use of ichnofabrics and sedimentology.

Directly or indirectly, ichnofabrics are extremely useful in deciphering a number of aspects of the depositional environment, such as: (1) the primary character of the sedimentary substrate (Ekdale & Bromley 1991, Lewis & Ekdale 1992); (2) interstitial oxygen levels in organic-rich sedimentary units (Ekdale & Mason 1988, Savrda & Bottjer 1986, 1987, 1989, 1994, Wignall 1991); (3) trophic level (eutrophic versus oligotrophic conditions) (Tunis & Uchman 1996b, Wetzel & Uchman 1998a); (4) intensity of bioturbation in stratigraphic sequences (Bottjer & Droser 1991, Droser & Bottjer 1986, 1988, 1989); (5) tiering patterns (Bromley & Ekdale 1986, Rajchel & Uchman 1998); (6) subsequent taphonomic history of one or more phases of biogenic activity (Taylor & Goldring 1993); (7) depth of erosion (Wetzel & Aigner 1986, Savrda & Bottjer 1994); (8) discontinuity surfaces (Ghibaudo *et al.* 1996); (9) sedimentary cycles (Erba & Premoli Silva 1994, Heard *et al. in review*); and (10) processes of deposition (Frey & Goldring). Consequently, ichnofabric analysis is one of the most dynamically developing fields of ichnology. There is no formal agreement as to the naming of ichnofabrics, though it is generally convenient to use a group designation

such as the '*Ophiomorpha*' ichnofabric. Bromley (1996) suggested that overall there might perhaps be a hundred or so different ichnofabrics.

Features to be recorded to allow a complete description of the ichnofabric include: (1) primary sedimentology (2) a measurement of the intensity of bioturbation; (3) ichnological diversity; (4) relative abundance; (5) burrow dimensions; (6) tiering; (7) burrow ordering; and (8) colonisation styles (Taylor & Goldring 1993, McIlroy 2004).

3.8.1. Primary sedimentology

In a detailed ichnofabric analysis, primary sedimentary characteristics of the bioturbated rock such as lithology, grain size, grain sorting, scale and type of preserved sedimentary structures should be recorded.

3.8.2. Intensity of bioturbation

The intensity of bioturbation is a major component of ichnofabric and is important because it reflects the duration of the colonisation events, which, in turn, is related to rates of sedimentation/erosion (Taylor & Gawthorpe 1993) and also reflects bottom-water oxygen conditions (e.g., Ekdale 1985, Ekdale & Mason 1988).

The importance of ichnology in palaeoenvironmental studies is reflected in the number of different methods developed for quantifying and describing sediment disruption by organisms. Two schemes for the assessment of bioturbation intensity are in current use, the descriptive bioturbation indices of Taylor *et al.* (1993) and the semi-quantitative ichnofabric index scheme of Droser & Bottjer (1986, 1991). The ichnofabric index scheme is based on the degree of biogenic disruption of the primary sedimentary fabric (see section 2.3.2). However, a problem lies in the fact that size variations of the trace fossils are not taken into account. For example, a single large trace fossil such as *Arenicolites,* when looking at a surface in vertical section, may indicate high levels of bioturbation, however, when cut in horizontal section, may indicate lower levels of bioturbation. This problem is addressed in the scheme of Taylor *et al.* (1993), as it is based on a measurement of the percentage area bioturbated with each grade of bioturbation clearly defined in terms of burrow density, amount of burrow overlap and the sharpness of the original sedimentary fabric. However, this scheme has

been less widely adopted than that of Droser and Bottjer (1986, 1991) due to its complexity and speed at which observations can be made. In the current study, the ichnofabric index scheme was used in conjunction with a quantitative measure of bioturbation intensity, outlined in section 2.3.2.

3.8.3. Diversity

Ichnological diversity is a simple process of counting the number of trace fossils present. Although trace-fossil diversity cannot be directly related to biological diversity, it is usually considered a reasonable proxy (McIlroy 2004). It can therefore be a useful indicator of environmental stress, with a low diversity trace-fossil assemblage indicative of high environment stress related to variable and low salinities, low oxygen levels, toxicity and biological factors such as competition and predation. It is also important to document the relative volumetric proportions of all traces within an ichnofabric because simply presenting data on the number of different trace fossils present may be misleading (McIlroy 2004).

3.8.4. Ichnometry

The dimensions of the burrows may also be of great importance (McIlroy 2004). Studies have shown that trace fossils become narrower in more stressed environments such as with increased salinity stress and decreasing dissolved oxygen in porewaters/bottom waters.

3.8.5. Infaunal tiering

Ecologic conditions change with depth below the sediment-water interface; sediment strength increases, porosity and permeability decrease, organic matter becomes decomposed, and oxygen content of the pore water decreases (Bąk 1994, Wetzel & Uchman 1997, Wetzel & Uchman 1998a). As a result, organisms and their traces below the sediment are subdivided into a vertical sequence known as tiering (Ausich & Bottjer 1982). The preservation of a tiering profile is reliant upon rapid killing off of the community (e.g., burial under an event bed), because with continued deposition, deeper burrows tend to overprint shallower ones (McIlroy 2004). Consequently, turbidite

sequences are suitable to study tiering because the rapid depositional events preserve the tiering structure of the bioturbate zone as a "frozen profile" (Wetzel & Uchman 1998a). In turbidite deposits, two levels of colonisers have a distinct influence on tiering. Deep-tier, generally opportunistic, multi-layer colonisers, which feed in the sediment of buried turbidites, are typically the first to colonise newly deposited turbidites from the bottom because they have the shortest path to the new substrate and form elite trace fossils. The shallow-tier, single-layer colonisers, which mainly represent equilibrium strategies come from outside the deposited sediment (Uchman 1995a, Tunis & Uchman 1996b).

In thin-bedded turbidite sequences or continuously accumulating deposits, tiering can be very complex due to the occurrence of multiple episodes of bioturbation as deeper burrows overprint shallower ones. In many cases, elite trace fossils, which are commonly late-stage bioturbators and may be visually striking due to a prominent fill/burrow lining, may visually dominate an ichnofabric (Bromley & Ekdale 1986, Bromley 1996, McIlroy 2004). It is therefore important to understand the succession of bioturbation when analysing tiering.

The tier structure and sequential changes in tier structure provide much information including: (1) ecological maturity, reflecting stability of the environment; (2) highlights omission and hiatuses in sedimentation, erosion or non-deposition (Wetzel & Aigner 1986); (3) reflects ecological changes; (4) provides information for the quantification of porosity and permeability of the sediment; and (5) appreciation of the effects of diagenesis and consolidation of the sediment (Taylor *et al.* 2003).

3.9. Ichnofacies and Ichnofabrics - Summary

As outlined above, there are two main methodologies for using ichnology in facies analysis, both of which take into consideration the primary sedimentary structures and other primary aspects of the sediment, the processes involved and their interpretation. One method uses the specific ichnotaxa as indicators of ichnofacies, linked to an environmental/bathymetric distribution model, and is adopted by, for example, Pemberton (1992). The second method is the ichnofabric approach (e.g., Martin & Pollard 1996, Taylor & Gawthorpe 1993). According to Taylor *et al.* (2003), the integrated ichnofabric analysis method provides far greater resolution than the ichnofacies analysis in the interpretation of ancient sedimentary environments and

enhances sequence stratigraphic interpretation. For example, in the Upper Jurassic Fulmar Formation of the Kittiwake Field, Western Platform of the north Central Graben, Martin and Pollard (1996) recognised ten ichnofabrics, which reflect environments from the offshore to shoreface setting, thus providing a greater resolution of environmental setting recognition than using ichnofacies or a simple quantitative study of the trace fossils.

However, the use of specific ichnotaxa as indicators of ichnofacies is a method that is particularly useful at outcrop, where the most common observation is the recognition of individual ichnotaxa. Ichnofabric analysis is most useful in unweathered vertical sections, such as in core, or polished outcrop sections. The ability to fully understand ichnofabrics at outcrop, particularly in turbidite successions where fine-grained intervals between sandstones are typically highly weathered, and commonly difficult to polish, means that studying ichnofabrics at outcrop is typically limited. Consequently, most studies in core are based on ichnofabrics whilst at outcrop, observations are based on bioturbation intensity and trace-fossil diversity.

3.10. Systematic descriptions of trace fossils at outcrop

Trace fossils have been observed on bedding and on parting surfaces and in vertical sections. Taphonomic description is arranged according to morphological groups defined by Książkiewicz (1977), with further modifications by Uchman (1995a). Ichnotaxa are only briefly described, as they are characterised more extensively in publications by Uchman (1995a, 1998, 1999, and references within). Collected specimens have been donated to the Department of Paleontology, Natural History Museum (London), and are awaiting catalogue numbers. They will be catalogued as the "Thomas Heard Collection".

3.10.1. Circular and Elliptical Structures

3.10.1.1. *Mammillichnis* CHAMBERLAIN 1971

Diagnosis: Hypichnial mound with a convex or concave apex and a teat-like tubercule at the centre of the apex.

Mammillichnis aggeris CHAMBERLAIN 1971

1971 *Mammillichnis aggeris* n. ichnog. and sp. – Chamberlain, p. 238, pl. 30, figs. 6-7.

Diagnosis: As for ichnogenus

Remarks: Small, circular or elliptical hypichnial mounds with apical depression and tubercule at the centre of the depression. The mound is 6 mm in diameter and 4 mm in height. According to Uchman (1998), *M. aggeris* represents the upper part of a thin vertical or subvertical cylindrical burrow, which displays a hemispherical funnel-like upper termination. The funnel was probably produced actively by the tracemaker and may have been filled with pellets or may have acted as a trap.

3.10.1.2. *Bergaueria* PRANTL 1945

Diagnosis: Cylindrical or hemispherical, vertical structures having smooth, unornamented walls, circular to elliptical in cross-section; fill essentially structureless;

rounded base, with or without shallow, central depression and radial ridges (after Pemberton *et al.* 1988).

Remarks: *Bergaueria* is probably a cubichnial or domichnial trace fossil produced by suspension-feeders, probably coelenterates, chiefly sea anemones (Fürsich 1975, Pemberton *et al.* 1988, Uchman 1998).

?*Bergaueria prantli* KSIĄŻKIEWICZ 1977 (Appendix 3.1.E)

Bergaueria prantli n. ichnosp. – Książkiewicz, p. 53, pl. 1, figs. 3-5, text-fig. 5c-e.

Diagnosis: *Bergaueria* displaying an irregular shape and apical, more or less distinct, irregular depression (after Uchman 1998).

Remarks: Large hypichnial mound 32 mm long, 25 mm wide, and 20 mm high. ?*B. prantli* was recently reviewed by Uchman (1998).

3.10.1.3. Plug-shaped form A (Appendix 3.1.B)

Description: Large hypichnial semi-relief mound with flat top, oval to circular in outline. Ranges between 32-38 mm long, 28-30 mm wide, and 25 mm high.

Remarks: A similar trace was described by Uchman (1995a) (Plug-shaped form A, p. 11, Pl. 2, Fig 7). Uchman (1995a) interpreted the trace as possibly being the cast of a sea-floor depression formed by burrowing fish.

3.10.1.4. *Lockeia* JAMES 1879

Diagnosis: Bilaterally symmetrical, elongated, commonly almond-shaped, heart-shaped, club-shaped to dumbbell-like or rarely of triangular shape, with smooth margin; predominantly preserved as isolated or row-like arrangements of, hypichnial mounds; single segments commonly with a distinct median crest. Vertical spreite may be present (after Schlirf *et al.* 2001).

Remarks: Isolated *Lockeia* is commonly interpreted as a bivalve resting trace most probably produced by an animal with a wedge-foot (Seilacher & Seilacher 1994).

Lockeia siliquaria JAMES 1879 (Appendix 3.1.A)

Diagnosis: Thin, elongated to stout, generally high relief, almond-shaped, smooth hypichnial ridges, with strongly arcuate to almost obtuse terminations; occasionally showing vertical spreite (after Schlirf *et al.* 2001).
Remarks: Almond-shaped hypichnial ridges, occurring in solitude or in groups of up to three on individual bedding planes.

3.10.1.5. *Circulichnis* VIALOV 1971

Diagnosis: Smooth, circular to irregularly ellipsoidal unlined burrows. Burrow fill identical to host rock (modified after Häntzschel 1975, McCann & Pickerill 1988).
Remarks: This trace is eurybathic. It has been reviewed by McCann & Pickerill (1988).

Circulichnis isp. (Appendix 3.1.C and 3.1.D)

Diagnosis: Two morphotypes of this ichnogenus have been identified. Form A is oval-shaped in outline, with inflection point located on both sides of the circle. The diameter of the trace is 15 mm with a string width of 0.6 mm. Form B consists of two symmetrical arcs. The diameter of the trace is 10 mm with a string width of 1 mm.
Remarks: Both forms are preserved as hypichnial semirelief ridges and the outline of both forms differs significantly from *C. montanus* Vialov, 1971 (McCann & Pickerill 1988).

3.10.2. Simple Branched structures

3.10.2.1. *Skolithos* HALDEMAN 1840

Diagnosis: Unbranched, vertical to steeply inclined, straight to slightly curved, cylindrical to subcylindrical, lined or unlined structures with or without funnel-shaped top. Wall distinct or indistinct, smooth to rough, some specimens annulated; fill massive; burrow diameter in some individuals slightly inconstant (after Schlirf 2000).

Remarks: Skolithos is a facies crossing trace fossil, but is most common in shallow-marine environments. It is interpreted as a domichnion produced by annelids or phoronids (Schlirf & Uchman 2005).

Skolithos isp. (Appendix 3.2.F)

Description: vertical to steeply inclined, straight, cylindrical, unlined burrows, 4-6 mm in diameter and 12-20 cm in length.
Remarks: The only occurrence of this trace fossil in the Ainsa-Jaca basin is in the upper slope gully head and associated upper slope / shelf edge sandstones at Formigales.

3.10.2.2. *Arenicolites* SALTER 1857

Diagnosis: Simple, U-shaped cylindrical structures without spreiten (after Ekdale & Lewis 1991).
Remarks: Arenicolites is interpreted as a dwelling and feeding burrow (domichnia) of suspension-feeding annelids or small crustaceans. It is typical of shallow-marine settings (Ekdale & Lewis 1991, Pervesler & Uchman 2004), and most commonly occurs in the Cruziana and Skolithos ichnofacies (Frey & Pemberton 1985).

Arenicolites isp. (Appendix 3.2.A, 3.2.B and 3.2.C)

Description: As for ichnogenus
Remarks: The burrows are preserved in full-relief and range in size, with cylinder diameters between 5-11 mm, and limbs 10-30 mm apart. The burrows are between 15-170 cm in length. The cylinders are rarely lined, and typically one cylinder is filled with coarser sand than the other. *Arenicolites* typically pervasively dominates certain horizons, with particular horizons either being dominated by small (<30 cm long) or large burrows (>30 cm long).

The bedding plane expression of *Arenicolites* is pairs of round knobs, separated by undisturbed sediment of the host rock. *Arenicolites* occurs mainly in fine- to medium-grained, very thin- to medium-bedded sandstones (facies C2.2 and C2.3), as

well as mud-silt couplets (facies D2.1) and has been observed within sandstone beds as thick as 30 cm.

3.10.2.3. *Nummulites*-lined burrow (Appendix 3.2.D and 3.2.E)

Description: Nummulites-lined vertical to horizontal, cylindrical burrows.
Remarks: The burrows are a maximum of 10 cm in length in vertical orientation, and 15 mm in diameter. In vertical section, the platy nummulites lining the burrows are stacked on top of each other, inclined at an angle of 10° away from the burrow centre. There is evidence that the trace making organism collected nummulites to line the tubes from buried nummulites rich layers. Similar nummulites-lined burrows include *Diopatrichnus roederensis* (Kern 1978), *Nummipera eocenica* (Hölder 1989) and a number of traces described from the Eocene of Poland (Roniewicz 1970, Olempska 1973). The nummulites-lined burrows observed by the current author differ to *Diopatrichnus roederensis* (Kern 1978) because the entire burrow is lined by organic fragments whilst *Nummipera eocenica* (Hölder 1989) is diagnosed as a vertical trace.

3.10.2.4. *Arthrophycus* HALL 1852

Diagnosis: Oblique to horizontal, cylindrical or subcylindrical structures with regular, perpendicular fine ribs and a tendency to plunge into bed surfaces. Commonly, the trace fossils are grouped in bundles (after Uchman 1998).

Arthrophycus ?strictus KSIĄŻKIEWICZ 1977 (Appendix 3.3.F)
Arthrophycus strictus n. ichnosp. – Książkiewicz, 57, pl. 1, figs. 11-12.

Diagnosis: Small *Arthrophycus*, approximately circular in cross-section, with very fine, delicate perpendicular ribs. Structures are distinctly arcuate in vertical plane and plunge into sole of beds (after Uchman 1998).
Remarks: Short, hypichnial, perpendicularly striated, simple ridges, which dip into the bed. The specimen observed is incompletely preserved, with half the trace missing. It is therefore unclear whether the other end of the trace dips into the bedding plane and the arcuate profile of the trace in vertical plane is not preserved. Consequently, the specimen is reservedly included in *A. strictus*.

3.10.2.5. *Halopoa* TORELL 1870

Diagnosis: Long, generally horizontal trace fossils covered with longitudinal irregular ridges or wrinkles, which are composed of several imperfectly overlapping cylindrical probes (after Uchman 1998).
Remarks: A post-turbidite trace fossil that commonly occur densely crowded on the soles of turbiditic beds. The unknown tracemaker was probably a deposit-feeder (pascichnion), specialising in the reworking of turbiditic sand (Uchman 1998).

Halopoa imbricata TORELL 1870 (Appendix 3.3.A)
1870 *Halopoa imbricata* n. sp. – Torell, 7 (no illustration)

Diagnosis: Simple, unbranched, cylindrical, hypichnial ridge, 7-12mm wide, preserved in full relief covered in horizontal, relatively long and continuous furrows and wrinkles (after Uchman 1998).
Remarks: This trace fossil can occur on the soles of turbidite sandstones as thick as 150 cm. Most commonly orientated horizontal, parallel to bedding and are straight, however, obliquely orientated trace fossils observed on the soles of beds are also common.

Halopoa storeana isp. n. (UCHMAN 2001) (Appendix 3.3.B)

Diagnosis: *Halopoa* with wrinkles arranged in distinct, oriented plait-like design (after Uchman 2001).
Remarks: Simple, unbranched, straight, cylindrical, hypichnial ridge, preserved in full relief covered with wrinkles inclined to the main axis at an angle of 10-20°, and arranged in distinct, plait-like design (Uchman 2001). The dimensions of this trace fossil are similar to *Halopoa imbricata.*

3.10.2.6. *Hormosiroidea* SCHAFFER 1928

Diagnosis: Subspherical bodies joined by horizontal string. Additional, usually oblique strings can emerge from the chambers (after Uchman 1998).

Remarks: This ichnotaxon was tentatively included in the graphoglyptids (Seilacher 1977). The bulbs may be breeding structures (Uchman 1998).

Hormosiroidea annulata (VIALOV 1971) (Appendix 3.3.C and 3.3.D)

1971 *Fustiglyphus annulatus* gen. et sp. n. – Vialov, 91, fig 3.

Diagnosis: Straight or rarely winding *Hormosiroidea* with angular, trapezoid, oval, semispherical or arcuate outline of chamber-like bodies, which are regularly or irregularly distributed along the string. Thin strings, locally branched, may emerge from the chamber-like bodies (after Uchman 1998).

Remarks: hypichnial ridge preserved in semirelief. The bulbs are much greater than the string diameter, with the string ranging in thickness from 2-5 mm, whilst the bulbs are between 4-10 mm across and tend to be bell-shaped or trapezoid in outline. Thin strings emerging from the bulb are not observed.

3.10.2.7. *Strobilorhaphe* KSIĄŻKIEWICZ 1968

Diagnosis: Horizontal trace fossils consisting of central stem and numerous lateral short, blunt, clevate branches (after Uchman 1998).

Remarks: *Strobilorhaphe* is interpreted as a post-depositional feeding trace (pascichnion). Książkiewicz (1977) interpreted the producer tentatively as a polychaete that burrowed along a central tunnel and laterally excavated small oblong holes, subsequently filling them with the reworked material.

Strobilorhaphe glandifer KSIĄŻKIEWICZ 1968 (Appendix 3.3.E)

1977 *Strobilorhaphe glandifer* n. Ichnosp. – Książkiweicz pl. 11, fig 16, text-fig. 11s-z

Diagnosis: Hypichnial full relief, more or less straight, with lateral knob-like lobate side-shoots branching from the thick stem (after Książkiewicz 1977).

Remarks: In general, the knobs are the same diameter as the stem (3 mm), and are more numerous on one side of the stem than on the other.

3.10.2.8. *Imponoglyphus* VIALOV 1971

Diagnosis: Horizontal, slightly winding trace fossil composed of invaginated, regularly spaced cones (after Uchman 1998).

Imponoglyphus torquendus Vialov 1971 (Appendix 3.4.D)

1971 *Imponoglyphus torquendus* gen. et sp. nov. Vialov, 89, pl. 2, figs. 1a-b, 2 (copied in Häntzschel, 1975, fig. 45. 1a-c).

Diagnosis: As for ichnogenus

Remarks: Two specimens were observed, both incomplete. The trace fossil is 8 mm wide.

3.10.2.9. *Planolites* NICHOLSON 1873

Diagnosis: Unlined, rarely lined, rarely branched, straight to tortuous, smooth to irregularly walled or annulated trace fossils, circular to elliptical in cross section, of variable dimensions and configurations. Fill is essentially structureless, differing in lithology from the host rock (after Uchman 1998).

Remarks: Dimensions commonly vary within given specimens and individual segments may be parallel, inclined or normal to bedding. Preserved as endichnia, hypichnial ridges and epichnial grooves (Pemberton & Frey 1982). *Planolites* is a eurybathic, extremely facies-crossing ichnogenus referred to polyphyletic vermiform deposit-feeders producing active backfilling. The taxonomy of *Planolites* has been reviewed by Pemberton and Frey (1982).

Planolites montanus RICHTER 1937 (Appendix 3.4.C)

1937 *Planolites montanus* – Richter, pl. 2, figs. 4, 7; pl. 3, fig. 9

Diagnosis: Small, curved to contorted burrows (after Pemberton & Frey 1982).

Remarks: Short, hypichnial, full-relief ridges rarely branching.

Planolites beverleyensis BILLINGS 1862 (Appendix 3.4.B)

1862 *Planolites beverleyensi* (n. sp.) – Billings, p. 97, text-fig. 86.

Diagnosis: Relatively large, smooth, straight to gently curved or undulose cylindrical burrows (after Pemberton & Frey 1982).

Remarks: Simple unlined trace fossils 4-9 mm in diameter.

Planolites ispp.

Description: Epichnial, hypichnial and more rarely, endichnial cylinders, 2-6 mm wide, rarely branching, meandering to straight.

Remarks: Poor preservation does not allow more exact determination.

3.10.2.10. *Palaeophycus* HALL 1847

Diagnosis: Branched or unbranched, smooth or ornamented, lined, essentially cylindrical, predominantly horizontal trace fossils of variable diameter: fill typically structureless, of the same lithology as the host rock (after Pemberton & Frey 1982).

Remarks: *Palaeophycus* is a eurybathic facies-crossing ichnogenus, produced probably by polychaetes (after Pemberton & Frey 1982).

Palaeophycus tabularis HALL 1847 (Appendix 3.4.A)

1847 *Palaeophycus tabularis* – Hall, pl. 1, figs. 1, 2, 5, 6, 8, 10; pl. 2, 1; pl. 3, figs. 3, 6; pl. 4, fig. 5

Diagnosis: Smooth, unornamented burrows of variable diameter, thinly but distinctly lined (after Pemberton & Frey 1982).

Remarks: Horizontal, straight to curved, rarely branched, smooth-walled burrows, distinctly lined, 4-6 mm in diameter. In cross section it is distinctly flattened and is filled with the same sediment as the host rock. Cross-cutting burrows and local collapse features are very common. Preserved as epichnial ridges or grooves.

?*Palaeophycus* isp. (Appendix 3.4.E)

Description: Cylindrical, horizontal, slightly curved, lined burrow with distinct, continuous, essentially parallel, longitudinal striations.
Remarks: Preserved as hypichnial ridge, 2 mm in diameter.

3.10.2.11. *Chondrites* STERNBERG 1833

Diagnosis: Regularly branching tunnel systems consisting of a small number of mastershafts open to the surface, which ramify at depth to form a dendritic network (after Uchman 1998).
Remarks: *Chondrites* is a feeding system of unknown trace makers related to infaunal deposit feeders. Seilacher (1990) and Fu (1991) postulated that the tracemaker of *Chondrites* may have been able to live under dysaerobic conditions as a chemosymbiotic organism.

Chondrites intricatus BRONGNIART 1823 (Appendix 3.5.B)
1823 *Fucoides intricatus* – Brongniart. 311, pl. 19, fig. 8.

Diagnosis: Small trace fossil composed of numerous downward radiating branches. The angle of branching is usually less than 45 degrees (Uchman 1998).
Remarks: There are first-, second-, and rarely third-order branches, which diverge at acute angles (after Fu 1991). The tunnels are filled with sediment lighter and, more rarely, darker than the host rock. *Chondrites intricatus* occurs in variable substrates including T_b turbiditic sandstones, but mostly in fine-grained siliciclastic and calcareous rocks.

Chondrites targionii (BRONGNIART 1828) (Appendix 3.5.C)
1823 *Fucoides targionii* – Brongniart. 56, pl. 4, figs. 2-6.

Diagnosis: *Chondrites* characterised by well expressed primary successive branchings, which are commonly slightly curved. The angle of branching is usually sharp (after Uchman 1998).

Chondrites patulus FISCHER-OOSTER 1858 (Appendix 3.5.E)

1858 *Chondrites patulus* – Fischer-Ooster, 48, pl. 8, figs. 6-7.

Diagnosis: Small *Chondrites* system with simple branches, which branches concordantly at an obtuse angle from the main stem (after Uchman 1998).

Chondrites recurvus (BRONGNIART 1823) (Appendix 3.5.D)

1823 *Chondrites recurvus* – Brongniart, 309, pl. 19, fig. 4.

Diagnosis: *Chondrites* system in which branches arise only on one side of the masterbranch and which are all bent in one direction in a lyre-shaped into two bilaterally opposed directions; there are commonly one or two orders of branching (after Fu 1991).

Chondrites isp. (Appendix 3.5.A)

Description: A system of horizontal to subhorizontal, branched tunnels. Tunnels are 0.5-1.5 mm wide. Fill differs to that of host rock in terms of colour and grain size. Occur as groups of small spots interpreted as cross-sections of *Chondrites*.

3.10.2.12. *Ophiomorpha* LUNDGREN 1891

Diagnosis: Simple to complex burrow systems lined at least partially with agglutinated pelletoidal sediment (after Uchman 1995a).

Remarks: Some burrow segments, which lack the knobbly exterior, resemble *Thalassinoides* and intergradation between *Ophiomorpha* and *Thalassinoides* is commonly observed. In Mesozoic-Cenozoic sediments, *Ophiomorpha* is produced mainly by shrimps comparable to the recent *Callianassa major*, which are partly suspension-, partly deposit-feeders (Uchman 1995a). In addition, other organisms, mainly arthropods, produce structures related to *Ophiomorpha* (Frey *et al.* 1978).

Ophiomorpha annulata KSIĄŻKIEWICZ 1977 (Appendix 3.6.B)

1977 *Arthrophycus annulata* n. ichnosp. – Książkiewicz, 56, pl. 1, figs. 8-10.

Diagnosis: Mainly horizontal or subhorizontal, cylindrical, rarely branched, covered with elongate pellets arranged perpendicularly to the long axis of the burrow. Sharp angles prevail at branching points. Swellings are common. Commonly hypichnial, smooth and straight small specimens (usually 2-6 mm in diameter) (after Uchman 1995a).

Remarks: *O. annulata* commonly occurs as small, straight or slightly curved, horizontal or slightly oblique, hypichnial full-relief, cylindrical, lined burrows, 2-10 mm in diameter. The cylinders are smooth or covered, commonly only partially, with small knobs and commonly occur in high density on the soles of some beds. Burrow fill is identical to the host rock. *O. annulata* was probably produced by extremely deep burrowing crustaceans, which were searching for deeply buried plant detritus. It occurs on the soles of turbidite beds as thick as 1.6 m (Channel-lobe transition).

Ophiomorpha rudis KSIĄŻKIEWICZ 1977 (Appendix 3.6.A)

1977 *Sabularia rudis* n. ichnosp. – Książkiewicz, pl. 2, fig. 4, text-fig. 7

Diagnosis: Horizontal, oblique to vertical branched, straight or slightly winding trace fossil. The cylinders are lined, with the exterior being smooth or covered with irregular ovoid sandy pellets, which are 3-4 mm in diameter.

Remarks: Preserved as endichnial, exhichnial, and more rarely hypichnial full relief trace fossils. Mainly concentrated on the top of thick turbidite beds. Some cylinders show meniscate back-filling. Diameter of the cylinders is variable, ranging from 7-25 mm.

Ophiomorpha isp. (Appendix 3.6.C and 3.6.D)

Description: Vertical to subvertical, straight or slightly winding, lined trace fossils, usually smooth or partially covered with poorly developed knobs.

Remarks: Commonly, the trace fossil is preserved in negative relief consisting of the mould of formerly pellet-lined burrows, with the mould of the pellets in the host

sediment clearly visable. Diameter of the cylinders is similar to *O. rudis*, and the trace fossil is characteristic of thick, coarse-grained amalgamated sandstone units.

3.10.2.13. *Thalassinoides* EHRENBERG 1944

Diagnosis: Three-dimensional burrow systems consisting predominantly of smooth-walled, essentially cylindrical components of variable diameter, branches; Y- to T-shaped, enlarged at points of bifurcation (after Uchman 1995a).
Remarks: *Thalassinoides* is a facies crossing form, most typical of shallow-marine environments, and is mainly produced by scavenging and deposit-feeder crustaceans (Uchman 1995a, Uchman *et al.* 2004).

Thalassinoides suevicus (Rieth 1932) (Appendix 3.6.E)

Diagnosis: Mostly horizontal, more or less regularly branching, essentially cylindrical burrow system; dichotomous bifurcations are more common than T-shaped branches (after Howard & Frey 1984).
Remarks: Preserved as epichnial, endichnial and hypichnial full relief cylinders. Diameter of the cylinders is variable, ranging from 6-30 mm.

Thalassinoides ispp. indet.

Description: Three varieties are recognised: (1) Epichnial and hypichnial full relief cylinders, 10-20 mm wide, and probably branched; (2) Hypichnial and epichnial mounds and short ridges of similar size, preserved as semirelief, can be interpreted as washed-out and cast parts of *Thalassinoides* burrow system; (3) vertical, sub-vertical and horizontal endichnial cylinders, 10-22 mm in diameter, found in turbidite capping shales (T*e*).
Remarks: Poor preservation does not allow more exact determination.

3.10.2.14. *Spongeliomorpha* DE SAPORTA 1887

Diagnosis: Sparsely developed burrow systems, components vertical to horizontal, characterised by sets of longitudinal or oblique, fine, elongate striation on exterior of burrow casts (Uchman 1998).
Remarks: The striations are interpreted as scratch traces produced in stiff substrate.

Spongeliomorpha oraviense KSIĄŻKIEWICZ 1977 (Appendix 3.7.A)
1961 *Halymenidium oraviensis* (n.f.) – Książkiewicz, 885, pl. 2, fig. 1

Diagnosis: *Spongeliomorpha* covered with short, fine, oblique ridges. Ridges are orientated parallel and grouped in small patches. The patches form a plaited design (after Uchman 1998).
Remarks: Preserved as epichnial and hypichnial full relief cylinders. Diameter of the cylinders is variable, ranging from 10-22 mm.

3.10.2.15. *Phycodes* RICHTER 1850

Diagnosis: Densely to loosely packed bundle of tunnels. These are joined as a single stem or tightly packed in the downward-penetrating to horizontal proximal part. The bundle is split and looser in the upward-penetrating distal part (after Uchman 1998).
Remarks: *Phycodes* is regarded as a subsurface food-mining structure (Miller III 2001).

Phycodes palmatum (HALL 1852) (Appendix 3.7.F)
1852 *Buthotrephis palmate* (n. sp.) – Hall, p. 20, pl. 3, fig. 1, pl. 7, fig. 1

Description: Large bundles of densely packed burrows with minimal spreite development joined to a single stem (after Crimes & Anderson 1985).
Remarks: Fan-shaped tunnel system that diverge and overlap to some extent. Tunnel terminations are rounded 5-7 mm in diameter and 20-40 mm in length. Each fan consists of up to 9 tunnels.

3.10.2.16. *Agrichnium* PFEIFFER 1968

Diagnosis: Groups of small sub-parallel smooth furrows of unequal moderate length (after Häntzschel 1975).
Remarks: Poorly known trace fossil. Probably represent grazing trails.

?*Agrichnium* isp. (Appendix 3.7.B)

Description: Preserved as epichnial grooves. Consists of many burrows running horizontal in more or less the same direction.

3.10.2.17. *Saerichnites* BILLINGS 1866

Diagnosis: Trace fossil comprising at least single parallel rows of semicircular or subquadrate, more or less regularly distributed pits or pustules on bedding planes (after Uchman 1998).

Saerichnites abruptus BILLINGS 1866 (Appendix 3.7.D)
1866 *Saerichnites abruptus* – Billings: 76.

Diagnosis: A double row of circular to oval hypichnial mounds located in alternating positions.
Remarks: The mounds are 5 mm in diameter, up to 3 mm high, and 10 mm apart in the same row. The rows are 8-12 mm apart.

Saerichnites canadiensis CRIMES & ANDERSON 1985 (Appendix 3.7.C)
1985 *Hormosiroidea canadiensis* n. ichnosp. – Crimes & Anderson, 325, figs. 8.1

Diagnosis: A meandering line of densely spaced vertical or steeply inclined shafts, which appear on the bedding plane as circular or semi-circular mounds (after Crimes & Anderson 1985).
Remarks: The mounds are 2-5 mm in diameter, up to 2 mm high and 1-10 mm apart.

Saerichnites isp. (Appendix 3.7.E)

Description: Well spaced circular to oval hypichnial mounds which occur as both double and single rows.
Remarks: The mounds are 5 mm in diameter, up to 2 mm high and 10-30 mm apart.

3.10.2.18. *Parahaentzschelinia* Chamberlain 1971

Diagnosis: Trace fossil composed of numerous vertical shafts radiating vertically from one mastershaft. It may be expressed on interfaces as groups of oval to circular pits, mounds, bulbs, and spots (after Uchman 1998).

Parahaentzschelinia isp. (Appendix 3.8.E and 3.8.G)

Description: Form A comprise small hypichnial mounds. They are semi-reliefs, 3-5 mm in diameter, up to 2 mm in height, circular to oval in cross-section and occur closely bunched together. The surface pattern of the group of mounds is crudely circular in outline and 200 mm in diameter. Form B consist of groups of hypichnial mounds. They are semi-reliefs, 4-7 mm in diameter, up to 2 mm in height, circular in cross-section and are randomly distributed 5-20 mm apart.
Remarks: The mounds represent casts of outlets of vertical or inclined burrows. However, these burrows were not observed and thus a more precise determination is not possible.

3.10.2.19. *Teichichnus* SEILACHER 1955

Diagnosis: Long, wall-shaped, septate structures consisting of a pile of gutter-shaped laminae (after Seilacher 1955).
Remarks: *Teichichnus* is interpreted to have been formed by deposit-feeders (Häntzschel 1975) and can be classified as a fodinichnion (Pickerill *et al.* 1984).

Teichichnus isp. (Appendix 3.8.D)

Description: Vertical to sub-vertical burrows formed of stacked dark, gutter-shaped horizontal laminae. Preserved as epichnial full relief traces. Burrow diameter is 12-30 mm, and depth of burrow is 29-50 mm.
Remarks: Observed in mudstones, which form the wall of a slope gully within the Guaso System, Ainsa basin.

3.10.3. Radial structures

3.10.3.1. *Lorenzinia* GABELLI 1900

Diagnosis: Simple, short, smooth hypichnial ridges, arranged in one or two circular rows, radiating from an oval or circular central area. The ridges are very similar or different in length and are regularly or irregularly distributed. Occasionally the ridges protrude from a ring surrounding the central area (after Uchman 1995a).
Remarks: In general, *Lorenzinia* is a three-dimensional burrow system of various radial elements forming a wreath joined by a central ring (Uchman 1998). *Lorenzinia* is interpreted as a graphoglyptid (Seilacher 1977) and has been interpreted as produced by holothurians, crabs, annelids, or sipunculids (Uchman 1998 and references within).

Lorenzinia plana (KSIĄŻKIEWICZ 1968) (Appendix 3.8.B)
1968 *Sublorenzinia plana* n. "sp." – Książkiewicz, 10, pl. 5, figs. 1-2.

Diagnosis: Irregular *Lorenzinia* with short radiating ridges with rounded external terminations, or composed of an irregular wreath of knobs (after Uchman 1998).
Remarks: Hypichnial trace fossil preserved in semi-relief, 50 mm in diameter, with short ridges 1-3 mm diameter and 15 mm long.

Lorenzinia nowaki KSIĄŻKIEWICZ 1970 (Appendix 3.8.A)
1970 *Asterichnus nowaki* ichnosp. n. – Książkiewicz, 310, fig. 7d (= *Glockerichnus glockeri*)

Diagnosis: Irregular *Lorenzinia*, with pointed external terminations and elevated internal terminations of the radiating ridges (after Uchman 1998).

Remarks: Hypichnial trace fossil preserved in semi-relief, ranging in diameter between 8-55 mm. Typically occur as pairs on the soles of beds. The burrow system is interpreted as a wreath of asymmetric, wide U-tubes, which are radially arranged around a central area (Uchman 1998).

3.10.3.2. *Glockerichnus* PICKERILL 1982

Diagnosis: Branched strings, usually dichotomous, radiating from a central point or hollow central area. In some cases, indistinct bilateral symmetry is developed (after Uchman 1995a).

Glockerichnus alata (SEILACHER 1977) (Appendix 3.8.F)

1977a *Glockeria alata* n. ichnosp. – Seilacher, 316, pl. 1d, fig.9e, 10b-c.

Diagnosis: Very large *Glockerichnus*, with U-bifurcation of the radiating ridges. A new U-element usually occurs at the limb of a former element of similar shape (after Uchman 1998).

Remarks: Hypichnial, very large trace fossil ranging in size between 22-65 cm, with approximately 12-36 radiating ridges, radiating from a well defined hollow central area. The specimens observed show evidence of current erosion, indicating it to be pre-depositional. This trace fossil has been classified as a graphoglyptid by Seilacher (1977).

?*Glockerichnus* isp. (Appendix 3.8.C)

Description: Hypichnial, small, radiating trace fossil, which displays at least 13 thin strings. The radiating strings are rarely branched and up to 20 mm long. The centre is eroded.

Remarks: The question mark is placed before the ichnogeneric name due to the poor preservation of the central part of the trace fossil. Consequently, the dichotomy of the radiating ridges is unclear.

3.10.3.3. *Arenituba* STANLEY & PICKERILL 1995

Diagnosis: Generally irregularly arranged, sometimes branched tubes radiating from a central gallery, single or bunched, straight, curved, winding or sinuous, smooth to annulated, sand-coated or –filled (after Stanley & Pickerill 1995).
Remarks: a worm-like organism that maintained a permanent dwelling, from which it repeatedly extended itself, or its tentacles out along the surface seeking food, may have produced this ichnotaxa. *Arenituba* is a facies-crossing ichnotaxon, occurring in both shallow- and deep-water (Stanley & Pickerill 1995, Uchman 1998).

?*Arenituba* isp. (Appendix 3.9.A)

Description: Hypichnial, meandering, branching burrows running to a vertical shaft.
Remarks: It is most probable that this trace fossil is *Arenituba* due to a number of features which distinguish it from other radiating ichnogenera, through its lack of: (1) straight, pointed rays that may branch in bedding plane view (*Glockerichnus)*; (2) an elevated central region and rays that branch in three dimensions (*Dactyloidites*); or (3) rays nearly equal in length that broaden at their extremities (*Stellascolites*). It can be distinguished from *Stelloglyphus* due to evidence of a central vertical component in *Arenituba* that is absent in *Stelloglyphus* (after Stanley & Pickerill 1995).

3.10.3.4. *Asterosoma* VON OTTO 1854

Diagnosis: Branched elongated bulbs with concentric internal lamination (after Pervesler & Uchman 2004).
Remarks: Interpreted as a selective feeding burrow of a worm, and occurs typically in shallow-marine settings (Pemberton *et al.* 2001).

Asterosoma ispp. (Appendix 3.9.D and 3.9.E)

Description: Large, radiating endichnial trace fossil consisting of elongated bulbs.
Remarks: Weathered traces, with concentric laminae rarely preserved. The trace fossil is 40-55 cm in diameter, with the individual bulbs being 6-10 cm long. *Asterosoma* occurs in great abundance in particular horizons of the Guaso system.

3.10.4. Spreite structures

3.10.4.1. *Zoophycos* MASSALONGO 1855

Diagnosis: Spreiten structures comprised of numerous small, U- or J-shaped protrusive burrows of variable length and orientation. Spreiten arranged in helicoid spirals with an overall circular, elliptical or lobate outline, a central vertical tunnel or marginal tube may be present (after Uchman 1999).

Remarks: *Zoophycos* is generally assumed to be the trace of an unknown deposit-feeding organism. Their producers are possibly found among sipunculids (Wetzel & Werner 1981), polychaete annelids, arthropods (Ekdale & Lewis 1991), and enteropneust hemichordates (Kotake 1992). According to Kotake (1989, 1991), *Zoophycos* is produced by surface ingestors or organic detritus. Frey and Pemberton (1984) and Miller (1990) consider that the *Zoophycos*-producing animal tolerated a broad range of environmental parameters, representing an opportunistic form. In contradistinction, Bromley (1996) indicated that *Zoophycos* is a once-in-a-lifetime structure, characterising specialised sediment reworking and thus lacks typical features of opportunistic forms, but also considered that it can occur associated with *Chondrites* in opportunistic situations.

Zoophycos ?brianteus MASSALONGO 1855 (Appendix 3.9.F)

1855 *Zoophycos brianteus* – Massalongo, p. 51, pl. 3, figs. 1, 2

Diagnosis: *Zoophycos* having a more or less circular to elliptical outline in planar view, without lobes.

Remarks: Endichnial, helicoidal structure. It contains small pellets along delicate spreiten laminae. The structure is incompletely preserved.

Zoophycos insignis SQUINABOL 1890 (Appendix 3.9.C)

1890 *Zoophycos insignis* n. sp. – Squinabol, p. 195, pl. 5, fig. 2, pl. 6, fig. 1

Diagnosis: *Zoophycos* composed mostly of distinct U-shaped lobes, which may protrude from an oval central spreiten (Uchman 1999).

Remarks: Endichnial spreiten structures, which measure up to 40 cm in diameter. Preservation of entire structure is rare.

Zoophycos isp. (Appendix 3.9.B and 3.10.F)

Description: Two morphotypes of this ichnogenus have been identified. Form A is an endichnial trace, straight or slightly curved, composed of tongue-like lobes filled with spreite laminae with or without an encircling marginal tunnel. Form B, are vertical cross-sections of the lobes filled with spreite laminae.
Remarks: Form A has been described as being *Rhizocorallium*-like (Pervesler & Uchman 2004), and is probably part of a larger *Zoophycos* structure, incompletely exposed. Form B is commonly observed in core and polished turbiditic mudcaps.

3.10.4.2. *Phycosiphon* FISCHER-OOSTER 1858

Diagnosis: Planar, horizontal, or oblique lobate spreiten structure encircled at least partially by a relatively thin marginal tunnel. The lobes are protrusive (after Uchman 1999).

Phycosiphon incertum FISCHER-OOSTER 1858 (Appendix 3.10.B)
1858 *Phycosiphon incertum* – Fischer-Ooster, p. 59, pl. 15, fig. 4

Diagnosis: Extensive small-scale spreite trace fossil comprising repeated narrow, U-shaped lobes enclosing a spreite in millimetre to centimetre scale, branching regularly or irregularly from an axial spreite of similar width. Lobes are protrusive, mainly parallel to bedding/seafloor. However, the plane enclosing their width may lie horizontally, obliquely, or even vertically to bedding/seafloor (after Wetzel & Bromley 1994).
Remarks: *Phycosiphon incertum* is common in poorly oxygenated sediments. This trace fossil is produced by a deposit feeder (Uchman *et al.* 2004).

3.10.4.3. *Lophoctenium* RICHTER 1850

Diagnosis: Branches of closely spaced, inwardly bent "twigs" with comb-like branches, joining to form main axis (after Häntzschel 1975).

Lophoctenium ramosum (TOULA 1900) (Appendix 3.10.E)

1900 *Criophycus ramosus* – Toula, p. 159, fig. 159

Diagnosis: A bunch-like trace consisting of incisions on the upper surface. From the main furrow branch lateral grooves, 1-2 mm wide, curved in one direction, occur. Usually the ramifications occur on one side of the main furrow (after Książkiewicz 1977).

Remarks: Preserved as epichnial semirelief ridges, which sometimes totally dominate the trace-fossil assemblage of the tops of turbidite sandstones.

3.10.5. Winding and meandering structures

3.10.5.1. *Nereites* MACLEAY 1839

Diagnosis: Usually selectively preserved, winding to regularly meandering, more or less horizontal trails, consisting of median back-filled tunnel enveloped by even to lobate zone of reworked sediment. Commonly only the external part of the enveloping zone is preserved as a dense packed chain of uni- or multi-serial small depressions of pustules (after Uchman 1995a).

Remarks: *Nereites* is a grazing trace (Pascichnion) and probably produced by a worm-like sediment feeder (Mangano *et al.* 2000).

Nereites circinalis (HEER 1877) (Appendix 3.10.D)

1877 *Theobaldia circinalis* – Heer, p. 114, pl. 54, figs. 7-10. (non pl. 54, figs. 11-15a)

Diagnosis: *Nereites* with segments of burrows arranged in one or two spiral whorls (after Wetzel & Uchman 1997).

Remarks: Preserved as epichnial spiral traces with indistinct lobate, reworked zone.

Nereites missouriensis (WELLER 1899) (Appendix 3.10.C)

1899 *Scalarituba missouriensis* n. gen. and sp. – Weller, p. 12, pl. 6, fig. 1

Diagnosis: Variably preserved, loosely meandering to winding *Nereites* with wide, central backfilled tunnel and envelope zone of similar thickness, which occasionally displays low side lobes. The interior may be preserved as a row of at least uniserial closely packed sediment depressions, or as strongly flattened burrows, which form usually colour-contrasted strips on parting surfaces with poorly preserved or not-preserved side lobes (after Uchman 1995a).

Nereites irregularis (SCHAFHÄUTL 1851) (Appendix 3.10.A)

1851 *Helminthoida irregularis* – Schafhäutl, pl. 9, fig. 10

Diagnosis: Relatively small *Nereites* with usually closely packed, multi-storey, gregarious, deep meanders, which tend to coil. Meanders usually of variable dimension and regularity in adjacent levels or even at the same level. Mantle usually thinner than the core; where closely packed, meanders touch or overlap with neighbouring segments, in looser meanders it displays low lobes. Commonly the mantle is not preserved. Backfill structure is poorly manifested (after Uchman 1998).

Remarks: Meandering, endichnial or epichnial full relief, ribbon-like trace fossil composed of a central string and thin, poorly preserved side lobes of reworked sediment (Uchman *et al.* 2004). The central zone is preferentially preserved and occurs in some specimens as slightly elevated, flattened ridge or shallow, flat-bottom trough. The fill of the central zone, where present, is lighter coloured than the host rock and shows an indistinct backfill structure appearing as transverse ribs (Uchman *et al.* 2004).

Nereites cambrensis Murchison 1839 (Appendix 3.11.A)

1839 *Nereites cambrensis* – Murchison, p. 700, pl. 27, fig. 1

Diagnosis: Nereites with leaf-like lobes with a central tunnel.

Remarks: The observed trace is preserved as an endichnial, trace that exhibits only partially a central tunnel. The lobes alternate on each side, and have rounded ends rather than pointed ends as described by Benton (1982). The lobes are 2-4 mm long.

Nereites isp. (Appendix 3.11.B)

Description: Three morphotypes of this ichnogenus have been identified. *Nereites* isp. pres var. *Neonereites multiserialis* is preserved as hypichnial, semi-relief ridges consisting of multiple rows of pellets. *Nereites* isp. pres. var. *Neonereites biserialis* consists of a double row of pellets. Form A is in vertical section and consists of an oval shaped dark mantle surrounded by a lighter halo.
Remarks: *N.* isp. pres var. *Neonereites multiserialis* and *N.* isp. pres. var. *Neonereites biserialis* are preserved as hypichnial traces. The diameter of the traces is ~8-12 mm, with the individual pellets ~1-2 mm in diameter. According to a number of authors (e.g., Uchman 1995a, Mangano *et al.* 2000), *Neonereites* is a preservational variant of several different ichnotaxa, including *Nereites*, and should be considered as a ichnosubspecies of *Nereites.* The nomenclature adopted herein is taken from Mangano *et al.* (2000).

3.10.5.2. *Scolicia* DE QUATREFAGES 1849

Diagnosis: Variably and commonly selectively preserved, simple, winding, meandering to coiling bilobate or trilobite back-filled trace fossils with two parallel, locally discontinuous, sediment strings along their underside. In cross-section, *Scolicia* is approximately oval in outline. The underside between the strings is flat or slightly convex up. Back-fill laminae are composite and may be biserial on the upper side. Washed out variants are preserved as hypichnial bilobate ridges (after Uchman 1998).
Remarks: It is most likely that Cretaceous and younger *Scolicia* are produced by echinoids (Uchman 1995a).

Scolicia prisca DE QUATREFAGES 1849 (Appendix 3.12.A)
1849 *Scolicia prisca* – De Quatrefages, p. 265 (no illustration)

Diagnosis: *Scolicia* preserved usually as epichnial trilobite furrow with slightly concave, semicircular bottom and oblique slopes, densely packed fine transverse ribs at the bottom, and looser, asymmetrical and thicker ribs on the slopes. Two parallel strings may occur along the edges of the bottom. Proportion of bottom to slopes may vary in different specimens (after Uchman 1995a).

Remarks: The parallel strings represent the drainage canals of spatangoid echinoids (Uchman 1998). Densely packed ribs at the bottom are probably produced by locomotion organs of the producer. The asymmetric thicker ribs on the slopes are remnants of the edges of backfill menisci. Proportion of bottom to slopes and depth of furrow depend strongly on preservation (Uchman 1998).

Scolicia plana KSIĄŻKIEWICZ 1970 (Appendix 3.11.5)

1970 *Scolicia plana* ichnosp. n. – Książkiewicz, p. 289, pl. 1c

Diagnosis: *Scolicia* in which the flat medial ridge is longitudinally divided by a shallow furrow or crest (after Uchman 1998).

Remarks: The shallow crest is generally poorly preserved.

Scolicia strozzii SAVI & MENEGHINI 1850 (Appendix 3.11.4)

1850 *Nemertilites strozzii* nob. – Savi & Meneghini, p. 421.

Diagnosis: Straight to tightly meandering hypichnial bilobate ridge, preserved as semi-relief. A median groove separates the prominent zones of the ridge. The prominent zones and the groove are more or less arcuate in cross-section. Tendency to meandering; width, height, and proportions of the morphological elements may vary from specimen to specimen (after Uchman 1995a).

Remarks: This ichnotaxon is a cast of the furrow formed after washing-out of the *Scolicia* burrow by erosion. *S. strozzii* was produced at shallow tiers (Uchman 1998).

Scolicia isp. (Appendix 3.11.C and 3.11.F)

Description: Two morphotypes of this ichnogenus has been identified. Form A. Endichnial, flat, meandering trace fossil of constant width. Consists of densely packed arcuate backfill structures, with or without marginal parallel strings. Form B. In vertical section consisting of arcuate, backfill structures.

Remarks: Form A. Relatively large trace, 22-30 mm diameter, with alternating dark and light arcuate backfill structures 1-2 mm wide.

3.10.5.3. *Taenidium* HEER 1877

Diagnosis: Unlined or very thinly lined, simple, straight to sinuous, cylindrical trace fossils with a fill of meniscus-shaped segments (after Uchman 1998).
Remarks: *Taenidium* was reviewed by D'Alessandro & Bromley (1987) who recognised three valid ichnospecies: *T. serpentinum, T. cameronensis* and *T. satanassi.*

Taenidium serpentinum HEER 1877 (Appendix 3.12.D)
1877 *Taenidium serpentinum* – Heer, p. 117, pl. 45, figs. 9 and 10a
Diagnosis: Well-spaced, arcuate menisci; distinct between menisci about equal to or a little less than burrow width. External moulds may show slight annulation corresponding to menisci, or fine transverse wrinkling. Secondary subsequent branching and intersections occur. Boundary sharp, lining lacking or insignificant (after D'Alessandro & Bromley 1987).
Remarks: The burrows are closely spaced and branching is common in the observed specimen. Burrows are 10-15 mm in diameter.

Taenidium cameronensis (BRADY 1949) (Appendix 3.12.E)
1949 Scolecocoprus cameronensis – Brady, p. 471, pl. 69, fig. 1

Diagnosis: *Taenidium* having intermeniscate segments generally longer than wide, and deeply concave menisci; secondary successive branching and intersection occur (after D'Alessandro & Bromley 1987).
Remarks: Differs from *T. serpentinum* on the basis of its distinctly longer packets of sediment between successive menisci in the backfill. The arc of the meniscus is also much deeper (D'Alessandro & Bromley 1987). The width of the burrows is the same as in *T. serpentinum.*

Taenidium ispp. (Appendix 3.12.C)

Description: *Taenidium* consisting of moderately spaced arcuate menisci. Boundary sharp, lining lacking.
Remarks: These traces are relatively small, with diameters of 7-10 mm, and were observed for a distance of 40 mm. The two traces included in *Taenidium* ispp. do not

conform to any of the three ichnospecies of *Taenidium* revised by D'Alessandro & Bromley (1987).

3.10.5.4. *Protovirgularia* MCCOY 1850

Diagnosis: Horizontal or subhorizontal cylindrical trace fossil, trapezoidal, almond or triangular in cross-section, distinctly or indistinctly bilobate. Internal structure can be preserved; it is formed by successive pads of sediment, which can be expressed on the exterior as ribs. The ribs are arranged in a chevron-like biserial pattern along the external or internal dorsal part. Exterior smooth mantle covering the structure and/or oval mound-like terminations of the trace fossil can be present (after Uchman 1998).
Remarks: According to Seilacher and Seilacher (1994), *Protovirgularia* is a molluscan trace fossil.

Protovirgularia ?rugosa (MILLER & DYER 1878) (Appendix 3.12.B)
1878 *Walcottia rugosa* n. sp. – Miller & Dyer, 39, pl. 2, figs. 11 and 11a

Diagnosis: Cubichnial, short version of *Protovirgularia,* recognised by a chevron-like escape burrow. Chevron marks very strong (modified after Seilacher & Seilacher 1994, Uchman 1998).
Remarks: The two specimens examined in the field are reservedly included in *P. rugosa* because they do not have the smooth, *Lockeia*-like termination. Similar specimens also described as *P. ?rugosa* by Uchman (1998), were previously determined as *Gyrochorte burtani* by (Książkiewicz 1977, pl. 11, fig 6, 8).

3.10.5.5. *Gordia* EMMONS 1844

Diagnosis: Unbranched, horizontal, winding, or irregularly meandering trace fossils, predominantly horizontal, that tend to form loops (after Uchman 1998).

Gordia marina EMMONS 1844 (Appendix 3.13.A)

1844 *Gordia marina* – Emmons, 24, pl. 2, fig. 2

Diagnosis: *Gordia* in which level crossing is fully developed and meanders are unguided (after Uchman 1998).

Remarks: Hypichnial ridges preserved in semirelief 0.5-1 mm diameter. Most of the ridge curvatures are gentle, but some are sharp.

Gordia arcuata KSIĄŻKIEWICZ 1977 (Appendix 3.13.B)

1977 *Gordia arcuata* n. ichnosp. – Książkiewicz, p. 156, pl. 20, fig. 8, text-fig. 36y

Diagnosis: *Gordia* in which only apical arcuate bends are developed in hypichnial reliefs (after Uchman 1998).

Remarks: Hypichnial ridges preserved in semirelief 0.3-1.2 mm diameter. Arcuate bends are open to tight.

3.10.5.6. *Cosmorhaphe* FUCHS 1895

Diagnosis: Unbranched graphoglyptid trace fossil with two orders of meanders or undulations (after Seilacher 1977).

Cosmorhaphe lobata SEILACHER 1977 (Appendix 3.13.D)

1977 *Cosmorhaphe lobata* n. ichnosp. – Seilacher, p. 299, fig. 3d

Diagnosis: First order meanders fairly dense, containing 15-20 turns of regular second order meanders, which are 2-3 times higher than wide and interlock strongly (after Seilacher 1977).

Remarks: Small delicate trace with string diameter of 1-3 mm.

Cosmorhaphe sinuosa (AZPEITIA MOROS 1933) (Appendix 3.13.C)

1933 *Helminthopsis sinuosa* Azpeitia n. sp. – Azpeitia Moros, p. 45, fig. 24b

Diagnosis: First-order meanders widely spaced; second-order undulations of greater wave length than amplitude. Occasional shortcuts may connect successive turns (after Seilacher 1977).

3.10.5.7. *Helicolithus* Azpeitia Moros 1933

Diagnosis: Small, horizontal, meandering trace fossils with horizontal, second order helicoidal turns. Changes of screw direction at every turn of first order meanders (after Uchman 1998).

Helicolithus ramosus (Vialov 1971) (Appendix 3.13.E)

Diagnosis: *Helicolithus* with densely packed meanders, and in which the radius of the helicoidal turns is very small and the amplitude is relatively high. Occasionally preserved as meandering rows of horizontally cross-sectioned vertical elements (after Tunis & Uchman 1996b).

Remarks: Hypichnial semirelief of tightly spaced, meandering rows of small dots, interpreted to represent washed-out parts of *H. ramosus.*

3.10.5.8. *Helminthorhaphe* SEILACHER 1977

Diagnosis: Non-branching trace fossil of small string diameter with only one order of smooth systematic meanders of very high amplitude, usually preserved as hypichnial semi-relief strings (Uchman 1998).

Remarks: *Helminthorhaphe* occurs in shallow tiers (Uchman 1995a).

Helminthorhaphe flexuosa UCHMAN 1995a (Appendix 3.14.A)

1977 *Helminthorhaphe crassa* – Seilacher, p. 300, fig. 3h

Diagnosis: *Helminthorhaphe* with relatively deep, commonly irregular and poorly guided meanders lacking distinct bulges in the curved portions (after Uchman 1998).

Remarks: Preserved as hypichnal semirelief ridges. Commonly exhibits tightly spaced meanders.

Helminthorhaphe japonica (Tanaka 1970) (Appendix 3.13.F)

1977 *Helminthoida crassa* - Książkiewicz, p. 159, text-fig. 34 I, m, pl. 21, figs. 5-6, 8

Diagnosis: Meanders of very high amplitude and densely guided, at least part of the meanders with the rounded and typically bulging turns (after Uchman 1998).
Remarks: Preserved as hypichnal semirelief ridges and characterised by tightly spaced meanders with bulges in the turning portions of the meanders.

3.10.5.9. *Helminthopsis* HEER 1877

Diagnosis: Simple, unbranched, elongate, cylindrical tube with curves, windings, or irregular open meanders (after Wetzel & Bromley 1996).
Remarks: *Helminthopsis* is a eurybathic facies crossing trace fossil, produced probably by polychaetes or priapulids (Książkiewicz 1977, Fillion & Pickerill 1990).

Helminthopsis abeli KSIĄŻKIEWICZ 1977 (Appendix 3.14.B)

1977 *Helminthopsis abeli* n. ichnosp. – Książkiewicz, p 117, pl. 12, fig 5

Diagnosis: *Helminthopsis* that commonly displays deep and bulged or horseshoe meanders (after Uchman 1998).
Remarks: Preserved as hypichnal semirelief ridges. *H. abeli* and *H. tenuis* has recently been reviewed by Uchman (1998).

Helminthopsis tenuis KSIĄŻKIEWICZ 1968 (Appendix 3.14.D)

1968 *Helminthopsis tenuis* n. "sp." – Książkiewicz, p. 7, pl. 4, fig. 1

Diagnosis: *Helminthopsis* with co-occurring wide, shallow meanders and deeper, narrow, but obtuse meanders (after Uchman 1998).
Remarks: Preserved as hypichnal semirelief ridges.

Helminthopsis ispp. (Appendix 3.14.F)

Description: Hypichnial semirelief ridge, which displays loose meanders. The meanders display both sharp and gentle curves, but their incomplete preservation does not allow determination at the species level.

3.10.6. Spiral structures

3.10.6.1. *Spirohaphe* FUCHS 1895

Diagnosis: Thin, spirally coiled trace fossil, supposedly multi-floored (after Uchman 1998).

Spirohaphe involuta (De stefani 1895) (Appendix 3.14.C)

1895 *Helminthopsis involuta* n. – De stefani, p. 168(16), pl. 14, fig. 1

Diagnosis: Two-way spirals consisting of an inward spiral, a central loop and an outward spiral, guided between the turns of the inward one (after Seilacher 1977).
Remarks: Preserved as hypichnal semirelief ridges. The trace is up to 11 cm in diameter.

Spirohaphe isp. (Appendix 3.14.E)

Description: Two morphotypes of this ichnogenus have been identified. Form A is a small, hypichnial trace consisting of at least one complete spiral and measures 5-7 mm across. Form B is much larger, consisting of multiple spirals and shows similarities to *S. involuta.*
Remarks: The incomplete preservation of Form B does not allow determination at the species level.

3.10.7. Branched winding and meandering traces

3.10.7.1. *Belorhaphe* FUCHS 1895

Diagnosis: Horizontal trace fossils with fine, angular zigzag second order meanders, which are thicker around points of curvature. Short lateral protrusions extending from the curved points can occur. The first order meanders are very wide (after Uchman 1998).

Belorhaphe zickzack HEER 1877 (Appendix 3.15.A)
1877 Cylindrites *zickzack* Hr – Heer, p. 159, pl. 68, fig. 10

Diagnosis: As for ichnogenus.
Remarks: Preserved as hypichnal semirelief ridges. Small incomplete traces with string diameter of 1-1.5 mm, which were observed for a maximum distance of 22 mm.

3.10.7.2. *Paleomeandron* PERUZZI 1880

Diagnosis: Meandering string, with small, more or less regular, three-dimensional, rectangular second-order meanders (after Uchman 1998).

Paleomeandron robustum KSIĄŻKIEWICZ 1968 (Appendix 3.15.B)
1968 *Paleomeandron robustum* n. "sp." – Książkiewicz, p. 4, pl. 1, fig. 3

Diagnosis: Large *Paleomeandron* with second-order undulations in one plane and with irregular corners. The first-order meanders are very wide (after Uchman 1998).
Remarks: Preserved as a hypichnial trace. The outer side of the meanders is rounded whilst the inner side is straighter.

3.10.7.3. *Desmograpton* FUCHS 1895

Diagnosis: Trace fossil preserved usually as hypichnial double rows of string-like U-, J-shaped, or angular semi-meanders. Their curved segments are inwardly oriented, in alternating position, and two opposite semi-meanders are joined by short bars.

Orientation of the bars variable. Some axial elements of the system may be elevated or depressed (after Uchman 1995a).

Remarks: Desmograpton is interpreted as a three-dimensional graphoglyptid burrow (Seilacher 1977).

Desmograpton dertonensis SACCO 1888 (Appendix 3.15.D)

1888 *Nemertilites? Dertonensis* Sacc. – Sacco, p. 42, pl. 2, fig. 19

Diagnosis: *Desmograpton* with narrow U- or J-shaped semi-meanders, commonly elevated in the curved segments. The connecting bars are parallel or sub-parallel (after Uchman 1995a).

Remarks: The parallel or sub-parallel connecting bars are poorly preserved. The string is 1-1.5 mm wide.

Desmograpton alternum (KSIĄŻKIEWICZ 1977) (Appendix 3.15.E)

1977 *Helminthoida alterna* n ichnosp. – Książkiewicz, p. 162, pl. 20, fig. 2, text-fig. 35a-m

Diagnosis: *Desmograpton,* which displays U- or J-shaped semi-meanders of moderate width, elevated in the curved portions. The connecting bars are obliquely orientated to the trace-fossil axis and form a zigzag pattern (after Uchman 1995a).

Remarks: The obliquely orientated connecting bars are poorly preserved. The strings are 0.8-1.4 mm wide.

Desmograpton ichthyforme (Macsotay 1967) (Appendix 3.15.C)

1977 *Desmograpton fuchsia* n. isp. – Książkiewicz, p. 182, pl. 29, fig. 5, text-fig. 43a-f, h-i

Diagnosis: *Desmograpton,* which displays angular narrow semi-meanders, which appear as parallel ridges, joined by short perpendicular bars. Axial part of trace fossil commonly elevated. Perpendicular bars may not be preserved (after Uchman 1998).

Remarks: Preserved as a small hypichnial semirelief ridge. Observed specimen displays parallel ridges, but the perpendicular ridges not preserved. The observed specimen is poorly preserved.

3.10.7.4. *Urohelminthoida* SACCO 1888

Diagnosis: Trace fossil preserved usually as string-sized, deep hypichnial meanders. Lateral appendages protrude outwardly from the curved segments of the meanders (after Uchman 1995a).
Remarks: *Urohelminthoida* is a typical graphoglyptid trace fossil (Seilacher 1977).

Urohelminthoida dertonensis SACCO 1888 (Appendix 3.15.F)
1888 *Urohelminthoida dertonensis* Sacc. – Sacco, 36, pl. 2, figs. 8, 16

Diagnosis: *Urohelminthoida* with lateral appendages that pass straight into one arm meander, but form an angle with the second arm (after Uchman 1995a).
Remarks: Preserved as hypichnial semirelief ridge. Meanders are tight to widely spaced. String diameter is between 1-1.4 mm.

Urohelminthoida appendiculata HEER 1877 (Appendix 3.16.A)
1877 *Urohelminthoida appendiculata* Hr. – Heer, p. 168, pl. 66, fig. 1a

Diagnosis: *Urohelminthoida* with very deep, narrow meanders. The string is usually slightly winding, and the appendages can be long and can turn towards meanders (after Uchman 1998).
Remarks: Preserved as hypichnial semirelief ridge. String diameter is between 0.8-1.2 mm. The observed specimen was poorly preserved however, the characteristic deep winding meanders of *U. appendiculata* are clear.

3.10.7.5. *Protopaleodictyon* KSIĄŻKIEWICZ 1958

Diagnosis: Hypichnial, wide first-order meanders and more or less regular second-order meanders with one or two appendages usually branching from the apex of the second-order meanders (after Uchman 1998).
Remarks: The ichnospecies of *Protopaleodictyon* are distinguished on the basis of the shape of the second-order meanders and number of appendages (Uchman 1998).

Protopaleodictyon incompositum KSIĄŻKIEWICZ 1958 (Appendix 3.16.E)

1958 *Protopaleodictyon incompositum* ichnogen. nov. – Książkiewicz, p. 303, figs. 4e1-4e2 (non fig. 4e3)

Diagnosis: *Protopaleodictyon* with sinuous second-order meanders and one appendage per undulation (after Uchman 1998).

Remarks: Meanders are relatively deep and unguided.

Protopaleodictyon spinata GEINITZ 1867 (Appendix 3.16.B)

1867 *Palaeophycus spinatus* Geinitz – Geinitz, p. 16, pl. 6, fig. 4

Diagnosis: *Protopaleodictyon* with zigzag-shaped second-order meanders and one appendage per undulation (after Uchman 1998).

Remarks: First order meanders not seen due to the size of the specimen observed. Between the inflection points of the zigzag, the string is slightly curved.

Protopaleodictyon bicaudatum SEILACHER 1977 (Appendix 3.16.C)

1977 *Protopaleodictyon bicaudatum* n. ichnosp. – Seilacher, p. 313, figs. 7h, 8b

Diagnosis: *Protopaleodictyon* with two appendages per undulation (after Uchman 1998).

3.10.8. Networks

3.10.8.1. *Megagrapton* KSIĄŻKIEWICZ 1968

Diagnosis: Trace fossil commonly preserved as hypichnial irregular nets (after Uchman 1998).

Remarks: *Megagrapton* has recently been reviewed by Uchman (1998).

Megagrapton irregulare KSIĄŻKIEWICZ 1968 (Appendix 3.16.D)

Diagnosis: *Megagrapton* with meshes bordered by only slightly winding strings, which commonly branch at approximately right angle (after Uchman 1998).

Remarks: Preserved as hypichnial ridges, with string diameters of 2-3 mm.

Megagrapton submontanum (AZPEITIA MOROS 1933) (Appendix 3.16.F)

1933 *Cylindrites submontanum* n. sp. – Azpeitia Moros, 44, fig. 21b

Diagnosis: *Megagrapton* with meshes bordered by distinctly winding strings. Acute angles of branchings are common (after Uchman 1998).

Remarks: Large hypichnial traces, with the meshes having been traced for 50 cm on the soles of turbidite sands and with string diameter of 1.5-3 mm.

3.10.8.2. *Paleodictyon* MENEGHINI 1850

Diagnosis: Three-dimensional burrow system consisting of horizontal net composed of regular to irregular hexagonal meshes and vertical outlets. Preferentially, the net is preserved (after Uchman 1995a).

Remarks: The *Paleodictyon* ichnospecies were classified according to the scheme of Uchman (1995a), which is based on the maximum mesh size and thickness of string. See Uchman (1995a) for a more detailed review of *Paleodictyon.*

Ichnosubgenus *Glenodictyon* VAN DER MARCK 1863

Paleodictyon (*Glenodictyum*) *minimum* SACCO 1888 (Appendix 3.17.A)

1888 *Paleodictyon minimum* Sacc – Sacco, p. 11, pl. 1, fig. 6

Diagnosis: Very small *Glenodictyum,* mesh-size up to 2 mm, string diameter up to 0.5 mm.

Paleodictyon (*Glenodictyum*) *latum* VIALOV & GOLEV 1965 (Appendix 3.17.C)

1965 *Paleodictyon latum* sp. Nova – Vialov & Golev, p. 100, pl. 2, fig. 2

Diagnosis: Very small *Glenodictyum,* mesh-size up to 2 mm, string diameter 0.5-1.0 mm.

Paleodictyon (*Glenodictyum*) *strozzii* MENEGHINI 1850 (Appendix 3.17.D)

1850 *Paleodictyon strozzii* nob. – Meneghini in Savi & Meneghini, 484

Diagnosis: Small *Glenodictyum*, mesh-size 2-6 mm, string diameter 0.2-1.0 mm.

Paleodictyon (*Glenodictyum*) *miocenicum* SACCO 1886 (Appendix 3.17.B)

1886 *Paleodictyon miocenicum* Sacc. – Sacco, p. 301, fig. 4

Diagnosis: Small *Glenodictyum*, mesh-size 2-6 mm, string diameter 1.0-1.6 mm.

Paleodictyon (*Glenodictyum*) *delicatulum* UCHMAN 1995a (Appendix 3.17.E)

Diagnosis: Small *Glenodictyum*, mesh-size 6-14 mm, string diameter up to 0.8 mm.

Paleodictyon (*Glenodictyum*) *majus* MENEGHINI in PERUZZI 1880

1880 *Paleodictyon majus* Mgh. – Peruzzi, p. 7, pl. 1, fig. 1

Diagnosis: Medium-sized *Glenodictyum*, mesh-size 6-14 mm, string diameter 0.8-1.6 mm.

Paleodictyon (*Glenodictyum*) *goetzingeri* VIALOV and GOLEV 1965 (Appendix 3.17.F)

1951 *Paleodictyon* – Götzinger, pl. 29, fig. a

Diagnosis: Medium-sized *Glenodictyum*, mesh-size 14-30 mm, string diameter 0.8-1.6 mm.

Paleodictyon (*Glenodictyum*) *maximum* EICHWALD 1868 (Appendix 3.18.A)

1868 *Cepholites maximus* – Eichwald, p. 82, pl. 7, fig. 12

Diagnosis: Medium-sized *Glenodictyum* with thick string; mesh-size up to 14 mm, string diameter 1.6-2.8 mm.

Paleodictyon (*Glenodictyum*) *arvense* BARBIER 1956 (Appendix 3.18.B)

1956 *Paleodictyon arvense*- Barbier, p. 127, fig. 1

Diagnosis: Medium-sized *Glenodictyum* with thick string; mesh-size 14-30 mm, string diameter 1.6-2.8 mm.

3.10.9. Trackways

3.10.9.1. Arthropod trackways (Appendix 3.18.C and 3.18.D)

Description: Two morphotypes have been recognised. Form A consists of two rows of paired, oval hypichnial mounds. The mounds are oval in shape, 0.8-1.1 mm diameter, 7-9 mm apart in the rows and the rows are 11-15 mm apart. Form B consists of two poorly developed rows of spherical to oval shaped endichnial grooves. The grooves are 3-4 mm diameter, 15-20 mm apart in the rows and the rows are 16-20 mm apart.
Remarks: Similar arthropod trackways were described from the Hecho Group by Uchman (2001).

Chapter 4

Facies and facies-associations, and terminology

4.1. Introduction

The deep-marine sediments of the Ainsa-Jaca basin are described using the hierarchical and descriptive facies classification scheme of Pickering *et al.* (1986, 1989). The general characteristics of the facies-associations recognised in the Ainsa-Jaca basin refers to the facies descriptions.

4.2. Environmental summary

Sixteen fan and related environments have been recognised in the Ainsa-Jaca basin. Diagnostic criteria used to recognise individual environments stem largely from the turbidite fan models of Mutti and Ricci Lucchi (1972, 1975), Mutti (1977), Walker (1978), Mutti and Johns (1979), and Reading and Richards (1994). A detailed sedimentological description of each environment is provided in Chapter 6 and 7. A summary of diagnostic criteria for the recognition of the most common fan and related environments is detailed below.

4.2.1. Canyon

- Erosive, V-shaped in cross section.
- Low net:gross fill characterised by abundance of MTCs
- Upper slope

4.2.2. Channel

- Act as a long-term conduit for sediment gravity currents and show a wide variety of sediment infill and geometry.
- Sub-environments of channels include channel axis, channel off-axis and channel margin.

Channel axis:

- Typically characterised by amalgamated, thick-bedded sandstones, but can be highly heterogeneous and low net:gross
- Erosional contacts common
- Mud clasts and bypass deposits common

Channel off-axis:

- semi- to non-amalgamated sandstones
- erosional contacts less common than axis

Channel margin:

- sandstones with well developed fine-grained intervals between beds
- Evidence for margin instability (e.g., Type Ib MTCs).

4.2.3. Channel-lobe transition (CLT)

- Environment between channel and lobe with deposits which can exhibit characteristics of both environments (Mutti & Normark 1987).
- The characteristic feature of the CLT is related to changes that occur when turbidity currents undergo a hydraulic jump or other rapid flow change due to a variation in gradient and channelised to non-channelised environment.

4.2.4. Lobe

- Lobes typically have a tabular or sheet-like geometry and accumulate downfan from sediment-supplying feeder conduits (channels). In some spectacular outcrops, lobes can be shown to have a wedge or lensoid shape over a few kilometres (Normark & Stuart 2000).
- Individual lobes may exhibit thickening-and-coarsening-upward (interpreted as lobe progradation) or thinning-and-fining-upward sequences (interpreted as lobe abandonment).
- The compensation stacking of lobes reflects the ephemeral nature of the shifting sandy depocentres in the basin (cf. Drinkwater & Pickering, 2001).
- Characterised by sandstone bodies several metres to tens of m thick which alternate with intervals characterised by mudstones and fine-grained thin-bedded sandstone (interlobe).

4.2.5. Lobe margin

- Medium- to thin-bedded turbidites peripheral to lobe deposits, as distal equivalents.
- Characterised by thin sandstone bodies up to several metres thick with coarsening- or fining-upward sequences. Sandstone bodies alternate with fine-grained intervals of the interlobe

4.2.6. Fan fringe

- Thin to very thin-bedded turbidites in regularly bedded packets, representing the most distal submarine fan deposits.

4.2.7. Distal basin floor

- Laterally continuous, very-thin-bedded sandstones, thick-bedded mudstones and pelagics / hemipelagics deposited beyond the submarine fan.
- Medium-bedded, medium-grained sandstones are associated with exceptional flows which reached the distal basin floor.

4.3. Channel hierarchy

The channelised turbidite systems of the Ainsa basin have been described using the element analysis scheme of Pickering *et al.* (1995) and Campion *et al.* (2000). Individual channel-fills are interpreted as second-order features and are referred to as storeys, defined as a "Volume of sediment within a channel which is separated by scour surfaces" (Friend *et al.* 1979). Channel elements (commonly referred to as depositional bodies) are typically third order features and comprise a volume of sediment deposited within a single cycle of deposition bounded by channel avulsion or abandonment. Amalgamated channel elements which appear to be genetically linked as manifest by grain size, bed thickness, and facies, typically form fourth-order channel complexes. The base of a channel complex is generally marked by erosion followed by a stack of amalgamated channels that may or may not exhibit a fining-upward grain size trend. A channel complex set comprises a number of channel complexes and is marked by a regional erosion surface at the base, with the top characterised by a regional abandonment surface. These are commonly fifth order features. Fifth order features are

typically individual turbidite systems (e.g., Guaso system) and are equivalent to second-order features of Mutti and Normark (1987).

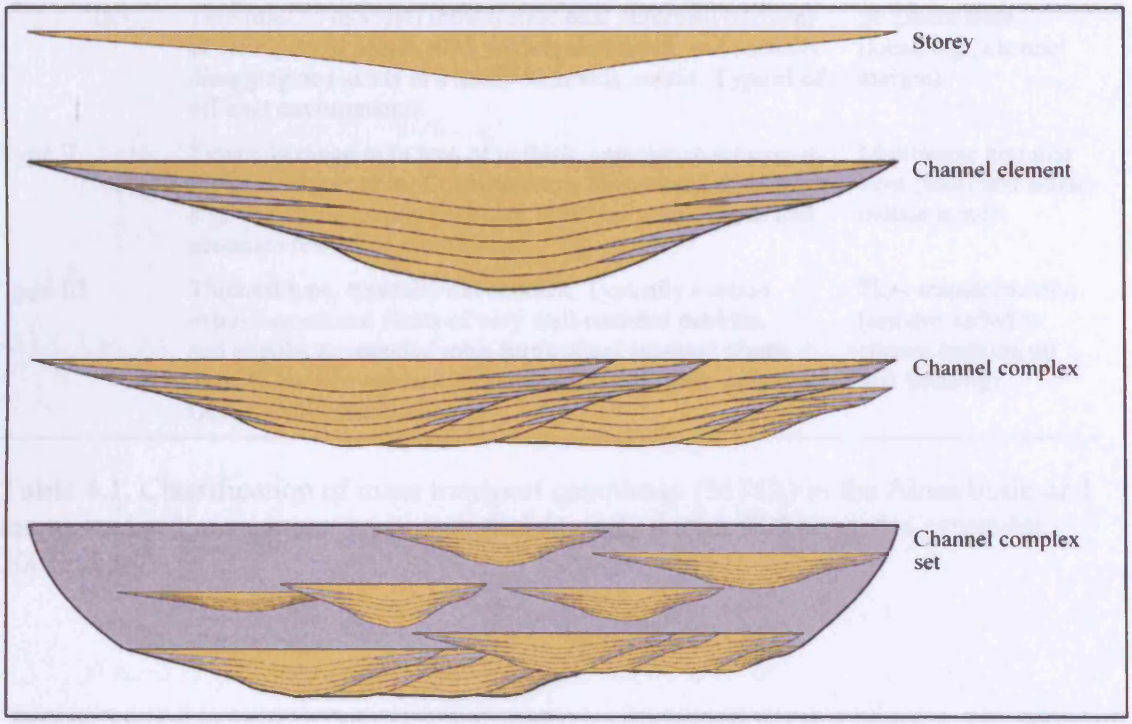

Fig. 4.1. Channel hierarchy model, see text for details.

4.4. MTCs

Chaotic deposits in the Ainsa-Jaca basin, typically with visco-plastically deformed rafts of disrupted bedding, cobble-pebble conglomerates, pebbly mudstones, mud-flake breccias, and pebbly sandstones, are classified as mass transport complexes (MTCs) *sensu* Pickering and Corregidor (2005a, b). Three broad categories of MTCs were recognised by Pickering and Corregidor (2005a, b) in the Ainsa basin, designated types I-III, with subdivisions of type Ia, Ib and Ic (Table 4.1). Where possible, the chaotic deposits studied as part of this thesis are classified according to this scheme. However, a number of MTCs cannot be classified according to this scheme and are therefore described in more detail (e.g., FA1d mud-poor turbidite sandstones and mud-rich chaotic sandstones).

Type I	Ia	Typically tens of m thick of essentially intra-formational muddy and heterolithic sediments. Generally occur between Visco-plastic deformation, varying degrees of disruption	Sediment slide (mid/upper basin bodies. sand slope)
	Ib	Thin (dm- to m-scale) intra-formational deformed horizons of clearly local origin, with folded, attenuated, and partially disaggregated sands in a sandy to muddy matrix. Typical of off-axis environments	Sediment slide (local, e.g., channel margin)
Type II		Typically range m to tens of m thick, cumulative erosion at the base of tens of m. Contains extra-formational material, e.g., very well-rounded pebbles, shallow-marine shells and abundant reworked nummulites	Multiphase granular flow (shelf and fluvio-deltaic input)
Type III		Thinnest type, typically dm-m thick. Typically contain extra-formational clasts of very well-rounded pebbles, and angular to rounded intra-formational silt-mud clasts. Tend to contain greatest proportion of sand-grade sediment. Occur within sandbodies	Flow transformation (erosive turbidity current bulking up and freezing)

Table 4.1. Classification of mass transport complexes (MTCs) in the Ainsa basin and interpreted sediment transport process(es) (modified after Pickering & Corregidor 2005a, b).

4.5. Facies descriptions

The deep-marine sediments of the Ainsa-Jaca basin are described using the hierarchical and descriptive facies classification scheme of Pickering *et al.* (1986, 1989). The reader is referred to the original facies scheme for more detailed descriptions of individual facies. In total, 31 facies have been recognised in the Ainsa-Jaca basin, of which only two are not described in the facies scheme of Pickering *et al.* (1986, 1989) (Facies H and I).

4.5.1. Facies Class A: gravels, muddy gravels, gravelly mudstones, pebbly sandstones 25% gravel grade

4.5.1.1. Facies GROUP A1 - Disorganised gravels, muddy gravels, gravelly muds and pebbly sands

4.5.1.1.1 Facies A1.1 - Disorganised gravel (Appendix 4.1.B)

This facies is typically in the order of several tens of centimetres thick (up to 2 m thick) or may occur as thin gravel lags. Beds typically have irregular erosive bases, which may be deeply scoured. Upper surface geometry may be irregular, wavy, or with individual clasts projecting out of the bed. Clast size ranges from fine pebble to boulder grade, and beds are characteristically poorly sorted and the clasts are typically angular to well-rounded. Intra-formational mud clasts are common. Facies A1.1 deposits were likely deposited from high-concentration turbidity currents or debris flows. This facies is rare in the Ainsa-Jaca basin.

4.5.1.1.2 Facies A1.2 - Disorganised muddy gravel (Appendix 4.1.C)

Facies A1.2 is matrix-supported, structureless muddy gravel with 10-50% mud- or clay-grade matrix. Individual deposits may be up to one metre thick and laterally discontinuous. The bases of beds are generally erosive (to several metres) and the tops of beds are commonly irregular. Large cobbles and boulders may be evenly dispersed throughout the bed, may project above the top of the unit, or may define a coarse-tail grading. This facies is commonly associated with other Class A deposits or with deposits of Class F and is the equivalent to the basal gravel deposits formed by bipartite debris flow described by Pickering and Corregidor (2005a, b).

4.5.1.1.3 Facies A1.3 - Disorganised gravelly mud (Appendix 4.1.D and 4.3.A)

Facies A1.3 is similar to that of Facies A1.2, except that the deposits contain 50-95% mud- or clay-grade sediment. Beds range from decimetres to tens of metres thick and the bases of beds are erosive (tens of metres) and the tops of beds are commonly irregular. Extra-formational carbonate clasts, sand rafts, shells, nummulites and sub-rounded pebbles are all common constituents as well as intra-formational folded and disaggregated heterolithics, irregular sand clasts and sand rafts and mud clasts. These are deposited from cohesive debris flows and are examples of Type II MTCs of Pickering and Corregidor (2005a, b). Thin pebble horizons (Facies A1.2) may occur towards the base of the mudstones, or punctuate the deposit throughout. This facies is common in the Ainsa basin.

4.5.1.1.4 Facies A1.4 - Disorganised pebbly sand (Appendix 4.1.A)

Facies A1.4 consists of larger clasts dispersed in a sandy matrix. These sandstones range in the order of tens of centimetres to several metres in thickness and are characterised by irregular erosive bases (up to several metres), with scour and load structures common, as well as well-developed sole marks. Clasts of fine to coarse pebble grade appear to be most common, with dispersed cobbles and boulders being less common. Clast concentration is variable, with irregular patches and stringers of more concentrated clasts occurring down to one pebble in thickness. Mudstone clasts are also common to Facies A1.4, and may form mud-flake breccias where they occur in high concentrations. The sandstones are disorganised, and rarely, larger clasts may be concentrated towards the base of a bed. These deposits are formed from high concentration turbidity currents.

4.5.1.2. FACIES GROUP A2 - Organised gravels and pebbly sands

4.5.1.2.1 Facies A2.1 - Stratified gravel (Appendix 4.2.A)

Stratified gravels are typically lens shaped, laterally discontinuous and several metres in thickness. The base of the beds is erosive, and the upper surface geometry may be irregular with individual clasts projecting out of the bed. Internal erosion surfaces are common. The deposits are clast-supported and clasts of coarse pebble grade appear to be most common. These are well-rounded to angular and up to 50 cm in diameter. Large, spherical sand clasts up to 130 cm in diameter also occur, as well as

intra-formational mud clasts. The gravels are well-stratified and characterised by a number of inclined, imbricated horizons. These deposits are formed from high concentration turbidity currents.

4.5.1.2.2 Facies A2.2 - Inversely graded gravel

Inversely graded gravels are commonly laterally discontinuous and lenticular. Individual beds are typically 0.5-1 m thick and the entire bed may be inversely graded or, more commonly, the basal part of the bed may be inversely graded. The bases of beds are generally erosive (to tens of centimetres) and the tops of beds are commonly irregular. Clast imbrication is well developed. These deposits are formed from high concentration turbidity currents undergoing late-stage flow transformations.

4.5.1.2.3 Facies A2.3 - Normally-graded gravel

Normally-graded gravels tend to be laterally discontinuous and lenticular. Beds range from tens of centimetres to several metres in thickness and are characterised by irregular erosive bases, with common basal scours and irregular tops. These deposits typically show a coarse-tail grading where the coarsest clasts occur in the lowest part of the bed and grade upward to fine pebbles. These gravels are formed from high concentration turbidity currents.

4.5.1.2.4 Facies A2.7 - Normally graded pebbly sandstones (Appendix 4.2.B)

Normally graded pebbly sandstones are the most common deposits of Facies Group A in the Ainsa-Jaca basin. Typically, beds range from tens of centimetres to several metres in thickness and are characterised by irregular erosive bases, with common basal scours and irregular tops. Clasts typically range between granules to medium pebbles in size. These deposits typically occur in amalgamated sandy units several metres in thickness. The normal grading is most commonly coarse-tail grading, although distribution grading also occurs. These pebbly sandstones are formed from high concentration turbidity currents.

4.5.1.2.5 Facies A2.8 - Graded-stratified pebbly,sandstones (Appendix 4.2.C)

Facies A2.8 is similar to Facies A2.7 in terms of bed thickness, bed shape and clast size. Beds show an overall grading from base to top, although layers of coarser clasts are repeated upward throughout beds. However, coarse clasts may be

concentrated at the base of the bed. Stratification typically comprises parallel, oblique or megaripple cross-bedding. Facies A2.8 is considered to be transitional between graded-stratified gravels of Facies A2.4 and the sandstones of Facies Class B. These pebbly sandstones are formed from high concentration turbidity currents which become more dilute with time at a single locality (i.e. waning conditions of Kneller 1995).

4.5.2. Facies Class B: sands, >80% sand grade, <5% pebble grade

4.5.2.1. FACIES GROUP B1 - Disorganised sandstones

4.5.2.1.1 Facies B1.1- Thick/medium-bedded, disorganised sandstones (Appendix 4.3.C)

Facies B1.1 consists of laterally continuous, parallel-sided to highly irregular, medium to thick beds. Sole marks are rare and grading is absent, except for the occurrence of basal layers of small pebbles. Fluid-escape structures may be well-developed. These deposits are formed from high concentration turbidity currents, sandy debris flows or liquefied flows.

4.5.2.1.2 Facies B1.2 - Thin-bedded, coarse-grained sandstones (Appendix 4.3.B)

Facies B1.2 sandstones are commonly irregular, with common wedge-shaped or pinch-and-swell geometry. The bases of beds are typically sharp and with a minor degree of erosion, and the tops are sharp. Pebbles are rare but intra-formational mud clasts including oversized mud clasts may occur. The beds are internally structureless and grading is absent. These sandstones were formed by bed-load transport beneath turbidity currents. Transport distances may have been short, and the major process may be winnowing out of finer grain sizes.

4.5.2.2 FACIES GROUP B2 - Organised sandstones

4.5.2.2.1 Facies B2.1 - Parallel-stratified sandstones (Appendix 4.4D)

These sandstones are typically medium- to very-thick-bedded, medium- to very-coarse-grained. The beds are parallel-sided to highly irregular, with common pinch-and-swell geometries. Erosive bases with intra-formational mud clasts are common. The sandstones are normally graded and characterised by bands, typically several

centimetres thick, each showing basal inverse grading as recognised by Hiscott and Middleton (1980). These sandstones are commonly amalgamated, or grade into siltstones and may display current ripples. These are deposited from high concentration turbidity currents.

4.5.2.2.2 Facies B2.2 - Cross-stratified sandstones (Appendix 4.3.D)

These sandstones are typically thin- to thick-bedded, coarse-grained to granule-grade. The beds consist of mega-ripple cross-stratification in sets that are typically from 5-25 cm thick. Beds are typically irregular, with lensing, splitting and amalgamation. The base of the sandstones may be erosive, and the tops sharp. These deposits are formed from bed-load transport beneath dilute turbidity currents.

4.5.3 Facies Class C: sandstone-mudstone couplets and muddy sandstones, 20-80% sand grade, <80% mud grade (mostly silt)

4.5.3.1 FACIES GROUP C1 - Disorganised muddy sandstones

4.5.3.1.1 Facies C1.1 - Poorly-sorted muddy sandstones (Appendix 4.4.A)

Facies C1.1 is characterised by a high content of silt- and clay-grade sediment (up to 80%) in poorly sorted beds. These deposits are typically medium- to very-coarse-grained, medium- to thick-bedded. The beds may be irregular, with the bases of beds commonly being erosive and characterised by sole structures. Grading may be crudely developed, with coarse-tail grading formed from very coarse to coarse grained sand in the lower part of the bed. The deposit may also be characterised by a lower muddy sandstone and upper silty mudstone division. Internal sedimentary structures are mainly absent, but convolute lamination associated with pseudonodules of mudstone 'chips' may occur giving the beds a swirled appearance. These sandstones may weather a blue-grey colour and are fissile. In some beds, large limestone and sandstones rafts up to 2 m in maximum dimension occur 'suspended' within the deposit. These sandstones are formed from mud-rich, very high density turbidity currents or fluid sand-mud debris flows.

4.5.3.1.2 Facies C1.2 - Mottled sandstones (Appendix 4.4.B)

Mottled muddy sandstones occur mostly as irregular, very-thin- to medium-bedded fine-grained sandstones. The tops and bases of the beds may be sharp or gradational, related to mixing due to bioturbation. Bioturbation is commonly pervasive and may destroy the primary physical structures. The beds may be laterally discontinuous due to intense bioturbation from large bulldozing (*sensu* Thayer 1979) trace-making organisms.

4.5.3.2 FACIES GROUP C2 - Organised sandstone-mudstone couplets

Facies Group C2 consists of moderately well sorted to poorly sorted sandstone-mudstone couplets showing partial or complete Bouma sequences. The bases of beds may be irregular and erosive, with sole structures common, as well as deep scour and load structures, or may be smooth and planar. The tops of beds may be flat or current rippled. Beds are typically normally graded.

4.5.3.2.1 Facies C2.1 - Very thick and thick-bedded sandstone-mudstone couplets (Appendix 4.1.A)

These sandstones generally begin with Bouma division T_a and are characterised by irregular erosive bases with common scour, load and sole structures. These sandstones are deposited from high concentration turbidity current flows.

4.5.3.2.2 Facies C2.2 - Medium bedded sandstone-mudstone couplets (Appendix 4.4.C)

Facies C2.2 sandstones typically begin with Bouma division T_b and are deposited from turbidity currents of intermediate character between high and low concentration flows.

4.5.3.2.3 Facies C2.3 - Thin-bedded sandstone-mudstone couplets (Appendix 4.5.A)

These deposits typically begin with Bouma division T_c and are characterised by smooth and planar bases. These sandstones are deposited from relatively dilute turbidity currents.

4.5.3.2.4 Facies C2.4 - Flow reflected sandstones (Appendix 4.5.B)

This facies comprises thick-bedded, mud-dominated sandstone-mudstone couplets, generally 0.5-2 m thick, which show internal evidence of flow reversals during deposition, and that commonly have a mud cap that accounts for about 80% of the thickness of the deposit. The sandy basal divisions are graded. Internal structures include megaripple form sets, ripple and climbing-ripple lamination, wavy and parallel lamination, and pseudonodules. On the top surface of the sandstones, megaripples may cross-cut one another (fig. 7.4). These are deposited from contained turbidity currents (*sensu* Pickering & Hiscott 1985) that are confined within small basins, such that multiple deflections and reflections of the initial current occur during deposition of the sand-silt load. The thick silty mud caps are deposited by rapid settling of flocs formed in the highly concentrated mud cloud that becomes ponded above the basin floor after cessation of flow (see section 7.5).

4.5.4 Facies Class D: siltstones, silty mudstones, and silt-mud couplets, >80% mud, ≥40% silt, 0-20% sand

4.5.4.1 FACIES GROUP D1 - Disorganised siltstones and silty mudstones

4.5.4.1.1 Facies D1.3 - Mottled siltstones and mudstones (Appendix 4.5.C)

Facies D1.3 consists of very thin beds, laminae, lenses and mottles of siltstone in mudstone. Bed shape is characteristically irregular and both bases and tops of the beds vary from sharp to gradational. Grading is mostly irregular in nature due to intense bioturbation. Sorting is poor to moderate. Bioturbation is intensive and may totally homogenise the sediments. If the siltstones have been totally bioturbated, they typically occur as patches of silt in bioturbated mudstones.

4.5.4.2 FACIES GROUP D2 - Organised siltstones and muddy siltstones

4.5.4.2.1 Facies D2.1 - Graded-stratified siltstones (Appendix 4.6.A)

The sediments of Facies D2.1 are typically thin- to medium-bedded, and rarely thick-bedded. The bases of beds are commonly sharp and scoured, and bed tops are gradational. The siltstones are typically normally graded. Internal sedimentary structures can be described using the Bouma (1962) turbidite model. Facies D2.1 beds

are commonly thoroughly laminated and were deposited by low concentration turbidity currents.

4.5.4.2.2 Facies D2.2 - Thick irregular siltstone and mudstone laminae

Facies D2.2 typically contains thick siltstone laminae with sharp, commonly rippled tops and scoured, sharp bases. Typically, siltstone:mudstone ratios exceed 2:1. Groups of laminae may be arranged in normally graded, laminated units showing partial structural sequences. These are deposited by low concentration turbidity currents, or relatively weak bottom currents.

4.5.4.2.3 Facies D2.3 - Thin regular siltstone and mudstone laminae (Appendix 4.6.B)

Facies D2.3 occurs as thin to medium beds of horizontal siltstone laminae in mudstone, with some slightly lenticular, indistinct and wispy silt laminae. Siltstone:mudstone ratios range from about 2:1 to about 1:2. The siltstone laminae show sharp to gradational tops and bases. This facies is particularly common in proximal axial environments in the Ainsa basin. These deposits were formed from low concentration turbidity currents, as well as weak bottom currents.

4.5.5 Facies Class E: ≥95% mud grade, <40% silt grade, <5% sand and coarser grade, <25% biogenic material

4.5.5.1 FACIES GROUP E1 - Disorganised mudstones and claystones

4.5.5.1.1 Facies E1.1 - Structureless mudstones

Structureless mudstones commonly occur in thick sections several metres thick. Bedding is poorly defined or absent, but colour banding or zones of burrow mottling, may be locally identifiable. The mudstones are either clay grade, or mixed silt and clay grades. Structureless mudstones are characteristically difficult to identify accurately at outcrop, with many mudstones appearing structureless at outcrop but showing clear structure in core or polished outcrop sections. These mudstones are probably formed by thick, mud-rich turbidity currents and lateral transfer of hemipelagic material by deep-ocean currents or by sliding.

4.5.5.1.2 Facies E1.3 - Mottled mudstones (Appendix 4.6.C)

Facies E1.3 consists of relatively uniform, thin to thick intervals of mudstone that are poorly bedded and intensely bioturbated. Relict primary sedimentary structures include wavy, indistinct, or fine parallel layering. Clay-grade material is dominant, but relatively silty patches may be common.

4.5.5.2 FACIES GROUP E2 - Organised mudstones

4.5.5.2.1 Facies E2.1- Graded mudstones

Facies E2.1 occurs both as single, isolated, graded beds >4 m thick, or as thick, repetitive successions of graded mudstones of variable thickness. Individual beds may show broad scoured bases with thin siltstone laminae at the base; thicker beds can be lenticular. Most beds show normal grading. These deposits are formed from high and low concentration turbidity currents.

4.5.6 Facies Class F: chaotic deposits

4.5.6.1 FACIES GROUP F2 - Coherent / disturbed strata

4.5.6.1.1 Facies F2.1 - Coherent folded and contorted strata (Appendix 4.6.E)

Facies F2.1 comprises folded and contorted, essentially coherent to semi-coherent intra-formational strata in irregularly-shaped layers or horizons from tens of centimetres to tens of metres thick. Discrete internal glide or shear surfaces may be visible and define the bounding surfaces of the deposit. The base of the deposit is typically erosive (tens of metres) and the upper surface is irregular, which commonly created significant seafloor topography. The deposits are characterised by common dramatic changes in layer thickness along strike. Typically these deposits comprise folded, attenuated and partially disaggregated thin-bedded sandstones and mudstones together with abundant redeposited nummulites, rarely as thin layers of concentrated nummulites in a fine-grained muddy matrix. The matrix typically comprises less than 20% sand. These deposits are deposited by slides and rotational slumps.

4.5.6.1.2 Facies F2.2 - Brecciated and balled strata (Appendix 4.6.D)

Facies F2.2 is characterised by entirely intra-formational, highly brecciated and balled strata in a chaotic disorganised mudstone matrix. Typically these deposits consist of a relatively fine grained muddy matrix with fragments of original bedding and laminae in angular to well rounded clasts and rafts. The layers of rounded balled strata are the most common variant of Facies F2.2. These deposits are characterised by irregular erosive bases (to several metres) and irregular tops, which commonly created significant seafloor topography. Relict bedding is visible as plastically deformed bundles of laminae/beds, or as 'wisps' within an almost 'homogenised' layer. These deposits are formed from gravity-induced sliding, during which internal deformation and brecciation occurs.

4.5.7 Facies Class G: biogenic oozes (>75% biogenics), muddy oozes (50-75% biogenics), biogenic muds (25-50% biogenics) and chemogenic sediments, <5% terrigenous sand and gravel

4.5.7.1 FACIES GROUP G2 - Biogenic mudstones

4.5.7.1.1 Facies G2.1- Biogenic mudstones

Facies G2.1 comprise mudstones with 25-50% biogenic content. These deposits are typically very-thin-bedded, poorly sorted and ungraded. Bedding is poorly defined and the deposits are commonly homogeneous and structureless. Bioturbation is typically intense, commonly resulting in the total homogenisation of sediment.

4.5.8 Facies H - Hemiturbidites / Calcilutites (Appendix 4.7.B)

These deposits comprise thin-bedded marly limestones. They are characterised by their white weathering colour compared to dark grey mudstones. As individual beds, they may be normally graded, become lighter towards the top, and commonly show parallel-laminated lower intervals (T_d).

According to Remacha *et al.* (2005), calcilutites (hemiturbidites) form due to hydraulic sorting of finer and lighter carbonate particles towards the top of the turbulent flow as a consequence of their poor ability to flocculate. This carbonate sediment was most probably incorporated into the flows by bulking through erosion. The fine-grained

carbonate sediment remains in suspension until the flow ceases, therefore representing the final deposits of dilute turbidity currents.

4.5.9 Facies I - Nummulites-rich bioclastic sandstones (Appendix 4.7.A)

These can be differentiated from other nummulites-rich sandstones in the Ainsa-Jaca basin (e.g., Facies Class B and C sandstones) based on the fact that they are not the products of turbidity currents. Typically the sandstones are very-fine- to fine-grained with a high silt content and are poorly sorted. They are internally structureless and ungraded, with sharp to gradational bases and gradational tops. The sandstones are rarely amalgamated, forming sandy units up to 2 m in thickness with intra-formational mud clasts common at amalgamation surfaces. Silty mudstones with abundant nummulites are typically well developed between the sandstones.

4.6 Facies-associations

The general characteristics of the facies-associations recognised in the Ainsa-Jaca basin refers to the facies descriptions above in section 4.5. In total, 29 facies-associations are recognised, which correspond to sixteen fan and related environments: (1) "Prodeltaic clastic ramp" sandbodies; (2) "Prodeltaic clastic ramp" thin-bedded sands at top of sandbodies; (3) Basin-slope; (4) Upper-slope gully; (5) Slope gully; (6) Canyon-fill; (7) Channel-axis; (8) Channel off-axis; (9) Channel margin; (10) Outermost channel-to-levee-overbank; (11) Proximal interfan; (12) Channel-lobe transition (CLT); (13) Lobe; (14) Lobe fringe; (15) Fan fringe; and (16) Distal basin-floor.

4.6.1 FA1 Disorganised chaotic deposits (MTCs)

4.6.1.1 FA1a Thick aerially extensive intra-formational chaotic mudstones (slumps and slides) (Appendix 4.8.A)

Facies-association 1a (FA1a) is characterised by thick-bedded (metres to tens of metres thick) commonly aerially extensive intra-formational disorganised chaotic deposits (Facies F2.1 and F2.2). These deposits are commonly erosive, with cumulative erosion of several tens of metres. Typically they comprise folded, attenuated and partially disaggregated thin-bedded sandstones and mudstones together with abundant redeposited nummulites, rarely as thin layers of concentrated nummulites in a fine-grained muddy matrix. The matrix typically comprises less than 20% sand. These deposits may form thick complexes (tens of metres thick) formed by several depositional events. Commonly, thin- to thick-bedded, irregular, laterally discontinuous sandstones punctuate these complexes.

Facies-association 1a occurs in a number of environments, such as canyon-fill, slope and between sandbodies. They formed depositional topography upon which sandbodies, or thin packets of sandy turbidites, accumulated. FA1a deposits are interpreted to have formed from sediment slides and slumps. These deposits are examples of Type Ia MTCs of Pickering and Corregidor (2005a, b).

4.6.1.2 FA1b Chaotic sandy-mudstones with intra-formational and extra-formational components and associated localised sandy conglomerate and gravel horizons (Appendix 4.8.B and 4.10.A)

Facies-association 1b (FA1b) is characterised by chaotic sandy-mudstones typically a few metres to tens of metres thick with both intra-formational and extra-formational components. These deposits are commonly erosive, with cumulative erosion of several tens of metres and have irregular tops, which may have created significant seafloor topography. Typically they may be stacked to create thick complexes punctuated by conglomerates, gravels and thick-bedded, coarse-grained sandstones (Facies Class A and B). These deposits are typically laterally discontinuous, with common pinch-and-swell geometries, as well as scour, load and sole structures at their bases. This facies-association is characterised by Facies A1.3 pebbly mudstones, as well as thin pebble horizons (Facies A1.2).

Although extra-formational pebbles are the most characteristic component of FA1b, they do not occur in all deposits. This is particularly true for turbidite systems characterised by an absence of extra-formational pebbles such as the Arro system (see section 5.4). FA1b deposits are interpreted to have formed from debris flows, including multiphase granular flows (*sensu* Pickering & Corregidor 2005a, b). These deposits are examples of Type II MTCs of Pickering and Corregidor (2005a, b). FA1b typically occur at the base of sandbodies, commonly defining erosion surfaces where they may be several tens of metres thick. Thinner FA1b deposits (<2 m) may occur within the sandbodies, where they may define the base of small channel elements. FA1b deposits are also common in the canyon-fill.

4.6.1.3 FA1c Chaotic thin-bedded sandy-mudstones (Appendix 4.9.A)

Facies-association 1c (FA1c) is characterised by thin (dm to m thick) chaotic sandy-mudstones. Typically the sand content of the mudstone matrix is >40%. These deposits are typically erosive (with up to 2 m of erosion), irregular, and laterally discontinuous. The deposits are typically entirely intra-formational, comprising angular mud clasts, and contorted sands of local origin, but may contain extra-formational material such as rounded pebbles, nummulites and shell fragments. FA1c is typically associated with Facies F2.1, F2.2, A1.2 and A1.3.

Facies-association 1c deposits differ to those of FA1b based on their high sand content, local nature of the deposits and thickness. FA1c deposits are similar to the

Type Ib and III MTCs of Pickering and Corregidor (2005a, b), interpreted to have formed from flow transformations, multiphase flows or sediment slides. Facies-association 1c may occur with FA3a and FA3e sandstones and is associated with the channel fill, and in particular, off axis environments such as the channel margin.

4.6.1.4 FA1d Mud-poor turbidite sandstones and mud-rich chaotic sandstones (Appendix 4.9.B)

Facies-association 1d (FA1d) is characterised by deposits comprising mud-rich sandstones (Facies C1.1) which overlie mud-poor turbidite sandstones (Facies C2.1 and C2.2) and are themselves overlain by fine-grained sandstones and/or graded mudstones (Facies E2.1). The base of the turbidite sandstones may be smooth and parallel, to irregular and scoured, whilst the surface between the mud-rich and mud-poor sandstones is typically planar to irregular. Extra-formational material is absent, but intra-formational, angular, mud clast are common. This facies-association is characteristic of the fan fringe, as well as the distal basin floor. These deposits have characteristics similar to those previously described as 'linked debrites' (Houghton *et al.* 2003), 'co-genetic debrite-turbidite' beds (Talling *et al.* 2004) and slurry beds (Lowe & Guy 2000).

Houghton *et al.* (2003) describe sharp-based, structureless and dewatered sandstones directly overlain by mud-clast breccias that are commonly rich in terrestrial plant fragments and fragments of exotic lithologies and capped by thin laminated sandstones. They interpret the breccias as deposition from debris flows that travelled on a carpet of wet and actively dewatering sand. The sedimentary characteristics, including internal structures of these linked debrites appear very different from the deposits described from the fan fringe of the Jaca basin.

Talling *et al.* (2004) described beds comprising mud-rich sandstones (sandy debrites) encased in mud-poor sandstones (turbiditic sandstones) from the Neogene Marnosa Arenacea Formation, Italian Apennines. These 'co-genetic debrite-turbidite' beds are believed to be particularly common in relatively distal fan fringe environments. They interpret these deposits as forming from erosion of the muddy seafloor by a turbidity current. The incorporation of muddy fluid into the flow leads to the development of a localised debris flow with cohesive strength. The muddy substrate commonly found in distal settings is interpreted as being fundamental to their occurrence in distal settings.

Mud-rich (debrite) sandstones described by Talling *et al.* (2004), and also those described herein are similar to deposits interpreted as slurry beds in the Lower Cretaceous Britannia Formation, UK North Sea by Lowe and Guy (2000). These mud-rich sandstones have been interpreted as the deposits of sediment flows transitional between debris flows and turbidity currents. They interpret these deposits as forming when mud was transported as sand- and silt-sized grains that were approximately hydrodynamically equivalent to suspended quartz and feldspar in initially fully turbulent turbidity currents. As the turbidity currents began to wane, particle settling resulted in the formation of strongly stratified flows with a lower part consisting of a cohesion-dominated viscous sublayer (debris flow) and an upper turbulent part (turbidity current). The lower part formed as a result of high particle contents, abundant mud and near-bed breakdown of sand-sized clay particles. The absence of sedimentary structures such as parallel lamination, meso- and macrobanding and other structures described by Lowe and Guy (2000), and the occurrence of basal turbidite sandstones, suggest that grain-size segregation resulting from traction movement and deposition beneath turbulent flows was not involved in the formation of the deposits described from the Jaca basin. A process more similar to that described by Talling *et al.* (2004) for the formation of the 'co-genetic debrite-turbidite' beds is favoured for FA1d.

4.6.2 FA2 Organised conglomerates and pebbly sandstones (>50% pebbles)

Facies-association 2 (FA2) comprises Facies Class A gravels and pebbly sandstones. Individual deposits are typically highly irregular and laterally discontinuous. FA2 comprises one group.

4.6.2.1 FA2a Lens-shaped sandy conglomerates with common inclined surfaces (Appendix 4.10.B)

Facies-association 2a (FA2a) is characterised by matrix- and clast-supported conglomerate beds with a coarse sandy matrix. These conglomerates are commonly associated with internal erosion surfaces and form lens-shaped, laterally discontinuous macroform elements. These macroform elements are characterised by erosive irregular bases with sole structures and scour depressions. The upper surface geometry is typically irregular and may form a convex-up surface, which is onlapped laterally by pebbly sandstones (Facies A1.4 and A2.7) or thin-bedded sandstones. Internal erosion

surfaces are common as well as dipping imbricated horizons, which typically dip perpendicular to palaeoflow. The conglomerates are typically well-stratified, or normal to inversely graded (Facies A2.1, A2.3 and A2.2 respectively). More rarely, they appear to be ungraded and disorganised (Facies A1.4).

The lens-shaped macroform elements of FA2a are interpreted as channel barforms formed as a result of gravity flows which underwent hydraulic jumps related to changes in seafloor gradient/flow confinement and reworked previously deposited gravels on the seafloor. The dipping imbricated horizons are interpreted as macroform accretion sets. These barforms may be point bars within a channel with some degree of sinuosity (cf. Abreu 2003), or bars formed in a braided submarine channel system. This facies-association commonly occurs with FA3g sandstones either defining the base, or occurring within sandy channelised units.

4.6.3 FA3 Thick-bedded, coarse-grained sandstones

This facies-association comprises Facies B1.1, B2.1 and C2.1 sandstones. Interbedded mudstones are typically not developed, but horizons of intra-formational rip-up mud clasts are common at amalgamation surfaces. This facies-association can be subdivided into four groups based on bed geometries.

4.6.3.1 FA3a Laterally discontinuous coarse-grained to pebbly sandstones (Appendix 4.11.A)

Facies-association 3a (FA3a) is characterised by laterally discontinuous coarse-grained to pebbly sandstones, with common pinch-and-swell bed geometries and more rarely, scour-and-fill structures. They are typically amalgamated in units up to ~11 m thick. The base of the sandstones is generally erosive (to 3 metres) with well-developed flutes and grooves. Current ripples are rarely developed. The sandstones are typically poorly sorted, normally graded and internal stratification is poorly developed, with only faint parallel stratification occurring (Facies B2.1, C2.1). This facies-association is also characterised by internally disorganised sandstones (Facies B1.1). Extra-formational nummulites are common. Some sandstones are characterised by abundant extra-formational rounded pebbles and shell fragments towards the base of the beds. These sandstones are normally graded and grade into structureless (Facies A2.7) or more rarely, planar stratified pebbly sandstones (Facies A2.8). Mud-flake breccias are also

characteristic of this facies-association and typically occur as disorganised, mud clast rich sandstones several tens of centimetres thick in amalgamated units (Facies A1.4).

. Bedding discontinuities associated with FA3a sandstones are developed as a result of underlying topographic relief associated with Facies Class A and F deposits, overlying erosive debris flow deposits or high concentration turbidity currents, or infill of erosion surfaces. Typically, this facies-association occurs towards the base of channel fills or as isolated amalgamated sandstone units within MTCs.

4.6.3.2 FA3b Laterally continuous amalgamated sandstones (at outcrop scale) (Appendix 4.11.B)

Facies-association 3b (FA3b) is characterised by laterally continuous, medium- to very-coarse-grained sandstones up to 4 m thick. Pinch-and-swell bed geometries and scour-and-fill structures occur, but the beds are typically more regular than those of FA3a. The base of the sandstones is typically erosive, and flutes and grooves are well-developed. Current ripples are rare. Most of the sandstones are normally graded and internal stratification is poorly developed, with only faint parallel stratification occurring (Facies B2.1 and C2.1). This facies-association frequently overlies FA3a in the axial fill of channels (e.g., Ainsa I sandbody), and more rarely, in channel off-axis environments.

4.6.3.3 FA3c Laterally continuous (at outcrop scale) amalgamated planar stratified sandstones (Appendix 4.12.A)

Facies-association 3c (FA3c) is very similar to FA3b, however, the sandstones are distinguished from those of FA3b by their well developed planar stratification and finer grain-size (typically fine- to coarse-grained). Pinch-and-swell bed geometries occur but scour-and-fill structures are rare. This facies-association is characteristic of the main sandy fill of prodeltaic clastic ramp sandbodies (Guaso system).

4.6.3.4 FA3d Laterally continuous (at outcrop scale) medium- to thick-bedded sandstones (Appendix 4.12.B)

Facies-association 3d (FA3d) is characterised by medium- to thick-bedded, medium- to very-coarse-grained sandstones which are amalgamated to non-amalgamated. Pinch-and-swell bed geometries occur, but scour-and-fill structures are rare. The base of the sandstones are typically erosive, and flutes and grooves are well-

developed. The top of the beds is typically flat, and rarely rippled. Most of the beds are internally structureless or display parallel stratification (Facies B1.1, B2.1 and C2.1). Normal grading is well-developed in most beds. Small extra-formational rounded pebbles at the base of the beds are very rare. Intra-formational mud clasts may occur at the base of the beds, particularly in amalgamated sandstones. This facies-association typically occurs in the channel off-axis.

4.6.3.5 FA3e Laterally continuous (at outcrop scale) medium-bedded sandstones (Appendix 4.13.A)

Facies-association 3e (FA3e) is characterised by medium-bedded, medium- to very-coarse-grained sandstones which are typically non-amalgamated. The bases of the sandstones are typically sharp and flat, whilst the tops typically have current ripples. Beds are generally tabular, laterally continuous and rarely display pinch-and-swell geometries. Internally the sandstones are typically normally graded and planar stratification is common, as well as wavy and cross-stratification (Facies B2.1, B2.2 and C2.1). Small rounded extra-formational pebbles occur rarely at the base of the sandstones, and intra-formational mud clasts are common. These sandstones are typical of the channel margin. Rarely, they may be laterally discontinuous pinching out onto the erosive margins of individual channel elements.

4.6.3.6 FA3f Medium-bedded, coarse-grained laterally continuous sandstones (Appendix 4.13.B)

Facies-association 3f (FA3f) is typical of proximal lobes and is characterised by laterally extensive medium-bedded tabular sandstones. Load structures at sand-mud contacts are common. Intra-formational mud clasts, scour-and-fill structures and pinch-and-swell geometries are rare. Current ripples are common and the sandstones are well sorted. Internal stratification is well developed, with parallel- and cross-stratification, including mega-ripple cross-stratification, common (Facies B2.2, C2.1 and C2.2). FA3f sandstones commonly overlie FA5f forming a coarsening-and-thickening-upward sequence over several metres.

4.6.3.7 FA3g Irregular, poorly sorted sandstones with scour-and-fill structures (Appendix 4.15.A)

Facies-association 3g (FA3g) is similar to that of FA3a and is characterised by medium- to thick-bedded sandstones. Sand-filled and more commonly mud-filled scour-and-fill structures, as well as pinch-and-swell bed geometries are common. Individual beds may be laterally discontinuous and are rarely amalgamated. When amalgamated, sandstone units do not exceed 1.5 m in thickness. Sole markings are common on the base of the beds as well as the sides of sand-filled scour elements. Intra-formational mud clasts typically occur at the base of beds. Current ripples are commonly developed on the tops of beds. The sandstones are typically poorly sorted, normally graded and internal stratification is rare, with only faint parallel stratification occurring (Facies B2.1, C2.1). This facies-association is also characterised by thin, erosive, disorganised chaotic deposits (Facies A1.3). These are irregular, laterally discontinuous and tend to have scour structures at their bases. FA3g typically occurs near the canyon mouth, and is formed by flows which underwent a hydraulic jump associated with changes in gradient and/or confinement at the canyon mouth. This facies-association may occur with FA3a discontinuous sandstones and FA2a lens-shaped sandy conglomerates.

4.6.3.8 FA3h Irregular, well sorted, internally stratified sandstones with scour-and-fill structures (Appendix 4.15.B)

Facies-association 3h (FA3h) is similar to that of FA3g, however, the beds are laterally more continuous and the sandstones are better sorted, with well developed internal stratification. Amalgamated sandstones are common, forming units several metres in thickness. The base of the beds is erosive (to 1.5 m) with well-developed flutes and grooves, as well as load structures at both sand/mud interfaces and amalgamation surfaces. Scour-and-fill structures are common, including both sand- and mud-filled scours. Intra-formational (rip-up) mud clasts may occur at the base of beds, and more rarely, small extra-formational rounded pebbles (<3 cm) occur at the base of normally graded sandstones (Facies A2.7). Cross-stratification, current ripples and mega-ripple cross-stratification are common features of the sandstones, as well as planar stratification (Facies B2.1, B2.2). This facies-association is typical of the channel lobe transition (CLT) and is associated with flows which underwent a hydraulic jump associated with a change in seafloor gradient and / or a change from a channelised to non-channelised environment.

4.6.4 FA4 Thin-bedded, coarse-grained sandstones

Facies-association 4 comprises Facies B1.2 thin-bedded, coarse-grained sandstones. Interbedded mudstones are commonly developed. This facies-association is typical of proximal off axis environments and can be subdivided into two groups based on bed geometries.

4.6.4.1 FA4a Lenticular mega-rippled sandstones (Appendix 4.15.A)

Facies-association 4a (FA4a) is characterised by medium- to gravel-grade, thin-bedded laterally continuous (at outcrop scale) sandstones (Facies B2.2). Individual beds have sharp bases and tops, and are generally associated with minor erosion (tens of centimetres) and some beds may exhibit load structures. The sandstones are rarely amalgamated and current ripples are common features. Lenticular bedding is common, with the sandstone lenses formed by discontinuous ripple crests associated with starved mega-ripples. These mega-ripples have crest-to-crest distances typically between 3-4 m, and up to 17 m, and amplitudes of up to 10 cm. Internally, the sandstones are typically ungraded, or more rarely, normally graded, and angular mud clasts including oversized red mud clasts are rare features.

This facies-association is typical of the outermost channel to levee-overbank and typically occurs with thin-bedded rippled sandstones of FA5b. These deposits do not form well-developed thickening- or thinning-upward sequences. The starved mega-ripples may have been deposited rapidly and then reworked by tractional processes.

4.6.4.2 FA4b Discontinuous isolated lens-shaped sandstones (in thin-bedded sandstones) (Appendix 4.15.B)

Facies-association 4b (FA4b) is characterised by laterally discontinuous (metres to tens of metres) lens-shaped medium- to coarse-grained thin-bedded sandstones. Typically they have erosive bases (to tens of centimetres) and are internally structureless. Intra-formational mud clasts and extra-formational nummulites are common constituents of these sandstones. These deposits typically occur as isolated beds within thin-bedded fine-grained sandstones, siltstones and mudstones (FA5d and FA6d) and are characteristic of the interfan and overbank. These deposits may have formed from erosive, isolated, high concentration turbidity currents as well as splay

deposits associated with channelised turbidity currents which overspilled into the genetically related levee-overbank environment.

4.6.5 FA5 Thin- to medium-bedded, fine- to medium-grained sandstone-mudstone couplets

Facies-association 5 is the most widespread in the Ainsa-Jaca basin. It is characterised by sandstone-mudstone couplets showing partial or complete Bouma sequences. Typical facies include C2.2 and C2.3 sandstones, and more rarely C2.1 and C2.4 sandstones. The mudstones are characterised by mottled D1.3 and E1.3 siltstones and mudstones, D2.3 siltstone and mudstone laminae and more rarely E2.1 and E1.1 siltstones and mudstones. Facies-association 5 is subdivided into 7 groups on the basis of bed thickness and/or geometry.

4.6.5.1 FA5a Laterally discontinuous thin- to medium-bedded sandstone-mudstone couplets with lensoid, concave-up geometry (Appendix 4.16.A)

Facies-association 5a (FA5a) is characterised by laterally discontinuous thin- to medium-bedded fine- to medium-grained sandstone-mudstone couplets (Facies C2.2 and C2.3). Individual beds are lens-shaped, concave-up and laterally discontinuous over ~7 m. The beds typically are parallel-sided, with flat non-erosive bases and flat or rarely current rippled tops. The sandstone/mudstone ratio is 1:1 and the sandstones are non-amalgamated. Internal stratification is typically well developed in thicker beds, characterised by planar stratification, and less well developed in thinner beds. Interbedded mudstones average 7.3 cm in thickness and are characterised by regular siltstone and mudstone laminae (Facies D2.3). This facies-association characterises the fill of a small (~14 m wide) slope gully.

4.6.5.2 FA5b Laterally continuous (at outcrop scale), thin- to medium-bedded sandstone-mudstone couplets (sandstone: mudstone ratio of 1:1) (Appendix 4.17A)

Facies-association 5b (FA5b) is characterised by laterally continuous (at outcrop scale), thin- to medium-bedded sandstone-mudstone couplets. The sandstones typically have sharp non-erosive bases and sharp, current rippled tops. Generally the sandstone/mudstone ratio is 1:1 and amalgamated sandstones are rare. Internal stratification is well-developed, with planar and cross-stratification common (Facies

C2.2 and C2.3). Thin-bedded sandstones may form packages of single-train rippled beds or are pervasively bioturbated (Facies C1.2). More rarely, sandstones in this facies-association have erosive bases and flat tops and are commonly amalgamated. These sandstones are characterised by poorly-developed internal stratification (Facies C2.1) and intra-formational mud clasts may occur at amalgamation surfaces. The interbedded mudstones are commonly intensely bioturbated (Facies D1.3 and E1.3) or comprise thin regular siltstone and mudstone laminae (Facies D2.3). Planar stratification and current ripples are common features of the siltstone laminae, and individual laminae may appear lenticular where starved current ripples are developed. This facies-association is characteristic of the channel margin.

4.6.5.3 FA5c Laterally discontinuous thin- to medium-bedded variable thickness sandstone-mudstone couplets (Appendix 4.11.B)

Facies-association 5c (FA5c) is characterised by laterally discontinuous thin- to medium-bedded sandstone-mudstone couplets. The deposits are very similar to those of FA5b, with flat, non-erosive bases and flat or current rippled tops. Internal stratification may be well-developed, with planar stratification common, and more rarely, cross-stratification (Facies C2.2 and C2.3). The sandstones are commonly ungraded, and more rarely, normally graded. Typically the sandstone/mudstone ratio is 1:0.5 and bedding may be indistinct due to the lack of mudstone partings. Where thin mudstones are developed, flaser bedding may be formed. This facies-association is characteristic of proximal axial environments such as the channel axis and channel off-axis. FA5c deposits commonly form the top of fining- and thinning-upward sequences associated with the channel-fill.

4.6.5.4 FA5d Laterally continuous tabular current rippled thin-bedded sandstone-mudstone couplets with poorly-developed internal stratification (Appendix 4.17.B)

Facies-association 5d (FA5d) is characterised by laterally continuous, sheet-like, tabular, thin- to medium-bedded, fine- to medium-grained sandstone-mudstone couplets. The sandstone beds typically have sharp, planar, non-erosive bases and sharp to gradational, commonly current rippled tops. Typically the sandstone/mudstone ratio is 1:1-1:2 and the sandstones are rarely amalgamated. The sandstones are typically ungraded to normally graded, and internal stratification is poorly-developed. However, individual beds may exhibit well-developed planar and cross-stratification. The

mudstones are commonly intensely bioturbated, with the preservation of primary bedding rare (Facies D1.3 and E1.3). In areas of reduced bioturbation, thin regular siltstone and mudstone laminae are developed (Facies D2.3).

This facies-association commonly forms heterolithic packages several tens of metres thick, and up to ~60 m thick, which exhibit no overall thickening- or thinning-upward trend. It is characteristic of the slope and interfan, as well as lower slope channel-overbank systems, and commonly occurs in association with siltstones, mudstones and biogenic mudstones (FA6c) and/or intra-formational chaotic mudstones (FA1a).

4.6.5.5 FA5e Laterally continuous thin- to thick-bedded fine- to medium-grained sandstones with interbedded siltstone-mudstone laminae. (Appendix 4.18.A)

Facies-association 5e (FA5e) is characterised by thin- to medium-bedded sheet-like sandstones with rare mud draped scours (Facies C2.2, C2.3). The sandstones have sharp bases and sharp, current rippled tops and are typically normally graded. Extra-formational reworked nummulites and organic detritus, as well as intra-formational (rip-up) mud clasts are rare. Internal stratification, where developed, is characterised by planar stratification. Interbedded mudstones comprise siltstone and mudstone laminae (Facies D2.3) with silt:mud ratios of 1:0.5. Flaser bedding and single-train ripple beds are commonly developed. The main characteristic of this facies-association is the paucity of bioturbation in the siltstone-mudstone laminae.

This facies-association is typical of the "prodeltaic clastic ramp" thin-bedded sandstones at the top of sandbodies.

4.6.5.6 FA5f Laterally continuous tabular current rippled sandstone-mudstone couplets with well-developed internal stratification (Appendix 4.13.B)

Facies-association 5f (FA5f) is characterised by laterally continuous, sheet-like, tabular, thin- to medium-bedded, fine- to medium-grained sandstone-mudstone couplets. The sandstone beds typically have sharp, planar, essentially non-erosive bases and sharp current rippled tops. Well-developed sole structures are formed at the base of some beds. Typically the sandstone/mudstone ratio is 1:1-1:2 and the sandstones are rarely amalgamated. Intra-formational mud clasts are uncommon. Internal stratification is typically well-developed, with cross and planar stratification common, and more rarely liquefaction structures such as convolute stratification (Facies C2.2 and C2.3),

and the sandstones are typically normally graded. The mudstones generally comprise thin regular siltstone and mudstone laminae (Facies D2.3), or are intensely bioturbated (Facies E1.3).

This facies-association is typical of the lobe. FA5f deposits are commonly overlain by FA3f sandstones forming coarsening- and thickening-upward sequences.

4.6.5.7 FA5g Laterally continuous tabular current rippled fine- to coarse-grained sandstone-mudstone couplets with well-developed internal stratification (Appendix 4.18.B)

Facies-association 5g (FA5g) is very similar to FA5f. However, this facies-association is characterised by thin- to medium-bedded, fine- to coarse-grained sandstones. Medium-bedded, medium- to coarse-grained sandstones (Facies C2.1) occur rarely in FA5g. The base of the sandstones is typically irregular and erosive, with flutes well developed on the soles of coarse-grained sandstones. The tops of the sandstones are sharp and rippled. The beds are normally graded and internal stratification is well developed, including planar, cross, wavy and convolute stratification. Rip-up mud clasts and extra-formational reworked nummulites are rare. The thin- to medium-bedded, fine- to medium-grained sandstones typically have sharp bases and sharp rippled tops. Mud clasts and extra-formational nummulites are rare. Internal stratification of the sandstones is well developed, with cross and planar stratification common, and more rarely, convolute stratification (Facies C2.2). Interbedded mudstones are well developed, but thin, typically with a sandstone:mudstone ratio of 1:1. The Facies C2.1 sandstones may overlie Facies C2.2 sandstones to form crude thickening- and coarsening-upward sequences. However, these sequences are rarely developed. This facies-association is typical of the lobe fringe.

4.6.5.8 FA5h Laterally continuous thin- to thick-bedded fine- to coarse-grained sandstones with thick mudstones and calcilutites (Appendix 4.19.A)

Facies-association 5h (FA5h) is characterised by laterally continuous tabular sandstones with thick mudstones. Sandstone:mudstone ratios are in the order of 1:5. The sandstones typically have sharp flat bases, with sole markings generally subdued, and sharp to gradational, commonly current rippled tops. Sandstones with evidence of flow reversals (reflected) during deposition are also common (Facies C2.4). Thick-bedded sandstones may be associated with mega-ripples which commonly cross-cut one another

when exposed on bedding planes. The sandstones of FA5g are well sorted, normally graded, and characterised by well-developed internal stratification, including cross and planar stratification, and more rarely convolute stratification (Facies C2.2 and C2.3). Typically the interbedded mudstones are thick, averaging 16.66 cm in thickness, and normally graded, and may have thin siltstone laminae at the base immediately overlying the sandstone division (Facies E2.1). The mudstones overlying the flow reflected sandstones (Facies C2.4) are thick (up to ~3 m thick) and structureless (Facies E1.1). Rarely, marly limestone beds (calcilutites/hemiturbidites) are associated with this facies-association.

The thick mudstones of FA5h were deposited by the slow-moving dilute turbulent upper part of the turbidity current and may be related to ponding of the turbidity currents. Correspondingly, flow reflected sandstones may be related to a nearby topographic high which may have caused the reflection and ponding of the gravity currents. This facies-association is characteristic of the fan fringe.

4.6.6 FA6 Very-thin-bedded sandstones, siltstones and mudstones

Facies-association 6 (FA6) is characteristic of mud-rich sequences which are typically intensely bioturbated. Where original sedimentary fabrics are preserved, typical facies include C2.3 sandstones, D2.3 and D2.1 siltstones as well as E1.1 and E2.1 mudstones. Intensely bioturbated sequences are characterised by Facies C1.3, D1.3 and E1.3 deposits.

4.6.6.1 FA6a Very-thin-bedded, intensely bioturbated sandstones, siltstones and mudstones (Appendix 4.12.B)

Facies-association 6a (FA6a) is characterised by very-thin-bedded, tabular, laterally continuous, thin-bedded, fine-grained sandstones, siltstones and mudstones. The sandstones and siltstones have sharp flat bases and sharp to gradational, current rippled tops. Internal stratification is typically well-developed, with planar and wavy stratification common (Facies C2.3). Siltstones typically are planar stratified and form siltstone-mudstone laminae (Facies D2.3). This facies-association is characterised by intense bioturbation. The sediments may be totally homogenised by bioturbation, with only remnant patches of silt and sand in mottled mudstones occurring. The most

common deposits therefore comprise bioturbated mudstones, siltstones and fine-grained sandstones (Facies E1.3, D1.3 and C1.3 respectively).

This facies-association typically occurs as thin packets, up to several metres thick (<10 m) at the top of individual channel elements and channel complexes, and is associated with the abandonment phase of the channel-fill.

4.6.6.2. FA6b Very-thin-bedded, sparsely bioturbated sandstones, siltstones and mudstones

Facies-association 6b (FA6b) is very similar to FA6a. However, it is characterised by non-bioturbated to sparsely bioturbated, very-thin-bedded deposits, including fine-grained sandstones, siltstones and mudstones. The sandstones and siltstones have sharp flat bases and sharp to gradational, current rippled tops. Internal stratification is typically well-developed, with planar and wavy stratification common (Facies C2.3). Siltstones typically are planar stratified and form siltstone-mudstone laminae (Facies D2.3). Similarly to FA6a, this facies-association occurs as thin packets at the top of individual channel elements and is associated with the abandonment phase of the channel-fill. It is typical of the older turbidite systems in the Ainsa basin, including Fosado and Los Molinos (see sections 5.2 and 5.3), which are characterised by a low bioturbation intensity compared to the younger systems in the Ainsa basin.

4.6.6.3. FA6c Thin-bedded laterally continuous sandstones and thick siltstones and mudstones (Appendix 4.19.B)

Facies-association 6c (FA6c) is characterised by laterally continuous, tabular, thin-bedded, very-fine to fine-grained sandstones, siltstones and mudstones. The sandstones and siltstones typically have sharp bases and gradational tops, and are normally graded. The deposits are typically bipartite or tripartite, comprising basal cross-laminated sandstones, which grade into parallel laminated siltstones ranging between 5-10 cm in thickness. These grade into structureless or parallel laminated mudstones (T_{cde}). In bipartite beds, the basal sandstone division is missing. In both cases, the mudstone division is typically as thick as the siltstone division, although this may vary. These deposits are characterised by Facies C2.3 sandstones, D2.1 siltstones and E2.1 graded mudstones. Facies-association 6c is characteristic of distal overbank environments.

4.6.6.4 FA6d Intensely bioturbated very-thin-bedded sandstones, siltstones, mudstones and biogenic mudstones (Appendix 4.20.A)

Facies-association 6d (FA6d) is characterised by very-thin-bedded current rippled sandstones and siltstones. Mudstone intervals are typically thicker than the underlying sandstones or siltstones (sandstone:mudstone ratio of 1:2-1:4). The deposits of this facies-association generally comprise laminated siltstones, overlain by graded mudstones which may be capped by a very thin hemipelagic layer. Typically the deposits are intensely bioturbated and may be completely homogenised. The preservation of siltstone and mudstone laminae is rare, and siltstones typically occur as patches within the mottled mudstones (Facies D1.3 and E1.3). Where the original sedimentary fabric is preserved, the most common deposits are graded-stratified siltstones (Facies D2.1), graded mudstones (Facies E2.1), and biogenic mudstones (hemipelagics) (Facies G2.1).

Facies-association 6d is characteristic of both the interfan and interlobe. In the interfan, FA6a deposits form thick packages several tens of metres thick in association with thick heterolithic packages (FA5d). In the interlobe, the packages are thinner (<5 m thick) and form laterally continuous muddy units between sandy units of the lobe

4.6.6.5 FA6e Laterally continuous thin-bedded sandstones, siltstones, mudstones and calcilutites (Appendix 4.20.B)

Facies-association 6e (FA6e) is characterised by thin-bedded sandstones (Facies C2.3), thin regular siltstone and mudstone laminae (Facies D2.3) as well as thin- to medium-bedded graded stratified siltstone (Facies D2.1). White weathering marly limestones (calcilutites) may also occur (Facies H). These deposits are laterally continuous and rarely display lateral changes in thickness. The thin-bedded sandstones and siltstones have sharp bases, and sharp or more rarely gradational flat tops. Internal stratification is poorly developed. Facies-association 6d is characteristic of the distal interlobe and occurs as mud-rich intervals ~1-2 m thick with sandstones of FA3f and FA5f.

4.6.6.6 FA6f Laterally continuous very-thin-bedded current rippled sandstones, siltstones and mudstones (Appendix 4.18.B)

Facies-association 6f (FA6f) is characterised by very-thin-bedded, fine-grained sandstones (Facies C2.3), siltstones (Facies D2.2) and associated mudstones. These

deposits typically have sharp flat bases and sharp to gradational, current rippled tops. Where the tops of the sandstones are gradational, sandstones may grade into a thin sandstone-siltstone division, and an upper mudstone division (Facies E2.1). In areas of intense bioturbation, the mudstones may be characterised by Facies E1.3. This facies-association typically occurs as thin (<3 m thick) intervals associated with FA5g, and is characteristic of the lobe fringe.

4.6.6.7 FA6g Laterally continuous thin-bedded very-fine- to fine-grained sandstones with thick mudstones and calcilutites (Appendix 4.21.A)

Facies-association 6g (FA6g) is characterised by laterally continuous tabular thin-bedded very-fine- to fine-grained sandstones with thick mudstones. The deposits of this facies-association can typically be divided into a number of divisions (or facies). The lower division is characterised by thin-bedded sandstones (Facies C2.3). These sandstones are typically overlain by sand-silt divisions, which appear graded and are commonly thoroughly laminated (T_d). These intervals range between 3-10 cm in thickness. Laminated siltstones may form individual beds when the sandstone division is absent (Facies D2.1). These intervals range in thickness between 1-6 cm. Immediately overlying the siltstone divisions are thick graded mudstones which may grade into structureless mudstones towards the top of the deposits. These mudstones are equivalent to the Piper (1978) E2 and E3 and Stow and Shanmugam (1980) T_{6-7} divisions (Facies E2.1, E1.1). In the absence of the silt division, these mudstones may immediately overlie the sand division. Typically, the mud, and more rarely, the silt divisions contain small dark muddy pseudonodules with diameters of 2-7 mm. Finally, a marly limestone (calcilutite) division may occur (Facies H). Less commonly, the marly limestones form either the mudstone division (T_e) when directly overlying rippled sandstones or may form individual beds.

The sandstones have sharp flat bases, with rare sole marks and sharp to gradational commonly current rippled tops. Amalgamated beds and intra-formational mud clasts are rare. The sandstones are well sorted and internal stratification is well-developed, with cross and planar stratification common, and more rarely convolute stratification (Facies C2.3). Medium-bedded, fine-grained sandstones with evidence of flow reflections are also developed in FA6g (Facies C2.4)

Facies-association 6g is characteristic of the distal basin floor. The most distinctive features which distinguish the deposits of FA6g from those of FA5h (fan

fringe) are the paucity of medium- to thick-bedded, medium- to coarse-grained sandstones, and the abundance of marly limestones (calcilutites).

4.6.7 FA7 Bioclastic sandstone / packstones

Facies-association 7 is characterised by sandstones rich in redeposited fossiliferous material. Facies-association 7 is subdivided into 3 groups, on the basis of bioclastic content and bed geometry.

4.6.7.1 FA7a Laterally continuous (at outcrop scale) nummulites-rich bioclastic sandstones (Appendix 4.21.B)

Facies-association 7a (FA7a) is characterised by poorly sorted, laterally continuous bioclastic sandstones with abundant nummulites (Facies I). The sandstones are rarely amalgamated, forming sandy units up to 2 m in thickness with intra-formational mud clasts common at amalgamation surfaces. This facies-association is characteristic of delta front lobe sandstones deposited near the shelf/slope break.

4.6.7.2 FA7b Discontinuous, concave-up, nummulites-rich bioclastic sandstones (Appendix 4.21.B)

Facies-association 7b (FA7b) is very similar to FA7a. However, these sandstones are laterally discontinuous over ~5-15 m, and have concave-up bed geometries. This facies-association occurs in the upper slope gully, which is incised into the delta front lobe sandstones of FA7a.

4.6.7.3 FA7c Concentrated nummulites beds (packstones)

Facies-association 7c (FA7c) is characterised by cm thick layers of nummulites (packstones). These deposits are not environmental specific, and occur throughout the proximal Ainsa basin. They are particularly common towards the base of channels, but generally occur in all environments. They are interpreted as storm beds, formed during exceptionally large storms in which large accumulations of nummulites stored on the shelf and upper slope were redeposited into deeper water.

Chapter 5

Ainsa basin:
Proximal turbidite systems of the Castisent Group

5.1 Introduction

The turbidite systems of the Castisent Group (Fosado, Los Molinos and Arro) are the least studied in the Ainsa basin. This is in part due to the limited size and extent of the outcrops, as well as the intense deformation associated with several major thrust zones. This chapter documents, for the first time, three discrete sandbodies stratigraphically between the Fosado and Arro turbidite systems, herein named the Los Molinos system (Section 5.3). The Arro system which has previously been interpreted as a canyon-mouth-of-canyon system (Millington and Clark 1995) is also reinterpreted (see Section 5.4).

5.2. Fosado System

The Fosado system is the least studied turbidite system in the Ainsa basin. This is due to poor exposure, which essentially consists of one main outcrop south of the village Fosado (Locality 1, Fig. 1.3), and a number of small sand ridges southeast of Los Molinos village. The Fosado system comprises at least three small-scale channelised sandbodies. The best-exposed sandbody is described below.

5.2.1. Channel axis

5.2.1.1. Sedimentology

The Fosado system is exposed as a small confined (channelised) sandbody immediately south of Fosado (Locality 1, Fig. 1.3) (Fig. 5.1). This channelised sandbody is 10 m thick and ~120 m wide (aspect ratio of 12:1). Palaeoflow ranges between 308°-335°. A normal fault striking east-west cuts through the axis of the channel, with a displacement of ~6 m. The section was logged ~20 m from the axis of the channel.

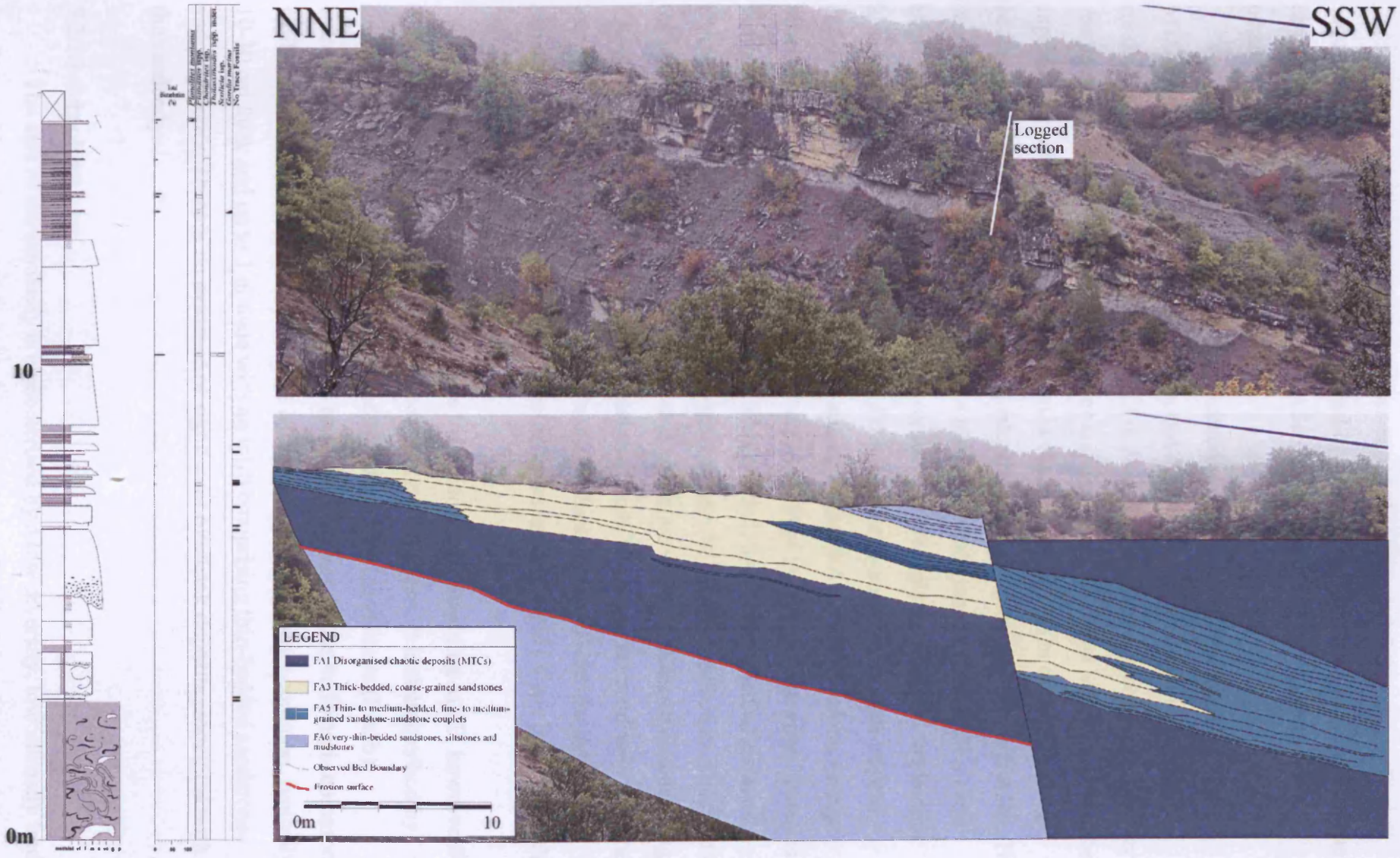

Fig. 5.1. Channelised sandbody of the Fosado system immediately south of Fosado, including interpreted photo panel and detailed bed-by-bed graphic sedimentary log (16 m thick) and trace-fossil data through the channel axis.

The channelised sandbody comprises two thinning- and fining-upward sequences that represent individual second-order channel fills (storey). The axis of the channel is characterised by FA3a and FA5c sandstones, with FA5b sandstones occurring at the margins.

The base of the sandbody is associated with a ~10.5 m thick muddy Type Ia MTC that overlies thin-bedded siltstones and mudstones. Deformed thin-bedded sandstones, mudstones and sand-rafts (<2 m diameter) are common constituents. Over the lateral extent of the outcrop, the lower and upper contact of the MTC appears to be regular. The base of the sandy succession is characterised by ~4 m of thin- to thick-bedded, typically amalgamated, erosive, laterally discontinuous sandstones (FA3a). The sandstones tend to be disorganised with a mud-rich sandy matrix (Facies B1.1) and abundant mud-clasts towards the base. Normally graded, planar stratified sandstones also occur. These are overlain by ~2 m of thin-bedded, commonly current-rippled sandstones with interbedded mudstones and siltstones (FA5c) which form a fining-upward sequence ~6 m thick. This represents the fill of the storey. The upper storey is characterised by ~4 m of amalgamated, thick-bedded, normally graded sandstones (FA3a) punctuated by thin-bedded, fine-grained current rippled sandstones. The base of the storey is associated with ~2 m of erosive cut-down which truncates the underlying FA5c sandstones resulting in channel amalgamation. The top of the sandbody comprises very-thin-bedded sandstones, siltstones and mudstones with well-developed current ripples (FA6b). These deposits are truncated by an erosive muddy Type Ia MTC, with cut-down in the order of several metres.

The margin of the upper storey is truncated by the overlying MTC, however the margin of the lower storey is clearly exposed at both margins. It is characterised by thin-bedded, fine-grained, current rippled sandstones and mudstones (FA5b). Interbedded mudstones may be thin and bedding indistinct. Flaser bedding is common, whilst starved ripples occur more rarely. Minor scour structures are common, typically 10-30 cm thick and up to 2 m wide with an infill comprising thin-bedded sandstones and mudstones. There is no evidence of significant overbank deposits associated with the sandbody.

5.2.1.2. Ichnology

The axis of the sandbody is characterised by a low diversity, low intensity trace-fossil assemblage dominated by post-depositional trace fossils. Mean bioturbation on

bedding planes is 8.35% and of the 19 bedding planes analysed, 10 were non-bioturbated. 6 ichnospecies from 5 ichnogenera were identified, of which 5 are post-depositional and 1 is pre-depositional. In vertical section, in the mudstones of FA5c, no bioturbation was observed. Bioturbation is also absent from the sandstones of FA3a. The trace-fossil assemblage is dominated by *pascichnia,* with the most common ichnotaxa including *Planolites* and *Scolicia. Domichnia* such as *Ophiomorpha* are absent from the section, as well as vertical burrows within the sandstones.

5.2.1.3. Interpretation

The channelised sandbody is interpreted as a lower slope channel system based on its geometry, the abundance of Type Ia MTCs associated with the surrounding deposits, and the proximity to temporal shelf deposits (see Remacha 2003) (c.f., Muñoz *et al.* 1994, Galloway 1998). It is unclear whether the base is located at the lower or upper surface of the basal MTC. The MTC may be contained within a larger erosional surface, or may have provided the substrate over which the channel developed. Based on the fan evolution model of Pickering and Corregidor (2005a, b), the base would be at the lower contact of the MTC, with the MTC representing the initial collapse of the basin slope. The absence of observed overbank deposits and the high aspect ratio of the channel suggest that deposition was confined within an erosional master surface.

The low intensity, low diversity trace-fossil assemblage of the axis of the channel may be indicative of environmental stress factors. The absence of burrow networks formed by large, robust, deeply burrowing organisms (e.g., *Ophiomorpha* and *Halopoa*), which are characteristic of proximal axial environments such as the channel axis of the Ainsa I sandbody (see Section 6.4.1.2) is indicative of low oxygen levels in the bottom waters. A paucity of *domichnia* in an oxygen-controlled trace-fossil model was interpreted by Ekdale and Mason (1988) as being indicative of reduced oxygen levels.

The paucity of pre-depositional trace-fossils in the axis may be related to the erosive nature of the depositing turbidity-current flows, which destroyed any shallow-tier burrow networks which, when preserved, typically form the pre-depositional trace-fossil assemblage. However, the paucity of pre-depositional trace-fossils associated with thin-bedded sandstones of FA5 which were deposited by weakly erosive, low concentration turbidity currents, suggests that a pre-depositional trace-fossil community was not established between deposition of turbiditic sandstones. The absence of a pre-

depositional equilibrium trace-fossil assemblage as well as burrow networks formed by large, robust, deeply burrowing organisms and the overall low bioturbation intensity suggests bottom waters were poorly oxygenated. Bioturbation is essentially associated with opportunistic post-depositional trace-forming organisms which may have colonised newly deposited sediments as a result of a temporary increase in oxygen levels upon deposition of turbiditic sands due to the transportation of gravity currents through shallow oxygenated water (e.g., Wilson *et al.* 1985, Orr 1995, Buatois *et al.* 2001, Wetzel & Uchman 2001). The fact that the channel is encased in thick MTCs may also have influenced the nature of the trace-fossil assemblage. This is because organisms may have had to migrate large distances from areas unaffected by MTC deposition to reach the channel.

5.3. Los Molinos system

Three discrete sandbodies have been recognised in the Barranco Sierra south of Los Molinos (Localities 2 and 4, Fig. 1.3) (Figs. 5.2 and 5.3). These sandbodies were first documented by Remacha *et al.* (2003) and interpreted as being part of the Arro system. However, the current author has interpreted them as belonging to a separate turbidite system, the Los Molinos system, named after the nearby village of Los Molinos. These sandbodies are not included in the Arro system due to: (1) the large volume of thin-bedded sandstones, siltstones and mudstones between the top of the Los Molinos system and base of the Arro system (~70 m); and (2) the angular unconformity at the base of the Arro system which is interpreted as a sequence boundary related to the first stages of the Los Molinos thrust and the Mediano detachment fold (Millington and Clark 1996) and the incision of the Charo-1 canyon (Section 5.4.1). Petrographic studies have also revealed that the sands of the Los Molinos system are distinct to those of the underlying Fosado system (Das Gupta & Pickering *in press*).

The three sandbodies are exposed in the Barranco Sierra where they outcrop in the river and adjacent cliff section (Locality 4 and 2 respectively, Fig. 1.3), which is orientated very oblique to palaeoflow (~20°). To the southeast, the sandbodies are truncated by the Los Molinos thrust system, whilst to the northwest, they form a ridge (Sierra Chica) to the west of Torrelisa (Locality 3, Fig. 1.3) beyond which they are

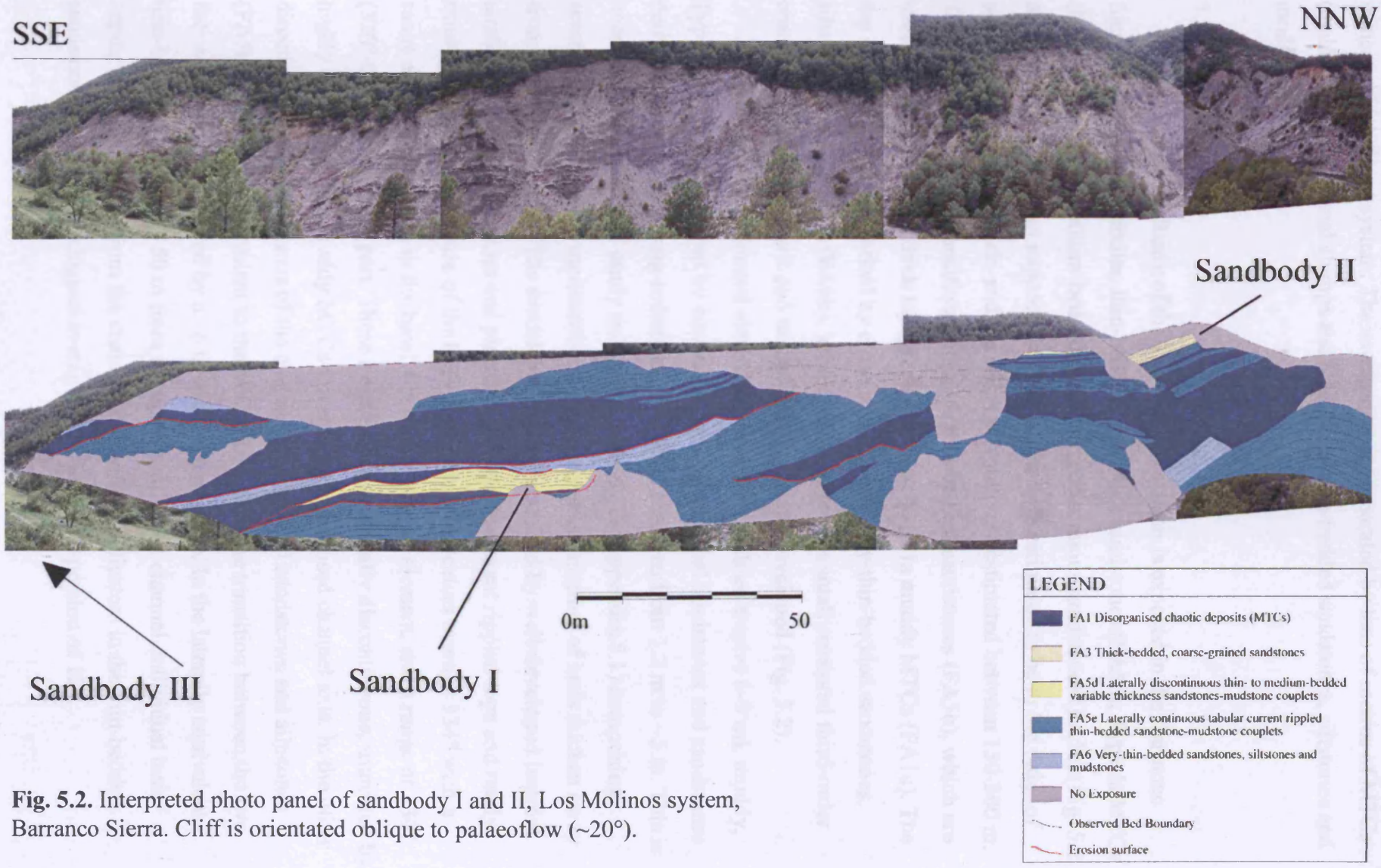

Fig. 5.2. Interpreted photo panel of sandbody I and II, Los Molinos system, Barranco Sierra. Cliff is orientated oblique to palaeoflow (~20°).

truncated by a thrust system. The sandbodies are separated by tens of metres of MTCs (mainly intraformational slumps and slides) and thin-bedded sandstones, siltstones and mudstones.

5.3.1. Sandbody I

The oldest sandbody of the Los Molinos system is exposed in the Barranco Sierra and comprises tabular, thin-bedded, sheet-like sandstones (FA5b), Type Ia MTCs (FA1a) and thin- to medium-bedded laterally discontinuous sandstones (FA5c) (Fig. 5.2 and 5.3). The base is not exposed, but the sandbody is estimated to be in the order of several tens of metres thick, and the width is tentatively estimated between 150-300 m. The dominant facies-association comprises thin-bedded sandstones (FA5b), which are truncated by, and onlap, thick topography forming Type Ia muddy MTCs (FA1a). The top of the sandbody is marked by erosive MTCs and very-thin-bedded sandstones, siltstones and mudstones (FA6b). Within the sandbody, a small erosional third-order channel element ~9 m thick and tens of metres wide is developed (Fig. 5.2).

The base of the channel element is associated with an erosive (~3 m), muddy, Type Ia MTC characterised by contorted, intra-formational mudstones and sandstones derived from the underlying sediments. The MTC thickens from 1.2 m to ~5 m. This is overlain by a 6.5 m thick sandy succession (see log D; Appendix 5.1) comprising essentially FA5c thin- to medium-bedded sandstones. A number of beds thicken away from the logged section. The sandstones are characterised by well-developed internal stratification including cross and planar stratification, current rippled tops and rarely, mud-clasts towards the base of the beds. Palaeoflow indicators average 334° with a range of 30° (320°-350°) in the basal 4 m of the channel element, and a range of 130° (320°-090°) in the upper part. These sandstones are laterally discontinuous, truncated by highly erosive Type Ia muddy MTCs towards the unexposed channel axis. In the other direction, away from the axis of the channel, thin-bedded sandstones and siltstones (FA5b) are laterally equivalent to the sandstones, with the transition between the two facies-associations covered by a ~6 m wide area of scree. In the laterally equivalent thin-bedded sandstones ~50 m from the upper part of the channel, individual beds appear to thicken away from the channel. Palaeoflow indicators in the thin-bedded sandstones lateral to the channel average 325°, with a dispersion of 12°.

5.3.2. Interpretation

The basal thin-bedded sandstones (FA5b) may represent sheet sandstones deposited by low volume, low concentration turbidity current flows, or channel margin / levee-overbank deposits associated with an unexposed channel. These sandstones are truncated by an erosional confined channel element, with the logged sandy succession (log D) interpreted as the margin of the channel element, and the axis characterised by Type Ia MTCs, which truncated the sandstones. The unexposed transition between the FA5c channelised sandstones and their lateral equivalent, the FA5b thin-bedded sandstones, is interpreted as a steep channel margin. Palaeoflow indicators from the channel margin sandstones support this interpretation, with palaeoflows becoming increasingly divergent towards the top of the channel, indicating that the gravity flows were confined towards the base. The lateral equivalent thin-bedded sandstones (FA5b) may therefore represent a small levee-overbank system created as a result of flow stripping of fines from bypassing gravity flows which underwent an up-depositional-dip hydraulic jump. Alternatively, the channel may have been incised into the thin-bedded sandstones, in which case, the two are genetically unrelated. Due to the absence of divergent palaeoflows in the thin-bedded sandstones characteristic of levee systems, the latter interpretation is preferred. However, towards the top of the channel fill, the flows became less confined, and overspilled the confines of the erosional surface, resulting in the formation of splay deposits. The thickening of these beds away from the channel suggests that some relief had been established in association with the channel margin.

5.3.3 Sandbody II

Sandbody II outcrops in a cliff section above the Barranco Sierra at Locality 2 (log E; Appendix 5.2) (Figs. 5.2 and 5.3) and in the Barranco Caixigosa, west of Torrelisa (Locality 3; Appendix 5.3). Mean palaeoflow is towards 320°. In the Barranco, the outcrop is orientated very oblique to main palaeoflow (~20°).

In the Barranco Sierra cliff section, the base of the sandbody is associated with a number of thin (<4 m thick) Type II MTCs (FA1b) characterised by intra-formational sand- and mud-clasts, as well as extra-formational pebbles in a sandy mudstone matrix. These MTCs are separated by a ~5 m thick interval of very-thin-bedded sandstones and siltstones and also a thin (<1 m thick) amalgamated gravely sandstone unit which has abundant fossiliferous material and small (<3 cm) pebbles. At an oblique angle to palaeoflow down the cliff, these basal deposits onlap a highly irregular surface

associated with an underlying thick (tens of metres) Type Ia MTC (FA1a). Here the ~5 m thick sandstone interval is characterised by distinct thickening of the beds, with thin-bedded sandstones most common. The main sandy succession is ~9 m thick and comprises thick-bedded amalgamated sandstones at the base (FA3a) and thin- to medium-bedded sandstones towards the top (FA5b) forming a clear fining-upward sequence. The sandstones are typically amalgamated, forming units up to 4 m thick, and are normally graded and characterised by abundant extra-formational pebbles (<2 cm diameter), shell fragments and nummulites, as well as intra-formational mud-clasts. These sandstones thin laterally over ~20 m to essentially non-amalgamated fine- to medium-bedded sandstones.

In the Barranco Caixigosa, the beds dip at ~90° forming a small waterfall. The sandstones are poorly exposed except in the stream, where the polishing effect of the water has made internal stratification clearly visible. The outcrop is underlain and overlain by large thrust systems and is the most northerly outcrop of the Los Molinos system in the Ainsa basin. The main sandy succession is ~14 m thick. The base is characterised by thin- to thick-bedded sandstones (FA3a/FA3d and FA5c/FA5b) with the top associated with thin- to medium-bedded sandstones (FA5b/FA5c) and interbedded thin siltstones forming a crude fining-upward sequence. All the beds display well-developed internal stratification, including planar and cross stratification. Some sandstones are characterised by mega-ripples. Towards the base, the sandstones may be amalgamated to form units up to 2 m thick. The beds typically have erosive bases and flat tops, are normally graded and mud clasts are common. Siltstones tend to be rippled, and may form single-train ripple beds.

5.3.4 Interpretation

The Los Molinos II sandbody can be interpreted as a confined (channelised) sandbody comprising at least two channel elements. The base of the sandbody is characterised by a master surface associated with a thick underlying MTC. This is probably a composite surface of erosion and deposition, in part a channel margin and in part controlled by seafloor topography. The basal Type II MTCs and thin-bedded sandstones of the sandbody are interpreted as the channel margin/overbank of an

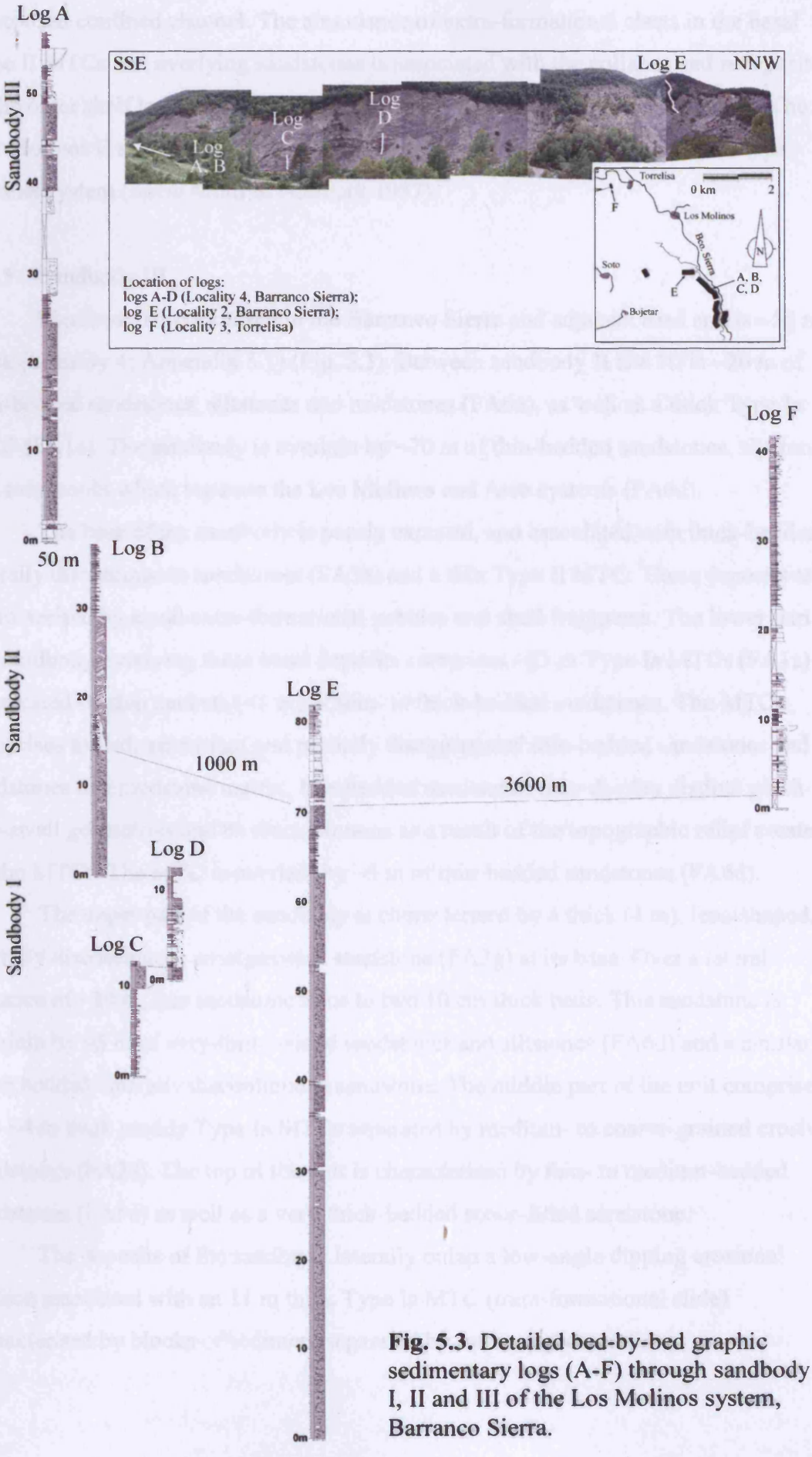

Fig. 5.3. Detailed bed-by-bed graphic sedimentary logs (A-F) through sandbody I, II and III of the Los Molinos system, Barranco Sierra.

unexposed confined channel. The abundance of extra-formational clasts in the basal Type II MTCs and overlying sandstones is associated with the collapse and redeposition of the outer shelf to littoral zone during the early phase of channel development. The Los Molinos II sandbody can be interpreted as a mixed erosional/depositional type channel system (*sensu* Mutti & Normark 1987).

5.3.5 Sandbody III

Sandbody III is exposed in the Barranco Sierra and adjacent road and is ~55 m thick (Locality 4; Appendix 5.1) (Fig. 5.3). Between sandbody II and III is ~20 m of thin-bedded sandstones, siltstones and mudstones (FA6d), as well as a thick Type Ia MTC (FA1a). The sandbody is overlain by ~70 m of thin-bedded sandstones, siltstones and mudstones which separate the Los Molinos and Arro systems (FA6d).

The base of the sandbody is poorly exposed, and associated with thick-bedded laterally discontinuous sandstones (FA3a) and a thin Type II MTC. These deposits are characterised by small extra-formational pebbles and shell fragments. The lower part of the sandbody overlying these basal deposits comprises ~23 m Type Ia MTCs (FA1a) punctuated by thin packets (<1 m) of thin- to thick-bedded sandstones. The MTC comprises folded, attenuated and partially disaggregated thin-bedded sandstones and mudstones in a mudstone matrix. Interbedded sandstones may display distinct pinch-and-swell geometries and be discontinuous as a result of the topographic relief created by the MTCs. The MTC is overlain by ~3 m of thin-bedded sandstones (FA6d).

The upper part of the sandbody is characterised by a thick (4 m), lens-shaped, laterally discontinuous amalgamated sandstone (FA3g) at its base. Over a lateral distance of ~30 m, this sandstone thins to two 10 cm thick beds. This sandstone is overlain by ~5 m of very-thin-bedded sandstones and siltstones (FA6d) and a similar, thick bedded, laterally discontinuous sandstone. The middle part of the unit comprises two ~4 m thick muddy Type Ia MTCs separated by medium- to coarse-grained erosive sandstones (FA3a). The top of the unit is characterised by thin- to medium-bedded sandstones (FA5c) as well as a very-thick-bedded scour-filled sandstone.

The deposits of the sandbody laterally onlap a low-angle dipping erosional surface associated with an 11 m thick Type Ia MTC (intra-formational slide) characterised by blocks of sediment separated by internal glide surfaces.

5.3.6 Interpretation

Sandbody III is interpreted as a confined system based on the lateral discontinuity of the deposits and lateral facies changes. These deposits were confined by an erosional master surface associated with the slide unit. Sandbody III is interpreted as a low net:gross slope valley fill.

5.3.7. Summary

The association of thick accumulations of Type Ia MTCs (FA1a) and small, confined, erosional sandbodies suggests deposition at or near the base of the morphological slope (c.f., Schultz *et al.* 2005 and references within). The three lower-slope, confined, erosional sandbodies of the Los Molinos system exhibit the importance of the interplay between depositional control on sand accumulation by MTCs and erosional confinement. The thin-bedded sandstones (FA5b) of sandbody I are confined by thick topography-forming MTCs, whilst the channel is confined within an erosional master surface. Sandbody II is interpreted to be controlled by the interplay between confinement by MTCs and erosion, whilst sandbody III was controlled by erosional confinement. The sandbodies therefore exhibit an increase in the degree of erosional confinement through time. This may be related to changes in slope gradient, with an increase in slope gradient related to an increase in channel incision (e.g., McCaffrey *et al.* 2002). Alternatively, it may be related to an increase in the volume of the gravity flows, associated with the progradation of the system.

The paucity of extra-formational rounded pebbles within the Los Molinos system is probably related to the maturity of the fluvial systems. It is postulated that there were very few pebbles stored in the shelf area which may be related to the maturity of the fluvial systems and the basin itself. It wasn't until the Gerbe system that large quantities of pebbles were deposited into the Ainsa basin (Section 6.2), suggesting that the system was not mature enough for significant volumes of pebbles to be transported down the system and stored on the shelf.

5.4. Arro System - Introduction

The Arro system is exposed at a number of localities in the Ainsa basin. The most proximal outcrop is to the southeast, at Charo hill (Locality 10, Fig. 1.3). It then forms a ridge, which runs northwards to the Rio Nata (Locality 7). From the Rio Nata, the Arro

system forms a ridge, the Sarreta d'Arro, which runs northwest to the Barranco Sierra, (Localities 5 and 6) and then outcrops at the Santa Catalina ridge (Locality 8) (Fig. 5.4). To the north, the Arro system is incorporated into a major thrust system where it has not been studied in detail due to intense tectonic deformation. The Arro system is 180 m thick, which differs to previous estimations, including 145 m by Mutti *et al.* (1985) and Clark and Pickering (1996) as well as 280 m by Remacha *et al.* (2003). This estimation by Remacha *et al.* (2003) erroneously included the underlying sandbodies of the Los Molinos system (see Section 5.3) into the Arro system. The study by Millington and Clark (1995, 1996) concluded that the Arro system is a canyon-mouth sheet system, sourced through the Charo-1 canyon, which outcrops at Charo hill (Section 4.1).

The Arro system developed coevally with the onset and first stages of the Los Molinos thrust and the Mediano detachment fold (Mutti 1992). Due to the close proximity of the Los Molinos and related thrusts, the Arro system is the most tectonically deformed system in the Ainsa basin. Consequently, it is also probably the most poorly understood. In the Rio Nata (Locality 7, Fig. 1.3), the Los Molinos thrust is located ~40 m below the base of the Arro system, and the beds are overturned, dipping at ~85°. Consequently, observations on lateral changes were not possible. The Arro system is less deformed at the Barranco Sierra (Localities 5 and 6), however, throughout the section there are numerous small- to large-scale thrust faults. Deformation is greatest at the base of the system, and also in the underlying basin slope thin-bedded sandstones siltstones and mudstones. The absence of slickenside fibres, fractures and joints associated with folds and faults suggests that much of the deformation was syn-sedimentary. The clearest example of this is a syntectonic angular unconformity at the base of the Arro system in the Barranco Sierra.

The sandstones of the Arro system are rich in organic detritus including wood fragments. This suggests that many of the deposits were directly sourced from fluvial systems on the delta. Although the high amount of organic detritus is not unique to the Arro system (cf. the interfan of the Ainsa system, Section 6.4.5), the Arro system contains a particularly high amount of organic detritus compared to many of the other turbidite systems. This is reflected in the organic carbon content (C_{org}) of mudstones from the Arro system. Despite C_{org} only crudely reflecting benthic food levels due to other factors on preserved C_{org} including sedimentation rates and oxygen supply (e.g., Wetzel 1991), the high C_{org} of the Arro system suggests that benthic food levels were high. C_{org} throughout the turbidite systems of the Ainsa basin averages 0.567%,

however, the average C_{org} from 3 samples in the Arro system is 1.29%. The Arro system also has the highest C_{org} from a single sample, at 2.48% (unpublished data, Das Gupta). However, these high C_{org} levels may also be related to differences in terms of oxygenation during the Arro system compared to the other turbidite systems.

Similarly to the Los Molinos and Fosado turbidite systems, the Arro system is characterised by a paucity of pebbles (see Section 5.3.7).

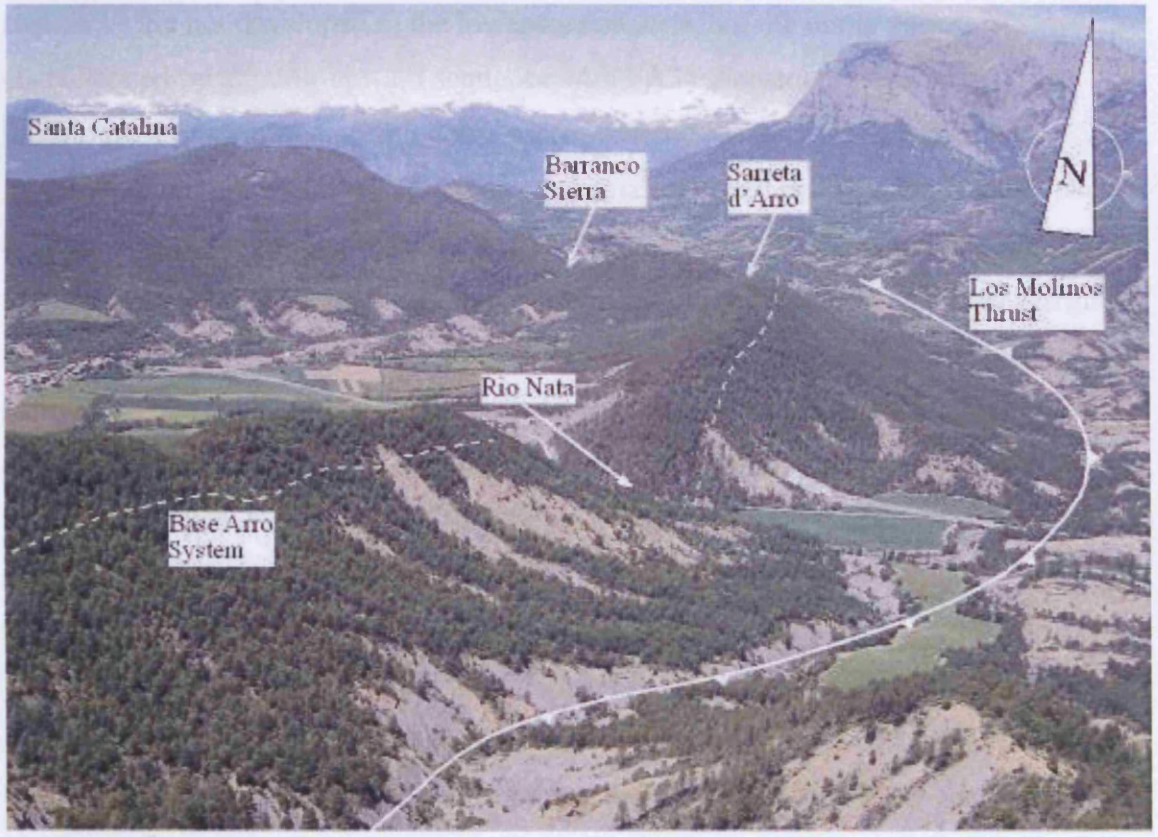

Fig. 5.4. The Arro system from Charo hill, facing northwest.

5.4.1 Charo hill

The sandbody at Charo hill is ~44 m thick and is overlain by ~65 m of poorly exposed thin-bedded turbiditic sandstones and MTCs (intra-formational muddy sediment slides and slumps) which together form the fill of the Charo-1 canyon (Millington & Clark 1996). Only the basal 44 m of the section were logged (Appendix 5.5). This sandbody overlies Type Ia MTCs, siltstones and mudstones of the basin slope. The Charo-1 canyon is erosively overlain by the Charo-2 canyon fill (Section 6.2.1), the base of which is characterised by thin-bedded sandstones and intra-

formational MTCs. The base of the Charo-2 canyon is marked by an angular unconformity formed as a result of a phase of thrusting at the onset of the Gerbe system (Millington & Clark 1996).

The sandbody is characterised by three sandy packets divided by Type II MTCs. Each sandy packet is characterised by FA3d laterally continuous (at outcrop scale) medium-to thick-bedded sandstones and FA5b laterally continuous (at outcrop scale), thin- to medium-bedded sandstone-mudstone couplets. Coarsening or fining-upward sequences are not developed in the lower two packets, but the upper packet is characterised by a fining-upward sequence with FA3a sandstones at its base. These sandstones are laterally discontinuous, coarse-grained and contain abundant extra-formational nummulites, shell fragments and small rounded pebbles. Each sandy packet is laterally continuous over the extent of the outcrop (~200 m), however, the sandstones thin away from the logged section and onlap an erosive surface at the channel margin.

These sandy packets are interpreted as individual channel elements, which form part of the Charo-1 canyon fill. The rapid lateral thinning of the sandstones and the absence of substantial overbank deposits, suggest that the channels were confined within the canyon.

5.4.2 Rio Nata

At the Rio Nata, the Arro system is exposed in the river and adjacent road, forming a ~160 m thick section through the entire system (appendix 5.6). The outcrop has been informally subdivided into five units based on its sedimentary characteristics. The base of the system is associated with a ~20 m thick muddy Type Ia MTC (FA1a) (Unit 1). The exact position of the base is ambiguous due to the intense tectonic deformation associated with the Los Molinos thrust system. Overlying the basal MTC is a ~15 m thick sandy succession (Unit 2) characterised by tabular, sheet-like, thin-bedded sandstones (FA3c) which are erosively overlain by medium- to thick-bedded sandstones characterised by scour-and-fill structures and pinch-and-swell geometries. These sandstones are punctuated by thin (<1 m) Type Ib MTCs (FA1c), which are characterised by a sand-rich mudstone matrix. This sandy succession is overlain by a number of muddy Type Ia MTCs (FA1a) punctuated by thin packets (<3 m thick) of thin-bedded sandstones (Unit 2: 0-35m, Appendix 5.6).

Unit 3 comprises ~18 m of thin- to thick-bedded sandstones (FA3e and FA5b). These sandstones are rarely amalgamated, have sharp flat to erosive bases and

commonly current rippled tops. Thin (<3 m thick) muddy Type Ia MTCs and Type II MTCs with a sand-rich mudstone matrix punctuate the sandstones. These are typically erosive (decimetres) and the Type II MTCs are characterised by a sand-rich base with abundant extra-formational shell fragments, nummulites and intra-formational sand clasts, overlain by a muddy MTC to form a bipartite deposit. There appears to be no packaging of the beds, and interbedded mudstones between the sandstones are well developed. This sandy succession is overlain by Type II MTCs which encase a thick amalgamated sandstone unit. This thick sandstone was used by Millington and Clark (1996) as a correlative horizon between the Rio Nata and the Barranco Sierra (see discussion below). The top of Unit 3 is marked by thin-bedded, current rippled sandstones (FA5b) (Unit 3: 35-70 m, Appendix 5.6).

Unit 4 comprises a ~9 m thick packet of tectonically deformed sandstones. These sandstones are medium- to thick-bedded, commonly rippled, with the basal ~3 m consisting of thin- to medium-bedded sandstones which are succeeded by thick-bedded sandstones (FA3d). No clear fining- or coarsening-upward sequences are developed (Unit 4: 70-81 m, Appendix 5.6).

The top of the section (Unit 5) comprises ~54 m of essentially thick (2-11 m thick) muddy Type Ia MTCs. Thinner (0.3-4.5 m thick) Type II MTCs characterised by abundant extra-formational shells and nummulites also occur. These MTCs are punctuated by thin packets (<1 m thick) of sandstones comprising thin- to thick-bedded sandstones. The base of the interbedded sandstones may be characterised by thin-bedded sandstones, which infilled the topography created by the underlying MTC, whilst the top of the packets may be truncated and incorporated into the overlying MTC (Unit 5: 81m-top of log, Appendix 5.6).

5.4.3 Barranco Sierra (Armita d'os Dolores)

The Arro system is exposed in the Barranco Sierra and adjacent road section, immediately north of the Armita d'os Dolores (Localities 5 and 6) where it is ~180 m thick. Two large cliff sections at the base of the outcrop above the river, and above the road (Fig. 5.5) exposing the middle part of the system, allow for a more detailed understanding of the geometries of the depositional elements of the Arro system than the Rio Nata section. Mean palaeoflow is towards 305°. For clarity, the outcrop has been informally divided into five units.

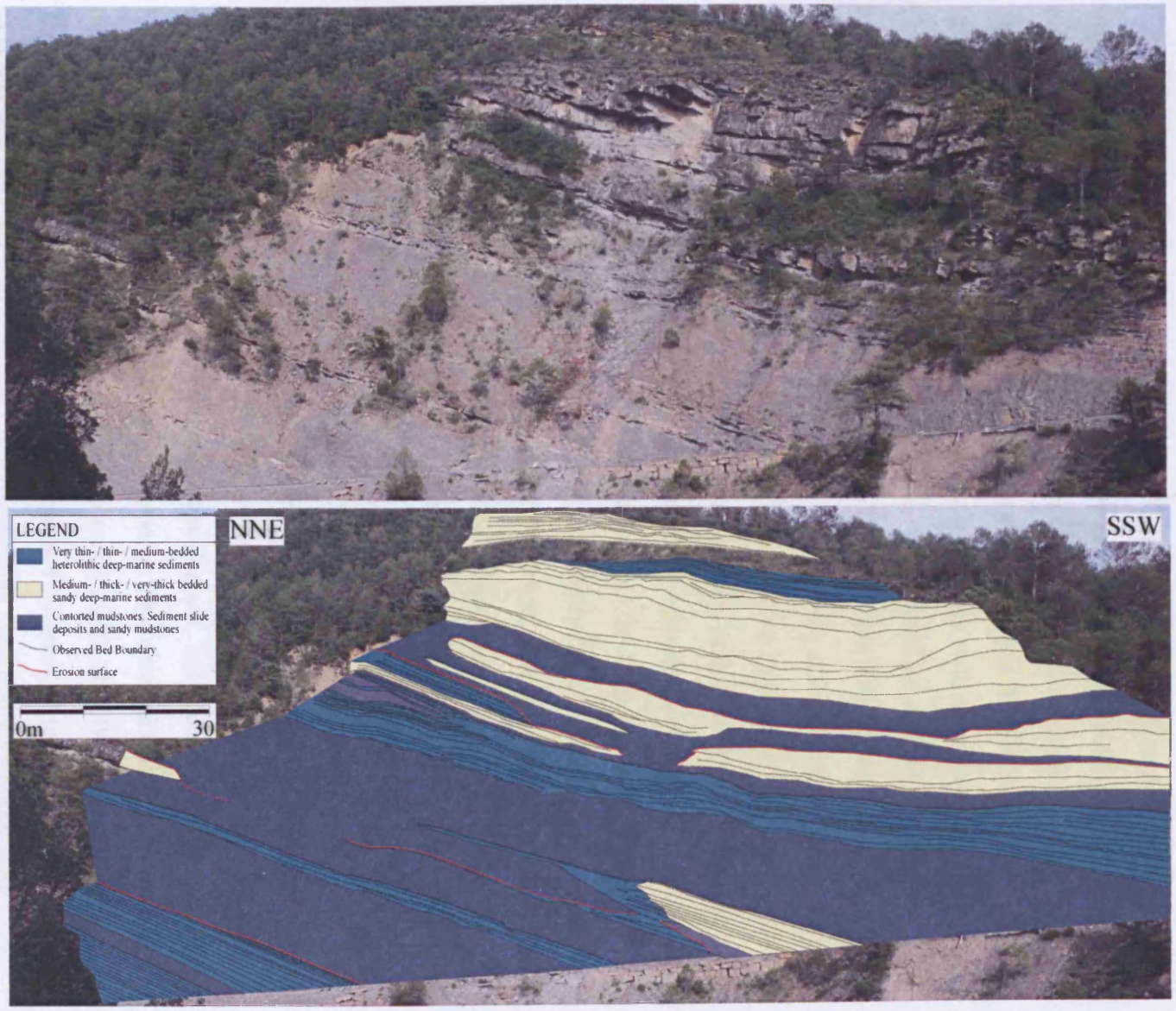

Fig. 5.5. Interpreted photo panel of the Arro cliff section above the road at the Barranco Sierra.

The base of the Arro system is associated with an angular unconformity marked by a 6° dip change. This is overlain by two thick (4-8 m thick) muddy Type Ia MTCs (FA1a) punctuated by a 1 m thick packet of thin-bedded, coarse-grained, laterally discontinuous sandstones (Unit 1: 5-18 m, Appendix 5.7).

These basal MTCs are overlain by ~51 m of thin- to medium-bedded tabular sandstones (FA5b) of Unit 2. This unit can be subdivided into 3 packets. The basal sandstone packet is 19 m thick and comprises tabular, thin- to medium-bedded sandstone-mudstone couplets and thin (<50 cm thick), Type Ib MTCs (FA1c). These MTCs are characterised by a sand-rich mudstone matrix with abundant mud-clasts. Crude packaging is developed, with the basal ~6 m exhibiting a poorly defined thinning-upward sequence, and the top ~4 m of the packet a thickening-upward sequence. The middle packet is ~22 m thick and consists of tabular, thin- to medium-bedded sandstones which are punctuated by thin, erosive Type Ia MTCs. The MTCs thicken away from the logged section in the river. This middle packet is deformed by southwest directed thrust faults and folds associated with the Los Molinos thrust system. The upper packet of sandstones comprise medium- to thick-bedded sandstones which thicken away from both logged sections into essentially thick-bedded, amalgamated sandstones. These sandstones appear relatively tabular, with scour structures and pinch-and-swell bed geometries rare. Unit 2 therefore displays an overall thickening and coarsening upward sequence (Unit 2: 18-69 m, Appendix 5.7).

Unit 3 essentially comprises three thick Type Ia and Type II MTCs up to 16 m thick with interbedded sandy packets (Figs. 5.5 and 5.6). The two lower MTCs are muddy Type Ia MTCs whilst the upper Type II MTC is characterised by a sand-rich mudstone matrix with large folded mudstones and thin-bedded sandstones. This is succeeded by a muddy MTC to form a bipartite deposit. Between the middle and upper MTCs is a small confined (channelised) sandbody. This channel thickens from 6 m in the road to 10.5 m in the river and has an estimated width of ~200 m (aspect ratio 19:1). The channel margin along the road is characterised by thin (<2 m thick) erosive Type Ib MTCs (FA1c) interbedded with thin- to thick-bedded commonly amalgamated sandstones. These sandstones tend to have well-developed internal stratification, and abundant intra-formational mud-clasts towards the base. Towards the axis of the channel in the river, the sandstones are medium- to thick-bedded, typically amalgamated with erosive bases (FA3a). Planar and cross stratification is developed in some beds and mud-clasts are common. These sandstones are laterally discontinuous,

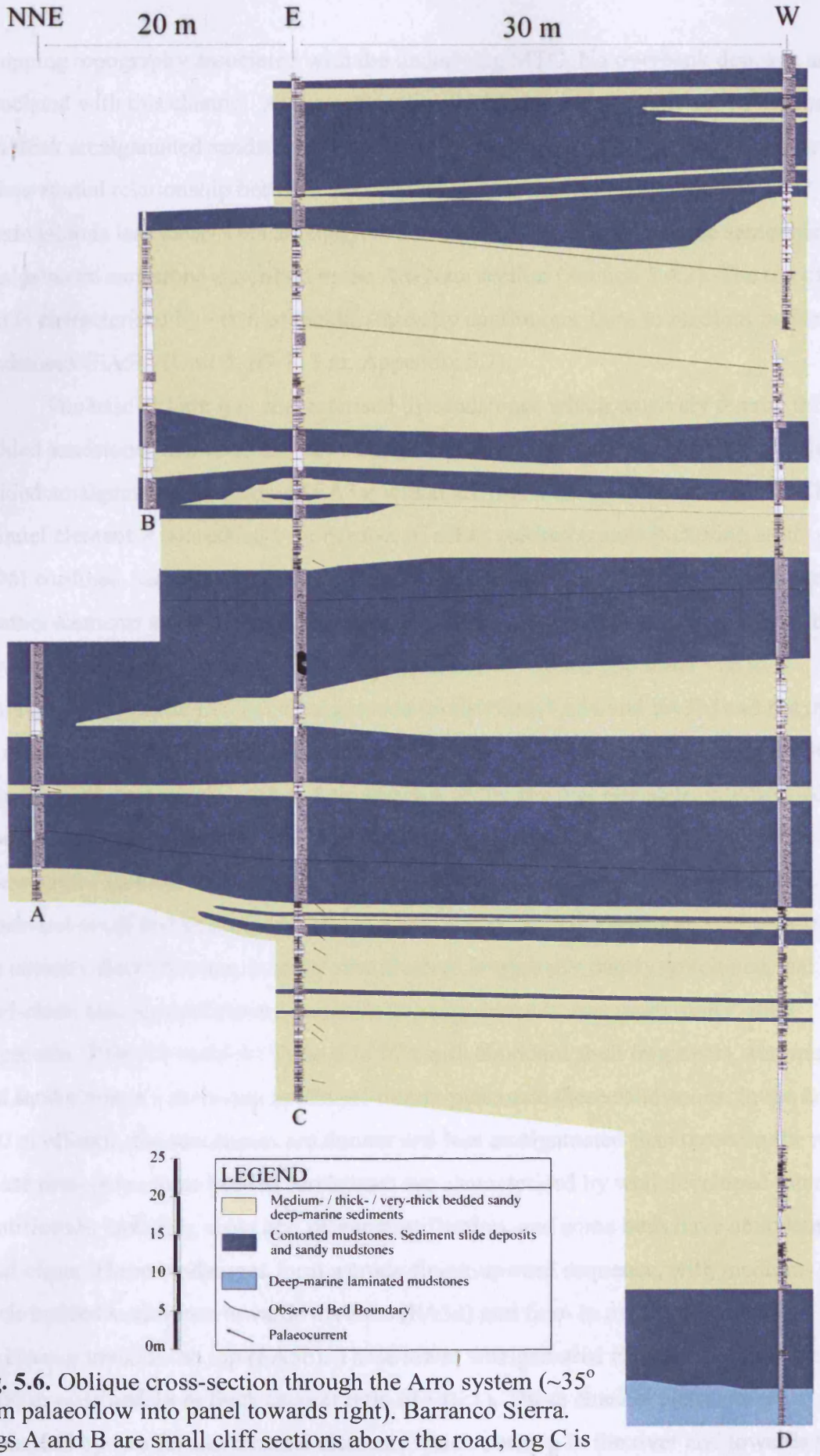

Fig. 5.6. Oblique cross-section through the Arro system (~35° from palaeoflow into panel towards right). Barranco Sierra. Logs A and B are small cliff sections above the road, log C is the road section (Appendix 5.8) and log D is the river log (Appendix 5.7).

onlapping topography associated with the underlying MTC. No overbank deposits are associated with this channel. At the same stratigraphic level in the cliff above the road, a 4 m thick amalgamated sandstone is truncated by the overlying MTC. Although there is a clear spatial relationship between the channel and the sandstone, the temporal relationship is less clear. This amalgamated sandstone is interpreted as the same thick amalgamated sandstone described in the Rio Nata section (Section 5.4.2). The top of the unit is characterised by ~6 m of tabular, laterally continuous, thin- to medium-bedded sandstones (FA5b) (Unit 3: 69-115 m, Appendix 5.7).

The base of Unit 4 is characterised by sandstones which erosively overlie thin-bedded sandstones and form an ~8-m-thick discrete channel element comprising thick-bedded amalgamated sandstones (FA3a) which are truncated by an erosive MTC. This channel element is succeeded by a number of offset stacked (*sensu* Pickering *et al.* 1996) confined, semi-amalgamated channel elements (Figs. 5.5 and 5.6). Two lower channel elements are exposed in the main cliff section above the road (Fig. 5.5) where they are amalgamated, with a cumulative thickness of ~24 m. The basal ~16 m is characterised by thick-bedded amalgamated sandstones (FA3a and FA3b) and the upper ~8 m consists of thin- to medium-bedded sandstones (FA5b) forming a thinning-upward sequence. Along the road, ~40 m from the axis of the channel elements, interbedded mudstones are developed between the medium- to thick-bedded sandstones (FA3d). These sandstones are characterised by erosive bases and flat to current rippled tops. Pinch-and-swell bed geometries are common, as well as load structures, and some beds are laterally discontinuous. Internal stratification is typically poorly developed, and mud-clasts and nummulites are common in many deposits, and more rarely, shell fragments. Thin (<2 m thick) Type II MTCs with abundant shell fragments, nummulites and sand clasts in a sand-rich mudstone matrix punctuate these sandstones. In the river ~90 m off-axis, the sandstones are thinner and less amalgamated than those on the road. These thin- to medium-bedded sandstones are characterised by well developed internal stratification including cross and planar stratification, and some beds have abundant mud-clasts. These sandstones form a crude fining-upward sequence, with medium- to thick-bedded sandstones towards the base (FA3d) and fine- to medium-bedded sandstones towards the top (FA5b). These lower amalgamated channel elements are ~400 m wide and 24 m thick (aspect ratio of ~16:1). These channel elements are succeeded by two further channel elements which outcrop in the river and towards the top of the cliff section above the road. Both are developed over the margins of the

underlying channel elements. In the river, the base of the channel element is defined by a thin (<20 cm thick) MTC and is overlain by thick bedded, rarely amalgamated sandstones with well-developed planar stratification (FA3d). This upper channel is truncated by erosive Type Ia MTCs (FA1a) (Unit 1: 115-162 m, Appendix 5.7). These overlying muddy MTCs are 1-6 m thick and punctuated by thin packets (<0.5 m) of thin-bedded sandstones (Unit 5). These are overlain by tens of metres of thin-bedded sandstones in the river section (Unit 5: 162-179 m, Appendix 5.7).

5.4.4 Santa Catalina

The Santa Catalina section (Locality 8, Fig. 1.3) is located down depositional-dip from the Barranco Sierra. The section is 42 m thick and incomplete due to tectonic deformation. Correlations between the other sections of the Arro system are ambiguous due to the lack of marker beds. The lower part of the section comprises thin- to medium-bedded sandstones (FA5b) interbedded with Type Ia and II MTCs. The sandstones are rarely amalgamated, current ripples are common and internal stratification is well developed, including planar and cross stratification, as well as mega-ripple cross stratification. These sandstones are not packaged into thinning- or thickening-upward sequences. The upper part of the section is characterised by a 3.5 m thick Type II MTC overlain by thick-bedded, commonly amalgamated sandstones (FA3a). These amalgamated sandstones are succeeded by medium-bedded sandstones (FA5b) punctuated by thin (<1 m) Type Ia and II MTCs to form a thinning-upward sequence. The MTCs in the section are markedly thinner than those in the Rio Nata or Barranco Sierra.

5.4.5 Interpretation / Correlation

Current understanding of the Arro system is restricted by the intense tectonic deformation and paucity of correlatable sections lateral to the main outcrops. Correlating between the Rio Nata and Barranco Sierra is complicated by tectonic deformation between the sections and the apparent heterogeneity of the system. Millington and Clark (1996) used a thick amalgamated sandstone overlain and underlain by MTCs as a correlative horizon between the sections. However, it is not possible to trace this sandstone between the two sections due to tectonic deformation, and there are several thick amalgamated sandstones in the Barranco Sierra section, all of which are discontinuous. In the absence of obvious marker horizons, the correlation proposed by

the current author is based on both sedimentological and ichnological observations (Fig. 5.7).

The first significant sandstone deposits of the Arro system immediately overlying the basal MTCs exhibit a down-depositional-dip change from erosive, scoured thick-bedded sandstones (FA3a) and interbedded thick MTCs of Unit 2 and 3 in the Rio Nata, to tabular, thin- to medium-bedded sandstones (FA5b) and thin MTCs of Unit 2 in the Barranco Sierra. This change in facies-associations may be related to a change in the nature of the gravity currents, from essentially erosional to depositional as the flows underwent a hydraulic jump due to changes in seafloor gradients or confinement. Alternatively, the observed down-dip change in facies-associations may simply reflect lateral changes in depositional environments within the channel system, with the Rio Nata section representing more axial deposits than the Barranco Sierra section, which may represent deposits associated with the margin of the channel system. The medium- to thick-bedded sandstones at the top of Unit 2 in the Barranco Sierra can be correlated up-depositional-dip with similar deposits in the Rio Nata (base Unit 3) and may be interpreted as more axial deposits.

The middle part of the Arro system differs greatly in both sections, with sandstones in the Rio Nata (Unit 3) correlating with the basal thick MTC of Unit 3 in the Barranco Sierra. The sandstones in the Rio Nata may be lateral to unexposed MTCs which correlate with those in the Barranco Sierra down depositional-dip. The MTCs, thick amalgamated sandstone and overlying thin-bedded sandstones and mudstones can be correlated between both sections. These thin-bedded sandstones overlying the MTCs may be associated with a period of reduced clastic input, and may mark a phase of abandonment.

The sandstones of Unit 4 in the Rio Nata correlate down depositional-dip with similar facies-associations at the base of Unit 4 in the Barranco Sierra. The basal tabular, laterally continuous sandstones immediately underlying the thick-bedded sandstones may be associated with initial sheet-like deposits prior to channel incision, or may represent the margin of an older channel element. The deposition of thick-bedded, channelised sandstones may be related to a renewed period of thrusting in the Los Molinos thrust system. This may have resulted in a change in dip that has been observed in the Barranco Sierra section. The thick unit of MTCs at the top of the Rio Nata correlate with the confined channel systems of Unit 4 in the Barranco Sierra. These MTCs may have acted to confine and funnel the gravity flows leading to the

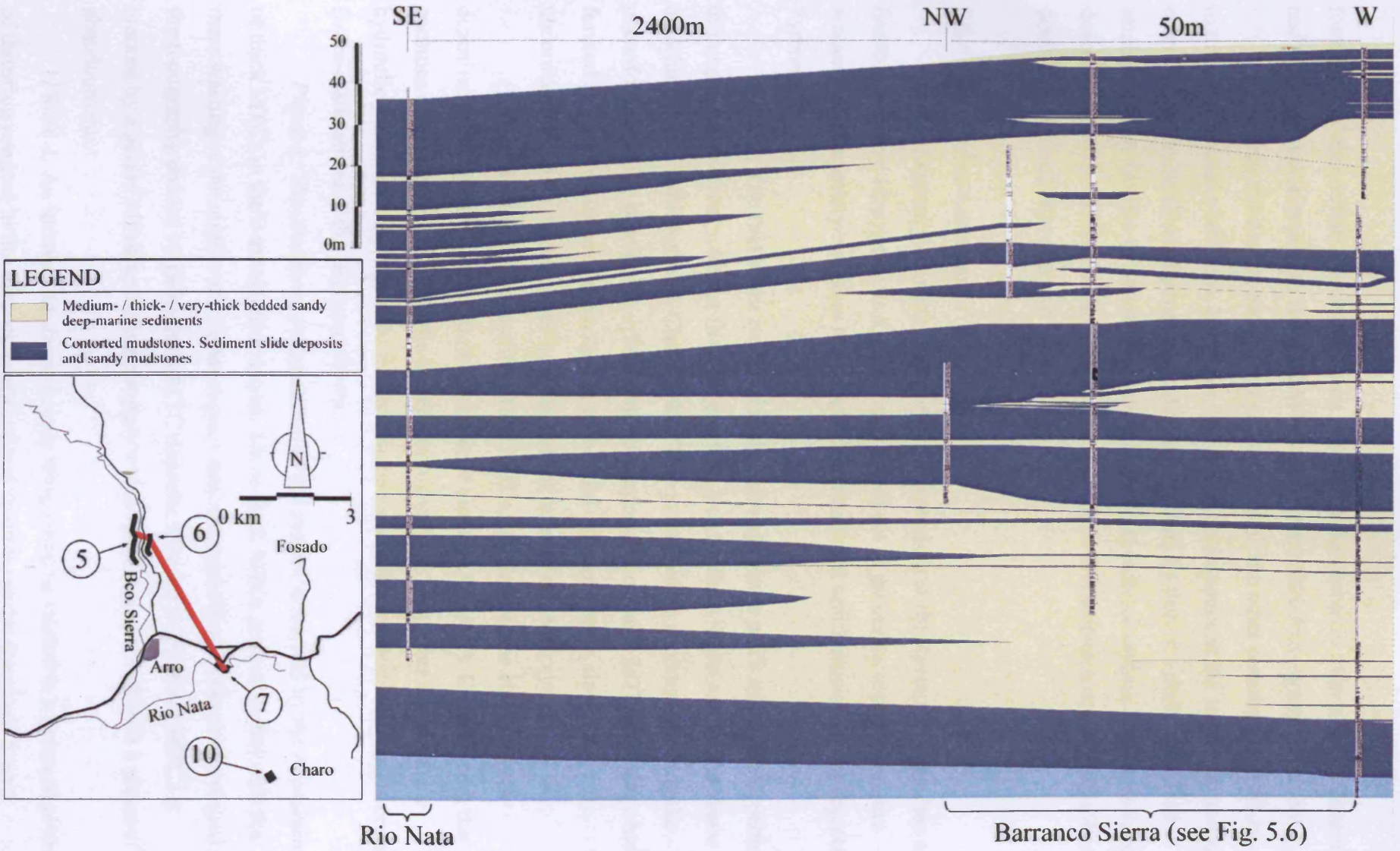

Fig. 5.7. Oblique cross-section through the Arro system between the Rio Nata and Barranco Sierra sections. See Appendices 5.6-5.8 for more detailed bed-by-bed graphic sedimentary logs.

formation of the confined channels which outcrop in the Barranco Sierra. Slope failure and healing is associated with the final MTCs at the top of the Arro system (Unit 5).

The Santa Catalina section is not correlated with the other outcrops studied due to the lack of marker horizons. However, the fining-up sequence at the top of the section characterised by thick amalgamated sandstones overlain by thin- to medium-bedded sandstones is indicative of deposition within a confined channel setting, similar to those described in Unit 4 of the Barranco Sierra section. Thus this section may represent the down-depositional equivalent of Unit 4.

5.4.6 Depositional summary

The sedimentary characteristics of the Arro system at the Barranco Sierra has a fivefold division, interpreted as a genetically linked set of processes representing the sequential sedimentary response to phases of thrust-related uplift-erosion in the adjacent Pyrenees.

Phase 1: The first event recorded in the Arro system is uplift and oversteepening of the slope associated with the first stages of the Los Molinos thrust and the Mediano detachment fold (Millington & Clark 1996). This is marked by a syntectonic angular unconformity at the base of the system and the deposition of basal MTC deposits which formed as a consequence of the collapse of the mid- to upper basin slope. The unconformity marks the sequence boundary at the base of the Arro system.

Phase 2: Following deposition of the MTCs, the first coarse clastics were deposited in the system sourced through a feeder canyon (Charo-1). Upon exiting the confines of the canyon, towards the lower-slope, the flows may have undergone a hydraulic jump resulting in erosive facies-associations in the Rio Nata and depositional facies-associations in the Barranco Sierra.

Phase 3: The continued progradation of the system is marked by the deposition of thick MTCs in the Barranco Sierra area. These thick MTCs are associated with the mass wasting of the middle and upper slope. Confined sand-filled channels developed in the topography created by these thick MTC deposits. The top of the thick MTCs is marked by a period of reduced clastic supply which may be associated with a phase of abandonment.

Phase 4: An increase in clastic supply which may be related to a renewed phase of thrusting resulted in the formation of confined channels in the Barranco Sierra.

Gravity current flows may have been confined by the thick MTC deposits in the Rio Nata.

Phase 5: The final phase in the Arro system is the deposition of thick MTCs in both sections. These MTCs mark the final collapse and healing of the slope. The final abandonment phase is marked by tens of metres of thin-bedded sandstones.

The thick accumulations of muddy slumps, facies-associations typical of flows which underwent hydraulic jumps, and the occurrence of confined channel elements suggests that deposition occurred on the lower slope. Overall, in the Barranco Sierra section, the Arro system displays a distinct coarsening-upwards, which may represent the overall progradation of the system. The Arro system may also represent a candidate for a tectonically controlled system, similar to the Lower Carboniferous Moravice Formation, Czech Republic (Babek *et al.* 2004).

5.4.7 Ichnology of the Arro System

The trace-fossil assemblage of the Arro system was studied along the road section at the Rio Nata (Locality 7), as well as the base of the road section at Barranco Sierra (Locality 6) (Units 1-3).

The Rio Nata section is characterised by a moderately low diversity and density trace-fossil assemblage. Average bioturbation is 15.13% on bedding planes. The trace-fossil assemblage consists of 9 ichnospecies from 5 ichnogenera. Of the 9 ichnospecies, 7 are post-depositional and 2 pre-depositional, including 1 graphoglyptid. The trace-fossil assemblage is dominated by *Pascichnia*, *fodinichnia* and *domichnia*. The most common taxa include *pascichnia* (*Scolicia* and *Planolites*), *fodinichnia* (*Thalassinoides*) and *domichnia* (*Ophiomorpha*). There is a paucity of vertically orientated trace fossils within the sandstones. The trace-fossil assemblage is characteristic of the *Ophiomorpha rudis* subichnofacies.

The Barranco Sierra section is characterised by a moderately high diversity, moderate density trace-fossil assemblage. Average bioturbation is 20.35% on bedding planes. In vertical section, within the turbiditic mudcaps, bioturbation is very low to absent (1.6%), with an ichnofabric index ranging between 1-2. The trace-fossil assemblage consists of 22 ichnospecies from 17 ichnogenera. Of the 22 ichnospecies, 13 are post-depositional and 9 pre-depositional, including 3 graphoglyptids. The trace-fossil assemblage is dominated by *pascichnia*, *fodinichnia* and *domichnia*, as well as some *agrichnia*. The most common taxa include *pascichnia* (*Halopoa, Planolites* and

Nereites), *fodinichnia* (*Thalassinoides*), *domichnia* (*Ophiomorpha*) and *agrichnia* (*Paleodictyon*). Like the Rio Nata section, there is a paucity of vertically orientated trace fossils within the sandstones. The Barranco Sierra section has an assemblage typical of the *Ophiomorpha rudis* subichnofacies, with some trace fossils more typical of the *Paleodictyon* subichnofacies.

The two sections differ greatly in terms of trace-fossil assemblages, with the Barranco Sierra section characterised by a higher diversity and intensity trace-fossil assemblage with a greater number of pre-depositional trace fossils, including graphoglyptids. This is directly related to the sedimentary characteristics of the sections studied. The sandstones of the Rio Nata section are coarser-grained and thicker-bedded than those at the base of the Barranco Sierra section, and were deposited by higher concentration turbidity currents associated with a greater amount of erosion. The more erosive sediment gravity flows probably removed the fertile top layer of the seafloor, resulting in the preservation of only the deepest tier trace fossils. The thick-bedded sandstones of the Rio Nata section may also have prevented all but the largest, most robust trace-making organisms to escape burial. As a consequence, this environment is dominated by large post-depositional trace fossils such as *Scolicia* and *Ophiomorpha*. The coarse-grained nature of the deposits in the Rio Nata section may also have excluded burrowers adapted only to fine-grained sediments (Tchoumatchenco & Uchman 1999). The paucity of vertically orientated burrows such as *O.* isp., which are in general common in proximal axial environments of the Ainsa basin (e.g., Ainsa I sandbody, Section 6.4.1), as well as the low bioturbation intensity on bedding planes and in vertical section, indicates that the Arro system may have been characterised by poorly oxygenated bottom waters.

Although the two sections are ichnologically very different, trace fossils have been used to correlate between the sections. The sandstones at the base of Unit 4 in both sections are characterised by very high bioturbation intensities relative to overlying and underlying deposits. In the Barranco Sierra, the bases of sandstones are heavily bioturbated by *H. imbricate*, whilst in the Rio Nata section, the bases are bioturbated by *O. annulata* and the tops by *O. rudis* and *Scolicia*. Although the ichnotaxa differ, the high intensity of bioturbation indicates that these sandstones were probably deposited coevally, in well-oxygenated bottom waters.

Chapter 6

Ainsa basin:
proximal fan and related environments

6.1. Introduction

The use of trace fossils stems from the fact that variations in trace-fossil assemblages and average bioturbation in fan and related environments reflect the varying, innate, dynamic controlling factors such as substrate consistency (e.g., sandy *versus* muddy, etc.), nutrient supply, level of oxygenation, hydrodynamic energy, rates of sediment accumulation, salinity, and any chemical toxicity (Frey *et al.* 1990). In this chapter, a detailed documentation of the different trace-fossil assemblages / abundances that characterise different fan and related environments in the deep-marine Ainsa basin is provided, together with a detailed sedimentological study of submarine fan and related environments recognised in the Ainsa basin. The principal observations of the sedimentological study are summarised in Table 6.1. A list of ichnotaxa identified is provided in Table 6.3. The results should find wide applicability in other deep-marine basins worldwide.

6.2. Gerbe system

The Gerbe system is a canyon-erosive submarine channel system (Clark & Pickering 1996). It consists of two sandbodies tens of metres thick separated by a thick muddy wedge. Both sandbodies are characterised by accumulations of conglomerates, pebbly sandstones and pebble-rich MTCs towards the base, which represent active stages of basinward transference. The older Gerbe I sandbody is a type I channel feature (*sensu* Mutti & Normark 1987), whilst the Gerbe II sandbody is a type II mixed channel, with a conglomeratic base and sandy fill. The Gerbe system is exposed southeast of Ainsa, along the Rio Nata (Locality 11, Fig. 1.3), as well as to the north of Ainsa. The point source of the Gerbe system, the Charo canyon (Mutti *et al.* 1985), is located ~2 km to the southeast of the Rio Nata sections near Charo village (Locality 9, Fig. 1.3; Appendix 6.1).

6.2.1. Canyon fill

6.2.1.1. Sedimentology

The Charo submarine canyon cuts into the underlying deltaic shelf and basin slope forming a v-shaped erosional surface with several 100 metres of cut down. Only the middle and top part of the Charo canyon fill was studied (Appendix 6.1). This section corresponds to the Santa Liestra Units b, c and d of Millington and Clark (1995b). Below the logged section, ~40 m of poorly exposed thin-bedded sandstones and thin MTCs (< 10 m) occur, which, according to Millington and Clark (1995a, b), are associated with the base of the Charo-2 canyon.

The base of the logged section is characterised by a 35 m thick, aerially extensive, Type Ia MTC (FA1a). The canyon fill is dominated by MTC formed by Type Ia (FA1a) and Type II MTCs (FA1b). These complexes are typically tens of metres thick and punctuated by thin (< 2 m thick), localised, lens-shaped, sandy and muddy conglomerate and gravel horizons and more rarely, medium-bedded sandstones. Small channel elements < 7 m thick may be developed between the MTC. These sandbodies typically have erosive bases, and may be partially confined by topography created by underlying MTCs. Typically, the sandbodies are several tens of metres in lateral extent and up to ~150 m wide. The main sandy succession is characterised by laterally discontinuous, thin- to medium-bedded sandstones of FA5c. These sandstones are typically internally structureless, tabular, and non-erosive. Extra-formational organic matter, shell fragments, nummulites and small rounded pebbles occur in some of the sandstones. Typically, the sandbodies display no thinning- or fining-upward sequences, however, such sequences are crudely developed in some sandbodies. The canyon fill is overlain by shelf sandstones.

6.2.1.2. Ichnology

The canyon fill is characterised by a very low diversity, low intensity trace-fossil assemblage (Fig. 6.1). Mean bioturbation on bedding planes is 15.87% with 4 ichnospecies from 2 ichnogenera recognised, all of which are post-depositional. The trace-fossil assemblage is dominated by *Thalassinoides* (*fodinichnia*) and

Table 6.1. Summary of sedimentary characteristics of fan and related environments in the Ainsa basin.

Environment	Section	Summary characteristics	S:M** ratio	Av. sand thickness	Facies***
"structurally-confined clastic ramp" sandbodies	1	Overall, sandbodies show sheet-like geometry with internal heterogeneity formed by laterally stacked, shallow channel elements, with aspect ratios of 200-300 Rare erosional and/or topography-forming MTCs* below and within sandbodies	90:10	14.42	B2.1, C2.1
"structurally-confined Clastic ramp" thin-bedded at top of sandbodies	2	Sandstones generally tabular and sheet-like, with rare mud- and sand-filled scours associated with broad sandstones shallow low net : gross channel elements MTCs are rare, and mudstones between sandstones and siltstones very thin, and ripple train beds common	66:34	3.33	C2.2, C2.3, D2.3
Basin slope	5	Thick packages of bioturbated mudstones and siltstones, intercalated with smaller. packages of heterolithics Sandstones are tabular and sheet-like	46:54	3.78	C2.3, D1.3, D2.3, E1.3
Upper-slope gully bioclastic sandstones	4	Gully is 5 m deep, 67.5 m wide, with an aspect ratio of 13.5 . Multi-storey master erosion surface that cuts down into delta front lobe sandstones Fill comprises nummulite-rich, structureless, very-fine- to fine-grained sandstones which pinch out at margins	58:42	13.83	
Slope gully	3	Gully is 14 m wide, 6 m deep with an aspect ratio of 2.3 Sandstones thicken in the centre of the gully, and pinch out at the margins, and form a concave up geometry	28:72	6.52	C2.2, C2.3
Canyon fill	6	Dominated by thick MTCs (mainly intra-formational sediment slides and slumps) up to 30 m thick Small lens-shaped channel elements typically <5 m thick, with erosive pebble-rich bases encased in MTCs	15:85	16.42	A1.2, A1.3, A1.4, C2.1, C2.2, F2.1
Channel axis, Fosado	9	Small channel encased in MTCs (mainly intra-formational slumps) 120 m wide, 10 m thick Comprises two vertically stacked fining-up channel elements with medium- to thick-bedded, medium- to coarse-grained amalgamated sands at the base	75:25	25.26	B2.1, C2.1, C2.2

Table 6.1. *(Continued)*

Environment	Section	Summary characteristics	S:M** ratio	Av. sand thickness	Facies***
Channel axis, Gerbe I	10	Multiple vertical and laterally offset-stacked channel elements between 80-250 m wide and 6-20 m thick Complex, heterogeneous fill with high frequency of laterally discontinuous MTCs Lens-shaped, pebbly macroform elements with internal dipping surfaces (macroform accretion sets) dipping oblique to palaeoflow	54:46	17.17	A1.3, A2.1, A2.7 B2.1, C2.1, C2.2, C2.3
Channel axis, Ainsa I	7, 8	Laterally stacked confined to poorly confined channel elements in an overall fining upward sequence Characterised by thick-bedded, coarse-grained amalgamated sandstones averaging 15 m in length and pebbly MTCs	85:15	18.25	A1.2, A2.7, C2.1, C2.2
Channel axis, Morillo	11	Complex, heterogeneous fill characterised by multiple laterally offset stacked channels Common MTCs, pebbly discontinuous sandstones and pebble-rich sandy macroform elements	65:35	28.33	A1.2, A2.7, B2.1, C2.1, C2.2
Channel off-axis	12, 13,	Fewer amalgamated sandstones and thick MTCs compared to channel axis Sandstones are laterally continuous to discontinuous	70:30	12.76	A1.2, B2.1, C2.1, C2.2, C2.3,

* MTC = mass transport complex (or deposit);
** S:M = sandstone : mudstone;
*** Facies after Pickering *et al.* (1986, 1989).

Ophiomorpha (*domichnia*). The diameter of these trace fossils can be very large, with the largest being 6 cm in diameter (*Thalassinoides* ispp. indet.). Obliquely orientated *Ophomorpha* burrow networks are particularly common within the sandstones. The trace-fossil assemblage is characteristic of the *Cruziana* ichnofacies.

6.2.1.3. Interpretation

The abundance of Type Ia and II MTCs is associated with the mass wasting and collapse of the slope which both excavated and infilled the canyon. Type Ia MTCs are probably locally derived, representing mass wastage from the mid and upper basin slope as well as intra-canyon slope failures. They are the products predominantly of sediment slides and slumps. In contrast, Type II MTCs were probably derived from the collapse of the upper slope and outer shelf to littoral zone, redeposited as sediment slides and debris flows. The canyon morphology probably induced lateral confinement and funnelling of high-intensity gravity flows. As a consequence, by-pass facies are abundant, such as scours and conglomerates. These probably represent lag deposits associated with by-passing high concentration turbidity currents and cohesive debris flows. Many of the fine-grained sandstones may represent suspension deposits of the fine-grained tail of by-passing gravity flows.

The low diversity trace-fossil assemblage is probably associated with the inferred high stress environment. Most organisms could probably not colonise the canyon due to the high frequency of erosive gravity-current flows. The only ichnotaxa recognised, *Thalassinoides* and *Ophiomorpha*, are interpreted to have been formed by crustaceans, mainly but not exclusively decapods (Frey *et al.* 1978). Unlined *Thalassinoides* characterise muddy sediments whilst lined *Ophiomorpha* characterise the sandstones, and in many cases, both ichnotaxa may have been formed by the same organism. Consequently, it is interpreted that in the canyon, only crustaceans, and mainly decapods, were able to colonise the sands. It is possible that the canyon was dominated by one single type of organism, which formed both *Thalassinoides* and *Ophiomorpha*. The trace-making organisms may have been transported directly from the shelf as doomed pioneers (*sensu* Föllmi & Grimm 1990).

A number of beds analysed are heavily bioturbated resulting in a low diversity, high intensity trace-fossil assemblage. This is characteristic of an opportunistic strategy of colonising the sea-floor, by organisms transported into the canyon or by those, which survived burial by newly deposited sands. The occurrence of *Ophiomorpha* burrows is

typical of medium- to thick-bedded sandstones in proximal axial environments (e.g., Ainsa I and Guaso channel axis sandstones, Section 6.3.2.2 and 6.4.1.2, respectively). These burrow networks were formed by large, robust, deeply burrowing organisms, which exploited organic rich layers within the sands. Such colonising strategies were well adapted to the canyon because the trace-making organisms were able to survive burial by newly deposited thick sands (Wetzel & Uchman 2001).

Outcrop Number / Environment	No bed. planes	Av bio (%)	Diversity	No. pre-turbidite	No. post-turbidite	No. graph.
(24) "Prodeltaic clastic ramp" sandbodies, Guaso system	37	4.67	7	1	6	0
(25) "Prodeltaic clastic ramp" thin-bedded sandstones at top of sandbody, Guaso system	48	39.27	20	8	12	3
(26) Slope gully, Guaso system	18	37.95	10	1	9	0
(12) Upper-slope gully, Formigales	19	8.21	5	0	5	0
(27) Basin-slope, Guaso system	29	39.93	14	4	10	2
(9) Canyon-fill, Charo Canyon	49	15.87	4	0	4	0
(15) Channel-axis, Ainsa I sandbody	23	34.79	6	0	6	0
(19) Channel-axis, Ainsa I sandbody	12	38.67	8	1	7	0
(1) Channel-axis, Fosado system	20	8.35	6	1	5	0
(11) Channel-axis, Gerbe I sandbody	26	14.46	17	4	13	3
(23) Channel-axis, Morillo system	34	11.12	9	0	9	0
(14) Channel off-axis, Banaston III sandbody	32	29.58	19	9	10	6
(16) Channel off-axis, Ainsa I sandbody	22	23.55	11	2	9	2
(17) Channel-margin, Ainsa I sandbody	23	44.85	21	10	11	5
(20) Channel-margin, Ainsa II sandbody	144	43.6	34	16	18	9
(22) Channel-margin, Morillo system	92	42.76	25	10	15	7
(18) Outermost channel-to-levee-overbank	30	31.03	15	5	10	4
(21) Proximal interfan, Ainsa system	29	55.51	18	4	14	3

Table 6.2. Average bioturbation, trace-fossil diversity, number of pre- and post-depositional trace fossils, and the number of graphoglyptids for eleven fan and related environments of the Ainsa basin. The outcrop number (see Fig. 1.3 and Table 1.1) and number of bedding planes studied at each section is also recorded.

6.2.2. Channel axis

6.2.2.1. Sedimentology

The axis of the Gerbe I sandbody is exposed to the east of Gerbe village in a large, essentially inaccessible cliff section above the Rio Nata (Locality 11, Fig. 1.3; Appendix 6.2 and 6.3). The outcrop is ~60 m thick and ~500 m wide. On the basis of facies changes throughout the section, the width of the sandbody can be estimated very approximately at between 2000-3000 m. The sandbody comprises a number of discrete, vertically and laterally offset stacked channel elements, forming a channel complex set.

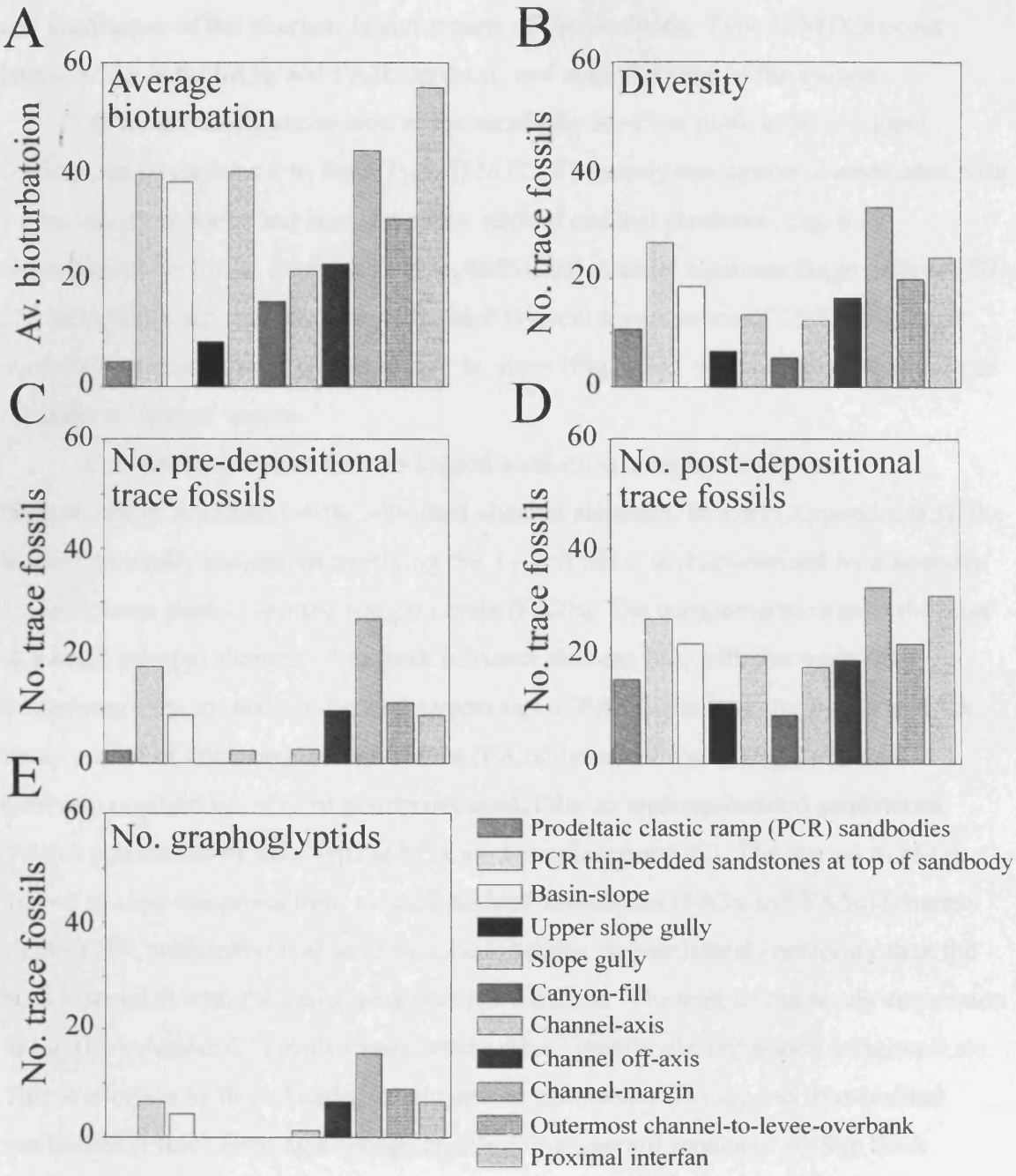

Fig. 6.1. (A) Average bioturbation in fan and related environments in the Ainsa basin; (B) Trace-fossil diversity; (C) Number of pre-depositional trace fossils; (D) Number of post-depositional trace fossils; (E) Number of graphoglyptids.

Two sections of the cliff were logged (Appendix 6.2 and 6.3), at a spacing of ~30 m. In each section, a number of channel elements were recognised (Fig. 6.2). Palaeoflow ranges between 304-330°, averaging 316°.

The base of the sandbody is strongly diachronous, and characterised by sand and mud-filled scours (FA3g), and laterally discontinuous, lens-shaped conglomerates (FA2b) (Figs. 6.3a, b and c). These basal deposits overlie FA6d thin-bedded sandstones

and mudstones of the interfan. In some parts of the sandbody, Type II MTCs occur lateral to the basal FA3g and FA2b deposits, and mark the base of the system.

The main sandy succession of the sandbody is ~15 m thick in both logged sections, and overlies a 4 m thick Type II MTC. The sandy succession is associated with a number of vertically and laterally offset stacked channel elements (Fig. 6.2), characterised by FA2b, FA3a and FA5c. Individual channel elements range between 80-250 m in width and typically are ~6 m thick (typical aspect ratios of 13:1). Erosional surfaces between channel elements may be steep (Fig. 6.3d), with cut-down typically in the order of several metres.

Correlating between the two logged sections is complicated by bed discontinuities associated with individual channel elements. In log I (Appendix 6.3), the base of the sandy succession overlying the Type II MTC is characterised by a laterally discontinuous clast-supported conglomerate (FA2b). The conglomerate marks the base of a small channel element ~4 m thick (channel element IA), with the main fill comprising thin- to medium-bedded sandstones of FA5c. It is overlain by a 3 m thick sandy packet of thick-bedded sandstones (FA3a) (channel element IB) which is erosively overlain by ~4 m of poorly exposed, thin- to medium-bedded sandstones (FA5c) punctuated by thin Type II MTCs (channel element IC). The top ~6 m of the logged section comprises thin- to thick-bedded sandstones (FA3a and FA5c) (channel element ID), with individual sandstone beds having greater lateral continuity than the beds associated with the underlying channel elements. The base of the sandy succession in log II (Appendix 6.2) is also associated with a laterally discontinuous conglomerate. This is overlain by thick-bedded amalgamated sandstones (FA3a) and thin-bedded sandstones (FA5c) forming a fining- and thinning-upward sequence ~4.5 m thick (channel element IIA). The basal deposits of this channel element truncate those of channel element IA. It is overlain erosively by a thin Type II MTC, which marks the base of a 4 m thick channel element (IIB). The main fill is characterised by thin- to medium-bedded sandstones (FA5c). Overlying these thin-bedded sandstones is a thick, lens-shaped, laterally discontinuous conglomerate with inclined surfaces (FA2b). Lateral to the conglomerate is an area of no exposure, probably marking a low net:gross channel-fill formed from thin-bedded sandstones and mudstones, or an MTC deposit (channel element IIC). The top of the sandbody is marked by several metres of thin-bedded


Log I
ID
IC
IB
IA
Log II
IIC
IIB
IIA
LEGEND
FA1b Chaotic sandy-mudstones with intra-formational and extra-formational components (MTCs)
FA2b Lens-shaped sandy conglomerates with common inclined surfaces
FA3a Laterally discontinuous coarse-grained to pebbly sandstones
Observed Bed Boundary
FA3g Irregular, poorly sorted sandstones with scour-and-fill structures
FA5d Laterally discontinuous thin- to medium-bedded variable thickness sandstone-mudstone couplets
FA6b Intensely bioturbated very-thin-bedded sandstones, siltstones, mudstones and biogenic mudstones
Observed Bed Boundary

Fig. 6.2. Detailed bed-by-bed graphic sedimentary logs and interpreted line drawing of the Gerbe I channel complex, Rio Nata.

sandstones (FA5c), which may represent an abandonment phase. Overall the sandbody shows a crude thinning- and fining-upward sequence.

The lens-shaped, laterally discontinuous conglomerates with inclined surfaces (FA2b) were studied in detail at this section. These pebbly macroform elements range between 2-4.5 m thick, are laterally discontinuous over ~40 m, and lens-shaped. They are clast-supported, normally graded and the clasts are typically imbricated. Dipping surfaces within the macroforms are interpreted as macroform accretion sets. Three macroforms were studied in detail: A, B and C. In macroform A (Fig. 6.3a), the surfaces dip between 20-21° towards the south (170°). In macroform B (Fig. 6.3b), the surfaces dip between 10-31° towards the WSW (253°) and the conglomerate is crudely graded. In macroform C, the surfaces dip between 24-28° towards the WSW (243°). The macroform accretion sets are therefore orientated oblique to the main palaeoflow.

6.2.2.2. Ichnology

The ichnology of the Gerbe I sandbody directly reflects the sedimentology of the section. Mean bioturbation on bedding planes is 14%, whilst in interbedded mudstones, bioturbation in vertical section is 10%, with an ichnofabric index of 2 (Fig. 6.1). 17 ichnospecies from 11 ichnogenera were recognised. Of these 17 ichnospecies, 13 are post-depositional and 4 are pre-depositional trace fossils, including 3 graphoglyptids. The trace-fossil assemblage is dominated by *domichnia* and *pascichnia*. Common ichnotaxa include *Arenicolites* and *Ophiomorpha* (*domichnia*); and *Halopoa* and *Scolicia* (*pascichnia*). The trace-fossil assemblage is also characterised by a number of *agrichnia* including *Megagrapton* and *Paleodictyon*.

Bioturbation intensity is highest in thin- to medium-bedded fine-grained sandstones of FA5c, whilst the conglomerates and gravels of FA2b are non-bioturbated. FA3a coarse-grained to pebbly sandstones are characterised by a very low diversity, low intensity trace-fossil assemblage. Mean bioturbation on bedding planes is 10%, and only five trace fossils are recognised, four of which are post-depositional. The trace-fossil assemblage is typical of the *Ophiomorpha rudis* subichnofacies of the *Nereites* ichnofacies. The sandstones of FA5c are characterised by a mean bioturbation of 17% and diversity of 14. Of these 14 trace fossils, 10 are post-depositional and 4 are pre-

depositional trace fossils, including 3 graphoglyptids. This facies association is dominated by *Arenicolites* isp. and has a trace-fossil assemblage that can be classified as a mixed *Cruziana-Nereites* ichnofacies.

Arenicolites commonly occurs below FA2b pebbly macroform elements, where particular horizons are commonly pervasively burrowed. *Arenicolites* is also associated with thicker sandstones, as well as the thin-bedded sandstones and siltstones of the underlying interfan/slope (FA6d). These ichnotaxa achieve a maximum vertical height of 55 cm and pass through sandstones as thick as 32 cm. The smallest *Arenicolites* are associated with the underlying basin slope deposits, whilst the largest ones occur below the pebbly macroform elements. Despite the abundance of vertically orientated *Arenicolites*, other vertical trace fossils such as *Skolithos* or vertically orientated *Ophiomorpha* are very rare. *Arenicolites* has also been observed in the overbank of the Banaston II sandbody (Section 6.3.3.2) and the interfan of the Ainsa system (Section 6.4.5.2).

6.2.2.3. Interpretation

The Gerbe I sandbody can be interpreted as a canyon-sourced, slope channel system. Although the lateral extent of the section does not allow detailed analysis of the geometries of the sandbody, it may be postulated that the base is marked by a broad, highly irregular erosion surface within which the channel system developed. This is similar to the turbidite systems recognised in the Oligocene of the Galio Field, Block 18, offshore Angola. The sandbody is characterised by a highly heterogeneous fill and is an example of a mixed erosional-depositional channel system (*sensu* Mutti & Normark 1987).

The abundance of lens-shaped conglomerates (FA2b), pebbly sandstones (FA3a), mud- and sand-filled scours (FA3g), truncated sandstones, well-developed cross bedding, and embedded pebbles in the tops of some sandstones (FA3a), is associated with erosive, high concentration turbidity currents and debris flows characterised by significant sediment bypass. This is related to possible changes in seafloor gradient on the slope and/or reduced lateral confinement of the flows as they exited the canyon. Consequently, a decrease in flow-energy favoured the formation of a hydraulic jump resulting in erosive flows characterised by bypass. Erosive processes

Ichnotaxa/Outcrops	24	25	26	12	27	9	15	19	1	11	23	14	16	17	20	22	18	21
Plug-shaped form A														0.5	0.04			
Lockeia siliquaria															0.04			
Skolithos isp.				1.68														
Arenicolites isp.										1.61								0.63
Nummulites-lined burrow				0.68														
Halopoa imbricate								1.41		1.32		0.37	4.48	0.9	9.65	6.91	0.73	0.11
Halopoa storeana										0.71					0.25	0.08		
Hormosiroidea annulata																	0.02	
Strobilorhaphe glandifer		0.09												0.23	0.03			
?Imponoglyphus isp.															0.03			
Planolites montanus									0.9							0.15		
Planolites beverleyensis		0.17		0.75											0.36			
Planolites ispp.	0.78	3.3	8.38		1.41			0.54	2.12		0.2	3.17	1.6	2.19	1.35	0.89	1.54	9.84
Palaeophycus tabularis										1.1						0.48		
Chondrites intricatus			0.06									0.46			0.06			0.34
Chondrites isp.									0.45	0.17	0.05	1.28		0.41	0.21		2.09	4.46
Ophiomorpha annulata	0.6	2.6	4.63		17.1	1.55	3.1	7.17		3.28	1.36	6.41	4.73	7.77	5.63	4.58	14	4.26
Ophiomorpha rudis	0.35	2.7	0.37		1.04	4.94	12.6	15		3	3.45	2.12	3.19	0.54	5.66	0.79	0.44	2.94
Ophiomorpha isp.	0.48		0.39	2.26	0.44		0.17	1.86		0.11	1.42		0.34	0.24	0.06	0.03	0.26	
Thalassinoides suevicus	0.91	0.08				2.88	2.5	6.28		1.05		3.62	1.62	19.2	3.08	5.67		1.7
Thalassinoides ispp, indet.		0.66	1.15	1.21	2.52	1.08			0.31		1.59		0.41	2.1	1.83	1.79	3.03	
Phycodes palmatum																0.23		0.17
?Agrichnium isp.		1.02																
Saerichnites canadiensis		0.07										0.15						
Lorenzinia plana		0.15																
Lorenzinia nowaki		0.07	0.21															
?Glockerichnus isp.															0.02			
?Arenituba isp.		1.56																
Asterosoma ispp.	0.1	8.81																
Zoophycos insignis		0.4																
Zoophycos isp.											0.25				0.19			
Phycosiphon incertum		6.59	1.87		6.96						0.03	2.42				0.45	0.47	0.63
Lophoctenium ramosum										0.45					1.85			
Nereites irregularis			3.85								0.03	0.35		1.11	0.03		0.97	5.95
Nereites cambriensis		0.37																
Nereites isp.	0.4																	
Scolicia prisca			4.66		1.18		0.65			0.69			1.03		2.11			3.83
Scolicia plana			1.15		1.18									0.2	0.46			2.06
Scolicia strozzii			5.15		1.22			0.15		0.26		0.31		1.69	0.43		0.32	
Scolicia isp.					1.18		0.56	0.8	0.31	0.51			0.66	2.52	1.22		0.28	1.05
Taenidium serpentinum																0.52		
Taenidium cameronensis												0.68				0.33		
Taenidium ispp.		0.1																
Gordia marina									0.64							0.56		
Gordia arcuata															0.08	1.62		
Cosmorhaphe lobata														0.54		0.02		
Cosmorhaphe sinuosa												0.25						
Helminthorhaphe flexuosa														0.68	0.05	0.22	0.08	0.44
Helminthorhaphe japonica												0.28				0.1		
Helminthopsis abeli		0.07																
Helminthopsis tenuis														0.31	0.02			
Helminthopsis ispp.	0.03	0.36								0.31		0.15			0.21	0.58		0.53
Spirohaphe isp.													0.21		0.04			
Belorhaphe zickzack			0.24											0.3				
Desmograpton alternum																0.27		
Megagrapton irregulare															0.19			
Megagrapton submontanum										0.76		0.32			0.04	0.36		
Paleodictyon minimum										0.19		0.32			0.6	0.46		0.48
Paleodictyon latum															0.12			
Paleodictyon strozzii		0.07	0.84							0.08		0.21	0.43		1.14	0.18		
Paleodictyon miocenicum														0.35	0.06			
Paleodictyon majus												0.43		0.47			0.83	0.26
Paleodictyon maximum														0.33			0.75	
Arthropod trackway																0.27		

Table 6.3. Distribution of trace fossils in the Ainsa basin. Individual numbers represent the areal percent of bedding planes at specific localities covered by individual ichnotaxa: (24) Prodeltaic clastic ramp sand bodies, Guaso system; (25) Prodeltaic clastic ramp thin-bedded sandstones at top of Guaso sandbody; (26) Basin-slope thin-bedded sandstones / mudstones, Guaso system; (12) Upper-slope sandstone-filled gully, Formigales; (27) Slope gully (sand filled), Guaso system; (9) Canyon fill (mudstones / siltstones / sandstones), Gerbe (Charo-2) Canyon; (15) Channel axis sandstones, Ainsa I sandbody; (19) Channel axis sandstones, Ainsa I sandbody; (1) Channel axis sandstones, Fosado system; (11) Channel axis sandstones, Gerbe I sandbody; (23) Channel-axis sandstones, Morillo system; (14) Channel off-axis sandstones (including mudstones), Banaston III sandbody; (16) Channel off-axis sandstones (incl. mudstones), Ainsa I sandbody; (17) Channel-margin sandstones / mudstones, Ainsa I sandbody; (20) Channel-margin sandstones / mudstones, Ainsa II System; (22) Channel-margin sandstones / mudstones, Morillo system; (18) Outermost channel-to-levee-overbank thin-bedded sandstones / mudstones; (21) Proximal interfan (mainly mudstones, some heterolithics), Ainsa system.

may also have been developed as a result of the potential funnelling of flows as they exited the canyon (Eschard *et al.* 2003).

The pebbly macroform elements (FA2b) characterised by macroform accretion sets (Figs. 6.3a and b) are interpreted as pebbly barforms, which are temporally and genetically related to the thalweg of individual channel elements. These barforms associated with lateral accretion surfaces may be point bars within a channel with some degree of sinuosity (cf. Abreu 2003), or bars formed in a braided submarine channel system. In the later case, the lateral accretion surfaces would therefore represent accretion at the lateral margin of the barform, and when observed along palaeoflow, down-flow macroform accretion sets would also be expected. In a barform recognised in the Morillo II sandbody (Section 6.5.1.1), macroform accretion sets were not observed dipping perpendicular to palaeoflow. The barforms in Gerbe I are interpreted as having formed in moderately sinuous channels. This is due to the consistent dip of the accretion sets perpendicular to palaeoflow and the 26° dispersion of palaeocurrent indicators throughout the channel complex set. Similar larger-scale deposits from the Miocene Cingöz Formation, southern Turkey, have been interpreted as point bars by Satur et al. (2000).

The abundance of pebbles in Gerbe I is significant because it marks the first time during the evolution of the Ainsa basin that considerable amounts of extra-formational pebbles were deposited in the deep-marine parts of the basin. In the underlying systems, pebbles are absent or very rare, and this has been interpreted as reflecting a lack of pebbles stored on the shelf due to the maturity of the fluvial systems (see Section 5.3.7). Gerbe I at Rio Nata is interpreted as a channel complex set characterised by a basal bypass dominated channel complex and an upper essentially depositional channel complex.

The trace-fossil assemblage dominated by vertically orientated *Arenicolites* supports the interpretation that the Gerbe I channel system was a high energy environment characterised by significant bypass. *Arenicolites* has previously been described in distributary bar facies of the Conway Flat fan delta depositional system (Ekdale & Lewis 1991) as well as in storm beds of the upper offshore-lower shoreface setting of the Grund Formation, in the Austrian molasses (Pervesler & Uchman 2004). The association with distributary bars and storm beds indicates that *Arenicolites* is very typical of high energy environments and should not be regarded exclusively as a shallow marine trace fossil. It is interpreted as a *domichnion* of a suspension feeder and

preferentially occurs where current activity is continuous / episodic (see Section 3.10.2.2). *Arenicolites* has been recognised in other submarine fan systems, such as the Wood River Formation, Pennsylvanian-Permian (Burton & Link 1991) and the Upper Cretaceous-Eocene Gurnigel flysch, Swiss Alps (Crimes *et al.* 1981). The association of *Arenicolites* with pebbly macroform elements indicates that *Arenicolites* may have been particularly abundant at the base of the channels.

The axis of Gerbe I exhibits a moderately high diversity trace-fossil assemblage. This is due to the occurrence of FA5c thin- to medium-bedded sandstones. Due to the abundance of these deposits, the trace-fossil assemblage is more diverse than other axial environments in the Ainsa basin, which are dominated by thick-bedded sandstones (c.f. Ainsa I sandbody; see Section 6.4.4.1 for discussion). The high diversity trace-fossil assemblage of FA5c with relatively high numbers of pre-depositional trace fossils suggests that equilibrium communities were developed during periods dominated by low concentration turbidity currents. Many shallow-tier burrows formed in the equilibrium community had a high preservation potential due to the dominance of low concentration turbidity currents characterised by low amounts of erosion. This is due to the fact that the majority of open burrow networks were formed only several millimetres below the sediment/water interface, and these burrows were preserved by shock erosion as casts on the soles of turbidite sandstones only when the net erosion associated with the turbidity currents did not exceed the depth of the burrows. In contrast, the thick-bedded sandstones of FA3a are dominated by traces formed by robust, deeply burrowing organisms (e.g., *Ophiomorpha*). Many smaller organisms were probably unable to escape burial by the thick-bedded sands and the coarse grain size may have prevented the preservation of the activities of smaller metazoans. The depositing high concentration turbidity currents were also highly erosive, meaning that shallow-tier burrows were not preserved.

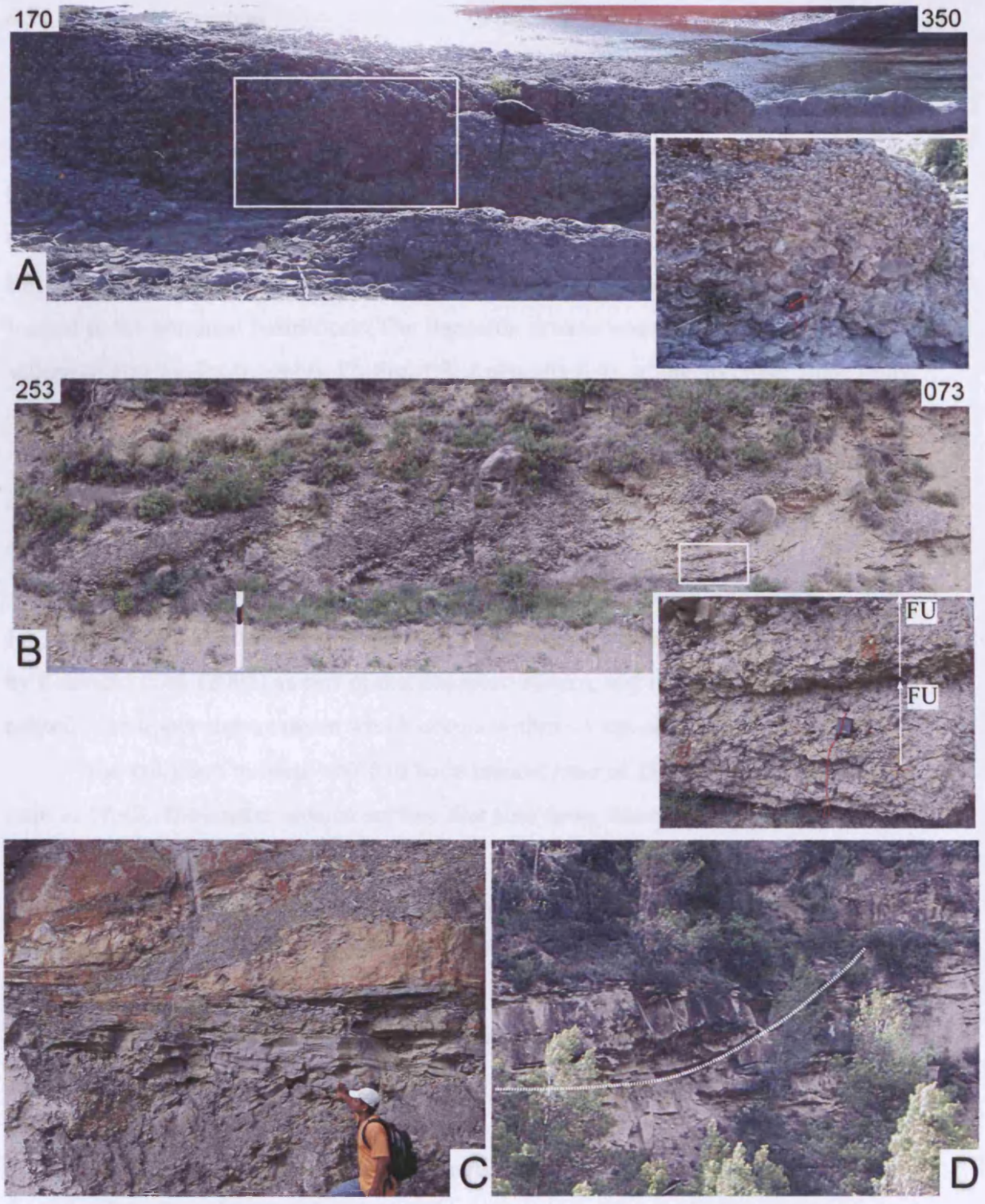

Fig. 6.3. Gerbe I sandbody A) Pebbly macroform element 'A' (FA2b). Inclined surfaces dip to the left (south). Rucksack for scale. Close-up image shows the imbricated pebbles aligned with the dipping surfaces, compass for scale; B) Pebbly macroform element 'B'. Inclined surfaces dip to the left (WSW). Road marker is 1 m high. Close-up image shows individual fining-up sequences, compass for scale; (C) Mud-draped scour; (D) steep erosive margin of channel element, height of cliff section is ~15 m.

6.3. Banastón system

The Banastón system comprises lower-slope erosional channels and proximal basin-floor submarine channel systems. It consists of 6 sandbodies, which can be traced from the lower slope to proximal basin-floor (Bayliss & Pickering, *in prep.* 2008). Only two outcrops were studied in detail, the overbank of the Banastón II sandbody (Locality 13, Fig. 1.3) and the channel off-axis of the Banastón III sandbody (locality 14, Fig. 1.3) located in the proximal basin-floor. The Banastón system was also studied near the village of Formigales (Locality 12, Fig. 1.3; Appendix 6.4), where an upper slope gully is preserved in the delta front sandstones.

6.3.1. Upper slope gully

6.3.1.1. Sedimentology

The upper slope gully outcrops near the village of Formigales (locality 12, Fig. 1.3; Appendix 6.4) and cuts into delta front sandstones. This feature has been mapped by Remacha *et al.* (2003) as part of the Banaston system, and is possibly genetically related to an upper slope canyon which occurs within ~1 km of the gully.

The gully is 5 m deep, ~67.5 m wide (aspect ratio of 13.5) and has a sand:mud ratio of 58:42. The master erosion surface that cuts down into the delta front sandstones is multi-storey (Fig. 6.4). The gully fill is very similar to that of the delta front sandstones, and is associated with laterally discontinuous, concave-up, nummulites-rich bioclastic sandstones (FA7b). A number of small normal faults cut these deposits. The delta front sandstones are laterally continuous and nummulites-rich. The sandstones are intensely deformed by normal faulting with minor displacement of up to several metres.

6.3.1.2. Ichnology

Both the gully fill and delta front sandstones are characterised by a low intensity, low diversity trace-fossil assemblage dominated by vertically orientated, post-depositional trace fossils. The gully fill is characterised by mean bioturbation on bedding planes of 4.1%, with 4 ichnospecies from 4 ichnogenera recognised, which are all post-depositional. The trace-fossil assemblage is dominated by *domichnia* and *fodinichnia*, including nummulites-lined burrows (*domichnia*) and *Thalassinoides* (*fodinichnia*).

The delta front sandstones have a mean bioturbation of 10.5% with 4 ichnospecies from 4 ichnogenera recognised, which are entirely post-depositional. Similarly to the gully fill, the trace-fossil assemblage is dominated by *domichnia* and *fodinichnia*, including: *Ophiomorpha* and *Skolithos* (*domichnia*); and *Thalassinoides* (*fodinichnia*). Nummulites-lined burrows, which occur in the gully fill, are absent from the delta front sandstones.

In both sections, the base of the sandstone beds are not characterised by semi-relief casts like in turbidite sandstones, due to the nature of the depositional processes involved. The trace-fossil assemblage of both sections is characteristic of the *Skolithos* ichnofacies.

6.3.1.3. Interpretation

The upper slope gully is an erosional feature characterised by a number of phases of incision, bypass and backfill. The sandy fill of the gully is the same as the surrounding delta front sandstones and was deposited during the backfilling phase of the gully. The low intensity, low diversity trace-fossil assemblages in both sections is typical of the *Skolithos* ichnofacies and is indicative of a moderate to high energy depositional environment (Frey & Pemberton 1985, Pemberton *et al.* 2001) in which only deep, and rarely middle tiers are preserved (Bromley 1996). The abundance of vertically orientated trace fossils is characteristic of suspension feeders, which seeked security by burrowing deeply and remaining stationary for long periods of time (Bromley 1996, Pemberton *et al.* 2001). The higher bioturbation intensity in the delta front sandstones is probably related to more stable, lower energy conditions than the gully, which enabled organism communities to become established, and also resulted in the increased preservation potential of burrows.

6.3.2. Channel off-axis

6.3.2.1. Sedimentology

The channel off-axis of Banastón III was studied on a path near the village of San Vicente (Locality 14, Fig. 1.3; Appendix 6.5). The base of Banaston III is not exposed in the section, however, laterally towards the axis of the sandbody, the base is expressed by a number of thick Type II MTCs and associated medium- to thick-bedded sandstones.

The channel off-axis of Banaston III is characterised by a number of fining-upward sequences, with medium- to thick-bedded sandstones at the base (FA3d), overlain by thin- to medium-bedded sandstones (FA5c) and very-thin-bedded sandstones, siltstones and mudstones (FA6a) at the top. These sequences range between 5-9 m thick, and average 6.9 m. The sandstones of FA3d are commonly amalgamated, forming amalgamated units up to 120 cm thick. Pinch-and-swell geometries are common, and the sandstones are typically normally graded and planar stratified. The thin- to medium-bedded sandstones of FA5c are typically non erosive, and characterised by well-developed planar stratification. These fining-upward sequences may represent individual channel elements. The entire section displays an overall fining- and thinning-upward sequence, with the top 4 m associated with very-thin-bedded sandstones, siltstones and mudstones of FA6a.

Throughout the section, MTCs are rare, with only one occurring, which forms the base of a fining-up channel element. This MTC has an erosive base and irregular top. The base is characterised by a mud-rich matrix with intra-formational sand rafts derived from the underlying bed. The top comprises folded, attenuated, and partially disaggregated sands in a sandy to muddy matrix. This is probably associated with a single thick sandstone bed that has been locally incorporated into the MTC. This MTC is typical of FA1c (Type Ib MTC).

6.3.2.2. Ichnology

The channel off-axis of the Banastón III sandbody is characterised by a relatively high diversity and intensity trace-fossil assemblage. Mean bioturbation on bedding planes is 29% with 19 ichnospecies from 15 ichnogenera identified, including 9 pre-depositional and 10 post-depositional trace fossils, as well as 6 graphoglyptids. The trace-fossil assemblage is dominated by *fodinichnia, domichnia* and *agrichnia.* The most common ichnotaxa include *Planolites, Thalassinoides* and *Phycosiphon* (*fodinichnia*); *Ophiomorpha* (*domichnia*); and *Paleodictyon* (*agrichnia*). The trace-fossil assemblage is characteristic of a mixed *Paleodictyon-Ophiomorpha rudis* subichnofacies of the *Nereites* ichnofacies.

The sandstones of FA3d are characterised by the lowest diversity and intensity trace-fossil assemblage, with an average bioturbation of 26%, with four ichnospecies identified, all of which are post-depositional. In contrast, FA5c thin- to medium-bedded, fine- to medium-grained sandstones are characterised by the highest diversity and

intensity trace-fossil assemblage, with an average bioturbation of 30.5% and 16 ichnospecies identified. Of these 16 ichnospecies, four are pre-depositional, including two graphoglyptids. FA6a very-thin-bedded sandstones, siltstones and mudstones have an average bioturbation of 27% and diversity of 7, of which 3 are pre-depositional, which are all graphoglyptids. In vertical section, the mudstones associated with FA6a are heavily bioturbated, with an average bioturbation of 86%, and an ichnofabric index of 3/6.

6.3.2.3. Interpretation

The channel off-axis comprises a number of fining- and thinning-upward sequences representing individual channel elements. The intensely bioturbated thin-bedded sandstones, siltstones and mudstones of FA6a which mark the abandonment phase towards the top of individual channel elements, suggests that sedimentation rates were low enough to allow organisms to totally bioturbate the newly deposited sediments. Similar bioturbation intensities in thin-bedded siltstones and mudstones (FA6a) of the abandonment phase have been observed in the channel margin of the Morillo system (Section 6.5.2.2). These FA6a deposits also form a thick interval at the top of the section interpreted as indicating a marked reduction in sediment supply to the active fan, and fan abandonment.

The high frequency of FA5 and FA6 deposits in the channel off-axis has greatly influenced the overall trace-fossil assemblage (c.f. channel axis of the Gerbe and Ainsa systems, Section 6.4.1.4). These deposits are characterised by a moderately high diversity and intensity trace-fossil assemblage, which is reflected in the overall trace-fossil assemblage of the section. In general, they were deposited by low concentration turbidity currents which were less erosive than those associated with the thick-bedded sandstones of FA3. This enabled the preferential preservation of shallow tier burrows, including many graphoglyptids. Thus, the trace-fossil assemblages of FA5c and FA6a are typified by a high number of pre-depositional trace fossils whilst the trace-fossil assemblage of the FA3d thick-bedded sandstones is characterised by a low proportion of shallow tier pre-depositional trace fossils because of their low preservation potential. The high frequency of thin- to medium-bedded sandstones of FA5c and FA6a may also have enabled many more organisms to escape burial from the newly deposited sediments compared to thicker sandstones of FA3d. The high variation in grain-sizes

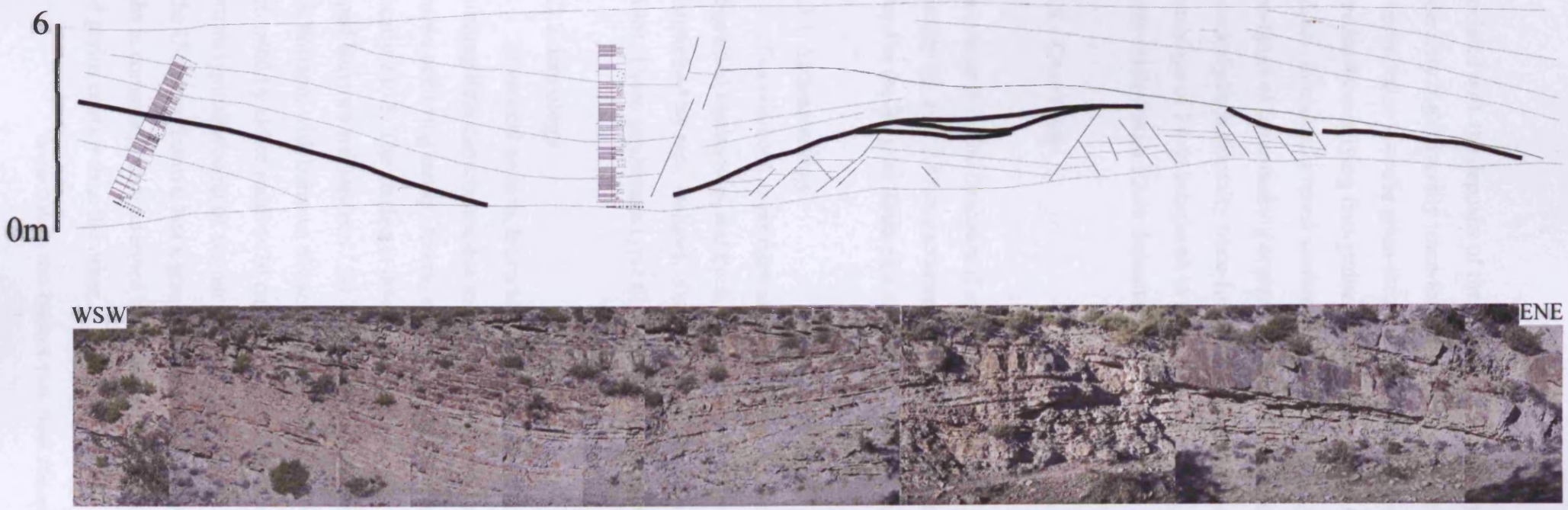

Fig. 6.4. Photomontage, field sketch and detailed bed-by-bed graphic sedimentary logs of upper slope gully and delta front sandstones, Formigales.

associated with the deposits of the channel off-axis may also have influenced the moderately high diversity trace-fossil assemblage due to the fact that many trace fossils are restricted to specific grain-sizes. For example, *Phycosiphon* typically occurs in silts immediately overlying fine-grained sandstones, whilst *Ophiomorpha* tends to occur in medium- to coarse-grained sandstones. Thus the large grain size variation enabled a wide-range of trace-making organisms to colonise the channel off-axis, resulting in the moderately high diversity trace-fossil assemblage. The reduced diversity trace-fossil assemblage of FA6a compared to FA5c may be related to the low number of bedding planes studied from FA6a deposits.

6.3.3. Overbank

The overbank of the Banastón II sandbody was studied at a small ~6 m thick horizon (Locality 13, Fig. 1.3) characterised by an abundance of *Arenicolites*. This section is located in the Bco. os Biñés east of the village San Vicente.

6.3.3.1. Sedimentology

The overbank comprises laterally continuous, tabular, thin-bedded, very-fine to fine-grained sandstones, and thick siltstones and mudstones of FA6c. It is also characterised by rare, isolated, coarse-grained, laterally discontinuous sandstones (FA4b). These sandstones typically have scoured erosive bases and sharp rippled tops.

6.3.3.2. Ichnology

In vertical section, bioturbation is low, with parallel laminated siltstones exhibiting little disturbance due to bioturbation, with only *Planolites* and *Thalassinoides* burrows occurring rarely. Average bioturbation is 10%, and the ichnofabric index is typically 2 to 3. The section is dominated by vertically orientated *Arenicolites*. These U-shaped burrows are between 15-170 cm deep and pervasively dominate a six metre thick horizon, with burrows occurring at intervals every 10 cm. Particular horizons are dominated by either small (<30 cm long) or large burrows (>30 cm long), with the burrows typically being of similar lengths at particular horizons. In most cases, one limb of the U-shaped burrow has a greater diameter than the other, and also the fill of the limbs is commonly characterised by different grain-sizes, with one limb in-filled with sand grains coarser than the other.

6.3.3.3. Interpretation

The section studied probably represents the very distal part of the overbank, characterised by low-concentration turbidity current deposits. The lens-shaped coarse-grained sands may represent channel-spillover sands deposited from high concentration turbidity currents. The occurrence of *Arenicolites*, which is more commonly associated with shallow marine settings (Ekdale & Lewis 1991, Pervesler & Uchman, 2004), is of particular interest in this section. In the Gerbe I sandbody (Section 6.2.2), *Arenicolites* was observed in great abundance, particularly towards the base of individual channel elements and was regarded as being typical of high energy environments. However, *Arenicolites* has also been observed in environments characterised by low concentration turbidity current deposits which were probably relatively stable environments, such as the proximal interfan underlying the Gerbe I sandbody, the proximal interfan of the Ainsa I sandbody (Section 6.4.5.2) and here, in the overbank of Banastón II. This suggests that *Arenicolites* is not restricted to high energy, channelised environments in the deep-marine realm. Instead, it is probably characteristic of environments which are associated with a relatively constant supply of nutrient-rich bottom currents. This is due to the fact that *Arenicolites* is interpreted as a dwelling and feeding burrow (*domichnia*) of suspension-feeding annelids or small crustaceans (Ekdale & Lewis 1991, Pervesler & Uchman, 2004).

6.4. Ainsa system

The Ainsa turbidite system has been referred to as lower-slope channels or basin-floor fans (for discussion see Pickering & Corregidor, 2005a, b). The turbidite system consists of three sandbodies (Ainsa I, II and III) of which only Ainsa I and II were studied in detail. The Ainsa I and II sandbodies are characterised by a number of vertically and laterally offset stacked channel elements forming a number of channel complexes. The Ainsa I sandbody is ~44 m thick, whilst the Ainsa II sandbody is ~75 m thick, and overlies ~80 m of MTCs, mudstones and thin-bedded sandstones and siltstones which represent the intrafan. The Ainsa system has also been studied in detail in the subsurface (see Chapters 9 and 10).

6.4.1. Channel axis

The channel axis was studied in the Ainsa I sandbody at two localities, in the quarry ~1 km south of Ainsa (Fig. 6.5) (Locality 15, Fig. 1.3; Appendix 6.7), and in the Bco. Fuen d'a Melonera, west of Labuerda (Locality 19, Fig. 1.3; Appendix 6.6), where it forms a poorly exposed cliff. The Ainsa quarry section has been studied extensively by a number of authors including Mutti and Normark (1987), Schuppers (1995), Clark and Pickering (1996), Pickering and Corregidor (2000), and Falivene *et al.* (2006a, b).

6.4.1.1. Sedimentology

The base of the Bco. Fuen d'a Melonera section is associated with a ~10 m thick muddy Type II MTC (FA1b). This is overlain by a sandy succession ~15 m thick which comprises thick-bedded, coarse-grained amalgamated sandstones at the base (FA3a) which form an amalgamated unit 11 m thick. These sandstones have erosive bases with incorporated mud clasts. The top of the section is characterised by FA5c thin- to medium-bedded sandstones and thin interbedded siltstone and mudstone laminae (Facies D2.3) to form a fining- and thinning-upward sequence. These sandstones are punctuated by a thin (35 cm thick) Type II pebbly MTC. Extra-formational organic matter is common in all the sandstones.

At the quarry section, the base is defined by a ~12 m thick Type II MTC (FA1b). This is poorly exposed at outcrop, but clear in core (see Section 8.4.3). This MTC is punctuated by thick-bedded conglomerates and coarse-grained sandstones. Individual MTCs typically have a sand-rich mudstone matrix with abundant pebbles at the base, and an upper mud-rich layer. Extra-formational pebbles with abundant molluscan borings occur throughout. The irregular upper surface of the MTC is onlapped by thin-bedded laterally discontinuous sandstones (FA5c) interpreted as a small levee-overbank system. These sandstones tend to have current ripples, and interbedded mudstones are thin. Bedding may be indistinct due to the lack of mudstone partings and flaser bedding may occur. The main sandy succession of the section is ~25 m thick and consists essentially of FA3a, FA3b and FA5c sandstones.

The basal ~5 m of the sandy succession is characterised by thick-bedded, irregular, erosive and laterally discontinuous sandstones (FA3a). These are characterised by abundant angular mud-clasts, commonly forming mud-flake breccias. Interbedded mudstones are thin and poorly preserved, and are typically pervasively

bioturbated. The sandstones are overlain by a ~12 m thick unit characterised by more sheet-like, laterally continuous, tabular, sandstones (FA3b). Within this unit are a number of broad, shallow erosion surfaces, which mark the base of weekly confined channel elements, which appear to be compensationally stacked. Towards the top of the section, thin- to medium-bedded sandstones occur (FA5c) forming a thinning-and-fining-upward sequence. The top of the sandbody is truncated by erosive (several metres to tens of metres), pebbly Type II MTCs.

Fig. 6.5. Ainsa I sandbody, Ainsa Quarry. Height of sandstone cliff ~35 m.

6.4.1.2. Ichnology

The axis of the Ainsa I sandbody is characterised by a low diversity, moderately high intensity, dominantly post-depositional trace-fossil assemblage. In the Bco. Fuen d'a Melonera section, mean bioturbation on bedding planes is 34.7%. The trace-fossil assemblage is comprised entirely of post-depositional trace fossils, with 6 ichnospecies from 3 ichnogenera. Vertically orientated *Ophiomorpha* isp. are particularly abundant in the thick amalgamated sandstones of FA3a towards the base of the sandy succession. These burrows have characteristic knobbly walls, are orientated vertical, oblique and horizontal to bedding and comprise essentially of shafts (Appendix 3.6C and 3.6D) (cf. Frey *et al.* 1978). The burrows range between 6-18 mm in diameter and the most deeply penetrating may pass through several beds and are over 1 m deep. The trace-fossil assemblage of the channel axis in the Ainsa Quarry is very similar, with an average bioturbation intensity of 38.6%. The trace-fossil assemblage consists of 8 ichnospecies from 5 ichnogenera, of which 7 are post-depositional. Like in the Bco. Fuen d'a Melonera section, vertically orientated *Ophiomorpha* isp. are abundant, particularly in thick-bedded sandstones of FA3a and FA3b. The trace-fossil assemblage of both

sections is dominated by *pascichnia*, *fodinichnia* and *domichnia*. The most common ichnotaxa include *pascichnia* (e.g. *Halopoa* and *Scolicia*), *fodinichnia* (e.g. *Thalassinoides*) and *domichnia* (e.g. *Ophiomorpha*). The trace-fossil assemblage is typical of the *Ophiomorpha rudis* subichnofacies of the *Nereites* ichnofacies.

6.4.1.3. Interpretation

The Ainsa I sandbody can be classified as a mixed erosional/depositional type channel system (*sensu* Mutti & Normark 1987). In the quarry section, basal conglomerates and Type II MTCs represent the initial erosional phase whilst the weekly confined channel elements mark the depositional phase and backfilling of the channel. The Type II MTCs with pebble-rich bases may have formed from deposition by multiphase granular flows (*sensu* Pickering & Corregidor, 2005a, b). The Ainsa I sandbody at the Bco. Fuen d'a Melonera is essentially a depositional type channel (*sensu* Mutti & Normark 1987). The Ainsa I sandbody can be defined as a channel complex set, with a basal MTC and upper axial dominated channel complex.

The low diversity, moderately high intensity, dominantly post-depositional trace-fossil assemblage of the channel axis occurs due to a number of factors; in this environment, the high concentration gravity flows tend to remove the fertile top layer of the seafloor, resulting in the preservation of only the deepest-tier trace fossils. As a consequence, shallow-tier pre-depositional trace fossils are rare, with graphoglyptids absent. In many cases, the muddy seafloor was totally eroded by high concentration turbidity currents resulting in the amalgamation of sands. As a consequence, only the burrows of deeply burrowing endobenthic organisms were preserved (e.g., *Ophiomorpha*). Due to this, the channel axis is dominated by endobenthic ichnotaxa such as *Halopoa* and *Scolicia* (*pascichnia*); and *Ophiomorpha* (*domichnia*), formed by large, robust, deeply burrowing organisms which were well adapted to surviving burial by newly deposited thick sands (Wetzel & Uchman, 2001). They may also have contributed to the low diversity trace-fossil assemblage by destroying any small burrows due to a bulldozing effect by the organisms (*sensu* Thayer 1979) in which relatively large burrowers prevented or reduced colonisation of the substrate by immobile suspension-feeders (Uchman 1999). The bulldozing effect of organisms such as those which formed *Scolicia* is clearest in core, where relict textures between the areas dominated by *Scolicia* reveal an older part of the ichnofabric dominated by smaller burrows (e.g., *Scolicia* Ichnofabric, Section 8.3.9). However, these large traces

are generally overprinted by later, smaller ichnotaxa and therefore do not totally inhibit the formation of small burrows (e.g., *Scolicia*-diverse-2 Ichnofabric, Section 8.3.11).

The high frequency of erosive gravity current flows associated with the channel axis may have inhibited colonisation by many organisms, except for those, which burrowed deeply into the newly deposited sediments. The duration of periods of quiescence between gravity current flows may also have been insufficient for colonisers to migrate from areas unaffected by the gravity currents resulting in the low diversity trace-fossil assemblage. The coarse-grained nature of the deposits in the proximal axial environments may also have excluded burrowers adapted only to fine-grained sediments (Tchoumatchenco & Uchman 1999) and may have inhibited the preservation of traces formed by smaller metazoans.

The low diversity trace-fossil assemblage dominated by a high abundance of individual ichnotaxa is indicative of an opportunistic colonising strategy of the sea floor, related to the pioneer stage during colonisation of newly deposited sediments (Uchman 1995a, Bromley 1996). The abundance of *domichnia* as well as the moderately high intensity bioturbation, abundance of deep burrows (e.g., *O. annulata, H. imbricata*) and endostratal *pascichnia* such as *Halopoa*, which did not maintain open connections to the seafloor, indicates that the channel axis environment was well-oxygenated. The abundance of organic matter in the sandstones, as well as the moderately high intensity bioturbation indicates that the channel axis was also characterised by a relatively high nutrient supply. This is probably related to the high frequency of sediment gravity currents associated with the channel axis, which may have incorporated or derived from organic rich slope or outer shelf sediments (Wilson *et al.* 1985) or been linked to direct river input, as indicated by the abundance of terrestrial organic material, including fossilised fern and wood fragments. This high frequency of sediment gravity currents may also have increased oxygen levels in the deep-marine environment by being transported through shallow oxygenated water (e.g., Wilson *et al.* 1985, Orr 1995, Buatois *et al.* 2001, Wetzel & Uchman, 2001). Due to this combination of high nutrient and oxygen levels, it is possible that preservation of organic matter at shallow levels was poor due to oxidation of the organic matter (e.g., Moodley *et al.* 2006).

After deposition of an oxygen rich turbidite sandstone, the lower part of the turbidite becomes oxygen deficient because oxygen consumption exceeds oxygen replacement by diffusion from the bottom water (Wilson *et al.* 1985). Trace-forming

organisms, which did not maintain open connections to the sea-floor, such as Halopoa, exploited, buried organic matter at the base of the turbidites in oxygenated conditions. These organisms therefore colonised the organic rich sediments in oxygenated sediments before both organic matter degradation took place and the redox boundary shifted up. After subsequent turbidite deposition, there was an upward shift of the redox boundary within the sediments (Rutgers van der Loeff 1990), and thus organic matter was preserved below the new turbidite. As a consequence, in oxygenated environments such as proximal axial environments, the trace-fossil assemblage is dominated by deep burrow networks formed by organisms which maintained open connection to the seafloor (e.g., *Ophiomorpha*) and exploited deeply buried organic rich layers.

6.4.1.4. The trace-fossil assemblages of the Ainsa I sandbody (Bco. Fuen d'a Melonera) and the Gerbe I sandbody: discussion

The trace-fossil assemblage of the Ainsa I sandbody at the Bco. Fuen d'a Melonera differs greatly to that of the Gerbe I sandbody (cf. Section 6.2.2.2 and 6.4.1.2). The Ainsa I sandbody at Bco. Fuen d'a Melonera is a depositional type channel (*sensu* Mutti & Normark 1987) comprising thick amalgamated sandstones (FA3a and FA5c) whilst the Gerbe I sandbody is a mixed erosional/depositional type channel system and is highly heterogeneous (Section 6.3.2.3). Due to the abundance of thin- to medium-bedded sandstones (FA5c) in Gerbe I, which were deposited principally by low concentration turbidity currents, interbedded mudstones are generally well preserved. In contrast, the thick-bedded sandstones which characterise the Ainsa I sandbody at Bco. Fuen d'a Melonera were in general deposited by erosive, high concentration turbidity currents, resulting in the poor preservation of interbedded mudstones. These fundamental sedimentological differences greatly influenced the trace-fossil assemblages of the two sections.

The moderately high intensity, low diversity, dominantly opportunistic trace-fossil assemblage of Ainsa I is related to the poor preservation potential of pre-depositional trace fossils and the high-stress environment associated with the channel system (see above for discussion). In contrast, the Gerbe I sandbody is characterised by a relatively high diversity, moderately low intensity trace-fossil assemblage including a number of pre-depositional trace fossils, and graphoglyptids (see Section 6.2.2.2). The trace-fossil assemblage of the thick-bedded sandstones (FA3a) is similar to that of Ainsa I, however, the thin- to medium-bedded sandstones which are common in the axis

of Gerbe I (FA5c) are characterised by a high diversity, moderate intensity trace-fossil assemblage more typical of proximal off-axis environments such as the channel margin (e.g., channel margin of the Morillo system, Section 6.5.2.2). The abundance of *Arenicolites* in the Gerbe I sandbody, particularly towards the base of individual channel elements, is indicative of the fact that the trace-making organisms were well adapted to such environments where there were high amounts of sediment bypass. In contrast, the dominant ichnotaxon in the Ainsa I sandbody, endichnial *Ophiomorpha* isp., was formed by trace-making organisms which exploited nutrient-rich horizons within the sediments and were able to survive burial from newly deposited turbidite sandstones because they formed deep burrow networks within the sandstones (see Section 6.4.1.3).

The contrasting trace-fossil assemblages of the Gerbe I and Ainsa I sandbodies clearly illustrates the close relationship between sedimentology and ichnology, and how important it is for both disciplines to be fully understood when utilising trace fossils as tools in palaeoenvironmental analysis.

6.4.2. Channel off-axis

The channel off-axis of the Ainsa I sandbody is exposed immediately north of the Ainsa quarry (Locality 16, Fig. 1.3; Appendix 6.8), ~400 m off axis. Only part of the channel-fill is exposed in the section, from the middle to the top of the sandbody, in a 10 m thick section.

6.4.2.1. Sedimentology

The channel off-axis is characterised by thin- to thick-bedded sandstones of FA3d and FA5c. The fine- to medium-bedded sandstones of FA5c occur at the base of the section and typically have sharp bases and tops, with occasional current ripples and are rarely amalgamated. Planar stratification is well-developed in many beds as well as cross-stratification and extra-formational organic matter is common. The thick-bedded sandstones of FA3d occur towards the top of the section forming amalgamated units up to 1.75 m thick. The base of the sandstones is typically erosive, and flutes and grooves are well-developed indicating a flow direction of 320°. Organic matter occurs in abundance near the top of many sandstones, and intra-formational mud-clasts are common, particularly along amalgamation horizons. Fining- or thickening-upward

sequences are not developed, however, this may be due to the incomplete nature of the section. Thin (tens of centimetres thick) Type II MTCs characterised by a sand-rich mudstone matrix, punctuate the sandy succession. Like in the quarry section (Section 6.4.1.1), the top of the sandbody is truncated by erosive (several metres to tens of metres), pebbly Type II MTCs (FA1b).

Approximately 400 m from the axis of the channel system, there is a distinct lateral thinning of the MTCs and sandstones and a decrease in the number of amalgamated sandstones. The beds are typically more tabular and laterally continuous than in the channel axis, and less erosive. Interbedded mudstones are thicker and there is a greater frequency of thin-bedded fine-grained sandstones (FA5c).

6.4.2.2. Ichnology

The channel off-axis is characterised by a low diversity and moderately low intensity trace-fossil assemblage. Mean bioturbation on bedding planes is 23.5% with 11 ichnospecies from 7 ichnogenera identified. Of these 11 ichnospecies, 9 are post-depositional and 2 are pre-depositional, both of which are graphoglyptids. The trace-fossil assemblage is dominated by *pascichnia, domichnia* and *agrichnia*. The most common ichnotaxa include: *Halopoa* and *Planolites* (*pascichnia*); *Thalassinoides* (*fodinichnia*); and *Ophiomorpha* (*domichnia*). The sandstones of FA3, like in the channel axis, are characterised by a low diversity trace-fossil assemblage dominated by vertical to sub-vertical *Ophiomorpha* isp. as well as *O. rudis*. The sandstones of FA3d have a lower average bioturbation (22%) than those of FA5c (29.5%). The trace-fossil assemblage associated with the thin-bedded sandstones, siltstones and mudstones of FA5c is also more diverse than the FA3d sandstones, and includes two graphoglyptids. The trace-fossil assemblage of the channel off-axis is typical of the *Ophiomorpha rudis* subichnofacies with some trace fossils more typical of the *Paleodictyon* subichnofacies of the *Nereites* ichnofacies.

6.4.2.3. Interpretation

The channel off-axis is characterised by a greater proportion of low concentration turbidity current deposits than the channel axis. Consequently, interbedded mudstones are thicker and more common, and the intensity and diversity of the trace-fossil assemblage is greater, partly as a result of an increase in the preservation potential of pre-depositional trace fossils.

The trace-fossil assemblage has several distinct differences to that of Banastón III (Section 6.3.2.2); both sections are characterised by similar bioturbation intensities, however, the channel off-axis of Ainsa I has a very low diversity trace-fossil assemblage with 81% of the ichnotaxa being post-depositional. In contrast, the trace-fossil assemblage of the Banastón III section is characterised by a moderate diversity trace-fossil assemblage, with only 52% of the ichnotaxa being post-depositional. This marked difference in the trace-fossil assemblages may be related to a number of factors including: (1) differences in environmental conditions such as oxygenation between the two systems; (2) the higher frequency of thin- to medium-bedded sandstones in Banastón III; and (3) the fact that a greater number of bedding planes were studied in the Banastón section (32 bedding planes) compared to the Ainsa section (22 bedding planes).

Although the Banastón system is the least documented in this thesis, the system has been extensively studied by the author. Field observations suggest that Banastón, along with Morillo, is the most similar turbidite system in terms of its ichnology, to the Ainsa system. Due to this, it is interpreted that environmental conditions such as oxygenation and nutrient supply were very similar. The greater diversity trace-fossil assemblage of Banastón III, characterised by a high abundance of pre-depositional trace fossils, is principally related to the higher frequency of thin- to medium-bedded, fine-grained sandstones (FA5c and FA6a). These sandstones form thinning-and-fining-upward sequences towards the top of individual channel elements, and also the abandonment phase (Section 6.3.2.1). In contrast, in the channel off-axis of Ainsa I, fining-upward sequences are less well-developed, and the top of the sandbody is truncated by an overlying MTC.

6.4.3. Channel margin

The channel margins of Ainsa I and II are both exposed in the Barranco Forcaz, ~2 km north of Ainsa (localities 17, Fig. 1.3; Appendix 6.9 and 20; Appendix 6.10, respectively). The margin of the Ainsa I sandbody is ~33 m thick and deformed by a SW trending thrust system towards its base. The northern margin of the Ainsa II sandbody is ~107 m thick.

6.4.3.1. Sedimentology

The channel margin of the Ainsa I sandbody comprises a lower and upper sandy packet 9 m and 11 m thick, respectively, and separated by an ~11 m thick muddy Type II MTC. Only the upper sandy packet was studied in detail, with the lower packet being intensely deformed by a SW directed thrust zone. The upper packet is dominated by thin- to medium-bedded sandstones of FA5b and very-thin-bedded sandstones, siltstones and mudstones of FA6a. Thick-bedded sandstones of facies association 3, which are common in more axial environments, are almost entirely absent from the section. Thinning- or thickening-upward sequences are not developed.

The base of the upper packet is characterised by concentrated nummulites beds (packstones) (FA7c). These are overlain by thin- to medium-bedded sandstones (FA5b), which dominate the section. These sandstones typically have parallel-sided flat bases and tops, with rare erosive bases, and may form amalgamated units <50 cm thick. Mud clasts are common along amalgamation surfaces and the sandstones tend to be internally structureless, with rarely developed cross stratification. Very-thin-bedded sandstones and siltstones (FA6a) are also common, and typically have current rippled tops, are internally structureless and may be intensely bioturbated. The upper packet is punctuated by a thin (35 cm thick), erosive, laterally discontinuous and highly localised muddy Type Ib MTC (FA1c). The margin of Ainsa I in the Bco. Forcaz is overlain by ~80 m of type Ia muddy MTCs punctuated by packets (<2 m thick) of thin-bedded sandstones.

The base of the Ainsa II sandbody is associated with moderately thick (< 10 m thick) muddy Type Ia MTCs (FA1a), which are punctuated by thin (<1.5 m) packets of concentrated nummulites beds (packstones) (FA7c) and thin-bedded fine-grained sandstones (FA5b). This basal MTC is overlain by a ~7 m thick sandy unit characterised by thin- to medium-bedded and more rarely thick-bedded sandstones (FA5b and FA3e respectively). These sandstones may be amalgamated forming units up to 1 m thick, and are tabular, with sharp flat bases and sharp tops which rarely display current ripples. Cross and planar stratification is typically well-developed and nummulites are common constituents. These sandstones are arranged into a crude coarsening- and thickening-upward sequence. This unit is overlain by a ~5 m thick erosive Type Ia MTC.

The main sandy unit is ~50 m thick and characterised by sandstones of FA5b, and more rarely, thick-bedded sandstones of FA3e and very-thin-bedded sandstones, siltstones and mudstones of FA6a. These are arranged into at least three thinning-and-

fining-upward sequences, that average 13.8 m in thickness. The base of the sequences may be defined by low-angle erosional scours and thick-bedded, rarely amalgamated sandstones (FA3e). These sandstones have sharp bases with common sole markings, and the tops are typically current rippled. Planar or cross stratification may be developed in some beds, whilst small extra-formational pebbles occur rarely at the base of the sandstones, as well as abundant mud-clasts. The most common deposits in the fining-upward sequences are thin- to medium-bedded sandstones of FA5b. These are characterised by sharp flat bases and current rippled tops and have well-developed internal stratification including planar and cross stratification. The top of the sequences may be characterised by very-thin-bedded sandstones, siltstones and mudstones of FA6a forming muddy intervals ~2-4 m thick. These fining-upward sequences are rarely punctuated by thin, sand-rich, intra-formational Type Ib MTCs (FA1c). These MTCs are typically erosive, laterally discontinuous and localised. The top of the section is characterised by ~8 m of fine-grained deposits of FA6a, and is overlain by intrafan siltstones and mudstones of FA6d.

6.4.3.2. Ichnology

The channel margins of Ainsa I and II are characterised by a moderate to high diversity, high intensity trace-fossil assemblage. In the margin of the Ainsa I sandbody, mean bioturbation on bedding planes is 44.8%, with 21 ichnospecies from 13 ichnogenera identified. Of these 21 ichnospecies, 11 are post-depositional and 10 are pre-depositional trace fossils, including 5 graphoglyptids. The margin of the Ainsa II sandbody is characterised by a higher diversity but similar intensity trace-fossil assemblage. Mean bioturbation on bedding planes is 43.6%, with 34 ichnospecies from 19 ichnogenera identified. Of these 34 ichnospecies, 18 are post-depositional, 16 are pre-depositional, including 9 graphoglyptids. Both trace-fossil assemblages are dominated by *pascichnia, fodinichnia, domichnia* and *agrichnia*. In Ainsa II, the most common ichnotaxa include: *Halopoa, Planolites, Scolicia* and *Helminthopsis* (*pascichnia*); *Thalassinoides* and *Lophoctenium* (*fodinichnia*); *Ophiomorpha* (*domichnia*); and *Paleodictyon* (*agrichnia*). The most common ichnotaxa in Ainsa I include: *Planolites, Nereites* and *Scolicia*; (*pascichnia*); *Thalassinoides* (*fodinichnia*); *Ophiomorpha* (*domichnia*); and *Helminthorhaphe* and *Paleodictyon* (*agrichnia*). The trace-fossil assemblage of the channel margins of Ainsa I and II are typical of a mixed *Paleodictyon-Ophiomorpha rudis* subichnofacies.

Like the channel axis and channel off-axis of the Ainsa I sandbody, the thick-bedded, coarse-grained sandstones of FA3e have a lower diversity and intensity trace-fossil assemblage than the thin- to medium-bedded sandstones of FA5b (Section 6.4.1.2 and 6.4.2.2). In the margin of the Ainsa II sandbody, mean bioturbation in FA3e sandstones is 37.3% with a diversity of 15. Of these 15 trace fossils, only 2 are pre-depositional, of which one is a graphoglyptid. The trace-fossil assemblage of these sandstones is typical of the *Ophiomorpha rudis* subichnofacies. FA5b sandstones have a mean bioturbation of 46% and a diversity of 31, including 10 pre-depositional trace fossils, of which 5 are graphoglyptids. These sandstones have a trace-fossil assemblage typical of the *Paleodictyon* subichnofacies with some trace fossils typical of the *Ophiomorpha rudis* subichnofacies. The very-thin-bedded sandstones, siltstones and mudstones of FA6a have a mean bioturbation of 51.7% and a diversity of 8. This low diversity assemblage may be in part a function of data collection due to the low number of FA6a deposits studied (8 beds, compared to 88 from FA5b sandstones).

6.4.3.3. Interpretation

The base of the Ainsa II sandbody characterised by subclass 1a MTCs and nummulites-rich beds (FA7c) marks the onset of sedimentation with the collapse of the slope and cleaning of the shelf. According to Pickering and Corregidor (2005a, b), the thick MTCs at the base of the section stacked to create seafloor relief of up to 35 m resulting in the onlap of the sandy turbidites of Ainsa II against this topography. The lower 9 m packet of coarsening-up sandstones represents deposition in a channel margin environment. The three fining- and thinning-upward sequences in the main body of sands may correlate with individual third-order channel elements in the cliff section to the south (Fig. 8.23). The localised intra-formational Type Ib MTCs (FA1c), which occur in both sections, were interpreted by Pickering and Corregidor (2005a, b) as being characteristic of off-axis channel environments associated with channel margin instability and localised sediment sliding.

The two sections differ greatly in terms of their sedimentological characteristics, with FA3e sandstones almost completely absent from the channel margin of the Ainsa I sandbody. This may be related to the proximity of the sections to the axis of the channels. It is interpreted that the channel margin section of Ainsa I was more off axis than the channel margin section studied in Ainsa II. This is supported by subsurface data (see Chapter 8).

The high diversity trace-fossil assemblage of the channel margin is related in part to the mixture of both FA3e and FA5b sandstones. These sandstones are characterised by different trace-fossil assemblages, with the FA3e sandstones dominated by trace fossils formed by large, robust trace-making organisms (e.g., *Scolicia* and *Ophiomorpha*). The higher diversity and intensity trace-fossil assemblages of FA5b sandstones, and to some extent, the fine-grained deposits of FA6a, are related to increased preservation potential and more stable environmental conditions. Equilibrium organism communities were established in the more stable conditions, resulting in diverse trace-fossil assemblages characterised by abundant pre-depositional trace fossils and graphoglyptids. The structures formed as a result of these equilibrium organism communities had a high preservation potential due to the dominance of low concentration turbidity currents.

Opportunistic colonising strategies are still common in the channel margin both in FA3e and FA5b sandstones, with some bedding planes dominated almost exclusively by endichnial *pascichnia* (e.g., *Halopoa, Scolicia*) and/or *fodinichnia* (e.g., *Lophoctenium*) to form high-intensity, low-diversity, opportunistic trace-fossil assemblages. The abundance of endostratal *pascichnia* such as *Halopoa*, formed by organisms, which did not maintain open connections to the seafloor, suggests that the channel margin was characterised by relatively high oxygenation levels in the interstitial waters, at least immediately after turbidite deposition.

6.4.4. Outermost channel to levee-overbank

The positive identification of ancient levees at outcrop is typically difficult. It is commonly the case that a spatial association between channels and overbank sediments can be recognised, but it is unclear as to their temporal associations, and whether overbank deposits in fact represent levees. In general, morphological evidence for ancient levees is also rarely preserved. In the Ainsa I sandbody, a thick well-developed levee-overbank system has been recognised in the subsurface (Pickering & Corregidor 2004, 2005a, b) (see Chapter 8). This levee-overbank system correlates with a section near the Barranco Forcaz (Locality 18, Fig. 1.3; Appendix 6.11) which is ~11 m thick and herein referred to as outermost channel to levee-overbank.

6.4.4.1. Sedimentology

The outermost channel to levee-overbank of the Ainsa I sandbody is characterised by deposits typical of FA1c, FA4a and FA5b. This section is dominated by thin-bedded, medium- to gravel-grade sandstones with well developed current ripples or starved mega-ripples (FA4a). Thin-bedded current-rippled sandstones (FA5b) occur with these sandstones and commonly form starved ripples or single-train rippled beds. No thickening- or thinning-upward sequences are developed. Two thin (<30 cm) Type Ib MTCs punctuate the sandstones, and comprise a sand-rich mudstone matrix with deformed sand rafts derived from underlying beds. These MTCs are laterally discontinuous and of local origin (FA1c). Mega-ripples and sole markings indicate a palaeoflow of 320°.

6.4.4.2. Ichnology

The outermost channel to levee-overbank of the Ainsa I sandbody is characterised by a low diversity, moderate intensity trace-fossil assemblage. Mean bioturbation on bedding planes is 31%, with 15 ichnospecies from 11 ichnogenera identified. Of these 15 ichnospecies, 10 are post-depositional and 5 are pre- depositional trace fossils, all of which are graphoglyptids. The trace-fossil assemblage is dominated by *pascichnia, fodinichnia, domichnia* and *agrichnia*. The most common ichnotaxa include *Halopoa* and *Planolites* (*pascichnia*); *Thalassinoides* and *Phycosiphon* (*fodinichnia*); *Ophiomorpha* (*domichnia*); and *Paleodictyon* (*agrichnia*). In vertical section within the interbedded mudstones, bioturbation is low (20%), with an ichnofabric index of 3. However, some mudstone intervals are completely bioturbated by *Scolicia* isp. The trace-fossil assemblage of the outermost channel to levee-overbank is typical of the *Paleodictyon* subichnofacies with some trace fossils more typical of the *Ophiomorpha rudis* subichnofacies.

6.4.4.3. Interpretation

The most distinctive feature of the section is the bed thickness and grain size of the sandstones. Thick-bedded sandstones typical of more axial environments are absent but the thin-bedded sandstones tend to be coarse-grained. Typically, levee-overbank deposits are characterised by fine- to medium-grained sandstones such as in the proximal levees recognised in the Pab Formation, Pakistan (Eschard *et al.* 2003). These sandstones may therefore represent spill-over or crevasse deposits similar to those

described in the upper Ross Formation (Lien *et al.* 2003). However, unlike the upper Ross Formation, palaeoflow is the same as in the channel axis (~320°). Extensive subsurface studies on the Ainsa I sandbody (e.g., Pickering & Corregidor 2004, 2005a, b; this study), suggest that it was characterised by a well-developed levee-overbank system. The occurrence of small MTCs formed from local sediment slides (FA1c), suggests that this section may be associated with localised slope instability. Due to the palaeoflow directions and the coarse-grained nature of the deposits, the depositional environment is interpreted tentatively as the channel margin/inner bank of the levee.

The moderately low intensity trace-fossil assemblage of the outermost channel to levee-overbank may be related to the coarse-grained, thin-bedded nature of the turbidite sandstones. The coarse-grained sands may have excluded burrowers adapted only to fine-grained sediments (Tchoumatchenco & Uchman 1999) and also hindered the preservation of the activities of small metazoans. The thin-bedded, coarse-grained sandstones were probably transported as a coarse bed-load beneath turbidity currents, with most of the finer-grained elements of the upper low concentration part of the turbidity current bypassing the area and deposited further down the system. These upper bypassing parts of the flow may have reworked the sands to form the starved mega-ripples. Despite the thin-bedded nature of the sandstones, the depositing turbidity-current flows may have been erosive, as indicated by the occurrence of angular mud-clasts within some of the sandstones. Consequently, the preservation potential of many shallow tier trace fossils may have been more similar to thick-bedded erosive sandstones of axial environments (e.g., FA3) rather than beds of a similar thickness in off-axis environments such as the channel margin.

6.4.5. Interfan

The interfan was studied between the Ainsa II sandbody and the base of the Morillo system between the Bco. o Solano and the Bco. Coda Sarten (Locality 21, Fig. 1.3; 6.12). The entire section has also been studied in the subsurface (Core A6) (Chapter 9). Consequently, the sedimentology and ichnology of the interfan is only briefly described, and the reader is referred to Chapter 9 for a more detailed description.

6.4.5.1. Sedimentology

The interfan comprises thick packets (tens of metres) of intensely bioturbated very-thin-bedded sandstones, siltstones, mudstones and biogenic mudstones (FA6d). Packets of heterolithics tens of metres thick, comprising current rippled thin-bedded sandstone-mudstone couplets (FA5d) are common. coarse-grained, thin-bedded, erosive, laterally discontinuous sandstones (FA4b) occur throughout the interfan as well as intra-formational muddy Type Ia MTCs, which range from several metres to 10s of metres in thickness.

6.4.5.2. Ichnology

The interfan is characterised by a moderately low diversity, very high intensity trace-fossil assemblage. Mean bioturbation on bedding planes is 54.5%, with 18 ichnospecies from 13 ichnogenera identified. Of these 18 ichnospecies, 14 are post-depositional and 4 are pre-depositional trace fossils, including 3 graphoglyptids. The trace-fossil assemblage is dominated by *pascichnia, fodinichnia, domichnia* and *agrichnia*. The most common ichnotaxa include *Planolites, Nereites* and *Scolicia* (*pascichnia*); *Thalassinoides* (*fodinichnia*); *Ophiomorpha* (*domichnia*); and *Chondrites* (*agrichnia*). The trace-fossil assemblage of the interfan is very mixed, with FA5d sandstones characterised by trace fossils typical of the *Paleodictyon* subichnofacies whilst others are more typical of the *Ophiomorpha rudis* subichnofacies. FA6d deposits are characterised by trace fossils typical of the *Nereites* subichnofacies (*sensu* Seilacher 1974), with an abundance of backfilled burrow systems formed by sediment feeders such as *Nereites, Phycosiphon* and *Scolicia.* In vertical section, bioturbation is very intense, with mudstones and siltstones intensely bioturbated and dominated by biodeformational structures, with an ichnofabric index typically of 2/6.

6.4.5.3. Interpretation

The interfan is characterised by the highest intensity trace-fossil assemblage in the Ainsa-Jaca basin. This is related to a number of factors; the totally bioturbated nature of many of the sediments suggests that the rate of biogenic reworking exceeded that of sedimentation (Bromley 1996). This may imply that sediment accumulation rates were lower than other, more axial environments in the Ainsa basin. The absence of thick-bedded sandstones may also have enabled many organisms to survive burial from the newly deposited sediments, which would have influenced the intensity of

bioturbation. The sediments of the interfan are also inferred to have had a high benthic food content. This is due to the high intensity of bioturbation and the abundance of biodeformational structures, and mobile deposit-feeders, including *bulldozer* traces (*sensu* Thayer 1979) such as *Scolicia*. These trace-fossils formed by mobile deposit-feeders have been inferred as being characteristic of high benthic food availability (Ekdale 1985, Uchman *et al.* 2004). A high benthic food content is also supported by the paucity of specialist feeding strategies typical of stable, but food-restricted settings (Ekdale 1985) such as many forms of graphoglyptids (e.g., *Paleodictyon*) and some *pascichnia* (e.g., *Nereites*), which covered a given surface in a systematic way (see Seilacher 1977, Miller 1991). The paucity of graphoglyptids and other shallow-tier trace fossils may also be related to their poor preservation potential, as a result of the abundance of biodeformational structures, as well as large *bulldozer* trace fossils.

The high bioturbation intensity of the mudstones in the interfan suggests that equilibrium organism communities became well established, as a result of long-term stable conditions between turbidite sand deposition (Uchman 1995a). However, opportunistic colonising strategies also occur in the interfan, and are common in FA5d sandstones. Newly deposited sandstones and siltstones are typically intensely bioturbated by low diversity trace-fossil assemblages, dominated by ichnotaxa such as *Phycosiphon* to form opportunistic trace-fossil assemblages.

Similar trace-fossil assemblages are observed in thin-bedded sandstones siltstones and mudstones (FA6) in the channel off axis of Banaston III , the channel margin of Ainsa II, and the slope of the Guaso system (sections 6.3.2.2, 6.4.3.2 and 6.6.1.2, respectively).

6.5. Morillo system

The Morillo system comprises three sandbodies interpreted as confined channel systems. The Morillo I sandbody was studied near the village of Morillo de tout (Locality 22, Fig. 1.3; Appendix 6.14) where the margin of the sandbody is exposed. Immediately to the north, the axis is exposed in a large cliff section. The Morillo II and III sandbodies are expressed as heterolithic packets in this part of the basin. Approximately 7 km to the northwest, in the Rio Sieste, all three sandbodies are exposed and stacked vertically (Locality 23, Fig. 1.3; Appendix 6.13).

The base of the Morillo system in the Rio Sieste is associated with a ~30 m thick Type II MTC. The MTCs is characterised by an abundance of pebbles and sand rafts, with pebble-rich scours and stringers commonly defining the base of individual MTCs. Laterally discontinuous irregular gravels and conglomerates punctuate these. The Morillo I sandbody is ~40 m thick and characterised by a number of fining- and thinning-upward channel elements and can be defined as a channel complex. The Morillo II and III sandbodies are ~50 m thick, vertically stacked, and comprise a complex heterogeneous fill formed by thick-bedded sandstones (FA3a), Type II MTCs (FA1b), and pebbly sandstones and conglomerates (FA2b). Palaeoflow is towards ~316° in the section.

6.5.1. Channel axis, Morillo II

6.5.1.1. Sedimentology

The channel axis of the Morillo II sandbody in the Rio Sieste (Locality 23, Fig. 1.3; Appendix 6.13) is dominated by FA1b, FA2b and FA3a. The base is associated with thick-bedded amalgamated sandstones (FA3a) which are erosively overlain by a 10-m-thick, Type II MTC. This MTC is characterised by abundant pebbles and sand rafts in a muddy matrix. Overlying the MTC is a ~5-m-thick unit of thin- to medium-bedded sandstones (FA5c). The base of the sandstones is sharp and commonly erosive, with the tops typically current rippled. Extra-formational organic matter and pebbles occur in some of the beds. Internal stratification is well developed with planar and cross stratification common. These deposits are erosively overlain by an amalgamated unit ~7 m thick comprising laterally discontinuous coarse-grained to pebbly sandstones and matrix-supported sandy conglomerates (FA3a). These deposits form a lens-shaped pebble-rich sandy macroform element (Fig. 6.6), which thins and pinches out at both margins, perpendicular to palaeoflow. The macroform element is 2 m thick and 8 m wide and is internally structureless. Laterally, it is onlapped by FA3a pebbly sandstones.

The top part of the sandbody is characterised by thick-bedded laterally discontinuous amalgamated sandstones with well-developed planar stratification (FA3a). This sandy succession is punctuated by erosive (to several metres), Type II MTCs with abundant pebbles and sand rafts in a muddy matrix. The base of the MTCs may be characterised by abundant sand rafts and pebbles forming a bipartite MTC. Towards the top of the sandbody, the MTCs and thick-bedded sandstones are characterised by increased amounts of pebble-grade material. Normally graded clast-

supported pebbly mudstones, as well as normally graded pebbly sandstones are common. The sandbody is overlain by a thick (tens of metres) Type II MTC.

6.5.1.2. Ichnology

The axis of Morillo II is characterised by a low diversity, low intensity trace-fossil assemblage. Mean bioturbation on bedding planes is 11%, with 9 ichnospecies from 7 ichnogenera identified, all of which are post-depositional. The trace-fossil assemblage is dominated by *pascichnia, fodinichnia,* and *domichnia.* The most common ichnotaxa include *Planolites* (*pascichnia*); *Thalassinoides* and *Zoophycos* (*fodinichnia*); and *Ophiomorpha* (*domichnia*). The trace-fossil assemblage is typical of the *Ophiomorpha rudis* subichnofacies of the *Nereites* ichnofacies. However, a small muddy horizon ~50 cm thick characterised by FA6a very-thin-bedded sandstones, siltstones and mudstones has a trace-fossil assemblage more typical of the *Zoophycos* ichnofacies. This horizon is interpreted as representing the abandonment phase of an individual channel-fill, and is dominated by *Zoophycos* isp., which pervasively bioturbates the horizon.

6.5.1.3. Interpretation

The Morillo II sandbody can be defined as a mixed erosional/depositional type channel complex. The highly heterogeneous fill characterised by rapid lateral changes in facies is in part related to the abundance of Type II MTCs which formed both the irregular topography upon which the sandstones were deposited, and also truncated many of the sandstones. These erosive deposits created significant topography, and may have contributed to the lateral confinement of the channelised sandbody. The pebble-rich sandy macroform element is interpreted as a barform, formed by flows, which reworked gravels on the seafloor (Fig. 6.6). Morillo II may therefore represent a confined braided channel system. The abundance of MTCs, truncated thick-bedded sandstones, pebble-rich deposits and barform indicates significant amounts of bypass and suggests that seafloor gradients were relatively high during deposition. The heterogeneous nature of the deposits and abundance of bypass facies, as well as the vertical stacking of the sandbodies in the Rio Sieste suggests the system may have been confined at this point.

Like many axial environments in the proximal Ainsa basin (e.g., Ainsa I sandbody, Section 6.4.1.2), this section is characterised by a high proportion of trace

fossils formed by deeply burrowing organisms (e.g., *Ophiomorpha*), and a low proportion of shallow-tier trace fossils such as graphoglyptids. This is related to the preservation potential of shallow-tier traces in axial environments (see Section 6.4.1.3 for discussion). However, the absence of pre-depositional trace-fossils on the soles of thin- to medium-bedded sandstones of FA5c, suggests that pre-depositional equilibrium trace-fossil communities were rarely developed. The low intensity trace-fossil assemblage suggests that there was a stress factor, which restricted bioturbation. It is possible this stress factor may have been reduced oxygen levels in the basin. The dominant ichnotaxon of the axis of the Morillo II sandbody, *Ophiomorpha*, was probably formed by opportunistic organisms, which colonised the newly deposited sands, possibly as doomed pioneers (*sensu* Föllmi & Grimm 1990). These organisms may have exploited organic rich horizons in the sands as a result of a temporary increase in oxygen levels transported in with the newly deposited turbidite sandstones (Wilson *et al.* 1985, Orr *et al.* 1996, Wetzel & Uchman 2001). The paucity of pre-depositional trace fossils preserved on the soles of both high concentration and low concentration turbidite sandstones may indicate that equilibrium trace fossil communities were not established due to low oxygen levels.

Fig. 6.6. Barform in Morillo II, Rio Sieste. Section is orientated approximately perpendicular to palaeoflow (315°).

6.5.2. Channel margin

6.5.2.1. Sedimentology

The southern margin of the Morillo I sandbody is exposed in the Bco. Cotón near Morillo de tout (Locality 22, Fig. 1.3; Appendix 6.14) and is 81 m thick. This section is characterised by three sandy units, with clearly developed fining-upward

sequences averaging 18 m in thickness and separated by several metres of thin-bedded sandstones and siltstones, and can be defined as a channel complex set.

The lower sandy unit is interpreted as a channel complex, the base of which is marked by a ~11 m thick Type 1a MTC, that is overlain by a 5-m-thick thickening-and-coarsening-upward sequence, to thin- to medium-bedded sandstones (FA5b) representing a channel margin element. The main sandy succession is ~10 m thick and is characterised by medium-bedded, commonly amalgamated sandstones at the base (FA3e), and thin- to medium-bedded sandstones (FA5b) at the top to form an overall thinning- and fining-upward sequence. Current ripples are common, and the medium-bedded sandstones (FA3e) typically have erosive bases with sole markings. The sandstones tend to have well-developed internal stratification, including planar stratification, and organic matter is common. These sandstones are punctuated by two thin (<35 cm), muddy, intra-formational MTCs. This sandy succession is overlain by ~6 m of thin-bedded sandstones (FA5b) and very-thin-bedded sandstones, siltstones and mudstones (FA6a).

The middle sandy unit comprises two semi-amalgamated, fining-upward channel margin elements (10 m and 11 m thick, respectively) and is interpreted as a margin dominated channel complex. The base of the unit is marked by ~3 m of laterally discontinuous medium- to thick-bedded sandstones (FA3a) which onlap a basal erosion surface. These sandstones are typically amalgamated, have erosive bases, and abundant mud-clasts at amalgamation surfaces. They are overlain by ~7 m of thin- to medium-bedded sandstones (FA5b) with well-developed planar and cross-stratification forming a fining-upward sequence. This sequence is truncated by an irregular erosion surface, with up to 5 m of cut-down. The basal deposits which infill this erosion surface comprise ~2 m of laterally discontinuous medium- to thick-bedded sandstones (FA3a) which are overlain by more laterally continuous medium- to thick-bedded sandstones (FA3e). These deposits are characterised by abundant extra-formational shells, nummulites and organic matter. The top part of the sequence is associated with two Type II MTCs overlain by very-thin-bedded sandstones, siltstones and mudstones (FA6a). These MTCs are characterised by a sand-rich mudstone matrix with abundant shell fragments, nummulites and sand clasts. The base of the upper MTC is formed of disaggregated sand rafts overlain by a mud-rich interval, forming a bipartite deposit.

The upper sandy unit is ~20 m thick and is interpreted as a channel margin element characterised by basal thick-bedded sandstones (FA3e). These sandstones are

rarely amalgamated, have flat bases with well developed sole markings, and current rippled tops. Internal stratification is common, including planar and wavy stratification, and organic matter typically occurs towards the top of the beds. These sandstones are overlain by thin- to medium-bedded sandstones forming a fining-upward sequence.

6.5.2.2. Ichnology

The channel margin is characterised by a moderate diversity, high intensity trace-fossil assemblage. Mean bioturbation on bedding planes is 42.7%, with 25 ichnospecies from 16 ichnogenera identified. Of these 25 ichnospecies, 15 are post-depositional and 10 are pre-depositional, including 7 graphoglyptids. The trace-fossil assemblage is dominated by *pascichnia, fodinichnia* and *domichnia*. The most common ichnotaxa include *Halopoa, Planolites, Gordia* and *Helminthopsis* (*pascichnia*); *Thalassinoides* (*fodinichnia*); *Ophiomorpha* (*domichnia*); and *Paleodictyon* (*agrichnia*). In vertical section, mudstones are moderately to intensely bioturbated. The mudstones within the sandy units have an average bioturbation of 25% and an ichnofabric index of 3. In contrast, the mudstones between the sandy units (FA6a) are intensely bioturbated (between 60-100%), with an ichnofabric index of between 5-2/6.

The thick-bedded sandstones of FA3a and FA3e have a mean bioturbation of 29% with 7 trace fossils identified, which are entirely post-depositional. These deposits are dominated by *fodinichnia* and *domichnia*, with a trace-fossil assemblage typical of the *Ophiomorpha rudis* subichnofacies. The thin- to medium-bedded sandstones of FA5b have a higher diversity and intensity trace-fossil assemblage with an average bioturbation of 46% and a diversity of 21. Of these, 11 are post-depositional and 10 are pre-depositional, including 7 graphoglyptids. The trace-fossil assemblage is characterised by abundant *pascichnia*, *fodinichnia* and *domichnia* and is typical of the *Paleodictyon* subichnofacies, with some trace fossils more typical of the *Ophiomorpha rudis* subichnofacies. The very-fine-grained sandstones, siltstones and mudstones (FA6a) are characterised by a high intensity, low diversity trace-fossil assemblage. Average bioturbation is 44.2% and 9 trace fossils were identified, of which only two are pre-depositional. The trace-fossil assemblage is very mixed, with trace fossils typical of the *Paleodictyon*, *Nereites* and *Ophiomorpha rudis* subichnofacies of the *Nereites* ichnofacies, and is dominated by *pascichnia*.

In terms of specific trace fossils, the channel margin of Morillo I is characterised by a high number of *Gordia arcuata*, a trace fossil which is unique to this section in the

Ainsa basin, and which only occurs in small numbers in the lobe of the Broto system at Aragues del Puerto (Section 7.3) and the fan fringe of the Cotefablo system at Jasa (Section 7.5). Like the channel margin of Ainsa II (Section 6.4.3), the channel margin of Morillo I is characterised by a high number of *Halopoa imbricata*. However, *H. imbricata* is only abundant in the lower and middle channel elements and is absent from the upper one. *H. imbricata* is particularly abundant in FA6a sandstones, siltstones and mudstones, where it forms 34% of the trace-fossil assemblage. Unlike the channel margin of Ainsa I and II though, *Scolicia* is absent.

6.5.2.3. Interpretation

The Morillo I sandbody is interpreted as a mixed erosional/depositional type channel system. The trace-fossil assemblage is very similar to the channel margin of Ainsa II (Section 6.4.3.2). This is due to the similar sedimentary characteristics of both sections, including bed thickness and grain size, as well as inferred environmental conditions such as oxygenation and nutrient supply. The thick-bedded sandstones of FA3a and FA3e are dominated by trace fossils formed by large, deeply burrowing organisms. The absence of pre-depositional trace fossils associated with these thick-bedded sandstones is related to their poor preservation potential (see Section 6.2.2.3).

In contrast, the more diverse trace-fossil assemblage of the thin- to medium-bedded sandstones of FA5b is associated with an increase in the preservation potential of shallow-tier burrows related to higher frequencies of low concentration turbidity current deposits. Increased long-term stability between turbidite deposition including lower sedimentation rates and the lower frequency of erosive gravity currents also enabled equilibrium communities to become established resulting in an increase in trace-fossil diversity. The reduced bed thickness may also have enabled more organisms to escape burial by the newly deposited sands.

The low diversity, high intensity trace-fossil assemblage of FA6a sandstones, siltstones and mudstones is similar to the interfan overlying the Ainsa system (Section 6.4.5). The trace-fossil assemblage is characterised by a low number of specialist feeding strategies such as many graphoglyptids and complex forms of *pascichnia* (e.g., *Nereites*). This is interpreted as being indicative of organic rich sediments (see Section 6.4.5.3). The abundance of *fodinichnia* and *pascichnia*, interpreted by Ekdale and Mason (1988) as being indicative of sediments, which were organic-rich, also supports this conclusion. The abundance of biodeformational structures may also be related to

the occurrence of organic-rich sediments, and may have resulted in the poor preservation potential of any shallow-tier burrows developed such as graphoglyptids.

The lower diversity trace-fossil assemblage may also be related to the number of bedding planes studied from FA6a, with less than half the number of bedding planes studied compared to FA5b. However, due to other low diversity, high intensity trace-fossil assemblages in FA6 deposits such as the channel margin of Ainsa II (Section 6.4.3.2), it may be interpreted that such trace-fossil assemblages are typical of FA6.

6.6. Guaso system

The Guaso system is the youngest depositional system in the Ainsa basin and is overlain by the Sobrarbe delta (Dreyer *et al.* 1999). It is the least deformed of the turbidite systems due to the fact that it is the youngest and furthest system from the thrust front to the southeast. It has been interpreted as the deep-marine part of a structurally confined sandy "prodeltaic clastic ramp" (Pickering & Corregidor 2005a, b). In contrast to the other depositional systems of the Ainsa basin, the Guaso system was probably fed by a number of small, active feeder channels and/or slope gullies. Two main sandbodies have been recognised by Sutcliffe & Pickering (*in review*). The Guaso I sandbody is analysed in detail in this chapter (see Section 6.6.3).

A number of different environments were studied in the Guaso system, including: (1) "prodeltaic clastic ramp" sandbody (Guaso I); (2) "prodeltaic clastic ramp" thin-bedded sandstones at the top of the Guaso I sandbody; (3) basin-slope thin-bedded sandstones / mudstones; and (4) slope gully (sandstone filled). The marine water depths during the Guaso system were below storm wave-base, but probably no more than several hundred metres, in upper bathyal water depths (Pickering & Corregidor 2005a, b).

6.6.1. Basin slope

6.6.1.1. Sedimentology

The section studied (Locality 27, Fig. 1.3; Appendix 6.15) is located stratigraphically above the main sandstones of the Guaso system and represents the youngest deposits studied in the Ainsa-Jaca basin. The basin slope is characterised by thin-bedded, fine- to medium-grained sandstones (FA5d) and very-thin-bedded sandstones, siltstones and mudstones (FA6d). The sandstones of FA5d form laterally

extensive sandstone packets several metres to tens of metres thick. Extra-formational organic matter is common. Between these sandstone packets are thick sequences of FA6d fine-grained sediments. These are typically intensely bioturbated. Although not recognised in the studied section, other characteristics typical of the basin slope include thick muddy intra-formational type Ia MTCs (sediment creep and slump features) (FA1a). These are particularly common within the slope deposits of the Castissent Group (see Chapter 5).

6.6.1.2. Ichnology

The basin slope is characterised by a low diversity, high intensity trace-fossil assemblage. Mean bioturbation on bedding planes is 37.9%, with 14 ichnospecies from 10 ichnogenera identified. Of these 14 ichnospecies, 10 are post-depositional and 4 are pre-depositional, including 2 graphoglyptids. The trace-fossil assemblage is dominated by *pascichnia*, *fodinichnia* and *domichnia*. The most common ichnotaxa include: *Nereites* and *Scolicia* (*pascichnia*); *Planolites, Thalassinoides* and *Phycosiphon* (*fodinichnia*); and *Ophiomorpha* (*domichnia*). The trace-fossil assemblage is characteristic of a mixed *Paleodictyon-Ophiomorpha rudis* subichnofacies (*sensu* Uchman 2001).

6.6.1.3. Interpretation

Mutti *et al.* (2003) interpreted similar basin slope deposits associated with deltaic systems from the Castissent Group as being deposited by hypopycnal and hyperpycnal flows. According to Mutti *et al.* (2003), mudstones similar to FA6d deposits may record the background hemipelagic sedimentation from hypopycnal plumes during periods of normal river discharge. Siltstones and mudstones were interpreted to have formed from silt rich buoyant plumes and lofting of dilute hyperpycnal flows whilst sandstones similar to those of FA5d were interpreted to have been deposited by turbulent low-intensity hyperpycnal flows.

The occurrence of intensely bioturbated mudstones, abundant organic matter, and the high proportion of deposit feeders suggest the basin slope was characterised by a high nutrient supply. The relative lack of graphoglyptids and complex forms of *pascichnia* (e.g., complex forms of *Nereites*), which covered a given surface in a systematic way, may be related to the inferred high nutrient supply (see Seilacher 1977, Miller 1991). This is also reflected in the abundance of *fodinichnia* and *pascichnia* in

the basin slope (see Section 6.4.5.3). Based on the model of Ekdale and Mason (1988), the high proportion of *domichnia* in the basin slope suggests that the sediments were relatively well oxygenated.

6.6.2. Slope gully

6.6.2.1 Sedimentology

The slope gully (Locality 26, Fig. 1.3; Appendix 6.16) is located stratigraphically above the main sandstones of the Guaso system, and erodes into the basin slope deposits described above (Section 6.6.1). A number of small gullies have been observed within the Guaso system, and are interpreted as similar sediment supply systems to those which may have fed the Guaso system. The gully is ~14 m wide and 6 m deep, (aspect ratio of 2.3:1) (Fig. 6.7). The margins of the gully are very steep, with angles of 47° and 77°. Beds within the gully have a concave-up geometry with beds dipping to the ESE on the western margin and to the SW on the eastern margin. Overlying the gully are basin slope sandstones and mudstones. The sandy fill of the gully is characterised by FA5a thin- to medium-bedded fine- to medium-grained sandstone-mudstone couplets. These beds thin and pinch out at the margins of the gully. Towards the top of the gully, many of the sandstone beds spill over the gully margin and are deposited in the basin slope. Individual beds typically thin over the margin of the gully and then thicken slightly into the adjacent basin slope.

6.6.2.2 Ichnology

The slope gully is characterised by a low diversity, high intensity trace-fossil assemblage. Mean bioturbation on bedding planes is 39.9%, with 10 ichnospecies from 5 ichnogenera identified. Of these 10 ichnospecies, 9 are post-depositional and 1 is pre-depositional. The trace-fossil assemblage is dominated by *pascichnia*, *fodinichnia* and *domichnia*. The most common ichnotaxa include: *Scolicia* (*pascichnia*); *Thalassinoides* and *Phycosiphon* (*fodinichnia*); and *Ophiomorpha* (*domichnia*). In contrast to the sandstones of the basin slope, vertically orientated burrows (*Ophiomorpha*) occur in the gully, principally within sandstones. With the absence of *agrichnia* and graphoglyptids, the trace-fossil assemblage is characteristic of the *Ophiomorpha rudis* subichnofacies (*sensu* Uchman 2001).

Near the upper margin of the gully, a 30 cm muddy interval occurs immediately below the erosion surface marking the margin. This muddy interval is characterised by a

number of distinct, well preserved, uncompacted *Thalassinoides* and *Teichichnus* burrows within the mudstones, and may be a candidate firmground.

6.6.2.3 Interpretation

The slope gully is a small erosional feature, with only one master erosion surface. This is in contrast to the upper slope gully at Formigales (Section 6.3.1), where the base is marked by multiple stepped erosion surfaces. This suggests the slope gully was a relatively short-lived feature on the basin slope acting as a short-term feeder system that was later back-filled.

The low diversity, high intensity trace-fossil assemblage dominated by post-depositional trace fossils is indicative of an opportunistic colonising strategy. The absence of trace fossils indicative of equilibrium colonising strategies, including shallow-tier pre-depositional trace fossils such as graphoglyptids, and the occurrence of deep burrow networks such as *Ophiomorpha*, indicates that the environment was probably hostile to many trace-forming organisms. This is related to the fact that the gully was probably a high-energy environment, characterised by a high frequency of topographically confined gravity currents.

6.6.3. Guaso prodeltaic clastic ramp sandbody

The Guaso I sandbody is thickest in the Rio Eña (Locality 24, Fig. 1.3; Appendix 6.17) and consists of two thinning-and-fining-upward channel complexes, herein referred to as 1A and 1B. Mapping has revealed the overall geometry of the channel elements to be weakly confined (Sutcliffe & Pickering *in review*) with internal complexities associated with laterally stacked weakly confined channel elements. Mean palaeoflow is towards 317°.

6.6.3.1. Sedimentology

Both channel complexes in Guaso I exhibit distinct thinning-and-fining-upward sequences and are separated by a ~3 m area of no exposure, probably a muddy chaotic deposit (MTC) or thin-bedded sandstones and siltstones. The lower channel complex (1A) is ~38 m thick, whilst channel complex 1B is ~32 m thick, and is overlain by intrafan mudstones and thin-bedded turbidite sandstones. The base of 1A is associated with a thin (~2-m-thick) muddy Type Ia MTC. This is overlain by ~31 m of sheet-like,

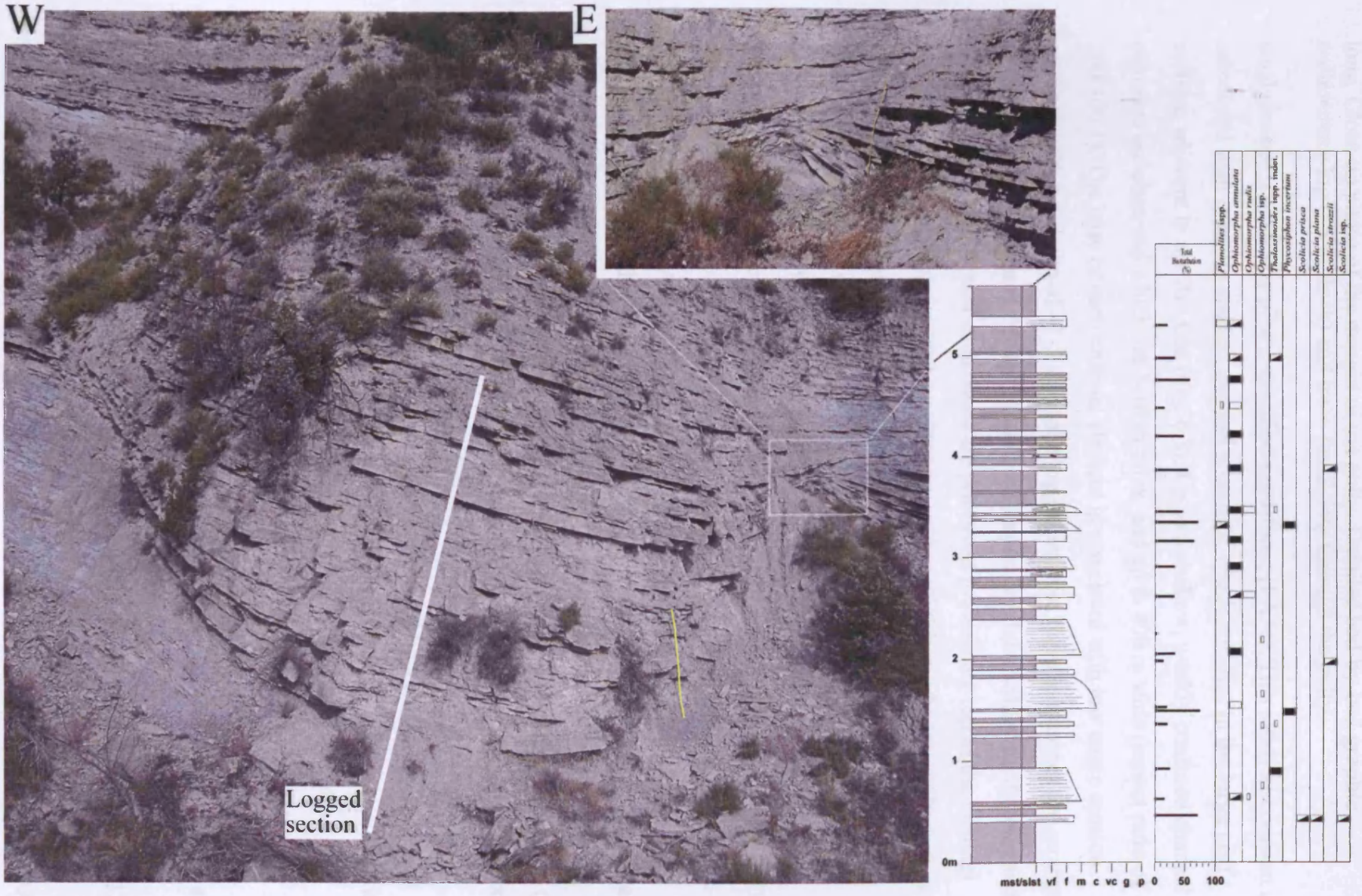
W
E
Logged section
5
4
3
2
1
0m
mst/sist vf f m c vc g p
0 50 100
Planolites ispp.
Ophiomorpha annulata
Ophiomorpha rudis
Ophiomorpha isp.
Thalassinoides ispp. indet.
Phycosiphon incertum
Scolicia prisca
Scolicia plana
Scolicia strozzii
Scolicia isp.

Fig. 6.7. Sand-filled gully in slope deposits, Guaso system. Scale bar (yellow) is 2 m long. Close-up photo of the margin of the gully. Detailed bed-by-bed graphic sedimentary log (~5 m thick) and trace fossil data through the gully.

amalgamated, commonly planar stratified sandstones (FA3c). This sandy succession is associated with laterally stacked channel elements, which are clear in the large cliff sections adjacent to the Rio Eña (Fig. 6.8). Up to 6 shallow, weakly confined channel elements are observed which are 5-10 m thick, and up to 400 m wide (aspect ratio of 200/300:1). The base of each channel element is associated with low angle erosion surfaces, with cut-down of ~1-3 m. In the logged section, these sandstones are arranged into crude coarsening- and thickening-upward sequences. Interbedded mudstones and siltstones between the thick sandstones are preserved towards the top of the channel complex. These are characterised by siltstones with very thin mudstones (silt:mud ratio of 1:0.5). Flaser bedding and single-train rippled beds are common. The top 6 m comprises thin-bedded sandstones and interbedded siltstone-mudstone laminae with common flaser and ripple-train bedding (FA5e).

Channel complex 1B is characterised by increased internal heterogeneities. The basal 14 m of the section is associated with laterally discontinuous medium- to thick-bedded sandstones (FA6a) with erosive bases. The sandstones are commonly amalgamated towards the base of the section, and characterised by abundant mud-clasts, nummulites and small rounded pebbles (<3 cm). Planar stratification is less well developed than the thick sandstones of 1A. These sandstones are punctuated by thin (<1 m thick) locally erosive Type Ib MTCs characterised by a sand-rich mudstone matrix (FA1c). The upper half of the channel complex comprises tabular, thin- to medium-bedded sandstones (FA5e). These sandstones are truncated by a small, low net:gross channel element. Only one margin of the channel is exposed, which dips at ~13° with cut-down of ~5.5 m. The channel-fill is similar to the sediments it erodes into. Individual beds thicken into the channel axis. A small package of FA5e sandstones thicken laterally away from the channel element and are interpreted as genetically related overbank deposits. The sandstones overlying the channel element thicken as a result of accommodation space created by the underlying, underfilled channel.

The thin- to medium-bedded sandstones (FA5e), which characterise the top 22 m of channel complex 1B, including the low net:gross channel element, have a very distinctive trace-fossil assemblage compared to the main sandstones of Guaso I. They

are therefore interpreted separately and referred to as "prodeltaic clastic ramp" thin-bedded sandstones at the top of the Guaso I sandbody (see below).

6.6.3.2. Ichnology

The thick-bedded sandstones (FA3a and FA3c) of Guaso I, which characterise the lower sequences of both channel complexes, are characterised by a low diversity, very low intensity trace-fossil assemblage. Mean bioturbation on bedding planes is 4.6% with 7 ichnospecies from 5 ichnogenera identified. Of these 7 ichnospecies, 6 are post-depositional and 1 is pre-depositional. The trace-fossil assemblage is dominated by *fodinichnia* and *domichnia* with the most common ichnotaxa including: *Planolites* and *Thalassinoides* (*fodinichnia*); and *Ophiomorpha* (*domichnia*). Only *Ophiomorpha* isp. occurs within the sandstones. The most distinct feature is the occurrence of flat-bottomed, non-bioturbated sandstones. Even thin-bedded sandstones of FA5e are rarely bioturbated. The trace-fossil assemblage of the Guaso I sandbody is characteristic of the *Ophiomorpha rudis* subichnofacies (*sensu* Uchman 2001).

The "prodeltaic clastic ramp" thin-bedded sandstones at the top of the sandbody have a high diversity, high intensity trace-fossil assemblage. Mean bioturbation is 39% with 20 ichnospecies from 15 ichnogenera. Of these, 12 are post-depositional and 8 are pre-depositional, including 3 graphoglyptids. The trace-fossil assemblage is dominated by *fodinichnia* and *domichnia*, with the most common ichnotaxa including: *Planolites*, *Thalassinoides*, *Asterosoma* and *Phycosiphon* (*fodinichnia*); and *Ophiomorpha* and *Arenituba* (*domichnia*).

The thin-bedded sandstones at the top of Guaso I are characterised by a number of trace fossils unique to the Guaso system in the Ainsa basin. These include *Nereites cambriensis*, *Agrichnium* and *Arenituba*, as well as abundant *Asterosoma*, which, outside the Guaso system, occur only rarely in the Morillo system. The thin-bedded sandstones at the top of Guaso I are characterised by an increase thickness of the fine-grained intervals between the sandstones compared to the main sandbody, as well as a decrease in the number of siltstone and mudstone laminae between the sandstones. The trace-fossil assemblage is mixed, comprising trace fossils typical of the *Paleodictyon* and *Ophiomorpha rudis* subichnofacies of the *Nereites* ichnofacies (*sensu* Uchman 2001) as well as others more typical of the *Cruziana* ichnofacies.

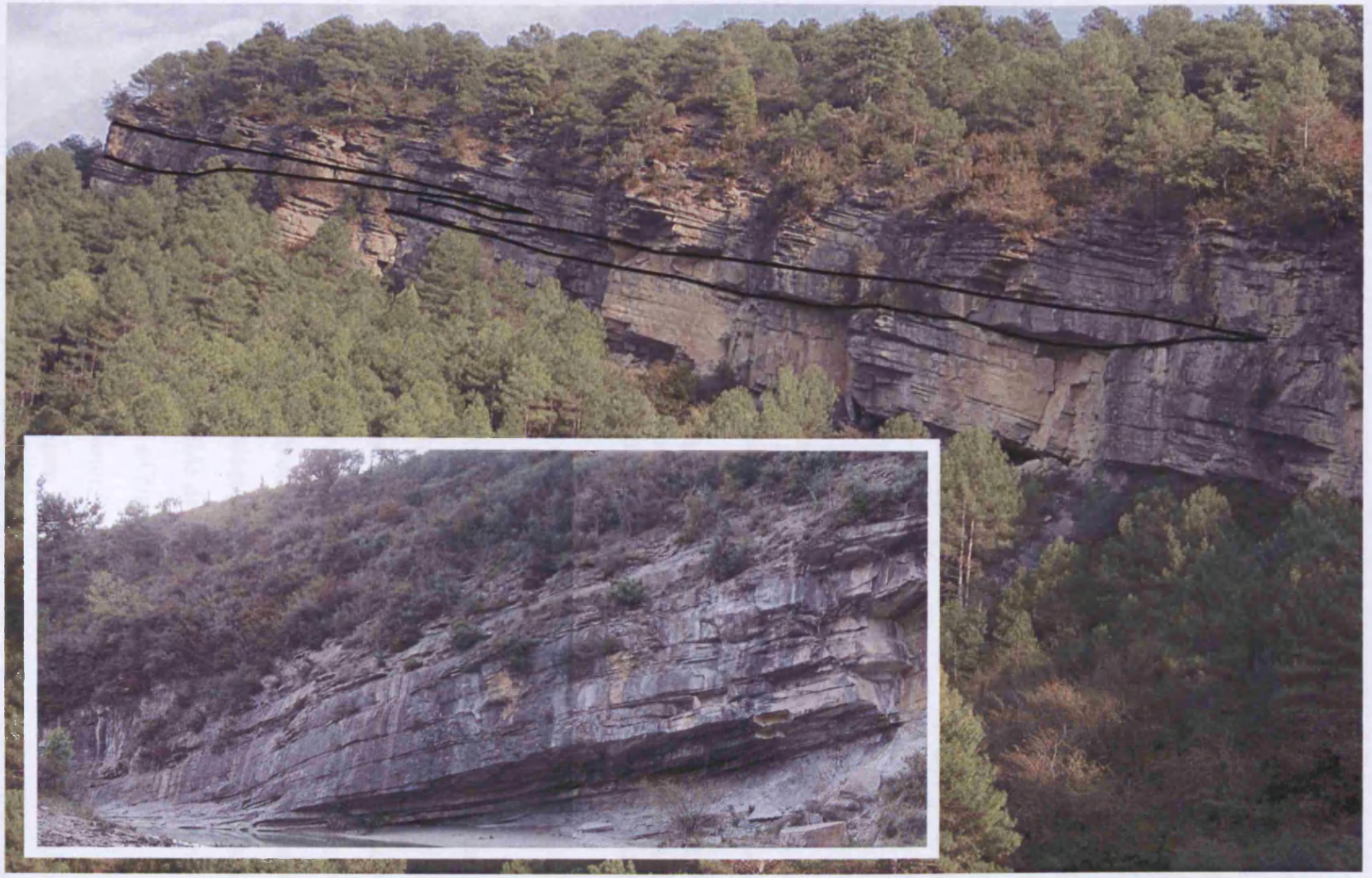

Fig. 6.8. Two of the six relatively unconfined channel elements, which are ~5-10 m deep at the base of the lower channel complex (1A) of Guaso I, in a large cliff section adjacent to the Rio Eña. Inset is the base of Guaso I in the Rio Eña. Height of exposure is ~20 m, characterised by sheet-like, amalgamated, commonly planar stratified sandstones (FA3c).

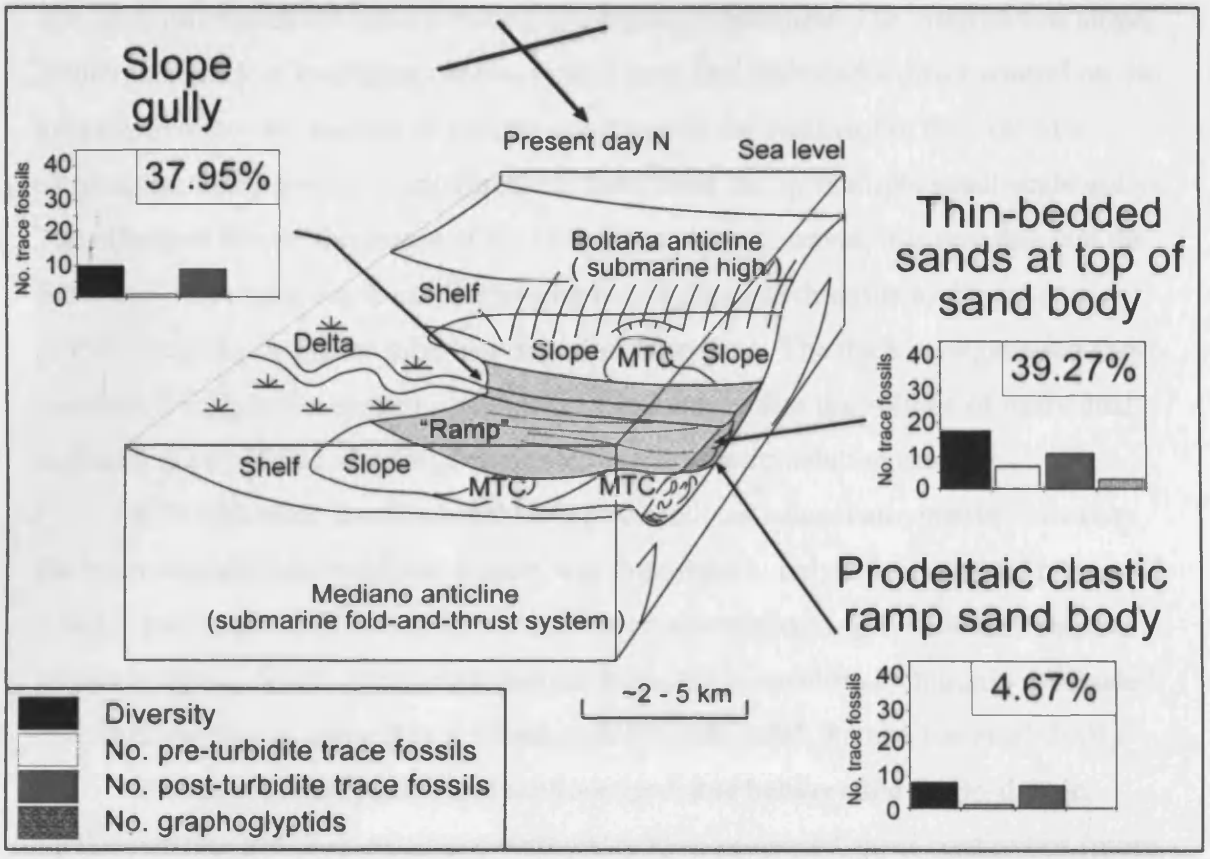

Fig. 6.9. Depositional model for Guaso system (modified after Sutcliffe & Pickering *in review*) with summary graphs showing the average bioturbation, trace-fossil diversity, number of pre- and post-depositional trace fossils and number of graphoglyptids.

6.6.3.3. Interpretation

In terms of both its sedimentology and ichnology, the Guaso system differs to the other turbidite systems of the Ainsa basin. Guaso I is characterised by a low frequency of MTCs compared to other sandy systems. This may be related to both the nature of the slope and tectonic activity at the time of deposition. The inferred low gradient of the slope may have resulted in increased slope stability and therefore reduced slope failure and the subsequent generation of MTCs. A reduction in slope failure may also be related to a possible decrease in tectonic activity during the Guaso system. This is indicated by the lack of significant structural deformation in the Guaso system (Sutcliffe & Pickering *in review*).

The paucity of thick MTCs upon which the sandbody accumulated may have resulted in a seafloor with minimal topographic relief, which had a first order control on the essentially weakly confined geometries associated with Gerbe I. The low frequency of erosive and/or topography forming MTCs within the sandy fill of the sandbody may

also have influenced the relatively simple internal architecture. The inferred low slope gradient and lack of confining canyon system may also have had a direct control on the internal architecture. Instead of a single-point source for sediment in the case of a canyon, the Guaso system is interpreted to have been fed by multiple small-scale gullys. The effects of this on the nature of the flows is unclear, however, it is possible that the flows may have been similar to the jet-plume pair deposits describe by Hoyal *et al.* (2003), resulting in a more lobe-like depositional system. The thick amalgamated sheet-sandstones suggest the system was broadly confined, or that the volume of individual sediment gravity flows was large compared to the accommodation space.

Although trace fossils cannot be used directly as palaeobathymetric indicators, the interpretation that the Guaso system was deposited in only a few hundred metres of water is consistent with the observed trace-fossil assemblage. *Agrichnium*, *Arenituba* and *Asterosoma*, which occur in abundance in Guaso I, are more commonly associated with shallow-marine settings (e.g., Stanley & Pickerill 1995, Pemberton *et al.* 2001).

The reduced bathymetry and seafloor gradients between the fluvio-deltaic, shallow-marine and deep-marine systems, may have promoted quasi-continuous (more steady and uniform) turbidity-current flows compared to steeper slopes, especially if associated with direct river input (Sutcliffe & Pickering *in review*). Consequently, many of the deposits associated with Guaso I may have originated from hyperpycnal flows and low concentration turbidity currents. The high frequency of low concentration turbidity currents is indicated by the abundance of sandstone and siltstone ripple-train beds formed by deposition from low concentration flows under seafloor traction conditions. These low concentration flows may have been between sub- and super-critical flow regimes and therefore non-erosive. This may have resulted in the paucity of grooves and flutes on the soles of most sandstones.

The low intensity trace-fossil assemblage characterised by a paucity of pre-depositional trace fossils on the soles of both high and low concentration turbidite sandstones suggests that bottom waters were poorly oxygenated. The occurrence of *Ophiomorpha* within the sandstones may be related to bioturbation by doomed pioneers (*sensu* Föllmi & Grimm 1990) due to a temporary increase in oxygen levels associated with the newly deposited turbidite sandstones (see Section 6.5.1.3). These low oxygen levels may be related to the palaeogeographic setting of the Guaso system, which may have formed in a slope mini-basin with restricted or no connectivity to the open ocean at the time of deposition (Pickering *pers. comm.* 2007).

The upper part of the section referred to as the thin-bedded sandstones at the top of Guaso I, are characterised by an increased diversity and intensity trace-fossil assemblage. This may be related to an increase in oxygen levels in the basin. The increased thickness of the interbedded mudstones, as well as a decrease in the number of siltstone and mudstone laminae between the sandstones, may be related to a reduction in the coarse clastic supply at the top of the sandbody, as well as an increase in bioturbation intensity which could have effected the preservation of the original sedimentary fabric.

6.7. Trace-fossil distributions in the Ainsa Basin: Summary

A distinct trace-fossil assemblage, diversity and abundance characterise each fan and related environment in the Ainsa basin (Figs. 6.11 and 6.12). The proximal and axial parts of the sandy systems, e.g., upper slope gully, canyon fill, channel axis, and intrachannel off-axis, all have low diversity, low intensity trace-fossil assemblages dominated by post-depositional trace fossils. Off-axis environments, e.g., channel margin and outermost channel-to-levee-overbank, show a general increase in trace-fossil diversity and intensity compared to more proximal and axial environments, with maximum intensity of bioturbation in the (commonly) totally bioturbated sediments of the proximal interfan, and greatest diversity occurring in the channel margin. Off-axis environments, in particular channel margins, are characterised by an increase in pre-depositional trace fossils, including graphoglyptids. The basin slope and slope gully settings are characterised by a moderately low diversity, high intensity trace-fossil assemblages, with the basin slope typified by a higher number of pre-depositional trace fossils including graphoglyptids compared to the slope gully. The trace-fossil assemblage of the basin slope is most similar to the proximal interfan, albeit with a markedly lower average bioturbation.

The low diversity trace-fossil assemblages typical of the channel axis are characterised by high abundances of individual ichnotaxa such as *Ophiomorpha* and *Thalassinoides*. The axis of the Gerbe I sandbody is characterised by abundant *Arenicolites*, which commonly occurs below pebbly macroform elements, some of which may represent base-of-channel deposits. The Banastón, Ainsa and Morillo systems are characterised by very similar trace-fossil assemblages and average bioturbation, with the most diverse and dense trace-fossil assemblages in the Ainsa

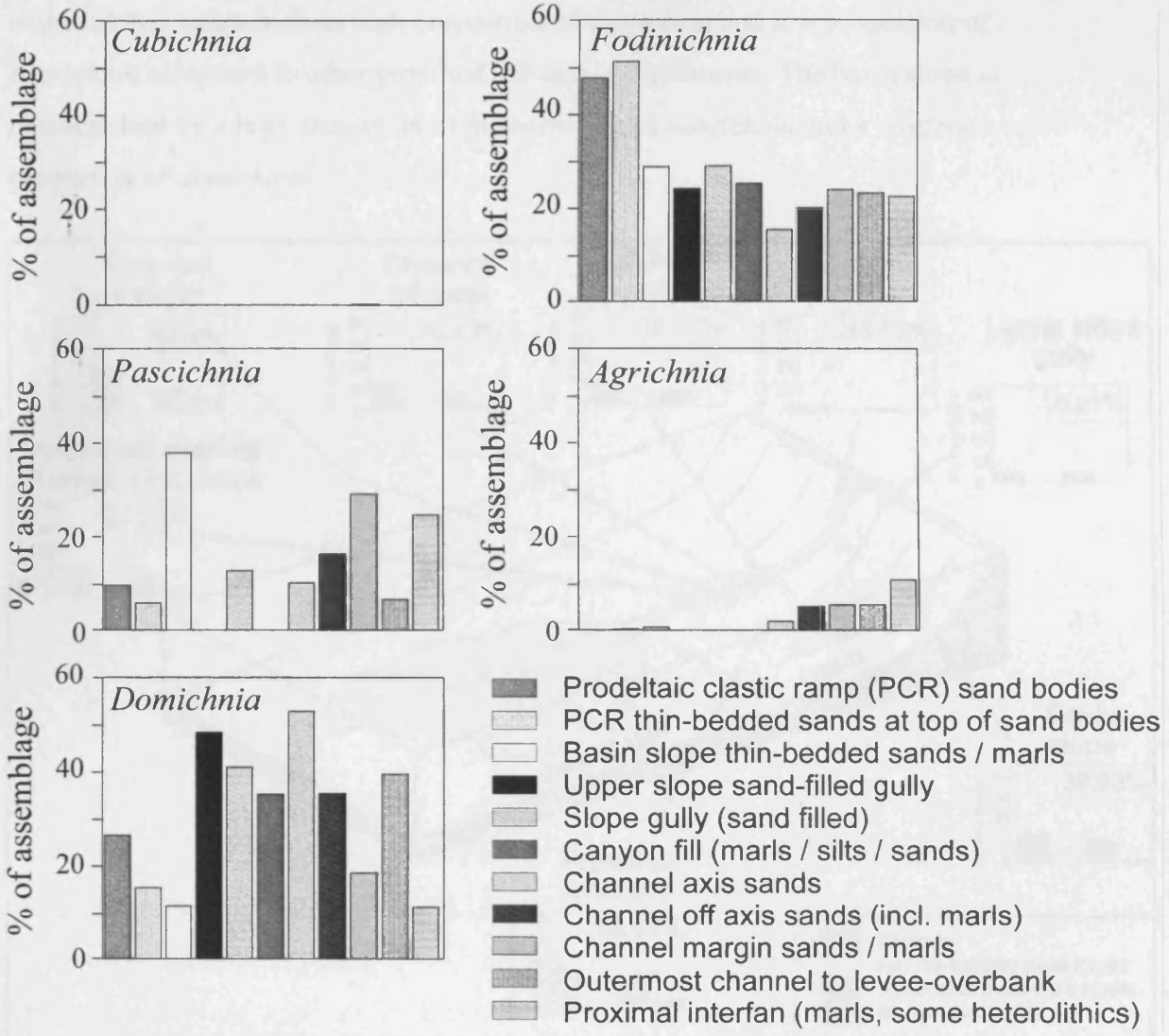

Fig. 6.10. The proportion of *cubichnia, pascichnia, fodinichnia, domichnia* and *agrichnia* in the trace-fossil assemblages of individual fan and related environments in the Ainsa basin.

basin. The Guaso system is characterised by a very distinct trace- fossil assemblage. The lowest diversity and intensity trace-fossil assemblage of any sandbody in the Ainsa basin occurs at the base of Guaso I.

The trace-fossil assemblages of the fan and related environments can also be distinguished by the characteristic behaviour of the trace-making organisms (Fig. 6.10 and 6.14). In proximal axial environments such as upper-slope gully, canyon or channel axis, the trace-fossil assemblages are dominated by *fodinichnia* and *domichnia*. In proximal off-axis environments such as the channel margin or interfan, the trace-fossil assemblages are characterised by a decrease in the proportion of *domichnia*, a general increase in *pascichnia* and an increase in *agrichnia*. The outermost channel-to-levee-

overbank has an anomalous high proportion of *domichnia* and low proportion of *pascichnia* compared to other proximal off-axis environments. The basin slope is characterised by a high proportion of *fodinichnia* and *pascichnia* and a moderate proportion of *domichnia*.

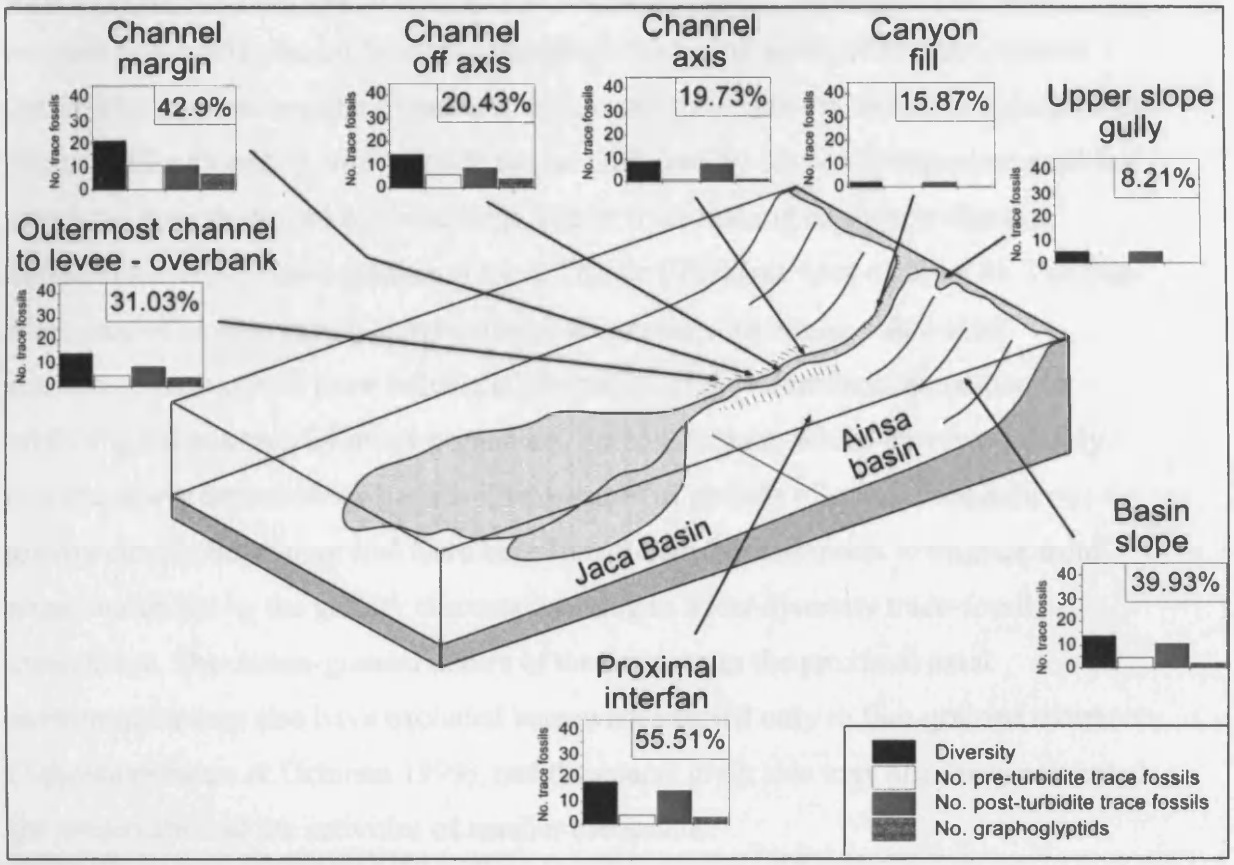

Fig. 6.11. Summary diagram of average bioturbation, trace-fossil diversity, number of pre- and post depositional trace fossils and number of graphoglyptids for the most characteristic environments of the turbidite complex of the Ainsa basin.

6.8. Interpretation

The low diversity, low intensity, dominantly post-depositional trace-fossil assemblages of the proximal and axial parts of the sandy systems occurs due to a number of factors. In these environments, sediment gravity flows are generally more erosive and, therefore, tend to remove the fertile top layer of the seafloor, resulting in the preservation of only the deepest burrowing trace fossils. Many of the trace-making organisms, which formed the pre-depositional trace-fossil assemblage, existed in this top layer of the seafloor, on or near the sediment/water interface. Consequently, such environments are associated

with low numbers of pre-depositional trace fossils due to their poor preservation potential. Endobenthic *pascichnia* (e.g., *Halopoa*, *Scolicia*) as well as *domichnia* (e.g., *Ophiomorpha*), formed by large, robust, deeply burrowing organisms, which exploited organic rich layers within the sandstones, are typical of these proximal axial sections. This is, at least in part, due to the fact that the trace-making organisms were well adapted to surviving burial by newly deposited thick sand beds (Wetzel & Uchman 2001). The traces of smaller organisms which may have survived burial or colonised the deposits after migrating from outside the area affected by the newly deposited sand bed, may have been destroyed by these large, robust trace making organisms due to a bulldozing effect by the organisms (*sensu* Thayer 1979) (see Section 6.4.1.3). The high frequency of erosive gravity current flows associated with the proximal axial environments may also have influenced the nature of the trace-fossil assemblages inhibiting colonisation by many organisms, except for those which burrowed deeply into the newly deposited sediments. The duration of periods of quiescence between gravity current flows may also have been insufficient for colonisers to migrate from areas unaffected by the gravity currents resulting in a low diversity trace-fossil assemblage. The coarse-grained nature of the deposits in the proximal axial environments may also have excluded burrowers adapted only to fine-grained sediments (Tchoumatchenco & Uchman 1999), and the coarse grain size may also have prevented the preservation of the activities of smaller metazoans.

In proximal off-axis environments, such as the channel margin, the high-diversity, high-intensity trace-fossil assemblages characterised by an abundance of pre-depositional trace fossils and graphoglyptids is related to a number of factors. The lower frequency of strongly erosive sediment gravity flows, compared to proximal axial environments, and meant that the preservation potential of shallow tier trace fossils, such as many graphoglyptids, was greater. The increase in average bioturbation from proximal axial to off-axis environments may be related, at least in part, to a decrease in bed thickness and grain size of the deposits. The reduction in grain size and bed thickness of the deposits in proximal off-axis environments may have promoted an increase in bioturbation. For example, in Recent turbidites east of the Cape Verde Islands, Wetzel (1991) observed an increase in bioturbation with a decrease in bed thickness and grain size of the sands. The reduced bed thicknesses compared to more axial environments may also have enabled more organisms to survive burial. Lower rates of sediment accumulation in off axis environments such as the overbank, as well

as the interfan and basin slope, enabled organisms greater time to colonise and bioturbate the newly deposited sediments resulting in higher bioturbation intensities than more axial environments. The fact that the proximal off-axis environments were generally closer to areas unaffected by the depositing sediment gravity flows also meant that the sediments may have been colonised by migrating organisms more quickly due to the reduced migration distances. The reduced diversity trace-fossil assemblages of off-axis environments such as the proximal interfan, as well as the basin slope and thin-bedded sandstones and mudstones of the channel abandonment phase may be related in part to the intensity of bioturbation. The fact that the sediments are commonly totally homogenised, interpreted as a result of high nutrient supply and low sediment accumulation rates, may have reduced the preservation potential of individual ichnotaxa, except for the deepest-tier trace fossils.

The distribution of trace fossils in the fan and related environments is also related to environmental stability. In general, the producers of post-depositional trace fossils followed an opportunistic strategy in colonising the seafloor, whereas pre-depositional forms represent an equilibrium strategy (Uchman 1995a). Examples of trace-fossil assemblages dominated by opportunistic colonising strategies include the

Environment	Bed thickness (cm)	Average Pre.	Average Post.	Average Graph.	No. Beds
Channel axis	0-3	0	3	0	1
Channel off-axis	0-3	1	2.5	1	2
Channel margin	0-3	1	3	0.5	2
Channel axis	3-10	0	3	0	2
Channel off-axis	3-10	0	2	0	1
Channel margin	3-10	4	8	3	3
Channel axis	10-30	0	2.5	0	6
Channel off-axis	10-30	0	1	0	5
Channel margin	10-30	2.33	2	1.33	3
Channel axis	30-100	0.125	2	0	8
Channel off-axis	30-100	0	2	0	4
Channel margin	30-100	1	1	0	1

Table 6.4. Variations in trace-fossil assemblages preserved on the soles of turbidite sandstones of varying thickness from channel axis to channel margin, Ainsa I sandbody.

channel axis and canyon environments. In environments such as the channel margin, examples of opportunistic colonising strategies are still common, with some bedding planes dominated almost exclusively by endichnial *pascichnia* (e.g., *Halopoa, Scolicia*) and/or *fodinichnia* (e.g., *Lophoctenium, Phycosiphon*) to form high-intensity, low-

diversity opportunistic trace-fossil communities. In general, the increase in the proportion of pre-depositional trace fossils including graphoglyptids in proximal off-axis environments is related to the establishment of equilibrium organism communities related to long-term stable conditions between turbidite sand deposition which enabled equilibrium communities to develop (Uchman 1995a). However, the importance of the preservation potential of pre-depositional trace fossils should not be under-estimated, with pre-depositional trace fossils having a higher preservation potential in off axis environments characterised by a lower frequency of high concentration turbidity currents than axial environments (see Section 6.9). It is also important to fully understand the colonising strategies of organisms, because many equilibrium communities may be associated with a high proportion or exclusive population of post-depositional trace fossils (e.g., Orr 1995).

6.9. Discussion: The importance of environmental conditions as controlling factors on trace-fossil assemblages in fan and related environments

It is clear that there are distinct variations in trace-fossil assemblages in different fan and related environments in the Ainsa basin. However, this study also illustrates the importance of the nature of the deposits to trace-fossil assemblages independent of the environment of deposition. It is clear that in general, sandstones of a similar thickness and grain size in different environments are characterised by similar trace-fossil assemblages. For example, thick-bedded coarse grained sandstones of FA3 in the channel axis, channel off axis and channel margin are characterised by a low diversity trace-fossil assemblage dominated by post-depositional trace fossils. Thin-bedded sandstones siltstones and mudstones of Facies-association 6 in the interfan, basin slope, channel margin, channel off-axis and channel abandonment, are characterised by a high intensity low diversity trace-fossil assemblage dominated by post-depositional trace fossils. In contrast, thin- to medium-bedded, fine- to medium-grained sandstones of Facies-association 5 in the channel off axis and channel margin are associated with high intensity, high diversity trace-fossil assemblages with a high proportion of pre-depositional trace-fossils including graphoglyptids. The trace fossil communities were therefore directly controlled by factors such as grain size, bed thickness and the nature

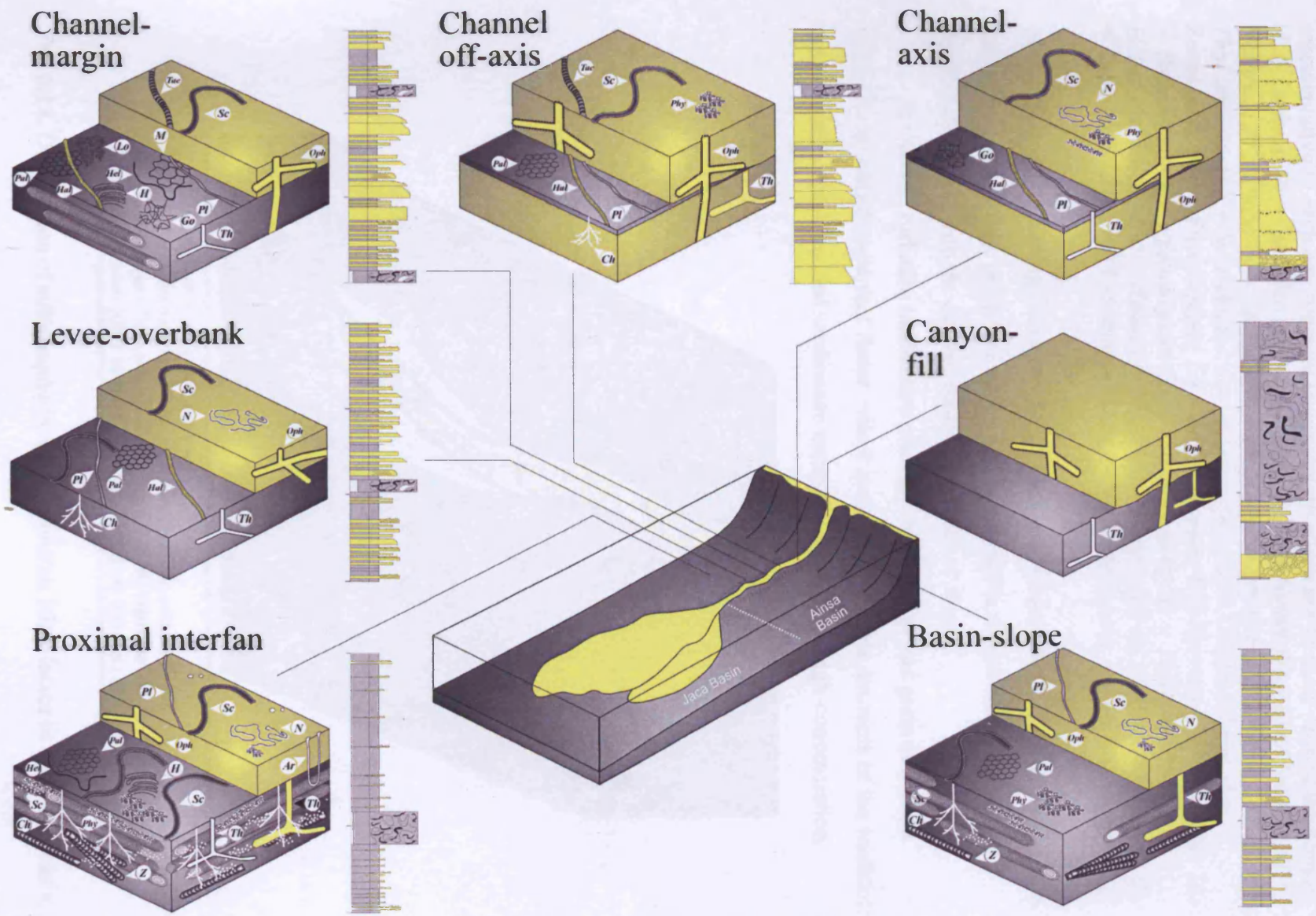
Channel-
margin
Channel
off-axis
Channel-
axis
Levee-overbank
Canyon-
fill
Proximal interfan
Basin-slope
Ainsa
Basin
Jaca Basin

Fig. 6.12. Summary of typical trace-fossil assemblages for the most characteristic environments of the turbidite complex of the Ainsa basin and example logs representative of each environment (representative logs are 15 m in vertical thickness). (*L = Lockeia; Sk = Skolithos; Ar = Arenicolites; Nu = Nummulites-lined burrow; H = Halopoa; Pl = Planolites; Ch = Chondrites; Oph = Ophiomorpha; Th = Thalassinoides; S = Saerichnites; Lor = Lorenzinia; Gl = Glockerichnus; Z = Zoophycos; Phy = Phycosiphon; Lo = Lophectenium; N = Nereites; Sc = Scolicia; Tae = Taenidium; Pr = ProtovirgularCos = Cosmorhaphe; He = Helicolithus; H = Helminthorhaphe; Hel = Helminthopsis; Sp = Spirohaphe; Pa = Palaeomeandron; De = Desmograpton; Ur = Urohelminthoida; M = Megagrapton; Pal = Paleodictyon*).

of the substrate (including firmness). One of the fundamental controlling factors on the trace-fossil assemblage preserved on the soles of turbidite sandstones is the depth of erosion associated with the depositing turbidity-current flow.

In general, turbidite sandstones of a similar thickness and grain size were deposited by turbidity-current flows, which eroded comparable amounts of the seafloor. Consequently, thick-bedded sandstones deposited by erosive, high-concentration

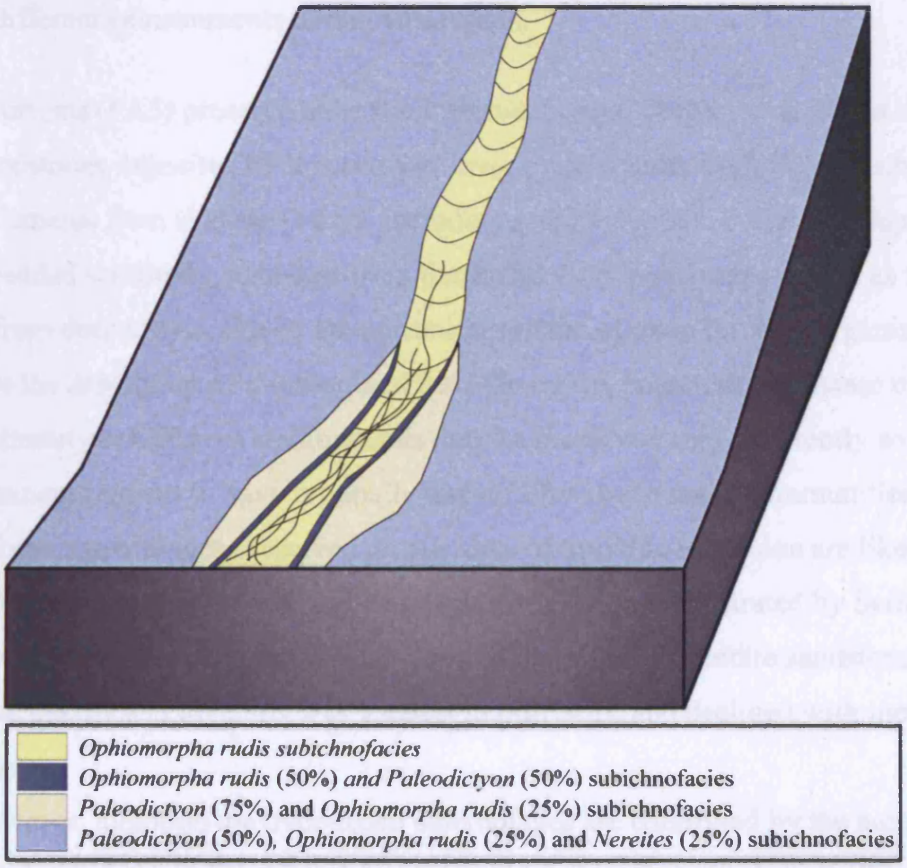

Fig. 6.13. Distribution of subichnofacies of the *Nereites* ichnofacies in the Ainsa basin.

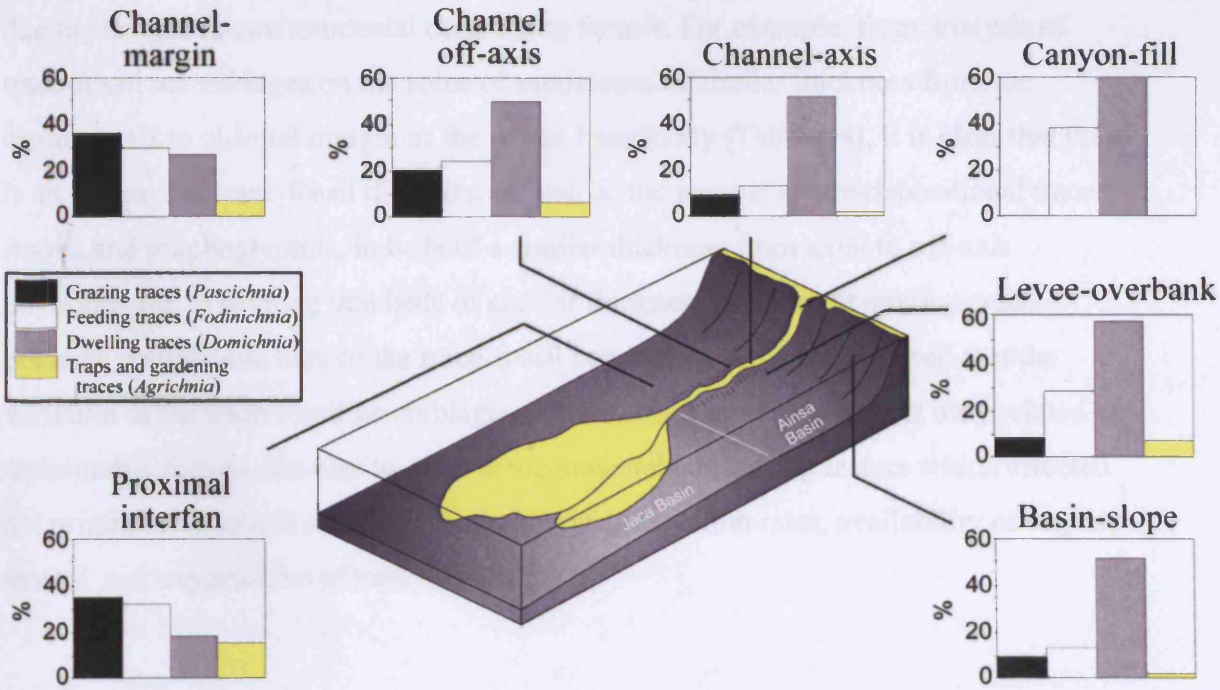

Fig. 6.14. Summary of the ethological behaviour of organisms established from trace fossils in different environments in the Ainsa basin.

turbidity currents (FA3) preserve trace fossil elements from deeper-tiers, whilst thin-bedded sandstones deposited by less erosive, low-concentration turbidity currents (FA5) preserve elements from shallower-tiers, including graphoglyptids. Following deposition of a thin-bedded sandstone, elements from the shallow tier may be preserved, as well as elements from deeper tiers, due to the upward migration of trace-forming organisms as a response to the deposition of a subsequent bed. Therefore, potentially the same trace fossil community in different environments may be preserved very differently so that the environments appear to have originally had different trace fossil communities. Thus, the trace-fossil assemblages preserved on the soles of turbidite sandstone are likely to be linked with the amount of erosion and bed thickness. This was illustrated by Seilacher (1962) where studies on trace-fossil diversities on the soles of turbidite sandstone showed that trace-fossil diversity was greatest in thin beds, and declined with increasing bed thickness.

However, although the trace-fossil assemblages are controlled by the nature of the deposits independent of the actual depositional environment, other controlling factors also play a major role in the distribution of trace-fossil assemblages. Thus, thick-bedded sandstones (FA3) or thin- to medium-bedded sandstones (FA5) may be associated with subtle differences in trace-fossil assemblages in different environments

due to changes in environmental controlling factors. For example, from analysis of trace-fossil assemblages on the soles of sandstones of similar thickness from the channel axis to channel margin of the Ainsa I sandbody (Table 6.4), it is clear that there is an increase in trace-fossil diversity, as well as the number of pre-depositional trace fossils and graphoglyptids, in beds of a similar thickness from axial to off-axis environments. Assuming that beds of similar thickness in different environments preserve comparable tiers of the trace-fossil community, it can be inferred that the variation in the trace-fossil assemblages in the Ainsa I sandbody are not only related to taphonomic factors, but also to other environmental controlling factors which effected the original trace-fossil community, such as sedimentation rates, availability of organic matter, and oxygenation of interstitial waters.

Chapter 7

Jaca basin: sedimentology and ichnology of distal submarine-fan and related environments

7.1. Introduction

Two turbidite systems were studied in the distal Jaca basin, the Arro-Broto and Gerbe-Cotefablo systems. Five fan and related environments are recognised from east of Fanlo to west of Roncal: (1) channel-lobe transition (CLT); (2) lobe; (3) lobe fringe; (4) fan fringe, and (5) distal basin floor. A summary of sedimentological and ichnological data for each individual fan and related environment is detailed in Table 7.1, and trace fossils identified at each outcrop are listed in Table 7.4.

In the past few decades, there has been less published research from the Jaca basin compared to the Ainsa basin. Although this study attempts to redress the balance, never-the-less, much of this work still has remained focused on the more proximal Ainsa basin (cf. Chapters 5 and 6). The reason for this is that detailed mapping and bed correlations in the Jaca basin were beyond the scope of this project, whereas such data is available from the Ainsa basin. In this study, the interpretation of fan and related environments in the Jaca basin is based on field observations by the author and published work by Mutti *et al.* (1985, 2003), Remacha and Fernandez (2003), and Remacha *et al.* (2003, 2005).

7.2. Channel-lobe transition (CLT)

7.2.1. Sedimentology

The channel-lobe transition (CLT) has been extensively studied in the Broto system, including Mutti and Normark (1987), and Remacha *et al.* (1998, 2003). The studied section is located near Fanlo, southeast of Broto (Locality 28, Fig. 1.3; Appendix 7.1) and was interpreted by Remacha *et al.* (2003) as the CLT of the Broto system. It is 72 m in thickness and represents an incomplete section through the Broto system. The CLT is characterised by relatively high net:gross sand-rich deposits including irregular, well-sorted, thick-bedded sandstones with common scour-and-fill

structures (FA3h), thin- to medium-bedded sandstone-mudstone couplets (FA5c) as well as chaotic sandy mudstones (FA1b). Sandstones are commonly amalgamated, with an average of 9.44% of all beds amalgamated (Fig. 7.1). Sandstones range between 3-164 cm in thickness and average 17.78 cm (Fig. 7.1). Interbedded fine-grained intervals between the sandstones are generally very thin, averaging 3.90 cm in thickness (Fig. 7.1).

The base of the section is marked by a muddy ~2-m-thick Type I MTC (*sensu* Pickering & Corregidor 2005a, b) (FA1a). Contorted sandstones and mudstones are rare, and the deposit is dominated by a mud-rich chaotic matrix. No thinning- or thickening-upward sequences are developed in the section, but overall, the entire section shows a crude thinning-and-fining-upward trend. The main sandy package is

Characteristics	**Channel-lobe transition**	**Muddy lobe**	**Distal sandy lobe**	**Lobe margin**	**Fan fringe**	**Distal basin floor**
Mean bed thickness (sandstone)	17.78	9.02	10.02	4.85	5.68	4.92
Mean mudstone thickness	3.90	4.65	4.98	3	16.66	19.18
Calcilutite divisions	None	None	Rare	None	Rare	Common
Dominant facies	A1.3, A1.4, A2.7, B2.1, B2.2, C2.1, C2.2, F2.1	B2.1, C2.1, C2.2, C2.3, E1.3, F2.1,	C2.1, C2.2	C2.2, C2.3	C2.2, C2.3, C2.4, D2.1, F2.1	C2.3, C2.4, D1.3, D2.3, E1.3, E2.1
Subordinate facies	C2.3, D2.1	A1.3, D1.3, D2.2, E2.1,	C2.3, D2.2	D2.2, E1.3, E2.1, F2.1	A1.3,	B1.1, C2.2, F2.1
Grain size range	silt-gravel	silt-v.c. sst.	silt-coarse sst.	silt-v.c. sst.	silt-c. sst.	Silt-m.c. sst.
Mean grain size	f	f	mf	f	f	F
Bed amalgamation (per 100 sst. Beds)	9.44	8.28	1.822	0.7	0	0.74
MTC's (per 100 sst. Beds)	3.54	0.63	0	0.1	1.95	1.48
Bioturbation intensity (%)	17.76	31.29	30.87	43.59	20.14	20.19
Ichnofabric index	4	2/6	3	4	4	3
Trace-fossil diversity	12	32	34	42	30	12
Pre-turbidite trace fossils	3	13	21	19	17.5	4
Post-turbidite trace fossils	9	15	15	23	13	9
Graphoglyptids	1	6	14	12	10.25	3
General Remarks	Lenticular, discontinuous sandstones and mud-draped scours.	Lobe sandstones are intercalated with muddy intervals of the inter-lobe	Internal sedimentary stratification poorly developed.	Tabular sheet sandstones Abundant ripple topped sandstones.	Tabular sheet sandstones with well developed internal sedimentary stratification	Tabular sheet sandstones with well developed internal sedimentary stratification

Table 7.1. Diagnostic features of distal deep-marine fan environments of the Broto and Cotefablo systems, Jaca Basin. Facies definitions after Pickering *et al.* (1986, 1989).

characterised by FA3h and FA5c, and is associated with a wide range of sediment facies, including Facies Classes A, B, C, D and F (Pickering *et al.* 1986, 1989). These deposits are punctuated by thin- to medium-thickness (decimetre to metre thick), Type II MTCs (FA1b). These MTCs typically have erosive bases, and are characterised by a sand-rich mudstone matrix, commonly with very-coarse-grained sand injections. Extra-formational pebbles and nummulites are rare. The lower net:gross upper part of the section is characterised by thin- to medium-bedded sandstone-mudstone couplets (Facies C2.2 and C2.3) typical of FA5c, as well as Facies D1.3, D2.1, D2.3 and E1.3 siltstones and mudstones.

7.2.2. Ichnology

The trace-fossil assemblage of the CLT is a low diversity, low intensity assemblage. Mean bioturbation on bedding planes is 17.58%, with 14 ichnospecies from 10 ichnogenera identified. Of these 14 ichnospecies, 11 are post-depositional and 3 are pre-depositional, including 1 graphoglyptid. The trace-fossil assemblage is dominated by *domichnia*, as well as *fodinichnia* and *pascichnia*. The most common ichnotaxa include *Scolicia* (*pascichnia*); *Thalassinoides* (*fodinichnia*); and *Ophiomorpha* (*domichnia*). In vertical section, within the turbiditic mudcaps, bioturbation is relatively high (40%), with an ichnofabric index of 4. Trace fossils are absent within sandstones, and no vertical burrows were recognised. The trace-fossil assemblage of the channel-lobe transition is characteristic of the *Ophiomorpha rudis* subichnofacies of the *Nereites* ichnofacies (*sensu* Uchman 2001) (Fig. 7.9).

The sandstones of FA3h have the highest intensity and diversity trace-fossil assemblage, however, this may be in part related to the number of bedding planes studied. These sandstones are characterised by a trace-fossil assemblage typical of the *Ophiomorpha rudis* subichnofacies with some ichnotaxa typical of the *Paleodictyon* subichnofacies. The post-depositional trace fossil *Halapoa imbricata* that occurs on the soles of beds is restricted to beds less than 48 cm thick.

7.2.3. Interpretation

According to Mutti and Normark (1987), the CLT is characterised by features related to changes that occur when gravity currents undergo an hydraulic jump or other rapid flow change associated with a change in seafloor gradient and / or a change from a channelised to non-channelised environment. Such features observed at the studied

section include mud-draped and sand-filled scours, pinch-and-swell geometries and coarse-grained, thick-bedded sandstones with relatively well developed internal stratification including mega-ripple cross-stratification. Mud-draped scours suggest the development of large-scale turbulence absent of sediment deposition implying that turbulence was sufficient enough to maintain even coarser particles within the flow after undergoing the hydraulic jump. The internal stratification of the sandstones is indicative of deposition under tractive conditions as the flow continued moving basinward. The thin-bedded nature of the Type II MTCs and paucity of extra-formational nummulites and pebbles compared to those of the Ainsa basin is probably related to the distal nature

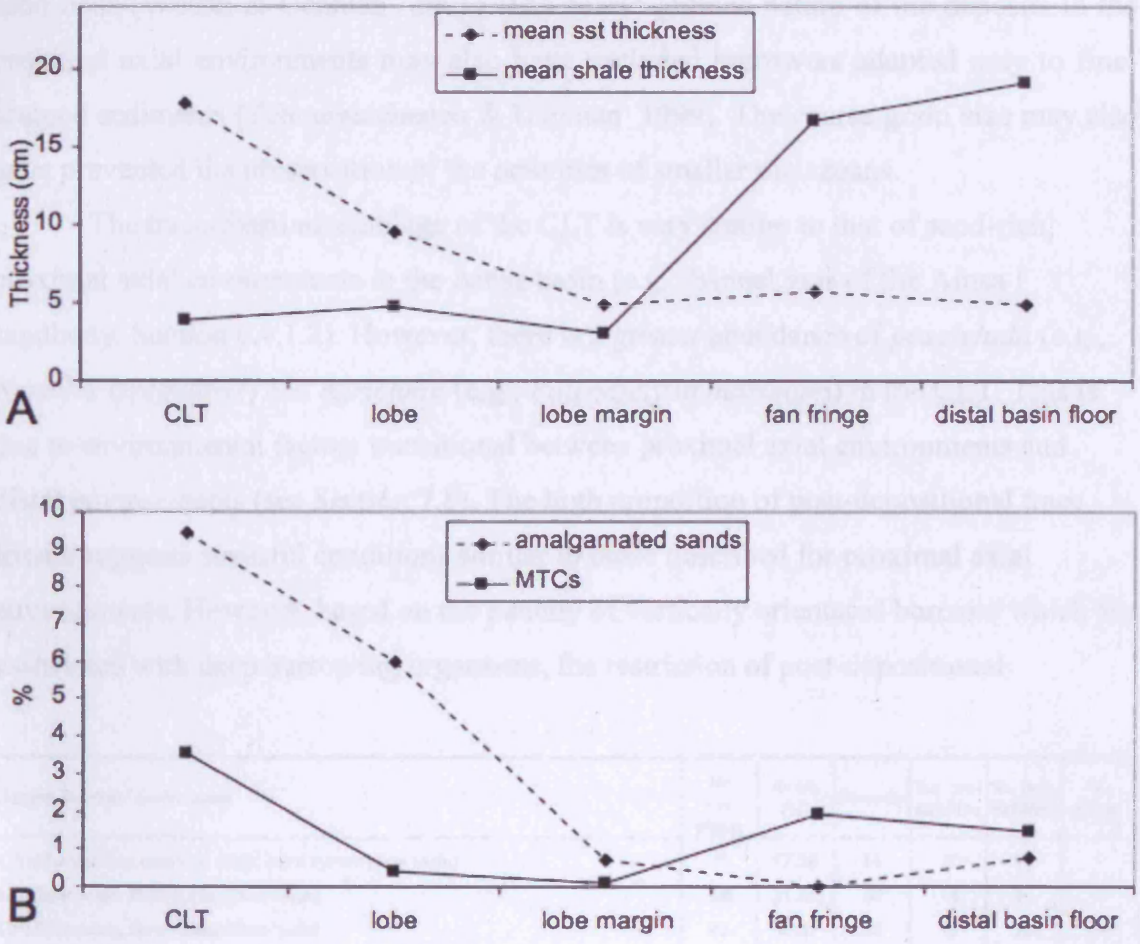

Fig. 7.1. (A) Average sandstone and mudstone thicknesses in the five fan and related environments of the Jaca basin. (B) Percentage of amalgamated sandstones and MTCs in the five fan and related environments of the Jaca basin.

of the section. The paucity of pebbles may also be related to the fact that the proximal, up-depositional-dip Arro system is characterised by low amounts of pebbles (see

Section 5.4). The deposits of the CLT of the Broto system are typical of a highly efficient system (*sensu* Mutti & Normark 1987).

The low diversity, moderately low intensity, dominantly post-depositional trace-fossil assemblage of the CLT occurs due to a number of factors. In this environment, the high intensity gravity flows tend to remove the fertile top layer of the seafloor, resulting in the preservation of only the deepest-tier trace fossils. As a consequence, pre-depositional trace fossils are rare. The CLT is dominated by trace-fossils formed by large, robust, deeply burrowing organisms (e.g., *Halopoa*, *Scolicia* and *Ophiomorpha*). These trace-forming organisms exploited organic rich layers buried within the sediment. As a consequence, they were well adapted to surviving burial by newly deposited thick sand beds (Wetzel & Uchman 2001). The coarse-grained nature of the deposits in the proximal axial environments may also have excluded burrowers adapted only to fine-grained sediments (Tchoumatchenco & Uchman 1999). The coarse grain size may also have prevented the preservation of the activities of smaller metazoans.

The trace-fossil assemblage of the CLT is very similar to that of sand-rich, proximal axial environments in the Ainsa basin (e.g. channel axis of the Ainsa I sandbody, Section 6.4.1.2). However, there is a greater abundance of *pascichnia* (e.g., *Nereites irregularis*) and *agrichnia* (e.g., *Paleodictyon maximum*) in the CLT. This is due to environmental factors transitional between proximal axial environments and distal environments (see Section 7.8). The high proportion of post-depositional trace fossils suggests stressful conditions similar to those described for proximal axial environments. However, based on the paucity of vertically orientated burrows which are associated with deep burrowing organisms, the restriction of post-depositional

Outcrop Number / Environment	No bed. planes	Av bio (%)	Diversity	No. pre-turbidite	No. post-turbidite	No. graph.
(28) Channel-lobe transition sands, Broto system (Jaca basin)	45	17.58	14	3	11	1
(29) Lobe sands, Broto system (Jaca basin)	208	31.29	30	14	16	8
(30) Lobe sands, Broto system (Jaca basin)	95	30.87	36	18	18	12
(31) Lobe-fringe sands, Cotefablo system (Jaca basin)	268	43.59	43	19	24	12
(32) Fan-fringe sands / marls, Cotefablo system (Jaca basin)	88	29.64	32	19	13	8
(33) Fan-fringe sands / marls, Cotefablo system (Jaca basin)	86	17.91	38	21	17	17
(34) Fan-fringe sands / marls, Cotefablo system (Jaca basin)	39	23.4	24	14	10	6
(36) Fan-fringe sands / marls, Cotefablo system (Jaca basin)	71	20.14	27	14	13	8
(37) Distal basin-floor marls (incl. thin sands), Cotefablo system (Jaca basin)	27	20.18	13	4	9	3

Table 7.2. Average bioturbation, trace-fossil diversity, number of pre- and post-depositional trace fossils, and the number of graphoglyptids for five fan and related

environments of the Jaca basin. The outcrop number (see Fig. 1.3 and Table 1.1) and number of bedding planes studied at each section is also recorded.

ichnotaxa such as *H. imbricata* to medium-bedded sandstones, and the relatively low intensity of bioturbation, it is postulated that interstitial waters in the CLT were characterised by lower oxygenation levels than in more proximal axial environments (cf. channel axis of the Ainsa I sandbody, Section 6.4.1.2).

7.3. Lobe

7.3.1. Sedimentology

Depositional lobes were studied in the Broto System in two sections, southeast of Broto on the road between Sarvise and Fanlo (Locality 29, Fig. 1.3; Appendix 7.2), and ~50 km basinward, north of Aragues del Puerto (Locality 30, Fig. 1.3; Appendix 7.3). The Sarvise-Fanlo section is ~76 m thick and the logged section at Aragues del Puerto is ~60 m thick. Both are incomplete sections through the Broto system. They are characterised by parallel-sided, sand-rich and mud-rich packets interpreted as depositional lobes and associated interlobes. In the Sarvise-Fanlo section, sandstones (incl. siltstones) range in thickness between 3-145 cm, averaging 9 cm (Fig. 7.1). Interbedded mudstones average 4.6 cm in thickness. At Aragues del Puerto, sandstones (incl. siltstones) range between 2-90 cm in thickness, and average 10 cm. Interbedded mudstones average 5 cm in thickness (Fig. 7.1). Mean palaeoflow at both sections is 295°. However, both sections are characterised by divergent palaeocurrents, with the soles of individual bedding planes at Aragues del Puerto displaying tool marks with up to 35° divergence.

The base of the Sarvise-Fanlo section is marked by a thick (>15 m) Type II MTC (FA1b). This deposit is characterised by a chaotic, mudstone matrix with intra-formational clast-rich breccia of variably deformed thin- to thick-bedded rafts of turbiditic sandstones and mudstones. Coarse sand injection occurs within the muddy matrix as well as extra-formational reworked nummulites. Small extra-formational well-rounded pebbles are rare. Thin packets (typically dm thick) of heterolithics above the irregular top surface of the MTC infill residual topography. The overlying sandy succession comprises sand-rich and mud-rich packets which average 4.5 m and 2.3 m in thickness respectively. A number of the sandy packets show clear coarsening- and thickening-upward sequences formed by FA5f sandstones which are overlain by FA3f

sandstones. Amalgamated beds are common within these packets, with 8% of all beds amalgamated, and organic matter is common. MTCs are very rare in the sandy succession, with only one thin (45 cm thick) type II MTC (Facies A1.3) occurring. The mud-rich packets are typically intensely bioturbated and characterised by Facies-association 6d (FA6d).

The more distal Aragues del Puerto section is characterised by less distinct sand-rich and mud-rich packets and has a higher overall net:gross. Sandy packets are characterised by FA3f and FA5f deposits, however, in general the sandstones are finer-grained than those at Sarvise-Fanlo, with Facies-association 5f (FA5f) more typical in this section. Coarsening and thickening-upward sequences over 1-3 m may be crudely developed, and muddy packets are typically thinner (~1-2 m thick) than those at Sarvise-Fanlo.

	CLT			**Lobe**		
FA	FA3	FA5	FA5	FA3	FA5	FA5
Facies		(C2.2)	(C2.3)		(C2.2)	(C2.3)
Av. Bio.	19.8	15.59	8.66	35	34.58	28.29
Diversity	9 (0.34)	8 (0.5)	3 (1)	7 (0.28)	15 (0.23)	24 (0.26)
Pre	2	0	0	0	3	9
Post	7	8	3	7	12	13
Graphs.	1	0	0	0	3	4
No Bed.	26	16	3	25	64	89
	Lobe Fringe			**Fan Fringe**		
FA	FA5	FA5	FA6	FA5	FA5	
Facies	(C2.1)	(C2.2/C2.3)		(C2.2)	(C2.3)	
Av. Bio.	17.25	45.51	44.56	11.25	35.01	
Diversity	3 (0.37)	24 (0.28)	40 (0.22)	4 (0.5)	30 (0.43)	
Pre	0	7	17	3	17	
Post	3	17	23	1	13	
Graphs.	0	4	11	1	7	
No Beds.	8	84	176	8	69	

Table 7.3. Summary of trace-fossil assemblages for different facies-associations in the CLT, lobe (Sarvise-Fanlo section), lobe fringe and fan fringe (Jasa section). Trace-fossil data includes average bioturbation, diversity (mean diversity in relation to number of bedding planes studied in brackets), number of pre- and post-depositional trace fossils, graphoglyptids and bedding planes studied. The Facies Group is used to subdivide facies-associations where necessary.

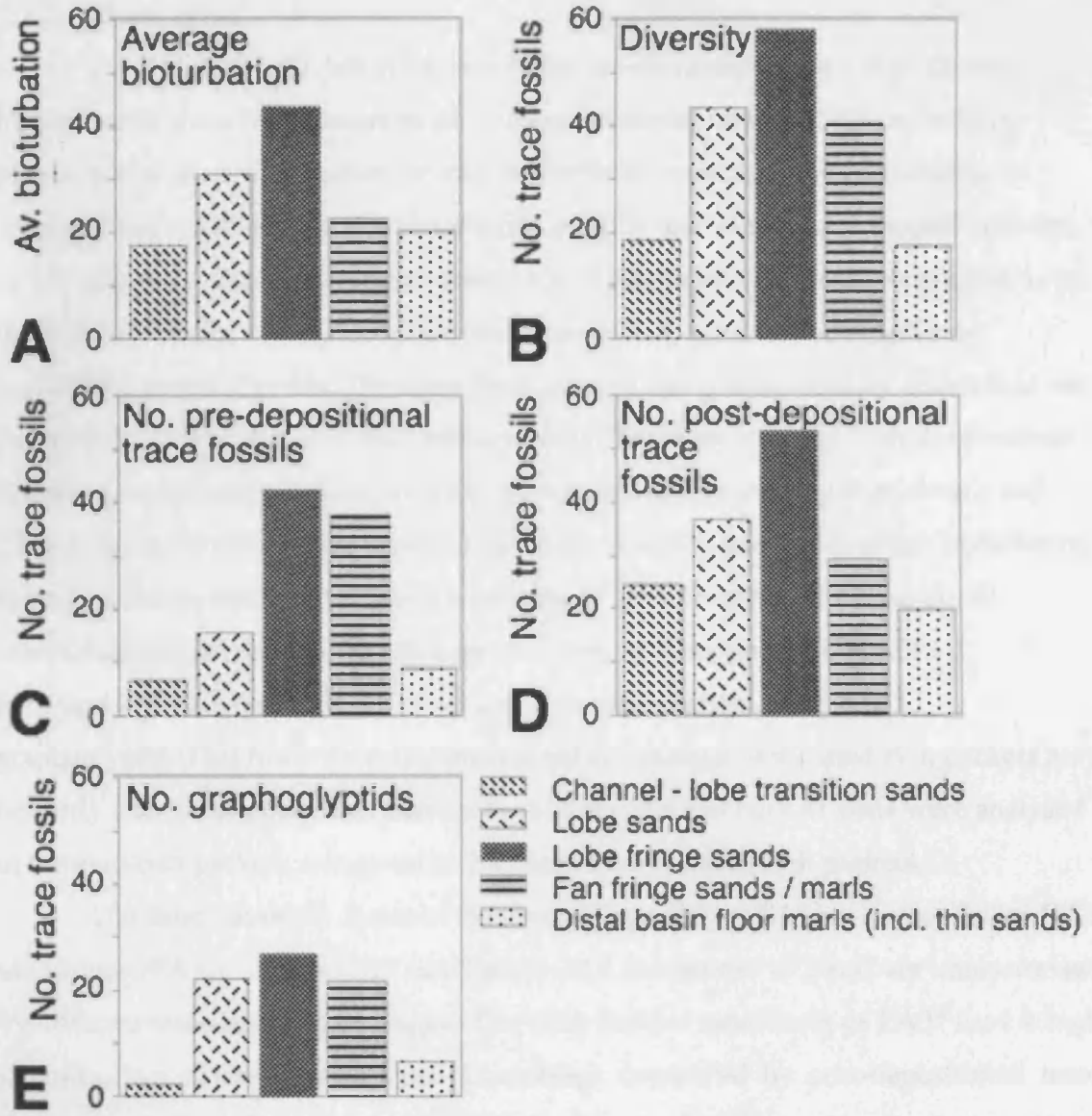

Fig. 7.2. A) Average bioturbation in fan and related environments in the Jaca basin; B) Trace-fossil diversity; C) Number of pre-depositional trace fossils; D) Number of post-depositional trace fossils; E) Number of graphoglyptids.

Amalgamated sandstones are rare, with only 1.82% of all sandstones in the sand-rich packets amalgamated. Current rippled sandstones are uncommon, and organic matter is rare. Internal stratification is typically poorly developed, with most beds being internally structureless. Erosional processes are less pronounced, with lower frequencies of scoured sandstones, amalgamated beds and mud-clasts compared to Sarvise-Fanlo. The muddy packets are characterised by FA6d fine-grained deposits. Unlike the muddy-intervals of the Sarvise-Fanlo section, these intervals are typified by low intensity bioturbation.

7.3.2. Ichnology

The depositional lobes at Sarvise-Fanlo are characterised by a high diversity, high intensity trace-fossil assemblage. Average bioturbation is 31.29% on bedding planes, whilst in vertical section, within the turbiditic mudcaps (T_e), bioturbation is relatively high, with an average bioturbation of 40%, and an average ichnofabric index of 2/6. The trace-fossil assemblage comprises 30 ichnospecies from 20 ichnogenera. Of the 30 ichnospecies identified, 16 are post-depositional and 14 pre-depositional, including 8 graphoglyptids. The trace-fossil assemblage is dominated by *domichnia* and *fodinichnia*, as well as *pascichnia* and *agrichnia*. The most common ichnotaxa include *Scolicia* (*pascichnia*); *Thalassinoides* (*fodinichnia*); *Ophiomorpha* (*domichnia*); and *Chondrites* and *Paleodictyon* (*agrichnia*). In the mud-rich packets, average bioturbation is very similar to that of the sand-rich packets, at 31%. However, the trace-fossil assemblage comprises only 13 ichnospecies from 11 ichnogenera. Of the 13 ichnospecies, 11 are post-depositional and 2 pre-depositional, including 1 graphoglyptid. This lower diversity trace-fossil assemblage of the mud-rich packets may be partly due to sampling, as a consequence of the fact that only 41 beds were analysed in the mud-rich packets, compared to 201 beds from the sand-rich packets.

The three dominant facies of the sand-rich packets at Sarvise-Fanlo; Facies C2.1 sandstones (FA3f), Facies C2.2 and Facies C2.3 sandstones of FA5f are characterised by different trace-fossil assemblages. The thick-bedded sandstones of FA3f have a high intensity, low diversity trace-fossil assemblage dominated by post-depositional trace fossils (Table 7.3). This facies-association is characterised by a trace-fossil assemblage typical of the *Ophiomorpha rudis* subichnofacies. Medium-bedded sandstones of FA5f are characterised by a higher diversity trace-fossil assemblage with a low number of pre-depositional trace fossils. The trace-fossil assemblage is typical of the *Ophiomorpha rudis* subichnofacies with some ichnotaxa typical of the *Paleodictyon* subichnofacies. The thin-bedded sandstones of FA5f are characterised by a lower intensity but higher diversity trace-fossil assemblage, with a high number of pre-depositional trace fossils. These sandstones have a trace-fossil assemblage typical of a mixed *Ophiomorpha rudis-Paleodictyon* subichnofacies.

At Aragues del Puerto, the trace-fossil assemblage is similar to that at Sarvise-Fanlo. Average bioturbation on bedding planes is 30.87%, whilst in vertical section,

Ichnotaxa/Outcrops	28	29	30	31	32	33	34	35	37
Mammillichnis aggeris	0.07								
?Bergaueria prantli					0.02				
Plug-shaped form A		0.03		0.01					
Lockeia siliquaria				0.01				0.23	
Circulichnis montanus				0.01			0.31		
Arthrophycus ?strictus		0.02							
Halopoa imbricate	0.79	0.78	0.12	1.17		0.01			
Halopoa storeana		0.05		0.02					
Hormosiroidea annulata		0.02					0.12		
Strobilorhaphe glandifer		0.05							
?Imponoglyphus isp.				0.01					
Planolites montanus	0.04						0.3		
Planolites beverleyensis			0.12	0.17					
Planolites ispp.	0.04	0.68	1.99	2.4	0.41	1.71	1.31	0.6	5.83
Palaeophycus tabularis	0.05								0.63
?Palaeophycus isp.			0.39	0.04					
Chondrites intricatus		0.9	0.23	6.11	4.09	1.27	0.89	1.54	1.11
Chondrites targionii				1.19	0.04	0.4		0.17	
Chondrites patulus			0.28		0.37	0.02		0.76	0.39
Chondrites recurvus						0.26			
Chondrites isp.	0.58	1.16	1.93	3.35	1.23	0.6	1.4	2.75	2.37
Ophiomorpha annulata	3.23	10.7	11.1	12	7.7	2.1	3.03	2.48	0.11
Ophiomorpha rudis	0.31	0.13	0.3	0.28		0.07	0.24	0.09	
Ophiomorpha isp.	0.06	0.02		0.08			0.21		
Thalassinoides suevicus	7.57		2.78	1.37	0.76	0.87	0.6	1.47	1.09
Thalassinoides ispp. indet.	0.14	5.08		0.35					
Spongeliomorpha oraviense			0.48	0.04	0.35	0.19		0.42	1.13
Phycodes palmatum		0.06							
Saerichnites abruptus					0.07		0.47	0.31	
Saerichnites canadiensis			0.05	0.01	0.05	0.03	0.27	0.24	
Saerichnites isp.					0.03				
Parahaentzschelinia isp.					0.07		0.21	0.78	0.54
Lorenzinia plana			0.05						
Lorenzinia nowaki			0.24	0.12		0.18		0.02	
Glockerichnus alata						1.14			
Zoophycos ?brianteus					0.32				
Zoophycos insignis						0.21			
Zoophycos isp.		0.09	0.09	0.43	0.14	0.3		0.25	
Phycosiphon incertum		0.16	0.51	0.74	2.78	0.28	0.2	1.3	1.17
Lophoctenium ramosum				0.07					
Nereites circinalis						0.03			
Nereites missouriensis				0.13	0.52			0.14	
Nereites irregularis	0.13	0.41	0.11	1.1	1.41	0.66	1.05	0.86	
Nereites isp.						0.19			
Scolicia prisca		0.68	0.54	0.26					
Scolicia plana			0.07	0.12					
Scolicia strozzii	1.04	0.04	1.02	0.22	0.46		0.76		
Scolicia isp.		0.83	0.13	1.1					
Taenidium ispp.				0.01					
Protovirgularia ?rugosa				0.01		0.03			
Gordia marina					0.32				
Gordia arcuata			0.03		0.27				
Cosmorhaphe lobata		0.09	0.29						
Cosmorhaphe sinuosa			0.13			0.38			
Helicolithus ramosus						0.05			
Helminthorhaphe flexuosa			0.13	0.02		0.3		0.16	
Helminthorhaphe japonica			0.05		0.37	0.33		0.08	
Helminthopsis abeli			0.03		0.08				
Helminthopsis tenuis			0.3		0.83	0.46	0.47	0.45	
Helminthopsis ispp.		0.12	0.33	0.19	0.67	0.78	0.32	0.5	
Spirohaphe involuta		0.02							
Spirohaphe isp.		0.01			0.36	0.13			
Belorhaphe zickzack		0.01					0.18		
Paleomeandron robustum				0.06					
Desmograpton dertonensis				0.04	0.44				
Desmograpton alternum							0.38		
Desmograpton ichthyforme			0.05				0.17		
Urohelminthoida dertonensis						0.43	1.15		
Urohelminthoida appendiculata							0.39		
Protopaleodictyon incompositum					0.69				
Protopaleodictyon spinata		0.09		0.05					
Protopaleodictyon bicaudatum					0.13				
Megagrapton irregulare			0.3			0.23		0.13	
Megagrapton submontanum					0.29	0.26		0.26	
Paleodictyon minimum				0.06					
Paleodictyon latum				0.02					
Paleodictyon strozzii		0.19	0.1	0.12	0.51	0.26		0.04	0.17
Paleodictyon miocenicum		0.05	0.03			0.03			
Paleodictyon delicatulum				0.06	0.07	0.11		0.02	0.72
Paleodictyon majus			0.24	0.13		0.35		0.08	
Paleodictyon goetzingeri						0.23	0.23		
Paleodictyon maximum	0.38	0.19	0.01	0.04		0.24			0.14
Paleodictyon arvense				0.73		0.06			
Arthropod trackway			0.79						

Table 7.4. Distribution of trace fossils in the Jaca basin. Individual numbers represent the areal percent of bedding planes at specific localities covered by individual ichnotaxa: (28) Channel-lobe transition sandstones, Broto system; (29) Lobe sandstones, Broto system; (30) Lobe sandstones, Broto system; (31) Lobe-fringe sandstones, Cotefablo system; (32) Fan-fringe sandstones / mudstones, Cotefablo system; (33) Fan-fringe sandstones / mudstones, Cotefablo system; (34) Fan-fringe sandstones / mudstones, Cotefablo system; (36) Fan-fringe sandstones / mudstones, Cotefablo system; (37) Distal basin-floor mudstones (incl. thin sandstones), Cotefablo system.

bioturbation is 51%, with an average ichnofabric index of 3. The trace-fossil assemblage consists of 36 ichnospecies from 20 ichnogenera. Of these 36 ichnospecies, 18 are pre-depositional, and 18 are post-depositional, including 12 graphoglyptids. The most common ichnotaxa include *Planolites, Lorenzinia, Nereites, Scolicia* and *Helminthopsis* (*pascichnia*), *Thalassinoides, Spongeliomorpha* and *Phycosiphon* (*fodinichnia*), *Ophiomorpha* (*domichnia*) and *Chondrites, Cosmorhaphe, Helminthorhaphe* and *Paleodictyon* (*agrichnia*). In terms of specific trace-fossil occurrences in the lobe, a number of ichnotaxa are unique to this environment, including *Arthrophycus ?strictus*, (Sarvise-Fanlo) *Spirohaphe involuta* (Sarvise-Fanlo) and *Lorenzinia plana* (Aragues del Puerto). The lobe is also the most proximal environment in which *Protopaleodictyon* is recognised and the most distal environment in which *Phycodes palmatum* and *Cosmorhaphe lobata* occur. Like in the CLT, there is a paucity of vertically orientated burrows. Post-depositional trace fossils typical of proximal axial environments such as *Ophiomorpha rudis*, *Halopoa*, and *Planolites* are less common in the lobe environment compared to more proximal environments, with *Halopoa* being particularly rare in the more distal Aragues del Puerto section. The lobes of the Jaca basin exhibits an assemblage more typical of the *Paleodictyon* subichnofacies, with some trace fossils such as *Ophiomorpha rudis* and *O. annulata* typical of the *Ophiomorpha rudis* subichnofacies (Fig. 7.9).

7.3.3. Interpretation

Although both outcrops are not sufficiently extensive to recognise convex-upward lobate geometry, the alternating mud-rich and sand-rich packets, and the occurrence of coarsening and thickening-upward sequences and divergent palaeocurrents in the sand-rich packets are the main evidence for interpreting these sections as depositional lobes (and associated interlobe).

The low frequency of MTCs within the lobes compared to the CLT is probably related to the capacity of the depositing flows to flow such distances. These MTCs were deposited by cohesive debris flows, and are probably the distal expression of the type II MTCs described by Pickering and Corregidor (2005a, b) from the Ainsa basin. The absence of MTCs in the Aragues del Puerto section is probably related to its distal location on the submarine fan. It is probable that the debris flows did not have the capacity to flow such distances down the system.

Although the lobes represent the depositional zone of the turbidite system, most gravity currents contained grain populations that were transported farther basinwards. This is indicated by the lithological divisions of the beds, with sandstones overlain sharply by mudstones. This suggests the bypass of the intermediate grain-sizes transported within the turbidity current. The internal stratification of the lobe sandstones, as well as the well-developed current ripples at the Sarvise-Fanlo section, are indicative of deposition under tractive conditions as the flow continued moving basinward. The paucity of evidence of erosional processes at Aragues del Puerto compared to Sarvise-Fanlo, is probably indicative of the more erosive nature of the sediment gravity flows in the more proximal Sarvise-Fanlo section. However, compared to the CLT, erosional processes are less pronounced in the lobe.

The two sections are probably from different stratigraphic positions within the Broto System, with the more distal Aragues del Puerto section positioned stratigraphically near the base of the Broto System and the more proximal Sarvise-Fanlo section from the upper part of the Broto System. The more distal lobes at Aragues del Puerto are higher net:gross than at Sarvise-Fanlo. This is due to the fact that the lower part of the Broto system has been interpreted as a basal lowstand system characterised by sandy, thick-bedded lobes (Mutti 1992), whilst the upper part of the Broto system has been interpreted as being an upper receding transgressive system characterised by muddy, thin-bedded lobes.

The high diversity, high intensity trace-fossil assemblage of the lobe occurs as a consequence of a number of factors. In the lobe, the mixture of coarse-grained, medium-bedded sandstones as well as thin-bedded, fine-grained sandstones means that a mixed trace-fossil assemblage occurs. Trace fossils formed by organisms adapted to coarse-grained substrates (e.g., *Ophiomorpha*) occur as well as those produced by burrowers adapted only to fine-grained sediments (e.g., graphoglyptids). This is illustrated with the variations in the trace-fossil assemblages in the different sandstone facies. Facies-association 3f (FA3f) has a trace-fossil assemblage similar to the CLT or proximal axial environments, such as the channel axis, dominated by deeply burrowing, robust trace-forming organisms, which were able, to survive burial by the thick erosive sands associated with this facies-association. The absence of pre-depositional trace-fossils may be associated with the erosive nature of the deposits, as well as potentially unstable conditions, such as high sediment accumulation rates, which may have prevented the establishment of equilibrium communities between turbidite deposition. The trace-fossil

assemblage of these thick-bedded sandstones differs to those in more proximal and axial environments (e.g., Ainsa I sandbody, see Section 6.4.1.2) due to the smaller size of the *Ophiomorpha annulata* burrows, as well as paucity of *Ophiomorpha rudis* and a high proportion of *Chondrites*. The increased diversity and intensity trace-fossil assemblages of the medium- and thin-bedded sandstones (Facies C2.2 and C2.3 respectively) of FA5f, is related to the reduced thickness and grain size of the deposits compared to those of FA3f, which enabled more organisms to survive burial and also increased the preservation potential of pre-depositional traces. The paucity of erosive high concentration turbidity currents and inferred lower sedimentation rates associated with Facies-association 5f (FA5f) suggests that equilibrium communities were able to become well established between turbidite deposition, and had a high preservation potential. The marked increase in trace-fossil diversity and number of graphoglyptids at Aragues del Puerto compared to Sarvise-Fanlo is related to the increased frequency of weakly erosive, Facies C2.3 sandstones.

The increase in *Chondrites,* decrease in the diameter of *Ophiomorpha annulata* burrows, the paucity of deep vertically orientated burrows within the sandstones, and the low amount of endostratal *pascichnia* such as *Halopoa*, which did not maintain open connections to the seafloor, suggests that the lobe may have been characterised by reduced oxygenation compared to more proximal and axial environments such as the channel axis.

7.4. Lobe fringe

7.4.1. Sedimentology

The lobe fringe was studied in the Cotefablo system, at a road cutting between Broto and Biescas, immediately west of the Cotefablo tunnel (Locality 31, Fig. 1.3) in an 88 m thick section. It is characterised by tabular, laterally extensive sheet sandstones. The beds in the lobe fringe are typically bipartite, consisting of a sand and mud division. Rarely, some beds are tripartite, comprising a sand division, a very thin (<3 cm) sand-silt division, and an upper mud division. Mean sand thickness (incl. silt) is 4.85 cm, whilst mean thickness of the mud division is 3 cm. Amalgamated beds are rare, with 0.7 of every 100 beds amalgamated. Palaeoflow is towards 280°.

Similar to the lobe, the lobe fringe is characterised by sand-rich packets (lobe fringe) and mud-rich packets (interlobe). The sand-rich packets are associated with

Facies-association 5g (FA5g) thin- to medium-bedded and rarely thick-bedded sandstones, which consist of Facies C2.1, C2.2 and C2.3 sandstones. These packets range between 2.5-6 m in thickness and typically the sandstones show no thinning- or thickening-upward sequences, or may rarely form coarsening- and thickening-upward sequences. The mud-rich packets are less distinct than in the lobe, and are between 1.5-6 m thick and characterised by FA6f fine-grained deposits.

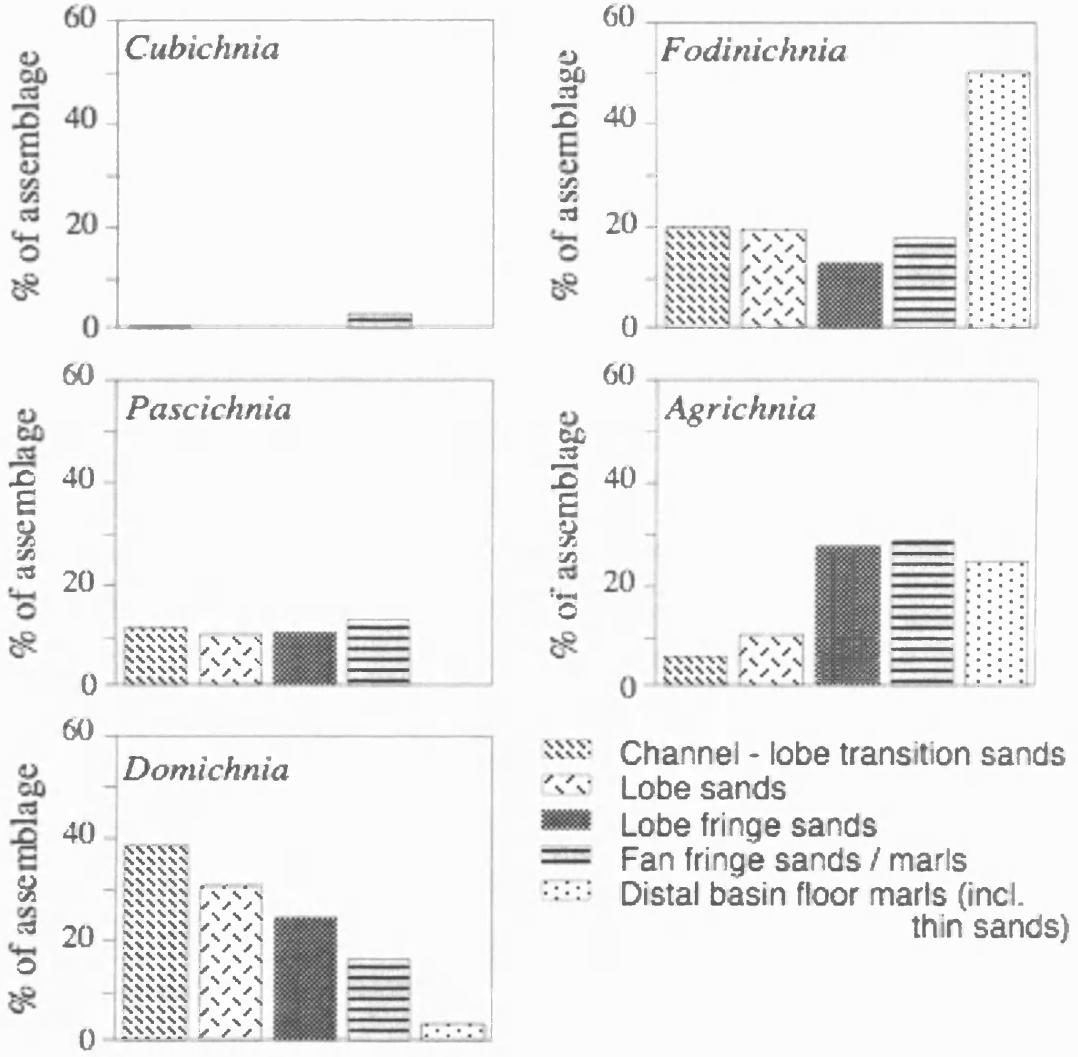

Fig. 7.3. The proportion of *cubichnia, pascichnia, fodinichnia, domichnia* and *agrichnia* in the trace-fossil assemblages of individual fan and related environments in the Jaca basin.

Only one MTC was observed in the studied section (FA1a). The deposit is 280 cm thick, with an erosive base with cut-down of up to 50 cm. It contains intra-formational, irregular shaped sand rafts up to 100 cm in diameter and smaller (<10 cm diameter), rounded sand clasts, in a chaotic muddy matrix. The sandstone underlying the MTC has

been jacked up by the depositing flow. A similar structure has been described within the Banaston system in the Ainsa basin by Pickering and Corregidor (2005a, Fig. 13).

7.4.2. Ichnology

The lobe fringe is characterised by a very high diversity, very high intensity trace-fossil assemblage. Average bioturbation is 43.59% on bedding planes, whilst in vertical section, within the turbiditic mudcaps (T_e), bioturbation is relatively high, with an average bioturbation of 43%, and an average bio-deformation index of 3. The trace-fossil assemblage is the most diverse in the Ainsa-Jaca basin, consisting of 43 ichnospecies and 25 ichnogenera. Of the 43 ichnospecies identified, 24 are post-depositional and 19 pre-depositional, including 12 graphoglyptids. The trace-fossil assemblage is dominated by *domichnia* and a*grichnia*, as well as *pascichnia* and *fodinichnia.* The most common ichnotaxa include: *Planolites, Nereites, Scolicia* and *Helminthopsis* (p*ascichnia*); *Thalassinoides, Phycosiphon* and *Zoophycos* (*fodinichnia*); *Ophiomorpha* (*domichnia*); and *Chondrites* and *Paleodictyon* (*agrichnia*). There is a paucity of vertically orientated trace fossils within the sandstones. The lobe fringe has an assemblage typical of the *Paleodictyon* subichnofacies with some ichnotaxa more typical of the *Ophiomorpha rudis* subichnofacies (Fig. 7.9).

The Facies C2.1 sandstones of FA5g are characterised by a low intensity, low diversity trace-fossil assemblage dominated by post-depositional trace fossils (Table 7.3). These sandstones have a trace-fossil assemblage typical of the *Ophiomorpha rudis* subichnofacies. The Facies C2.2, and more rarely, Facies C2.3 sandstones of FA5g have a high intensity, moderately high diversity trace-fossil assemblage with trace-fossils typical of the *Ophiomorpha rudis* subichnofacies with some ichnotaxa more typical of the *Paleodictyon* subichnofacies. Very-thin-bedded sandstones siltstones and mudstones of FA6f are characterised by a high intensity, high diversity trace-fossil assemblage, with a high number of pre-depositional trace fossils. The trace-fossil assemblage is typical of the *Paleodictyon* subichnofacies with some ichnotaxa typical of the *Ophiomorpha rudis* subichnofacies.

In terms of specific trace fossils, a number of ichnotaxa are unique to the lobe fringe including ?*Imponoglyphus* isp., ?*Palaeophycus isp., Taenidium* ispp. and *Paleomeandron robustum.* The lobe fringe is also the most proximal environment in which *Lockeia siliquaria, Circulichnis montanus, Chondrites targionii, Protovirgularia* ?*rugosa* and *Desmograpton dertonensis* occur and is the most distal environment in

which *Halopoa storeana, Lophoctenium ramosum, Scolicia prisca, Sc. Plana, Sc.* isp., and *Protovirgularia ?rugosa* occur.

7.4.3. Interpretation

The lobe-fringe sandstones of the Cotefablo system are generally thinner, finer grained and less amalgamated than lobe sandstones of the Broto system (Fig. 7.1). Despite the fact that lobe sandstones of the Cotefablo system were not studied, it is reasonable to assume that they are similar to those studied in the Broto system. Like in the lobe, the bipartite nature of many beds as well as well developed current ripples and cross-stratification indicate that part of the turbidity flow bypassed this area of the fan. However, the occurrence of poorly developed thin sand-silt divisions indicates increased deposition of the finer constituents of the flow compared to the lobe environment. The mean mudstone thickness in the lobe fringe of the Cotefablo system is less than that of the lobes of the Broto system (Fig. 7.1). This is probably related to differences in sediment supply and sedimentation rates between the sections studied in the Broto and Cotefablo systems. From general field observations, the lobe fringe of the upper part of the Broto system stratigraphically similar to the Sarvise-Fanlo section is characterised by thinner bedded sands and thicker mudstone divisions than the lobe.

The high intensity, high diversity trace-fossil assemblage is related to a number of factors; in the lobe fringe, a mixture of mudstones and fine to coarse-grained sandstones supports both trace-forming organisms suited to coarse substrates as well as those adapted to fine-grained substrates. An inferred lower nutrient supply probably resulted in the development of more specialist feeding strategies such as graphoglyptids resulting in a greater trace-fossil diversity. The high number of pre-depositional trace fossils suggests that long-term stable ecological conditions were established between turbidite deposition. This high number of pre-depositional trace fossils, including shallow-tier graphoglyptids, is also related to an increase in preservation potential of shallow-tier burrows, due to the low frequency of Facies C2.1 sandstones deposited by erosive high concentration turbidity currents. A decrease in sediment accumulation rates compared to the lobe may also have enabled organisms longer time to migrate and colonise the newly deposited sediment, resulting in increased bioturbation intensities. In terms of trace-fossil assemblages in specific facies-associations/facies, the lobe fringe has a similar trend to that of the lobe, with an increase in trace-fossil diversity as well as proportions of pre-depositional trace fossils from Facies C2.1 sandstones of FA5g to

Facies C2.3 sandstones of FA5g and FA6f, albeit with a higher diversity than the lobe sandstones. This is probably related to similar controlling factors on the trace-fossil assemblages.

7.5. Fan fringe

The fan fringe of the Cotefablo system was studied southeast of Hecho at four sections; on the road between Hecho and Urdués (Locality 34, Fig. 1.3; Appendix 7.7), at the village of Urdués (Locality 33, Fig. 1.3; Appendix 7.6) along the road east of Jasa (Locality 32, Fig. 1.3; Appendix 7.5) and between Hecho and Anso, at Puerto d' Anso (Locality 35, Fig. 1.3; Appendix 7.8).

7.5.1. Sedimentology

The fan fringe consists of tabular, laterally extensive sheet sandstones. A number of sedimentary features are characteristic of the fan fringe, including: (1) abundance of MTCs; (2) abundance of flow reflected sandstones (Facies C2.4); and (3) occurrence of medium-bedded sandstones overlain by thick mudstones. Sandstones range between 2-36 cm in thickness, and average 5.68 cm. Interbedded mudstones average 16.66 cm in thickness. Amalgamated sandstones are absent (Fig. 7.1).

The fan fringe is characterised by FA5h thin- to thick-bedded, fine- to coarse-grained sandstones, as well as FA1d chaotic sandstones. No thinning- or thickening-upward sequences are developed. One of the main characteristics of the fan fringe is the relative abundance of MTCs, with 1.95 MTCs occurring for every 100 beds logged (Fig. 7.1). A number of MTCs comprise mud-rich sandstones which overlie mud-poor turbiditic sandstones (FA1d). However, there is also an abundance of MTCs similar to the Type II MTCs of Pickering and Corregidor (2005a, b) (FA1b). These deposits average 73 cm in thickness and have a muddy, chaotic matrix with a relatively high sand content (<50%). Some deposits characterised by a fine-grained muddy matrix have coarse sand grains injected throughout the matrix. The base of the deposits is flat to erosive, and the top is irregular. Extra-formational material such as small (<5 cm) pebbles, nummulites and shells are common as well as intra-formational mud-clasts and more rarely, sand rafts. A number of the Type II MTCs are overlain by thick structureless mudstones. These mudstones may be genetically related to the underlying deposits forming bipartite deposits.

Sandstones with evidence of flow reversals (reflected) during deposition are also very common in the fan fringe (Facies C2.4), and particularly well developed at the Urdués section (Fig. 7.4). Mega-ripples at the top of beds commonly cross-cut one another indicating deposition by contained turbidity currents (Pickering & Hiscott 1985). Two beds were studied in detail at Urdués, beds 9 and 13. Bed 9 is 13 cm thick, with a 7 cm mud cap, whilst bed 13 is 19 cm thick with a 10 cm mud cap. Both bed 9 and 13 are normally graded, with medium-grained, planar stratified bases and fine-grained cross-stratified tops. Sole marks are absent. The mega-ripples have a wavelength between 30-75 cm and amplitude of 4-8 cm. The values for the ripple form index (wavelength/amplitude ratio) range from ~5-9. Crests are slightly rounded, asymmetrical to symmetrical, and tend to have gently dipping up-current slopes (4-7°) and more steeply dipping down-current slopes (22-23°). In plan form, the crests are laterally continuous and commonly sinuous. Mega-ripples of bed 13 indicate palaeocurrent directions of 270° whilst on bed 9, mega-ripples indicating flows towards 120° are cross-cut by mega-ripples indicating later flows towards 040°. The mega-ripples of bed 13 were probably formed by primary turbidity currents. The dominant palaeoflow in the fan fringe is towards 290°.

7.5.2. Ichnology

The fan fringe is characterised by a high diversity and intensity trace-fossil assemblage. Average bioturbation ranges between 17.91% at Urdués to 29.64% at Jasa, with trace-fossil diversity ranging between 24 (Hecho-Urdués) to 38 (Urdués). At Urdués, the trace-fossil assemblage consists of 17 post- and 21 pre-depositional ichnotaxa, as well as 17 graphoglyptids. At Jasa, where trace-fossil diversity is slightly less with 32 ichnospecies from 20 ichnogenera, 13 post-depositional, 19 pre-depositional, and 8 graphoglyptids were recognised. The least diverse trace-fossil assemblage is the Hecho-Urdués section, consisting of 10 post- and 14 pre-depositional trace fossils, as well as 6 graphoglyptids. At Puerto d' Anso, average bioturbation is 20.14% on bedding planes. The trace-fossil assemblage comprises 27 ichnospecies from 16 ichnogenera. Of the 27 ichnospecies identified, 13 are post-depositional and 14 pre-depositional, including 8 graphoglyptids.

The trace-fossil assemblage of the fan fringe is dominated by a*grichnia, domichnia* and *fodinichnia* as well as some *pascichnia.* Common ichnotaxa include

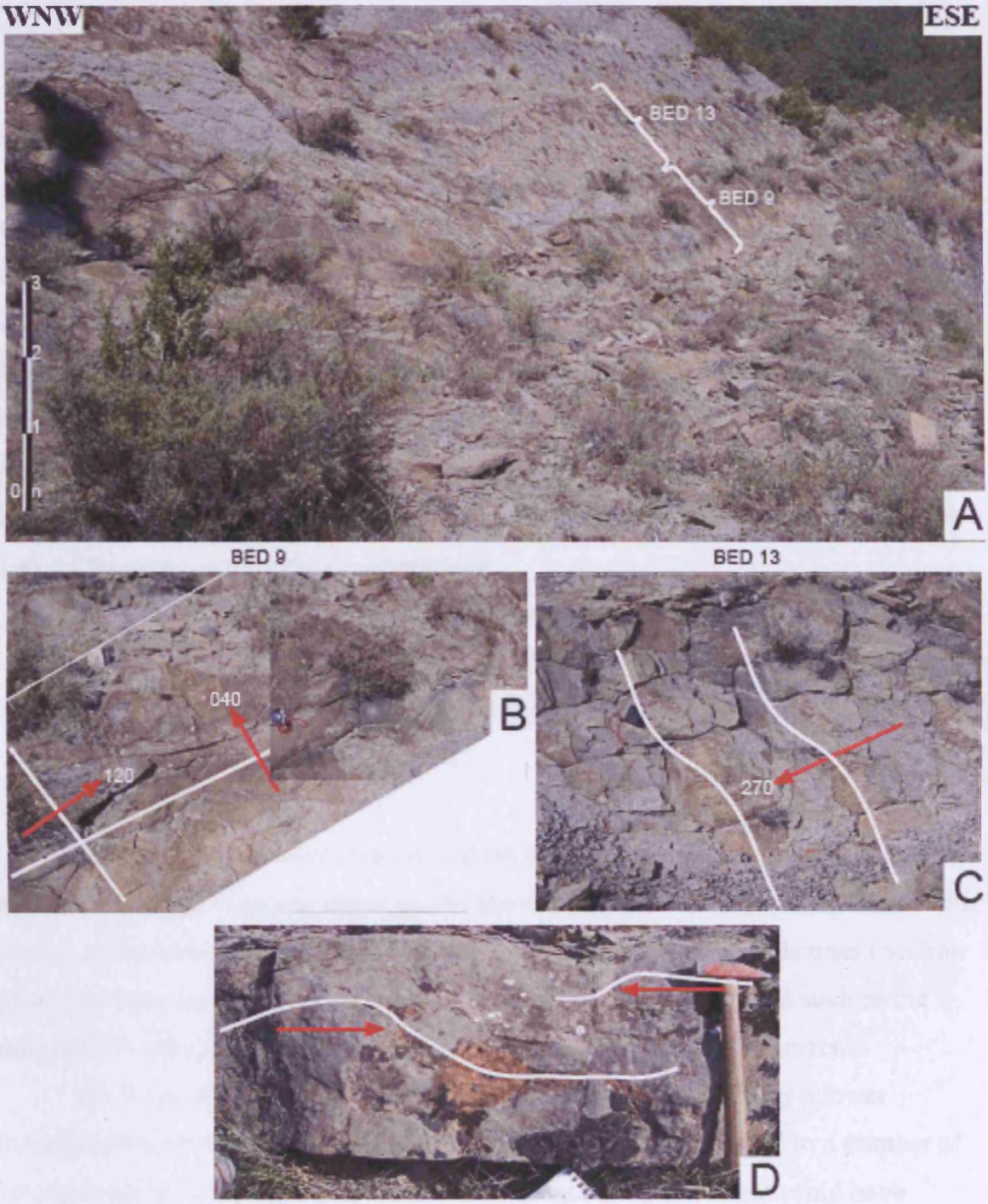

Fig. 7.4. Flow reflection facies (Facies C2.4), fan fringe, Urdues (Locality 33, Fig. 1.3). (A) General view of mega-ripples on bedding planes; (B) Cross-cutting mega-ripples on bed 9, indicating palaeoflows of 120 and 040; (C) Mega-ripples on bed 13 with sinuous crests and palaeoflows of 270; (D) Mega-ripples within a bed indicating deposition by currents flowing in opposite directions.

Planolites, Nereites and *Helminthopsis* (*pascichnia*); *Thalassinoides, Zoophycos* and *Phycosiphon* (*fodinichnia*); *Ophiomorpha annulata* (*domichnia*); and *Chondrites, Urohelminthoida,* and *Paleodictyon* (*agrichnia*). The fan fringe has an assemblage typical of the *Paleodictyon* subichnofacies (Fig. 7.9).

Like the other fan and related environments of the Jaca basin, individual facies at the Jasa section have distinctive trace-fossil assemblages. Facies C2.2 sandstones are characterised by a low intensity, low diversity trace-fossil assemblage with a mixture of both pre- and post-depositional trace fossils (Table 7.3). These sandstones are characterised by abundant *Ophiomorpha annulata* with a trace-fossil assemblage typical of a mixed *Ophiomorpha rudis-Paleodictyon* subichnofacies. The Facies C2.3 sandstones have a high intensity moderately high diversity trace-fossil assemblage dominated by pre-depositional trace-fossils, with a mixed *Paleodictyon-Ophiomorpha rudis* subichnofacies trace-fossil assemblage.

In terms of specific trace fossils, a number of traces are unique to the fan fringe including *?Bergaueria prantli, Glockerichnus alata, Zoophycos ?brianteus, Helicolithus ramosusm, Protopaleodictyon* and *Urohelminthoida.*

7.5.3. Interpretation

The thick mudstone intervals of the fan fringe which were deposited by the slow-moving dilute turbulent upper part of the turbidity current may be associated with ponding of the turbidity currents. Correspondingly, flow reflected sandstones (Section 7.5.4) may have formed as a consequence of a nearby topographic high such as the basin margin, which caused the reflection and ponding of the gravity currents.

The trace-fossil assemblage of the fan fringe is characterised by a lower diversity and bioturbation intensity than the lobe fringe. This is related to a number of factors; Ponding of the finer-grained elements of the turbidity current could have resulted in the formation of thick accumulations of soupy soft muds (soupground substrate) which may have been unfavourable to many trace-forming organisms. The destabilising nature of the reflected flows on a trace-fossil community that was probably adapted to stable conditions may also have influenced the nature of the trace-fossil assemblage. The abundance of fine-grained sands may also have excluded burrowers adapted to medium- or coarse-grained sediments resulting in lower abundances of trace-fossils more typical of coarse-grained substrates, such as those of the *Ophiomorpha*

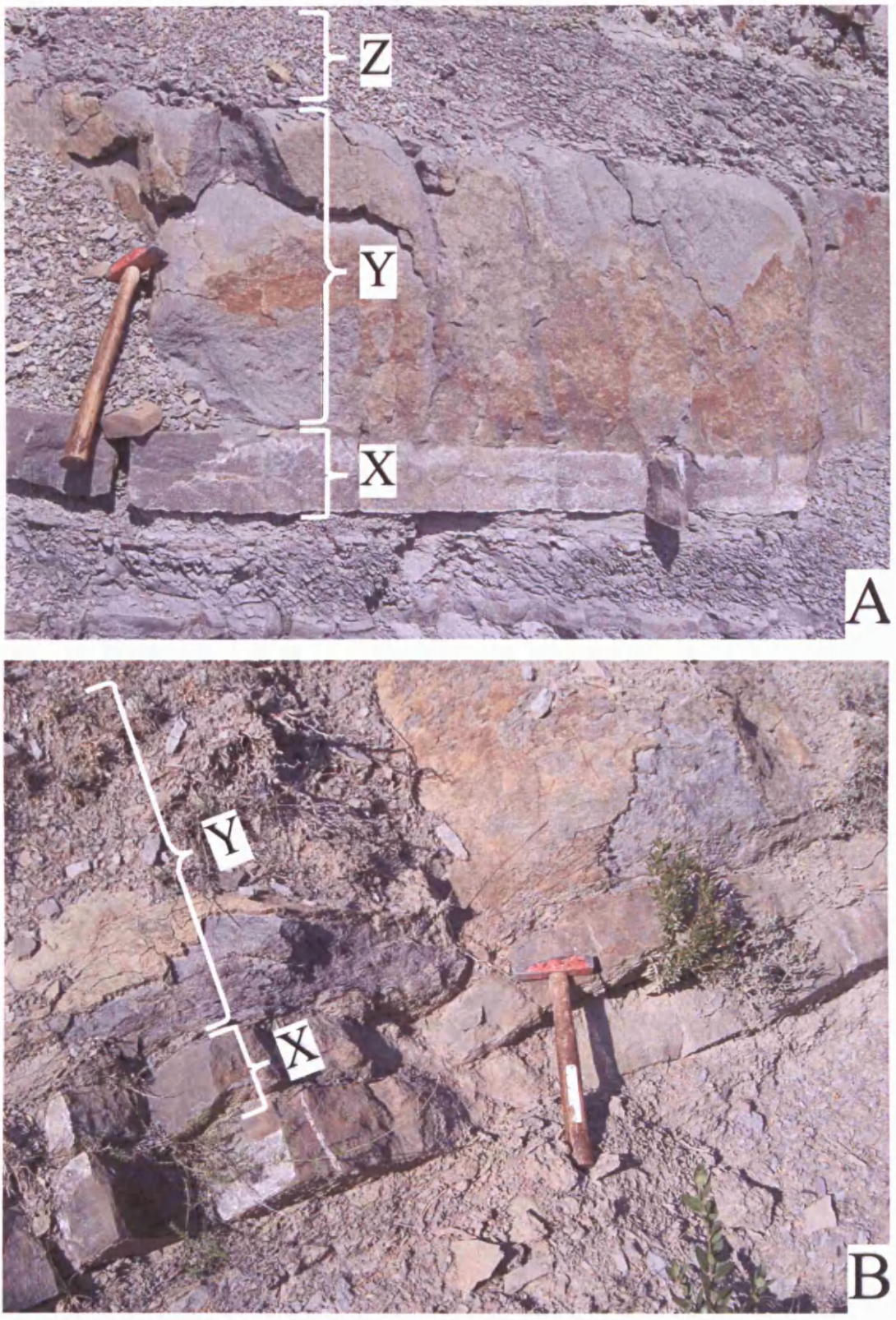

Fig. 7.5. FA1d Mud-poor turbidite sandstones and mud-rich chaotic sandstones. (A) Chaotic sandstone (Facies C1.1) (Y) underlain by turbiditic sandstone (Facies C2.2) (X) and overlain by graded mudstone (Facies E2.1) (Z), fan fringe, Jasa (Locality 32, Fig. 1.3); (B) Chaotic sandstone (Y) overlaying turbiditic sandstone (X), distal basin floor, Anso-Roncal (Locality 37, Fig. 1.3).

rudis subichnofacies. The lower intensity of bioturbation may also be related to decreased oxygenation in this distal fan setting. However, the tiering profile with relatively deep tier traces such as *O. annulata* and *Planolites* suggests that oxygen levels were still relatively high.

7.5.4. Discussion

The Facies C2.4 sandstones with evidence of flow reversals (reflected) during deposition are similar to those described by Pickering and Hiscott (1985). They interpreted such facies as the deposits of large volume, high concentration turbidity currents confined within small basins, such that multiple deflections and reflections of the initial current occur during deposition of the sand-silt load. Remacha *et al.* (2005) interpreted flow-reflected deposits in the Banaston system in the Jaca basin as being indicative of basin plain (= distal basin floor in this thesis) environments in the Jaca basin. They interpreted similar deposits as having been deposited by flows undergoing multi-source reflections. It was concluded that flows firstly encountered the southern basin margin. The lower higher-intensity part of the flow was deflected and continued evolving with a simple waning behaviour, whilst the upper lower-intensity part of the flow was reflected and changed to a composite waning flow. This flow is interpreted to have also reflected off the northern margin. Successive reflections by both margins and also from the western closure of the basin (structural rise related to the Oroz-Betulu thrust) led to ponding in this part of the basin.

A paradox of the fan fringe is the abundance of MTCs compared to more proximal fan and related environments in the Jaca basin (Fig. 7.1). Only the CLT of the Broto system has more MTCs than the fan fringe of the Cotefablo system. It can be argued that this is simply a function of the stratigraphic sections studied, with more proximal environments studied essentially from the Broto system and more distal environments from the Cotefablo system. Thus the relative abundance of MTCs in the fan fringe of the Cotefablo system may simply be due to the fact that MTCs are more common in the Cotefablo system than the Broto system. However, due to the fact that only one MTC was observed in the lobe fringe of the Cotefablo system, and general field observations revealed no significant differences in the frequency of MTCs in depositional lobes of the Cotefablo and Broto systems, it is reasonable to conclude that the fan fringe contains a higher number of MTCs than the lobe fringe and lobe in the Jaca basin.

The second paradox of the fan fringe is that MTCs at Urdues (Locality 33, Fig. 1.3) can be distinguished from other MTCs in the Jaca basin by their abundance of extra-formational material such as pebbles, nummulites and shell fragments. Deposits in the Jaca basin which contain extra-formational material are observed only in the CLT and fan fringe. If it is assumed that the debris flows which deposited the MTCs were derived from the same source as the other gravity flows of the Jaca basin, then it must be questioned as to why extra-formational shelf-derived material is absent in the more proximal lobe and lobe-margin MTCs. It is therefore concluded that these MTCs are probably locally sourced, from a nearby submarine high or basin margin. The abundance of Facies C2.4 sandstones indicates the existence of a nearby topographic high such as the basin margin. These reflected depositional turbidity currents may have generated the collapse of the margins and the formation of MTCs. The MTCs probably originated from the same shallow water platform to the north and south of the basin from where many of the carbonate-rich megabeds were sourced from (see Section 1.2.2.2). However, not all the MTCs were sourced from local topographic highs, with the chaotic mud-rich sandstones of FA1d interpreted as having been transported basinally through the Ainsa basin from the southeast.

7.6. Distal basin-floor

The distal basin-floor was studied at two localities in the Cotefablo system. From proximal to distal: Hecho (Locality 36, Fig. 1.3; Appendix 7.9) and west of Anso (Anso-Roncal section, Locality 37, Fig. 1.3; Appendix 7.10).

7.6.1. Sedimentology

The distal basin floor is characterised by thin-bedded, fine-grained, tabular, laterally extensive sheet sandstones with thick mudstones and calcilutites (marly limestones) (FA6g), as well as a relatively high number of FA1d MTCs (Fig. 7.1). These deposits can typically be divided into a number of divisions (or facies). The lower division is characterised by thin-bedded sandstones which are typically overlain by a sandstone-siltstone division. These are overlain by thick mudstones, which may be overlain by a calcilutite division (see Section 4.17.7).

At the more proximal Hecho section, the sandstones average 5.94 cm in thickness, and are a maximum of 30 cm thick. The overlying lithological divisions

including siltstones, mudstones and calcilutites average 17.59 cm in cumulative thickness. At the more distal Anso-Roncal section, sandstones average 5.04 cm in thickness and are a maximum of 50 cm thick. Overlying fine-grained lithological divisions average 20.15 cm in cumulative thickness. Calcilutites are more common at Anso-Roncal, where they range in thickness between 3-19 cm, with a mean thickness of 6.72 cm. Tool marks indicate palaeoflow was towards 290° / 300°.

7.6.2. Ichnology

The distal basin floor has a moderate diversity and intensity trace-fossil assemblage. The lithological divisions of the turbidite beds have distinct trace-fossil signatures (Fig. 7.6). In vertical section, the most intense bioturbation occurs in the sandstone-siltstone division. Average bioturbation is approximately 50%, with a typical ichnofabric index of 4. Bioturbation is relatively high in the mudstone division (T_e), with an average bioturbation of 28-40%, and a typical ichnofabric index of 3 or 4, whilst within the sandstone and calcilutite divisions, bioturbation is very low, with an average bioturbation of between 14-21%, and a typical ichnofabric index of 2 or 3. However, in the distal Anso-Roncal section, unlike the Hecho section, calcilutites are intensely bioturbated, with average bioturbation ranging between 35-50%, and a typical ichnofabric index of 3 or 4. On bedding planes, average bioturbation is moderately high, with an average bioturbation of 20%. Within the sandstones, there are abundant vertical to sub-vertical burrows. Where sandstones immediately overlie calcilutites, average bioturbation on the soles of beds is typically lower than when sandstones overlie mudstone divisions, reflecting the lower intensity of bioturbation in the calcilutites. Post-depositional trace-fossils associated with newly deposited turbidite sandstones such as *Planolites* and *Thalassinoides* commonly bioturbate the top few centimetres of the underlying mudstones and calcilutites. Laminated siltstones are characterised by a lower average bioturbation than the sandstone-siltstone division, and the trace fossils are generally smaller, with *Chondrites* (*agrichnia*) and *Phycosiphon* (*fodinichnia*) being most common. Beneath thicker sandstones, bioturbation is generally more intense, with large-scale, uncompacted, well-defined *Thalassinoides* networks developed up to 40 cm beneath the turbidite sandstones. In general, thicker-bedded sandstones are associated with more intense surrounding bioturbation.

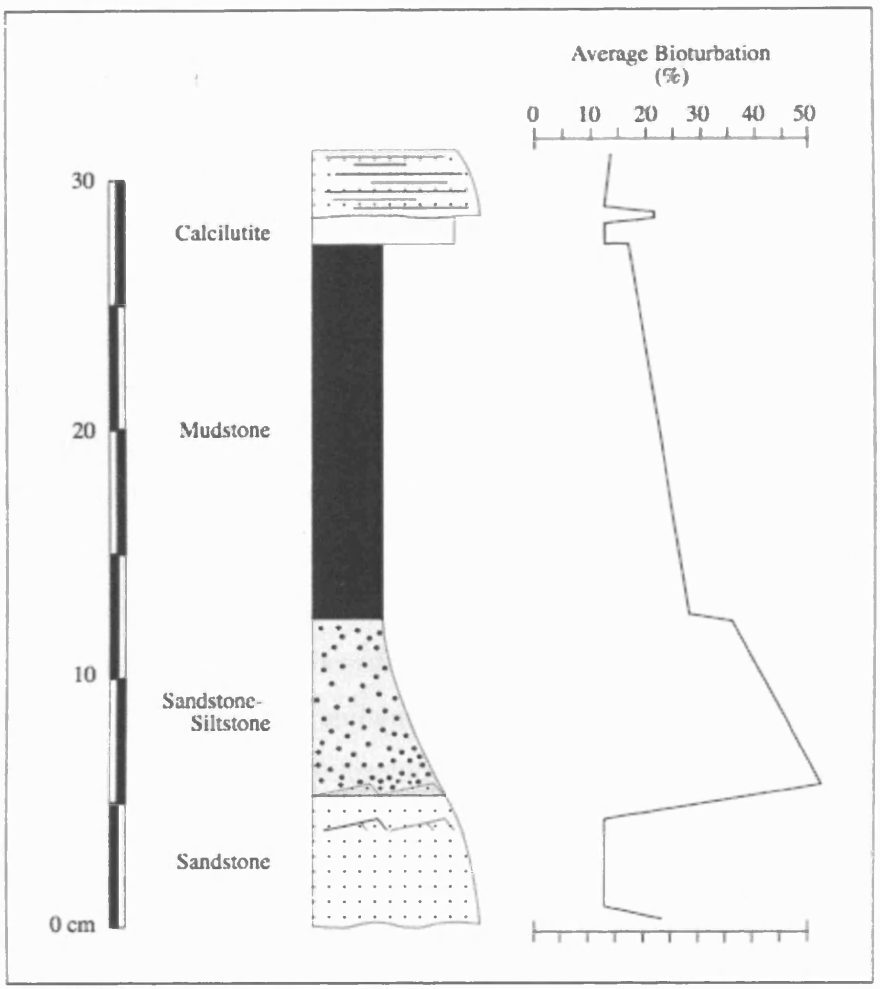

Fig. 7.6. Typical lithological divisions in the distal basin floor, with distinctive bioturbation intensities.

In the Anso-Roncal section the trace-fossil assemblage comprises 13 ichnospecies from 9 ichnogenera. Of the 13 ichnospecies, 9 are post-depositional and 4 pre-depositional, including 3 graphoglyptids. The trace-fossil assemblage is dominated by *fodinichnia.* Common ichnotaxa include *Planolites* (p*ascichnia*); *Thalassinoides* and *Spongeliomorpha* (f*odinichnia*); and *Chondrites* and *Paleodictyon* (a*grichnia*). The deepest-tier traces are *Chondrites, Thalassinoides* and *Planolites,* which may bioturbate up to 50 cm below the sediment-water interface. *Nereites* occurs just below the sediment-water interface, but cross-cuts *Phycosiphon*. The trace-fossil assemblage of the distal basin floor is transitional between the *Nereites* and *Paleodictyon* subichnofacies (*sensu* Seilacher, 1974) (Fig. 7.9).

7.6.3. Interpretation

The lithological divisions of the deposits, the relatively high numbers of MTCs, and the low diversity trace-fossil assemblage are characteristic features of the distal basin floor in the Jaca basin.

Evidence of intra-bed bypass still exists in the distal basin floor, with sandstones immediately overlain by mudstones or calcilutites, with the intermediate grain-size population being deposited in more distal regions. This may be a consequence of the relatively proximal positions of the sections studied in the distal basin floor, with more distal sections such as at Roncal, ~12 km basinward of the Anso-Roncal section, and beyond, characterised by finer-grained sediments than those studied.

The high ratio of post-depositional traces to pre-depositional traces, as well as low diversity trace-fossil assemblages, is indicative of stressed environmental conditions. This is related to a number of factors such as the nature of the substrate, preservation potential, oxygenation and nutrient supply. It is possible that due to ponding of turbidity currents and the formation of thick turbiditic mudstones, the substrate was very muddy and relatively unstable (soupground substrate). This may have influenced the nature of the trace fossils formed and diversity of the trace-fossil assemblage. However, individual burrows of post-depositional ichnotaxa such as *Thalassinoides* and *Spongeliomorpha* are generally clearly defined, with sharp walls, and uncompacted, indicating that following deposition of the successive turbidite sandstone, the underlying muddy substrate probably became well consolidated. The low intensity of bioturbation as well as low diversity trace-fossil assemblage may also be associated with the limited preservation potential of traces due to the low frequency of taphonomically beneficial turbidity currents (Seilacher *pers. comm.* 2006).

The relatively low number of graphoglyptids in the trace-fossil assemblage could be related to oxygenation, with graphoglyptids being most common in moderate oligotrophic conditions (Uchman 1995a). According to Ekdale and Mason (1988), *fodinichnia-pascichnia* dominated trace-fossil assemblages reflect a lack of abundant oxygen within the substrate. The high proportion of post-depositional trace fossils is also probably indicative of low oxygenation levels. Episodic increased oxygen levels in the substrate due to the introduction of oxygenated bottom-water and organic matter by gravity currents may have fostered an increase in macrobenthic burrowing and the developing of an oxygen-related post-depositional trace-fossil assemblage. After deposition of turbidite sandstones, *pascichnia* were more common, however, as oxygen

levels decreased, *fodinichnia* became more common. Such a scenario was postulated by Burton and Link (1991) in the Wood River Formation, Pennsylvanian-Permian.

7.7. Sedimentological and ichnological characteristics of fan and related environments in the Jaca Basin: summary

Although the different fan and related environments studied in the Jaca basin are not time equivalent sections through the turbidite complex, and thus changes between fan and related environments do not equate to changes in individual flows, the distinct characteristics of the fan and related environments studied are believed to represent an accurate summary of sedimentological and ichnological characteristics of particular fan and related environments in the Jaca basin.

In terms of lithological divisions, the CLT and lobe are characterised by bipartite beds comprising a lower sandstone and upper mudstone division. This is also typical for the lobe fringe, however, a number of beds are tripartite, with a thin sandstone-siltstone division developed. The fan fringe and distal basin floor are characterised by a lower sandstone division, sandstone-siltstone or siltstone division, mudstone and upper calcilutite division. These changes reflect deposition from waning turbidity-current flows as they travelled basinward and became increasingly dilute. This is also reflected in the decrease in amalgamated sandstones, and bed thickness, as well as the increase in mudstone thickness from CLT to distal basin floor (Fig. 7.1). This increase in thickness of the mudstone interval is also related to ponding of composite flows due to flow reflection off adjacent basin margins. There is also a basinward decrease in the frequency of MTCs from the CLT to lobe fringe, however, there is an increase in MTCs in the fan fringe and distal basin floor (Fig. 7.1). This is due to a number of factors, including instability and collapse of local slopes in the distal part of the fan, as well as debris flow deposits associated with flow transformations (see Section 4.12.4).

The trace-fossil assemblages of the distal Jaca basin show clear variations between different fan and related environments (Figs. 7.7 and 7.8). The CLT has a trace-fossil assemblage characterised by the lowest bioturbation intensity, and the second lowest diversity in the Jaca basin, dominated by post-depositional ichnotaxa. The greatest average bioturbation and trace-fossil diversity occurs in the lobe fringe, with the lobe also showing a relatively high diversity and average bioturbation. A general trend of decreasing average bioturbation and trace-fossil diversity occurs from

fan-fringe to distal basin floor. A similar trend is observed in the number of pre- and post-depositional trace fossils and graphoglyptids. In terms of the characteristic behaviour of the trace-making organisms, there is also a clear trend in different environments (Figs 7.3 and 7.10). The trace-fossil assemblage of the CLT is characterised by a high proportion of *domichnia* and a relatively low proportion of *pascichnia* and *agrichnia*. From the CLT to the fan fringe, the trace-fossil assemblages are characterised by decreasing proportions of *domichnia*, and increasing proportions of *agrichnia*. The trace-fossil assemblage of the distal basin floor is characterised by a sharp increase in the proportion of *fodinichnia*, as well as a high proportion of *agrichnia*, and a decrease in *domichnia*.

In terms of ichnofacies, the trace-fossil assemblage of the CLT is characteristic of the *Ophiomorpha rudis* subichnofacies of the *Nereites* ichnofacies (*sensu* Uchman 2001) (Fig. 7.9). Depositional lobes exhibit a trace-fossil assemblage more typical of the *Paleodictyon* subichnofacies, with some trace fossils typical of the *Ophiomorpha rudis* subichnofacies. The lobe-fringe and fan-fringe are characterised by trace-fossil assemblages typical of the *Paleodictyon* subichnofacies, whilst the distal basin floor has a trace-fossil assemblage transitional between the *Nereites* and *Paleodictyon* subichnofacies.

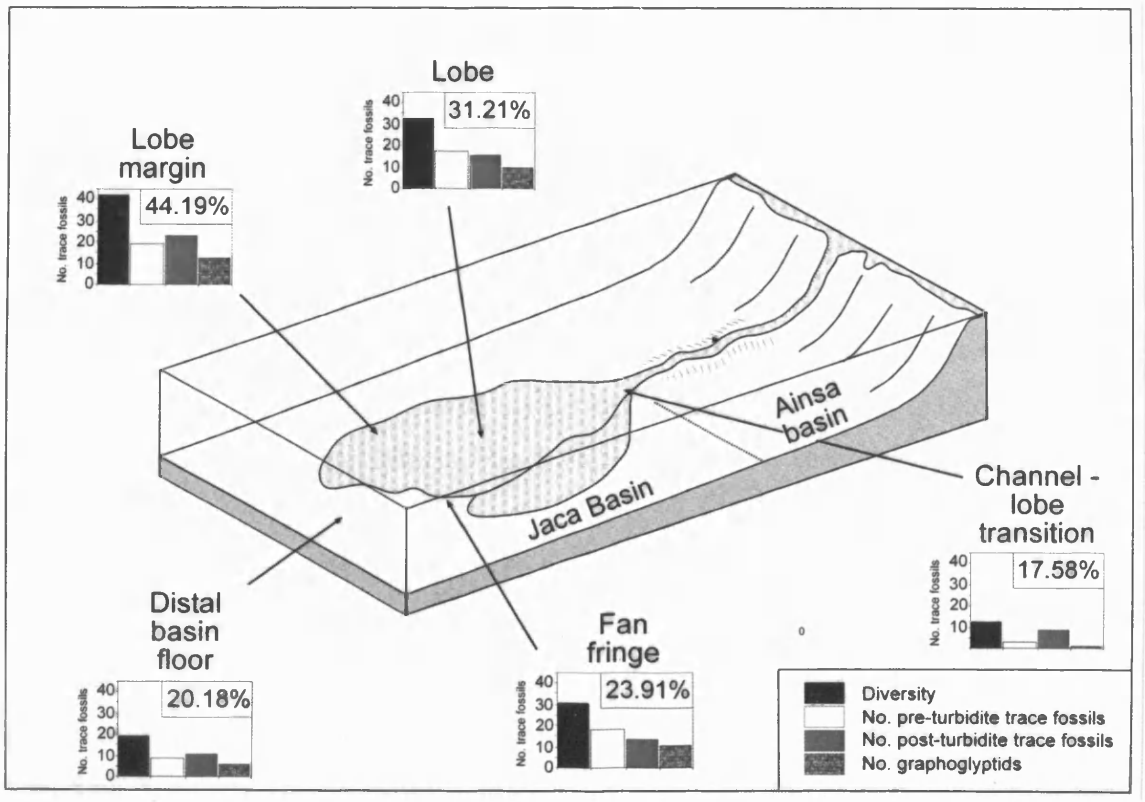

Fig. 7.7. Summary diagram of average bioturbation, trace-fossil diversity, number of pre- and post depositional trace fossils and number of graphoglyptids for the most characteristic environments of the turbidite complex in the Jaca basin.

7.8. Interpretation

The low-diversity, low-intensity, dominantly post-depositional trace-fossil assemblage of the CLT is related to a number of factors including: (1) the poor preservation potential of shallow-tier pre-depositional trace-fossils related to the high frequency of erosive high concentration turbidity currents; (2) the limited number of trace-forming organisms able to survive burial by newly deposited thick sands (Wetzel and Uchman 2001); (3) the coarse-grained nature of the deposits which may have excluded burrowers adapted only to fine-grained sediments (Tchoumatchenco & Uchman 1999); and (4) the potentially highly unstable nature of the environment related to the high frequency of high concentration turbidity currents which may have restricted the development of equilibrium communities and resulted in the high proportion of opportunistic trace-fossils.

In the lobe, lobe fringe and fan fringe, the high-diversity, high-intensity trace-fossil assemblages characterised by an abundance of pre-depositional trace fossils and graphoglyptids suggests that equilibrium organism communities may have become established due to long-term stable conditions between turbidite sandstone deposition (Uchman, 1995a). The lower frequency of strongly erosive sediment gravity flows compared to the CLT meant that the preservation potential of shallow-tier trace fossils, such as many graphoglyptids, was greater. The high bioturbation intensities associated with these environments may be related, at least in part, to decreased rates of sediment accumulation and a decrease in bed thickness and grain size of the deposits compared to the CLT. The slower rates of sediment accumulation meant that organisms had greater time to colonise and bioturbate the newly deposited sediments whilst the fine-grained, thin-bedded nature of the sediments may have enabled many organisms to survive burial.

From the fan fringe to the distal basin floor, there is a distinct decrease in average bioturbation and trace-fossil diversity, as well as the number of pre- and post-depositional trace fossils and graphoglyptids. This may be associated with the limited preservation potential of trace fossils due to the low frequency of taphonomically beneficial sediment gravity flows. The thick turbiditic mudstones characteristic of the

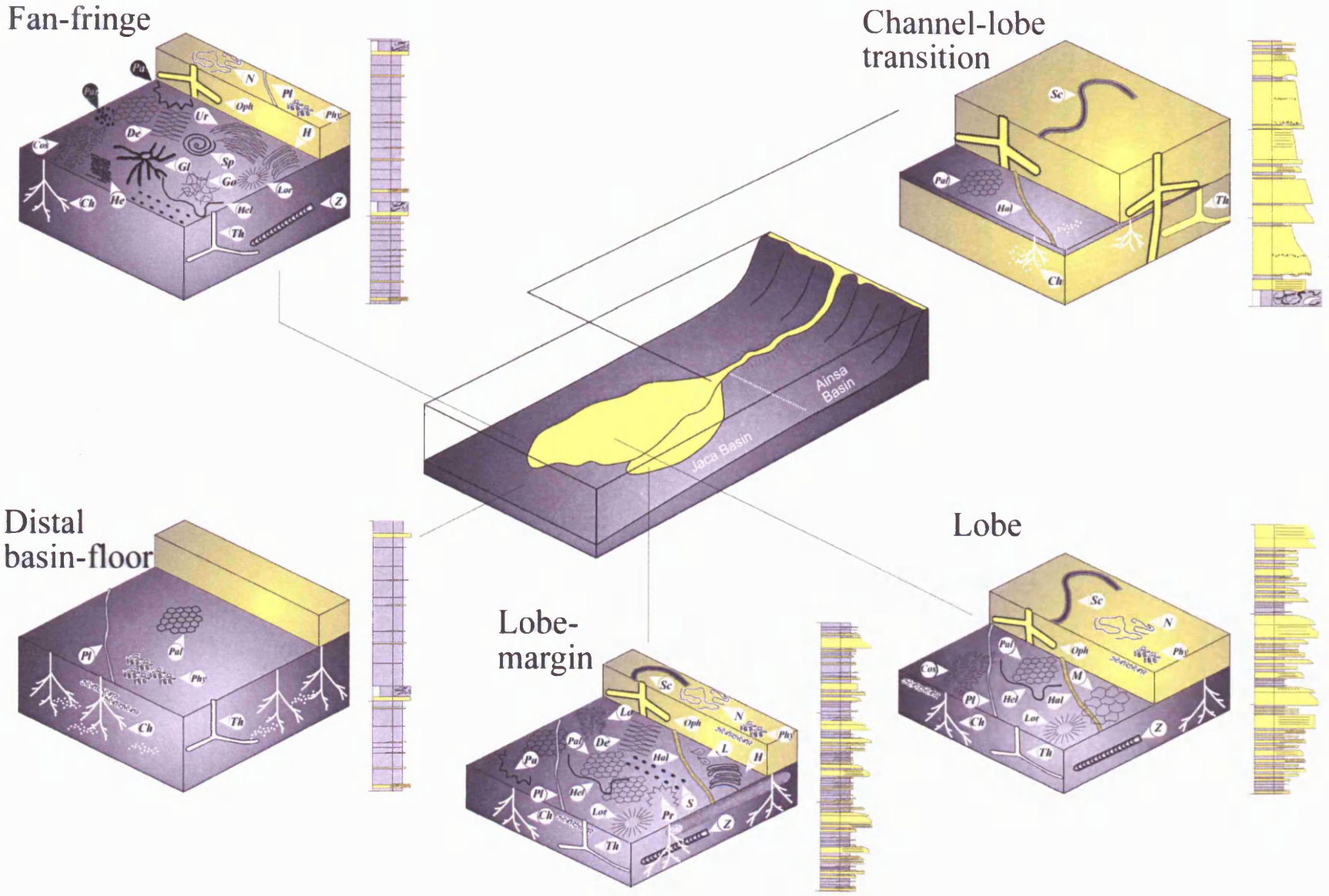
Fan-fringe
Channel-lobe transition
Ainsa Basin
Jaca Basin
Distal basin-floor
Lobe-margin
Lobe

Fig. 7.8. Summary of typical trace-fossil assemblages for the most characteristic environments of the turbidite complex of the Jaca basin. (*L = Lockeia; Sk = Skolithos; Ar = Arenicolites; Nu = Nummulites-lined burrow; H = Halopoa; Pl = Planolites; Ch = Chondrites; Oph = Ophiomorpha; Th = Thalassinoides; S = Saerichnites; Lor = Lorenzinia; Gl = Glockerichnus; Z = Zoophycos; Phy = Phycosiphon; Lo = Lophectenium; N = Nereites; Sc = Scolicia; Tae = Taenidium; Pr = ProtovirgularCos = Cosmorhaphe; He = Helicolithus; H = Helminthorhaphe; Hel = Helminthopsis; Sp = Spirohaphe; Pa = Palaeomeandron; De = Desmograpton; Ur = Urohelminthoida; M = Megagrapton; Pal = Paleodictyon*).

distal basin floor may also have had a strong control on the trace-fossil assemblages. The muddy, relatively unstable substrate ("soupground") that may have formed would have been unfavourable to many trace-making organisms. The observed decrease in the proportion of *domichnia* and *pascichnia* and increase in *fodinichnia* in the distal basin floor may be associated with changes in oxygen concentrations in interstitial waters.

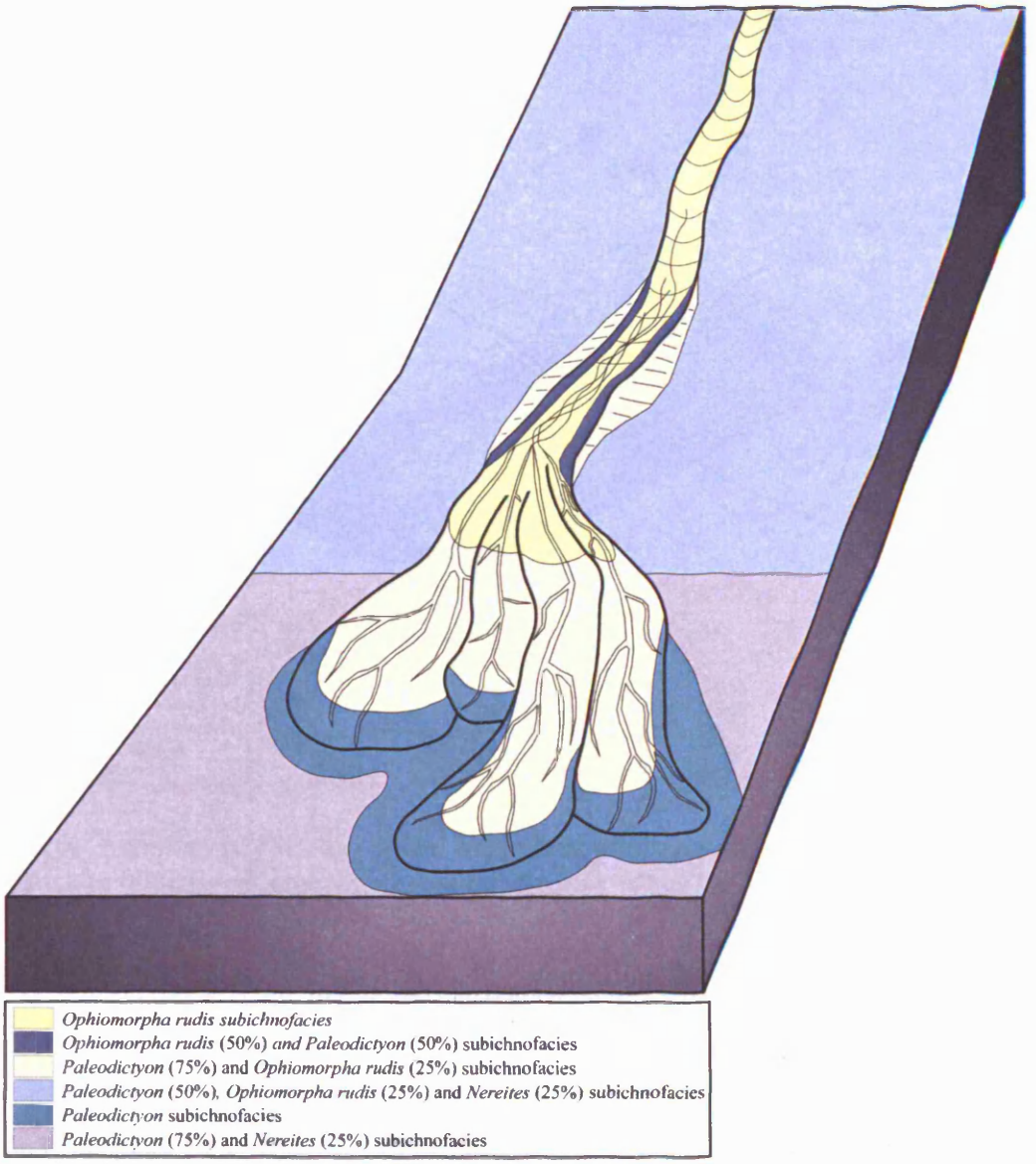

Fig. 7.9. Distribution of subichnofacies of the *Nereites* ichnofacies in the Ainsa - Jaca basin.

7.9. Discussion

In the proximal Ainsa basin, a general trend was recognised in which the same facies or facies-association is characterised by a similar trace-fossil assemblage independent of the environment of deposition (Section 6.9). However, subtle variations in the trace-fossil assemblages exist between different environments due to variations in environmental controlling factors. In the distal Jaca basin, similar facies and facies-associations in different environments have comparable trace-fossil assemblages, but the variations between the assemblages are more distinct (Table 7.3). This may be

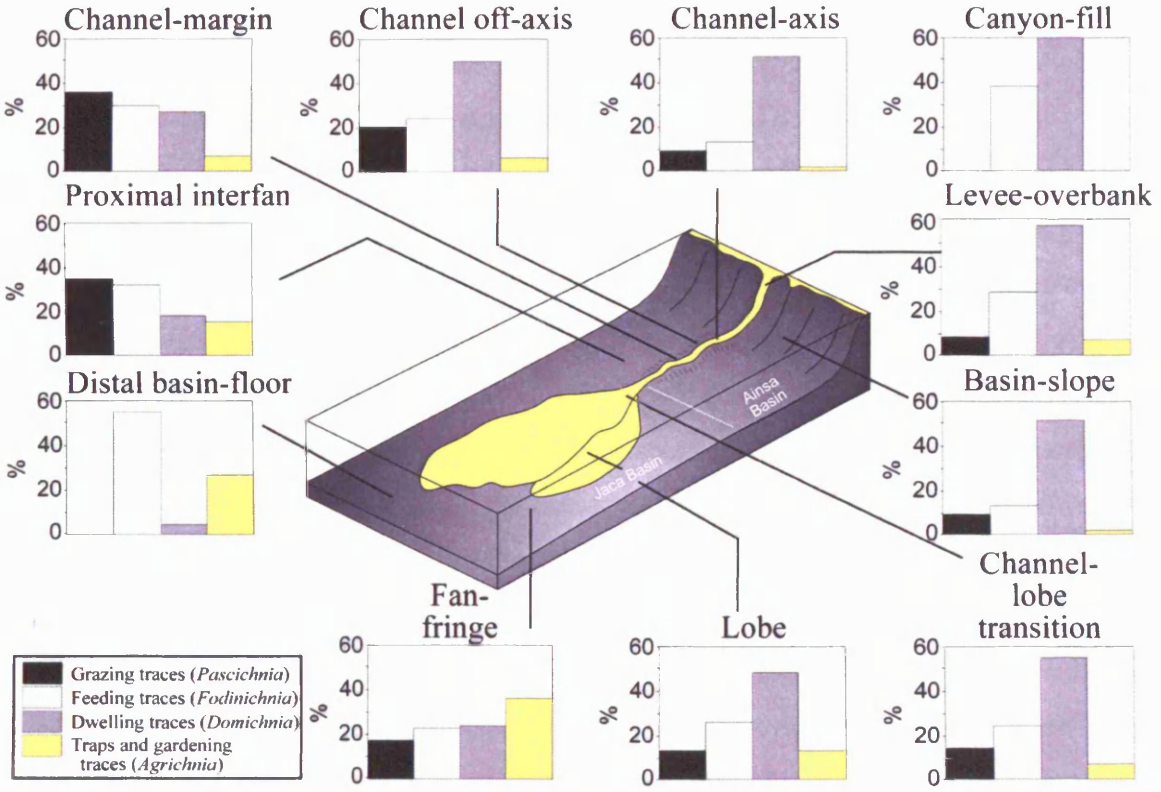

Fig. 7.10. Summary of the ethological behaviour of organisms established from trace fossils in different environments in the Ainsa - Jaca basin.

related to greater changes in environmental controlling factors between the more distal fan and related environments.

In the Jaca basin, the thin-bedded sandstones and mudstones (Facies C2.3), which are associated with Facies-associations 5 and 6, are characterised by the highest

diversity trace-fossil assemblages, with a high proportion of pre-depositional trace fossils. This is in contrast to the Ainsa basin, where the highest diversity trace-fossil assemblages occur in medium-bedded sandstones of FA5 (typically Facies C2.2). The thin-bedded sandstones and mudstones (Facies C2.3) which characterise FA6a and FA6d in the Ainsa basin typically have a very high intensity but low diversity trace-fossil assemblage. This is in part related to the predominance of biodeformational structures rather than distinct trace fossils, which is associated with high levels of benthic food content in the sediments. In the distal Jaca basin, inferred lower levels of oxygenation enabled a more diverse trace-fossil assemblage to become established, due to the absence of large bulldozing traces such as *Scolicia* and biodeformatioal structures. As a result, the thin-bedded sandstones and mudstones (Facies C2.3) of Facies-association 6 are characterised by a moderate intensity, high diversity trace-fossil assemblage. Nutrient supply is interpreted as having less of an influence on bioturbation than oxygenation because terrestrial carbon is typically carried and deposited distally due to low settling velocities (Haughton, *pers. comm.*, 2007).

Preservation potential may also have influenced the lower diversity trace-fossil assemblage associated with medium-bedded sandstones in the Jaca basin (Facies C2.2) compared to those in the Ainsa basin. The turbidity currents associated with the Facies C2.2 sandstones may have been more erosive in the distal parts of the fan due to the muddy, fine-grained nature of the sea-floor. This is indicated by the abundance of flutes and grooves on the soles of Facies C2.2 sandstones in the distal Jaca basin compared to those in the Ainsa basin. As a result, the preservation potential of shallow-tier burrows may have been poor, resulting in the dominantly post-depositional trace-fossil assemblages of these deposits. Burrow networks may also have been shallower than those in the Ainsa basin due to inferred reduced oxygen supply to the distal parts of the fan. This would therefore have greatly influenced the preservation potential of pre-depositional burrow networks in the Jaca basin. It is therefore clear that similar facies and facies-associations in different fan and related environments may be associated with very different trace-fossil assemblages based on varying environmental controls. It is on this basis that trace fossils and trace-fossil assemblages can be very powerful discriminators of deep-marine clastic fan and related environments.

7.10. Trace-fossil distributions in the Ainsa-Jaca basin, a comparison with previous studies

The distribution of trace fossils in the Ainsa-Jaca basin is consistent with other studies on deep-marine sediments, including submarine fans. For example, a similar distribution of trace fossils has been observed in the Eocene Jaizkibel fan of northern Spain (Crimes 1977), the Cretaceous-Eocene Gurnigel and Schlieren Flysch of Switzerland (Crimes *et al.* 1981), the upper Palaeocene-Lower Eocene flysch del Grivó in the Julian Prealps of Italy and Slovenia (Tunis & Uchman 1992, 1996a), the Miocene Marnoso-arenacea Formation of the Northern Apennines (Uchman 1995a), the Eocene turbidites of the Istria Peninsula (Tunis & Uchman 1996b), the Miocene Cingöz Formation of the Adana Basin (Uchman & Demircan 1999), the Eocene Greifensteiner Schichten of Austria (Uchman 1999), the Eocene Tarcau sandstone of the Eastern Carpathians, Romania (Buatois *et al.* 2001) and the Early-Middle Eocene Kusuri Formation of the Sinop-Boyabat Basin, Turkey (Uchman *et al.* 2004). The exact same trace-fossil distributions observed in the Ainsa-Jaca basin, however, may not necessarily be applicable as a general rule as these vary between basins. For example, in the Upper Jurassic-Lower Cretaceous turbidites of SW Bulgaria, most ichnotaxa occur in the proximal facies (Tchoumatchenco & Uchman 2001) whilst McCann and Pickerill (1988) proposed that proximal and distal lobe-fringe facies in the Cretaceous turbidite sands of the Kodiak Formation of Alaska contain a lower diversity and low intensity trace-fossil assemblage compared with channel-levee or interchannel environments.

The high-diversity trace-fossil assemblages and high average bioturbation of the Ainsa-Jaca basin, supports the view of Uchman (2001) that the basin was characterised by well oxygenated oligotrophic conditions. This is typical of many other documented Paleogene and Miocene turbidite systems (cf. Uchman 1995a 2001). Comparing this study to that of Uchman (2001), Uchman recognised 63 ichnotaxa belonging to 40 ichnogenera compared to the 95 ichnotaxa from 49 ichnogenera identified in this study. This difference is probably related to the fact that this study was conducted systematically in more areas and in more fan and related environments. Uchman (2001) concluded that the greatest diversity trace-fossil assemblage occurred in lobe and lobe-fringe deposited and is distinctly less in fan-fringe and basin-plain (= distal basin-floor in this thesis) facies. The interchannel deposits studied by Uchman (2001), and in this paper referred to as proximal interfan, were characterised by a low-diversity and low-

intensity trace-fossil assemblage, which contrasts with the very high average bioturbation and moderate diversity trace-fossil assemblage recognised in this study (Section 6.4.5.2).

Chapter 8

Trace fossils in the subsurface

8.1. Introduction

The detailed study of the uses of trace fossils as diagnostic indicators of deep-marine clastic fan and related environments at outcrop clearly indicates that trace fossils and trace-fossil assemblages can be very powerful discriminators of deep-marine environments (Chapters 6 and 7). This chapter includes a detailed sedimentological and ichnological study of six cores through the Ainsa I and II sandbodies. This includes a quantitative ichnological study and detailed ichnofabric analysis with the aim of fully understanding the uses of trace fossils as diagnostic indicators of deep-marine clastic fan and related environments in the subsurface. This study is of particular relevance to the petroleum industry where the analysis of ichnofabrics in core has been used in paleoenvironmental studies for many years.

The Ainsa turbidite system comprises three sandbodies (Ainsa I, II and III) (fig. 8.1) of which only the Ainsa I and II were studied in core. The Ainsa I and II sandbodies are characterised by a number of vertically and laterally offset stacked channel elements. The Ainsa I sandbody is up to 85.3 m thick in the subsurface and is classified as a channel complex set, comprising a basal MTC and overlying channel complex. The Ainsa II sandbody is up to 101 m thick and comprises two channel complexes forming a channel complex set. Ainsa I and II are separated by a thick MTC. A detailed architectural element analysis of the Ainsa system is beyond the scope of this thesis, and individual channel elements are divided on the basis of work by Clark (1995), and Pickering *et al.* (*in review*). The reader is referred to these references for a detailed analysis of the architectural elements. For ichnological descriptions, a statistical summary of relevant core data is provided in Tables 8.1, 8.2 and 8.3.

8.2. Trace fossils in core

In core, trace fossils were identified in vertical cross-sections, and defined at the ichnogenus level, as described by Häntzschel (1975). Trace fossils recorded include

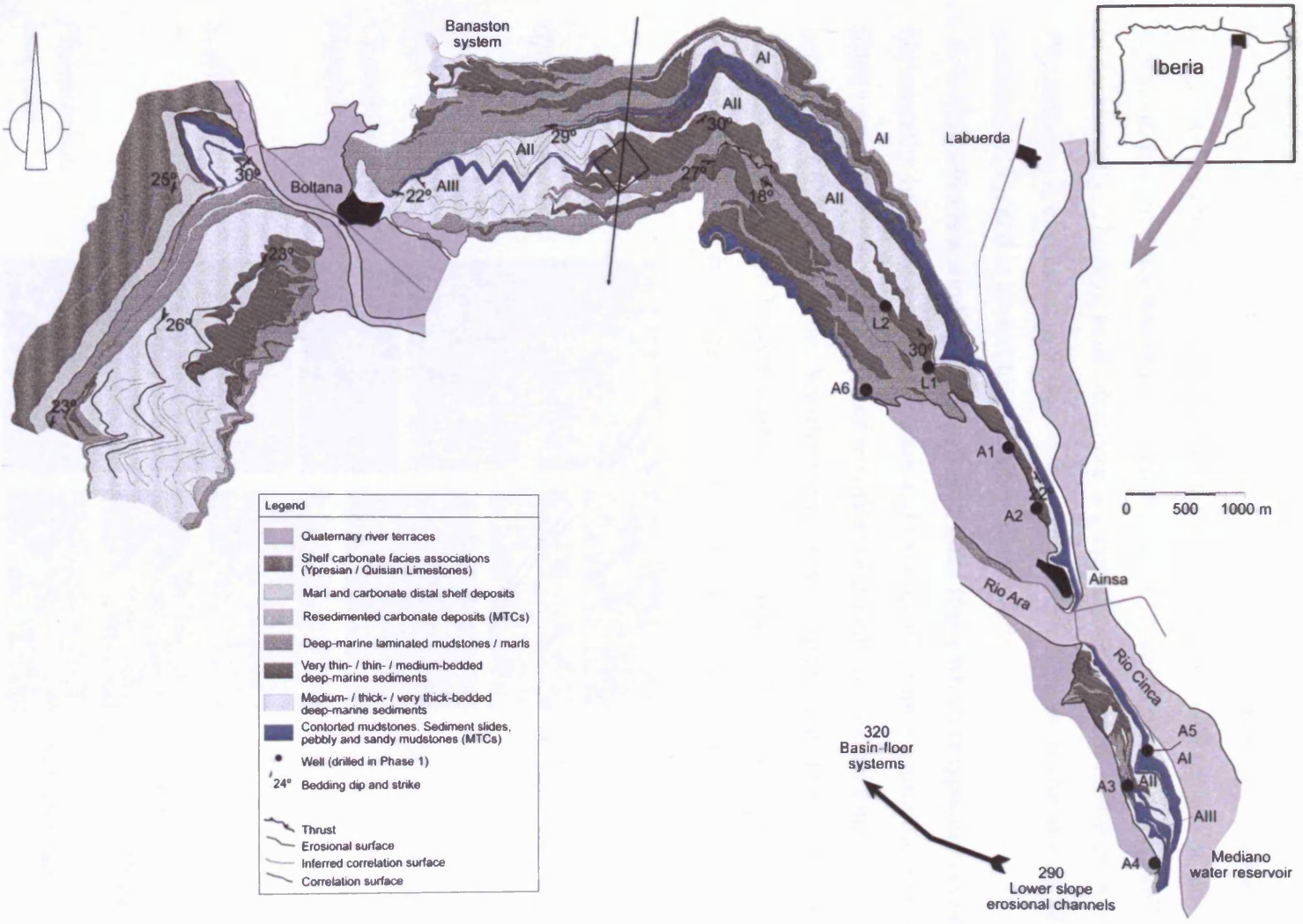

Fig. 8.1. Geological map of the Middle Eocene Ainsa deep-marine system, Ainsa basin, Spanish Pyrenees (modified after Pickering and Corregidor 2005). Well locations are projected onto the map.

lined and unlined vertical burrows, *Halopoa, Planolites, Palaeophycus, Chondrites, Trichichnus, Ophiomorpha, Thalassinoides, Zoophycos, Phycosiphon, Nereites, Scolicia* and *Teichichnus*. The most common trace fossils are described below, and illustrated in Figure 8.2.

Phycosiphon is a small complexly lobed spreite fossil (Bromley 1996). In core it is characterised by a dark backfilled centre surrounded by a thin mantle of pale sediment. It commonly occurs in small dense patches which penetrate vertically as well as horizontally. The dark backfilled core is generally <1.5 mm in diameter. At outcrop, *Phycosiphon* is expressed as *P. incertum*, and is very common on the tops of silty sandstones (T_d) and is crosscut by all other trace fossils.

Nereites is a winding or meandering trace fossil which is typically orientated horizontally. In core it has a dark centre and pale mantle, representing the median back-filled tunnel enveloped by a zone of reworked sediment. Individual tunnel zones range between 1-4 mm in diameter. *Nereites* commonly occurs in association with, and crosscuts *Phycosiphon*. In some cases, *Nereites* may crosscut shallow *Scolicia*. The *Nereites* recognised in core is probably *N. irregularis*, which is common at outcrop.

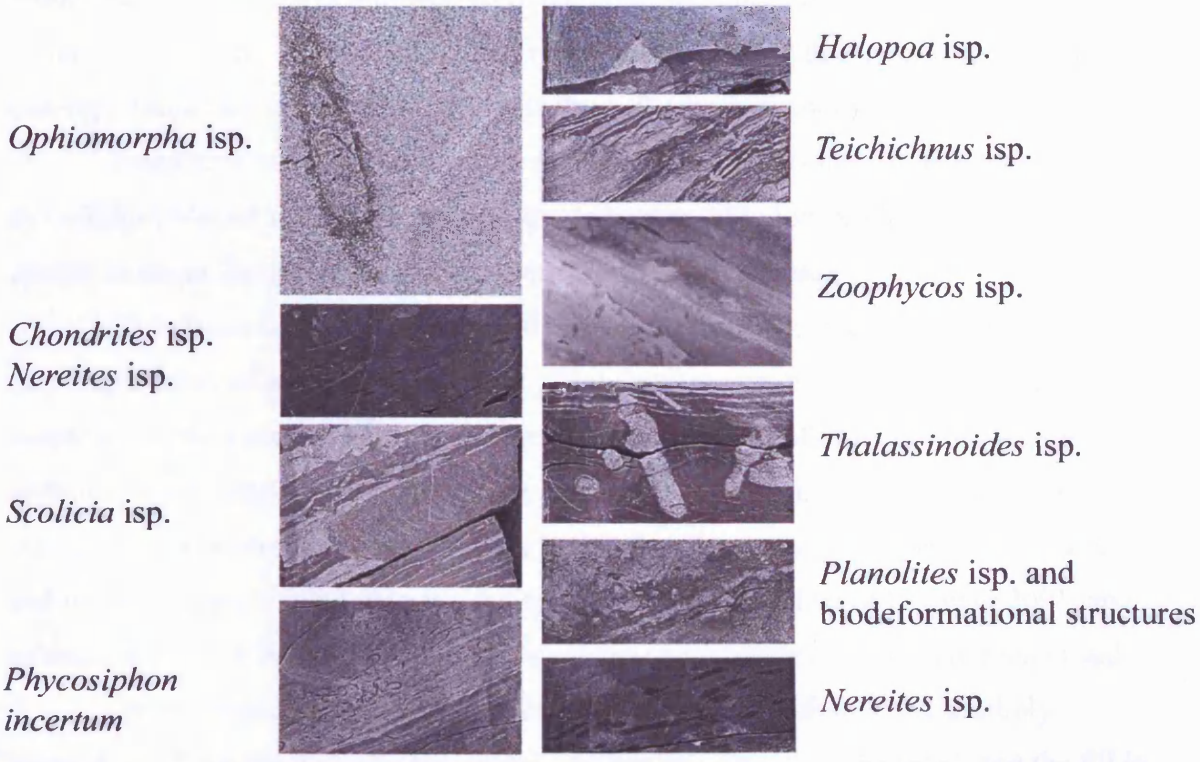

Fig. 8.2. Images of common trace fossils in core. The core is ~6 cm wide.

Planolites is typically unlined, rarely branched, straight to tortuous, horizontal to inclined cylindrical tunnels. The tunnels were actively filled, with the fill essentially being structureless and differing in lithology from the host rock. Typically, the diameter of *Planolites* is between 3-7 mm. Commonly, *Planolites* has secondary *Chondrites* within its burrows. At outcrop, only *Planolites* isp. was identified.

Scolicia occurs as large, essentially horizontal burrows filled with meniscate laminae. These large trace fossils are commonly referred to as bulldozer traces (*sensu* Thayer 1979), because they commonly form thick vertical intervals of homogenised sediment (e.g., Wetzel & Uchman 1997). Each burrow is 9-20 mm thick and may totally bioturbate core intervals to >1 m vertically. *Scolicia* is commonly crosscut by *Chondrites*. At outcrop, both *S. prisca* and *S. plana* are common, as well as *Scolicia* isp.

Thalassinoides is a three-dimensional burrow system. Branching is rarely preserved in core, but evidence of branching may be preserved in the rough outer surface of the core. The cylindrical burrows are typically horizontal, between 5-20 mm in diameter, and connected by vertical shafts. The burrows were actively filled, with the fill differing in lithology from the host rock. Secondary *Chondrites* may be developed within the *Thalassinoides* burrows. At outcrop, most *Thalassinoides* were identified as *T. suevicus*. In core, *Thalassinoides* can easily be confused with *Planolites*, however, at outcrop, *Thalassinoides* burrows are typically >10 mm in diameter.

Zoophycos is a spreiten structure that surrounds a central shaft in distinct levels or coilings (Wetzel 1991). In core it occurs as horizontal to low angle tubes with distinct spreite laminae. Each tube ranges between 2-7 mm in thickness.

Chondrites is a three-dimensional burrow system with intense branching forming clusters of small tunnels in core. *Chondrites* occurs throughout the core, crosscutting most trace fossils, and occurs in abundance in both totally homogenised sediments, and intervals characterised by low intensity bioturbation. Observations from core A6 are consistent with other studies in that the producers of *Chondrites* tolerate, and in many cases, exploit extreme ecological situations (Wetzel & Uchman 2001, and references within). At outcrop, both *C. intricatus* and *Chondrites* isp. were recognised.

Ophiomorpha is easily recognisable in core due to its distinctive knobbly exterior. Burrows are typically horizontal, oblique or vertically orientated, and the fill is the same lithology as the host rock. *Ophiomorpha* typically occurs within turbidite sandstones and ranges between 3-25 mm in diameter, and averages 9 mm. The trace-forming organism penetrated deep into the sediment maintaining an open connection to

the seafloor. At outcrop, *Ophiomorpha* typically occurs on the soles of sandstones, with *O. annulata* common, and more rarely *O. rudis*.

Halopoa is a cylindrical, hypichnial ridge, 7-12 mm wide preserved in full relief and typically occurs at the base of thin- to medium-bedded sandstone beds. The *Halopoa* producers reworked the sandstone/mudstone interface, back-filling their burrows. In general, *Halopoa* is difficult to recognise in core due to difficulties in observing the furrows and wrinkles, which characterise the surface of the cylindrical burrows.

Teichichnus is a vertical to sub-vertical burrow formed of stacked, dark, gutter-shaped horizontal laminae. This trace fossil is rare in the Ainsa cores, and occurs in intensely bioturbated thin-bedded sandstones.

8.3. Ichnofabrics

Eleven ichnofabrics have been established in this study. The recognition of individual ichnofabrics is based on quantitative ichnological analysis such as bioturbation intensity and diversity, as well as semi-quantitative analysis including infaunal tiering and colonisation styles. These ichnological observations are combined with a detailed sedimentological study.

8.3.1. *Planolites-Phycosiphon* ichnofabric

8.3.1.1. Diagnosis

Thin horizons of *Planolites* and bedding parallel patches of *Phycosiphon* in thin-bedded sandstones and siltstone-mudstone laminae characterised by low bioturbation intensities (<25%).

8.3.1.2. Description

The *Planolites-Phycosiphon* ichnofabric is characterised by thin-bedded sandstones and siltstone-mudstone laminae (Facies C2.3 and D2.3). Bioturbation intensities are low, ranging between 0-25% and averaging 10.2%. Ichnofabric indices average 2.09 and typically range between 2-3. Biodeformational structures are generally absent to very minor, averaging 3%. *Phycosiphon* and *Planolites* are the most common ichnotaxa and

typically occur parallel to bedding in muddy siltstones. Other ichnotaxa include *Chondrites, Planolites, Scolicia, Thalassinoides, Zoophycos* and *Nereites,* which form very minor constituents of the trace-fossil assemblage.

Cross-cutting relationships are poorly defined due to the low intensity of bioturbation. In general, Phycosiphon is cross-cut by *Chondrites* and *Planolites*, whilst *Chondrites* cross-cuts *Planolites*. Depth of bioturbation is restricted to only a few centimetres, and up to 3 cm.

Fig. 8.3. *Planolites-Phycosiphon* ichnofabric, Well A3. Core is ~6 cm wide.

8.3.1.3. Occurrence

This ichnofabric commonly occurs in fine-grained intervals between medium- to thick-bedded sandstones or as relatively thin horizons (<20 cm thick) which punctuate fine-grained homogenised sections. The *Planolites-Phycosiphon* ichnofabric is most clearly developed in the fine-grained deposits of the abandonment phase at the top of the Ainsa II sandbody in Wells A3, A2, A1 and L1. It also occurs in the levee-overbank deposits of Ainsa I, Well A2, the upper part of the margin of channel element I.4, Ainsa II, Well A1 and between thick-bedded sandstones in the channel off-axis of channel element II.3, Ainsa II, Well A3.

8.3.1.4. Discussion

The low bioturbation intensity, small burrow diameters, absence of biodeformational structures and the restriction of bioturbation to a narrow zone is interpreted as being indicative of poorly oxygenated bottom-water conditions. *Phycosiphon* has been interpreted as an opportunistic trace fossil produced by organisms which bioturbated the top part of the turbidite sandstone/siltstone immediately after deposition (Wetzel & Uchman 2001). Bioturbation is restricted to newly deposited sandstones / siltstones which may be associated with a temporary increase in oxygen levels in an otherwise oxygen deprived environment. This temporary increase in oxygen levels is related to the depositing gravity currents, which may have been transported through oxygenated water at shallow depths (e.g., Wilson *et al.* 1985, Orr 1995, Buatois *et al.* 2001, Wetzel & Uchman 2001). Consequently, opportunistic deposit feeding organisms such as *Phycosiphon*- and *Planolites*-producing organisms exploited the newly deposited oxygenated sediments. As oxygen levels returned to their original levels, bioturbation ceased.

8.3.2. *Planolites* Ichnofabric

8.3.2.1. Diagnosis

Thin-bedded sandstones and siltstone-mudstone laminae intensely bioturbated by a diverse ichnofauna dominated by *Planolites* and biodeformational structures.

Fig. 8.4. *Planolites* ichnofabric, Well L1. Core is ~6 cm wide.

8.3.2.2. Description

The *Planolites* ichnofabric is associated with thin-bedded sandstones and siltstone-mudstone laminae (Facies C2.3 and D2.3). These thin-bedded deposits typically occur in intervals between thick-bedded sandstones. Bioturbation is typically high, averaging 55.78%, of which 56% is biodeformational structures. Ichnofabric indices average 3.77. The deposits are rarely totally homogenised. The trace-fossil assemblage is dominated by *Planolites* and biodeformational structures. The layers associated with biodeformational structures are between several millimetres to several centimetres thick. Other common ichnotaxa include *Scolicia, Phycosiphon,* and *Thalassinoides.* From shallowest to deepest tier these trace fossils are: biodeformational structures, *Phycosiphon, Planolites, Thalassinoides* and *Chondrites.* Due to the thin-bedded nature of the siltstone-mudstone laminae, the tiering relationship is generally complex as a result of overprinting of tiers associated with successive event beds.

8.3.2.3. Occurrence

The *Planolites* ichnofabric is the most widespread ichnofabric other than the *Ophiomorpha* ichnofabric. It typically occurs in thin muddy intervals between medium- to thick-bedded sandstones.

8.3.2.4. Discussion

This ichnofabric is indicative of highly oxygenated, nutrient-rich environments characterised by thin-bedded sandstones and siltstone-mudstone laminae. Biodeformational structures are interpreted to have been formed near the sediment/water interface by deposit-feeding organisms in nutrient-rich, well-oxygenated, soupy sediment with low cohesion strength. These structures form a thin (<3 cm) homogenised layer which is cross-cut by distinct trace fossils. The most distinct trace fossils occur below the homogenised layer thus forming two layers, a homogenised layer cross-cut by distinct trace fossils, and a non-homogenised layer associated with deeper tier ichnotaxa such as *Planolites, Thalassinoides* and *Chondrites.* Cross-cutting relationships are generally complicated because some deeper-tier trace fossils bioturbate to older turbidites overprinting the ichnofabric. As a consequence, application of the toponomic position to the recognition of tiering patterns is limited in deeply-burrowed thin-bedded turbidite sandstones and siltstones (Rajchel & Uchman 1998). The two layers observed in the *Planolites* ichnofabric are commonly developed

in turbidite successions and have been referred to as the *spotty layer* and *elite layer* by Uchman (1999).

8.3.3. *Phycosiphon* ichnofabric

8.3.3.1. Diagnosis

Thin, bedding parallel patches of *Phycosiphon* in laminated siltstones and mudstones.

8.3.3.2. Description

This ichnofabric is characterised by very-thin-bedded sandstones, siltstone-mudstone laminae, laminated mudstones and biogenic mudstones (hemipelagites) (Facies C2.3, D2.3, E2.2 and G2.1 respectively). Bioturbation intensities are low, ranging between 0-28% with an average of 9%. Ichnofabric indices average 1.8 and biodeformational structures form 15% of the trace-fossil assemblage. *Phycosiphon* is the most common trace fossil, forming 79% of the trace-fossil assemblage and typically occurs parallel to bedding in thin muddy siltstones. Other ichnotaxa are rare, and include *Planolites, Thalassinoides* and *Chondrites.*

Cross-cutting relationships are poorly defined due to the low bioturbation intensity. In general, Phycosiphon is cross-cut by *Chondrites* and *Planolites*, whilst *Chondrites* cross-cuts *Planolites*. The depth of bioturbation is restricted to only a few centimetres.

8.3.3.3. Occurrence

The *Phycosiphon* ichnofabric typically occurs as relatively thick intervals (tens of centimetres thick) punctuated by thin homogenised horizons, or as thin (<10 cm thick) laminated horizons in homogenised intervals. This ichnofabric occurs as thick horizons in the levee-overbank of Ainsa I, Well A4 and A2, and the intrafan of Well A4. It occurs as thin horizons in the Ainsa I channel off-axis deposits, Well A3, the margin of channel element II.2, Ainsa II, Well A3, the interfan of Well A1 and the margin of channel element I.3, Ainsa II, Well L1.

Fig. 8.5. *Phycosiphon* ichnofabric, Well A3. Core is ~6 cm wide.

8.3.3.4. Discussion

This ichnofabric is similar to the *Planolites-Phycosiphon* ichnofabric, but is generally associated with finer-grained deposits. The paucity of *Planolites* in the *Phycosiphon* ichnofabric is probably directly related to oxygenation. Like the *Planolites-Phycosiphon* ichnofabric, the *Phycosiphon* ichnofabric is interpreted as representing bioturbation by opportunistic deposit feeding organisms in poorly oxygenated bottom-waters associated with a temporary increase in oxygen levels related to the depositing gravity flows. From cross-cutting relationships in the *Planolites-Phycosiphon* ichnofabric, it is clear that *Phycosiphon*-producing organisms colonised the newly deposited sediments first (see Section 8.3.1.2). The paucity of *Planolites* in the *Phycosiphon* ichnofabric suggests that after the temporary increase in oxygen levels, oxygenation rapidly returned to the original background level, thus inhibiting bioturbation from the later *Planolites*-producing organisms. This inferred lower oxygenation level is also supported by the lower bioturbation intensity, average ichnofabric index and trace-fossil diversity. This may be related to the finer-grained nature of the deposits, which is probably indicative of a lower frequency and/or concentration of oxygenated gravity currents.

8.3.4. *Phycosiphon-Planolites* homogenised ichnofabric

8.3.4.1. Diagnosis

A trace-fossil assemblage dominated by *Phycosiphon* and *Planolites* emplaced on a totally homogenised background of intensely bioturbated silty mudstone.

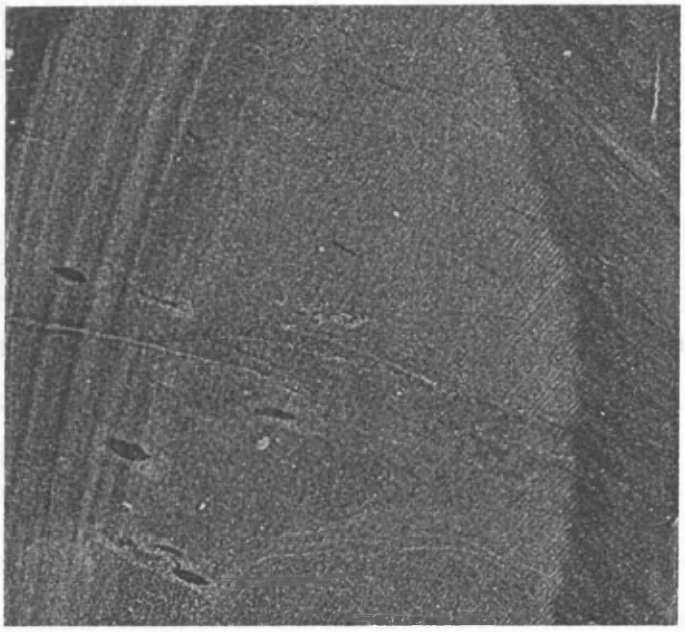

Fig. 8.6. *Phycosiphon-Planolites* homogenised ichnofabric, Well A1. Core is ~6 cm wide.

8.3.4.2. Description

This ichnofabric is associated with totally bioturbated siltstones, mudstones, and more rarely, thin-bedded sandstones (Facies D1.3, E1.3 and C1.2 respectively). Primary sedimentary structures are rarely preserved.

Bioturbation intensities are high, averaging 97%, whilst ichnofabric indices average 6.39. The high bioturbation intensity is related to the abundance of biodeformational structures associated with the homogenised background sediments. This homogenised background may also be characterised by poorly preserved *Scolicia.* The overprinting trace-fossil assemblage is characterised by well-defined, sharp-walled burrows emplaced on the homogenised background. The bioturbation intensity is low, averaging 11%. This trace-fossil assemblage is dominated by *Phycosiphon* and *Planolites.* Other common ichnotaxa include *Chondrites, Thalassinoides* and *Nereites.*

Tiering patterns are complex as a result of multiple colonisation. Cross-cutting relationships are poorly defined due to the low intensity of bioturbation of the overprinting trace-fossil assemblage. Typically, poorly preserved *Scolicia* as well as

biodeformational structures form the homogenised background sediments and are cross-cut by all other ichnotaxa. Using cross-cutting relationships as a proxy to tiering, trace fossils from shallowest to deepest tiers are *Phycosiphon*, *Nereites, Planolites, Thalassinoides* and *Chondrites*. Ichnotaxa such as *Nereites* and *Phycosiphon* which are characteristically orientated parallel to bedding in the *Phycosiphon* ichnofabric and *Planolites-Phycosiphon* ichnofabric tend towards an oblique orientation.

8.3.4.3. Occurrence

This ichnofabric is characteristic of the interfan in Well A2 and A1. It is also common in the levee-overbank of Ainsa I, Well A4 and A2. The *Phycosiphon-Planolites* homogenised ichnofabric also occurs in thin muddy intervals between medium-bedded sandstones in off-axis deposits of channel element II.3, Ainsa II, Well A3, and the margin of channel element I.4c, Ainsa II, Well A2.

8.3.4.4. Discussion

The homogenised background was formed in nutrient rich fluid softground (e.g., "soupground") in which biodeformational structures predominate. The abundance of biodeformational structures rather than distinct trace fossils is related to the fact that in sediments with high nutrient supply, behavioural specialisation by organisms is typically not developed leading to the formation of biodeformational structures rather than distinct trace fossils (cf. Wetzel 1991). Any distinct burrows developed may also have become indistinguishable due to the intensity of bioturbation, as well as compaction and smearing upon burial. The overprinting trace-fossil assemblage was formed in the sediment after partial dewatering and consolidation which enabled the formation and preservation of burrows with distinct structures. The low bioturbation intensities associated with this secondary trace-fossil assemblage is probably related to a reduction in oxygen levels and/or nutrient levels in the sediment.

The occurrence of *Chondrites,* which cross-cuts all other ichnotaxa, suggests that the trace-forming organism bioturbated the sediments last, and was able to tolerate and exploit extreme ecological conditions such as oxygen-poor sediments (Wetzel & Uchman 2001).

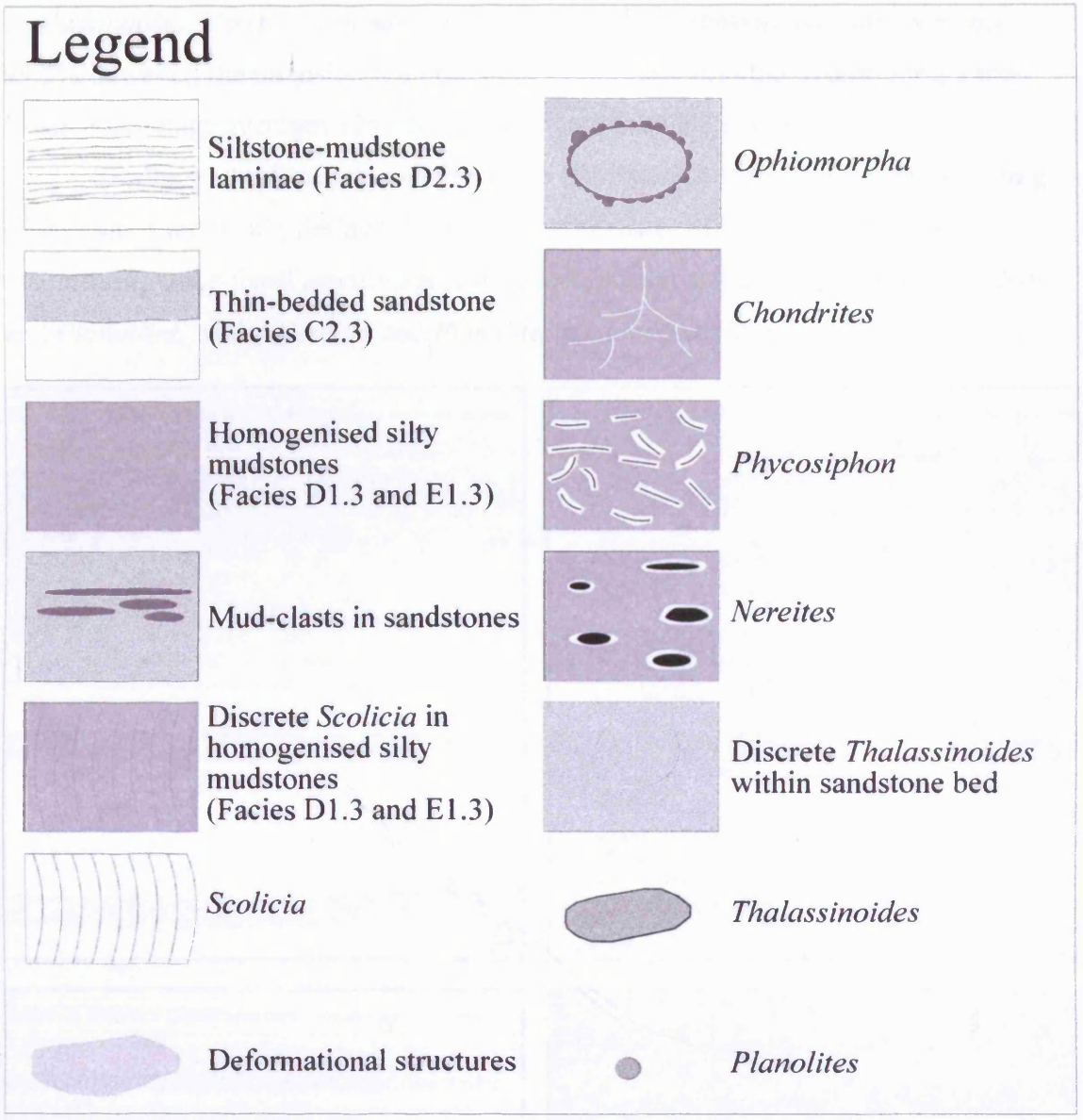

Fig. 8.7. Key for symbols used in the ichnofabric models (Figs. 8.8, 8.13, 8.17).

8.3.5. *Phycosiphon*-diverse homogenised ichnofabric

8.3.5.1. Diagnosis

A diverse trace-fossil assemblage dominated by *Phycosiphon* emplaced on a background of totally homogenised silty mudstone.

8.3.5.2. Description

This ichnofabric is associated with totally homogenised siltstones, mudstones, and more rarely, thin-bedded sandstones (Facies D1.3, E1.3 and C1.2, respectively). Primary sedimentary structures are rarely preserved. The trace-fossil assemblage is dominated by *Phycosiphon* and *Planolites*. Other common ichnotaxa include

Thalassinoides, Nereites, Chondrites and *Scolicia.* Bioturbation intensity averages 99.5% however, the intensity of bioturbation associated with the overprinting trace-fossil assemblage averages 12%. Ichnofabric indices average 6.6.

Similar to the *Phycosiphon-Planolites* homogenised ichnofabric, cross-cutting relationships are poorly defined due to the low intensity of bioturbation of the overprinting trace-fossil assemblage. *Phycosiphon* is cross-cut by *Nereites, Chondrites* and *Planolites,* whilst *Nereites* and *Planolites* are cross-cut by *Chondrites.*

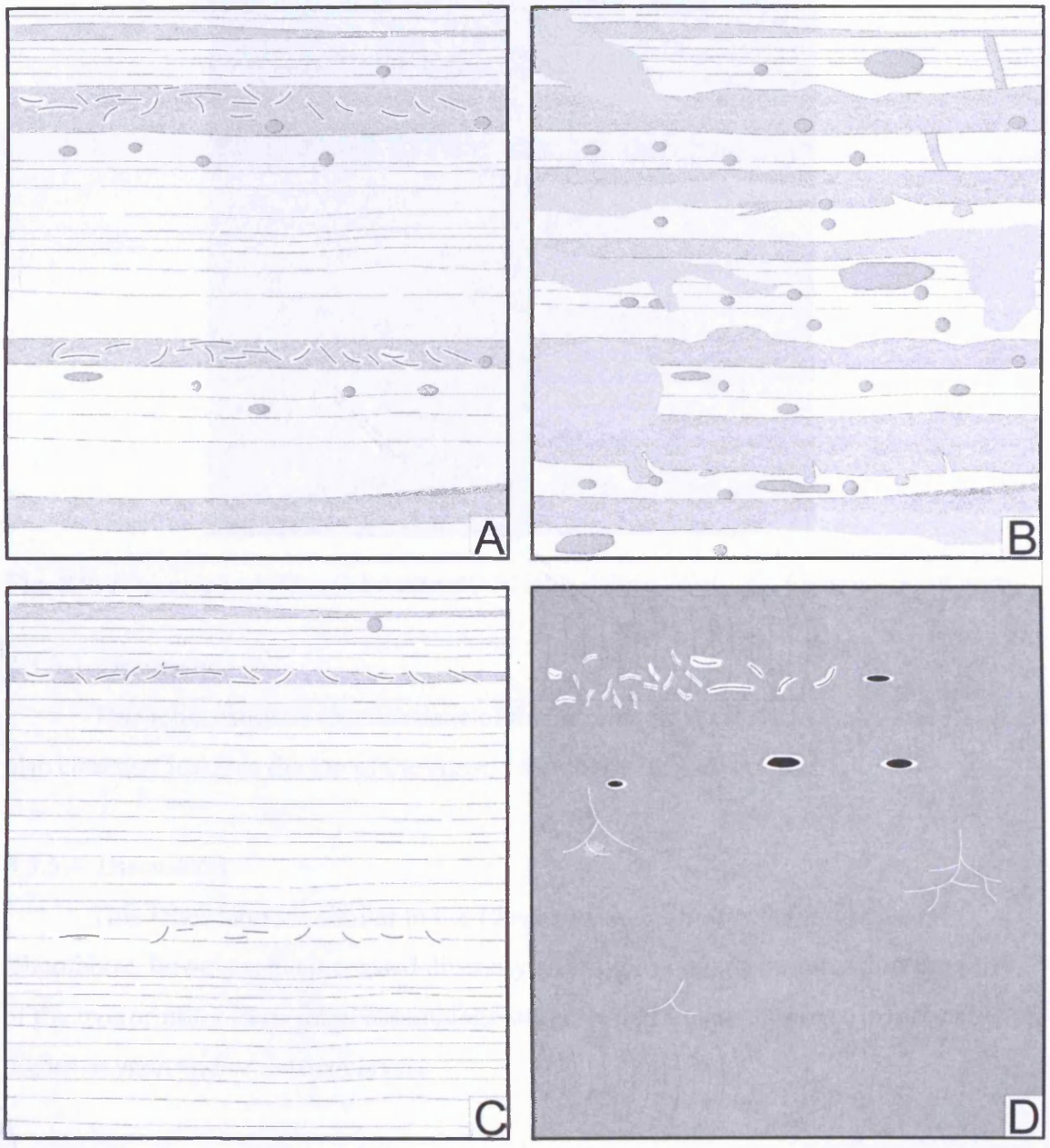

Fig. 8.8. Ichnofabric models: A) *Planolites-Phycosiphon* ichnofabric; B) *Planolites* Ichnofabric; C) *Phycosiphon* ichnofabric; D) *Phyc osiphon-Planolites* homogenised ichnofabric.

Fig. 8.9. *Phycosiphon*-diverse homogenised ichnofabric, Well A1. Core is ~6 cm wide.

8.3.5.3. Occurrence

This ichnofabric is characteristic of the intrafan in Well A4, A2, A1 and L1. It is also common towards the top of the Ainsa I sandbody in Well A1 and L1.

8.3.5.4. Discussion

This ichnofabric is similar to the *Phycosiphon-Planolites* homogenised ichnofabric, however, the increased diversity and slightly raised bioturbation intensity of the overprinting trace-fossil assemblage suggests that this ichnofabric is indicative of higher oxygen and/or nutrient levels.

8.3.6. *Ophiomorpha* ichnofabric

8.3.6.1. Diagnosis

Vertical to horizontal orientated *Ophiomorpha* within medium- to thick-bedded sandstones.

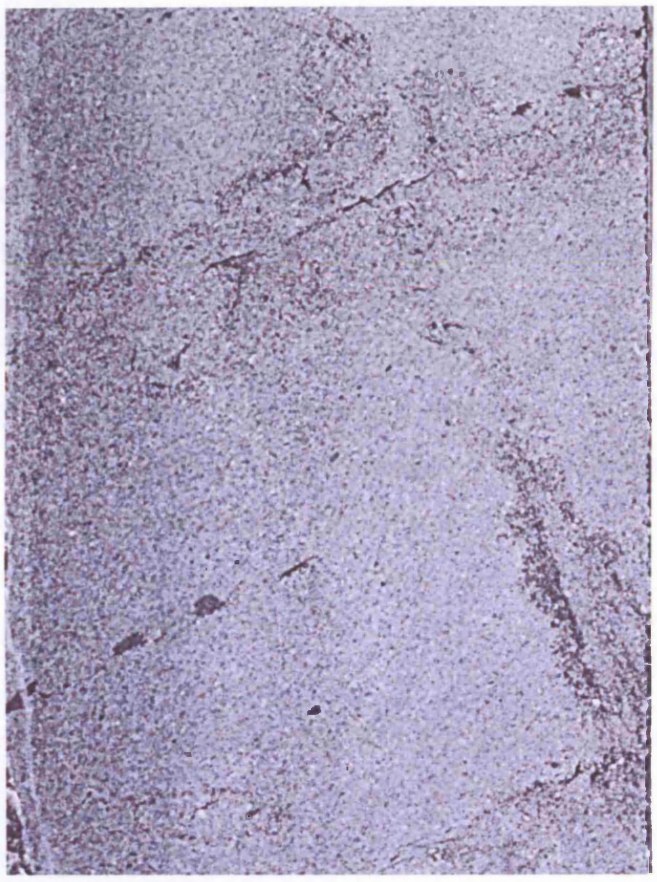

Fig. 8.10. *Ophiomorpha* ichnofabric, Well L1. Core is ~6 cm wide.

8.3.6.2. Description

This ichnofabric is associated with medium- to thick-bedded, commonly amalgamated, coarse-grained sandstones (Facies Group B and C). It is characterised by the almost exclusive occurrence of *Ophiomorpha* which can bioturbate amalgamated sandstone units several metres in thickness. Individual burrows are commonly truncated at amalgamation surfaces and particular horizons within the sandstones may be pervasively bioturbated by *Ophiomorpha*. Bioturbation intensities are low, typically <10% and ichnofabric indices range between 2 to 3. Biodeformational structures are rarely developed.

8.3.6.3. Occurrence

This is the most widespread ichnofabric and is characteristic of most sand-rich successions such as the channel axis and off-axis channel.

8.3.6.4. Discussion

The occurrence of *Ophiomorpha* burrows within medium- to thick-bedded sandstones has also been observed at outcrop (e.g., channel axis sandstones of Ainsa I and Guaso I, section 6.4.1.2 and 6.6.3.2, respectively). These burrow networks were formed by large, robust, deeply burrowing organisms which exploited organic rich layers within the sands. Such colonising strategies were well adapted to thick-bedded axial sandstone deposits because the trace-making organisms were able to survive burial by newly deposited thick sands (Wetzel & Uchman 2001).

In terms of specific ichnospecies, the majority of *Ophiomorpha* identified in core have been recognised at outcrop as *O. rudis* and *O.* isp. *O. annulata,* which is generally smaller, with a thinner, less distinct lining and typically occurs on the soles of turbidite sandstones, is less conspicuous in core than *O. rudis*.

8.3.7. *Thalassinoides*-1 ichnofabric

8.3.7.1. Diagnosis

Intensely bioturbated, coarse-grained, thick-bedded sandstones dominated by *Thalassinoides*.

8.3.7.2. Description

The sandstones are typically structureless, completely mixed and mud-rich (Facies B1.1 and C1.2). This is related to mixing of the deposits associated with intense bioturbation. *Thalassinoides* has structureless fills that contrasts little with the host sediments. Consequently, burrow walls are typically poorly defined resulting in a mottled appearance. Only *Thalassinoides* occurs in this ichnofabric. Bioturbation intensities are typically 70-100%.

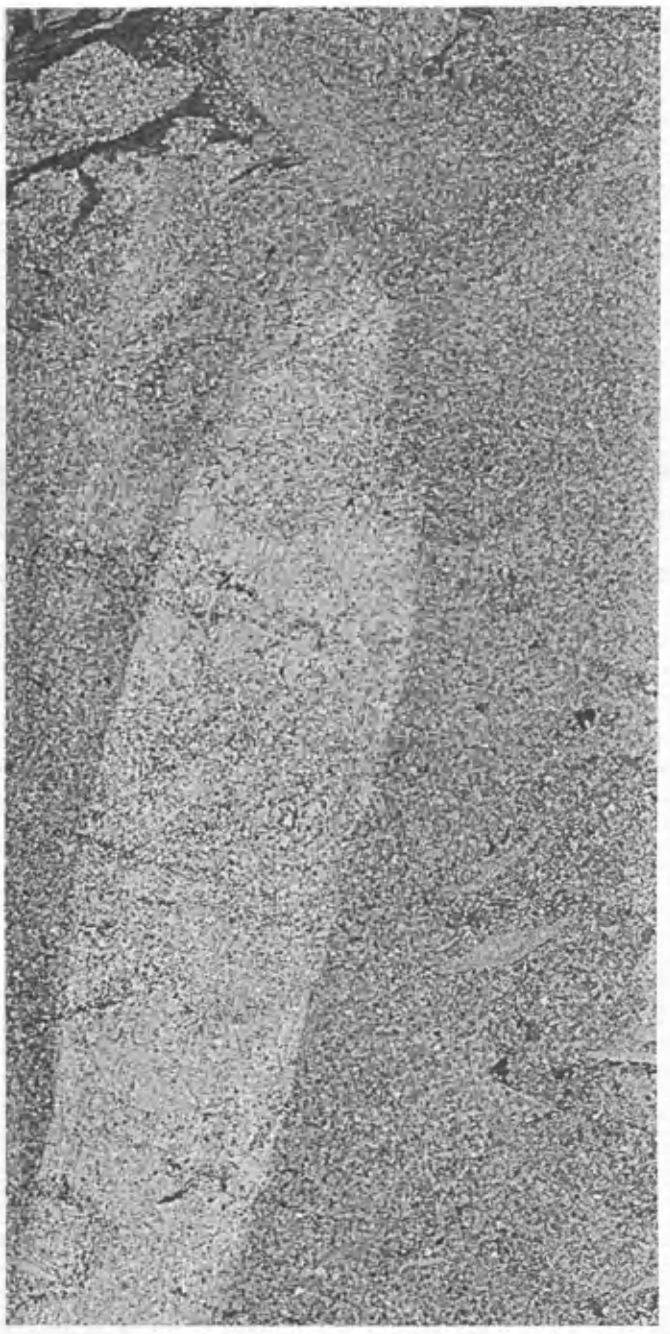

Fig. 8.11. *Thalassinoides*-1 ichnofabric, Well L1. Core is ~6 cm wide.

8.3.7.3. Occurrence

This ichnofabric is typical of thick-bedded sandstones in the channel axis to channel margin.

8.3.7.4. Discussion

Thick-bedded, coarse-grained sandstones tend to be associated with the *Ophiomorpha* ichnofabric, with *Ophiomorpha* representing domiciles excavated by

organisms, which burrowed deeply into the sands to exploit organic rich horizons. *Ophiomorpha* is absent from the *Thalassinoides*-1 ichnofabric, which is dominated by backfilled *Thalassinoides* burrows formed by deposit feeders. In the *Ophiomorpha* ichnofabric, organic matter was concentrated in bedding parallel layers. These organic-rich horizons were intensely bioturbated by *Ophiomorpha*-forming organisms which were able to burrow deeply into the sands because they maintained an open connection to the sea-floor. In the *Thalassinoides*-1 ichnofabric, the intense bioturbation of the sands suggests that organic matter was abundant and the interstitial waters were well-oxygenated. The high bioturbation intensity throughout the sands suggests that organic matter was randomly distributed rather than concentrated in organic rich layers. This suggests that the original deposit was disorganised, and thus this ichnofabric may be associated with Facies B1.1 sandstones deposited by high concentration turbidity currents or hyperconcentrated flows. The intense bioturbation promoted enhanced oxygenation of the interstitial waters in the sands and thus the maintaining of an open connection to the sea-floor was not required.

8.3.8. *Thalassinoides*-2 ichnofabric

8.3.8.1. Diagnosis

Sharp-walled, undeformed, horizontal to vertical orientated *Thalassinoides* in mudstones and siltstones below an erosion surface typically marked by a thick-bedded, coarse-grained sandstone.

8.3.8.2. Description

The *Thalassinoides*-2 ichnofabric typically occurs in siltstone-mudstone laminae (Facies D2.3) or mottled silty mudstones (Facies D1.3) beneath erosion surfaces. These erosion surfaces are typically overlain by coarse-grained sandstones (Facies Group B or C). This ichnofabric is characterised by *Thalassinoides* and, less commonly, *Planolites*, which commonly cross-cut an earlier phase of bioturbation which is characterised by a diverse trace-fossil assemblage, including *Planolites, Phycosiphon, Chondrites, Nereites* and biodeformation structures. The *Thalassinoides* burrows typically have sharp walls, are uncompacted, and orientated horizontal to vertical. The fill of the burrows is the same as the overlying coarse-grained sandstone. Vertical burrows associated with this ichnofabric may be as deep as 15 cm. Bioturbation intensities are

typically moderately high, ranging between 25-75% and ichnofabric indices range between 3 to 3/6. Biodeformation is absent.

8.3.8.3. Occurrence

This ichnofabric is typical of the channel axis and channel off-axis, with examples from Well A3, A5, A1, A2 and L1.

Fig. 8.12. *Thalassinoides*-2 ichnofabric, Well L1. Core is ~6 cm wide.

8.3.8.4. Discussion

This ichnofabric represents colonisation of firmgrounds (*Glossifungites* ichnofacies). These firmgrounds were formed when semi-consolidated mudstones and siltstones were exhumed by erosive bypassing gravity currents. *Thalassinoides*-forming

organisms produced open burrow networks in the semi-consolidated sediment which were later infilled by the overlying sandstone. This ichnofabric is most common in channel axis and channel off-axis environments.

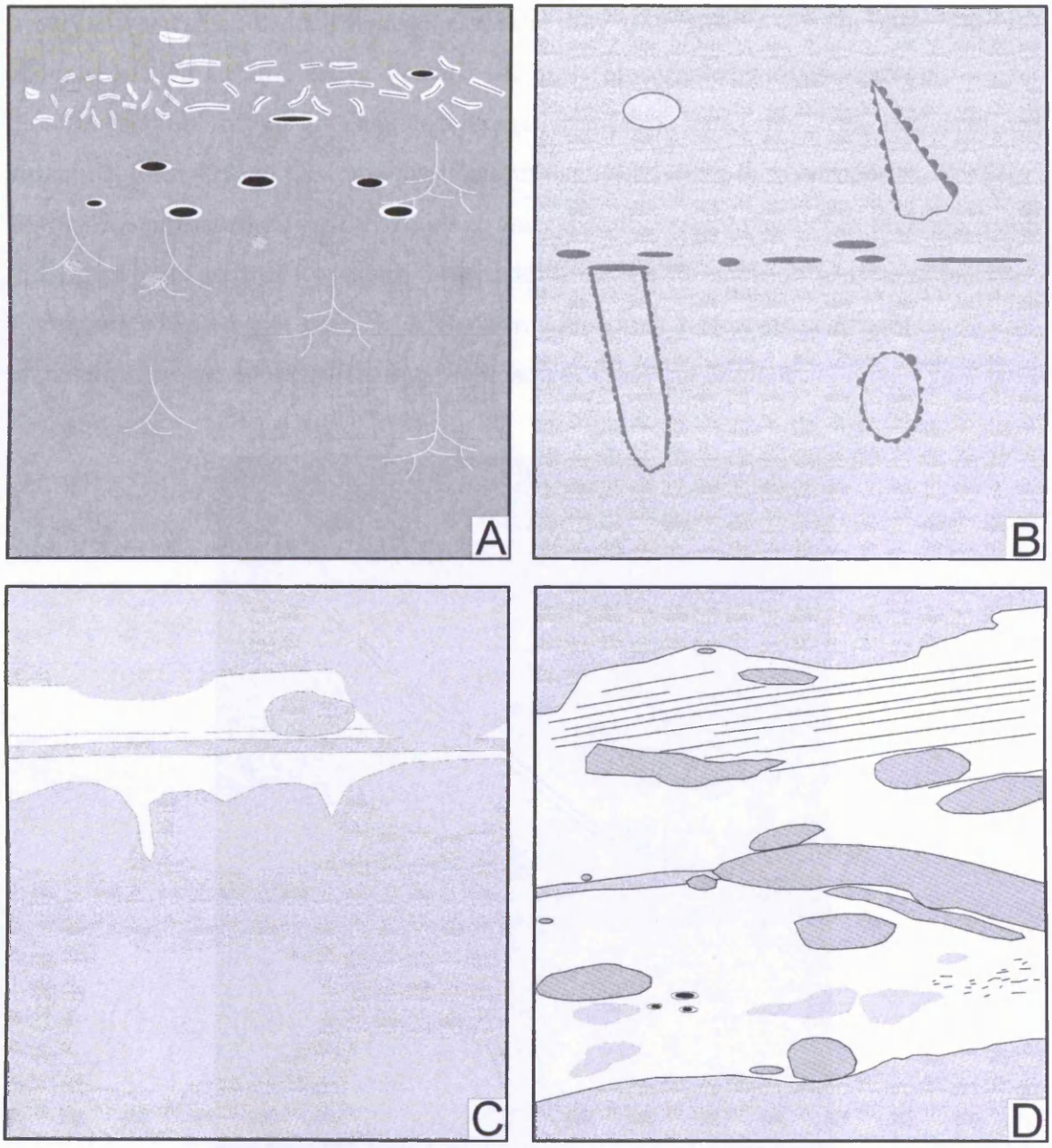

Fig. 8.13. Ichnofabric models: A) *Phycosiphon*-diverse homogenised ichnofabric; B) *Ophiomorpha* ichnofabric; C) *Thalassinoides*-1 ichnofabric; D) *Thalassinoides*-2 ichnofabric.

8.3.9. *Scolicia* Ichnofabric

8.3.9.1. Diagnosis

Siltstone-mudstone laminae intensely bioturbated by *Scolicia*

8.3.9.2. Description

The *Scolicia* ichnofabric is associated with silty mudstone intervals characterised by siltstone-mudstone laminae (Facies D2.3). These intervals commonly occur between thick-bedded sandstones where they are typically <20 cm thick. The siltstone-mudstone laminae are typically intensely bioturbated with an average bioturbation intensity of 51% and an average ichnofabric index of 4.2. Biodeformational structures form 47% of the trace-fossil assemblage. Including these structures, *Scolicia* forms 42% of the trace-fossil assemblage and typically occurs parallel to bedding. Each individual trace generally overlaps the previous one. Other common ichnotaxa include *Planolites, Phycosiphon* and *Thalassinoides,* which may bioturbate sediments undisturbed by the *Scolicia*-forming organism, or cross-cut *Scolicia*.

Fig. 8.14. *Scolicia* ichnofabric, Well L1. Core is ~6 cm wide.

8.3.9.3. Occurrence

This ichnofabric is typical of the levee-overbank of Ainsa I, occurring as thin horizons (<20 cm thick) in Well A4 and A2. It is also common as thin intervals in the channel margin deposits of channel element I.3, Ainsa II, Well A1 and L1. The *Scolicia*

ichnofabric also occurs in the thin-bedded deposits of the abandonment phase at the top of Well L1, Ainsa II sand body.

8.3.9.4. Discussion

In total, 89% of the *Scolicia* ichnofabric comprises biodeformational structures and *Scolicia.* This is indicative of sediments with a high nutrient supply in which behavioural specialisation by organisms was not developed, or restricted to large deposit feeding, *Scolicia*-forming organisms. Other ichnotaxa were probably destroyed by the bulldozer-like trace-forming organisms associated with *Scolicia* or were never developed, with trace-making organisms forming biodeformational structures rather than discrete trace fossils due to the high nutrient supply. The paucity of trace fossils developed after the initial high intensity bioturbation associated with the biodeformational structures and *Scolicia* suggests that oxygen levels and/or nutrient levels were not high enough to support a later diverse trace-fossil assemblage. This is in contrast to the *Scolicia*-diverse-2 ichnofabric (Section 8.3.11).

It is possible that in fine-grained sediments with only minor grain-size contrasts between beds, a high proportion of biodeformational structures may in fact be *Scolicia,* with the absence of contrasting grain-sizes hindering the recognition of spreiten, which characterise *Scolicia.*

8.3.10. *Scolicia*-diverse-1 ichnofabric

8.3.10.1. Diagnosis

Intensely bioturbated, thin-bedded sandstones and siltstone-mudstone laminae with a diverse trace-fossil assemblage dominated by *Scolicia.*

8.3.10.2. Description

This ichnofabric is characterised by thin-bedded sandstones (Facies C2.3), and siltstone-mudstone laminae (Facies D2.3). Bioturbation is intense, averaging 65%, with an average ichnofabric index of 4.5. Biodeformational structures form 64% of the trace-fossil assemblage. Including biodeformational structures, *Scolicia* forms 16% of the trace-fossil assemblage. Other common ichnotaxa include *Phycosiphon, Planolites, Thalassinoides* and *Chondrites.*

In terms of cross-cutting relationships, *Scolicia* is typically cross-cut by all other ichnotaxa and is commonly associated with the biodeformational structures. *Scolicia* is

cross-cut by *Phycosiphon* but is deeper burrowing than *Phycosiphon. Planolites* cross-cuts *Phycosiphon,* which in turn is cross-cut by *Thalassinoides. Chondrites* typically cross-cuts all ichnotaxa.

Fig. 8.15. *Scolicia*-diverse-1 ichnofabric, Well L1. Core is ~6 cm wide.

8.3.10.3. Occurrence

The *Scolicia*-diverse-1 ichnofabric is abundant throughout the Ainsa cores, commonly occurring in muddy intervals between medium- to thick-bedded sandstones, including: (1) the margin of channel element II.2, Ainsa II, Well A3; (2) the margin of channel element 4b, Ainsa II, Well A2; (3) the channel off-axis of Ainsa I, Well A1; (4) the margin of channel element I.3, Ainsa II, Well A1 and Well A3; and (5) channel off-axis deposits of channel element I.1a, Ainsa II, Well L1.

This ichnofabric also occurs as thicker intervals tens of centimetres thick, generally in finer-grained deposits rather than thin muddy intervals between sandstones. These intervals occur in: (1) the levee-overbank of Ainsa I, Well A2; (2) the intrafan, Well A1; and (3) the abandonment deposits at the top of Ainsa II, Well A1.

8.3.10.4. Discussion

This ichnofabric has a higher proportion of biodeformational structures but a lower proportion of *Scolicia* than the *Scolicia* ichnofabric. In general, the biodeformational structures were formed near the sediment/water interface representing structures formed by grazing organisms in soft sediment. The preservation of primary sedimentary features such as bedding, in contrast to the totally homogenised sediments of the *Scolicia*-diverse-2 ichnofabric (Section 8.3.11), may be related to a lower nutrient supply, which restricted bioturbation associated with large deposit-feeders such as *Scolicia*-forming trace-makers, as well as biodeformational structures. However, the high bioturbation intensity suggests that oxygen and nutrient supply were still high.

8.3.11. *Scolicia*-diverse-2 Ichnofabric

8.3.11.1. Diagnosis

Siltstone-mudstone laminae intensely bioturbated by *Scolicia* and a diverse ichnofauna.

8.3.11.2. Description

This ichnofabric is similar to the *Scolicia*-diverse-1 ichnofabric but is associated with intensely bioturbated, commonly homogenised sediments. It is characterised by silty mudstone intervals formed of thin siltstone-mudstone laminae (Facies D2.3). These intervals commonly occur between thick-bedded sandstones where they are typically <20 cm thick. Bioturbation intensity averages 87%, with the siltstone-mudstone laminae commonly totally homogenised. The average ichnofabric index is 6.8 and biodeformational structures form 76% of the trace-fossil assemblage. Including biodeformational structures, *Scolicia* forms 24% of the trace-fossil assemblage. Biodeformational structures typically occur as homogeneous background sediment along with some *Scolicia*. A diverse secondary trace-fossil assemblage is emplaced on this background of totally homogenised sediment and is associated with *Planolites, Phycosiphon* and *Thalassinoides*.

Fig. 8.16. *Scolicia*-diverse-2 ichnofabric, Well A1. Core is ~6 cm wide.

8.3.11.3. Occurrence

This ichnofabric is less common than the *Scolicia*-1 diverse ichnofabric, occurring towards the top of the levee-overbank of Ainsa I, Well A2, where it is punctuated by thin laminated horizons. It also occurs in thin muddy intervals between sandstones in the channel off-axis deposits of Ainsa I, Well A1.

8.3.11.4. Discussion

This ichnofabric is associated with totally homogenised sediments similar to the *Phycosiphon-Planolites* homogenised ichnofabric and the *Phycosiphon*-diverse homogenised ichnofabric. However, these ichnofabrics are characteristic of finer-grained deposits in which homogenisation of the substrate is associated with biodeformational structures formed in fine-grained, soupy substrates.

This ichnofabric is similar to both the *Scolicia* ichnofabric and the *Scolicia*-diverse-1 ichnofabric. However, in both cases, the *Scolicia*-diverse-2 ichnofabric, with its greater intensity trace-fossil assemblage, is interpreted to represent bioturbation in substrates characterised by higher levels of oxygen and/or nutrient supply. Alternatively, sedimentation rates may have been lower resulting in more intense bioturbation.

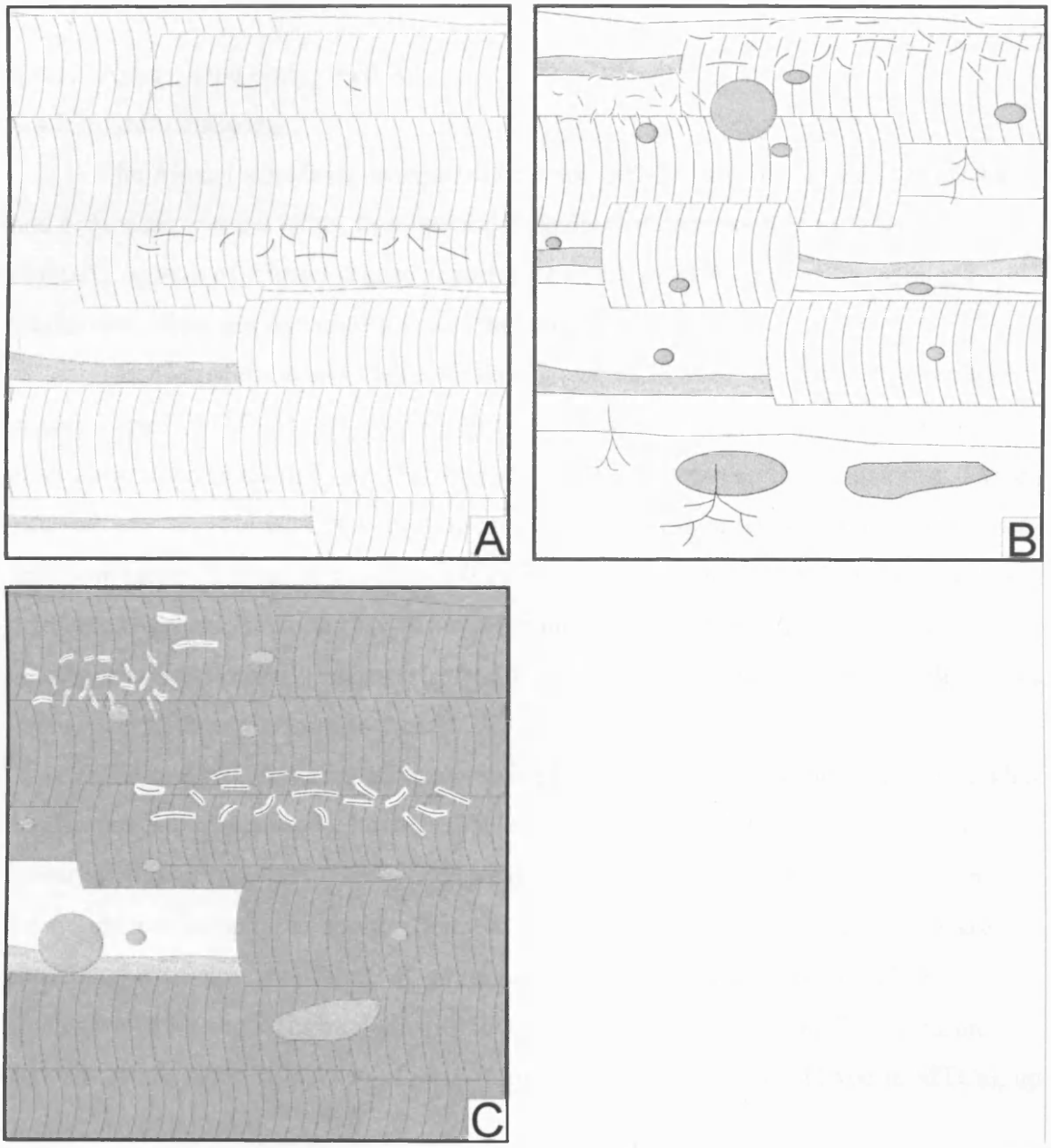

Fig. 8.17. Ichnofabric models: A) *Scolicia* Ichnofabric; B) *Scolicia*-diverse-1 ichnofabric; C) *Scolicia*-diverse-2 ichnofabric.

8.4. Sedimentology and Ichnology

Sedimentological and ichnological descriptions for each Well are detailed below. A summary of ichnological data is provided in Table 8.1 and 8.2 and downhole data is illustrated in Fig. 8.18 (Well A4), Fig. 8.19 (Well A3), Fig. 8.20 (Well A5), Fig. 8.21 (Well A2), Fig. 8.22 (Well A1), and Fig. 8.23 (Well L1).

8.4.1. Ainsa I sand body, Well A4

8.4.1.1. Sedimentology

The Ainsa I sand body is exposed between 209-244 m subsurface in Well A4 and comprises low net:gross, fine-grained deposits that correspond to the levee-overbank system of Ainsa I. These deposits are overlain by 35.6 m of fine-grained sandstones, siltstones and mudstones of the intrafan.

The base of the Ainsa I levee-overbank system in Well A4 is associated with a muddy Type Ia MTC. This is overlain by thin- and rarely medium-bedded, fine- to medium-grained sandstones with thick muddy intervals between the sandstones. These intervals are characterised by very-thin-bedded sandstones, siltstone-mudstone laminae, and more rarely, laminated mudstones (Facies C2.3, D2.3 and E2.2). Towards the top of the levee-overbank, the intensity of bioturbation increases, resulting in mottled siltstones and mudstones (Facies D1.3 and E1.3). Overall, the levee-overbank displays a fining- and thinning-upward sequence.

The overlying intrafan is characterised by thick intervals of mottled thin-bedded sandstones, mudstones and siltstones (Facies C1.2, D1.3 and E1.3). In less intensely bioturbated intervals, very-thin-bedded sandstones, siltstone-mudstone laminae, and laminated mudstones are common (Facies C2.3, D2.3 and E2.2). The intrafan is also associated with rare, very thin (<30 cm thick) intra-formational Type Ib MTCs characterised by abundant mud-clasts in a sand-rich mudstone matrix. The intrafan deposits are overlain by 82.8 m of intra-formational muddy slumps (Type Ia MTCs), up to the base of Ainsa II.

8.4.1.2. Ichnology

The levee-overbank of Ainsa I in Well A4 is intensely bioturbated (45.9%), with an average ichnofabric index of 4. Biodeformational structures are abundant, representing 39% of the deposits and 85% of the trace-fossil assemblage. The basal

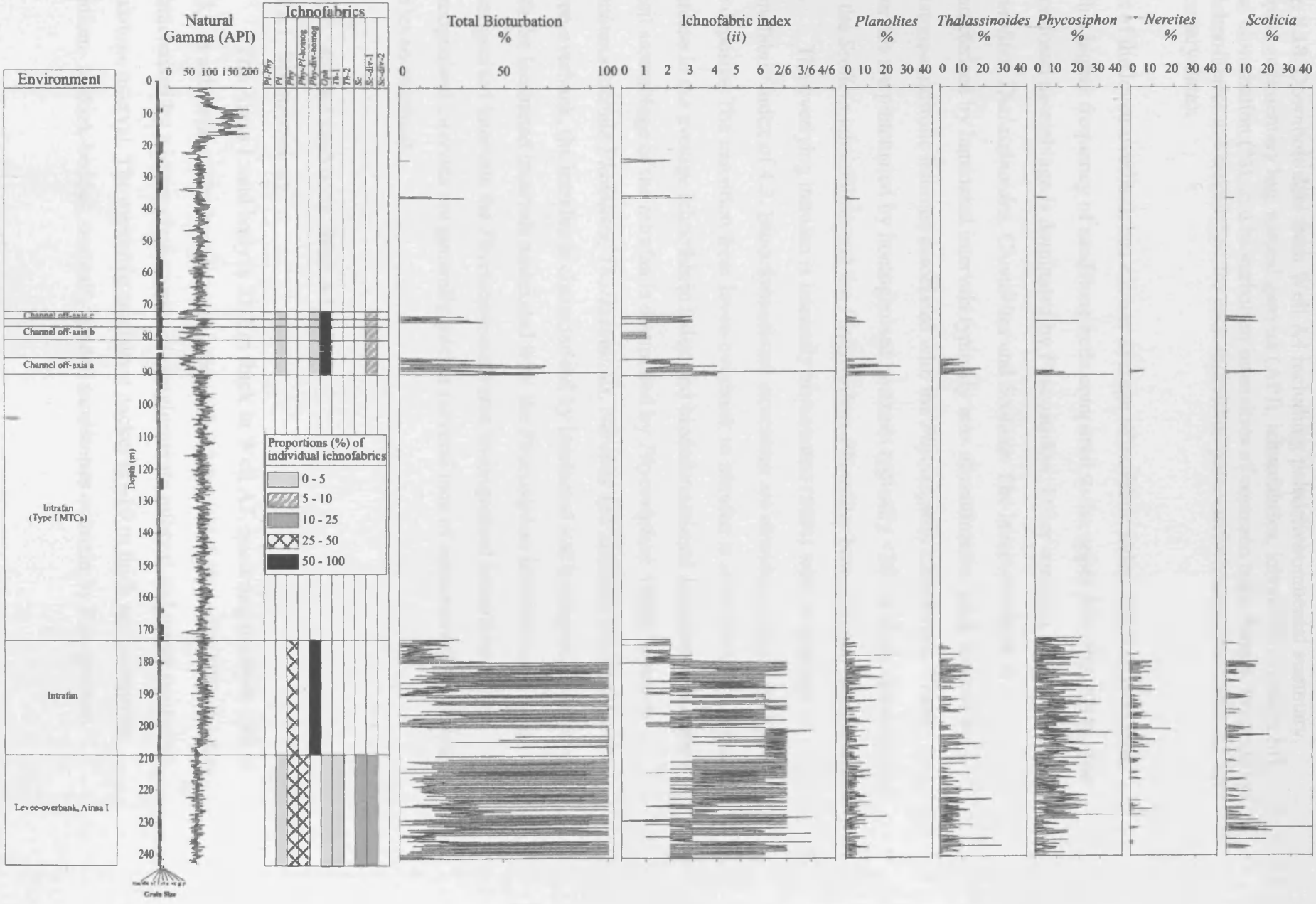
Environment
Natural Gamma (API)
0 50 100 150 200
Ichnofabrics
Pi-Phy
Pi
Phy
Phy-Pi-homog
Phy-div-homog
Opk
Th-1
Th-2
Sc
Sc-div-1
Sc-div-2
Total Bioturbation %
0 50 100
Ichnofabric index (ii)
0 1 2 3 4 5 6 2/6 3/6 4/6
Planolites %
Thalassinoides %
Phycosiphon %
Nereites %
Scolicia %
0 10 20 30 40
Depth (m)
0 10 20 30 40 50 60 70 80 90 100 110 120 130 140 150 160 170 180 190 200 210 220 230 240
Channel off-axis c
Channel off-axis b
Channel off-axis a
Intrafan (Type I MTCs)
Intrafan
Levee-overbank, Ainsa I
Proportions (%) of individual ichnofabrics
0 - 5
5 - 10
10 - 25
25 - 50
50 - 100
Grain Size

Fig. 8.18. Downhole date from Well A4 including; paleoenvironmental summary, graphic sedimentary log, natural gamma (API), ichnofabrics, ichnofabric indices (ii), total bioturbation (%), and bioturbation intensities of common trace fossils. Proportions of ichnofabrics are established for each individual paleoenvironment (see Table 8.2 for summary data).

part of the levee-overbank has a lower average ichnofabric index which is associated with a higher frequency of sandstone beds compared to the upper part (Fig. 8.18). The trace-fossil assemblage is dominated by *Phycosiphon*. Other common ichnotaxa include *Planolites, Thalassinoides, Chondrites* and *Scolicia*. The levee-overbank is characterised by laminated intervals typically tens of centimetres thick formed by siltstone-mudstone laminae associated with the *Phycosiphon* ichnofabric. These intervals are punctuated by homogenised horizons typically <20 cm thick characterised by the *Scolicia* ichnofabric and the *Phycosiphon-Planolites* homogenised ichnofabric.

The overlying intrafan is intensely bioturbated (56%) with an average ichnofabric index of 4.2. Biodeformational structures are abundant, representing 51% of the deposits. The transition from levee-overbank to intrafan is associated with a marked increase in the average ichnofabric index and biodeformational structures. The trace-fossil assemblage of the intrafan is dominated by *Phycosiphon.* Other common ichnotaxa include *Planolites, Thalassinoides, Nereites* and *Scolicia.* Similarly to the levee-overbank, the intrafan is characterised by laminated and homogenised intervals, with the laminated intervals associated with the *Phycosiphon* ichnofabric and the homogenised intervals the *Phycosiphon*-diverse homogenised ichnofabric. The homogenised intervals are generally thicker (several tens of centimetres) than those in the levee-overbank.

8.4.2. Ainsa I sand body, Well A3

8.4.2.1. Sedimentology

The Ainsa I sand body is 23.2 m thick in Well A3, occurring between 180.5-203.7 m subsurface. The base is associated with a 3.5 m thick Type II MTC which is characterised by a lower clast-supported conglomerate interval and upper contorted mudstone interval. The overlying sandstone packet is ~10 m thick and comprises medium- to thick-bedded, normally graded sandstones overlain by fine-grained

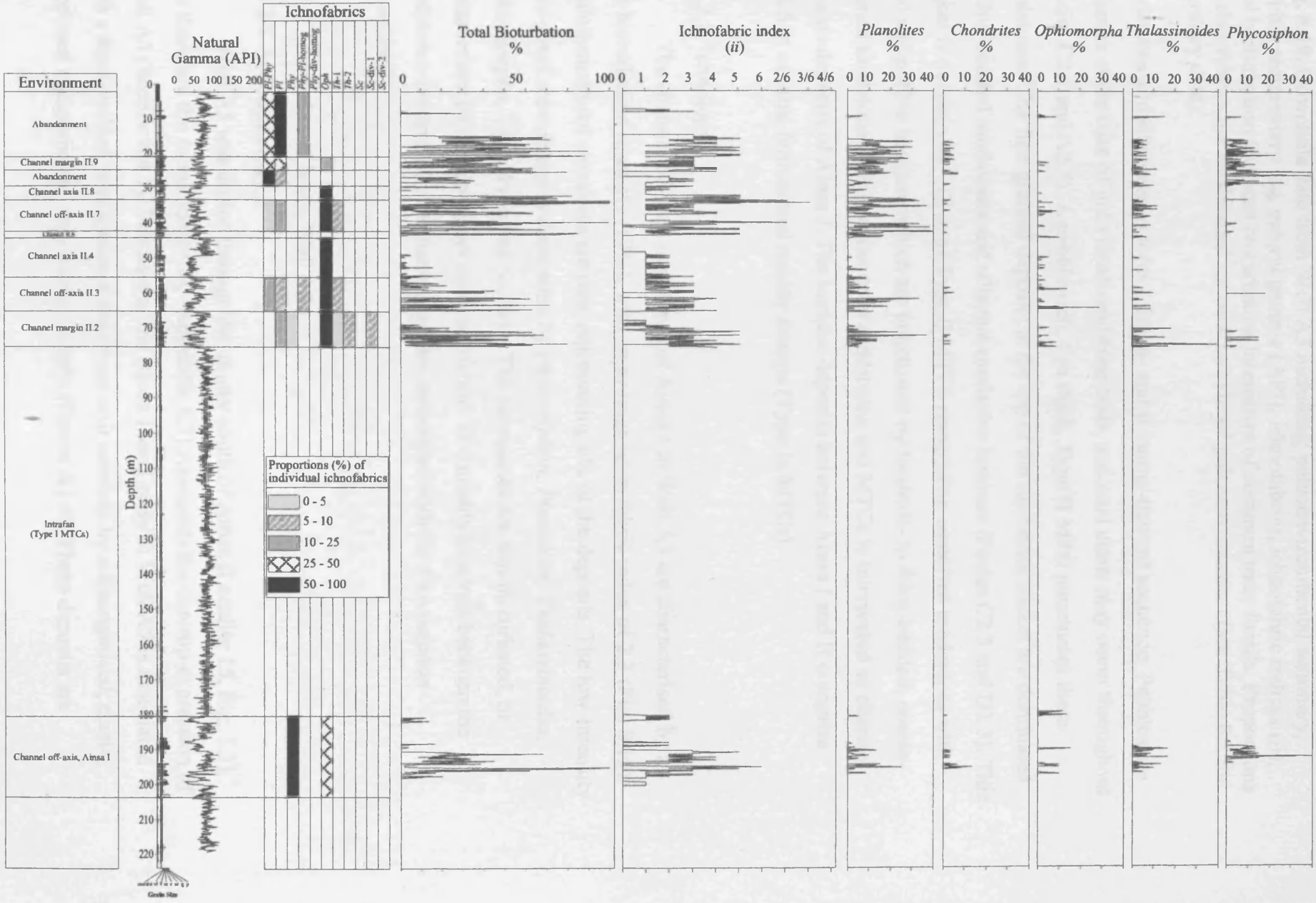
Environment
Natural Gamma (API)
Ichnofabrics
Total Bioturbation %
Ichnofabric index (ii)
Planolites %
Chondrites %
Ophiomorpha %
Thalassinoides %
Phycosiphon %
Depth (m)
Abandonment
Channel margin II.9
Abandonment
Channel axis II.8
Channel off-axis II.7
Channel II.6
Channel axis II.4
Channel off-axis II.3
Channel margin II.2
Intrafan (Type I MTCs)
Channel off-axis, Ainsa I
Proportions (%) of individual ichnofabrics
0 - 5
5 - 10
10 - 25
25 - 50
50 - 100

Fig. 8.19. Downhole date from Well A3 including; paleoenvironmental summary, graphic sedimentary log, natural gamma (API), ichnofabrics, ichnofabric indices (ii), total bioturbation (%), and bioturbation intensities of common trace fossils. Proportions of ichnofabrics are established for each individual paleoenvironment (see Table 8.2 for summary data).

sandstones and siltstones to form a fining- and thinning-upward sequence. Pebbles are common at the base of individual sandstone beds, and mud clasts may occur throughout (Facies C2.1 and A2.7). A pebble-rich, 1 m thick, Type II MTC punctuates these sandstones. The fine-grained deposits at the top of the sandstone packet are dominated by thin-bedded sandstones and siltstone-mudstone laminae (Facies C2.3 and D2.3). This packet is overlain by ~12 m of Type II MTCs comprising contorted mudstones with sand and pebble horizons which are punctuated by medium- to thick-bedded, coarse-grained sandstones. This sequence of sandstones and MTCs is interpreted as channel off-axis deposits of Ainsa I. The intrafan deposits between Ainsa I and II comprise 102.5 m of intra-formational muddy slumps (Type Ia MTCs).

8.4.2.2. Ichnology

The channel off-axis sandstones of Ainsa I in Well A3 are characterised by a low bioturbation intensity (17%), with an average ichnofabric index of 2.3 (Fig. 8.19). Biodeformational structures are rare, representing 6% of the deposits. The low-intensity trace-fossil assemblage is dominated by *Phycosiphon, Planolites, Thalassinoides, Ophiomorpha, Chondrites* and *Scolicia.* The sandstones are non-bioturbated, or characterised by the *Ophiomorpha* ichnofabric. The muddy intervals between the sandstones are typically laminated, and are associated with the *Phycosiphon* ichnofabric.

8.4.3. Ainsa I sand body, Well A5

8.4.3.1. Sedimentology

Well A5 was drilled through the quarry south of Ainsa (Locality 15, Fig. 1.3), and therefore the Ainsa quarry log (Appendix 6.7) represents the outcrop expression of Well A5 (Section 6.4.1). The base of the Ainsa I sand body in Well A5 is associated with a thick-bedded, amalgamated sandstone unit overlain by a disorganised, clast-supported conglomerate with a sandy matrix (Facies A1.4). These deposits are

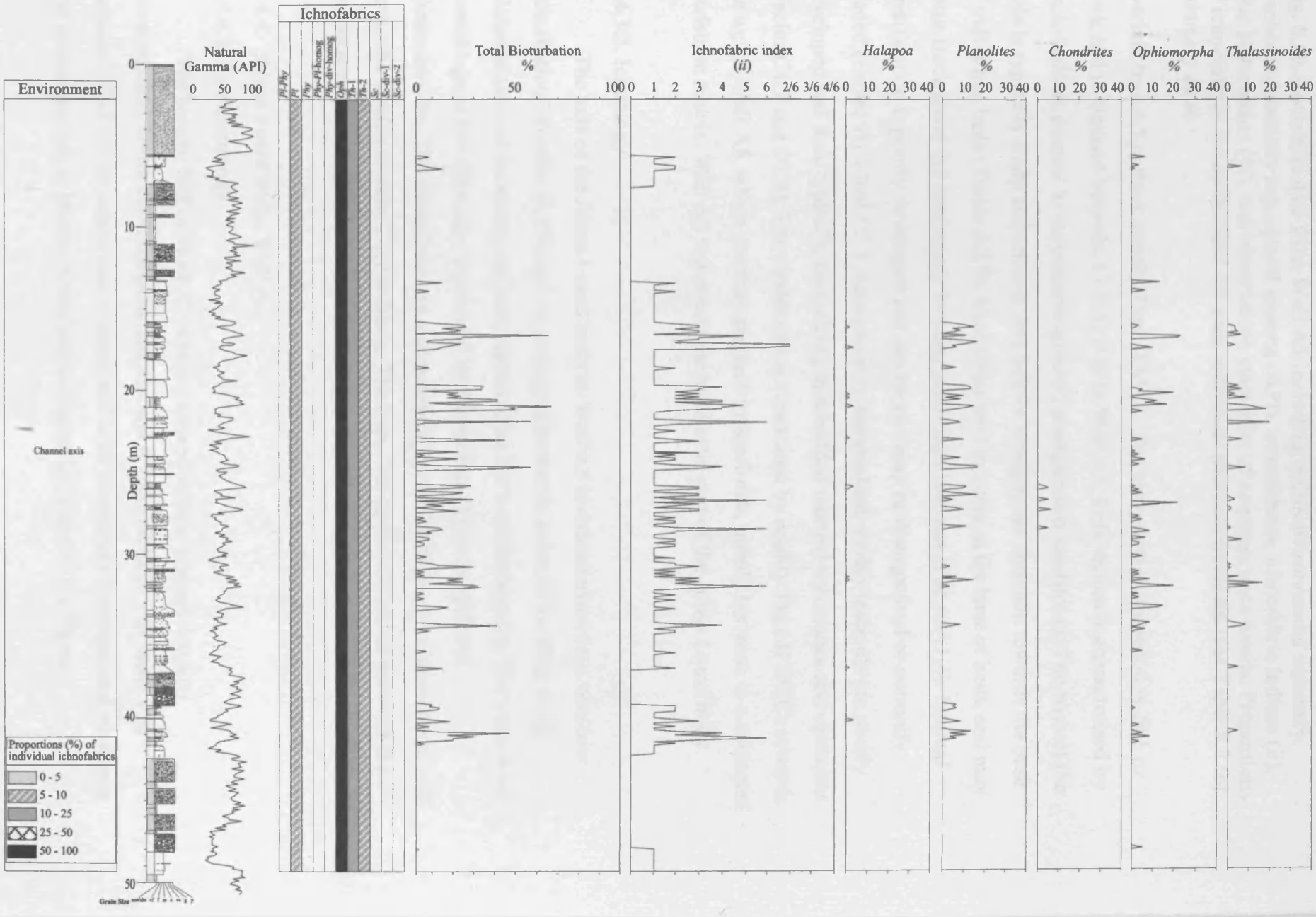
Environment
Channel axis
Proportions (%) of individual ichnofabrics
0 - 5
5 - 10
10 - 25
25 - 50
50 - 100
Depth (m)
0
10
20
30
40
50
Natural Gamma (API)
0 50 100
Ichnofabrics
Pf-Phy
Pf
Phy
Phy-Pf-homog
Phy-div-homog
Cyls
Th-1
Th-2
Sc
Sc-div-1
Sc-div-2
Total Bioturbation %
0 50 100
Ichnofabric index (ii)
0 1 2 3 4 5 6 2/6 3/6 4/6
Halapoa %
0 10 20 30 40
Planolites %
0 10 20 30 40
Chondrites %
0 10 20 30 40
Ophiomorpha %
0 10 20 30 40
Thalassinoides %
0 10 20 30 40

Fig. 8.20. Downhole date from Well A5 including; paleoenvironmental summary, graphic sedimentary log, natural gamma (API), ichnofabrics, ichnofabric indices (ii), total bioturbation (%), and bioturbation intensities of common trace fossils. Proportions of ichnofabrics are established for each individual paleoenvironment (see Table 8.2 for summary data).

overlain by a 4.5 m thick pebbly Type II MTC. The main sandy succession is 29.1 m thick and is exposed between 13.3-42.4 m in Well A5. This section is characterised by thick-bedded, coarse- to very-coarse-grained amalgamated sandstones. The base of the beds is typically sharp and erosive, and pebble stringers are common towards the base of individual beds (Facies A2.7). Mud clasts tend to occur at the base of beds, and may occur throughout the sandstones forming mud-flake breccias (Facies A1.4). Internal stratification is poorly developed and sandstones may be disorganised or normally graded (Facies B1.1 and C2.1, respectively). Interbedded muddy intervals are poorly developed and thin, typically comprising thin-bedded mottled sandstones and siltstones (Facies C1.2 and D1.3). The sandstones are truncated by muddy Type II MTCs towards the top of Well A5, which are characterised by sand-rich, pebbly horizons in a contorted mudstone matrix. Well A5 represents the most axial part of the Ainsa I sand body.

8.4.3.2. Ichnology

The axis of the Ainsa I sand body in Well A5 is characterised by a very low bioturbation intensity (4.2%) and an average ichnofabric index of 1.1 (Fig. 8.20). Biodeformational structures are rare, representing 3.1% of the deposits. The trace-fossil assemblage is low diversity, dominated by *Planolites, Ophiomorpha* and *Thalassinoides*. The sandstones are characterised by the *Ophiomorpha* ichnofabric, and rarely the *Thalassinoides*-2 ichnofabric. The thin, fine-grained intervals between the sandstones are associated with the *Planolites* ichnofabric.

8.4.4. Ainsa I sand body, Well A2

8.4.4.1. Sedimentology

The bottom half of Well A2 is characterised by fine-grained deposits corresponding to two environments, interfan and levee-overbank. The basal 8 m between 242.7-251 m subsurface is associated with completely homogenised siltstones and mudstones due to intense bioturbation (Facies D1.3 and E1.3). These

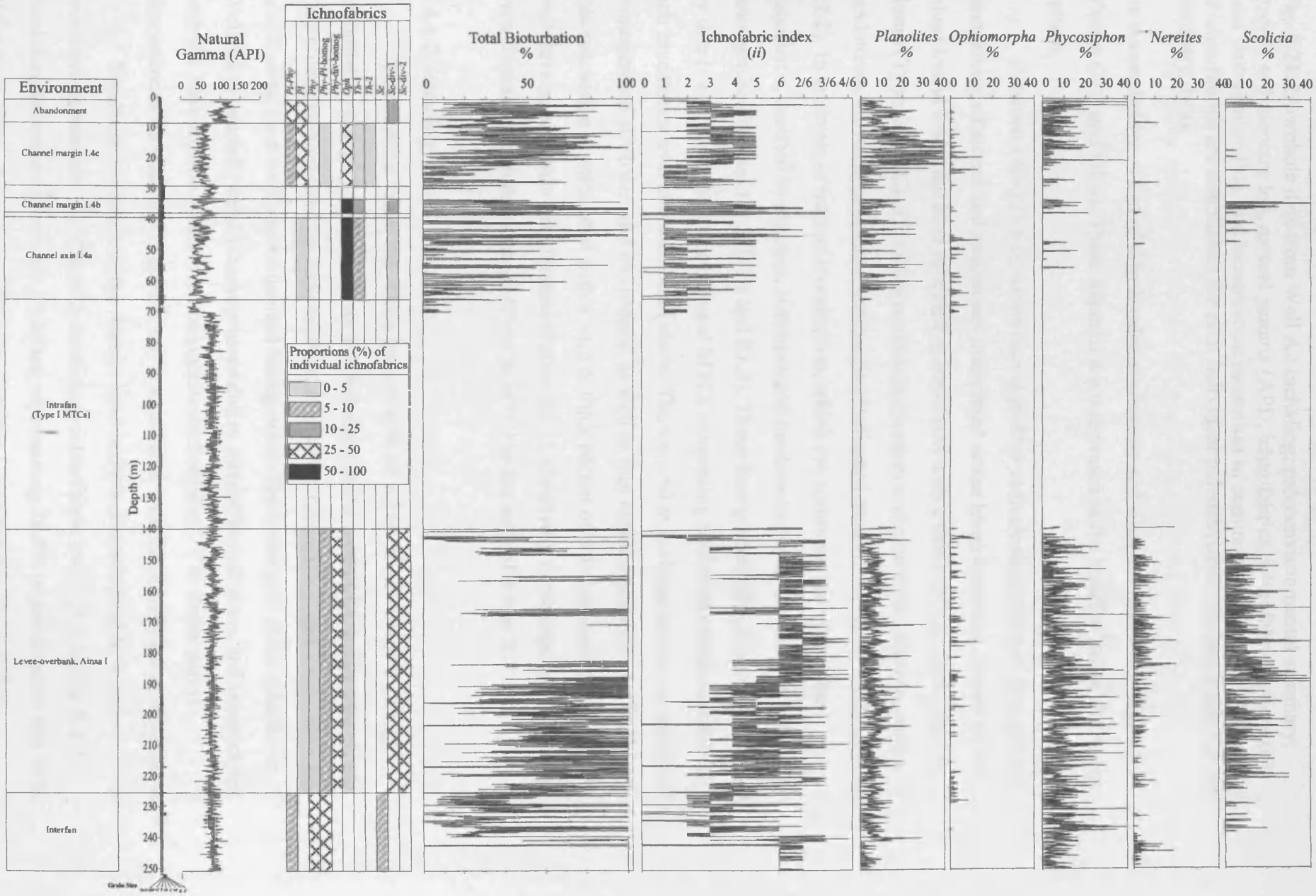
Environment
Abandonment
Channel margin I.4c
Channel margin I.4b
Channel axis I.4a
Intrafan
(Type I MTCs)
Levee-overbank, Ainsa I
Interfan
Depth (m)
Natural
Gamma (API)
0 50 100 150 200
Ichnofabrics
Pl-Php
Pl
Php
Php-Pl-homog
Php-dw-homog
Oph
Ps-1
Ps-2
Sc
Sc-div-1
Sc-div-2
Proportions (%) of
individual ichnofabrics
0 - 5
5 - 10
10 - 25
25 - 50
50 - 100
Total Bioturbation
%
0 50 100
Ichnofabric index
(ii)
0 1 2 3 4 5 6 2/6 3/6 4/6
Planolites
%
Ophiomorpha
%
Phycosiphon
%
Nereites
%
Scolicia
%
0 10 20 30 40

Fig. 8.21. Downhole date from Well A2 including; paleoenvironmental summary, graphic sedimentary log, natural gamma (API), ichnofabrics, ichnofabric indices (ii), total bioturbation (%), and bioturbation intensities of common trace fossils. Proportions of ichnofabrics are established for each individual paleoenvironment (see Table 8.2 for summary data).

are succeeded by ~15 m of thin-bedded sandstones and siltstone-mudstone laminae (Facies C2.3 and D2.3). These deposits are interpreted as the interfan below the Ainsa system.

Between 140-225.6 m subsurface is an 85.6 m thick succession of fine-grained sandstones, siltstones and mudstones interpreted as the levee-overbank system of the Ainsa I sand body, the base of which is associated with a thin (<30 cm thick) muddy slump (Type Ia MTC). This 85.6-m-thick succession is characterised by thin-bedded sandstones, siltstone-mudstone laminae and laminated mudstone (Facies C2.3, D2.3 and E2.2). In intervals of intense bioturbation, which are common throughout the succession, mottled sandstones, siltstones and mudstones occur, and may be totally homogenised (Facies C1.2, D1.3 and E1.3). These fine-grained deposits are punctuated by thin (<1 m thick) intra-formational MTCs comprising contorted mudstones and sand-rich mudstones with abundant sand clasts. The top ~50 m is characterised by completely homogenised siltstones and mudstones, as well as thin mottled sandstones. The top of this succession is associated with a ~1.5 m thick packet of amalgamated sandstones with well developed planar stratification (Facies B2.1). Overlying these deposits is 70 m of intra-formational muddy slumps (Type Ia MTC) to the base of Ainsa II.

8.4.4.2. Ichnology

The interfan below the Ainsa system in Well A2 is characterised by a high bioturbation intensity (64%) with an average ichnofabric index of 4.6. The trace-fossil assemblage is dominated by *Phycosiphon, Planolites, Chondrites,* and *Thalassinoides,* which occur on a totally homogenised background. The lower part of the interfan in Well A2 is generally totally homogenised due to intense bioturbation, and is associated with the *Phycosiphon-Planolites* homogenised ichnofabric. The upper part is characterised by laminated deposits and is associated with the *Phycosiphon* ichnofabric.

The levee-overbank of the Ainsa I sand body is characterised by a high bioturbation intensity (83.9%) with an average ichnofabric index of 5.8 (Fig. 8.21). Biodeformational structures are abundant, representing 78.8% of the deposits and 94% of the trace-fossil assemblage. The most common ichnotaxa are *Phycosiphon,*

Planolites, Scolicia, Thalassinoides, Chondrites and *Nereites.* The levee-overbank is characterised by the *Phycosiphon-Planolites* homogenised ichnofabric, *Scolicia*-diverse-1 ichnofabric and the *Scolicia*-diverse-2 ichnofabric, with the *Scolicia*-diverse-1 ichnofabric more dominant at the base and the *Scolicia*-diverse-2 ichnofabric at the top.

8.4.5. Ainsa I sand body, Well A1

8.4.5.1. Sedimentology

The lower half of Well A1 is associated with three environments; interfan, channel off-axis, and intrafan. The basal 20.2 m of Well A1 which represent the interfan deposits comprise essentially totally bioturbated sandstones, siltstones and mudstones (Facies C1.2, D1.3 and E1.3). These interfan deposits are overlain by the Ainsa I sand body, which is 21.6 m thick in Well A1, occurring between 179.8-201.4 m subsurface. The base is associated with a 3.2-m-thick packet of thin (<1 m thick) intra-formational Type I MTCs comprising both contorted mudstones (slumps) and sand-rich mudstones (debris flow deposits), interbedded with intensely bioturbated thin-bedded sandstones, siltstones and mudstones (Facies C1.2, D1.3 and E1.3). Overlying the basal MTCs is ~11 m of medium- to thick-bedded, medium- to coarse-grained amalgamated sandstones. A number of beds exhibit normal grading, and internal stratification is well developed in many sandstones, including planar stratification (Facies B2.1 and C2.1). Mud clast horizons are common in many beds. Towards the top of the sandstone packet, amalgamated sandstones are less frequent, and muddy intervals between beds are preserved, and characterised by intensely bioturbated siltstones (Facies D1.3). The top ~6 m of the channel off-axis deposits are associated with thin-bedded sandstones, and intensely bioturbated sandstones, siltstones and mudstones (Facies C2.3, C1.2, D1.3 and E1.3, respectively), forming a fining- and thinning-upward sequence. These fine-grained deposits probably represent a channel abandonment phase. Overlying these deposits is 30.2 m of intensely bioturbated sandstones, siltstones and mudstones (Facies C1.2, D1.3 and E1.3) as well as horizons of thin- to medium-bedded sandstones interbedded with intensely bioturbated siltstones and mudstones (Facies C2.3, D1.3 and E1.3). These fine-grained deposits of the intrafan are overlain by 49.6 m of intra-formational muddy slumps (Type Ia MTC), to the base of Ainsa II.

8.4.5.2. Ichnology

The interfan below the Ainsa system is characterised by a high bioturbation intensity (90%) and high average ichnofabric index (5.9). Biodeformational structures are common and form 88% of the deposits. The trace-fossil assemblage is dominated by *Phycosiphon.* Other common ichnotaxa include *Chondrites, Planolites, Nereites* and *Thalassinoides*. The interfan is characterised by the *Phycosiphon-Planolites* homogeneous ichnofabric. Thin laminated horizons typically <10 cm thick punctuate these homogenised intervals and are associated with the *Phycosiphon* ichnofabric.

The channel off-axis of Ainsa I is characterised by a high bioturbation intensity (41.9%) with an average ichnofabrc index of 3.5 (Fig. 8.22). Biodeformational structures represent 35% of the deposits. The trace-fossil assemblage is dominated by *Thalassinoides, Planolites, Phycosiphon* and *Scolicia*. The fining-upward sequence associated with the channel off-axis deposits is clearly represented in the trace-fossil assemblages, with an increase in bioturbation intensity and average ichnofabric indices from the base to the top of Ainsa I. The fine-grained deposits immediately overlying the basal MTC are associated with the *Scolicia*-diverse-1 ichnofabric. The main body of sandstones is associated with the *Ophiomorpha* ichnofabric, and more rarely, the *Thalassinoides*-1 ichnofabric. Thin muddy intervals between the sandstones are dominated by the *Scolicia*-diverse-1 ichnofabric and the *Scolicia*-diverse-2 ichnofabric. Towards the top of the channel off-axis, the most common ichnofabrics are the *Phycosiphon*-diverse homogeneous ichnofabric and the *Scolicia*-diverse-2 ichnofabric.

The intrafan is characterised by a high bioturbation intensity (88%) with an average ichnofabric index of 6.1. Biodeformational structures represent 84% of the deposits. The trace-fossil assemblage is dominated by *Planolites* and *Phycosiphon.* Other common ichnotaxa include *Thalassinoides, Chondrites* and *Nereites.* The intrafan is characterised by the *Phycosiphon*-diverse homogeneous ichnofabric.

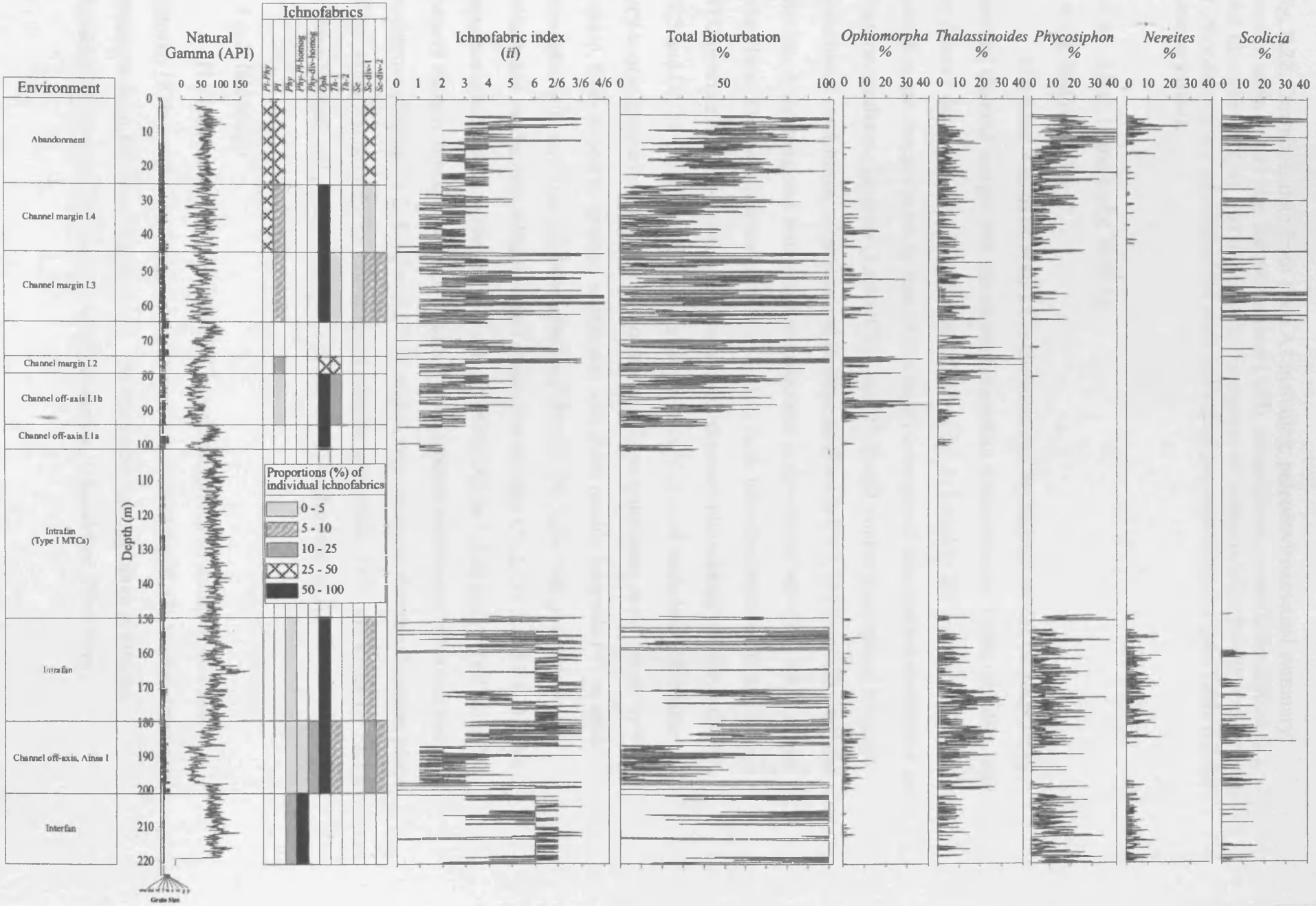
Environment
Natural Gamma (API)
0 50 100 150
Ichnofabrics
Pl-Phy
Pl
Phy
Phy-Pl-homog
Phy-div-homog
Ophi
Th-1
Th-2
Sc
Sc-div-1
Sc-div-2
Ichnofabric index (ii)
0 1 2 3 4 5 6 2/6 3/6 4/6
Total Bioturbation %
0 50 100
Ophiomorpha %
0 10 20 30 40
Thalassinoides %
0 10 20 30 40
Phycosiphon %
0 10 20 30 40
Nereites %
0 10 20 30 40
Scolicia %
0 10 20 30 40
Depth (m)
0 10 20 30 40 50 60 70 80 90 100 110 120 130 140 150 160 170 180 190 200 210 220
Abandonment
Channel margin I.4
Channel margin I.3
Channel margin I.2
Channel off-axis I.1b
Channel off-axis I.1a
Intrafan (Type I MTCs)
Intrafan
Channel off-axis, Ainsa I
Interfan
Proportions (%) of individual ichnofabrics
0 - 5
5 - 10
10 - 25
25 - 50
50 - 100

Fig. 8.22. Downhole date from Well A1 including; paleoenvironmental summary, graphic sedimentary log, natural gamma (API), ichnofabrics, ichnofabric indices (ii), total bioturbation (%), and bioturbation intensities of common trace fossils. Proportions of ichnofabrics are established for each individual paleoenvironment (see Table 8.2 for summary data).

8.4.6. Ainsa I sand body, Well L1

8.4.6.1. Sedimentology

The basal ~30 m of Well L1 is characterised by deposits which correspond to interfan, channel margin and abandonment/intrafan environments. These correlate with the Ainsa I deposits in the Bco. Forcaz (Section 6.5.3; Locality 20; Appendix 6.10). The basal 8 m are characterised by thin (<1 m thick) intervals of thin-bedded sandstones and siltstone-mudstone laminae (Facies C2.3 and D2.3) and thicker intervals of intensely bioturbated sandstones, siltstones and mudstones (Facies C1.2, D1.3 and E1.3) of the interfan. A thinning and fining-upward sequence is developed between 204-218.3 m subsurface. The base is associated with a ~1 m thick intra-formational muddy Type I MTC overlain by thin-bedded sandstones and intensely bioturbated siltstones (Facies C2.3 and D1.3). Overlying these basal deposits is ~1.5 m of thick-bedded, coarse- to very-coarse-grained amalgamated sandstones. These sandstones are overlain by thin-bedded, fine- to coarse-grained sandstones with thick muddy intervals (<1 m thick) associated with siltstone-mudstone laminae (Facies D2.3), as well as intensely bioturbated sandstones, siltstones and mudstones (Facies C1.2, D1.3 and E1.3). This sequence corresponds to the channel margin of the Ainsa I sand body. Overlying the channel margin deposits is 8 m of intensely bioturbated sandstones, siltstones and mudstones (Facies C1.2, D1.3 and E1.3), which may represent the abandonment phase of the Ainsa I sand body, or fine-grained intrafan sediments. This is overlain by 73.1 m of intra-formational muddy slumps (Type Ia MTC) to the base of Ainsa II.

8.4.6.2. Ichnology

The interfan at the base of Well L1 is characterised by a high bioturbation intensity (87%) with an average ichnofabric index of 6.3 (Fig. 8.23).Biodeformational structures form 83.4% of the deposits. The trace-fossil assemblage is diverse, characterised by high abundances of *Phycosiphon, Chondrites, Planolites,*

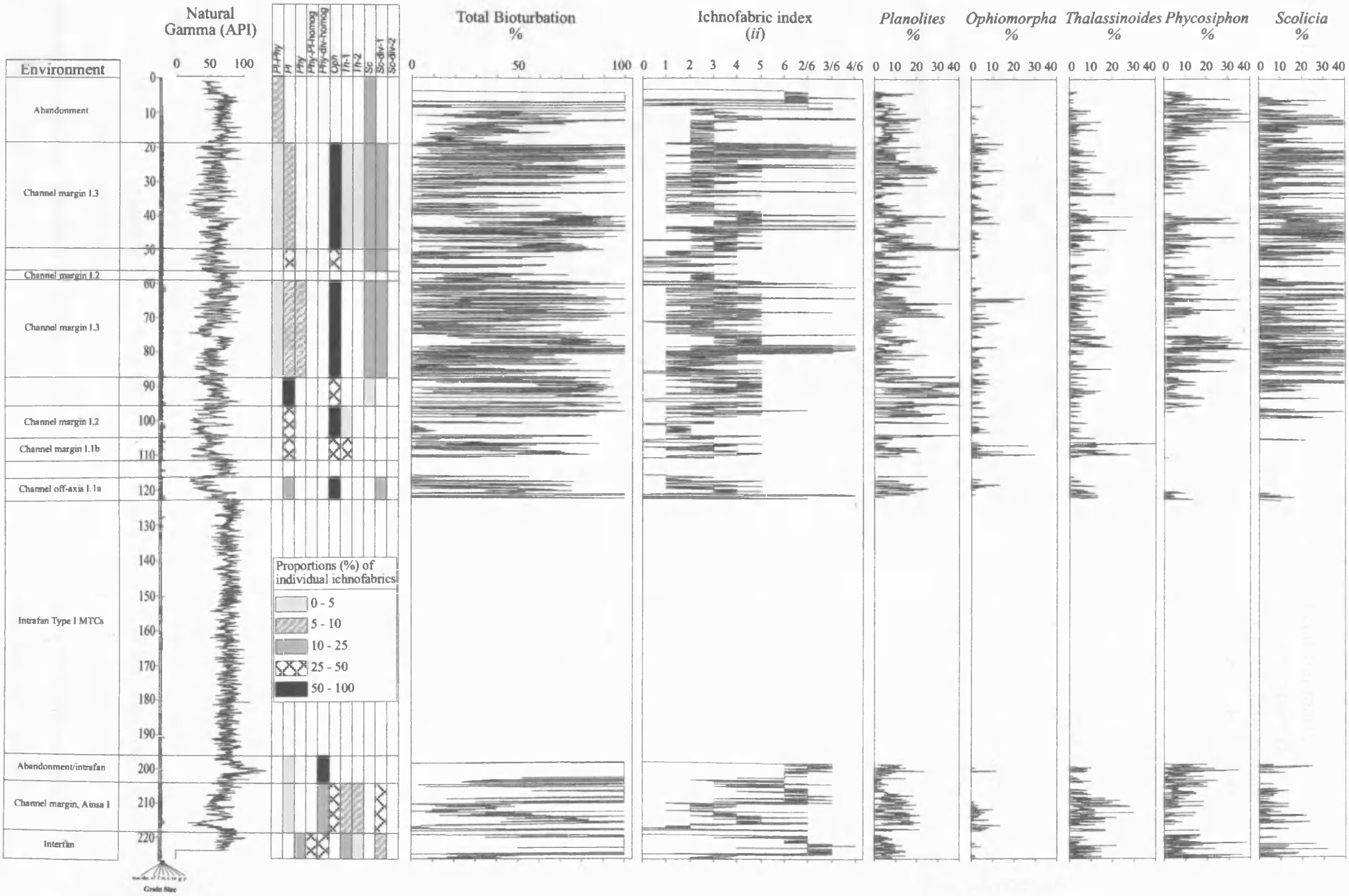
Environment
Natural Gamma (API)
0 50 100
Abandonment
Channel margin 1.3
Channel margin 1.2
Channel margin 1.3
Channel margin 1.2
Channel margin 1.1b
Channel off-axis 1.1a
Intrafan Type I MTCs
Abandonment/intrafan
Channel margin, Aimsa 1
Interfan
Grain Size
Pl-Phy
Pl
Phy
Phy-Pl-homog
Phy-div-homog
Cplx
Th-1
Th-2
Sc
Sc-div-1
Sc-div-2
Proportions (%) of individual ichnofabrics
0 - 5
5 - 10
10 - 25
25 - 50
50 - 100
Total Bioturbation %
0 50 100
Ichnofabric index (ii)
0 1 2 3 4 5 6 2/6 3/6 4/6
Planolites %
Ophiomorpha %
Thalassinoides %
Phycosiphon %
Scolicia %
0 10 20 30 40

Fig. 8.23. Downhole date from Well L1 including; paleoenvironmental summary, graphic sedimentary log, natural gamma (API), ichnofabrics, ichnofabric indices (ii), total bioturbation (%), and bioturbation intensities of common trace fossils. Proportions of ichnofabrics are established for each individual paleoenvironment (see Table 8.2 for summary data).

Thalassinoides, Scolicia and *Nereites.* The interfan is dominated by the *Phycosiphon*-diverse homogenised ichnofabric and the *Phycosiphon-Planolites* homogenised ichnofabric. Thin intervals of laminated sediments characterised by the *Phycosiphon* ichnofabric occur throughout the interfan.

The channel margin of Ainsa I is characterised by a high bioturbation intensity (43%) with an average ichnofabric index of 3.5. Biodeformational structures form 32% of the deposits. The trace-fossil assemblage is dominated by *Planolites* and *Thalassinoides.* The base of the channel margin is associated with the *Ophiomorpha* ichnofabric in the sandstones and the *Planolites* ichnofabric in the muddy intervals between the sandstones. The middle and upper part of the channel margin is associated with the Scolicia-diverse-1 ichnofabric and the *Phycosiphon*-diverse-homogenised ichnofabric. The medium-bedded sandstones are characterised by the *Ophiomorpha* ichnofabric.

The abandonment/intrafan overlying the channel margin has a bioturbation intensity of 94.8% with an average ichnofabric index of 6.3. Biodeformational structures form 94% of the deposits. The trace-fossil assemblage is dominated by *Phycosiphon.* Other common ichnotaxa include *Planolites, Nereites, Chondrites, Thalassinoides* and *Scolicia.* The abandonment/intrafan is characterised by the *Phycosiphon*-diverse homogenised ichnofabric.

8.4.7. Ainsa II sand body, Well A4

8.4.7.1. Sedimentology

The Ainsa II sand body in Well A4 is characterised by three small sandstone packets encased in MTCs. The lower sandstone packet is ~5 m thick and characterised by thick-bedded, amalgamated sandstones. Planar stratification is common, and a number of beds are normally graded (Facies B2.1 and C2.1). The lower and middle sandstone packet is separated by a 4.8-m-thick Type Ia muddy MTC (Pickering and Corregidor 2005). The middle packet is 4 m thick and comprises thick-bedded, coarse-grained sandstones. The base is characterised by a chaotic sandstone with abundant mud clasts and pebbles (Facies A2.7). This is overlain by medium-bedded, normally-graded

sandstones, and thin (<60 cm thick) Type Ia MTCs. The upper packet is 2.5 m thick and is separated from the middle packet by a 2.5-m-thick muddy Type II MTC. The base is associated with a 65 cm thick, disorganised, clast-supported conglomerate with a sandy matrix. This is overlain by medium-bedded, planar stratified sandstones. These sandstones are typically normally graded and siltstone-mudstone laminae are developed between the beds. The top 72 m of Well A4 is characterised by thick, muddy Type Ia MTCs punctuated by thick-bedded sandstones (Facies C2.1).

These sandstone packets are interpreted as axial or off-axis channel deposits of isolated channel elements encased within MTCs.

8.4.7.2. Ichnology

The three small sandstone packets are characterised by a low bioturbation intensity (15%) and a low average ichnofabric index (2). Biodeformational structures are rare, representing 7% of the deposits. The trace-fossil assemblage is dominated by *Planolites* and *Ophiomorpha.* Other common ichnotaxa include *Thalassinoides, Phycosiphon* and *Scolicia.* These sandstone packets are dominated by the *Ophiomorpha* ichnofabric. The thin mudstone intervals between the sandstones are characterised by the *Scolicia*-diverse homogenised ichnofabric, as well as the *Planolites* mottled ichnofabric.

8.4.8. Ainsa II sand body, Well A3

8.4.8.1. Sedimentology

The Ainsa II sand body is ~75 m thick in Well A3 and comprises a number of individual channel elements. The base is associated with a 6 m thick sandstone packet characterised by thin- to medium-bedded sandstones, which overlie Type Ia MTCs of the intrafan. These sandstones are typically normally graded, and planar stratification is developed in some beds (Facies C2.2 and B2.1). Thin-bedded sandstones, siltstones and mudstones are preserved between the sandstones, and tend to be intensely bioturbated (Facies C1.2, D1.3 and E1.3). These deposits represent the margin of channel element II.2. These sandstones are overlain by a 4 m thick Type II MTC characterised by a sand-rich, mudstone matrix with abundant extra-formational nummulites and pebbles, which is punctuated by a medium-bedded sandstone (Facies C2.2). This MTC marks the base of the overlying sandstone packet. This packet is ~10 m thick and occurs between 55.5-65.2 m depth. It is characterised by thick-bedded, coarse-grained sandstones towards the

base. These sandstones are commonly amalgamated, planar stratification is well developed in some beds, as well as mud clast horizons along amalgamation surfaces (Facies B2.1 and C2.1). The middle part of the packet is associated with a ~1.5 m thick Type II MTC characterised by a sand-rich mudstone matrix. The top is formed of medium- to thick-bedded, parallel stratified sandstones (Facies B2.1). These sandstones are commonly amalgamated, or have thin mudstone partings with intensely bioturbated siltstones (Facies D1.3) or siltstone-mudstone laminae (Facies D2.3). These deposits represent the off-axis of channel element II.3.

The overlying sandy succession is ~6 m thick and is associated with thick-bedded, coarse-grained, amalgamated sandstones which tend to be normally graded (Facies C2.1). These are axial deposits of channel element II.4. Overlying these sandstones is a 5 m thick muddy Type II MTC with large rounded pebbles. This MTC is overlain by an 11 m thick sandstone packet characterised by medium- to thick-bedded, mud-rich sandstones with well developed parallel stratification (Facies B2.1), as well as normally graded sandstones (Facies C2.1) and normally graded pebbly sandstones (Facies A2.7). These sandstones are typically amalgamated, and intra-formational mud clasts are common in many beds. Mudstone partings are typically thin and intensely bioturbated (Facies D1.3). A thin (30 cm thick) Type II MTC punctuates this sandy packet and is characterised by a sand-rich, mudstone matrix and abundant rounded extra-formational pebbles. This sandstone packet represents the off-axis deposits of channel element II.7.

A 3.7 m thick sandstone packet overlies channel element II.7 and is characterised by thick-bedded, amalgamated, normally graded sandstones (Facies C2.1) and coarse-grained, parallel stratified sandstones (Facies B2.1). These deposits represent the axis of channel element II.8 and are overlain by ~5 m of thin-bedded, current rippled sandstones, siltstones-mudstone laminae and graded stratified siltstones (Facies C2.3 D2.3 and D2.1, respectively). These fine-grained deposits are punctuated by thin (<1 m thick) Type II MTCs which typically have a mudstone matrix with abundant nummulites, small pebbles, and injected coarse-grained sandstone. These fine-grained deposits probably represent the abandonment phase of channel element II.8.

These deposits are overlain by a 3 m thick interval between 21-24.8 m subsurface which is characterised by thin- to medium-bedded normally graded sandstones commonly with abundant mud clasts (Facies C2.1 and C2.2), and intensely bioturbated thin-bedded sandstones, siltstones and mudstones (Facies C1.2, D1.3 and

E1.3). These deposits are interpreted as the distal margin of channel element II.9. These are overlain by a 5 m thick packet of thin-bedded sandstones, and siltstone-mudstone laminae (Facies C2.3 and D2.3), as well as intensely bioturbated sandstones, siltstones and mudstones (Facies C1.2, D1.3 and E1.3), which represent the abandonment phase at the top of Ainsa II. These thin-bedded deposits are truncated by a thick, muddy, Type Ia MTC at the top of Well A3.

8.4.8.2. Ichnology

The margin of channel element II.2 is characterised by a low bioturbation intensity (16%) and an average ichnofabric index of 2.1. The trace-fossil assemblage is dominated by *Thalassinoides, Planolites, Scolicia, Phycosiphon* and *Ophiomorpha*. The sandstones are dominated by the *Ophiomorpha* ichnofabric and rarely, the *Thalassinoides*-1 ichnofabric. The mudstone intervals are dominated by the *Planolites* ichnofabric, as well as the *Scolicia*-diverse-1 ichnofabric and *Phycosiphon* ichnofabric.

The channel off-axis deposits of channel element II.3 are associated with a low bioturbation intensity (10%) and low average ichnofabric index (1.7). The trace-fossil assemblage is dominated by *Planolites* and *Ophiomorpha*. The sandstones are characterised by the *Ophiomorpha* ichnofabric, and, more rarely, the *Thalassinoides*-1 ichnofabric. The muddy intervals between the sandstones in the lower part of the channel are associated with the *Planolites* ichnofabric, whilst the upper part is associated with the *Phycosiphon-Planolites* homogenised ichnofabric and the *Planolites-Phycosiphon* ichnofabric.

The axis of channel II.4 is dominated by amalgamated sandstones. Bioturbation intensity is very low (<1%) and the average ichnofabric index is 1.1. The trace-fossil assemblage is dominated by *Ophiomorpha, Planolites* and *Thalassinoides*. These deposits are associated with the *Ophiomorpha* ichnofabric.

The channel off-axis deposits of channel element II.6 are characterised by a moderately low bioturbation intensity (25%) with an average ichnofabric index of 2.6. Biodeformational structures are rare, representing 6% of the deposits and the trace-fossil assemblage is dominated by *Ophiomorpha, Planolites* and *Thalassinoides*. The sandstones are associated with the *Ophiomorpha* ichnofabric, and more rarely, the *Thalassinoides*-1 ichnofabric. The mudstone intervals between the sandstones are associated with the *Planolites* ichnofabric.

The channel off-axis deposits of channel element II.7 are associated with a moderately low bioturbation intensity (20%) and an average ichnofabric index of 1.9. Biodeformational structures are rare, representing 15% of the deposits. The trace-fossil assemblage is dominated by *Planolites,* and more rarely, *Thalassinoides.* The sandstones are characterised by the *Ophiomorpha* ichnofabric, and rarely, the *Thalassinoides*-1 ichnofabric. The mudstone intervals between the sandstones are associated with the *Planolites* ichnofabric.

Similar to the channel axis deposits of II.4, the axial sandstones of channel element II.8 are characterised by a low bioturbation intensity (1.6%) and low average ichnofabric index (1.1). *Planolites* is the most common trace fossil, as well as *Ophiomorpha*, and the sandstones are associated with the *Ophiomorpha* ichnofabric. The fine-grained deposits of the abandonment phase have a moderate bioturbation intensity (29.2%) with an average ichnofabric index of 2.6. Biodeformational structures represent 13% of the deposits compared to 1.4% for the axial deposits. The trace-fossil assemblage is dominated by *Phycosiphon* and *Planolites.* Other common ichnotaxa include *Thalassinoides* and vertical unlined burrows. The abandonment phase is dominated by the *Planolites-Phycosiphon* ichnofabric, and rarely, the *Planolites* ichnofabric.

The margin of channel element II.9 is characterised by a moderate bioturbation intensity (26%) with an average ichnofabric index of 2.5. Biodeformational structures represent 16% of the deposits. The trace-fossil assemblage is dominated by *Planolites* and *Phycosiphon.* Towards the base of the channel element, the most dominant ichnofabric is the *Planolites-Phycosiphon* ichnofabric. The medium-bedded sandstones are associated with the *Ophiomorpha* ichnofabric, whilst the top of the channel element is associated with the *Planolites* ichnofabric. The abandonment phase is characterised by a moderately high bioturbation intensity (35%) and an average ichnofabric index of 2.9. Biodeformational structures represent 19% of the deposits. The trace-fossil assemblage is dominated by *Planolites*, as well as *Phycosiphon* and *Thalassinoides.* The fine-grained deposits of the abandonment phase are associated with the *Planolites* ichnofabric. Less intensely bioturbated horizons are associated with the *Planolites-Phycosiphon* ichnofabric.

HOLE	ENVIRONMENT	i	ii	Biodef	% BIODEF
A2	A1 INTERFAN	64.40	4.68	55.72	86
A1	AI INTERFAN	90	5.9	88	97
L1	AI INTERFAN	87	6.3	83	95
	Mean	**80.5**	**5.6**	**75.6**	**92.7**
	StDev.	**14.0**	**0.8**	**17.4**	**5.9**
A4	A1 LEV OVERBANK	45.9	4	39	85
A2	A1 LEV-OVERBANK	83.9	5.78	78.89	94
	Mean	**64.9**	**4.9**	**58.9**	**89.5**
	StDev.	**26.9**	**1.3**	**28.2**	**6.4**
A5	AXIS	4.2	1.1	3.1	7.3
	Mean	**4.2**	**1.1**	**3.1**	**7.3**
A3	AI OFF AXIS	17	2.3	6	35
A1	AI OFF AXIS	41	3.5	35	85
	Mean	**29**	**2.9**	**20.5**	**60**
	StDev.	**17**	**0.8**	**20.5**	**35.3**
L1	I MARGIN	43	3.5	32	74
	Mean	**43**	**3.5**	**32**	**74**
A4	INTRAFAN	56	4.2	51	91
A1	INTRAFAN	88	6.1	84	95
L1	INTRAFAN	94.8	6.3	94	99
	Mean	**82.3**	**5.7**	**79.2**	**95.2**
	StDev.	**17.7**	**1**	**19.1**	**3**
A3	AII II.4 AXIS	1	1.1	0.2	25
A3	AII II.8 AXIS	1.6	1.1	1.4	87
A2	AII I.4a AXIS	12	1.8	9	75
	Mean	7.4	1.5	4.4	62.3
	StDev.	6.1	0.4	4.7	32.8

HOLE	ENVIRONMENT	i	ii	Biodef	% BIODEF
A4	AII CHANNELS	15	2	7	4.6
A3	AII II.3 OFF AXIS	10	1.7	6	60
A3	AII II.6 OFF AXIS	25	2.6	6	24
A3	AII II.7 OFF AXIS	20	1.9	15	75
A1	AII I.1a OFF AXIS	7.3	1.5	6	82
A1	AII I.1b OFF AXIS	19.9	2.2	12.5	62
L1	AII I.1a OFF AXIS	34	2.9	28	82
	Mean	**18.7**	**2.1**	**11.5**	**55.6**
	StDev.	**9**	**0.5**	**8.1**	**30**
A3	AII II.2 MARGIN	16	2.1	9.6	60
A3	AII II.9 MARGIN	26	2.5	16	61
A2	AII I.4b MARGIN	38	3.2	28	73
A2	AII I.4c MARGIN	33	2.9	16	48
A1	AII I.2 MARGIN	31	2.9	23.8	76
A1	AII I.3 MARGIN	31	3	21	67
A1	AII I.4 MARGIN	17	2.1	7.9	46
L1	AII I.1b MARGIN	32	2.8	22	68
L1	AII I.2 MARGIN	21	2.1	13	61
L1	AII I.3 MARGIN	33	3	17	51
L1	THRUST I.3 MARGIN	36	3.1	17	47
	Mean	**28.5**	**2.7**	**17.3**	**59.8**
	StDev.	**7.5**	**0.4**	**6**	**10.6**
A3	AII II.8 ABANDONMENT	29.2	2.6	13	44
A3	AII II.9 ABANDONMENT	35	2.9	19	54
A2	AII ABANDONMENT	34	3	18	52
A1	AII ABANDONMENT	52	3.6	29.5	56
L1	AII ABANDONMENT	55	4	41.6	75
	Mean	**41**	**3.2**	**24.22**	**56.2**
	StDev.	**11.6**	**4**	**11.4**	**11.4**

Table 8.1. Ichnological data for individual fan and related environments in each well including; mean bioturbation intensity (%) (i), mean ichnofabric indices (ii); mean biodeformational structures (%), mean percentage of the trace-fossil assemblage formed by biodeformational structures. The mean value for each fan and related environment as well as standard deviation is also presented.

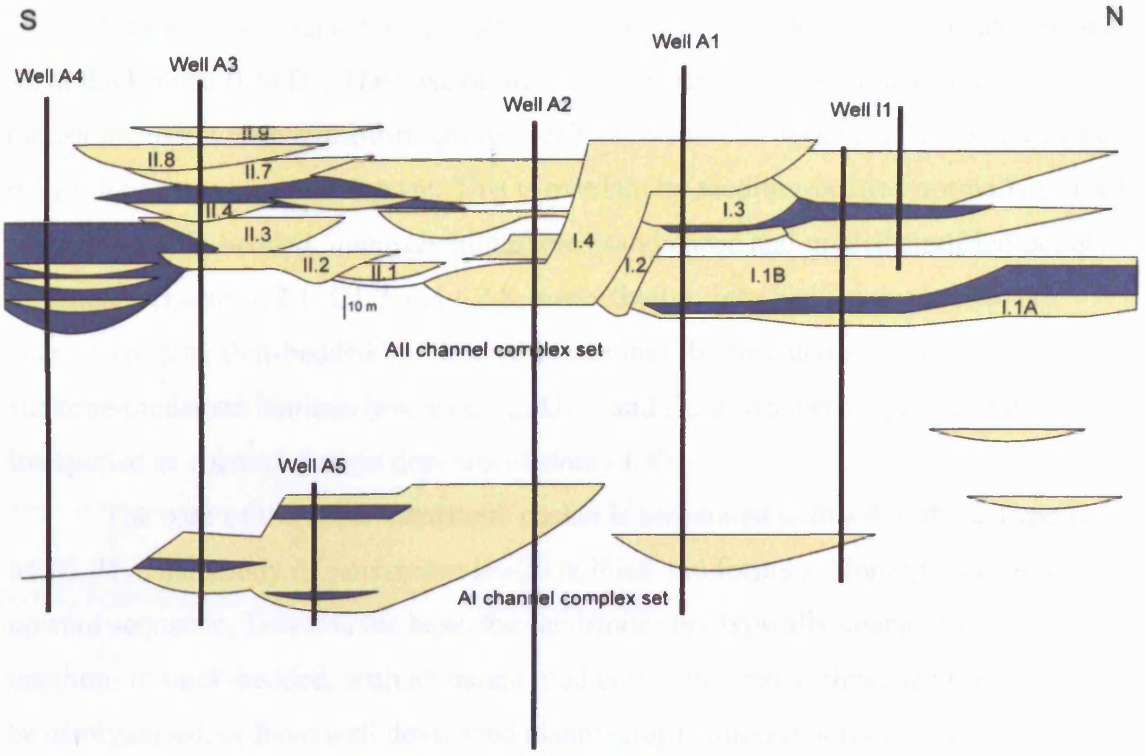

Fig. 8.24. Correlation panel of the Ainsa I and II sand body (redrawn after Clark, 2006).

8.4.9. Ainsa II sand body, Well A2

8.4.9.1. Sedimentology

The Ainsa II sand body is 70 m thick in Well A2 and cuts channel elements I.2 and I.4. Channel element I.4 (channel element 4 in Fig 8.24) comprises a number of fining-upward sequences interpreted as second-order storeys.

The basal 4 m of the Ainsa II sand body is characterised by thick-bedded, coarse-grained amalgamated sandstones. These sandstones are typically normally graded, commonly with extra-formational pebbles at the base (Facies C2.1 and A2.7) or are disorganised (Facies B1.1). These are interpreted as off-axis channel deposits of channel element I.2. The main sandstone packet in Well A2 is ~57 m thick and occurs between ~9-66 m subsurface. This packet represents sandstones of channel element I.4.

The base is associated with a ~1 m thick Type II MTC characterised by abundant extra-formational pebbles in a sand-rich mudstone matrix. This is succeeded by a ~25 m thick packet of essentially amalgamated, medium- to thick-bedded sandstones. Normal grading is well developed in many sandstones, and planar stratification is common in many beds (Facies C2.1 and B2.1). These sandstones are punctuated by metre-thick Type II MTCs characterised by abundant pebbles in a sand-rich mudstone matrix. This packet is interpreted as channel axis deposits (storey I.4a).

The overlying sandstone packet is ~6.5 m thick, with the base associated with a ~2 m thick Type II MTC. The base of the MTC deposit is characterised by a sand-rich mudstone matrix with extra-formational pebbles, whilst the upper part has a mudstone matrix forming a bipartite deposit. This is overlain by medium-bedded normally graded sandstones, thin-bedded, intensely bioturbated sandstones and graded stratified pebbly sandstones (Facies C2.1, C1.2 and A2.8, respectively). Interbedded mudstones are characterised by thin-bedded bioturbated sandstones, bioturbated siltstones and siltstone-mudstone laminae (Facies C1.2, D1.3 and D2.3, respectively). This packet is interpreted as channel margin deposits of storey I.4b.

The base of the upper sandstone packet is associated with a 4 m thick Type II MTC. The main body of sandstones is ~20 m thick and forms a thinning-and-fining-upward sequence. Towards the base, the sandstones are typically coarse-grained, medium- to thick-bedded, with abundant mud clasts. Internally, these sandstones may be disorganised, or have well developed planar stratification (Facies B1.1 and B2.1, respectively). Interbedded mudstones are typically thin, and associated with thin-bedded sandstones, siltstone-mudstone laminae and intensely bioturbated sandstones (Facies C2.3, D2.3 and C1.2, respectively). The upper part of the packet is associated with thin- and rarely medium-bedded sandstones with relatively thick mudstone partings associated with intensely bioturbated sandstones and siltstones, as well as siltstone-mudstone laminae (Facies C1.2, D1.3 and D2.3, respectively). This packet is interpreted as channel margin deposits of storey I.4c.

The upper ~8 m of Well A2 is associated with thin-bedded sandstones and siltstone-mudstone laminae (Facies C2.1 and D2.3), as well as intensely bioturbated sandstones and siltstones (Facies C1.2 and D1.3). These fine-grained deposits represent the abandonment phase.

8.4.9.2. Ichnology

The axis of storey I.4a is characterised by a low bioturbation intensity (12.2%) with an average ichnofabric index of 1.8. The most common ichnotaxa include *Planolites, Thalassinoides* and *Ophiomorpha.* Biodeformational structures represent 9% of the deposits. The thick-bedded commonly amalgamated sandstones of the channel axis are associated with the *Ophiomorpha* ichnofabric, and more rarely, the *Thalassinoides*-1 ichnofabric. Where muddy intervals are preserved between sandstone beds, the *Planolites* ichnofabric typically occurs.

HOLE	ENVIRONMENT	Pl-Phy	Pl	Phy	Phy-Pl homog	Phy-div homog	Oph	Th-1	Th-2	Sc	Sc-div-1	Sc-div-2
A2	A1 INTERFAN	6.9		41.5	43.8					7.6		
A1	AI INTERFAN			10.47	89.52							
L1	AI INTERFAN			14	30	38		10	2		6	
	Mean	**2.3**		**22.0**	**54.4**	**12.7**		**3.3**	**0.7**		**2**	
A4	A1 LEVEE OVERBANK		0.87	35.08	31.87		0.58	0.87		13.74	16.95	
A2	A1 LEVEE OVERBANK		0.17	4.65	5.18	29.69	0.01				28.63	30.11
	Mean		**0.5**	**19.9**	**18.5**		**0.3**	**0.4**		**6.9**	**22.8**	**15.1**
A5	AI AXIS		5				80	10	5			
	Mean		**5**				**80**	**10**	**5**			
A3	AI OFF AXIS			52.91			47.05					
A1	AI OFF AXIS			2.72	2.27	19.09	52.27	6.81			10	6.81
	Mean			**27.8**	**1.1**	**9.5**	**49.7**	**3.4**			**5**	**3.4**
L1	AI MARGIN		3.8			12.3	41.9	6.1	7.6		28	
	Mean		**3.8**			**12.3**	**41.9**	**6.1**	**7.6**		**28**	
A4	INTRAFAN			40		60						
A1	INTRAFAN			0.7		92.9					6.38	
L1	INTRAFAN			4		96						
	Mean			**14.9**		**83.0**					**2.1**	
A3	AII II.4 AXIS						100					
A3	AII II.8 AXIS						100					
A2	AII I.4a AXIS		4.84				85.46	8.43			1.25	
	Mean		**1.6**				**95.2**	**2.8**			**0.4**	
A4	AII OFF AXIS		4.61			7.69	78.46				9.23	
A3	AII II.3 OFF AXIS	10	6		7		72	5				
A3	AII II.6 OFF AXIS		10				80	10				
A3	AII II.7 OFF AXIS	2.22	15.55				75.55	6.66				
A1	AII I.1a OFF AXIS						100					
A1	AII I.1b OFF AXIS		3.75				72.5	23.75				
L1	AII I.1a OFF AXIS		17.85				60.71				21.42	
	Mean	**1.7**	**8.3**		**1**	**1.1**	**77.0**	**6.5**			**4.4**	
A3	AII II.2 MARGIN		10	3.33			70	3.33	6.66		6.66	
A3	AII II.9 MARGIN	43.33	40				16.66					
A2	AII I.4b MARGIN						68	12			20	
A2	AII I.4c MARGIN	8.43	48.71		2.34		34.19	4.91	1.4			
A1	AII I.2 MARGIN		14				48	38				
A1	AII I.3 MARGIN		14.28				70.47	1.9		2.38	5.23	5.71
A1	AII I.4 MARGIN	40.57	5.75				51.57				2.09	
L1	AII I.1b MARGIN		25.38				39.23	35.38				
L1	AII I.2 MARGIN		34				65	1				
L1	AII I.3 MARGIN	3.44	6.72	5.17			50			23.1	11.55	
L1	THRUSTED I.3 MARGIN	1.29	8.06				50.16	0.8	0.32	18.7	20.64	
	Mean	**8.8**	**18.8**	**0.8**	**0.2**		**51.2**	**8.8**	**0.8**	**4.0**	**6.0**	**0.5**
A3	AII II.8 ABANDONMENT	92	8									
A3	AII II.9 ABANDONMENT	26.66	62.22		11.11							
A2	AII ABANDONMENT	42.5	45								12.5	
A1	AII ABANDONMENT	35	35								30	
L1	AII ABANDONMENT	8.4								12.6		
	Mean	**40.9**	**30.0**		**2.2**					**2.5**	**8.5**	

Table 8.2. Summary of the proportion (%) of ichnofabrics in individual fan and related environments.in each well. The mean value for each fan and related environment is also presented.

The margin of storey I.4b is characterised by a high bioturbation intensity (38%) with an average ichnofabric index of 3.2. Biodeformational structures represent 28% of the deposits. The trace-fossil assemblage is dominated by *Planolites, Scolicia, Thalassinoides* and *Phycosiphon.* The sandstones are characterised by the *Ophiomorpha* ichnofabric with the fine-grained intervals between the sandstones associated with the *Scolicia*-diverse-1 ichnofabric and the *Scolicia-Planolites* ichnofabric.

The margin of storey I.4c is characterised by a moderately high bioturbation intensity (33%) with an average ichnofabric index of 2.9. Biodeformational structures represent 16% of the deposits. The trace-fossil assemblage is dominated by *Planolites.* Other ichnotaxa include *Thalassinoides* and *Phycosiphon.* The sandstone-rich base of I.4c is dominated by the *Ophiomorpha* ichnofabric. Rarely, the sandstones are characterised by the *Thalassinoides*-1 ichnofabric. The muddy intervals between the sandstones are associated with the *Phycosiphon-Planolites* homogeneous ichnofabric. Towards the top, the dominant ichnofabric is the *Planolites* ichnofabric, with the medium-bedded sandstones associated with the *Ophiomorpha* ichnofabric.

The abandonment phase has a moderately high bioturbation intensity (34%) with an average ichnofabric index of 3. The trace-fossil assemblage is dominated by *Planolites* and *Phycosiphon.* Other common ichnotaxa include *Thalassinoides* and *Scolicia.* Biodeformational structures represent 18% of the deposits. The abandonment phase is associated with the *Planolites-Phycosiphon* ichnofabric. More intensely bioturbated horizons are associated with the *Planolites* ichnofabric.

8.4.10. Ainsa II sand body, Well A1

8.4.10.1. Sedimentology

The Ainsa II system is ~101 m thick in Well A1, and comprises a number of fining- and thinning-upward sequences associated with individual channel elements. The base of the Ainsa II system is characterised by thick-bedded, amalgamated sandstones (Facies C2.1) which represent off-axis deposits of channel element I.1a. These are overlain by a ~5 m thick muddy Type II MTC which is characterised by a sand-rich basal division with abundant oversized mud clasts and pebbles (Facies A1.4), overlain by a mud-rich division (Facies F2.2) forming a bipartite deposit. This MTC is overlain by a 15 m thick fining- and thinning-upward sandy sequence between 79-94 m subsurface. This is characterised by thick-bedded, coarse-grained amalgamated sandstones towards the base with abundant mud clasts (Facies C2.1 and B1.1). These

sandstones are overlain by medium-bedded, medium-grained sandstones (Facies C2.2 and B1.1) interbedded with thin-bedded, intensely bioturbated sandstones and siltstone-mudstone laminae (Facies C1.2 and D2.3, respectively). This fining-upward sequence represents the channel off-axis of channel element I.1b (channel element 1 in Fig. 8.24).

This sequence is overlain by a 5 m thick packet of thick-bedded, normally graded sandstones (Facies C2.1) interbedded with thin-bedded, intensely bioturbated sandstones and siltstone-mudstone laminae forming a crude fining- and thinning-upward sequence which represents the margin of channel element I.2 (channel element 2 in Fig. 8.24). Between channel element I.2 and I.3 is a 10 m thick packet of Type II MTCs punctuated by medium-bedded, coarse-grained, planar stratified sandstones (Facies B2.1) and intensely bioturbated sandstones, siltstones and mudstones (Facies C1.2, D1.3 and E1.3). This is overlain by ~20 m of sandstones which represents the margin of channel element I.3 (channel element 3 in Fig. 8.24) between 44-64 m subsurface. These sandstones form a crude thinning-and-fining-upward sequence, and are associated with thin- to medium-bedded and rarely thick-bedded sandstones, with well developed internal stratification, including planar stratification (Facies B2.1 and C2.1). Thin-bedded sandstones are typically intensely bioturbated (Facies C1.2), as well as interbedded siltstones and mudstones (Facies C1.2, D1.3, D2.3 and E1.3).

The top packet of sandstone is 19 m thick, occurring between 25-44 m subsurface. The base is characterised by a thin Type II MTC which is overlain by medium-bedded, medium-grained sandstones, commonly with well developed planar stratification and more rarely, extra-formational mud-clasts (Facies C2.1 and B2.1). These sandstones are interbedded with thin-bedded sandstones, siltstones and mudstones (Facies C2.3, D2.3 and E2.2, respectively). Towards the top of the packet, the medium-bedded sandstones are succeeded by thin-bedded, current rippled sandstones, as well as siltstones and mudstones (Facies D2.3 and E2.2). This packet represents the margin of channel element I.4 (channel element 4 in Fig. 8.24). The top 25 m of Well A1 is characterised by thin-bedded sandstones, siltstones and mudstones (Facies C1.2, C2.3, D1.3, D2.3, E1.3 and E2.2) which represent the abandonment phase at the top of the Ainsa II sand body.

HOLE	ENVIRONMENT	No. TFs	>1%	>2%
A2	A1 INTERFAN	12	4	3
A1	AI INTERFAN	12	5	3
L1	AI INTERFAN	12	6	5
	Mean	**12**	**5**	**3.6**
A4	A1 LEVEE OVERBANK	8	5	3
A2	A1 LEVEE OVERBANK	14	6	4
	Mean	**11**	**5.5**	**3.5**
A5	AI AXIS	9	2	0
	Mean	**9**	**2**	**0**
A3	AI OFF AXIS	13	3	2
A1	AI OFF AXIS	14	4	4
	Mean	**13.5**	**3.5**	**3**
L1	AI MARGIN	12	6	3
	Mean	**12**	**6**	**3**
A4	INTRAFAN	10	3	1
A1	INTRAFAN	14	5	5
L1	INTRAFAN	11	6	3
	Mean	**11.6**	**4.6**	**3**
A3	AII II.4 AXIS	3	0	0
A3	AII II.8 AXIS	2	0	0
A2	AII I.4a AXIS	11	2	1
	Mean	**5.3**	**0.6**	**0.3**
A4a	AII OFF AXIS	10	4	3
A4b	AII OFF AXIS	0	0	0
A4c	AII OFF AXIS	5	3	1
A3	AII II.3 OFF AXIS	8	2	1
A3	AII II.7 OFF AXIS	10	2	1
A1	AII I.1a OFF AXIS	3	0	0
A1	AII I.1b OFF AXIS	7	2	2
L1	AII I.1a OFF AXIS	10	2	2
	Mean	**6.6**	**1.8**	**1.2**
A3	AII II.2 MARGIN	9	3	1
A3	AII II.9 MARGIN	10	2	2
A2	AII I.4b MARGIN	10	4	4
A2	AII I.4c MARGIN	14	4	3
A1	AII I.2 MARGIN	7	3	3
A1	AII I.3 MARGIN	12	5	3
A1	AII I.4 MARGIN	12	4	2
L1	AII I.1b MARGIN	10	3	3
L1	AII I.2 MARGIN	7	2	2
L1	AII I.3 MARGIN	13	4	4
L1	THRUSTED I.3 MARGIN	11	5	4
	Mean	**10.4**	**3.5**	**2.8**
A3	AII II.8 ABANDONMENT	7	4	3
A3	AII II.9 ABANDONMENT	10	3	2
A2	AII ABANDONMENT	12	5	3
A1	AII ABANDONMENT	10	7	4
L1	AII ABANDONMENT	12	3	3
	Mean	**10.2**	**4.4**	**3**

Table 8.3. Summary of trace-fossil diversity in individual fan and related environments.in each well. Data presented include the number of individual ichnotaxa identified (No. TFs), the number of trace fossils which bioturbate >1% of the deposits and number of ichnotaxa which bioturbate >2% of the deposits. The mean value for each fan and related environment is also presented.

8.4.10.2. Ichnology

The off-axis channel deposits of channel element I.1a are characterised by a low bioturbation intensity (7.3%) with an average ichnofabric index of 1.5. Biodeformational structures represent 6% of the deposits. The trace-fossil assemblage is low diversity, and dominated by *Thalassinoides, Ophiomorpha* and *Planolites*. The sandstones of channel element I.1a are characterised by the *Ophiomorpha* ichnofabric.

The off-axis channel deposits of channel element I.1b are characterised by a low diversity trace-fossil assemblage (19.9%) with an average ichnofabric index of 2.2. Biodeformational structures represent 12.5% of the deposits. Channel element I.1b is characterised by a low diversity trace-fossil assemblage. The most common ichnotaxa include *Planolites* and *Thalassinoides*. The off-axis channel deposits are associated with the *Ophiomorpha* ichnofabric. Rarely, the sandstones are intensely bioturbated by *Thalassinoides* to form the *Thalassinoides*-1 ichnofabric.

The margin of channel element I.2 is characterised by a moderate bioturbation intensity (31%) with an average ichnofabric index of 2.9. The trace-fossil assemblage is dominated by *Planolites, Thalassinoides* and *Ophiomorpha.* Biodeformational structures represent 23.8% of the deposits. The basal sand-rich part of the channel margin is associated with the *Ophiomorpha* ichnofabric, as well as the *Thalassinoides*-1 ichnofabric. The upper part is characterised by the *Thalassinoides*-1 ichnofabric and muddy intervals associated with the *Planolites* ichnofabric.

The margin of channel element I.3 is characterised by a moderate bioturbation intensity (31.9%) with an average ichnofabric of 3. Biodeformational structures form 21% of the deposits. The trace-fossil assemblage is diverse, and dominated by *Planolites* and *Scolicia.* Other common ichnotaxa include *Thalassinoides, Phycosiphon* and *Ophiomorpha*. The sandstones of the channel margin are dominated by the *Ophiomorpha* ichnofabric, and rarely, the *Thalassinoides*-1 ichnofabric. The muddy intervals are characterised by the *Planolites* ichnofabric, and more rarely, the *Scolicia*-diverse-1 ichnofabric towards the base of the channel, and the *Scolicia* ichnofabric towards the top.

The channel margin deposits of channel element I.4 are characterised by a low bioturbation intensity (17.6%) with an average ichnofabric index of 2.1. Biodeformational structures are rare, forming only 7.9% of the deposits. The trace-fossil assemblage is dominated by *Planolites* and *Phycosiphon*. Other common ichnotaxa include *Thalassinoides* and *Scolicia.* The sand-rich base of the channel is dominated by

the *Ophiomorpha* ichnofabric with thin muddy intervals associated with the *Planolites-Phycosiphon* ichnofabric. The finer-grained upper part of the channel is dominated by the *Planolites-Phycosiphon* ichnofabric, and rarely the *Planolites* ichnofabric.

The abandonment phase at the top of Ainsa II is characterised by a high bioturbation intensity (52%), but the deposits are generally non homogenised. The average ichnofabric index is 3.6 and biodeformational structures form 29.5% of the deposits. The trace-fossil assemblage is dominated by *Phycosiphon, Planolites* and *Scolicia.* The lower part of the abandonment phase is associated with the *Planolites* ichnofabric and the *Planolites-Phycosiphon* ichnofabric, and more rarely, the *Scolicia*-diverse-1 ichnofabric. The upper part is associated with an increase in *Scolicia* and is characterised by the *Scolicia*-diverse-1 ichnofabric.

8.4.11. Ainsa II sand body, Well L1

8.4.11.1. Sedimentology

The Ainsa II sand body is thickest in Well L1 where it is ~125 m thick. This is due to a major thrust zone which cuts the Well at 59 m subsurface resulting in the repetition of ~40 m of stratigraphy (Pickering *pers. comm.,* 2007). Well L1 represents the subsurface equivalent of Bco. Forcaz (Section 6.4.3, Locality 17; Appendix 6.9).

The base of Ainsa II in Well L1 is characterised by a ~2 m thick packet of thin-bedded sandstones and interbedded siltstone-mudstone laminae (Facies C2.3 and D2.3, respectively) overlain by a thick Type Ia MTC. These basal deposits are succeeded by a ~6 m thick packet of sandstones which form a distinctive coarsening-and thickening-upward sequence, and correlate with the basal thickening-upward packet of sandstones in the Bco. Forcaz (Section 6.4.3.1). The base of the packet is associated with a nummulites-rich packstone with a muddy sandstone matrix (Facies I), overlain by intensely bioturbated thin-bedded sandstones, siltstones and mudstones (Facies C1.2, D1.3 and E1.3). The middle part of the packet comprises thin- to medium-bedded, normally graded sandstones (Facies C2.2) with the top characterised by thick-bedded, normally graded sandstones (Facies C2.1). These deposits represent the off-axis sandstones of channel element I.1a. A ~5 m thick muddy Type Ia MTC separates channel elements I.1a and I.1b. Channel element I.1b is 6 m thick and occurs between 105-111 m subsurface. It is essentially characterised by intensely bioturbated thin- to medium-bedded sandstones (Facies C1.2), medium-bedded sandstones (C2.1) and intensely bioturbated siltstones and mudstones (Facies D1.3 and E1.3, respectively). No

distinct thinning- or thickening-upward sequences are developed, and these deposits represent the margin of the channel element.

The base of channel element I.2 erosively overlies I.1b, and is ~9 m thick. The base is associated with a Type Ib sand-rich MTC with abundant contorted mud-clasts. This is overlain by thick-bedded, coarse-grained, commonly amalgamated sandstones (Facies C2.1). These deposits are typically normally graded and intra-formational mud-clasts are common. The top of channel element I.2 is characterised by thin- to medium-bedded sandstones (Facies C2.2 and C2.3) as well as intensely bioturbated siltstones and mudstones (Facies D1.3 and E1.3) forming a thinning- and fining-upward sequence. These deposits represent the margin of channel element I.2.

Between channel elements I.2 and I.3 is a thin packet of sandstones and MTCs. At the base of this packet is ~8 m of sandstones, the base of which is associated with a ~1 m thick Type III MTC comprising extra-formational nummulites and rounded pebbles in a sand-rich, muddy matrix.

Channel element I.3 is 29 m thick in Well L1 occurring between 59-87.6 m subsurface. The base is associated with a 1 m thick Type Ib MTC characterised by a sand-rich mudstone matrix. The main sandstone packet is characterised by two thinning-upward sequences, ~10 m, and ~15 m thick, respectively. The base of each sequence is associated with non-amalgamated, thick-bedded, coarse-grained sandstones, with common planar stratification and current ripples (Facies B1.2, B2.1 and C2.1). These sandstones are overlain by medium-bedded sandstones (Facies C2.1 and C2.2) with well developed mudstone intervals. The mudstone intervals are characterised by intensely bioturbated siltstones and mudstones (Facies D1.3 and E1.3), thin-bedded sandstones (Facies C2.3), graded-stratified siltstones (Facies D2.1), and structureless siltstones and mudstones (Facies D1.1 and E1.1, respectively). These deposits represent the margin of channel element I.3. The top of the channel element is characterised by 3 m of thin-bedded sandstones, siltstones and mudstones (Facies C2.3, D1.3, D2.3 and E1.3), as well as thin (decimetres) sand-rich Type III MTCs with rare extra-formational pebbles. These deposits are truncated by the thrust fault and may represent the abandonment phase at the top of Ainsa II.

The stratigraphy is repeated in Well L1 between ~19-59 m subsurface, with channel elements I.2, and I.3 repeated. Although exact bed-to-bed correlations cannot be made, the sedimentology of this repeated section is very similar to that described above. However, the upper fining-upward sequence of channel element I.3 is associated

with thicker-bedded sandstones in the repeated section, and may represent more axial deposits, such as channel off-axis / channel-margin than those described above. The top ~19 m of Well L1 is associated with intensely bioturbated thin-bedded sandstones, siltstones and mudstones (Facies C1.2, D1.3 and E1.3) as well as less intensely bioturbated siltstone-mudstone laminae (Facies D2.3) and laminated mudstones (Facies E2.2). These deposits represent the abandonment phase at the top of Ainsa II.

8.4.11.2. Ichnology

The channel off-axis deposits of channel element I.1a are characterised by a moderate bioturbation intensity (34.8%) with an average ichnofabric index of 2.9. The trace-fossil assemblage is dominated by *Planolites.* Other common ichnotaxa include *Thalassinoides, Scolicia, Phycosiphon* and *Ophiomorpha.* Biodeformational structures form 28% of the deposits. The fine-grained base of I.1a is characterised by the *Scolicia*-diverse-1 ichnofabric whilst the sandstone-rich deposits are associated with the *Ophiomorpha* ichnofabric with thin muddy intervals between the sandstones associated with the *Planolites* ichnofabric.

The margin of channel element I.1b is characterised by a moderate bioturbation intensity (32%) and average ichnofabric index of 2.8. This environment is dominated by *Planolites, Thalassinoides, Ophiomorpha* and biodeformational structures. Medium- to thick-bedded sandstones have a low bioturbation intensity characterised by the *Ophiomorpha* ichnofabric. The muddy intervals and thin-bedded sandstones between these deposits are associated with the *Planolites* ichnofabric.

The margin of channel element I.2 has a low intensity trace-fossil assemblage (21%) characterised by an average ichnofabric index of 2.1. The most common ichnotaxa include *Planolites, Scolicia, Phycosiphon* and *Ophiomorpha.* The medium- to thick-bedded sandstones are associated with the *Ophiomorpha* ichnofabric, and rarely, the *Thalassinoides*-1 ichnofabric. Finer-grained intervals between the sandstones are characterised by the *Planolites* ichnofabric.

The margin of channel element I.3 has a moderate intensity trace-fossil assemblage (33%) with an average ichnofabric index of 3. The trace-fossil assemblage is dominated by *Scolicia*, with other common ichnotaxa including *Phycosiphon, Planolites, Thalassinoides* and *Ophiomorpha.* The sandstones are associated with the *Ophiomorpha* ichnofabric, whilst the finer-grained intervals between the sandstones are dominated by the *Scolicia* ichnofabric, *Scolicia*-diverse-1 ichnofabric and the *Planolites*

ichnofabric. The repeated section towards the top of Well L1 has a similar moderate intensity trace-fossil assemblage dominated by the *Scolicia* ichnofabric.

The thin-bedded fan abandonment deposits at the top of Well L1 have a high bioturbation intensity (55.5%) with an average ichnofabric index of 4. Biodeformational structures form 41.6% of the deposits. The trace-fossil assemblage is dominated by *Phycosiphon, Scolicia* and *Planolites*. The fan abandonment deposits are characterised by the *Planolites-Phycosiphon* ichnofabric and intervals of intense bioturbation are associated with the *Scolicia* ichnofabric.

8.5. Environmental summary of the Ichnology of the Ainsa system

The interfan is characterised by the highest bioturbation intensity, comprising almost entirely of completely homogenised sediment. The trace-fossil assemblage is generally diverse and the dominant ichnofabric is the *Phycosiphon-Planolites*-homogenised ichnofabric. The homogenised deposits in Well L1 are also characterised by an abundance of *Phycosiphon*-diverse-homogenised ichnofabric. Non-homogenised intervals are typically <20 cm thick, except for a ~15 m succession in Well A2, and are characterised by the *Phycosiphon* ichnofabric.

A number of different environments were studied in the Ainsa I sand body from channel axis to levee-overbank. Bioturbation intensities increase from axial to off-axis environments. The axis of the Ainsa I sand body is characterised by the lowest average bioturbation in the Ainsa cores. It is also associated with a low diversity trace-fossil assemblage and is dominated by the *Ophiomorpha* ichnofabric with the *Planolites* ichnofabric developed in the thin muddy intervals between the sandstones. The channel off-axis is characterised by an increase in bioturbation intensity and trace-fossil diversity and is dominated by the *Ophiomorpha* ichnofabric. Muddy intervals between the sandstones may be well-developed and in Well A3, are associated with the *Phycosiphon* ichnofabric. The off-axis deposits in Well A1 have a much greater bioturbation intensity, with the muddy intervals characterised by a high intensity, high diversity trace-fossil assemblage dominated by the *Phycosiphon*-diverse ichnofabric, *Scolicia*-diverse-1 ichnofabric and *Scolicia*-diverse-2 ichnofabric. Laminated sections associated with the *Phycosiphon* ichnofabric are rarely developed in Well A1. The channel margin is characterised by a high bioturbation intensity and high trace-fossil diversity. It is dominated by the *Ophiomorpha* ichnofabric with the thick muddy

intervals between the sandstones associated with the *Scolicia*-diverse-1 ichnofabric, as well as the *Phycosiphon*-diverse-homogenised ichnofabric.

The levee-overbank is characterised by the highest bioturbation intensity in the Ainsa I sand body. It is also characterised by a high diversity trace-fossil assemblage. The levee-overbank displays a distinct fining-upward sequence. This is also reflected in bioturbation intensities, with the lowest bioturbation intensities occurring towards the base of the levee-overbank, and increasing towards the top, where the deposits are typically totally homogenised. The base of the levee-overbank is characterised by the *Phycosiphon* ichnofabric (Well A4) and *Scolicia*-diverse-1 ichnofabric (Well A2) with thin homogenised horizons characterised by the *Scolicia* ichnofabric (Well A4) or the *Phycosiphon*-diverse-homogenised ichnofabric (Well A2). The top of the levee-overbank is associated with thick, intensely bioturbated and homogenised intervals punctuated by laminated horizons, characterised by the *Scolicia*-diverse-2 ichnofabric and the *Phycosiphon*-diverse-homogenised ichnofabric.

The intrafan has a high intensity trace-fossil assemblage, second only to the interfan, as well as a high diversity. It is characterised by thick homogenised intervals associated with the *Phycosiphon*-diverse homogenised ichnofabric, whilst thin laminated intervals which punctuate the homogenised sediments are associated with the *Phycosiphon* ichnofabric.

The Ainsa II sand body is characterised by a lower bioturbation intensity than Ainsa I. The channel axis has a very low bioturbation intensity and is dominated by the *Ophiomorpha* ichnofabric. The trace-fossil assemblage is the lowest diversity assemblage of any environment in the Ainsa system. Muddy intervals between the sandstones are rarely developed, but where they do occur, are characterised by the *Planolites* ichnofabric.

The channel off-axis of Ainsa II is characterised by an increased bioturbation intensity and diversity compared to the axis. The *Ophiomorpha* ichnofabric is the most common ichnofabric, whilst thin muddy intervals between the sandstones are characterised by intensely bioturbated, non-homogenised deposits associated with the *Planolites* ichnofabric and the *Scolicia*-diverse-1 ichnofabric.

The channel margin has a higher bioturbation intensity and trace-fossil diversity than the channel off-axis, but a lower bioturbation intensity than the channel margin deposits of the Ainsa I sand body. The dominant ichnofabric is the *Ophiomorpha* ichnofabric, whilst many sandstones are associated with the *Thalassinoides*-1

ichnofabric. The muddy intervals are generally non-homogenised, with low to high bioturbation intensities characterised by the *Planolites-Phycosiphon, Planolites* and *Scolicia*-diverse-1 ichnofabrics. More intensely bioturbated homogenised intervals are associated with the *Scolicia* ichnofabric.

The abandonment phase at the top of the Ainsa II sand body is characterised by a moderately low bioturbation intensity but a high diversity trace-fossil assemblage. The fine-grained deposits are dominated by the *Planolites-Phycosiphon* and *Planolites* ichnofabrics.

8.6. Interpretation

8.6.1. Interfan

The intensely bioturbated, almost totally homogenised deposits of the interfan is indicative of biogenic reworking that exceeded sedimentation rates. High bioturbation intensities suggest that equilibrium organism communities became well established, as a result of long-term stable conditions. The abundance of homogenised background sediment associated with the *Phycosiphon-Planolites*-homogenised ichnofabric and the *Phycosiphon*-diverse-homogenised ichnofabric suggests that bioturbation initially occurred in nutrient-rich, soupy sediment dominated by biodeformational structures. The density and diversity of the overprinting trace-fossil assemblage is controlled by the remaining oxygen levels and nutrient supply. It can be postulated that the increase in bioturbation intensity and diversity associated with the *Phycosiphon*-diverse-homogenised ichnofabric compared to the *Phycosiphon-Planolites*-homogenised ichnofabric is indicative of higher oxygen and/or nutrient levels. The thin laminated horizons associated with the *Phycosiphon* ichnofabric are related to periods of reduced oxygenation, and may represent basin-wide events. The ~15 m thick succession of laminated sediments in Well A2 is indicative of a period of long-term reduced oxygenation.

The lower intensity but higher diversity trace-fossil assemblage of the interfan in Well L1 compared to Well A2 may be related to greater bed thicknesses and grain-size variations in Well L1. As a consequence, the greater range of sedimentary facies and associated grain-sizes may have supported a more diverse community of organisms, whilst the increase in sandstone bed thickness may have also resulted in a reduction in bioturbation intensities (cf. Wetzel 1991).

8.6.2. Channel axis

The low diversity and intensity trace-fossil assemblage of the channel axis is related to the abundance of thick-bedded, amalgamated sandstones characterised by the *Ophiomorpha* ichnofabric. These sandstones have low bioturbation intensities, with the exception of those associated with the *Thalassinoides*-1 ichnofabric. Due to the highly erosive nature of the depositing gravity currents associated with the sandstones, only the burrows created by large, robust, deeply burrowing endobenthic organisms were preserved as they were well adapted to surviving burial by newly deposited thick sands (Wetzel and Uchman 2001). The coarse-grained nature of the sandstones may also have excluded burrowers adapted only to fine-grained sediments (Tchoumatchenco & Uchman 1999). Due to the erosive nature of the gravity currents associated with the channel axis, this environment is also characterised by the common occurrence of the *Thalassinoides*-2 ichnofabric, representing the colonisation of firmgrounds (*Glossifungites* ichnofacies) formed by erosive bypassing gravity currents. Where preserved, the thin muddy intervals between sandstone beds are characterised by moderately high bioturbation intensities associated with the *Planolites* ichnofabric. This suggests that despite low overall bioturbation intensities related to the abundance of sandstones in the channel axis, this environment was well oxygenated and the fine-grained deposits were intensely bioturbated between turbidite deposition. The abundance of organic matter in the sandstones, as well as the development of biodeformational structures in the muddy intervals also suggests that the channel axis was characterised by a high nutrient supply.

8.6.3. Channel off-axis

The increase in bioturbation intensity and trace-fossil diversity from the channel axis to channel off-axis is associated with the increased frequency and thickness of fine-grained intervals between sandstone beds. Consequently, the low intensity *Ophiomorpha* ichnofabric which characterises most of the sandstone beds is less dominant than in the channel axis. The fine-grained intervals are typically intensely bioturbated but non-homogenised. This is probably related to both the coarse-grained nature of the thin-bedded sandstones and/or high sedimentation rates. The high bioturbation intensity of the muddy intervals is indicative of a high oxygen and nutrient supply. However, in the off-axis deposits of the Ainsa I sand body, Well A3, the fine-grained intervals which are up to 4 m thick have very low bioturbation intensities

associated with the *Phycosiphon* ichnofabric, whilst the medium- to thick-bedded sandstones are non bioturbated. The laminated sediments and paucity of bioturbation suggests periods of reduced sea-floor oxygenation.

Throughout the Ainsa system in all of the Wells, there are horizons associated with the *Phycosiphon* ichnofabric and the *Planolites-Phycosiphon* ichnofabric which represent periods of reduced sea-floor oxygenation. These horizons should in theory provide robust marker horizons to correlate between Wells. However, correlations on the basis of ichnofabrics has not been achieved due to two main factors: (1) the complex architecture of the Ainsa system, characterised by a number of third-order channel elements, means that most deposits are laterally discontinuous; and (2) unlike in pelagic sediments, the use of ichnofabrics to correlate sections is complicated by secondary factors on bioturbation intensity such as grain size and bed thickness. However, in more sheet-like systems, such as the Guaso system, or in more distal fan and related environments such as the lobe, the application of ichnofabrics in Well correlations may be achieved. In previous studies, hardgrounds similar to the *Thalassinoides*-1 ichnofabric have been used to recognise regionally extensive discontinuity surfaces, which have been applied to Well correlations (e.g., MacEachern & Burton 2000). However, such correlations have only been attempted in shallow marine settings, with the hardgrounds associated with the Ainsa system representing localised horizons formed by erosive, high concentration turbidity currents and debris flows.

8.6.4. Channel margin

The increase in bioturbation intensity from the channel off-axis to the channel margin is related to the increased thickness of intensely bioturbated, finer-grained intervals between the sandstones. From outcrop observations, the high intensity, high diversity trace-fossil assemblage of the channel margin is directly related to the high preservation potential of the pre-depositional trace-fossil assemblage (Section 6.4.3). However, in core, because analysis is in vertical section and does not emphasise the trace-fossil assemblage preserved on bedding planes, taphonomic processes have less influence on observed bioturbation intensities. From analysis of the finer-grained intervals between the medium- to thick-bedded sandstones in the channel off-axis and channel margin of the Ainsa I sand body (Well A1 and L1, respectively), it is clear that there is an increase in bioturbation intensity from axial to off-axis environments (45.9% and 50%, respectively). In terms of ichnofabrics, the fine-grained intervals in the

channel off-axis are dominated by the *Scolicia*-diverse-1 and *Scolicia*-diverse-2 ichnofabrics, whilst in the channel margin they are dominated by the *Scolicia*-diverse-1 ichnofabric. This change in bioturbation intensities and ichnofabrics from the channel off-axis to the channel margin is related to varying environmental controlling factors such as sedimentation accumulation rates and environmental stability. This observation supports the conclusions of the outcrop study, in that despite preservation potential playing a fundamental role in the diversity of the trace-fossil assemblage and the intensity of bioturbation, other environmental controlling factors have a direct control on the trace-fossil assemblage.

The muddy intervals between the sandstones in the channel margin are characterised by a higher bioturbation intensity and degree of homogenisation in the Ainsa I sand body compared to the Ainsa II sand body. This is probably related to the finer-grained nature of the muddy intervals in Ainsa I. The finer-grained deposits may be associated with lower sedimentation rates, more stable ecological conditions and a more soupy substrate with low cohesion strength. However, it cannot be discounted that the Ainsa I sand body may have had higher levels of oxygen and nutrient supply.

8.6.5. Levee-overbank

The levee-overbank of the Ainsa I sand body differs greatly between Wells A4 and A2, with the levee-overbank in Well A4 being 32.7 m thick compared to 85.6 m in Well A2. According to Pickering and Corregidor (2000), the thickening of the levee-overbank into Well A2 is related to the fact that it is also the levee-overbank to a channel element to the east, which is not preserved in core or outcrop. The levee-overbank therefore represents significant flow-stripped contributions from channel elements at different times. The top and base of the levee-overbank in Wells A4 and A2 has been positioned on the basis of bio-events, which represent major palaeo-environmental phases that appear to provide a robust means of lateral correlation between wells (Pickering *et al.* 2004). These depths have been modified and refined, where necessary on the basis of bioturbation intensities.

The increase in bioturbation intensity and homogenisation of the sediments from the base to the top of the levee-overbank mirrors the fining and thinning-upward sequence. The low bioturbation intensity towards the base is related to the coarser-grained, thicker-bedded nature of the deposits. As observed by Wetzel (1991) in Recent turbidites, bioturbation decreases with increasing bed thickness and grain size. Lower

bioturbation intensities at the base of the levee-overbank may also be related to higher sediment accumulation rates, as well as the ability of organisms to escape burial from newly deposited sediments. Towards the top of the levee-overbank, the intensely bioturbated, finer-grained, homogenised deposits are associated with slower rates of sediment accumulation, more stable environmental conditions and the substrate was probably soupy with low cohesion strength (soupground). The reduced bed thicknesses may also have enabled more organisms to survive burial by newly deposited sediments.

The levee-overbank in Well A2 is characterised by a higher bioturbation intensity and a greater proportion of homogenised deposits than in Well A4. This is related to the top half of the levee-overbank in Well A2, which is typically totally homogenised, and is poorly developed in Well A4. This fine-grained homogenised top part of the levee-overbank is associated with the channel element to the east, and suggests that this channel element may have been a lower net:gross channel element. Alternatively, the levee-overbank preserved in Well A2 is laterally distal to the axis of the channel element.

The overall high bioturbation intensity of the levee-overbank is indicative of high nutrient and oxygen supply. However, the occurrence of laminated sections associated with the *Phycosiphon* ichnofabric, which is particularly common in Well A4, indicates periods of reduced sea-floor oxygenation.

8.6.6. Intrafan

The high diversity, high intensity trace-fossil assemblage of the intrafan, which is dominated by homogenised sediment, is indicative of a nutrient- and oxygen-rich environment. The dominance of the *Phycosiphon*-diverse-homogenised ichnofabric suggests that the substrate was initially soupy with low cohesion strength and abundant nutrients. Nutrient supply and oxygenation were high enough to support a secondary overprinting trace-fossil assemblage. The intense bioturbation suggests that sediment accumulation rates were low enough to enable the complete homogenisation of sediments. Laminated intervals characterised by the *Phycosiphon* ichnofabric which are well-developed in Well A4 but rare in Well A1 and L1, indicate periods of reduced sea-floor oxygenation.

The trace-fossil assemblage of the intrafan is very similar to the interfan. However, the intrafan is characterised by a slightly higher bioturbation intensity in the secondary overprinting trace-fossil assemblage (1.3% higher bioturbation intensity).

This is interpreted to reflect a higher nutrient and/or oxygen supply in the intrafan and may suggest that the system was not completely shut down during the intrafan.

8.6.7. Abandonment

The fine-grained deposits of the abandonment phase are characterised by a moderately low intensity, high diversity trace-fossil assemblage with a paucity of homogenised sediments. This is in part related to the grain size and thickness of individual beds, which typically comprise very-thin-bedded sandstones. Due to the nature of the deposits, it can be postulated that sediment accumulation rates were probably moderately high, which may also have influenced bioturbation intensities. Fluctuations in oxygen levels are recorded in the change from diverse, intensely bioturbated intervals associated with the *Planolites* ichnofabric and the *Scolicia*-diverse-1 ichnofabric, to the low intensity, low diversity *Planolites-Phycosiphon* ichnofabric. Bioturbation intensities in the abandonment phase are generally lower than in the fine-grained intervals between thick-bedded sandstones of the channel axis to channel margin, despite both being characterised by deposits of a comparable grain size and bed thickness. This may be related to a decrease in nutrient supply and oxygenation in the abandonment phase compared to channelised environments.

8.7. Discussion

Direct comparisons between ichnological studies at core and outcrop are complicated by the major differences in the datasets, with outcrop studies focused on the three-dimensional analysis of trace fossils on horizontal bedding planes whilst core studies are focused on two-dimensional analysis of bioturbation in vertical profile. Consequently, studies at outcrop are focused on the identification of ichnospecies on bedding planes and analysing changes in diversity, whilst core studies are typically based on ichnofabrics and are focused on analysis of thin-bedded successions and the fine-grained intervals between sandstone beds. Trace fossils are typically identified to the ichnogenus level whilst many ichnotaxa such as graphoglyptids cannot be identified in core.

Despite the differences in the nature of the datasets, both outcrop and core studies reveal similar trends in trace-fossil assemblages. For example, both studies show that there is a general trend of increasing trace fossil diversity and bioturbation intensity

from the channel axis to channel margin. However, unlike in the core study in which the levee-overbank of Ainsa I is characterised by a high bioturbation intensity, the levee-overbank of Ainsa I in the outcrop study has a lower diversity and intensity trace-fossil assemblage compared to the channel margin. This may be a result of the coarse-grained nature of the beds studied at outcrop which differ greatly to the levee-overbank deposits studied in core (see section 6.4.4). In both studies, the highest average bioturbation was recognised in the proximal interfan. The fine-grained thin-bedded deposits of the abandonment phase are characterised by high bioturbation intensity trace-fossil assemblages in both core and outcrop.

Despite these similarities, there are also many differences between the datasets. This is clearly illustrated when comparing the results of the core analysis from Ainsa II in Hole L1 and outcrop analysis from the Barranco Forcaz (locality 20) where the lateral distance between core and outcrop at this section is between ~ 25 – 200 m. The margin of channel elements I.1a, I.1b, I.2 and I.3 have an average bioturbation intensity of 42 % on bedding planes at outcrop whilst the average bioturbation intensity in vertical section in core is 30 %. The most common trace fossil at outcrop, *Halopoa imbricata,* is rarely observed in core partly due to difficulties in identification in vertical section. However, in core, the most common trace fossil is *Planolites*, which is rare at outcrop. Only in channel element I.3 are there great similarities between core and outcrop, with *Scolicia* abundant in both datasets. It is therefore clear that there are many differences between both datasets, however, overall they show similar trends in trace-fossil assemblages between different environments.

8.8. Conclusions

The complex ichnofabrics and high intensity of bioturbation recorded in the Ainsa system is indicative of well-oxygenated bottom waters. Similarly to the outcrop study, there is a clear trend in both Ainsa I and II from axial to off-axis environments, with an increase in bioturbation intensity from channel axis to levee-overbank. This is essentially related to the increased thickness of intensely bioturbated, fine-grained intervals between the poorly bioturbated sandstone beds. The high bioturbation intensity associated with these finer-grained intervals is interpreted as reflecting lower rates of sediment accumulation, more stable environmental conditions, and a paucity of erosive, high concentration turbidity currents. The reduced bed thicknesses associated with the

finer-grained intervals may also have enabled more organisms to survive burial by newly deposited sediments. These finer-grained intervals are dominated by the *Planolites* ichnofabric and the *Scolicia*-diverse-1 ichnofabric.

The interfan and intrafan are very similar, associated with totally homogenised sediments indicative of biogenic reworking that exceeded sedimentation rates in nutrient-rich, well-oxygenated soupy sediment with low cohesion strength. The slightly higher bioturbation intensity of the overprinting secondary trace-fossil assemblage in the intrafan, associated with the *Phycosiphon*-diverse-homogenised ichnofabric, suggests that the system was still active. In contrast, the abandonment deposits at the top of the Ainsa II sand body are rarely homogenised, and associated with a lower bioturbation intensity. This is in part related to the grain size and bed thickness of the deposits of the abandonment phase compared to the intrafan or interfan. However, overall the Ainsa I sand body is characterised by a higher bioturbation intensity than the Ainsa II sand body. This is probably related to the fact that the muddy intervals in Ainsa I are finer-grained, and have a lower net:gross. These deposits may therefore be associated with lower sedimentation rates, more stable ecological conditions and the substrate may have been more soupy, with low cohesion strength. However, it cannot be discounted that the Ainsa I sand body may be associated with higher levels of oxygenation and nutrient supply.

Chapter 9

Well A6 Core: Milankovitch control of bioturbation intensity in deep-marine thin-bedded siliciclastic turbidites

9.1 Introduction

Trace fossils are important tools for recognising and interpreting changing environmental conditions in bottom waters (e.g., oxygen and nutrient supply). To date, trace fossils have been used to infer a Milankovitch-type control on pelagic / hemipelagic deposits, e.g., to construct palaeo-oxygenation curves (Savrda & Bottjer 1989, 1994), bioturbation intensities (Damholt & Surlyk 2004), and quantitative studies applying spectral analysis to ichnological data (Erba & Primoli Silva 1994). However, there have been no comparable studies in deep-marine siliciclastic turbidite successions. Core A6 is 230-m-long, comprising very thin- and thin-bedded siliciclastic turbidites stratigraphically overlying the Ainsa II sandbody. A detailed quantitative geochemical and ichnological study was made, including bioturbation intensity, inorganic and organic carbon and gamma-ray logs, to determine whether Milankovitch-type processes were exerting an environmental control on bottom-water conditions during the Middle Eocene.

The middle Eocene is an important time period for understanding the link between the global deterioration in climate associated with the onset of Antarctic ice development and any possible responses in marine sedimentary systems. Studies suggest that ice may have begun to form on Antarctica by the Middle Eocene (Tripati *et al.* 2006), but the extent of the ice and its influence on sedimentary systems remains poorly understood.

Sequence-boundary ages determinations in shallow-water sediments obtained from ODP Leg 189 Site 1171 (South Tasman Rise), and other stratigraphic records (New Jersey, United States, and NW Europe), together with $\delta^{18}O$ variations from deep-sea records, suggest that significant (>10 m) eustatic changes occurred during the early to middle Eocene (51-42 Ma), i.e., at the same time as deep-marine deposition in the Ainsa basin (Pekar *et al.* 2005). The synchronous nature of sequence boundary

development from globally distant sites suggest a global control, with glacio-eustasy as the most plausible mechanism. The amplitude of eustatic sea-level changes is estimated as ~20 m for the early Eocene (51-49 Ma) and ~25 m to ~45 m for the middle Eocene (48-42 Ma) (Pekar *et al.* 2005). These results and conclusions open up the distinct possibility that glacio-eustasy may have been the primary driver in switching on and off the supply of sand to the Ainsa basin deep-water systems.

Many studies have demonstrated the presence of cycles in Paleogene pelagic and lacustrine sediments with periodicities consistent with orbital (so-called Milankovitch) forcing (e.g. Machlus *et al.* 2001, Pälike *et al.* 2001, Coxall *et al.* 2005). However, our knowledge is poor as to whether orbital forcing impacted on clastic marine sedimentation during the Eocene. Using stable isotopes from microfossils, Burgess and Pearson (2007) have identified a Milankovitch control on the clay-rich shelf sediments of the Middle Eocene Hampden Formation in New Zealand. However, the role of orbital forcing on cyclic sedimentation in deep-marine clastic environments has not yet been explored for the Eocene.

9.2 Well A6 Core - sedimentology

Core A6 comprises essentially very thin- and thin-bedded sandy, silty and muddy siltstone turbidites, with very minor amounts of mudstone, together with some chaotic muddy deposits, of Facies Classes C, D, E and F as defined by Pickering *et al.* (1986, 1989). The base of the core comprises thin-bedded sandstones (Facies C2.3), siltstone-mudstone laminae (Facies D2.3), and intervals of intensely bioturbated siltstone and silty mudstone (Facies D1.3 and E1.3, respectively), which correspond to the top of Ainsa II and depositional off-axis from the sand-rich axial, sandy, basin floor Ainsa III sandbody (Fig. 8.1) (Pickering & Corregidor 2005). The middle section of the core (~210 to ~64 m) is characterised by packets of siltstone-mudstone laminae, stratified siltstones, graded mudstones and thin biogenic mudstones (Facies D2.1, D2.3, E2.1 and G2.1, respectively). These are separated by more intensely bioturbated packets of mottled siltstones and mudstones (Facies D1.3 and E1.3 respectively). Representative core sections, showing the range of sediment facies are shown in Figure 9.1. This middle unit is interpreted as interfan between the Ainsa and Morillo systems. The upper part of core A6 contains dm- to m-scale sediment slides and debris flows (type I MTCs

of Pickering & Corregidor 2005), thin-bedded sandstones and siltstone-mudstone laminae (Facies F2.1, C2.3 and D2.3). This upper part of the core respresents the base of the Morillo system. Based on detailed micropalaeontological studies, the cored interval in Well A6 appears to have accumulated in the upper mid Lutetian, very close to the P11-P12 planktonic foramifera boundary (Pickering & Corregidor 2005). There is a pronounced gamma-ray peak at 71.2 m below ground level corresponding to a thrust zone showing a duplex structure ~10 cm thick. Spectral analysis therefore only uses data below the depth of the thrust.

9.3 Trace fossils

In core, trace fossils recorded include *Skolithos*, *Halopoa, Planolites, Palaeophycus, Chondrites, Trichichnus, Ophiomorpha, Thalassinoides, Zoophycos, Phycosiphon, Nereites, Scolicia* and *Teichichnus*. The most common ichnotaxa, from shallowest to deepest tier, are *Phycosiphon, Nereites, Planolites, Scolicia, Thalassinoides, Zoophycos* and *Chondrites* (see section 8.2 for detailed descriptions).

Phycosiphon and *Nereites* commonly occur together in core A6, with *Nereites* typically cross-cutting *Phycosiphon.* In some cases, *Nereites* may crosscut shallow *Scolicia.* At outcrop, *Phycosiphon* is expressed as *P. incertum*, and is very common on the tops of silty sandstones (T_d) whilst *Nereites* is expressed as *N. irregularis* at outcrop. *Planolites* cross-cuts these ichnotaxa, and is characterised by burrow diameters of between 3-7 mm. Commonly, *Planolites* has secondary *Chondrites* within its burrows. At outcrop, only *Planolites* isp. was identified. *Scolicia* ranges in thickness between 9-20 mm and may totally bioturbate core intervals to >1 m vertically. *Scolicia* is commonly crosscut by *Chondrites*. At outcrop, both *S. prisca* and *S. plana* are common, as well as *Scolicia* isp. *Thalassinoides* burrows typically range between 5-20 mm in diameter, and secondary *Chondrites* may be developed within the *Thalassinoides* burrows. At outcrop, most *Thalassinoides* were identified as *T. suevicus. Zoophycos* tubes range between 2-7 mm in thickness and commonly cross-cut *Scolicia. Chondrites* occurs throughout the core, crosscutting most trace fossils and is abundant in both totally homogenised sediments, and intervals characterised by low intensity bioturbation. At outcrop, both *C. intricatus* and *Chondrites* isp. were recognised.

9.4 Results

9.4.1 Ichnology

A summary of relevant core data from Well A6 is shown in Figure 9.2. Based on variations in the intensity of bioturbation, the core can be divided into two broad intervals, only one of which was analysed. The lower unit from the base of the core to the thrust, at ~71.2 m subsurface, is associated with a number of sequences characterised by totally bioturbated, homogenised sediment (*ii* = 6 - 4/6). These average 13.8 m in thickness and are separated by less intensely bioturbated sequences in which the primary sedimentary fabric is preserved (*ii* = 1-5). These sequences average 18.2 m in thickness and are best developed towards the top of the unit, where the deposits are generally finer-grained. The upper unit above the thrust is characterised by intense bioturbation in which primary sedimentary fabrics are preserved (*ii* = 2 - 5). This upper unit is associated with a paucity of *Scolicia* in the top 55.3 m of the core. For the purpose of this study, emphasis shall be put on the lower unit of core A6.

In the lower unit, the almost totally homogenised sediments have an average bioturbation intensity of 87% and are associated with an ichnofabric dominated by *Scolicia*, as well as biodeformational structures. Other trace fossils such as *Planolites, Phycosiphon* and *Zoophycos* are less abundant. Typically these trace fossils occur discretely on the homogenised background. In contrast, the trace-fossil assemblage of the non-homogenised sequences has an average bioturbation intensity of 46% and is characterised by high abundances of *Planolites, Phycosiphon, Thalassinoides, Zoophycos* and *Nereites*. *Scolicia* and biodeformational structures are less abundant. These sequences are characterised by the *Phycosiphon-Planolites* ichnofabric, named after the two most common ichnotaxa. *Chondrites* is common throughout the core. *Nereites*, which is very common in other cores through more axial fan and related environments in the Ainsa system, is less abundant in core A6. In terms of burrow diameters, the average size of *Planolites, Thalassinoides* and *Zoophycos* was recorded in both the homogenised and non-homogenised sequences. No distinct pattern was observed, with *Thalassinoides* and *Zoophycos* having larger burrow diameters, and *Planolites* smaller burrows in the homogenised sequences.

In the equivalent outcrop section that core A6 is drilled through, a similar high intensity trace-fossil assemblage is observed (see section 6.4.5.2). On horizontal bedding planes, mean bioturbation is 54.51%, with 18 ichnospecies from 13

ichnogenera identified, of which 3 are graphoglyptids. Sand-rich horizons characterised by Facies C2.3 sandstones and D2.3 siltstone-mudstone laminae have a trace-fossil assemblage typical of the *Paleodictyon* subichnofacies (*sensu* Seilacher 1974) with some trace fossils more typical of the *Ophiomorpha rudis* subichnofacies (*sensu* Uchman 2001), whilst muddier intervals are characterised by a trace-fossil assemblage typical of the *Nereites* subichnofacies (*sensu* Seilacher 1974), with an abundance of backfilled burrow systems associated with *Nereites, Phycosiphon* and *Scolicia.* Trace fossils recognised at outcrop but not in core include *Arenicolites* isp., *Phycodes palmatum, Helminthorhaphe flexuosa, Helminthopsis* isp., *Paleodictyon minimum* and *Paleodictyon majus.*

9.4.2 Inorganic and organic geochemistry

Core A6 is characterised by a high TOC content, with an average of 1.27%, and range of 0.11-2.98%. This high TOC is also reflected in the abundance of pyrite in the core, which is a common mineral product of early diagenesis in organic-rich sediments (Taylor & Macquaker 2000) and is preferentially concentrated within the burrows. There is no significant difference between the homogenised and non-homogenised sequences in terms of TOC (1.15% and 1.12%, respectively). There is a gradual decrease in TOC between ~200-90 m subsurface, whilst the top of the core is characterised by increased TOC levels.

9.4.3 Spectral Analysis

Spectral analysis of the bioturbation intensity data from the base of the core to the thrust (i.e., between 230-71.2 m subsurface) produces two large power peaks at 0.03 and 0.082 cycles m^{-1} (Fig. 9.3). If the smaller peak at 0.082 cycles m^{-1} represents the 41 k.yr. Milankovitch frequency, then the larger peak at 0.03 cycles m^{-1} would equate to cycles with a frequency of ~112 k.yr.. Assuming that the peak at 0.082 cycles m^{-1} represents obliquity forcing (41 k.yr.), a sediment accumulation rate for the fine-grained sediments of ~30 cm ka^{-1} is calculated. This is consistent with an independent age

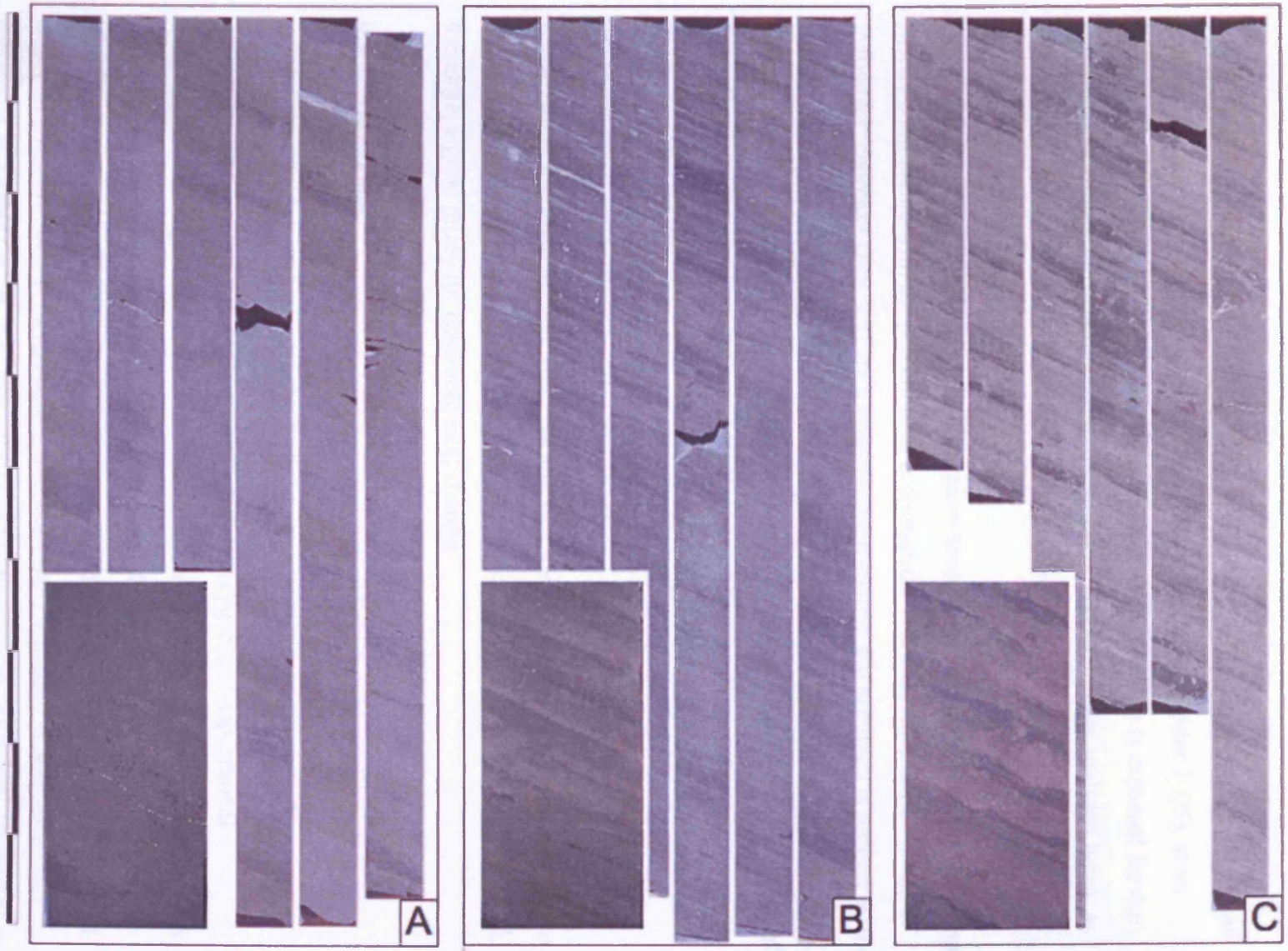
A
B
C

Fig. 9.1. A) Examples of totally homogenised sediment from the middle unit of the core, with close-up of the core (~6 cm wide); B) Non-homogenised sediment from the middle unit of the core, with close-up of the core (6 cm wide); C) Non-homogenised sand-rich sediment from the upper unit of the core, with close-up image (~6 cm wide).

model for the deep-marine sediments in the Ainsa basin which suggests that ~4 km of sediments accumulated in ~10 million years (Pickering & Corregidor 2005), at an average rate of ~40 cm ka^{-1}. A higher sediment accumulation rate is expected for the entire basinal stratigraphy (compared to the fine-grained sediments analysed here), as this includes large sandbodies and mass transport complexes that would have been deposited at much greater rates.

Time-series analysis for individual trace fossil data is not presented as this is not strictly comparable with the percent total bioturbation. Although abundance levels of individual ichnotaxa (Fig. 9.2) are a quantitative measure, the accuracy is limited by the nature of the trace-fossil assemblage. For example, larger traces such as *Scolicia* may destroy significant amounts of smaller trace fossils. Measurements of the abundance of *Scolicia* may also not reflect the original intensity of bioturbation associated with *Scolicia*-forming organisms. This is because the recognition of *Scolicia* is in part controlled by the nature of the substrate, with individual spreiten characteristic of *Scolicia,* only preserved where grain-size variations are sufficient to permit their preservation. For these reasons, only the analysis for the percent bioturbation is shown as this is an accurate record of the degree of biological disruption of the sediment and, therefore, a good proxy for environmental change.

9.5 Discussion

The overall high bioturbation intensity and TOC in core A6, as well as the paucity of graphoglyptids at outcrop, is indicative of a highly oxygenated depositional environment with high benthic food content. The low frequency of intervals with very low bioturbation intensities (*ii* = 1 - 2) suggest that dysaerobic conditions were rarely developed. Changes in the bioturbation intensity and particular ichnotaxa suggest that controlling factors such as oxygenation, nutrient supply and rates of sediment accumulation varied temporally. The effects of fluctuating environmental conditions are clearest in the homogenised and non-homogenised sequences.

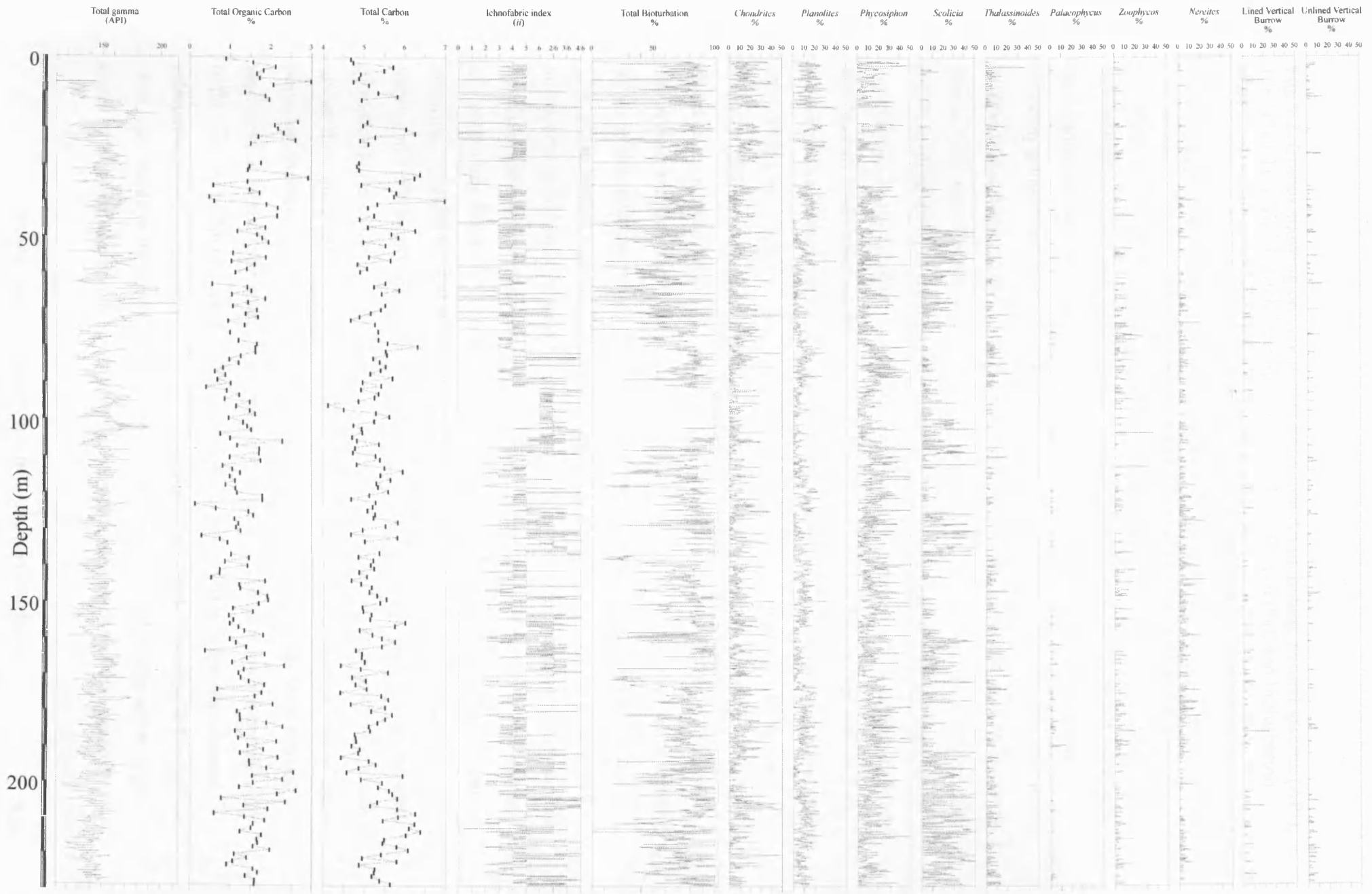
Total gamma (API)
Total Organic Carbon %
Total Carbon %
Ichnofabric index (ii)
Total Bioturbation %
Chondrites %
Planolites %
Phycosiphon %
Scolicia %
Thalassinoides %
Palaeophycus %
Zoophycos %
Nereites %
Lined Vertical Burrow %
Unlined Vertical Burrow %
Depth (m)
0
50
100
150
200

Fig. 9.2. Graphs showing downhole date from core A6 including; natural gamma (API), TOC (%), TC (%), ichnofabric indices (*ii*), total bioturbation (%), and bioturbation intensities of common trace fossils.

Although variations in bioturbation intensity at a Milankovitch scale are recognised in these sequences, it is not possible to unequivocally identify a specific environmental controlling factor for these fluctuations. A number of models have been established utilising ichnofabrics to interprete environmental controlling factors, including palaeo-oxygenation and benthic food content. The palaeo-oxygenation model of Savrda and Bottjer (1986, 1989) is based on pelagic sediments and uses sedimentary fabric, composition of trace-fossil assemblages, burrow size and tiering. However, this model is more suited to continuously accumulating pelagic sediments and has limited applicability in siliciclastics. An alternative palaeo-oxygenation model is that of Ekdale and Mason (1988) based on the ethological character of trace fossils (see section 3.4). However, this method cannot be fully utilised in core due to limitations associated with determining the ethological character of trace fossils in vertical profile. Wetzel and Uchman (1998) established a model to interprete benthic food content from ichnofabrics based on trace fossil tiering. However, the models of Savrda and Bottjer (1986, 1989) and Wetzel and Uchman (1998) cannot be applied to core A6 due to the homogenised nature of the sediment, which prevents the accurate analysis of trace fossil tiering. Changes in burrow size and TOC can be used as proxies to variations in oxygenation and benthic food levels, however, these datasets show no clear fluctuations between the homogenised and non-homogenised sequences. Despite the difficulties in elucidating any controlling factors in causing the changes in bioturbation intensity, the fact that significant changes in TOC throughout the A6 core are not measured (suggesting varying nutrient supply and/or changing oxidation of organic matter), and the presence of sections of core that show almost no bioturbation or only micro-bioturbation, tends to favour fluctuating levels of oxygenation of bottom waters as the principal control on bioturbation intensity. Furthermore, the Ainsa and Jaca basins appear to have been separated, at least during some of the depositional interval of time, by a submarine sill in the position of the present-day Boltaña anticline, known to be a syn-depositional submarine growth structure at the time (Fernandez *et al.* 2004, Pickering & Corregidor 2005, Das Gupta & Pickering, in press) (see Section 1.2.2). Such a submarine ridge could have provided a suitable barrier to the thorough mixing of well-oxygenated

marine bottom-waters on a Milankovitch time scale. This, in turn, would have led to periods of very low oxygen levels at the seafloor within the Ainsa basin.

The homogenised core intervals are interpreted as recording periods of increased oxygenation compared to non-homogenised intervals. The absence of significant changes in burrow diameter, together with the TOC values, also supports the view that nutrient supply was not an important variable in the Ainsa basin. The *Scolicia*-forming organisms associated with the homogenised core intervals may have been particularly sensitive to environmental changes. This may explain why there is a sudden, almost total disappearance of *Scolicia* in the top 55.3 m of the core whilst there is no change in the intensity of bioturbation of other ichnotaxa (Fig. 9.2).

Previous studies have emphasised the affinity of *Scolicia*-forming organisms to specific conditions created in coarse silty to fine sandy sediments, and in particular at the sandstone: siltstone/mudstone interface (e.g., Wetzel 1991, Fu & Werner 2000, Heard & Pickering *in press*). However, in core A6, *Scolicia* is most abundant in silty mudstone intervals rather than sandy intervals. The abundance of *Chondrites* throughout the core, which cross-cuts all other ichnotaxa, including *Scolicia* and biodeformational structures, suggests that the trace-forming organism bioturbated the sediments last, and was able to tolerate extreme ecological conditions such as oxygen-poor sediments.

The apparent absence of any cyclicity in bioturbation intensities in the upper core interval (i.e., between 0 and 71.2 m depth in Fig. 9.2) is probably related to the thicker-bedded, coarser-grained nature of the sediments, as large grain sizes and bed thicknesses tend to impede intense bioturbation processes (cf. Wetzel 1991).

The high TOC in core A6 suggests that sedimentation rates were high enough to preserve considerable amounts of organic carbon. This is because rapid burial can result in increased preservation of organic matter, even in well-oxygenated bottom-waters (e.g., Miller & Suess 1979, Moodley *et al.* 2005). Typically, the preservation of organic matter is related to low levels of oxygenation, which is reflected in a low intensity, low diversity trace-fossil assemblage (Ekdale 1985). This is because increased bottom-water oxygenation generally results in increased rates of degradation of organic matter (Moodley *et al.* 2005). However, due to the interpretation that the deposits of core A6 were formed in a well-oxygenated environment with high nutrient supply, rapid burial associated with high sedimentation rates are invoked from the high TOC. The complex interplay between nutrient supply, oxygenation and sedimentation rates on the levels of TOC is clear throughout the core. For example, the decrease in TOC from ~200-90 m is

interpreted as being due to a gradual increase in bottom-water oxygenation. This is reflected in the intensity of bioturbation, which successively increases in each sequence from older to younger. The absence of observed grain size changes or sandstone:mudstone ratios suggests that the increase in TOC in this interval is not related to changes in sedimentation rates. However, the increased TOC levels in the top ~90 m of the core is interpreted as being due to increased increased sedimentation rates. This increase in sedimentation rates is predicted from the change in sedimentology in the upper unit of the core.

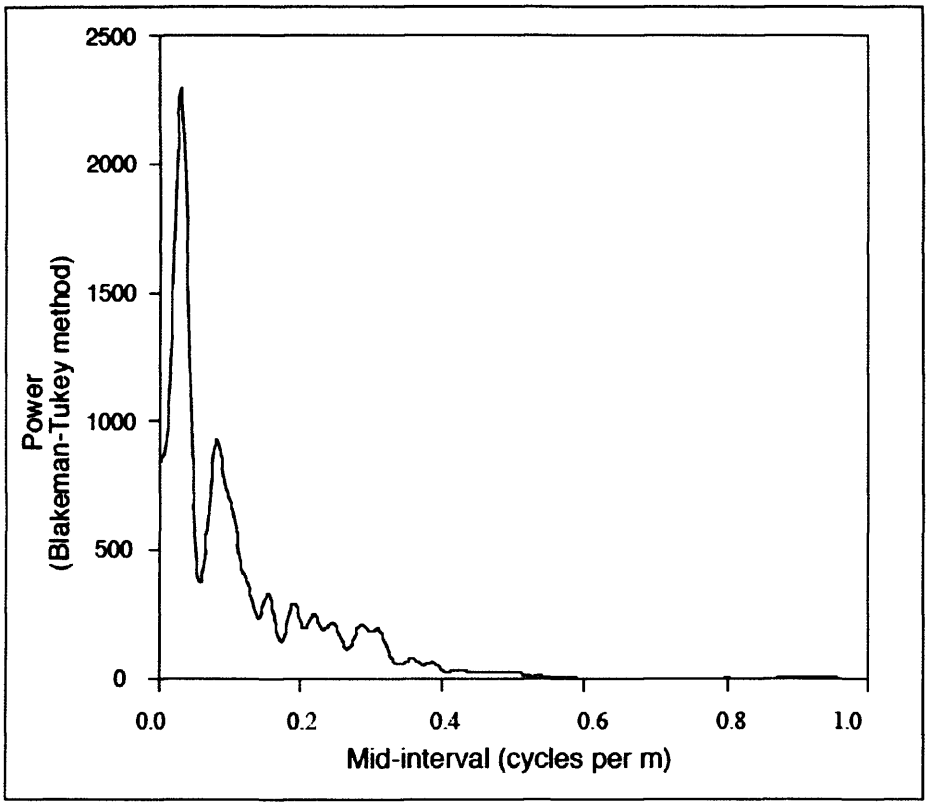

Fig. 9.3. Spectral Analysis graphs. Blackman-Tukey spectrum using a Bartlett window. The bandwidth is 0.0327781. The error estimation on the power spectrum is 0.625579 <ΔPower / Power <2.05482. Power peaks at 0.03 and 0.082. If the smaller peak represents the 41 k.yr. cycle, then the large peak would be ~112 k.yr.

In summary, spectral analysis of bioturbation intensity in the A6 core suggests that bioturbation was controlled by periodic changes in bottom-water oxygenation conditions at two different frequencies, that could be related to obliquity (41 k.yr. frequency) and short eccentricity forcing (~112 k.yr. in our analysis, but likely to be an unresolved average of the 95 and 125 k.yr. frequencies). It is hypothesised that the changes in bottom-water conditions may have resulted from processes that could have

been influenced by Milankovitch-scale climate change, such as ocean circulation and sea-level change. The latter may have been especially important for controlling mixing of the water-masses in the Ainsa and Jaca basins.

Although the cored interval in Well A6 appears to have accumulated close to the P11-P12 planktonic foraminifera boundary, and therefore probably including at least part of the time interval in which researchers recognise the so-called "Middle Eocene Climatic Optimum", at ~44-42 Ma (e.g., based on $\delta^{18}O$ stratigraphy of foraminifera from Demerara Rise, Sexton *et al.* 2006), and interpreted to reflect a temporary warming punctuating middle Eocene cooling, the record is not sufficiently long enough to identify this oceanographic event if it were present.

If the ~25 discrete deep-marine sandbodies in the Ainsa basin, representing ~10 million years of deposition (Pickering & Corregidor 2005), reflect the ~400 k.yr. Milankovitch frequency, then it can be concluded that eccentricity and obliquity are dominant in controlling deep-marine sedimentation in the Ainsa basin, between tectonic events. A precessional signal is not recognised and the dominance of eccentricity and obliquity is quite similar to results from the continental, lacustrine, Eocene Green River Formation (Machlus *et al.* 2001). A longer term, 2-3 million-year, compressional tectonic driver is also recognised in the Ainsa basin, manifest as angular-unconformity-bound "tectono-stratigraphic units" (Fernandez *et al.* 2004, Pickering & Corregidor 2005), at the same temporal scale as identified by Burbank *et al.* (1992) for broadly contemporaneous non-marine and marginal marine sediments immediately east of the Ainsa basin, in the Tremp-Graus basin. Thus, an important outcome of this research is the recognition of climatic and tectonic drivers, at a variety of time scales, in a deep-marine, turbiditic, siliciclastic succession that accumulated at a tectonically very active convergent plate margin (foreland basin).

Chapter 10

Conclusions

10.1. Proximal turbidite systems of the Castisent Group

The Castisent Group comprises the oldest turbidite systems in the Ainsa basin, Fosado and Arro. A new turbidite system, the Los Molinos system, has also been recognised stratigraphically between Fosado and Arro.

The Fosado system, which previously has not be documented in detail, is interpreted as a lower slope channel system based on its geometry, the abundance of Type Ia MTCs associated with the surrounding deposits, and the proximity to temporal shelf deposits (see Remacha, 2003) (c.f., Muñoz et al. 1994; Galloway, 1998).

The three sand bodies which form the Los Molinos system are interpreted as lower-slope, confined, erosional sand bodies. They exhibit an increase in the degree of erosional confinement through time. This may be related to changes in slope gradient, with an increase in slope gradient resulting in increased channel incision (e.g., McCaffrey et al. 2002). Alternatively, it may be related to an increase in the volume of the gravity flows, associated with the progradation of the system.

The Arro system has been reinterpreted as a tectonically controlled channelised system comprising thick accumulations of mass transport complexes (MTCs) and semi-amalgamated confined channel elements. The thick accumulations of muddy slumps, facies associations typical of flows which underwent hydraulic jumps, and the occurrence of confined channel elements, suggests that deposition occurred on the lower slope to proximal basin-floor. This differs to the original interpretation by Millington and Clark (1995, 1996), who concluded that the Arro system is a canyon-mouth sheet system. Overall, in the Barranco Sierra section, the Arro system displays a distinct coarsening-upwards, which may represent the overall progradation of the system.

10.2. Trace fossils as diagnostic indicators of deep-marine environments, in core and outcrop, Ainsa-Jaca basin

The quantitative study of trace fossils from the Middle Eocene deep-marine clastic systems, Ainsa-Jaca basin, shows that they are powerful discriminators of deep-marine

fan and related environments. Sixteen fan and related environments were recognised, from "Prodeltaic clastic ramp" sandbodies to the distal basin floor. A total of 95 ichnospecies from 49 ichnogenera were identified in this study. A distinct trace-fossil assemblage, diversity and abundance characterise each fan and related environment.

The proximal and axial parts of the sandy systems all show low diversity, low-density trace-fossil assemblages dominated by post-depositional trace fossils, which followed an opportunistic colonising strategy of the newly deposited sediments. A similar trace-fossil assemblage also occurs in the channel-lobe transition (CLT) in the Jaca basin. These environments are characterised by a trace-fossil assemblage dominated by *fodinichnia* and *domichnia.* This low diversity, low density trace-fossil assemblage is related to a number of factors: (1) In proximal and axial parts of the sandy systems, sediment gravity flows tend to be highly erosive resulting in the preservation of only the deepest burrowing trace fossils. Shallow-tier trace fossils which typically formed the pre-depositional trace-fossil assemblage were typically destroyed by these erosive gravity flows; (2) The thick-bedded sandstones of the proximal and axial parts of the sandy systems are dominated by endobenthic *pascichnia* and *domichnia* formed by large, robust, deeply burrowing organisms which were well adapted to surviving burial by newly deposited thick sand beds. The traces of smaller organisms which may have survived burial or colonised the deposits after migrating from outside the area affected by the newly deposited sand bed, may have been destroyed by these large, robust trace making organisms; (3) The inferred high sedimentation rates may have resulted in the time between the deposition of sand beds being insufficient for colonisers to migrate from areas unaffected by the newly deposited sediment; and (4) The coarse-grained nature of the deposits in the proximal axial environments may have excluded burrowers adapted only to fine-grained sediments.

Off-axis environments show a general increase in trace-fossil diversity and density compared to more proximal and axial environments, with maximum density of bioturbation in the (commonly) totally bioturbated sediments of the proximal interfan, and greatest diversity occurring in the channel margin and thin-bedded sands at the top of sandbodies. Off-axis environments, in particular channel margins, are characterised by an increase in pre-depositional trace fossils, including graphoglyptids. This increase in trace-fossil diversity and density compared to more proximal and axial environments is related to a number of factors: (1) the lower frequency of strongly erosive sediment gravity flows, compared to proximal axial environments, meant that the preservation

potential of shallow tier trace fossils, such as many graphoglyptids, was greater; (2) decreased rates of sediment accumulation meant that organisms had greater time to colonise and bioturbate the newly deposited sediments. This is coupled with the fact that the proximal off-axis environments were generally closer to areas unaffected by the depositing sediment gravity flows resulting in more rapid colonisation of the newly deposited sediment by migrating organisms due to the reduced migration distances; (3) a decrease in bed thickness and grain size of the deposits in proximal off-axis environments may have promoted an increase in bioturbation and enabled more organisms to survive burial; (4) the reduced diversity trace-fossil assemblages of off-axis environments such as the proximal interfan, basin slope or channel abandonment may be related in part to the high intensity of bioturbation. The fact that the sediments are commonly totally homogenised may have reduced the preservation potential of individual ichnotaxa, except for the deepest-tier trace fossils; and (5) the increase in the proportion of pre-depositional trace fossils including graphoglyptids in proximal off-axis environments, is related to the establishment of equilibrium organism communities related to long-term stable conditions between turbidite sand deposition.

Off-axis environments are characterised by a decreased proportion of *domichnia*, a general increase in *pascichnia* and an increase in *agrichnia* compared to more axial environments. This may be related to a decrease of oxygen levels in the interstitial waters. An increase in the number of ichnotaxa associated with specialist feeding strategies such as many forms of graphoglyptids and some *pascichnia* which covered a given surface in a systematic way suggests that off-axis environments may have been associated with reduced organic matter in the substrate. The basin slope and slope gully have relatively low-diversity, high-density trace-fossil assemblages, with the basin slope typified by a higher number of pre-depositional trace fossils including graphoglyptids compared to the slope gully.

In the distal Jaca basin, similar to the proximal and axial parts of the sandy systems in the Ainsa basin, the CLT is characterised by a low-diversity, low-density, dominantly post-depositional trace-fossil assemblage. The CLT is characterised by a high proportion of *domichnia* and a relatively low proportion of *pascichnia* and *agrichnia*. The greatest average bioturbation and trace-fossil diversity occurs in the lobe fringe, with the lobe and fan fringe also showing a relatively high diversity and average bioturbation. This is related to a number of factors including: (1) the lower frequency of strongly erosive sediment gravity flows; (2) lower rates of sediment accumulation; (3) a

decrease in bed thickness and grain size of the deposits; (4) a reduction in nutrient supply related to the distal location of these environments; and (5) the establishment of equilibrium organism communities due to long-term stable conditions between turbidite sandstone deposition. These environments are characterised by decreasing proportions of *domichnia*, and increasing proportions of *agrichnia* compared to the CLT. A general trend of decreasing average bioturbation and trace-fossil diversity, as well as the number of pre- and post-depositional trace fossils and graphoglyptids occurs from the fan-fringe to distal basin floor. This decrease in bioturbation intensity and diversity is interpreted as being due to a number of factors, including: (1) the limited preservation potential of trace fossils due to the low frequency of taphonomically beneficial sediment gravity flows; (2) the thick turbiditic mudstones characteristic of the distal basin floor may have resulted in a muddy, relatively unstable substrate ("soupground") which may have been unfavourable to many trace-making organisms. The observed decrease in the proportion of *domichnia* and *pascichnia* and increase in *fodinichnia* in the distal basin floor may be associated with changes in oxygen concentrations in interstitial waters.

It is therefore clear that there are distinct variations in trace-fossil assemblages in different fan and related environments in the Ainsa-Jaca basin. However, this study has also illustrated the direct control bed thickness and grain size has on trace-fossil assemblages independent of the environment of deposition. In general, sandstones of a similar thickness and grain size in different environments are characterised by comparable trace-fossil assemblages. This is because the trace fossil communities were directly controlled by factors such as grain size, bed thickness and the nature of the substrate (including firmness). The degree of erosion associated with individual turbidity-current flows also has a direct control on the preserved trace-fossil assemblage. This is most apparent in proximal environments such as the channel axis to channel margin. However, although trace-fossil assemblages are controlled by the nature of the deposits independent of the environment, other controlling factors such as nutrient supply, sediment accumulation rates and oxygenation, which vary between environments also play a major role in trace-fossil assemblages. This is reflected in the fact that sandstones of a similar thickness and grain-size are associated with small, but significant variations in trace-fossil assemblages in different environments. In more distal fan and related environments such as those of the Jaca basin, variations between the trace-fossil assemblages in beds of a similar thickness and grain size are more distinct. This is related to greater changes in environmental controlling factors between

the more distal fan and related environments. The importance of environmental controlling factors is also clear from core analysis, where changes in bioturbation intensity and ichnofabrics in fine-grained intervals between the medium- to thick-bedded sandstones are observed from the channel axis to channel margin.

In core, eleven ichnofabrics have been recognised in the Ainsa system. The detailed ichnofabric study clearly indicates that trace fossils and ichnofabrics can be very powerful discriminators of deep-marine clastic fan and environments.

Similarly to the outcrop study, there is a clear trend in both Ainsa I and II from axial to off axis environments, associated with an increase in bioturbation intensity from channel axis to levee-overbank. This is essentially related to the increased thickness of intensely bioturbated, fine-grained intervals between the poorly bioturbated sandstone beds. The high bioturbation intensity associated with these finer-grained intervals is interpreted as reflecting lower rates of sediment accumulation, more stable environmental conditions, and a paucity of erosive, high concentration turbidity currents. The reduced bed thicknesses associated with the finer-grained intervals may also have enabled more organisms to survive burial by newly deposited sediments. These finer-grained intervals are dominated by the *Planolites* ichnofabric and the *Scolicia*-diverse-1 ichnofabric.

The interfan and intrafan are very similar, associated with totally homogenised sediments indicative of biogenic reworking that exceeded sedimentation rates in nutrient-rich, well-oxygenated soupy sediment with low cohesion strength. The slightly higher bioturbation intensity of the overprinting secondary trace-fossil assemblage in the intrafan, associated with the *Phycosiphon*-diverse-homogenised ichnofabric, suggests that the system was still active. In contrast, the abandonment deposits at the top of the Ainsa II channel complex set are rarely homogenised, and associated with a lower bioturbation intensity. This is in part related to the grain size and bed thickness of the deposits of the abandonment phase compared to the intrafan or interfan. However, overall the Ainsa I channel complex set is characterised by a higher bioturbation intensity than the Ainsa II channel complex set. This is probably related to the fact that the muddy intervals in Ainsa I are finer-grained. These deposits may therefore be associated with lower sedimentation rates, more stable ecological conditions and the substrate may have been more soupy, with low cohesion strength. However, it cannot be discounted that the Ainsa I channel complex set may be associated with higher levels of oxygenation and nutrient supply.

10.3. Milankovitch beat of bioturbation intensity in deep-marine thin-bedded siliciclastic turbidites, Well A6 core

Because trace fossils are important tools for recognising and interpreting changing environmental conditions in bottom waters (e.g., oxygen and nutrient supply), they can be used to infer a Milankovitch-type control on deposits. The study from Well A6 shows for the first time that bioturbation intensity can be used to infer a Milankovitch-type control on a deep-marine siliciclastic turbidite succession. Spectral analysis of bioturbation intensity suggests that bioturbation was controlled by periodic changes in bottom-water oxygenation conditions at two different frequencies, that could be related to obliquity (41 k.yr frequency) and short eccentricity forcing (~112 k.yr. in our analysis, but likely to be an unresolved average of the 95 and 125 k.yr frequencies). It can therefore be postulated that the changes in bottom-water conditions may have resulted from processes that could have been influenced by Milankovitch-scale climate change, such as ocean circulation and sea-level change.

If the ~25 discrete deep-marine sandbodies in the Ainsa basin, representing ~10 million years of deposition (Pickering & Corregidor 2005), reflect the ~400 k.yr Milankovitch frequency, then it can be concluded that eccentricity and obliquity are dominant in controlling deep-marine sedimentation in the Ainsa basin, between tectonic events. A longer term, 2-3 million-year, compressional tectonic driver is also recognised in the Ainsa basin, manifest as angular-unconformity-bound "tectono-stratigraphic units" (Fernandez *et al.* 2004, Pickering & Corregidor 2005). Thus, an important outcome of this research is the recognition of climatic and tectonic drivers, at a variety of time scales, in a deep-marine, turbiditic, siliciclastic succession that accumulated at a tectonically very active convergent plate margin (foreland basin).

10.4. Lessons learnt and exportability of analysis

This study has demonstrated, in the most detailed analysis to date, that trace fossils and trace-fossil assemblages can be very powerful discriminators of deep-marine clastic fan and related environments and provide important tools for identifying changes in environmental conditions in the deep-marine environment. It has shown that trace fossils can and therefore should be utilised just like sedimentary structures, with the type, distribution and assemblage of trace fossils, their abundance and diversity, being

used as an additional (complementary) tool in paleoenvironmental analysis. Where outcrop or core data is very limited, and environmental interpretations correspondingly uncertain, the efficacy of the methodological approach undertaken in this study may be considerable, particularly for the Paleogene and Miocene.

The successful application of bioturbation intensity as a proxy to Milankovitch-style forcing of environmental change has illustrated that in heavily bioturbated successions in which conventional methods such as bed thickness and grain size analysis is not possible, bioturbation intensity can be used as a proxy to Milankovitch-style forcing of environmental change. It also shows that using bioturbation intensity to identify Milankovitch cycles should not be restricted to pelagic successions, but can also be applied to fine-grained clastic environments.

This study also illustrates the uses of both the ichnofabric and ichnofacies methodologies in trace fossil studies. The use of ichnofacies in palaeoenvironmental studies has recently been questioned by a number of authors (e.g. Goldring, 1995; Bromley, 1996; Goldring, 1999; McIlroy, 2004), however, this study has illustrated the importance of both methods. The use of applying subichnofacies of the *Nereites* ichnofacies as defined by Seilacher (1974) and Uchman (2001) to outcrop studies has been shown to be significant. In core, the more recent ichnofabric methodology will continue to grow in its applicability to core analysis as more studies are undertaken.

A number of significant lessons were learnt from this study. An important lesson was the importance of accurate identification of trace fossils. Key taxonomic papers such as Uchman (1995, 1998, 2001) should provide the basis of all taxonomic studies and where ichnotaxa are currently poorly defined (e.g., *Zoophycos*), care should be taken to prevent misidentification. In core, problems in identifying trace fossils due to the 2D vertical nature of the dataset means that great care should be taken when identifying trace fossils. This is particularly relevant for small, horizontal burrow networks which could be any number of ichnotaxa. The ichnofabric index scheme of Droser and Bottjer (1986, 1991) was also shown to be a quick and reliable semi-quantitative method to record bioturbation intensity.

10.5. Future research

Nummulites-lined burrow – a new ichnotaxon:

The *Nummulites*-lined burrows observed at Formigales require further study. These burrows show similarities to both *Diopatrichnus roederensis* (Kern 1978) and *Nummipera eocenica* (Hölder 1989) and a number of traces described from the Eocene of Poland (Roniewicz 1970, Olempska 1973). However, there are clear differences between the traces described in this thesis and previously described *nummulites*-lined burrows. For example, *Diopatrichnus roederensis* (Kern 1978) is only partially lined by organic fragments whilst *Nummipera eocenica* (Hölder 1989) is diagnosed as a vertical trace. The completely *nummulites*-lined vertical and horizontal burrow systems described in this thesis therefore may represent a new ichnotaxon and therefore require further analysis.

More detailed work on the Fosado, Los Molinos and Arro turbidite systems in the Ainsa basin:

The work presented in chapter 5 on the Castisent Group in the Ainsa basin was not a fundamental part of the thesis and thus there is great scope for continued work on these systems. In particular, a detailed geological map of the systems has not yet been constructed and the interaction between tectonics and sedimentation has not yet been fully investigated. There is also great scope to do a detailed structural study on the systems, due to the fact that they are the most structurally complex in the basin. The understanding of the interaction between tectonics and sedimentation during the early phase of the Ainsa basin as well as the evolution of the Ainsa basin during this time requires further analysis.

Detailed bed-to-bed analysis (including sedimentological, ichnological, micropalaeontological and geochemical) from channel axis to overbank:

One of the fundamental conclusions of this thesis is that controls such are grain-size, bed thickness and substrate are the prime controlling factors on trace fossil distributions, rather than environmental setting *per se.* It is because these variables change in different environments that trace-fossils are powerful discriminators of deep-marine fan and related environments. A number of systems including Banaston, Ainsa and Guaso have excellent sections where beds can be traced from the channel axis to overbank. A detailed study

quantifying variations in the sedimentology (including bed thickness and grain size) ichnology (including diversity and intensity bioturbation, ichnofabrics and ichnofacies, and ethological characteristics), micropalaeontology and geochemistry from axis to overbank will provide a detailed understanding of lateral changes in environmental conditions in a deep-marine channelised system.

More detailed work on comparing trace fossils in core and outcrop using bed-to-bed correlations:

This study is unique in that it provides a quantitative ichnological study in a deep-marine turbidite system (the Ainsa system) at outcrop and in the subsurface. Detailed correlations between core and outcrop allow the opportunity to study the subsurface and outcrop expression of trace fossils on the same beds. This study should increase our understanding of the differences and similarities between the two datasets, and should improve our understanding of trace fossils in core and the use of trace fossils in the subsurface.

Core A6 – more detailed study on understanding the principal controlling factor(s) on cyclical changes in bioturbation intensity:

Cyclical changes in bioturbation intensity recorded in core A6 were tentatively assigned to changes in oxygenation. However, a more detailed analysis including further, more detailed geochemical analysis is required to fully understand the main controlling factor(s). Analysis of changes in grain size in the core may provide an answer as to whether changes in bioturbation intensity are due to changes in clastic supply (such as sedimentation rate and / or nature of the depositing turbidity current flows), nutrient supply or oxygenation. A more detailed age dating of the core should also result in increased confidence in the spectral analysis of the bioturbation intensity data.

Chapter 11

References cited

Abreu, V., Sullivan, M., Pirmez, C., Mohrig, D., 2003. Lateral accretion packages (LAPs): an important reservoir element in deep water sinuous channels. Marine and Petroleum Geology. 20, 631-648.

Ausich, W.I., and Bottjer, D.J., 1982. Tiering in suspension-feeding communities on soft substrata throughout the Phanerozoic. Science. 9, 173-174.

Azpeitia M.F., 1933. Datos para el studio paleontólogico del Flysch de la Costa Cantábrica y de algunos otros puntos de España. Boletín. Instituto Geológico y Minero de España. 53, 1-65.

Babek, O., Mikulas, R., Zapletal, J., and Lehotsky, T., 2004. Combined tectonic-sediment supply-driven cycles in a Lower Carboniferous deep-marine foreland basin, Moravice Formation, Czech Republic. International Journal of Earth Sciences. 93(2), 241-261.

Bak, K., 1995. Trace fossils and ichnofabrics in the Upper Cretaceous red deep-water marly deposits of the Pieniny Klippen Belt, Polish Carpathians. Annales Societatis Geologorum Poloniae. 64, 81-97.

Bann, K.L., Fielding, C.R., MacEachern, J.A., and Tye, S.C., 2004. Differentiation of estuarine and offshore marine deposits using integrated ichnology and sedimentology: Permian Pebbley Beach Formation, Sydney Basin, Australia, in: McIlroy, D., (Ed.), The Application of Ichnology to Palaeoenvironmental and Stratigraphic Analysis. Geological Society of London, Special Publication. 228, pp. 179-211.

Barbier, R., 1956. Découverte d'un *Palaeodictyon* dans le Dogger ultradauphinois de la region des Aiguilles d'Arves. Travaux du Laboratoire de la Faculté des Sciences de l'Universite de Grenoble. 33, 125-133

Benton, M.J., 1982. Trace fossils from Lower Palaeozoic ocean-floor sediments of the Southern Uplands of Scotland. Transactions of the Royal Society of Edinburgh: Earth Sciences. 73, 67-87.

Billings, E., 1862. New species in fossils from the different parts of the lower, Middle and Upper Silurian rocks of Canada, in: Palaeozoic Fossils, volume 1 1861-1865. Geological Survey of Canada, Dawson Brothers, Montreal, pp. 96-168.

Billings, E., 1866. Catalogues of the Silurian fossils. Geological Survey of Canada, Dawson Brothers, Montreal, pp. 93.

Bottjer, D.J., and Droser, M.L., 1991. Ichnofabric and basin analysis. Palaios. 6, 199-205.

Brady, L.F., 1947 Invertebrate tracks from the Coconino Sandstone of northern Arizona. Journal of Paleontology. 21, 466-472.

Brady, L.F., 1949 *Oniscoidichnus*, new name for *Isopodichnus* Brady 1947 not Bornemann 1889. Journal of Paleontology. 23, 573.

Bromley, R.G., 1996. Trace fossils. Biology, taphonomy and applications. Chapman and Hall, London, pp. 361.

Bromley, R.G., and Ekdale, A.A., 1986. Composite ichnofabrics and tiering of burrows. Geological Magazine. 123(1), 59-65.

Brongniart, A.T., 1823. Observations sur les Fucoids. Société d'Hist Natur. Paris. Mémoir. 1, 301-320.

Brongniart, A.T., 1828. Histoire des végétaux fossils ou recherches botaniques et géologiques sur les végétaux renfermés dans les diverses couches du globe. Volume 1. G. Dufour and E. d'Ocagne, Paris. pp. 136.

Buatois, L.A., Mangano, M.G., and Sylvester, Z., 2001. A diverse deep-marine Iihnofauna from the Eocene Tarcau Sandstone of the Eastern Carpathians, Romania. Ichnos. 8, 23-62.

Burbank, D.W., Puigdefabregas, C., Munoz, J.A., 1992. The chronology of the Eocene tectonic and stratigraphic development of the eastern Pyrenean foreland basin, north-east Spain. Geological Society of America, Bulletin. 104, 1101-1120.

Burgess, C.E., and Pearson, P.N., 2007. Milankovitch scale cyclicity in the Eocene Southern Ocean - an integrated micropalaeontological and geochemical approach. Geophysical Research Abstracts. 9, 03065.

Burton, B.R., and Link, P.K., 1991. Ichnology of fine-grained mixed carbonate-siliciclastic turbidites, Wood River Formation, Pennsylvanian-Permian, South-Central Idaho. Palaios. 6, 291-301.

Chamberlain, C.K., 1971. Morphology and ethology of trace fossils from the Ouachita Mountains, Southeast Oklahoma. Journal of Paleontology. 45(2), 212-246.

Clark, J.D. 1995. Detailed section across the Ainsa II Channel complex, South Central Pyrenees, Spain, in: Pickering, K.T., Hiscott, R.N., Kenyon, N.H., Ricci Lucchi, F., and

Smith, R.D.A., (Eds.). Atlas of deep water environments: architectural style in turbidite systems. Chapman and Hall. London. pp. 139-144.

Clark, J.D. 2006. Architectural hierarchy in deepwater channel systems: Applications of Outcrop analogues to integrated subsurface characterization. Chevron SSC Forum. Poster.

Clark, J.D., and Pickering, K.T., 1996. Submarine channels: Processes and architecture. Vallis Press, London. pp. 232.

Coxall, H.K., Wilson, P.A., Palike, H., Lear, C.H., and Backman, J., 2005. Rapid stepwise onset of Antarctic glaciation and deeper calcite compensation in the Pacific Ocean. Nature, 433, 53-57.

Crimes, P.T., 1977. Trace fossils of an Eocene deep-sea fan, northern Spain, in: Trace Fossils 2 (Eds.) Crimes, P.T., and Harper, J.C. Geological Journal Special Issue 9, 71-90.

Crimes, P.T. and Anderson, M.M., 1985. Trace Fossils from Late Precambrian-Early Cambrian strata of Southeastern Newfoundland, Canada: temporal and environmental implications. Journal of Paleontololgy. 59, 310-343.

Crimes, P.T. Goldring, R., Homewood, P., Stuijvenberg, J., and Winkler, W., 1981. Trace fossil assemblages of deep-sea fan deposits, Gurnigel and Schlieren flysch Cretaceous-Eocene, Switzerland. Eclogae Geologicae Helveticae. 74, 953-995.

Cronin, B.T., Hartley, O.D., and Kneller, B., 1998. Slumps, debris flows and sandy deep-water channel systems: implications for the application of sequence stratigraphy to deep water clastic sediments. Geological Society of London, Journal. 155, 429–432.

Das Gupta, K., and Pickering, K.T., in review. Sandstone petrography of Eocene deep-marine Ainsa-Jaca basin.

D'Alessandro, A., and Bromley, R.G., 1987. Meniscate trace fossils and the *Muensteria-Taenidium* problem. Palaeontology. 30, 743-763.

Damholt, T., Surlyk, F., 2004. Laminated-bioturbated cycles in Maastrichtian chalk of the North Sea: oxygenation fluctuations within the Milankovitch frequency band. Sedimentology. 51, 1232-1342.

Dreyer, T., Corregidor, J., Arbues, P., and Puigdefabregas, C., 1999 Architecture of the tectonically influenced Sobrarbe deltaic complex in the Ainsa Basin, northern Spain. Sedimentary Geology. 127, 127-169.

Droser, M.L., Bottjer, D.J., 1986. A semiquantitative field classification of ichnofabric. Journal of Sedimentary Petrology. 56, 558-559.

Droser, M.L., Bottjer, D.J., 1988. Trends in depth and extent of bioturbation in Cambrian carbonate marine environments, Western United States. Geology. 16, 233-236.

Droser, M.L., Bottjer, D.J., 1989. Ichnofabric of Sandstones Deposited in High-Energy Nearshore Environments: Measurement and Utilization. Palaios. 4(6), 598-604.

Drinkwater, N. J., and Pickering, K. T., 2001. Architectural elements in a high-continuity sand-prone turbidite system, Late Precambrian Kongsfjord Formation, Northern Norway: Application to hydrocarbon reservoir characterization. AAPG Bulletin. 85(10), 1731-1757.

Droser, M.L., and Bottjer, D.J., 1988. Trends in depth and extent of bioturbation in Cambrian carbonate marine environments, western United States. Geology. 16, 233-236.

Droser, M.L., and Bottjer, D.J., 1989. Ichnofabric of sandstone deposited in high-energy nearshore environments: measurement and utilization. Palaios. 4, 598-604.

Droser, M.L., Bottjer, D.J., 1991. Trace fossils and ichnofabric in leg 119 cores. Proceedings of the Ocean Drilling Program, Scientific Results. 119, 635-641.

Eichwald, E., 1860-1868. Lethaea Rossica ou paléontologie de la Russie. Décrite et Figurée. Volume 1. 1860, Atlas. 1868. E Schweizerbart, Stuttgart. pp. 1657.

Ekdale, A.A., 1985. Paleoecology of the marine endobenthos. Palaeogeography, Palaeoclimatology, Palaeoecology. 50, 63-81.

Ekdale, A.A., and Bromley, R.G., 1982. Trace fossils and ichnofabrics in the Kjølby Gaard Marl, uppermost Cretaceous, Denmark. Bulletin of the Geological Society of Denmark. 31, 107-119.

Ekdale, A.A., and Bromley, R.G., 1991. Analysis of Composite Ichnofabrics: An Example in Uppermost Cretaceous Chalk of Denmark. Palaios. 6, 232-249.

Ekdale, A.A., and Lewis, D.W., 1991. Trace fossils and paleoenvionmental control of ichnofacies in a late Quaternary gravel and loess fan delta complex, New Zealand. Palaeogeography, Palaeoclimatology, Palaeoecology. 81, 253-279.

Ekdale, A.A., and Mason, T.R., 1988. Characteristic trace-fossil associations in oxygen-poor sedimentary environments. Geology. 16, 720-723.

Ekdale, A.A., Bromley, R.G., and Pemberton, G., 1984. Ichnology, trace fossils in sedimentology and stratigraphy. SEPM Short Course, 15.

Emmons, E., 1844. The Taconic System based on observations in New-York, Massachusetts, Maine, Vermont, and Rhode-Island. Caroll and Cook, Albany. pp. 63.

Erba, E., Silva, I.P., 1994. Orbitally driven cycles in trace-fossil distribution from the Piobbico core late Albian, central Italy, in: Deboer, P., Smith, D (Eds.). Orbital forcing and cyclic sequences: International Association of Sedimentologists, Special Publication. 19, pp. 211-225.

Eschard, R., Albouy, E., Deschamps, R., Euzen, T., and Ayub, A., 2003. Downstream evolution of turbiditic channel complexes in the Pab Range outcrops, Maastrichtian Pakistan. Marine and Petroleum Geology. 20, 691-710.

Falivene, O., Arbués, P., Gardiner, A., Pickup, G., Muñoz, J.A., and Cabrera, L., 2006a. Best practice stochastic facies modeling from a channel-fill turbidite sandstone analog (the Quarry outcrop, Eocene Ainsa basin, northeast Spain). AAPG Bulletin 90(7). 1003-1029.

Falivene, O., Arbués, P., Howell, J., Muñoz, J.A., and Fernandez, O., 2006b. Hierarchical geocellular facies modelling of a turbidite reservoir analogue from the Eocene of the Ainsa basin, NE Spain. Marine and petroleum geology. 23(6), 679-701.

Fernandez, O., Muñoz, J.A., Arbues, P., Falivene, O., and Marzo, M., 2004. Three-dimensional reconstruction of geological surfaces: An example of growth strata and turbidite systems from the Ainsa basin, Pyrenees, Spain. AAPG Bulletin. 88, 1049–1068.

Fillion, D., and Pickerill, R.K., 1990. Ichnology of the Upper Cambrian to Lower Ordovician Bell Island and Wabana groups of eastern Newfoundland, Canada. Palaeontology Canada. 7, 1-119.

Fischer-Ooster, C., 1858. Die fossilen Fucoiden der Schweizer Alpen, nebst Erörterungen über deren geologisches Alter. Huber, Bern. pp. 72.

Flood, R.D., Piper, D.J.W., and Klaus, A., et al., 1995. Proceedings of the Ocean Drilling Program, Initial reports, Volume 155. College Station, Texas, Ocean Drilling Program. pp. 1233.

Föllmi, K.B., and Grimm, K.A., 1990. Doomed pioneers: Gravity-flow deposition and bioturbation in marine oxygen-deficient environments. Geology. 18, 1069-1072.

Frey, R.W., and Seilacher, A., 1980. Uniformity in marine invertebrate ichnology. Lethaia. 13, 183-207.

Frey, R.W., and Pemberton, S.G., 1984. Trace fossil facies models, in: Walker, G (Ed.). Facies Models (2nd ed.). Geoscience. Canada. Reprint Series 1, pp. 189-207.

Frey, R.W., and Pemberton, S.G., 1985. Biogenic structures in outcrops and cores. 1. Approaches to Ichnology. Bulletin of Canadian Petroleum Geology. 33, 72-115.
Frey, R.W., and Goldring, R., 1992. Marine event beds and recolonization surfaces as revealed by trace fossil analysis. Geology Magazine. 129(3), 325-335.
Frey, R.W., Howard, J.D., and Pryor, W.A., 1978. *Ophiomorpha*: Its morphologic, taxonomic, and environmental significance. Palaeogeography, Palaeoclimatology, Palaeoecology. 23, 199-229.
Frey, R.W., Howard, J.D., and Hong, J.S., 1987. Prevalent lebensspuren on a modern macrotidal flat, Inchon, Korea: Ethological and environmental significance. Palaios. 2, 517-593.
Frey, R.W., Pemberton, S.G., and Saunders, T.D., 1990. Ichnofacies and bathymetry: A passive relationship. Journal of Paleontology. 64, 155-158.
Friend, P.F., Slater, M.J., and Williams, R.C., 1979. Vertical and lateral building of river sandstone bodies, Ebro Basin, Spain. Journal of the Geological Society of London. 136, 39-46.
Fu, S., 1991. Funktion, verhalten und einsteilung fucoider und lophoctenoider lebensspuren. Courier Forschung Institut Senckenberg. 135, 1-79.
Füchs, T., 1895. Studien über fucoiden und hieroglyphen. Denkschr Akad Wiss Wien Math-Naturwiss Kl. 62, 369-448.
Fürsich, F.T., 1975. Trace fossils as environmental indicators in the Corallian of England and Normandy. Lethaia. 8, 151-172.
Gabelli, L. De., 1900. Sopra un interessante impronta medusoidae. Il Pensiero Aristotelico della Scienza Moderna. 1(2), 74-78.
Galloway, W.E., 1998. Siliciclastic slope and base-of-slope depositional systems; component facies, stratigraphic architecture, and classification. AAPG Bulletin. 82(4), 569-595.
Geinitz, H.B., 1867. Die organischen ueberreste im dachschiefer von wurzbach bei lobenstein. Nova Acta Acad. Caes. Leop. Carol., German. Natur. Curios. 33, 1-24.
Ghibaudo, G., Grandesso, P., Massari, F., and Uchman, A., 1996. Use of trace fossils in delineating sequence stratigraphic surfaces, Tertiary Venetian Basin, northeastern Italy. Palaeogeography, Palaeoclimatology, Palaeoecology. 120, 261-279.
Gibert, J.M. de, Arbues, P., Puig, M., and Marzo, M., 2003. Ichnological signatures of turbidite channels from the Eocene Ainsa Slope Complex (Spanish Pyrenees). AAPG Conference Abstract.

Goldring, R., 1999. Field Palaeontology. Longman. Harlow.
Haldeman, S. S., 1840. Supplement to Number One of "A monograph of the Limniades, or freshwater univalve shells of North America." Containing descriptions of apparently new animals in different classes, and the names and characters of the subgenera, in: Paludina and Anculosa. J. Dobson, Philadelphia.
Hall, J., 1847. Paleontology of New York. Volume 1. C. Van Benthuysen, Albany. pp. 338.
Hall, J., 1852. Paleontology of New York. Volume 2. C. Van Benthuysen, Albany. pp. 362.
Häntzschel, W., 1975. Trace fossils and problematica, in: Teichert, C (Ed.). Treatise on invertebrate paleontology. Geological Society of America and Kansas University Press.
Haughton, P.W., Barker, S.P., and McCaffrey, W.D., 2003. 'Linked' debrites in sand-rich turbidite systems – origin and significance. Sedimentology. 50, 459–482.
Heard, T., and Pickering, K.T., 2008. Trace fossils as diagnostic indicators of deep-marine environments, Middle Eocene Ainsa - Jaca basin, Spanish Pyrenees: Sedimentology, in press.
Heard, T., Pickering, K.T., and Robinson, S.A., In Review. Milankovitch forcing of bioturbation intensity in deep-marine thin-bedded siliciclastic turbidites. Earth and Planetary Science Letters.
Heer, O. 1877. Flora fossilis helvetiae. Vorweltliche flora der Schweiz. J. Wurster and Comp. Zürich. pp. 182.
Hiscott, R.N., and Middleton, G.V., 1980. Fabric of coarse deep-water sandstones, Tourelle Formation, Quebec, Canada. Journal of Sedimentary Research. 50(3), 703-721.
Holder, H., 1989. Spuren auf der Spur. Palichnologische und. verwandte Notizen über Teredolites, Entobia, Nummipera nov. gen. und einiges andere Münstersche Forschungen zur Geologie und Paläontologie. 69.
Howard, J.D., and Frey, R.W., 1984. Characteristic trace fossils in nearshore to offshore sequences, Upper Cretaceous of east-central Utah. Canadian Journal of Earth Sciences. 21, 200-219.
Hoyal, D.C.J.D., Van Wagoner, J.C., Adair, M., Deffenbaugh, N.L., Sun, D. Li, T., Huh C., and Giffin, D.E., 2003. Sedimentation from jets: a depositional model for clastic deposits of all scales and environments. AAPG Conference Abstract.
James, U.P., 1879. Description of new species of fossils and remarks on some other, from the Lower and Upper Silurian rocks of Ohio. The Paleontologists. 3, 17-24

Jones, R.W., Pickering, K.T., Boudagher-Fadel, M., and Matthews, S., 2005. Preliminary observations on the micropalaeontological characterization of submarine fan/channel sub-environments, Ainsa System, south-central Pyrenees, Spain, in: Powell, A. J., and Riding, J. B. (Eds.). Recent developments in applied biostratigraphy. The Micropalaeontological Society, Special Publications, 55–68.

Kern, J.P., 1978. Paleoenvironment of new trace fossils from the Eocene Mission Valley Formation, California. Journal of Paleontology. 52, 186-194.

Kern, J.P., 1980. Origin of trace fossils in Polish Carpathian flysch. Lethaia. 13, 347-362.

Kneller, B., 1995. Beyond the turbidite paradigm: physical models for the deposition of turbidites and their implications for reservoir prediction, in: (Hartley, A.J., and Prosser, D.J. (Eds.) Characterisation of deep marine clastic systems. Geological Society of London Special Publication. 94, 31-49.

Kotake, N., 1989. Paleoecology of the *Zoophycos* producers. Lethaia. 22, 327-341.

Kotake, N., 1991. Packing process for filling material in *Chondrites.* Ichnos. 1, 277-285.

Kotake, N., 1992. Deep-sea echiurans: possible producers of *Zoophycos.* Lethaia. 25, 311-316.

Książkiewicz, M., 1958. Stratigraphy of the Magura Series in the Średni Beskid Carpathians. Inst. Geol. Biul. 153, 43-96.

Książkiewicz, M., 1968. On some problematic organic traces from the flysch of the Polish Carpathians, Part 3. Rocznik Polskiego Towarzystwa Geologicznego. 38, 3-17.

Książkiewicz, M., 1970. Observations on the ichnofauna of the Polish Carpathians, in: Crimes, P.T., and Harper, C., (Eds.). Trace Fossils. Geological Journal special Issue, 3. pp. 283-322.

Książkiewicz, M., 1977. Trace fossils in the flysch of the Polish Carpathians. Palaeontologica Polonica. 36, 1-208.

Labaume, P., Mutti, E., and Seguret, M., 1987. Megaturbidites: a depositional model from the Eocene of the SW-Pyrenean Foreland Basin, Spain. Geomarine Letters. 7, 91-101.

Lewis, D.W., and Ekdale, A.A., 1992. Composite ichnofabric of a Mid-Tertiary unconformity on a pelagic limestone. Palaios. 7(2), 222-235.

Lien. T., Walker, R.G., Martinsen, O.J., 2003. Turbidites in the Upper Carboniferous Ross Formation, western Ireland: reconstruction of a channel and spillover system. Sedimentology. 50, 113-148.

Lowe, D.R., and Guy, M., 2000. Slurry-flow deposits in the Britannia Formation (Lower Cretaceous), North Sea: a new perspective on the turbidity current and debris flow problem. Sedimentology. 47, 31-70.

Lundgren, B., 1891. Studier ofver fossilforande losa block. Geologiska Föreningens i Stockholm Förhandlingar. 13, 111-121.

Maceacherni, J.A., and Burton, J.A., 2000. Firmground *Zoophycos* in the Lower Cretaceous Viking Formation, Alberta: a distal expression of the Glossifungites Ichnofacies. Palaios. 15, 387-398.

Machlus, M., Olsen, P.E., Christie-Blick, N., Hemming, S.R., 2001. Milankovitch cyclicity in the Eocene Green River Formation of Colorado and Wyoming. American Geophysical Union. Abstract U12A-0005.

MacLeay, W.S., 1839. Note on the Annelida, in: Murchinson, R.I. (Ed.). The Silurian System, Part II, organic remains. J. Murray, London. pp. 699-701.

Macsotay, O., 1967. Huellas problematicas y su valor paleoecologico en Venezuela. Géos. 16, 7-39.

Mangano, M.G., Buatois, L.A., Maples, C.G., and West, R.R., 2000. A new Ichnospecies of Nereites from Carboniferous tidal-flat facies of eastern Kansas, USA: implications for the Nereites-Neonereites debate. Journal of Paleontology. 74(1), 149-157.

Martin, M.A., 1993. Trace fossil analysis and sequence stratigraphy of the Upper Jurassic Fulmar Formation, Western Central Graben, UKCS . Unpublished Ph.D. Thesis, Manchester University.

Martin, M.A., and Pollard, J.E., 1996. The role of trace fossil ichnofabric analysis in the development of depositional models for the Upper Jurassic Fulmar Formation of the Kittiwake Field Quadrant 21 UKCS, in: Hurst, A., et al. (Eds.). Geology of the Humber Group: Central Graben ad Moray Firth, UKCS. Geological Society Special Publication. 114. 163-183.

Martinsson, A., 1965. Aspects of a Middle Cambrian thanatotope on Öland. Geologiska Förening in Stockholm Förhandlingar. 87, 181-230.

Martinsson, A., 1970. Toponomy of trace fossils, in: Crimes, T.P. and Harper, J.C. (Eds.). Trace Fossils. Geological Journal Special Issues, 3, pp. 323-330.

Massalongo, A., 1855. Zoophycos, novum genus plantorum fossilium, Antonelli, Verona. pp. 52.

McCaffrey, W.D., Gupta, S., and Brunt, R., 2002. Repeated cycles of submarine channel incision, infill and transition to sheet sandstone development in the Alpine Foreland Basin, SE France. Sedimentology. 49(3), 623–635.

McCann, T., and Pickerill, R.K., 1988. Flysch trace fossils from the Cretaceous Kodiak Formation of Alaska. Journal of Paleontology. 62, 330-348.

McCoy, F., 1850. On some genera and species of Silurian Radiata in the collection of the University of Cambridge. Annual Magazine of Natural History, Series 2. 6, 270-290.

McIlroy, D., 2004. Some ichnological concepts, methodologies, applications and frontiers, in: The application of ichnology to palaeoenvironmental and stratigraphic analysis. Geological Society, London, Special Publications, 228. pp. 3-27.

Meigs, A.J., and Burbank, D.W., 1997. Growth of the South Pyrenean orogenic wedge. Tectonics. 16, 239–258.

Meneghini, G., 1850. *Paleodictyon,* in: Savi, P., and Meneghini, G., (Eds.). Osservazioni stratigrafiche e paleontologicke concernati la geologie della Toscana e dei paesi limitrofi (Appendix to R.R. Murchinson, Memoria sulla struttura geol. Dlle Alpi). Firenze. pp. 246.

Miller, S.A., and Dyer, C.B., 1878. Contribution to paleontology, no 1. Journal of Cincinnati Soc. Natural History 1, 24-39.

Miller, M.F., and Smail, S.E., 1997. A semiquantitative field method for evaluating bioturbation on bedding planes. Palaios. 12, 391-396.

Miller, W. III., 1991. Paleoecology of graphoglyptids. Ichnos. 1, 305-312.

Miller, W. III., 2001. *Thalassinoides-Phycodes* compound burrow systems in Paleocene deep-water limestones, Southern Alps of Italy. Palaeogeography, Palaeoclimatology, Palaeoecology. 170, 149-156.

Millington, J., and Clark, J.D., 1995. Submarine canyon and associated base-of-slope sheet system: the Eocene Charo-Arro system, south-central Pyrenees, Spain, in: Pickering, K.T., and Hiscott, R.N., Atlas of Deep Water Environments: Architectural style in turbidite systems. 150-156.

Millington, J., and Clark, J.D., 1996. The Charo/Arro canyon mouth sheet system, South-Central Pyrenees, Spain: a structurally influenced zone of sediment dispersal. Journal of Sedimentary Research. B65b, 443-454.

Müller, P.J., and Suess, E., 1979. Productivity, sedimentation rate, and sedimentary organic matter in the oceans – I. Organic carbon preservation. Deep-Sea Research. 26, 1347-1362.

Muñoz, J.A., Arbués, P., and Serra-Kiel, J., 1998. The Ainsa Basin and the Sobrarbe oblique thrust system: Sedimentological and tectonic processes controlling slope platform sequences deposited synchronously with a submarine emergent thrust system, in: Association of Sedimentologists, 15th International Sedimentological Congress field trip guidebook, Universite d'Alacant. Alacant. 213-223.

Murchison, R.I., 1839. The Silurian System. John Murray, London, pp. 768.

Mutti, E., 1977. Distinctive thin-bedded turbidite facies and related depositional environments in the Eocene Hecho Group South-central Pyrenees, Spain. Sedimentology. 24, 107-131.

Mutti, E., 1985. Turbidite systems and their relations to depositional sequences, in: Provenance of arenites. Zuffa, G.G., (Ed.). Dordrecht, Holland, NATO, Advanced Scientific Institute, D. Reidel. pp. 65-93.

Mutti, E., 1992. Turbidite Sandstones. Agip and Instituto di Geologia, University of Parma. Parma. pp. 275.

Mutti, E., and Ricci Lucci, F., 1972. Turbidites of the Northern Appenines: introduction to facies analysis. International Geology Review. 20, 125-166.

Mutti, E., and Ricci Lucci, F., 1975. Turbidite facies and facies associations, in: Examples of turbidite facies and associations from selected formations of the northern Apennines. IX Int. Congress of Sedimentology, Field TripA-11, 21-36.

Mutti, E., and Johns, D.R., 1978. The role of sedimentary by-passing in the genesis of fan-fringe and basin plain turbidites in the Hecho Group System, South-Central Pyrenees. Memorie della Società Geoligica Italiana 18. 15-22.

Mutti, E., and Normark, W.R., 1987. Comparing examples of modern and ancient turbidite systems: problems and concepts, in: Legget, J.K., and Zuffa, G.G., (Eds.). Marine Clastic Sedimentology: Concept and case studies. Graham and Trotman, London. pp. 1-38.

Mutti, E., Remacha, E., Sgavetti, M., Rosell, J., Valloni, R., and Zamorano, M., 1985. Stratigraphy and facies characteristics of the Eocene Hecho Group turbidite systems, south-central Pyrenees, in: Mila, M.D., and Rosell, J., (Eds.). International Association of Sedimentologists, 6th European Regional Meeting, Llerida, Excursion Guidebook. pp. 521-576.

Mutti, E., Seguret, M., and Sgavetti, M., 1988. Sedimentation and deformation in the Tertiary sequences of the Southern Pyrenees. Special Publication of the American Association of Petroleum Geology, Mediterranean Basin Conference. Institute of Geology, University of Parma. Field trip 7. pp. 153.

Mutti, E., Tinterri, R., Benevelii, G., di Biase, D., and Cavanna, G., 2003. Deltaic, mixed and turbidite sedimentation of ancient foreland basins. Marine and Petroleum Geology. 20, 733-755.

Nicholson, H.A., 1873. Contributions to the study of the errant annelids of the older Palaeozoic rock. Proceedings of the Royal Society of London. 21, 288-290.

Olempska, E., 1973. The genus *Discocyclina* foraminiferida from the Eocene of the Tatra Mts, Poland. Acta Palaeontologica Polonica. 18, 71-89.

Oms, O., Turrel, D.S., and Remacha, E., 2003. Magnetic stratigraphy from deep clastic turbidites: An example from the Eocene Hecho Group (Southern Pyrenees): Studia Geophysica et Geodaetica. 47, 275–288.

Orr, P.J., 1995. A deep-marine ichnofaunal assemblage from Llandovery strata of the Welsh Basin, west Wales, UK. Geological Magazine. 132, 267-285.

Orr, P.J., 2001. Colonization of the deep-marine environment during the early Phanerozoic: the ichnofaunal record. Geology Journal. 36, 265-278.

Orr, P.J., Benton, M.J., and Trewin, N.H., 1996. Deep marine trace fossil assemblages from the Lower Carboniferous of Menorca, Balearic Islands, western Mediterranean. Geological Journal. 31, 235-258.

Orr, P.J., Benton, M.J., and Briggs, D.E.G., 2003. Post-Cambrian closure of the deep-water slope-basin taphonomic window. Geology. 31, 769-772.

Otto, von, E., 1854. Additamente zur Flora des Quadergebirges, in: Sachsen. G. M (Ed.). Leipzig, Part 2, pp. 53.

Paillard D., Labeyrie, L., and Yiou, P., 1996. Macintosh Program Performs Time-Series Analysis: Eos, Transactions, American Geophysical Union. 77, 379.

Pälike, H., Shackleton, N.J., and Röhl, U. 2001. Astronomical forcing in late Eocene marine sediments. Earth and Planetary Science Letters. 193, 589-602.

Payros, A., Pujalte, V., and Orue-Etxebarria, X., 1999. The South Pyrenean Eocene carbonate megabreccias revisited: new interpretation based on evidence from the Pamplona Basin. Sedimentary Geology. 125, 165-194.

Pekar, S.F., Hucks, A., Fuller, M., and Li, S., 2005. Glacioeustatic changes in the early and middle Eocene 51–42 Ma: Shallow-water stratigraphy from ODP Leg 189 Site

1171 South Tasman Rise and deep-sea $\delta^{18}O$ records. Geological Society of America Bulletin, 117, 1081–1093.

Pemberton, S.G., and Frey, R.W., 1982. Trace fossil nomenclature and the *Planolites-Palaeophycus* dilemma. Journal of Paleontology. 56, 843-881.

Pemberton, S.G., Frey, R.W., and Bromley, R.G., 1988. The ichnotaconomy of *Conostichus* and other plug-shaped ichnofossils. Canadian Journal of Earth Sciences. 25, 866-892.

Pemberton, S.G., MacEachern, J.A., and Frey, R.W., 1992. Trace fossil facies models: environmental and allostratigraphic significance, in: Walker, R.G., and James, N.P., (Eds.). Facies models – response to sea level change. Geological Association of Canada, Ottowa. pp. 47-72.

Pemberton, S.G. Zhou, Z. and MacEachern, J. 2001. Modern ecological interpretation of opportunistic r-selected trace fossils and equilibrium K-selected trace fossils. Acta Palaeontologica Sinica. 40, 134-142.

Peruzzi, D.G., 1880. Osservazioni sui generi *Paleodictyon* e *Paleomeandron* dei trreni cretacei ed eocenici dell' Appennino sett. E centrale. Atti della Società Toscana di Scienze Naturali Residente in Pisa. 5, 3-8.

Pervesler, P., and Uchman, A., 2004. Ichnofossils from the type area of the Grund Formation Miocene, Lower Badenian in Northern Lower Austria Molasse Basin. Geologica Carpathica. 55, 103-110.

Pfeiffer, H., 1968. Die Spurenfossilien des Kulms (Dinants) und Devons der Frankenwalder Querzone (Thuringen). Jahrbuch der Geologie. 2, 651-717.

Pianka, E. R., 1970. On r- and K-selection. American Naturalist. 104, 592–597.

Pickerill, R.K., 1982. Glockerichnus, a new name for the trace fossil ichnogenus Glockeria Książkiewicz, 1968. Journal of Paleontology. 56(3). 816.

Pickerill, R.K., Fillion, D., Harland, T.L., 1984. Middle Ordovician trace fossils in carbonates of the Trenton Group between Montreal and Quebec City, St. Lawrence Lowland, Eastern Canada. Journal of Paleontology. 58(2), 416-439.

Pickering, K.T., and Hiscott, R.N., 1985. Contained (reflected) turbidity currents from the Middle Ordovician Cloridorme Formation, Quebec, Canada: an alternative to the antidune hypothesis. Sedimentology. 32(3), 373–394.

Pickering, K.T., and Corregidor, J., 2000. 3D reservoir scale study of Eocene confined submarine fans, South Central Spanish Pyrenees, in: Weimer. P., Slatt. R.M., Coleman. J., Rosen, N.C., Nelson, H., Bouma, A.H., Styzen, M.J., and Lawrence. D.T., (Eds.).

Deep water reservoirs of the world: Gulf Coast Section. SEPM Foundation 20th Annual Bob F. Perkins Research Conference, pp. 776-781.

Pickering, K.T. and Fadell, M. 2004. Micropalaeontology of the Mid Eocene Ainsa I fan channel-levee-overbank complex, Ainsa system, South Central Pyrenees, Spain. Unpublished Report (BP and UCL).

Pickering, K.T. and Corregidor, J., 2005a. Mass-transport complexes (MTCs) and tectonic control on basin-floor submarine fans, Middle Eocene, South Central Spanish Pyrenees. Journal of Sedimentary Research. 75, 761-783.

Pickering, K.T., Corregidor, J., 2005b. Mass transport complexes and tectonic control on confined basin-floor submarine fans, Middle Eocene, Spanish Pyrenees, in: Hodgson, D. M. and Flint, S. S. (Eds.). Submarine slope systems: Processes and products. Geological Society of London Special Publication.

Pickering, K.T., Clark, J.D., Smith, R.D.A., Hiscott, R.N., Ricci Lucchi, F., and Kenyon, N.H., 1995. Architectural element analysis of turbidite systems, and selected topical problems for sand-prone deep-water systems, in: Pickering, K.T., Hiscott, R.N., Kenyon, N.H., Ricci Lucchi, F., and Smith, R.D.A., (Eds.). Atlas of deep water environments: architectural style in turbidite systems. Chapman and Hall. London. pp. 1-10.

Pickering, K.T., Stow, D., Watson, M., and Hiscott, R., 1986. Deep-Water facies, processes and models: A review and classification scheme for modern and ancient sediments. Earth-Science Reviews. 23, 75-174.

Pickering, K.T. Hiscott, R.N. and Hein, F.J., 1989. Deep marine environments. London. Harper-Collins (now Chapman and Hall). pp. 416

Piper, D.J.W., 1978. Turbidite muds and silts on deep sea fans and abyssal Plains, in: Stanley, D.J., and Kelling, G. (Eds.). Sedimentation in submarine canyons, fans and trenches. Stroudsburg, PA (Dowden, Hutchinson and Ross). pp. 163-175.

Quatrefages, De M.A., 1849. Note sur la *Scolicia prisca* A. de Q. annélide fossile de la Craie. Annales des Sciences Naturelles, 3 série, Zoologie. 12, 265-266.

Rajchel, J., and Uchman, A., 1998. Ichnological analysis of an Eocene mixed marly-siliciclastic flysch deposits in the Nienadowa Marl Member, Skole Unit, Polish Flysch Carpathians. Annales Societatis Geologorum Poloniae. 68, 61-74.

Reading, H.G., and Richards, M., 1994. Turbidite systems in deep-water basin margins classified by grain size and feeder system. AAPG Bulletin. 78(5). 792-822.

Remacha, E., Oms, O., Gual, G., Bolaño, F., Climent, F., Fernandez, L.P., Crumeyrollle, P., Pettingill, H., Vicente, J.C., and Suarez, J., 2003. Sand-rich turbidite systems of the Hecho Group from slope to basin plain. Facies, stacking patterns, controlling factors and diagnostic features. Geological Field Trip 12. South-Central Pyrenees. AAPG International Conference and Exhibition, Barcelona, Spain, September 21-24. pp. 78.

Remacha, E., and Fernández, L.P., 2003. High resolution correlation patterns in the turbiditic systems of the Hecho Group South-Central Pyrenees, Spain. Marine Petroleum Geology. 20, 711-726.

Remacha, E., and Fernandez, L.P., 2005. The Ttransition between sheet-like lobe and basin-plain turbidites in the Hecho Basin (South-Central Pyrenees, Spain). Journal of Sedimentary Research. 75(5), 798-819.

Remacha, E., Oms, O., and Coello, J., 1995. The Rapitan turbidite channel and its related eastern levee-overbank deposits, Eocene Hecho group, south-central Pyrenees, Spain, in: Pickering, K.T., and Hiscott, R.N., Atlas of deep water environments: architectural style in turbidite systems. pp. 145-149.

Remacha, E., Fernández, L.P., Maestro, E., Oms, O., Estrada, R., and Teixell, A., 1998. The Upper Hecho Group turbidites and their vertical evolution to deltas Eocene, south-central Pyrenees, in: Association of Sedimentologists 15th International Sedimentological Congress field trip guidebook, University d'Alacant. Alacant. 1-25.

Remacha, E., Fernández, L.P., and Maestro, E., 2005. The transition between sheet-like lobe and basin-plain turbidites in the Hecho Basin South-Central Pyrenees, Spain. Journal of sedimentary research. 75, 795-819.

Richter, R., 1850. As der Thuringischen Grauwacke. Zeitschrift Deutsche Geologische Gesellschaft. 2, 198-206.

Richter, R., 1937. Marken und spuren aus allen Zeiten. I-11, Senckenbergiana. 19, 150-169.

Rieth, A., 1932. Neue Funde spongeliomorpher Fucoiden aus dem Jura Schwabens. Geologie Paläontologie Abhandlung. 19, 257-294.

Roniewicz, P., 1970. Borings and burrows in the Eocene littoral deposits of the Tatra Mountains, Poland, in: Crimes T.P., and Harper, J.C., (Eds.). Trace Fossils. 439-446. Liverpool.

Rutgers v. d. Loeff, M.M., 1990. Oxygen in pore waters of deep-sea sediments. Philosophical Transactions of the Royal Society, A. 331, 69-84.

Sacco, F., 1886. Impronte organiche dei terreni terziari del Piemonte. Atti Reale Accad. Sci. Torino. 21, 297-348.

Sacco, F., 1888. Note di Paleoicnologia Italiana. Atti Soc. Ital. Sci. Nat. 31, 151-192.

Salter, J.W., 1857. On annellide burrows and surface markings from the Cambrian rocks of the Longmynd. No. 2. Quarterly Journal of the Geological Society of London. 13, 199-206.

Saporta, G., 1887. Nouveaux documents relatifs aux organismes problematiques. Bulletin. Société Géologique de France, Serie 3. 15, 286-302.

Satur, N., Hurst, A., Cronin, B.T., Kelling, G., and Gürbüz, K., 2000. Sand body geometry in a sand-rich, deep-water clastic system, Miocene Cingöz Formation of southern Turkey. Marine and Petroleum Geology. 17, 239-252.

Savi, P., and Meneghini, G.G., 1850. Osservazioni stratigrafische e paleontologische concernati la geologia della Toscana e dei paesi limitrofi. Appendix in: Memoria sulla struttura geologica delle Alpi, degli Apennini e dei Carpazi. R.I. Murchison Stemparia granucale, Firenze.

Savrda, C.E., Bottjer, D.J., 1986. Trace-fossil model for reconstruction of paleo-oxygenation in bottom waters. Geology. 14, 3-6.

Savrda, C.E., and Bottjer, D.J., 1987. The exaerobic zone, a new oxygen-deficient marine biofacies. Nature. 327, 54-56.

Savrda, C.E., and Bottjer, D.J., 1989. Trace-fossil model for reconstructing oxygenation histories of ancient marine bottom waters: application to Upper Cretaceous Niobrara Formation, Colorado. Palaeogeography, Palaeoclimatology, Palaeoecology. 74, 49-74.

Savrda, C.E., and Bottjer, D.J., 1994. Ichnofossils and ichnofabrics in rhythmically bedded pelagic/hemi-pelagic carbonates: recognition and evaluation of benthic redox and scour cycles, in: Deboer, P., and Smith, D (Eds.). Orbital forcing and cyclic sequences. International Association of Sedimentologists, Special Publication. 19, pp. 195-210.

Schäfer, F.X., 1928. *Hormosiroidea florentina* n.g., n. sp., ein *Fuchs* aus der Kreide der Umbegung von Florenz. Paläontologishe Zeitscrift. 10, 212-215.

Schäfer, W., 1956. Wirkungen der Benthos-Organismen auf den jungen Schichtverband: Senckengergiana. Lethaea. 37, 183-263.

Schafhäutl, K.E. 1851. Geognostische Untersuchungen des südbayerischen Alpengebirges. Literarisch-artistische Anstalt, München, pp. 208.

Schlirf, M., 2000. Upper Jurassic trace fossils from the Boulonnais northern France . *Geol. Palaeontol.*, 34, 145-213.

Schlirf, M., Uchman, A., 2005. Revision of the Ichnogenus *Sabellarifix* Richter, 1921 and its relationship to Skolithos Haldeman, 1840 and Polykladichnus Fursich, 1981. Journal of Systematic Palaeontology. 32, 115-131.

Schlirf, M., Uchman, A. and Kummel, M., 2001. Upper Triassic Keuper non-marine trace fossils from the Hassberge area Franconia, south-east Germany. Palaontologische Zeitschrift. 75(1). 71-96.

Schluter, C., W. Von Der Marck, W., and Schluter, C., 1868. Neue fische und krebse aus der kreide von westphalens. Palaeontographica. 15, 269-305.

Schultz, M.R., Fildani, A., Cope, T.D., and Graham, S.A., 2005. Depositional and stratigraphic architecture of an outcropping ancient slope system: Tres Pasos Formation, Magallanes Basin, southern Chile, in: Hodgson, D.M., and Flint, S.S (Eds.). Submarine slope systems: processes and products. Geological Society of London, Special Publications. London. 244, 27-50.

Schuppers, J. D., 1995. Characterization of deep-marine clastic sediments from foreland basins-outcrop-derived concepts for exploration, production and reservoir modeling. Ph.D. thesis. Technische Universiteit Delft, Netherlands. pp. 272.

Seilacher, A., 1955. Spuren und fazies im unterkambrium, in: Schindewolf, O.H. and Seilacher, A. (Eds.). Beiträge zur Kenntnis des Kambrium in der Salt Range Pakistan. Akad. Wiss. Lit. Mainz. Abh. Math.-Naturwiss. K1. 10, 11-143.

Seilacher, A., 1962. Paleontological studies on turbidite sedimentation and erosion. Journal of Geology. 70, 227-234.

Seilacher, A. 1964a. Biogenic sedimentary structures, in: Imbrie, J., and Newell, N., (Eds.). Approaches to Paleoecology. Wiley, New York, pp. 296-316.

Seilacher, A., 1964b. Sedimentological classification and nomenclature of trace fossils. Sedimentology. 3, 253-256.

Seilacher, A., 1967. Bathymetry of trace fossils. Marine Geology. 5, 413-428.

Seilacher, A., 1974. Flysch trace fossils: Evolution of behavioural diversity in the deep-sea. Neues Jahrbuch für Geologie und Paläontologie. 233-245.

Seilacher, A., 1977. Pattern analysis of *Paleodictyon* and related trace fossils, in: Crimes, T.P., and Harper, J.C., (Eds.). Trace Fossils 2, Geology Journal Special Issue 9. pp. 289-334.

Seilacher, A., 1990. Aberration in bivalve evolution related to photo- and chemosymbiosis. Historical Biology 3. 289-311.

Seilacher, A. and Seilacher, E., 1994. Bivalvian Trace Fossils: A lesson from actuopaleontology. CFS. 169, 5-15.

Sexton, P.F., Wilson, P.A., Norris, R.D., 2006. Testing the Cenozoic multisite composite D18O and D13C curves: New monospecific Eocene records from a single locality, Demerara Rise Ocean Drilling Program Leg 207. Paleoceanography. 21, 2019-2036.

Simpson, S., 1957. On the trace fossil *Chondrites*. Quarterly Journal of the Geological Society of London. 112, 475-499.

Squinabol, S., 1890. Alghae und Pseudoalghae fossili ilatiane. Atti. Soc. Ling. Sci. Nat. Geogr. 1, 29-49 166-199.

Stanley, D.C.A., and Pickerill R.K., 1995. Arenitube, a new name for the trace fossil Ichnogenus Micatuba Chamberlain, 1971. Journal of Paleontology. 69, 612-614.

Sternberg, G.K., 1833. Versuch einer geognostisch, botanischen Darstellung der Flora der Vorvwelt. IV Heft. Brenck, C.E. Regensburg. pp. 48.

Stow, D. A. V., and Shanmugam, G., 1980. Sequence of structures in fine-grained turbidites: Comparison of recent deep-sea and ancient flysch sediments. Sedimentary Geology. 25, 23-42.

Stow, D.A.V., and Wetzel, A., 1990. 3. Hemiturbidite: a new type of deep-water sediment, in: Cochran, J.R., and Stow, D.A.V., (Eds.). Proceedings of the Ocean Drilling Program, Scientific Results, 116, 25-34.

Sutcliffe, C., and Pickering, K.T., In review. End-signature of deep-marine basin-fill, as a structurally confined low-gradient clastic slope: the Middle Eocene Guaso system, south-central Pyrenees.

Talling, P. J., Amy, L. A., Wynn, R. B., Peakall, J., and Robinson, M., 2004. Beds comprising debrite sandwiched within co-genetic turbidite: origin and widespread occurrence in distal depositional environments. Sedimentology. 51(1), 163–194.

Taylor, A.M., and Gawthorpe, R.L., 1993. Application of sequence stratigraphy and trace fossil analysis to reservoir description: examples from the Jurassic of the North Sea, in: Parker, J.R. (Ed.). Petroleum Geology of Northwest Europe: Proceedings of the 4th Conference. 317-335.

Taylor, A.M., and Goldring, R., 1993. Description and analysis of bioturbation and ichnofabric. Journal of the Geological Society, London. 150, 141-148.

Taylor, A.M., Goldring, R., and Gowland, S., 2003. Analysis and application of ichnofabrics. Earth-Science Reviews. 60, 227-25.

Tanaka, K., 1970. Sedimentation of the Cretaceous flysch sequence in the Ikushumbetsu area, Hokkaido, Japan. Geological Survey of Japan, Report. 236, 1-102.

Taylor, A.M., Goldring, R., and Gowland, S., 2003. Analysis and application of ichnofabrics. Earth-Science Reviews. 60, 227-259.

Tchoumatchenco, P., and Uchman, A., 1999. Lower and Middle Jurassic flysch trace fossils from the eastern Stara Planina Mountains, Bulgaria: A contribution to the evolution of Mesozoic ichnodiversity. Neues Jahrbuch für Geologie und Paläontologie. 213(2), 169-199.

Tchoumatchenco, P., and Uchman, A., 2001. The oldest deep-sea *Ophiomorpha* and *Scolicia* and associated trace fossils from the Upper Jurassic-Lower Cretaceous deep-water turbidite deposits of SW Bulgaria. Palaeogeography Palaeoclimatology and Palaeoecology. 169, 85-99.

Thayer, C.W., 1979. Biological bulldozers and the evolution of marine benthic communities. Nature. 203, 458-461.

Torell, O.M., 1870. Petrifacta Suecana Formationis Cambricae. *Lunds University.* 6(2). 1-14.

Toula, F., 1900. Lehrbuch der Geologie. Ein Leitfaden fur Studierende. Holder, A., Wien. pp. 410.

Tripati, A., Backman, J., Elderfield, H., and Ferretti, P., 2006. Eocene bipolar glaciation associated with global carbon cycle changes. Nature. 436, 341-346.

Tunis, G., and Uchman, A., 1992. Trace fossils in the "Flysch del Grivó" Lower Tertiary in the Julian Prealps, NE Italy: Preliminary observations. Gortania. 14, 71-104.

Tunis, G., and Uchman, A., 1996a. Trace fossils and changes in Cretaceous-Eocene flysch deposits of the Julian Prealps Italy and Slovenia: consequences of regional and world-wide changes. Ichnos. 4, 169-190.

Tunis, G., and Uchman, A., 1996b. Ichnology of Eocene flysch deposits of the Istria Peninsula, Croatia and Slovenia. Ichnos. 5, 1-22.

Uchman, A., 1995a. Taxonomy and palaeocology of flysch trace fossils: The Marnoso-arenacea Formation and associated facies, Miocene, Northern Apennines, Italy . Beringeria. 15, 3-115.

Uchman, A., 1995b. Tiering patterns of trace fossils in Paleogene flysch deposits of the Carpathians, Poland. Geobios, Memoir Special. 18, 389-394.

Uchman, A., 1998. Taxonomy and ethology of flysch trace fossils: revision of the Marian Książkiewicz collection and studies of complementary material. Annales Societatis Geologorum Poloniae. 68, 105-218.

Uchman, A., 1999. Ichnology of the Rhenodanubian Flysch Lower Cretaceous-Eocene in Austria and Germany. Beringeria. 25, 67-173.

Uchman, A., 2001. Eocene flysch trace fossils from the Hecho Group of the Pyrenees, northern Spain. Beringeria. 28, 3-41.

Uchman, A., 2003. Trends in diversity, frequency and complexity of graphoglyptid trace fossils: evolutionary and palaeoenvironmental aspects. Palaeogeography Palaeoclimatology and Palaeoecology. 192, 123-142.

Uchman, A., and Demircan, H., 1999. Trace fossils of Miocene deep-sea fan fringe deposits from the Cingöz Formation, southern Turkey. Annales Societatis Geologorum Poloniae. 69, 125-153.

Uchman, A., Bubniak, I. and Bubniak, A., 2000. Glossifungites ichnofacies in the area of its nomenclatural archetype, Lviv, Ukraine. Ichnos. 7(3), 183-193.

Uchman. A., Janbu, N.E., and Nemec, W., 2004. Trace Fossils in the Cretaceous-Eocene flysch of the Sinop-Boyabat Basin, Central Pontides, Turkey. Annales Societatis Geologorum Poloniae. 74, 197-235.

Verges, J., Marzo, M., Santaeularia, T., Serra-Kiel, J., Burbank, D.W., Munoz, J.A., Gimenez-Montsant, J., 1998. Quantified vertical motions and tectonic evolution of the SE Pyrenean foreland basin, in: Mascle, A., Puigdefabregas, C., Luterbacher, H.P., Fernandez, M., (Eds.). Cenozoic foreland basins of western europe, Geological Society of London, Special Publication. 134, pp. 107-134.

Vialov, O.S., 1971. The rare Mesozoic problematica from Pamir and Caucasus. Paleontologica Sbornik. 7, 85-93.

Vialov, O.S., and Golev, B.T., 1965. O drobnom podrazdieleni gruppy Paleodictyonidae. Byulletin Moskovskovo Obshczhestva Ispityvania Prirody, Odtiel Gieologii. 40, 93-114.

Walker, R.G., 1978. Deep-water sandstone facies and ancient submarine fans: models for exploration for stratigraphic traps. AAPG 62(6), 932-966.

Wetzel, A., 1983. Biogenic Sedimentary structures in a modern upwelling region: Northwest African continental margin, in: Thiede, J and Suess, E. (Eds.). Coastal upwelling and its sediment record, Part B, sedimentary records of ancient coastal upwelling, Plenum, New York. 123-144.

Weller, S., 1899. Kinderhook faunal studies. I. The fauna of the vermicular sabdstone at Northview, Webster Couty, Missouri. Transaction of the Academy of Sciences St Louis. 9, 9-51.

Wetzel, A., 1983. Biogenic structures in modern slope to deep-sea sediments in the Sulu Sea Basin Philippines. Palaeogeography, Palaeoclimatology, Palaeoecology. 42, 285-304.

Wetzel, A., 1991. Ecologic interpretation of deep-sea trace fossil communities. Palaeogeogaphy Palaeoclimatology Palaeoecology. 85, 47-69.

Wetzel, A., and Werner, F., 1980. Morphology and ecological significance of *Zoophycos* in deep-sea sediments off NW Africa. Palaeogeography, Palaeoclimatology, Palaeoecology. 32, 185-212.

Wetzel, A., and Aigner, T. 1986. Stratigraphic completeness: Tiered trace fossils provide a measuring stick. Geology. 14, 234-237.

Wetzel, A., and Bromley, R.G., 1994. *Phycosiphon incertum* revisited: *Anconichnus Horizontalis* is its junior subjective synonym. Journal of Paleontology. 68(6), 1396-1402.

Wetzel, A., and Bromley, R.G., 1996. Re-evaluation of ichnogenus *Helminthopsis* Heer 1877 – a new look at the type material. Palaeontology. 39, 1-19.

Wetzel, A., and Uchman, A., 1997. Ichnology of deep-sea fan overbank deposits of the Ganei Slates Eocene, Switzerland – a classical flysch trace fossil locality studied first by Oswald Heer. Ichnos. 5, 139-162.

Wetzel, A., and Uchman, A., 1998a. Deep-sea benthic food content recorded by ichnofabrics: A conceptual model based on observations from Paleogene Flysch, Carpathians, Poland. Palaios. 13, 533-546.

Wetzel, A., and Uchman, A., 1998b. Biogenic sedimentary structures in mudstones - an overview, in: Schieber, J., Zimmerle, W. and Sethi, P.S. (Eds.). Shales and Mudstones. I. basin studies, sedimentology, and paleontology. E. Schweitzerbart, Stuttgart, pp. 351-369. Stuttgart.

Wetzel, A., and Uchman, A., 2001. Sequential colonization of muddy turbidites: examples from Eocene Beloveža Formation, Carpathians, Poland. Palaeogeography, Palaeoclimatology, Palaeoecology. 168, 171-186.

Wignal, P.B., 1991. Dysaerobic Trace Fossils and Ichnofabrics in the Upper Jurassic Kimmeridge Clay of Southern England. Palaios. 6, 264-270.

Wilson, T.R.S., Thomson, J., Colley, S., Hydes, D.J., and Higgs, N.C., 1985. Early diagenesis: the significance of progressive subsurface oxidation fronts in pelagic sediments. Geochimica et Cosmoschimica Acta. 49, 811-822.

Ichnology and Sedimentology of deep-marine clastic systems, Middle Eocene,

Ainsa - Jaca basin, Spanish Pyrenees

Appendices

Thomas George Heard

2007

University College London,

University of London

Chapter 3

Trace Fossil Images at outcrop

Appendix 3.1

Appendix 3.1.A. *Lockeia siliquaria* JAMES 1879. Hypichnial full-relief. Lobe fringe, Cotefablo System, Cotefablo tunnel. Scale bar: 1 cm.

Appendix 3.1.B. Plug-shaped form A. Hypichnial semi-relief. Lobe fringe, Cotefablo System, Cotefablo tunnel. Scale bar: 2 cm.

Appendix 3.1.C. *Circulichnis* isp. Form B. Hypichnial semi-relief. Lobe fringe, Cotefablo System, Cotefablo tunnel. Scale bar: 2 cm.

Appendix 3.1.D. *Circulichnis* isp. Form A. Hypichnial semi-relief. Fan fringe, Banaston System, Hecho-Urdues. Scale bar: 2 cm.

Appendix 3.1.E. ?*Bergaueria prantli* KSIAZKIEWICZ 1977. Hypichnial semi-relief. Fan fringe, Cotefablo System, Jasa. Scale bar: 2 cm.

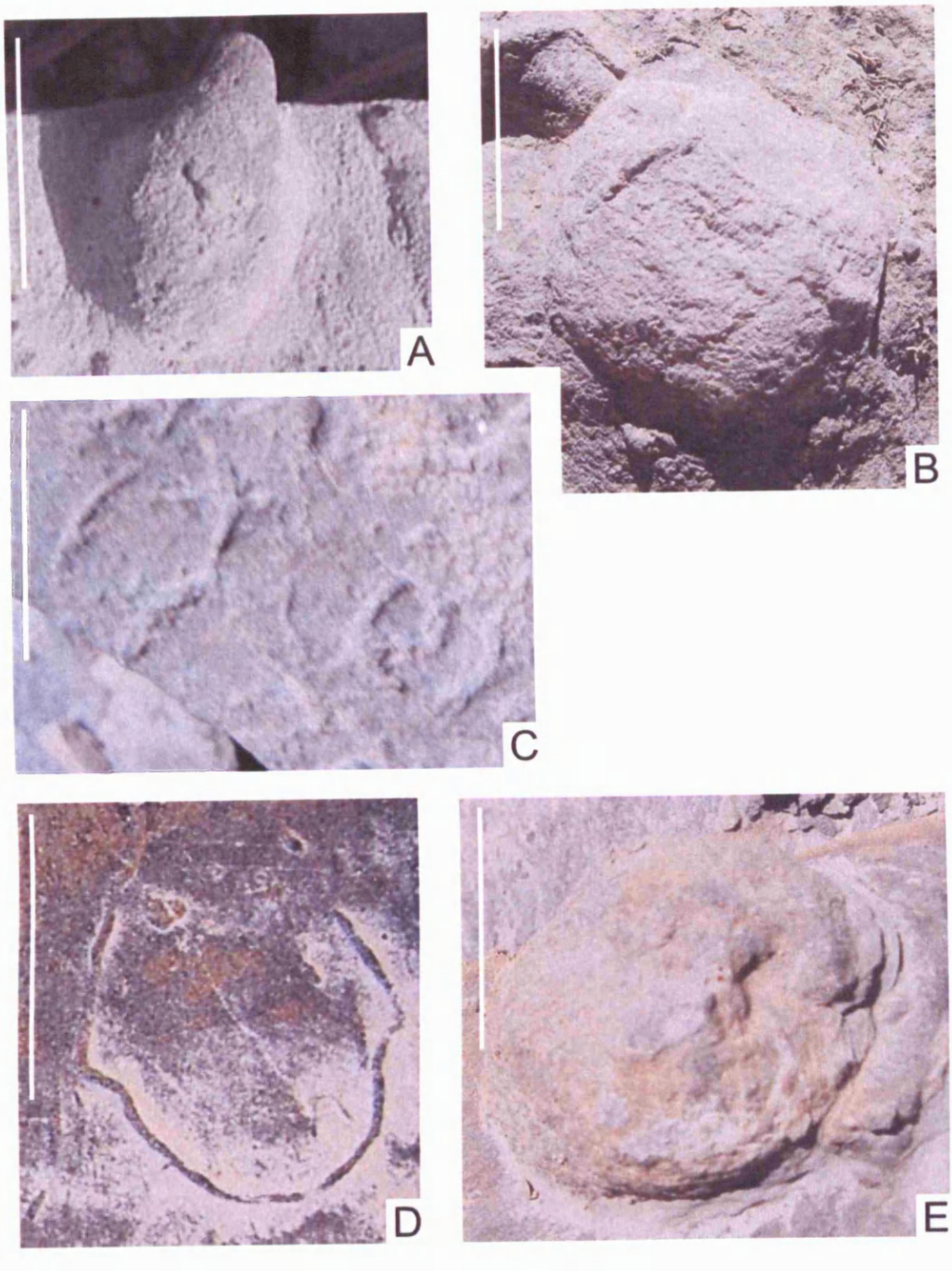
A
B
C
D
E

Appendix 3.2

Appendix 3.2.A. *Arenicolites* isp. Epichnial full-relief. Overbank, Banaston System, Labuerda. Scale bar: 2 cm.

Appendix 3.2.B. *Arenicolites* isp. Epichnial full-relief. Overbank, Banaston System, Labuerda. Scale bar: 2 m tape measure.

Appendix 3.2.C. *Arenicolites* isp. Endichnial full-relief. Overbank, Banaston System, Labuerda. Scale bar: 2 cm.

Appendix 3.2.D. Nummulite lined burrow. Epichnial full-relief. Upper slope gully, Formigales Scale bar: 2 cm.

Appendix 3.2.E. Nummulite lined burrow. Epichnial full-relief. Upper slope gully, Formigales Scale bar: 2 cm.

Appendix 3.2.F. *Skolithos* isp. Epichnial full-relief. Upper slope gully, Formigales Scale bar: 2 cm.

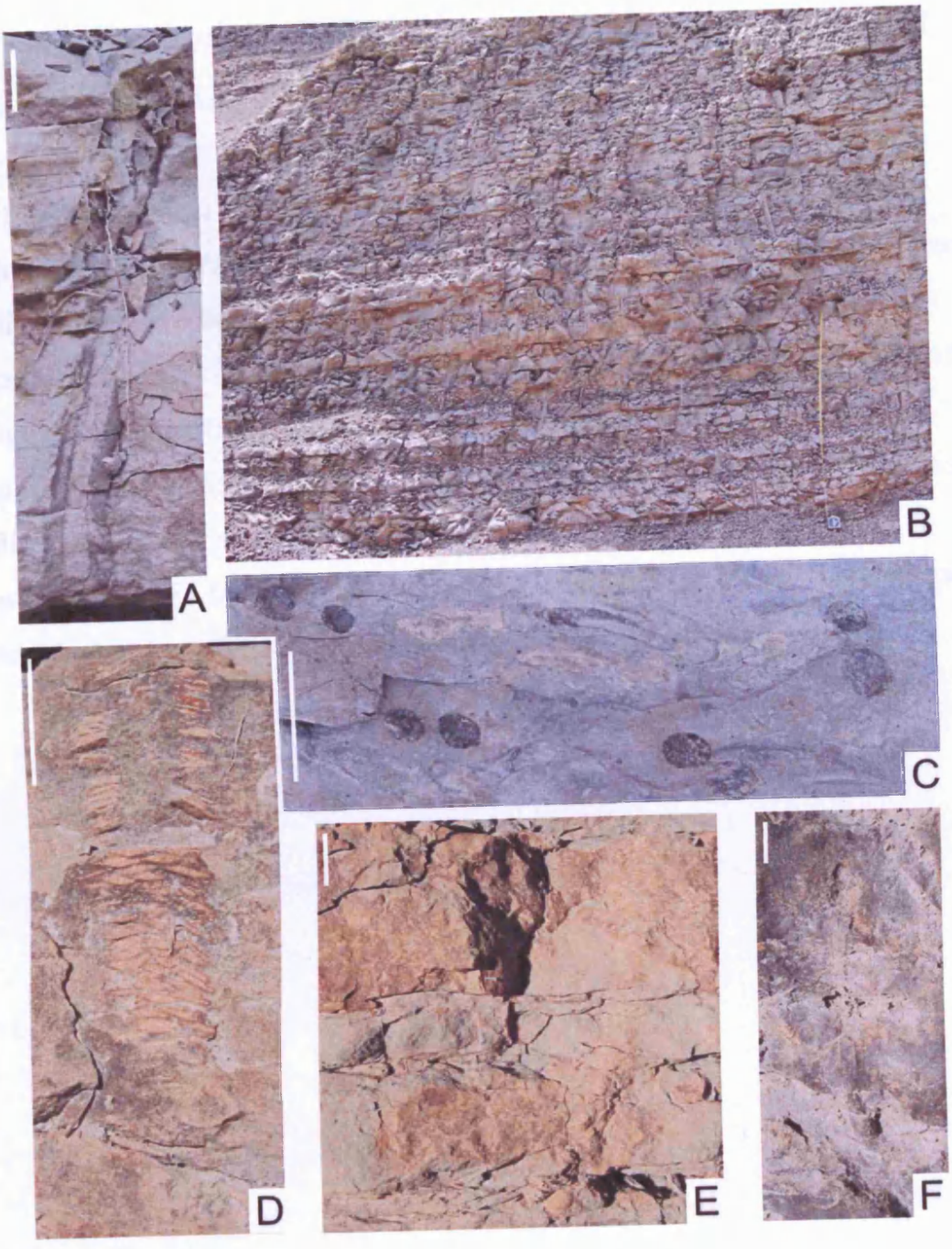
A
B
C
D
E
F

Appendix 3.3

Appendix 3.3.A. *Halopoa imbricata* TORELL 1870. Hypichnial full-relief. Channel margin, Arro System. Scale bar: 2 cm.

Appendix 3.3.B. *Halopoa storeana* isp. n. (UCHMAN, 2001). Hypichnial full-relief. Channel axis, Gerbe I sandbody, Rio Nata. Scale bar: 2 cm

Appendix 3.3.C. *Hormosiroidea annulata* (VIALOV 1971). Hypichnial semi-relief. Levee-overbank, Ainsa I sandbody. Scale bar: 2 cm.

Appendix 3.3.D. *Hormosiroidea annulata* (VIALOV 1971). Hypichnial semi-relief. Fan fringe, Banaston System, Hecho-Urdues. Scale bar: 2 cm.

Appendix 3.3.E. *Strobilorhaphe glandifer* KSIAZIEWICZ 1968. Hypichnial full-relief. Lobe, Broto System, Sarvise-Fanlo. Scale bar: 2 cm.

Appendix 3.3.F. *Arthrophycus* ?*strictus* KSIAZKIEWICZ 1977. Hypichnial trace. Lobe, Broto System, Sarvise-Fanlo. Scale bar: 2 cm.

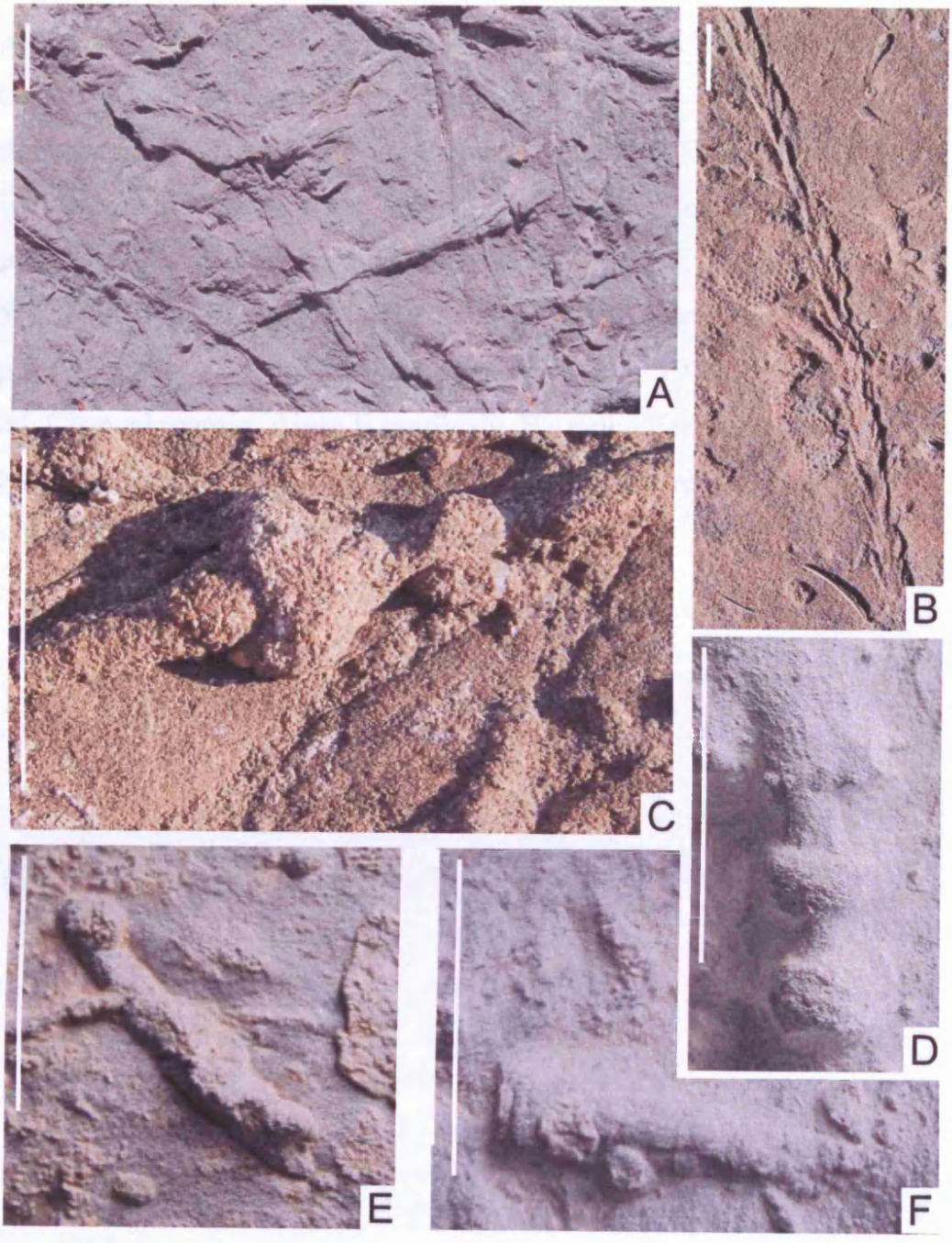
A
B
C
D
E
F

Appendix 3.4

Appendix 3.4.A. *Palaeophycus tabularis* HALL 1847. Epichnial full-relief. Channel axis, Gerbe I sandbody. Scale bar: 2 cm

Appendix 3.4.B. *Planolites beverleyensis* BILLINGS 1862. Epichnial full-relief. Proximal interfan, Ainsa System, Bco. Forcaz. Scale bar: 2 cm

Appendix 3.4.C. *Planolites montanus* RICHTER 1937. Hypichnial trace. Lobe, Broto System, Aragues del Puerto. Scale bar: 2 cm.

Appendix 3.4.D. *Imponoglyphus torquendus* Vialov 1971 Hypichnial full-reief. Channel margin, Ainsa II sandbody, Barranco Forcaz. Scale bar: 2 cm.

Appendix 3.4.E. ?*Palaeophycus* isp. Hypichnial full-reief. Lobe fringe. Cotefablo System, Cotefablo tunnel. Scale bar: 2 cm

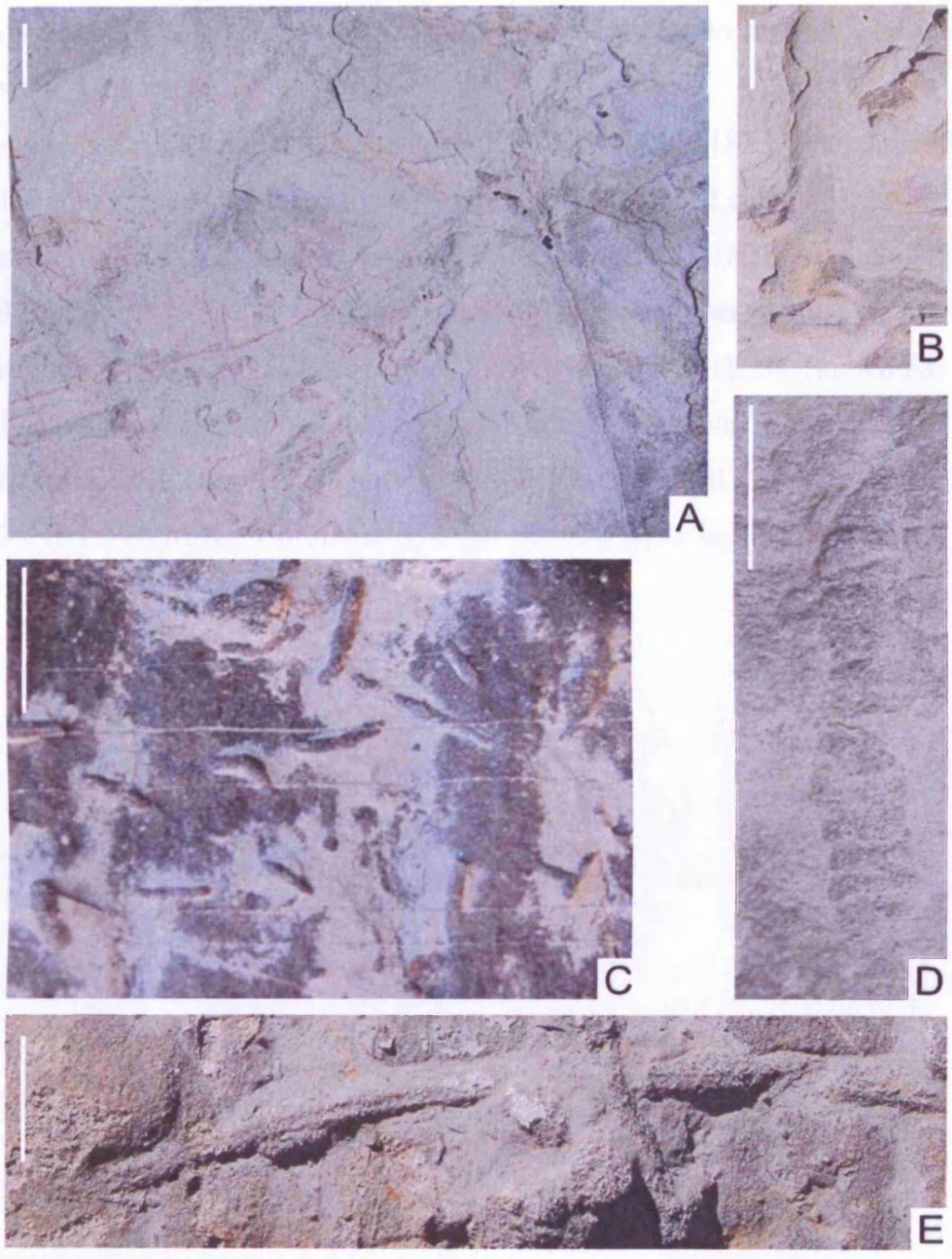
A
B
C
D
E

Appendix 3.5

Appendix 3.5.A. *Chondrites* isp. Epichnial full-relief. Fan fringe, Cotefablo System, Urdues. Scale bar: 2 cm.

Appendix 3.5.B. *Chondrites intricatus* BRONGNIART 1823. Endichnial full-relief. Fan fringe, Cotefablo System, Urdues. Scale bar: 2 cm.

Appendix 3.5.C. *Chondrites targionii* (BRONGNIART 1828). Endichnial full-relief. Fan fringe, Cotefablo System, Urdues. Scale bar: 2 cm.

Appendix 3.5.D. *Chondrites recurvus* (BRONGNIART 1823). Endichnial full-relief. Fan fringe, Cotefablo System, Urdues. Scale bar: 2 cm.

Appendix 3.5.E. *Chondrites patulus* FISCHER-OOSTER 1858. Endichnial full-relief. Fan fringe, Cotefablo System, Urdues. Scale bar: 2 cm.

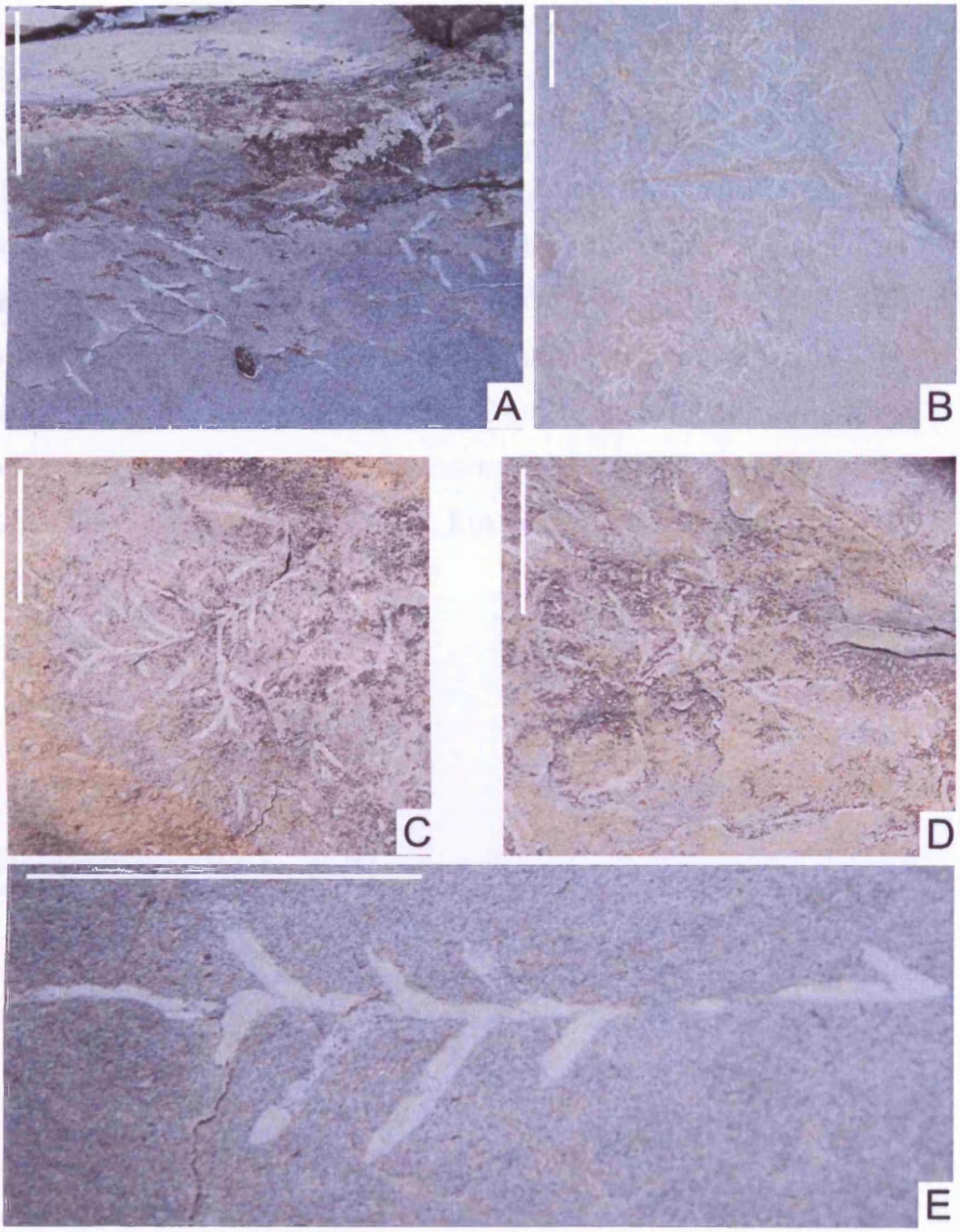
A
B
C
D
E

Appendix 3.6

Appendix 3.6.A. *Ophiomorpha rudis* (KSIAZIEWICZ 1977). Epichnial full-relief. Channel axis, Ainsa I sandbody, Ainsa. Scale bar: 2 cm.

Appendix 3.6.B. *Ophiomorpha annulata* KSIAZIEWICZ 1977. Hypichnial full-relief. Channel axis, Ainsa I sandbody, Ainsa. Scale bar: 2 cm.

Appendix 3.6.C. *Ophiomorpha* isp. Endichnial full-relief. Channel axis, Ainsa I sandbody, Labuerda. Scale bar: 10 cm.

Appendix 3.6.D. *Ophiomorpha* isp. Endichnial full-relief. Channel axis, Ainsa I sandbody, Labuerda. Scale bar: 2 cm.

Appendix 3.6.E. *Thalassinoides suevicus* (RIETH 1932). Hypichnial full-relief. Channel axis, Morillo system, Rio Sieste. Scale: Hand.

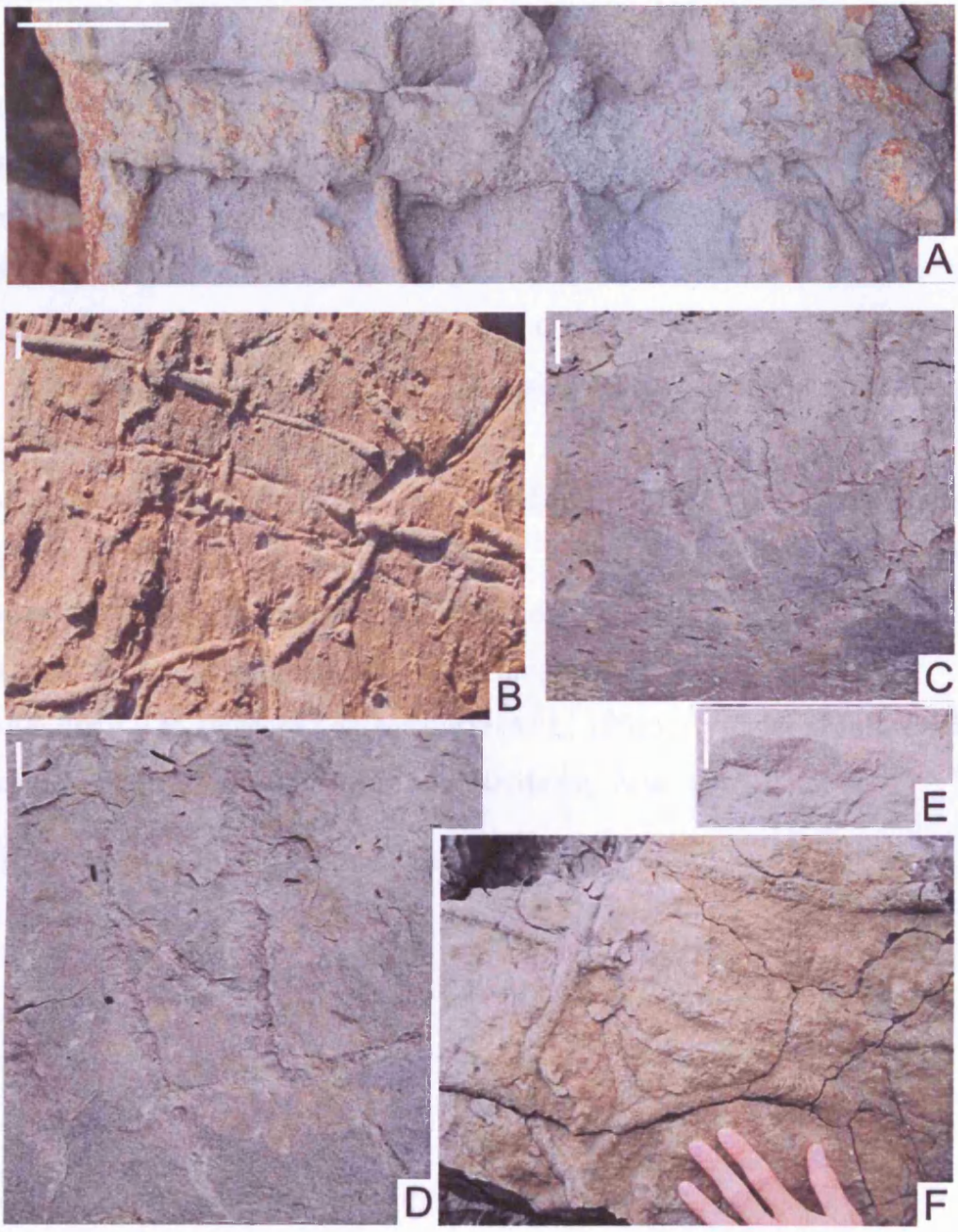
A
B
C
D
E
F

Appendix 3.7

Appendix 3.7.A. *Spongeliomorpha oraviense* KSIAZIEWICZ 1977. Hypichnial full-relief. Distal basin floor, Cotefablo system, Puerto d' Anso. Scale bar: 2 cm.

Appendix 3.7.B. ?*Agrichnium* isp. Epichnial full-relief. Prodeltaic clastic ramp thin-bedded sands at top of sandbody, Guaso system, Rio Ena. Scale bar: 2 cm.

Appendix 3.7.C. *Saerichnites canadiensis* CRIMES & ANDERSON 1985. Hypichnial semi-relief. Lobe fringe, Cotefablo system, Cotefablo tunnel. Scale bar: 2 cm.

Appendix 3.7.D. *Saerichnites abruptus* BILLINGS 1866. Hypichnial semi-relief. Distal basin floor, Cotefablo system, Puerto d' Anso. Scale bar: 2 cm.

Appendix 3.7.E. *Saerichnites* isp. Hypichnial semi-relief. Fan fringe, Banaston System, Hecho-Urdues. Scale bar: 2 cm.

Appendix 3.7.F. *Phycodes palmatum* (HALL, 1852). Hypichnial full-relief. Channel margin, Morillo system, Morillo de tou. Scale bar: 2 cm.

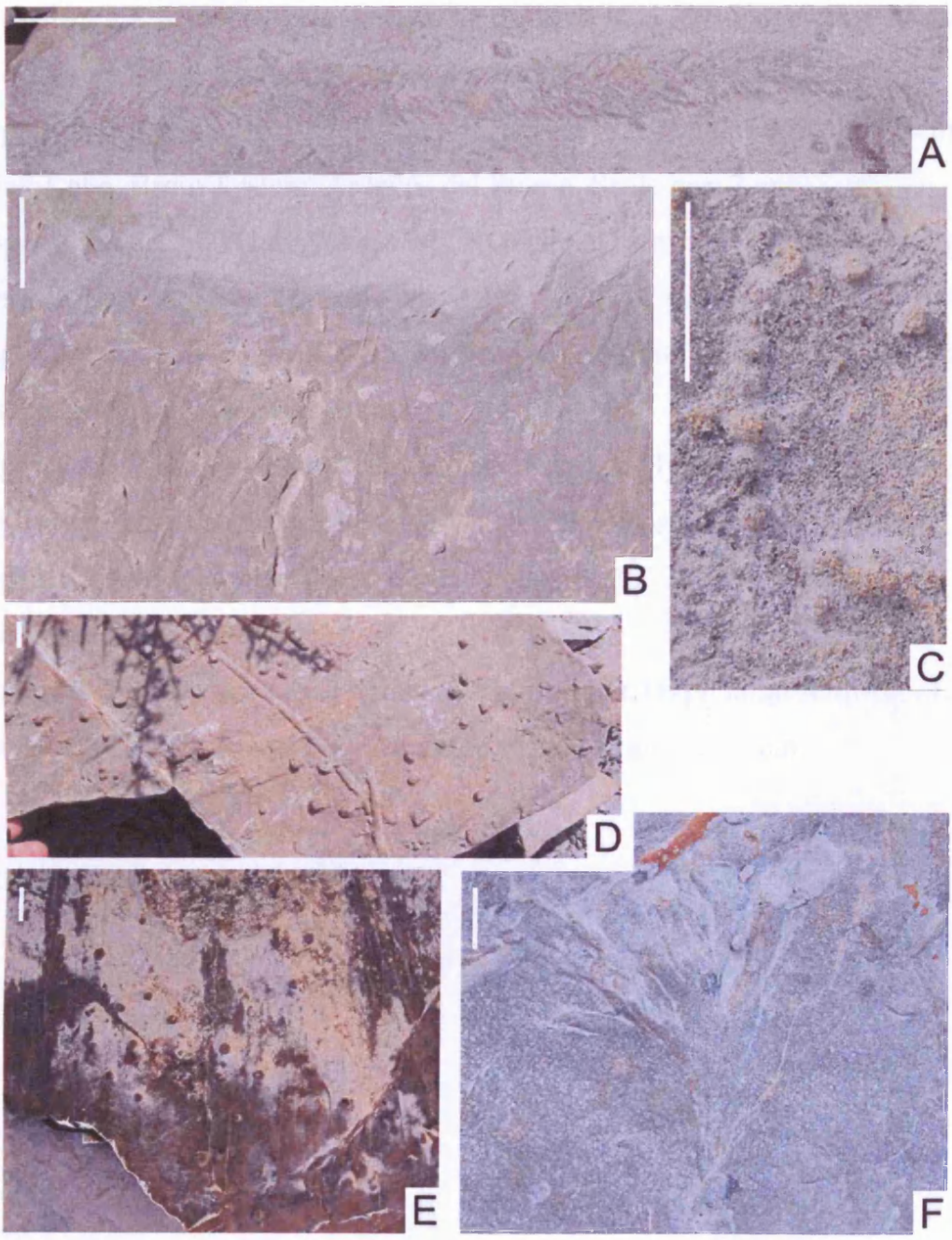
A
B
C
D
E
F

Appendix 3.8

Appendix 3.8.A. *Lorenzinia nowaki* KSIAZIEWICZ 1970. Hypichnial semi-relief. Lobe, Broto System, Aragűés del Puerto. Scale bar: 2 cm.

Appendix 3.8.B. *Lorenzinia plana* (KSIAZIEWICZ 1968). Hypichnial semi-relief. Lobe, Broto System, Aragűés del Puerto. Scale bar: 2 cm.

Appendix 3.8.C. ?*Glockerichnus* isp. Hypichnial semi-relief. Channel margin, Ainsa II, Barranco Forcaz. Scale bar: 2 cm.

Appendix 3.8.D. *Teichichnus* isp. Endichnial full-relief. Slope gully, Guaso System, Rio Ena. Scale bar: 2 cm.

Appendix 3.8.E. *Parahaentzschelinia* isp. Form A. Hypichnial semi-relief. Fan fringe, Banaston System, Hecho-Urdues. Scale bar: 2 cm.

Appendix 3.8.F. *Glockerichnus alata* (Seilacher, 1977). Hypichnial semi-relief. Scale bar: 2 cm.

Appendix 3.8.G. *Parahaentzschelinia* isp. Form B. Hypichnial semi-relief. Fan fringe, Cotefablo System, Cotefablo tunnel. Scale bar: 2 cm.

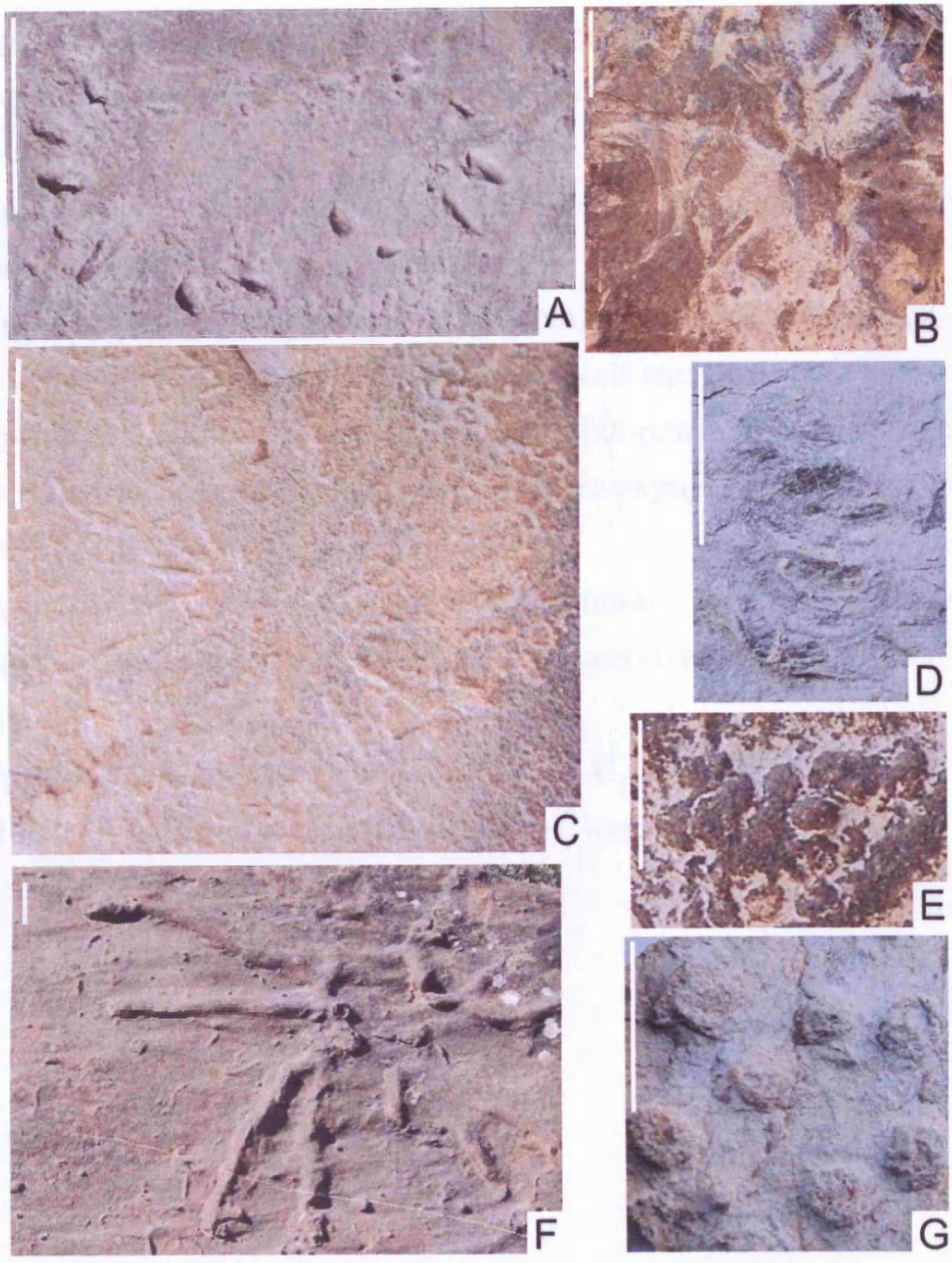
A
B
C
D
E
F
G

Appendix 3.9

Appendix 3.9.A. ?*Arenituba* isp. Hypichnial semi-relief. Prodeltaic clastic ramp thin-bedded sands at top of sandbody, Guaso system, Rio Ena. Scale bar: 2 cm.

Appendix 3.9.B. *Zoophycos* isp. Form B. Endichnial full-relief. Channel axis, Morillo system, Rio Sieste. Scale bar: 2 cm.

Appendix 3.9.C. *Zoophycos insignis* SQUINABOL 1890. Endichnial full-relief. Fan fringe, Cotefablo System. Urdues. Scale bar: 2 cm.

Appendix 3.9.D. *Asterosoma* ispp. Endichnial full-relief. Prodeltaic clastic ramp thin-bedded sands at top of sandbody, Guaso system, Rio Ena. Scale: feet.

Appendix 3.9.E. *Asterosoma* ispp. Endichnial full-relief. Prodeltaic clastic ramp thin-bedded sands at top of sandbody, Guaso system, Rio Ena. Scale bar: 2 cm.

Appendix 3.9.F. *Zoophycos ?brianteus* MASSALONGO 1855. Endichnial full-relief. Fan fringe, Cotefablo system, Jasa. Scale bar: 2 cm.

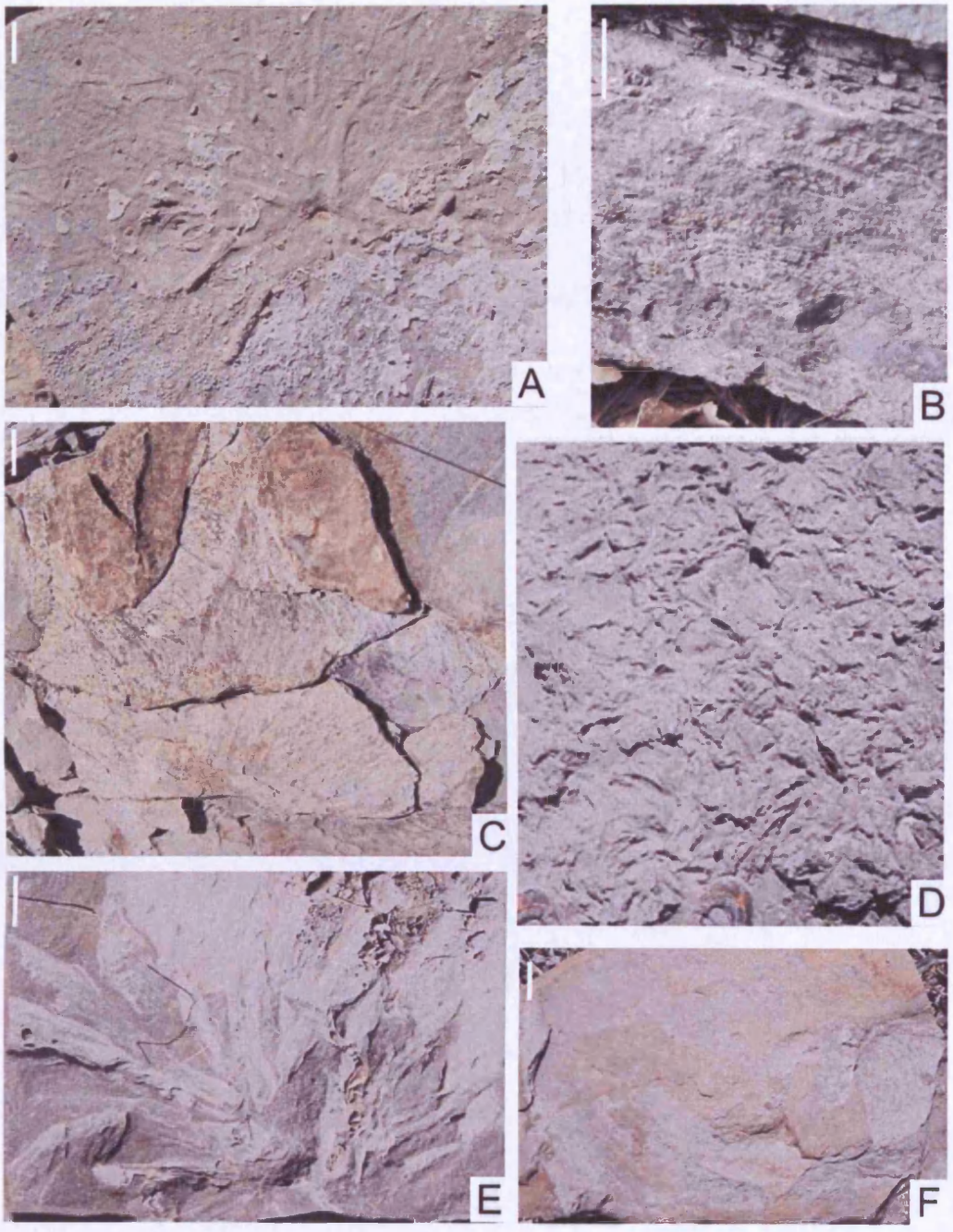
A
B
C
D
E
F

Appendix 3.10

Appendix 3.10.A. *Nereites irregularis* SCHAFHÄUTL 1851. Endichnial full-relief. Proximal interfan, Ainsa system, Bco Forcaz. Scale bar: 2 cm.

Appendix 3.10.B. *Phycosiphon incertum* FISCHER-OOSTER 1858. Endichnial full-relief. Lobe fringe, Cotefablo System, Cotefablo tunnel. Scale bar: 2 cm.

Appendix 3.10.C. *Nereites missouriensis* (WELLER 1899). Endichnial full-relief. Channel margin, Arro System, Bco. Sierra. Scale bar: 2 cm.

Appendix 3.10.D. *Nereites circinalis* (HEER 1877). Endichnial full-relief. Proximal interfan, Ainsa system, Bco Forcaz. Scale bar: 2 cm.

Appendix 3.10.E. *Lophoctenium ramosum* (TOULA, 1900). Endichnial full-relief. Channel margin, Ainsa II sandbody, Bco. Forcaz. Scale bar: 2 cm.

Appendix 3.10.F. *Zoophycos* isp. Form A. Endichnial full-relief. Fan fringe, Cotefablo System. Urdues. Scale bar: 2 cm.

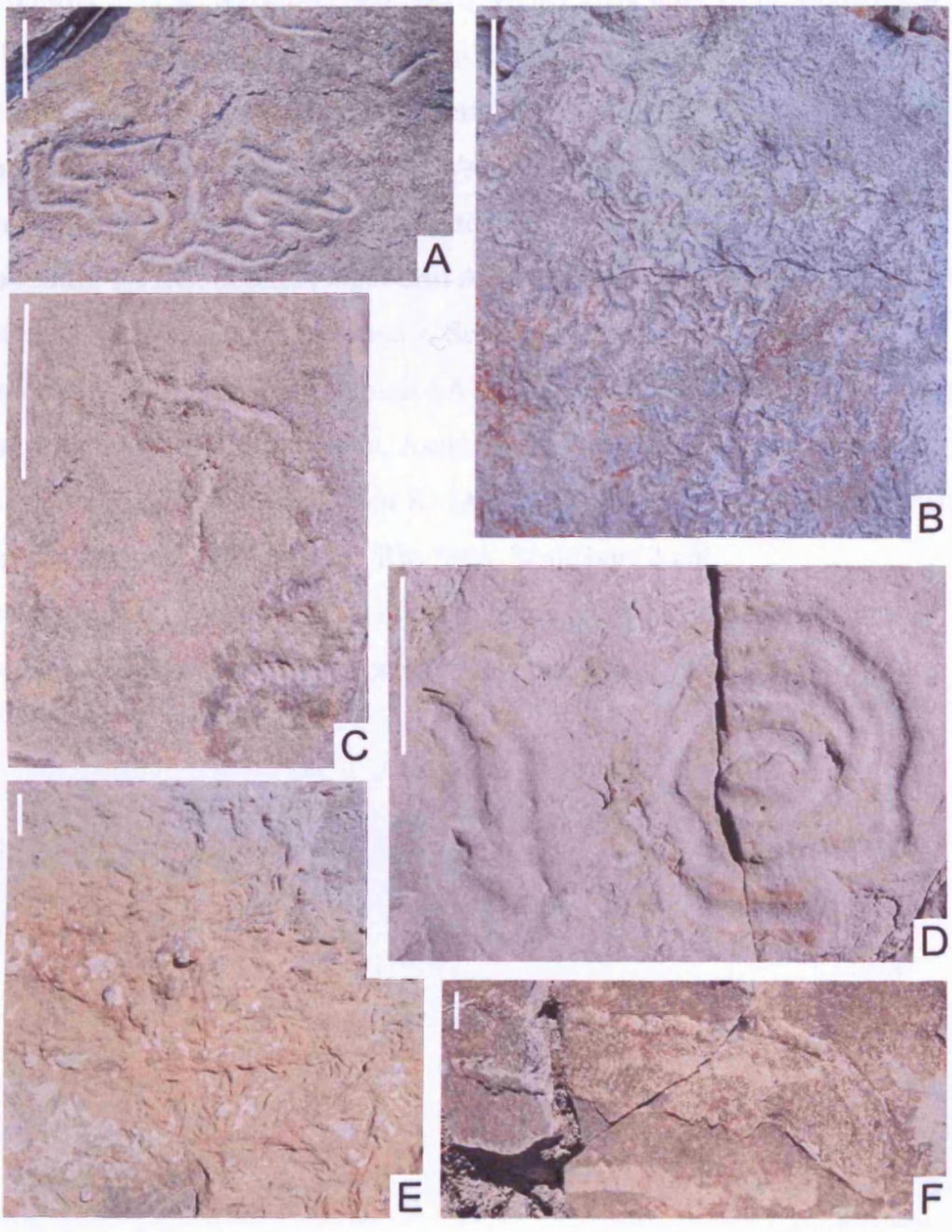
A
B
C
D
E
F

Appendix 3.11

Appendix 3.11.A. *Nereites cambrensis* MURCHINSON 1839. Endichnial full-relief. Prodeltaic clastic ramp thin-bedded sands at top of sandbody, Guaso system, Rio Ena. Scale bar: 2 cm.

Appendix 3.11.B. *Nereites* isp. var. *Neonereites multiserialis.* Hypichnial semi-relief. Fan fringe, Cotefablo System. Urdues. Scale bar: 2 cm.

Appendix 3.11.C. *Scolicia* isp. Form A. Endichnial full-relief. Proximal interfan, Ainsa system, Bco. Forcaz. Scale bar: 2 cm.

Appendix 3.11.D. *Scolicia strozzii* SAVI & MENEGHINI 1850. Hypichnial semi-relief. Lobe, Broto System, Aragues del Puerto. Scale bar: 2 cm.

Appendix 3.11.E. *Scolicia plana* KSIĄŻIEWICZ 1970. Endichnial full-relief. Channel off axis, Arro System, Rio Nata. Scale bar: 2 cm.

Appendix 3.11.F. *Scolicia* isp. Form B. Endichnial full-relief. Proximal interfan, Ainsa System, Bco. Forcaz. Scale bar: 2 cm.

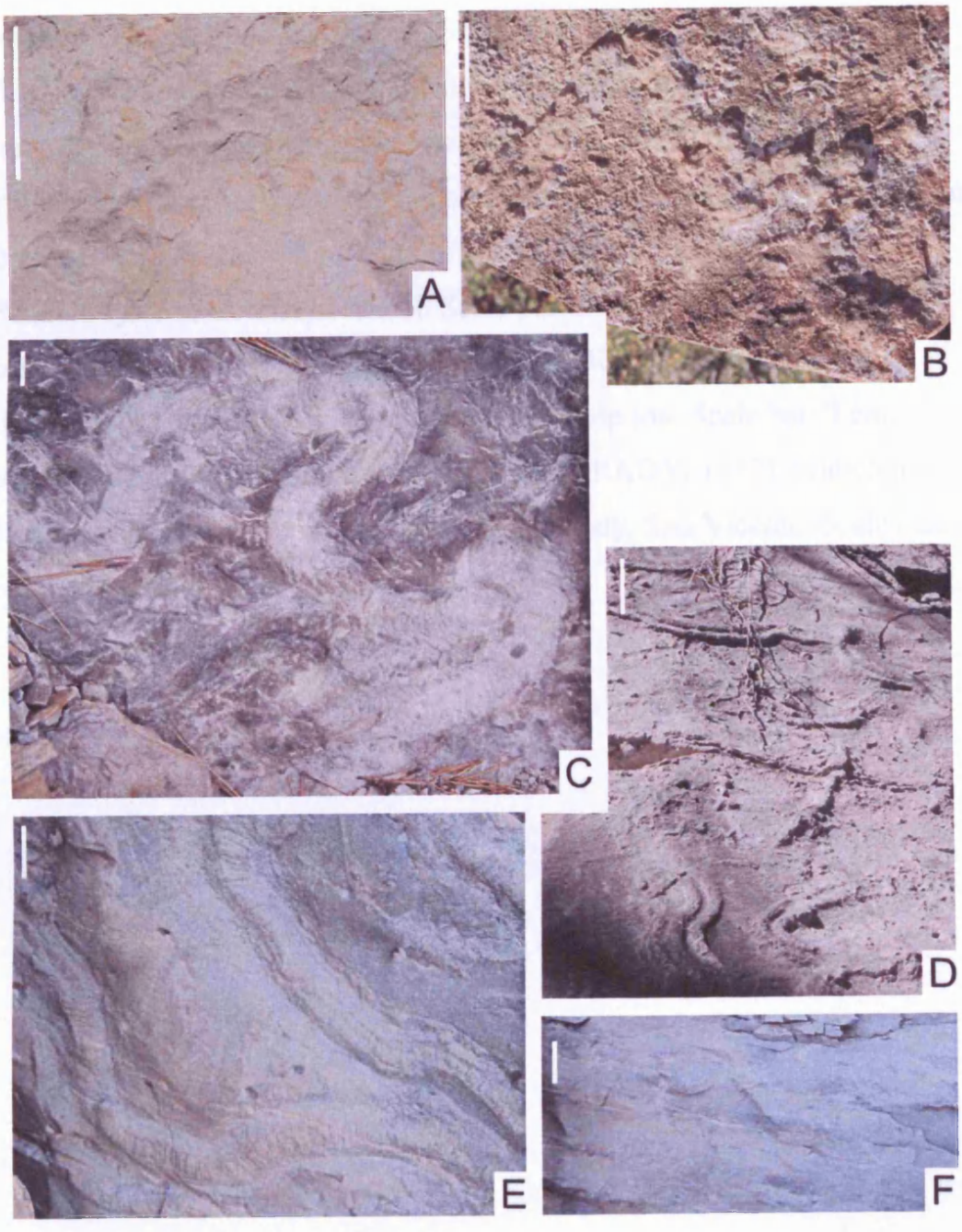
A
B
C
D
E
F

Appendix 3.12

Appendix 3.12.A. *Scolicia prisca* DE QUATREFAGES 1849. Endichnial full-relief. Channel off axis, Arro System, Rio Nata. Scale bar: 2 cm.

Appendix 3.12.B. *Protovirgularia ?rugosa* (MILLER & DYER 1878). Hypichnial semi-relief. Fan fringe, Cotefablo system, Urdues. Scale bar: 2 cm.

Appendix 3.12.C. *Taenidium* ispp. Endichnial full-relief. Fan fringe, Cotefablo system, Cotefablo tunnel. Scale bar: 2 cm.

Appendix 3.12.D. *Taenidium serpentinum* HEER, 1877. Endichnial full-relief. Channel margin, Morillo system, Morillo de tou. Scale bar: 2 cm.

Appendix 3.12.E. *Taeniudium cameronensis* (BRADY, 1947). Endichnial full-relief. Channel off axis, Banaston III sandbody, San Vicente. Scale bar: 2 cm.

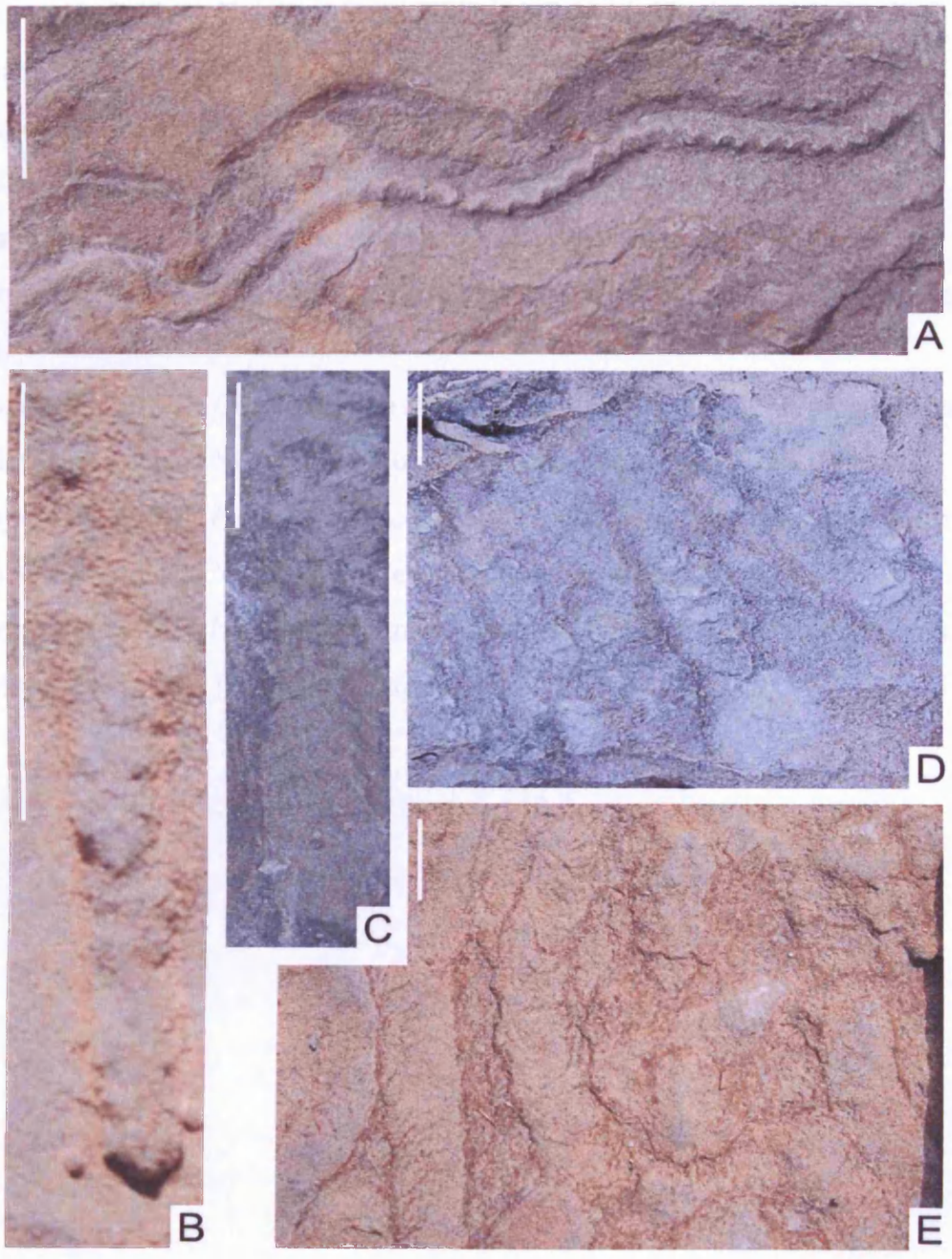
A
B
C
D
E

Appendix 3.13

Appendix 3.13.A. *Gordia marina* EMMONS 1844. Hypichnial full-relief. Channel margin, Morillo System, Morillo de tou. Scale bar: 2 cm.

Appendix 3.13.B. *Gordia arcuata* KSIĄŻIEWICZ 1977, Hypichnial full-relief. Channel margin, Morillo System, Morillo de tou. Scale bar: 2 cm.

Appendix 3.13.C. *Cosmorhaphe sinuosa* (AZPEITIA MOROS 1933). Hypichnial semi-relief. Lobe, Broto System, Aragues del Puerto. Scale bar: 2 cm.

Appendix 3.13.D. *Cosmorhaphe lobata* SEILACHER 1977. Hypichnial semi-relief. Lobe, Broto System, Aragues del Puerto. Scale bar: 2 cm.

Appendix 3.13.E. *Helicolithus ramosus* (VIALOV 1971). Hypichnial semi-relief. Fan fringe, Cotefablo System, Urdues. Scale bar: 2 cm.

Appendix 3.13.F. *Helminthorhaphe japonica* (TANAKA 1970). Fan fringe, Cotefablo System, Jasa. Scale bar: 2 cm.

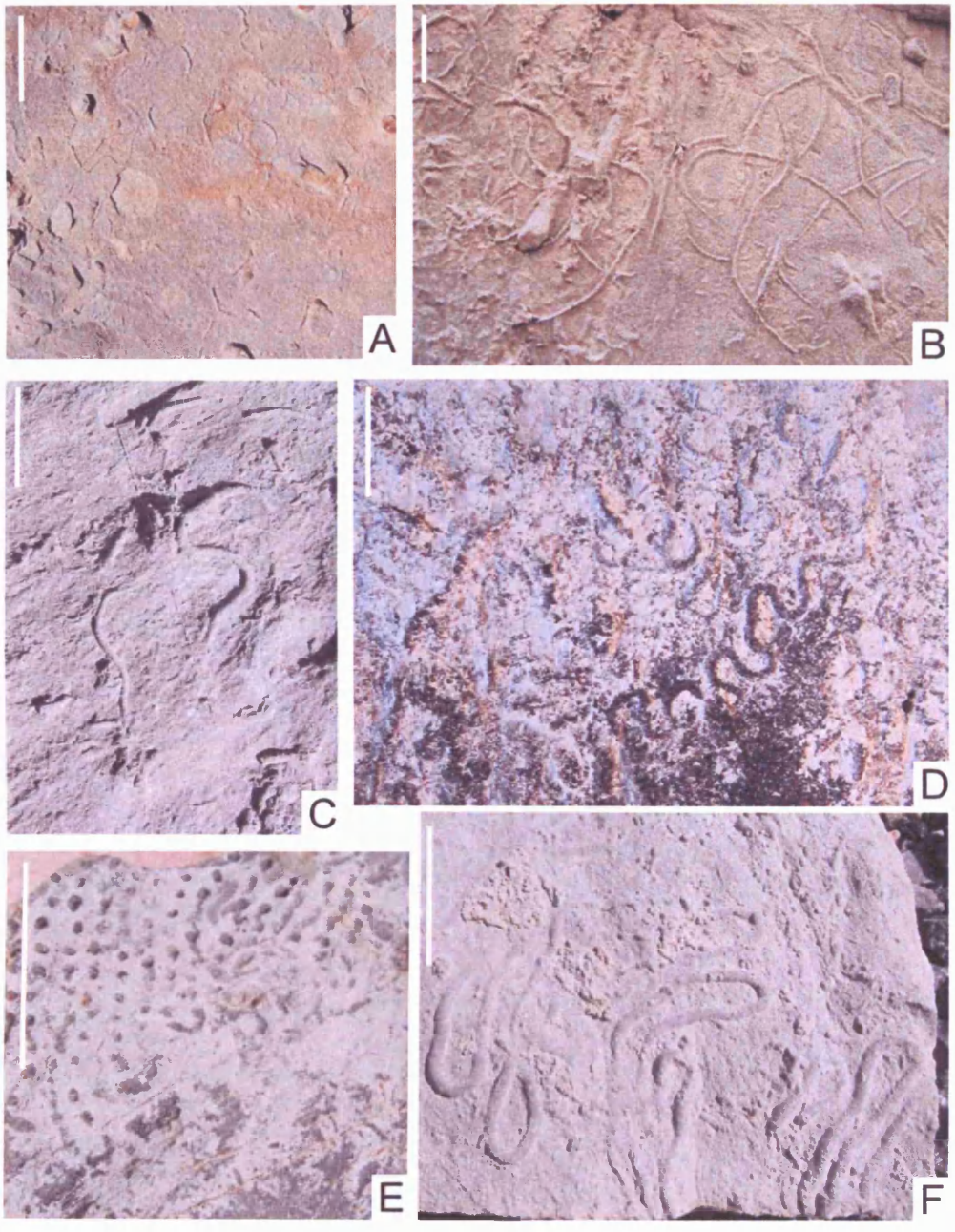
A
B
C
D
E
F

Appendix 3.14

Appendix 3.14.A. *Helminthorhaphe flexuosa* UCHMAN 1995. Hypichnial semi-relief. Channel margin, Morillo System, Morillo de tou. Scale bar: 2 cm.

Appendix 3.14.B. *Helminthopsis abeli* KSIĄŻIEWICZ 1977. Hypichnial full-relief. Fan fringe, Cotefablo System, Jasa. Scale bar: 2 cm.

Appendix 3.14.C. *Spirohaphe involuta* (DE STEFANI 1895). Hypichnial full-relief. Lobe, Broto System, Sarvise-Fanlo. Scale bar: 2 cm.

Appendix 3.14.D. *Helminthopsis tenuis* KSIĄŻIEWICZ 1978. Hypichnial full-relief. Lobe, Broto System, Aragues del Puerto. Scale bar: 2 cm.

Appendix 3.14.E. *Spirohaphe* isp. Hypichnial semi-relief. Channel off axis, Ainsa I sandbody, Ainsa. Scale bar: 2 cm.

Appendix 3.14.F. *Helminthopsis* ispp. Hypichnial full-relief. Lobe, Broto System, Aragues del Puerto. Scale bar: 2 cm.

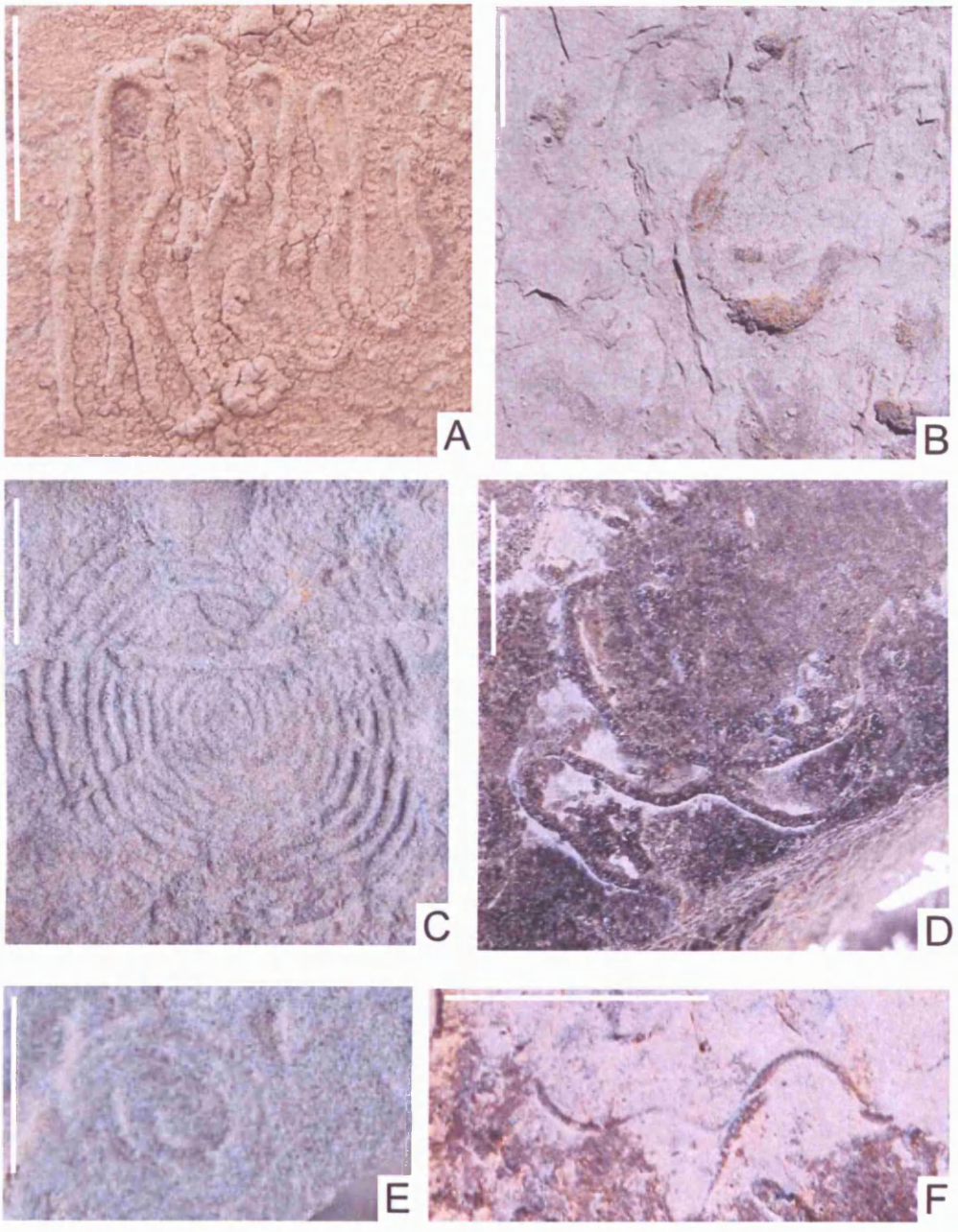
A
B
C
D
E
F

Appendix 3.15

Appendix 3.15.A. *Belorhaphe zickzack* HEER 1877. Hypichnial semi-relief. Lobe, Broto System, Sarvise-Fanlo. Scale bar: 2 cm.

Appendix 3.15.B. *Paleomeandron robustum* KSIĄŻIEWICZ 1968. Hypichnial semi-relief. Fan fringe, Cotefablo System, Jasa. Scale bar: 2 cm.

Appendix 3.15.C. *Desmograpton ichthyforme* (MACSOTAY 1967). Hypichnial semi-relief. Fan fringe, Banaston System, Hecho-Urdues Scale bar: 2 cm.

Appendix 3.15.D. *Desmograpton dertonensis* SACCO 1888. Hypichnial semi-relief. Fan fringe, Cotefablo System, Jasa. Scale bar: 2 cm.

Appendix 3.15.E. *Desmograpton alternum* (KSIĄŻIEWICZ 1977). Hypichnial semi-relief. Fan fringe, Banaston System, Hecho-Urdues Scale bar: 2 cm.

Appendix 3.15.F. *Urohelminthoida dertonensis* SACCO 1888. Hypichnial semi-relief. Fan fringe, Banaston System, Hecho-Urdues Scale bar: 2 cm.

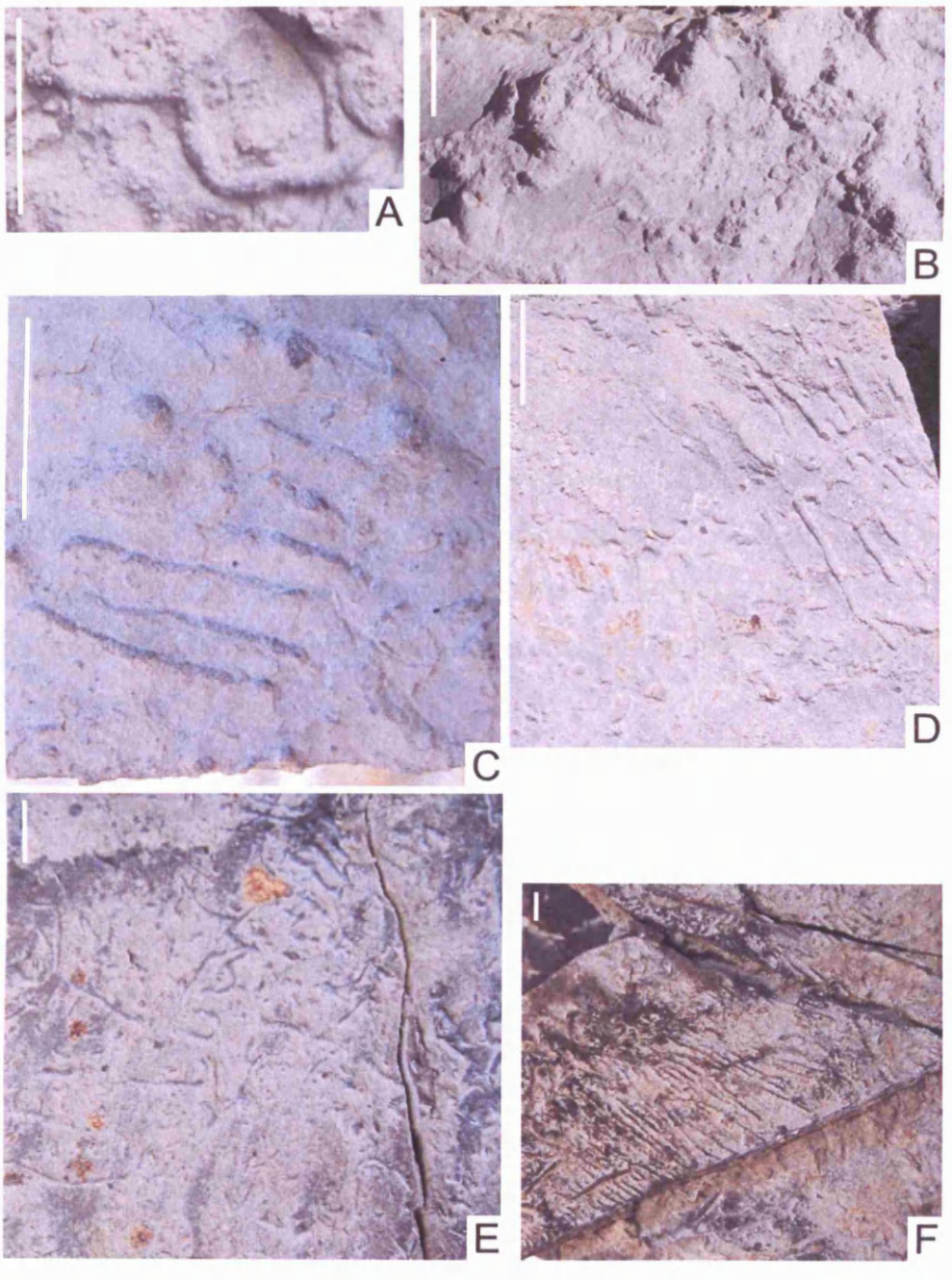
A
B
C
D
E
F

Appendix 3.16

Appendix 3.16.A. *Urohelminthoida appendiculata* HEER 1877. Hypichnial semi-relief. Fan fringe, Banaston System, Hecho-Urdues Scale bar: 2 cm.
Appendix 3.16.B. *Protopaleodictyon spinata* GEINITZ 1867. Hypichnial semi-relief. Lobe fringe, Cotefablo System, Cotefablo tunnel. Scale bar: 2 cm.
Appendix 3.16.C. *Protopaleodictyon bicaudatum* SEILACHER 1977. Hypichnial semi-relief. Fan fringe, Cotefablo System, Jasa. Scale bar: 2 cm.
Appendix 3.16.D. *Megagrapton irregulare* KSIĄŻIEWICZ 1968. Hypichnial semi-relief. Lobe, Broto System, Aragues del Puerto. Scale bar: 2 cm.
Appendix 3.16.E. *Protopaleodictyon incompositum* KSIĄŻIEWICZ 1958. Hypichnial semi-relief. Fan fringe, Cotefablo System, Jasa. Scale bar: 2 cm.
Appendix 3.16.F. *Megagrapton submontanum* (AZPEITIA MOROS 1933). Hypichnial semi-relief. Channel axis sands, Gerbe I sandbody, Rio Nata. Scale bar: 10 cm.

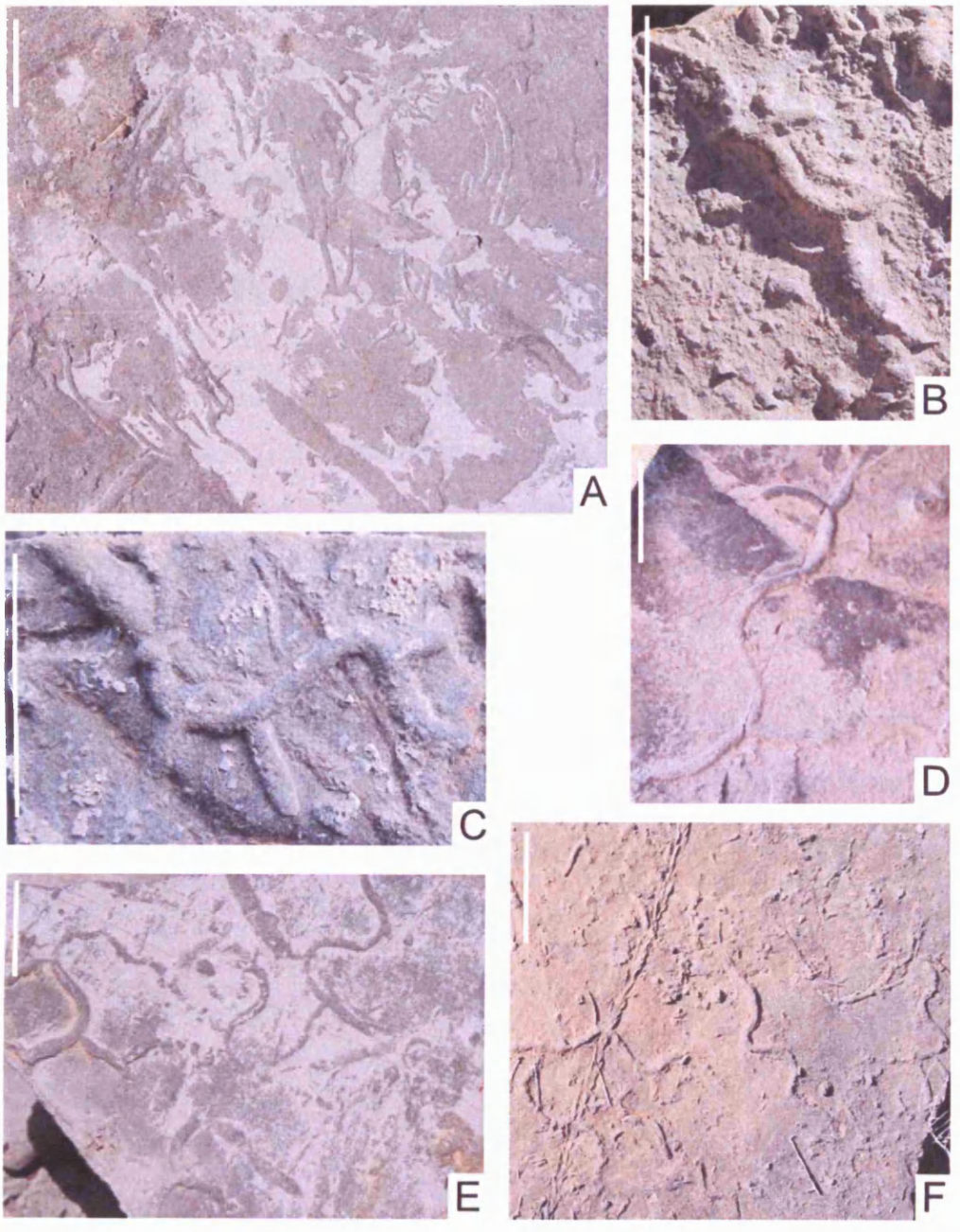
A
B
C
D
E
F

Appendix 3.17

Appendix 3.17.A. *Paleodictyon minimum* SACCO 1888. Hypichnial semi-relief. Channel margin, Arro System, Bco. Sierra. Scale bar: 1 cm.

Appendix 3.17.B. *Paleodictyon miocenicum* SACCO 1886. Hypichnial semi-relief. Lobe, Broto System, Aragues del Puerto. Scale bar: 2 cm.

Appendix 3.17.C. *Paleodictyon latum* VIALOV & GOLEV 1965. Hypichnial semi-relief. Lobe fringe, Cotefablo System, Cotefablo tunnel. Scale bar: 1 cm.

Appendix 3.17.D. *Paleodictyon strozzii* MENEGHINI 1850. Hypichnial semi-relief. Slope gully, Guaso System, Rio Ena. Scale bar: 2 cm.

Appendix 3.17.E. *Paleodictyon delicatulum* UCHMAN 1995. Hypichnial semi-relief. Fan fringe, Cotefablo System, Jasa. Scale bar: 2 cm.

Appendix 3.17.F. *Paleodictyon goetzingeri* VIALOV & GOLEV 1965. Hypichnial semi-relief. Fan fringe, Banaston System, Hecho-Urdues Scale bar: 2 cm.

Appendix 3.17.G. *Paleodictyon majus* MENEGHINI in PERUZZI 1880. Hypichnial semi-relief. Fan fringe, Cotefablo System, Urdues. Scale bar: 2 cm.

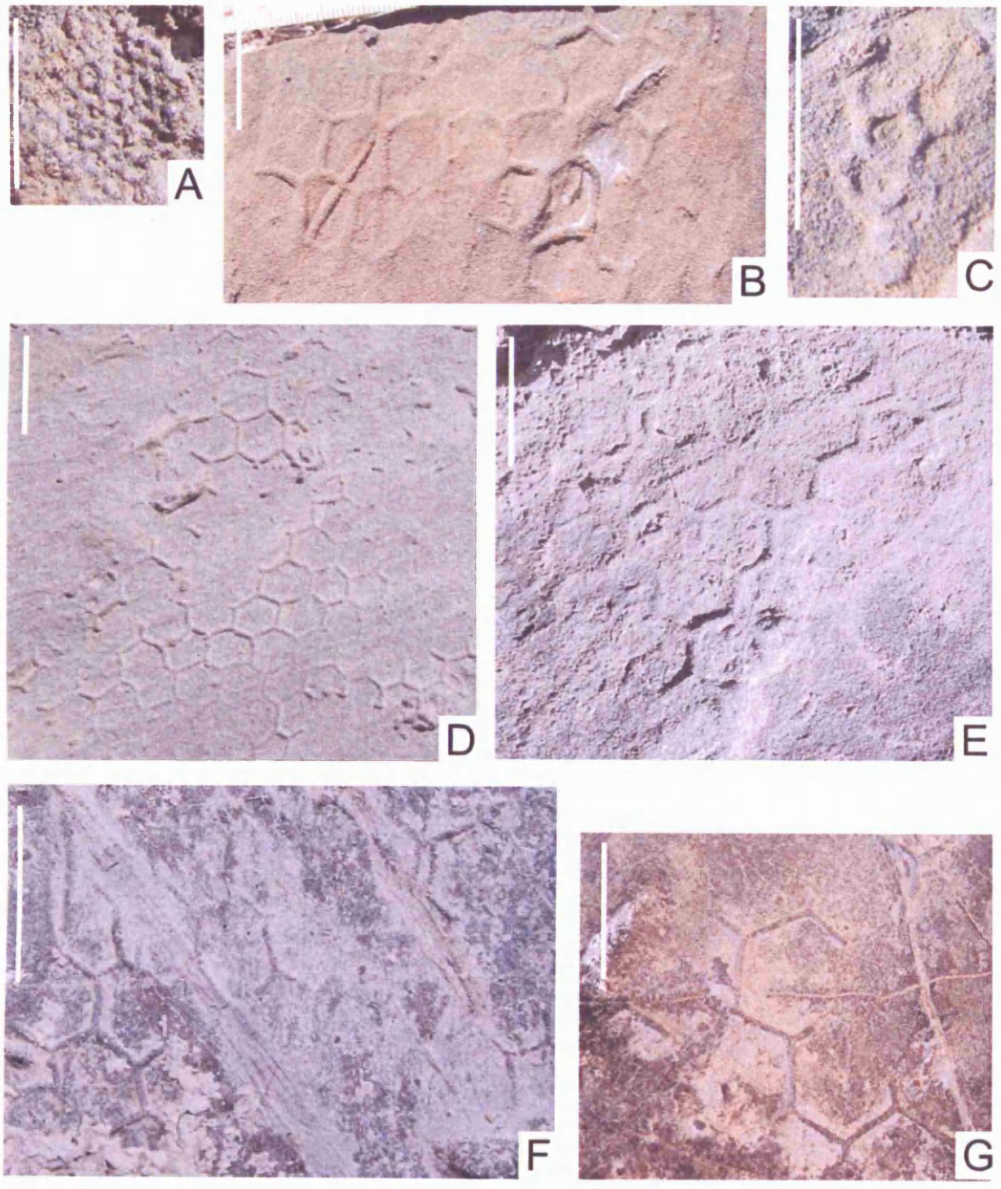
A
B
C
D
E
F
G

Appendix 3.18

Appendix 3.18.A. *Paleodictyon maximum* EICHWALD 1868. Hypichnial semi-relief. Fan fringe, Cotefablo System, Urdues. Scale bar: 2 cm.

Appendix 3.18.B. *Paleodictyon arvense* BARBIER 1956. Hypichnial semi-relief. Fan fringe, Cotefablo System, Urdues. Scale bar: 2 cm.

Appendix 3.18.C. Arthropod trackway, Hypichnial Form A. Lobe, Broto System, Aragues del Puerto. Scale bar: 2 cm.

Appendix 3.18.D. Arthropod trackway, Endichnial Form B. Channel margin, Morillo system, Morillo de tou. Scale bar: 2 cm.

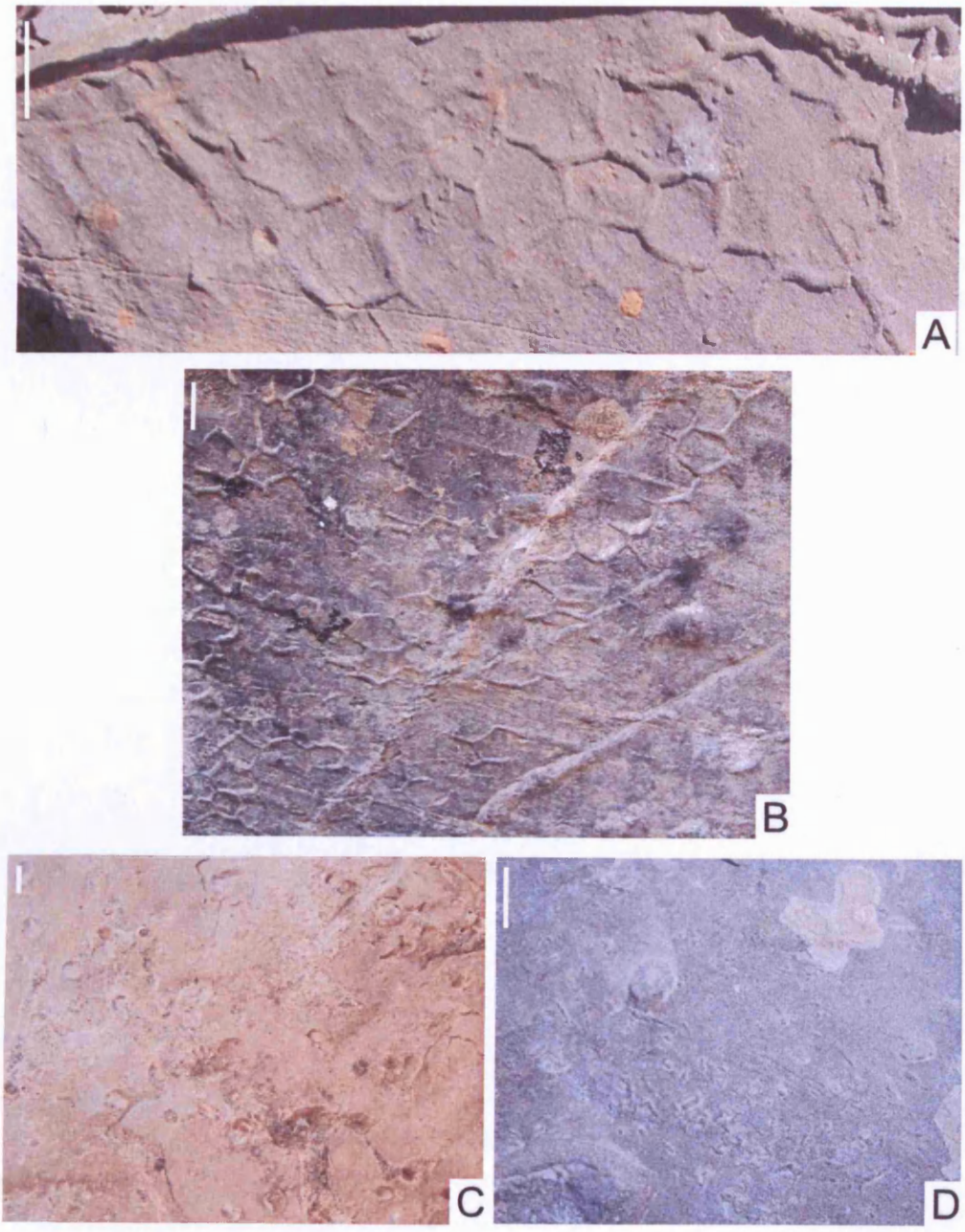
A
B
C
D

Chapter 4

Facies and Facies Associations

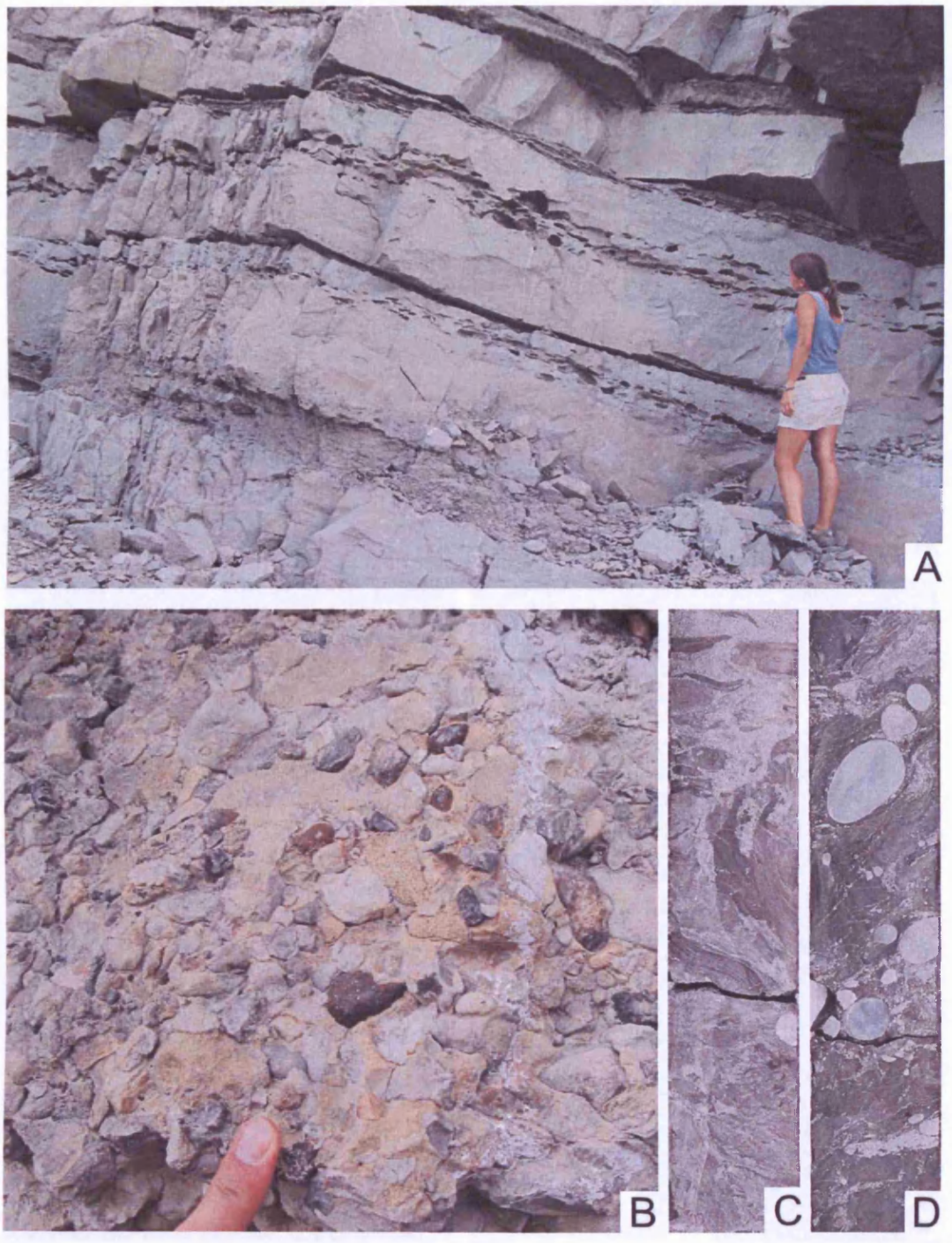

Appendix 4.1. A) Facies A1.4 mud-flake breccia and C2.1 sandstones, Ainsa I Fan, locality 15; B) Facies A1.1 disorganised gravel, Gerbe I; C) Facies A1.2 Ainsa II fan, Core A1 (6 cm wide); D) Facies A1.3, Ainsa II fan, Core A2 (6 cm wide).

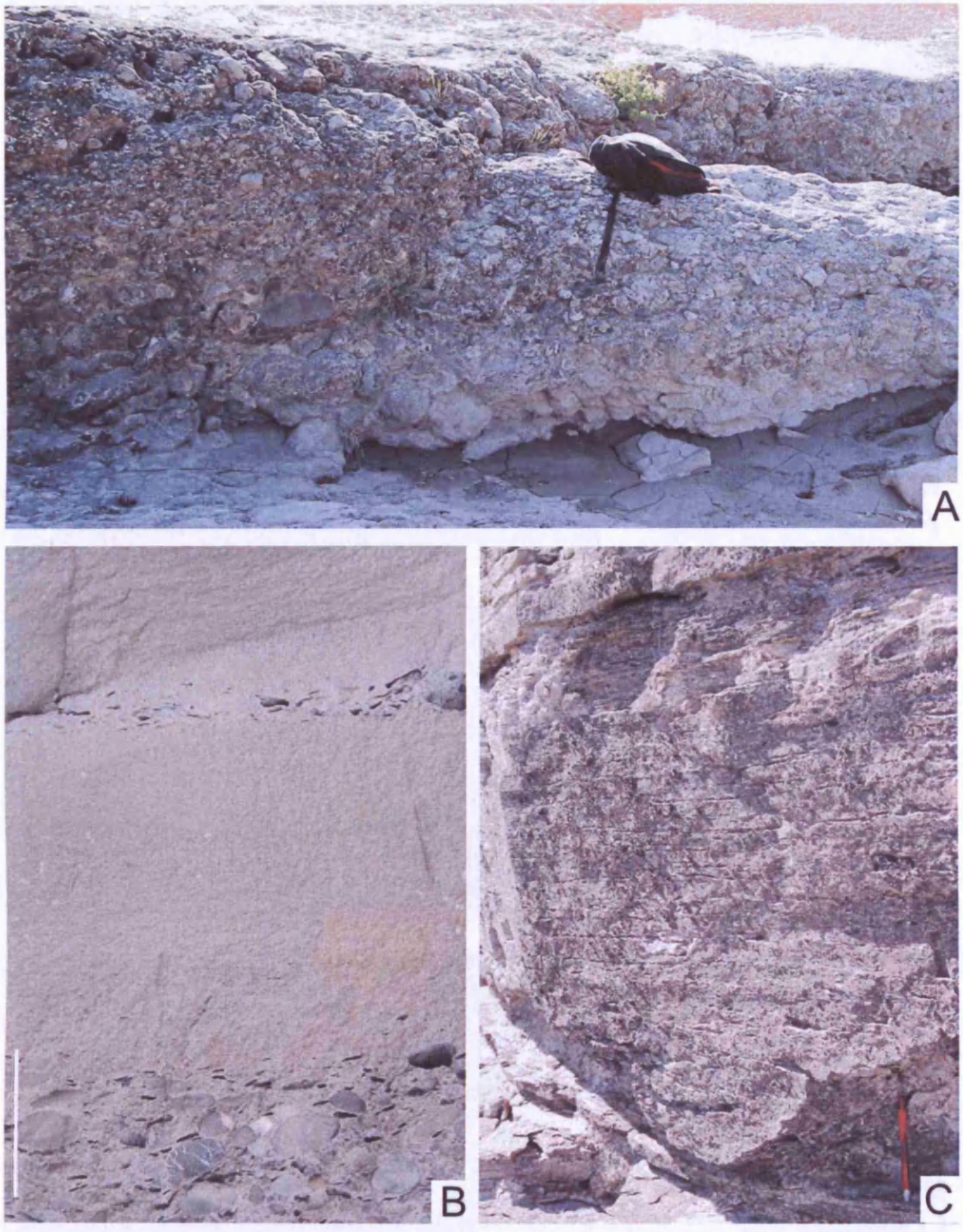

Appendix 4.2. A) Facies A2.1 stratified gravel, Gerbe I, locality 11; B) Facies A2.7 normally graded pebbly sandstone, Ainsa I, locality 15 (20 cm scale bar); C) Facies A2.8 graded-stratified pebbly sandstone, Morillo I, locality 22.

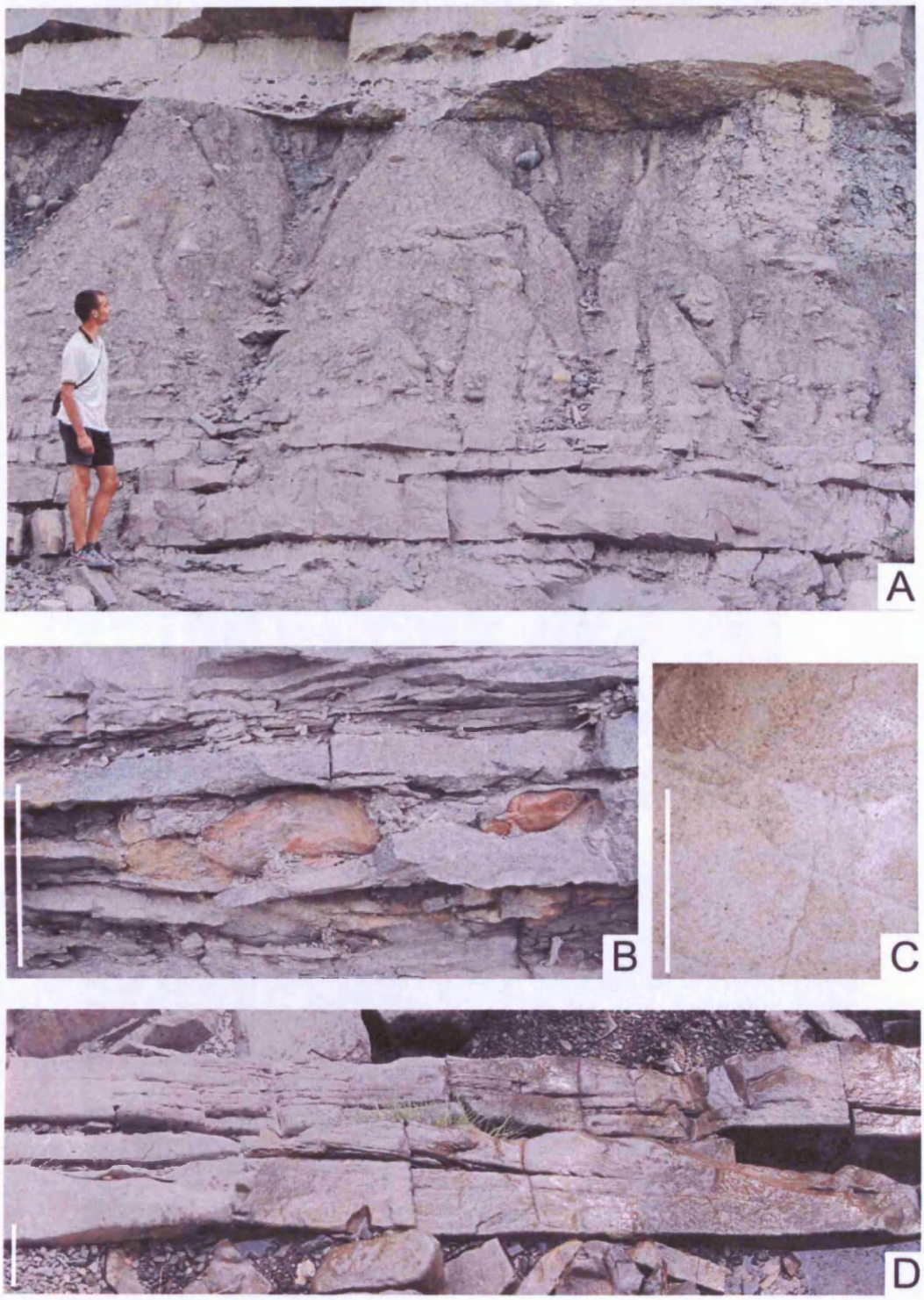

Appendix 4.3. A) Facies A1.3 disorganised gravely mudstone, Ainsa I, locality 15; B) Facies B1.2 thin-bedded coarse-grained sandstones, Ainsa I, locality 18 (10 cm scale); C) Dish structures, Facies B1.1 disorganised sandstones, Los Molinos II, locality 8 (10 cm scale); D) Facies B2.2 cross-stratified sandstones, Los Molinos II, locality 8 (20 cm scale).

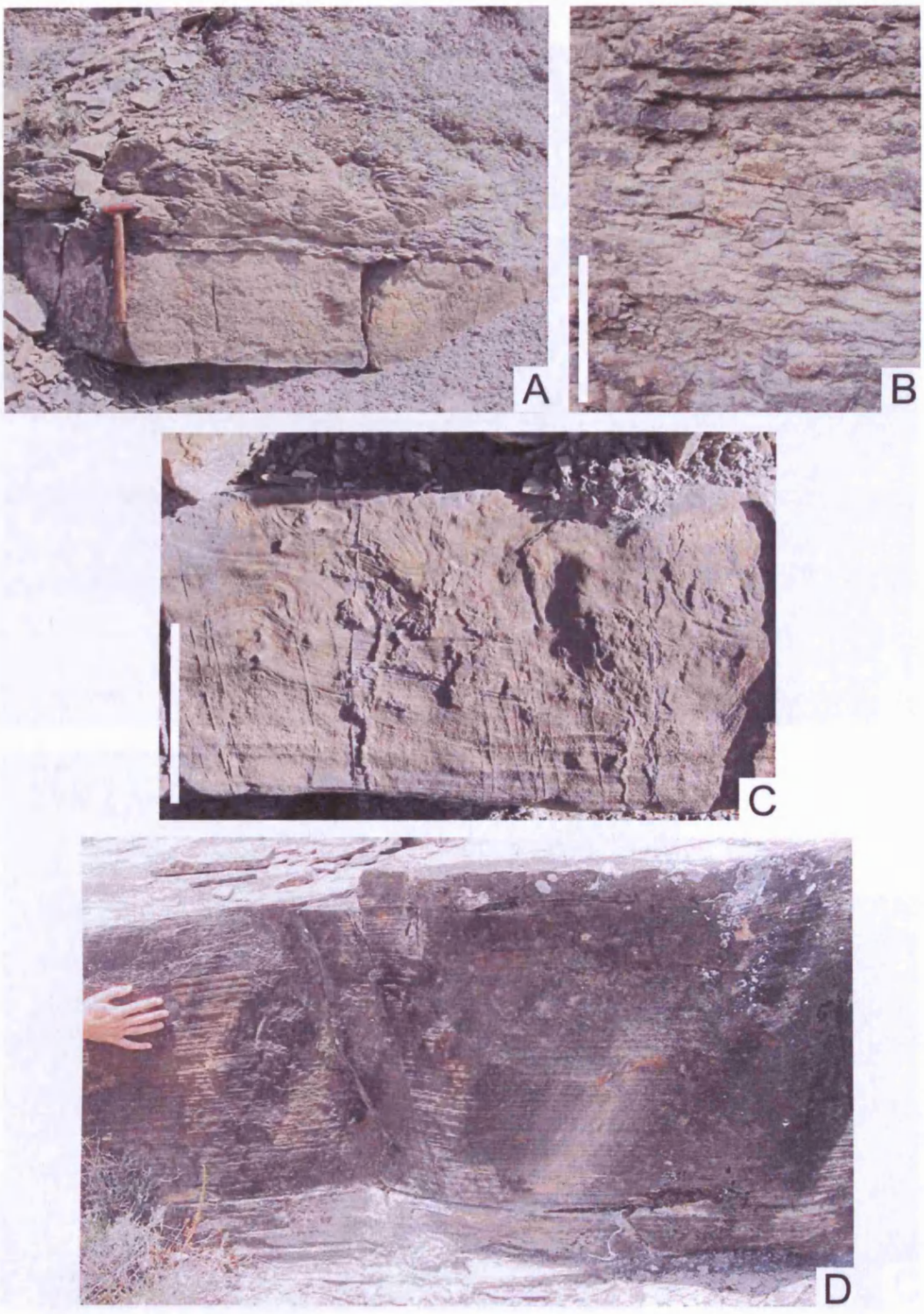

Appendix 4.4. A) Facies C1.1 poorly sorted muddy sandstones, Cotefablo system, locality 32; B) Facies C1.2 mottled muddy sandstones (10 cm scale), Broto system, locality 29; C) Facies C2.2 sandstone-mudstone couplet (T_{bc}), Cotefablo system, locality 32 (10 cm scale); (D) Facies B2.1 planar stratified sandstone, Ainsa I, locality 15.

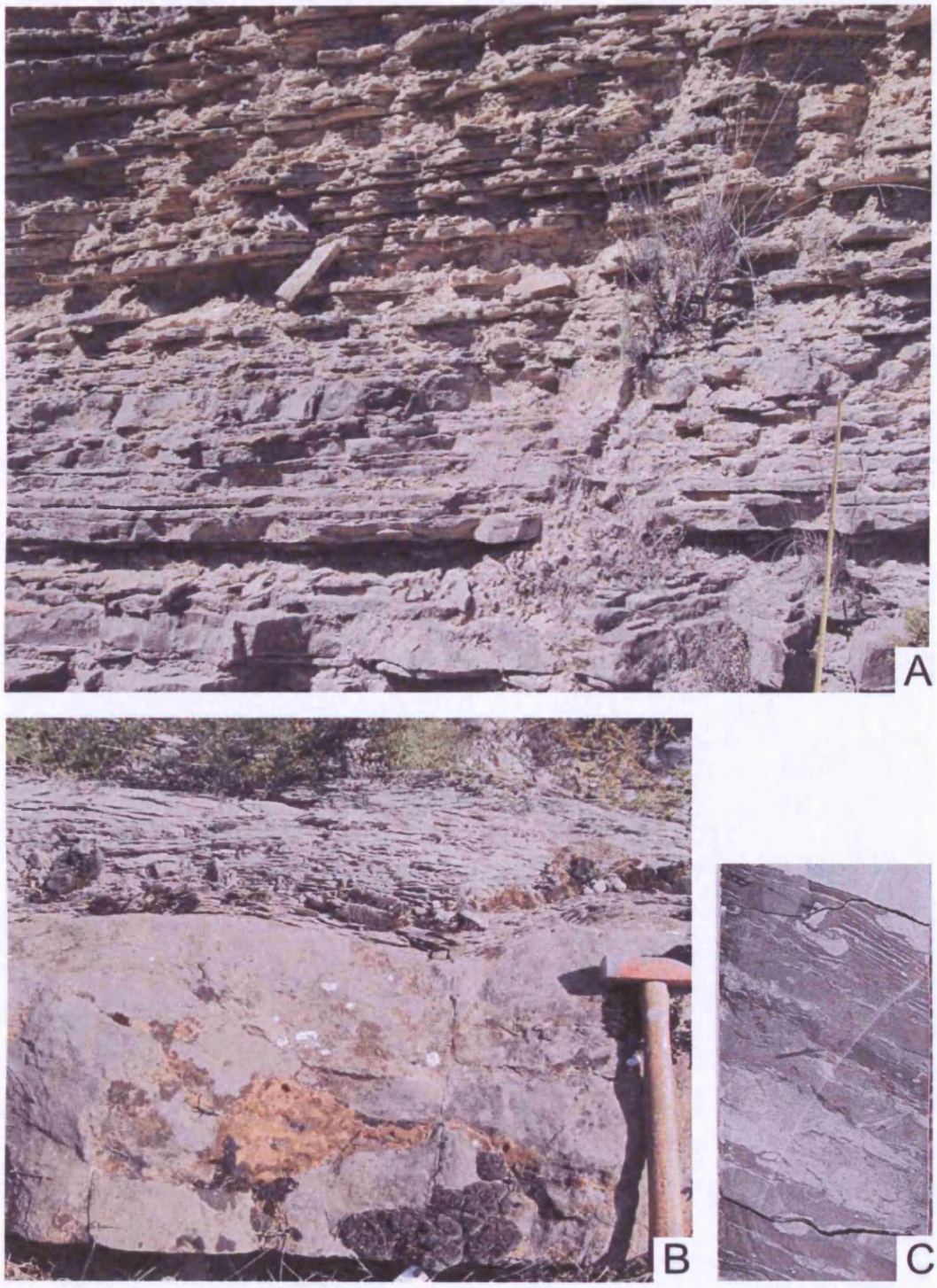

Appendix 4.5. A) Facies C2.3 sandstone-mudstone couplets, Morillo I, locality 22 (1 m scale); B) Facies C2.4 Flow reflected sandstone, Cotefablo system, locality 33; C) Facies D1.3 and E1.3 mottled siltstones and mudstones, and mottled mudstones, Ainsa II, Core L1 (core 6 cm wide).

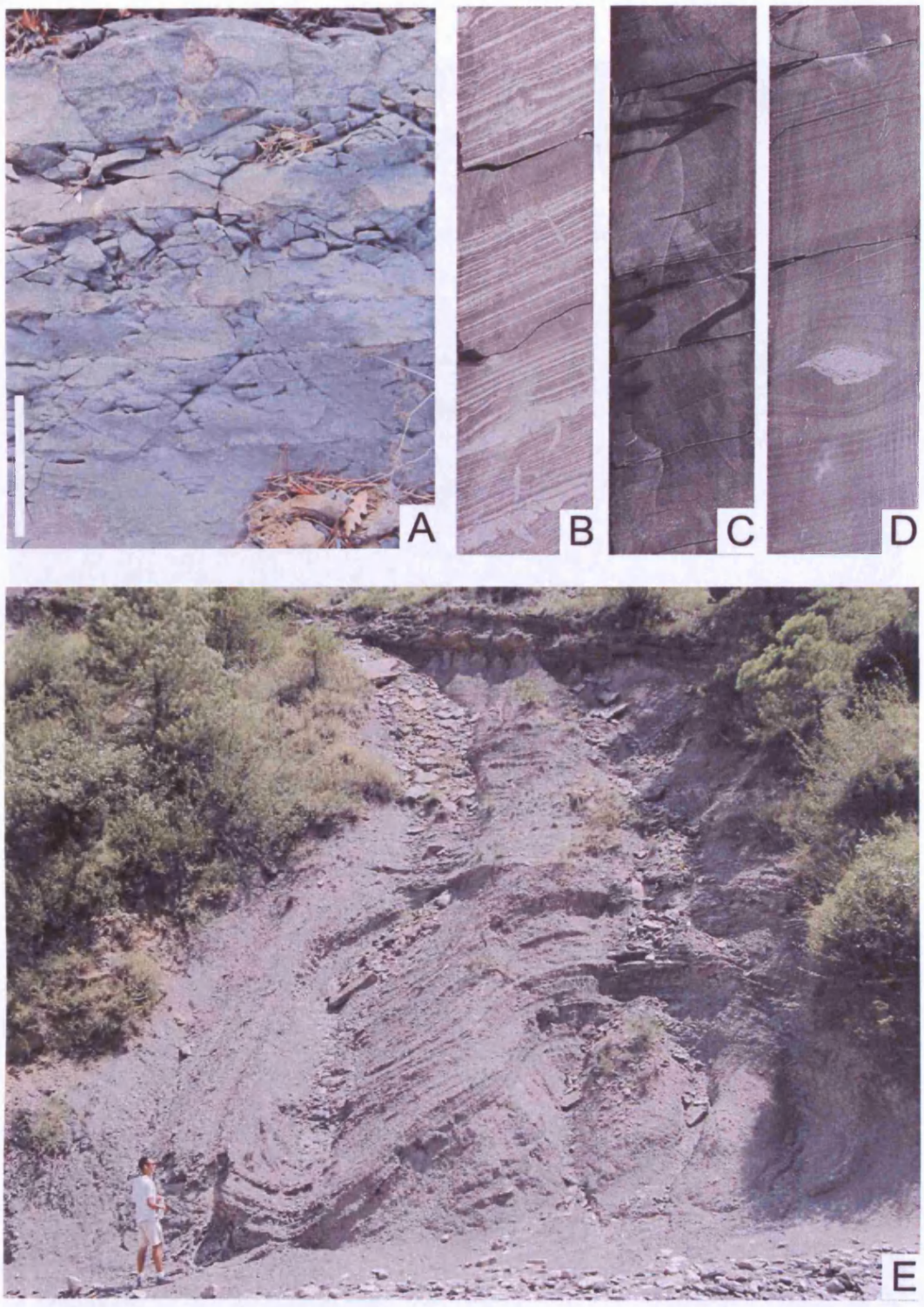

Appendix 4.6. A) Facies D2.1 graded stratified siltstones, Broto system, locality 28 (10 cm scale); B) Facies D2.3 silt and mud laminae, Ainsa II, Core L1 (Core 6 cm wide); C) Facies E1.3, mottled mudstones, Ainsa I, Core A4 (Core 6 cm wide); D) Facies F2.2, Ainsa II, Core L1 (Core 6 cm wide); E) Facies F2.1, Ainsa system, locality 20.

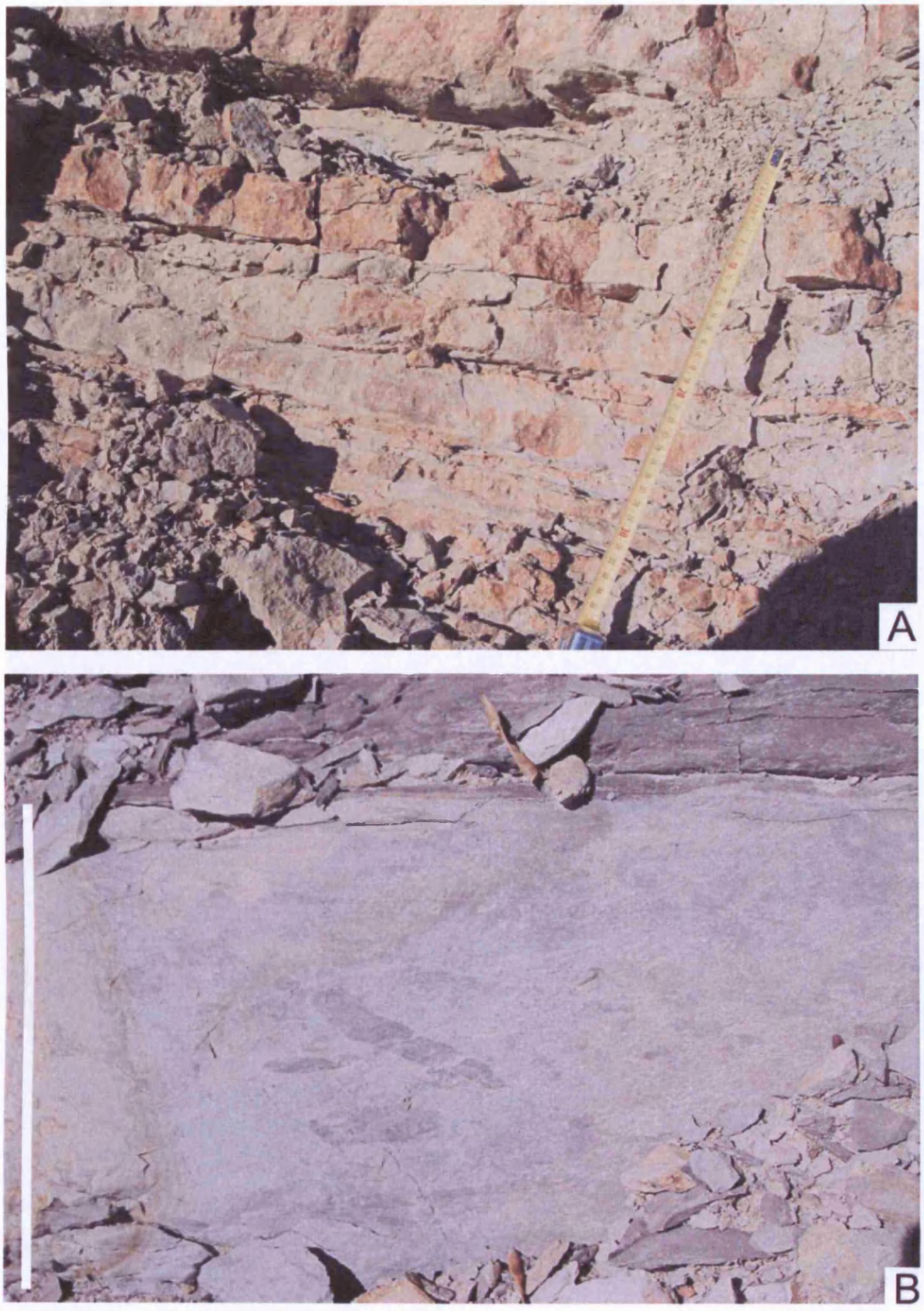

Appendix 4.7. A) Facies I nummulites-rich bioclastic sandstones, locality 12 (40 cm scale); B) Facies H, hemiturbidite / calcilutite, Cotefablo system, locality 37 (10 cm scale).

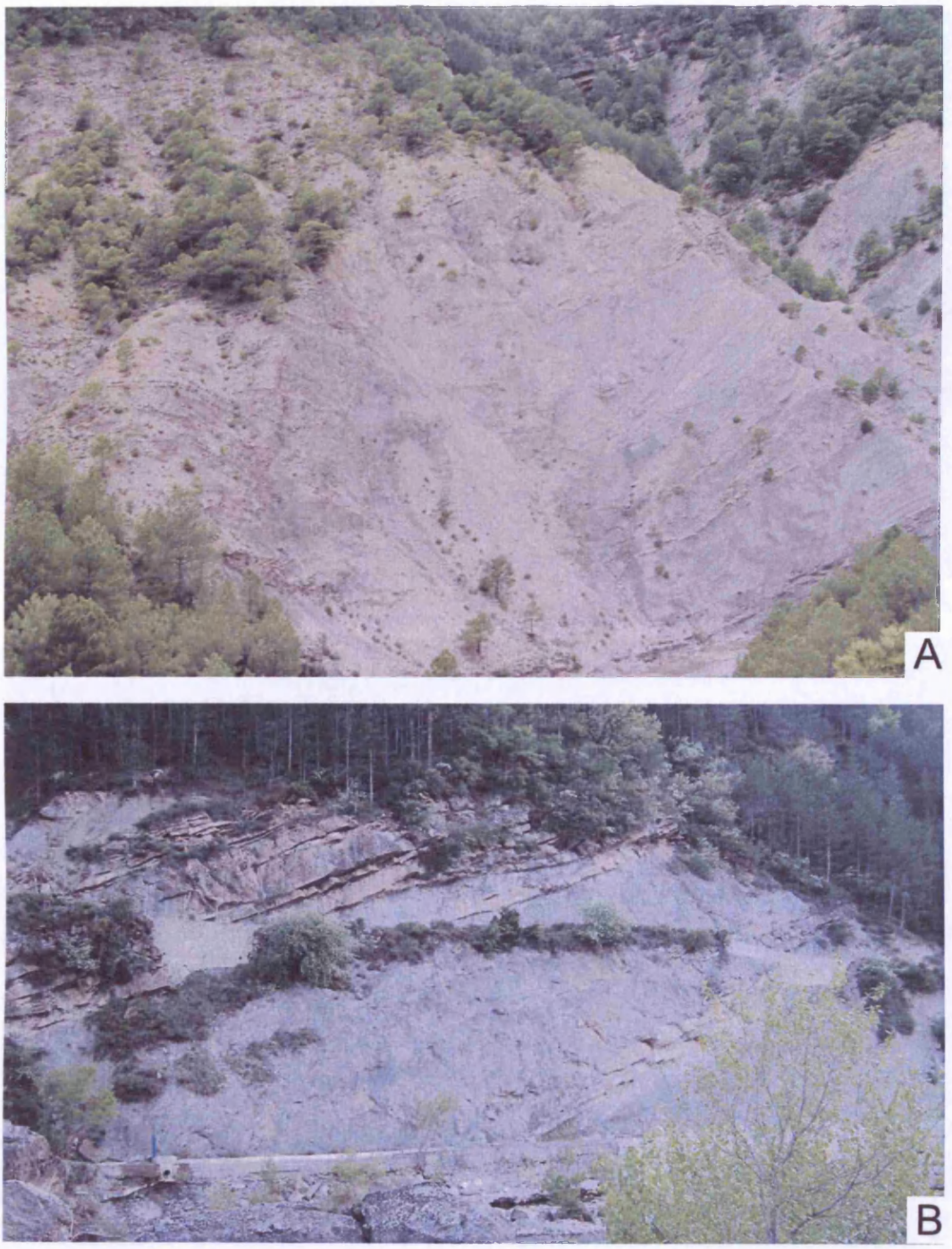

Appendix 4.8. A) FA1a, Los Molinos system, locality 4; B) FA1b, Morillo I, Rio Ara

Appendix 4.9. A) FA1c, Arro system, locality 6; B) FA1d, Cotefablo system, locality 36

Appendix 4.10. A) Pebble-filled scour, FA1b, Gerbe system, locality 9; B) FA2a, Gerbe I, locality 11 (Road marker 1 m high).

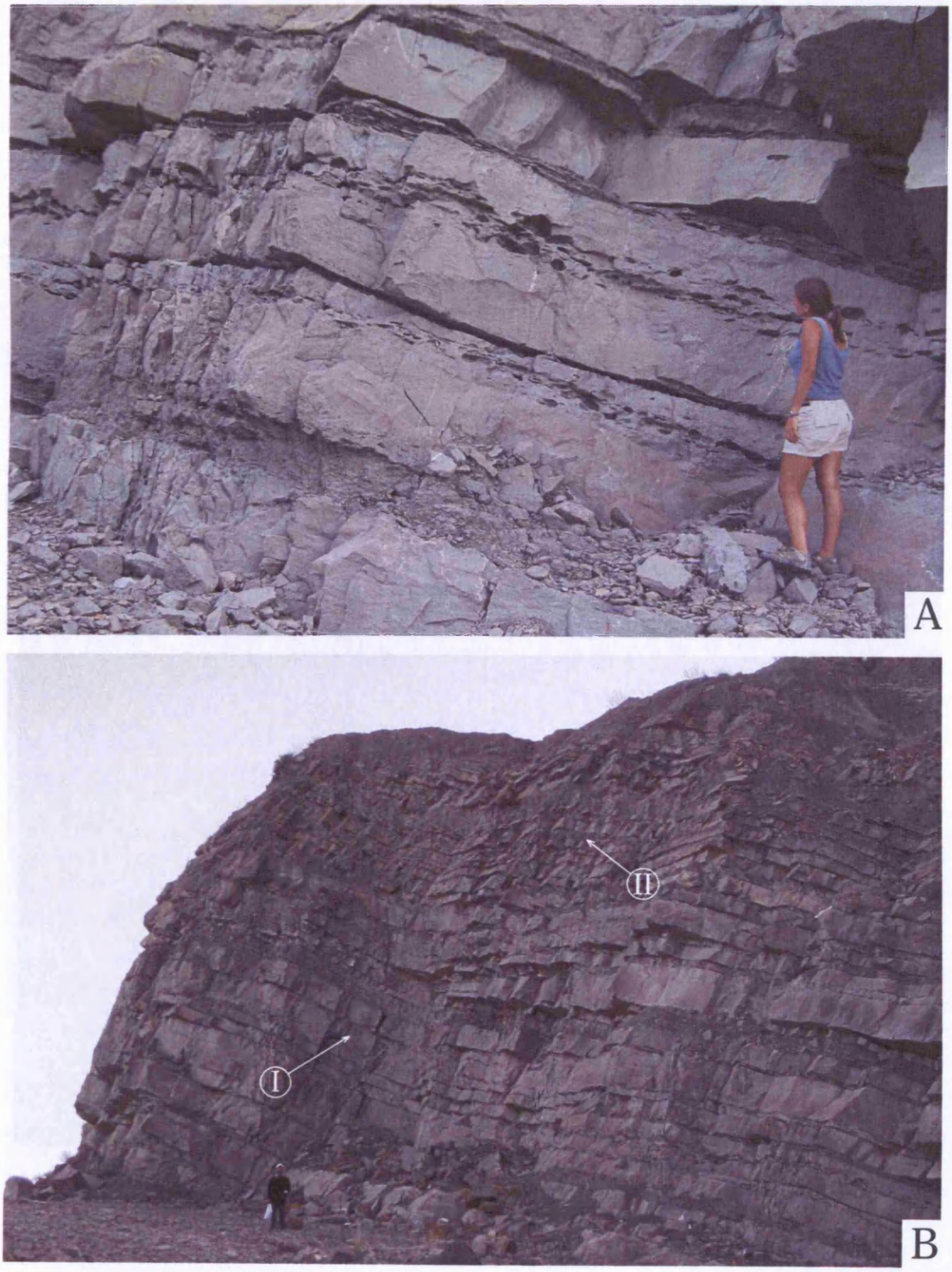

Appendix 4.11. A) FA3a, Ainsa I, locality 15; B) FA3b (I) and FA5c (II), Ainsa I, locality 15.

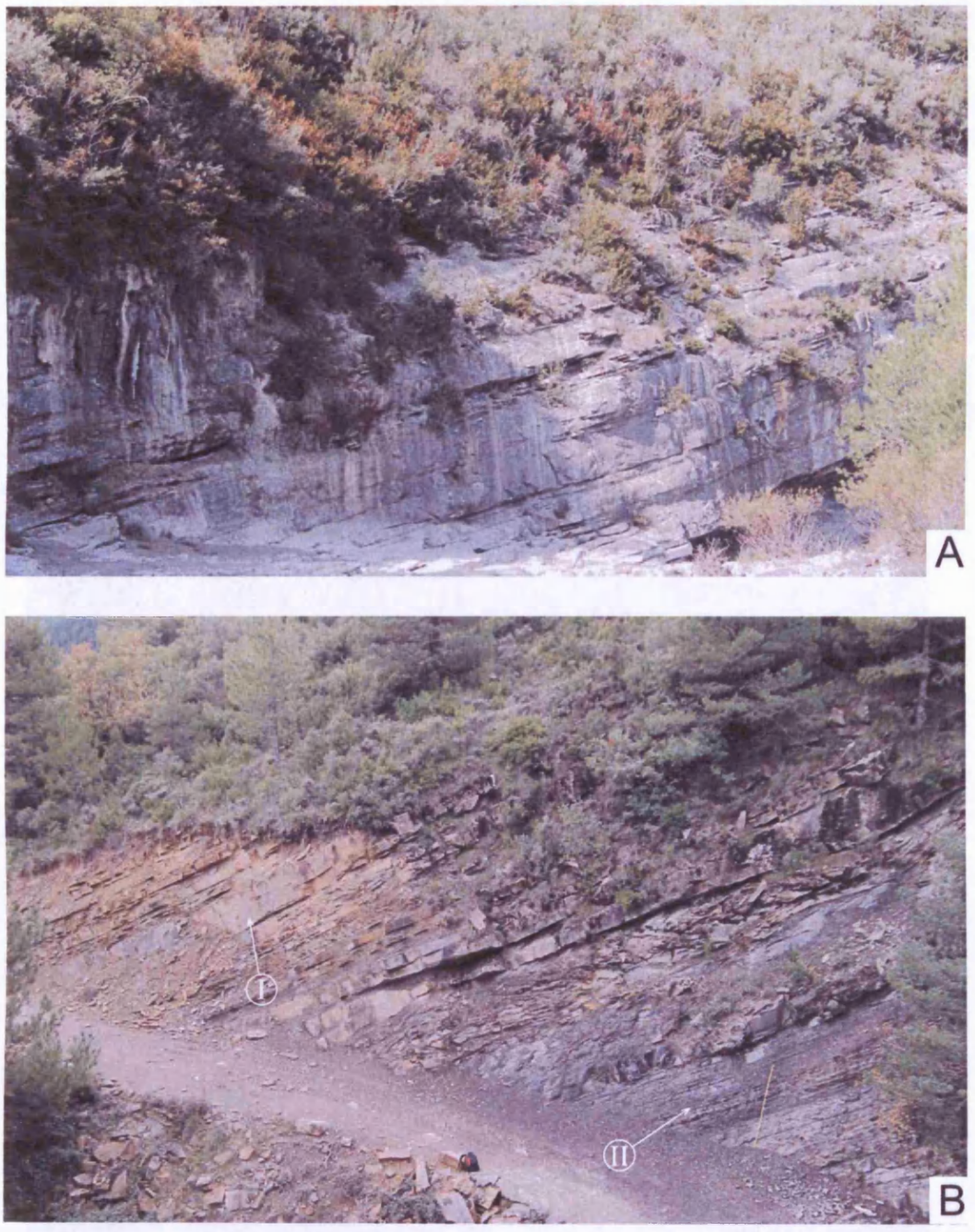

Appendix 4.12. A) FA3c, Guaso I, locality 24; B) FA3d (I) and FA6a (II), Banaston II, locality 14.

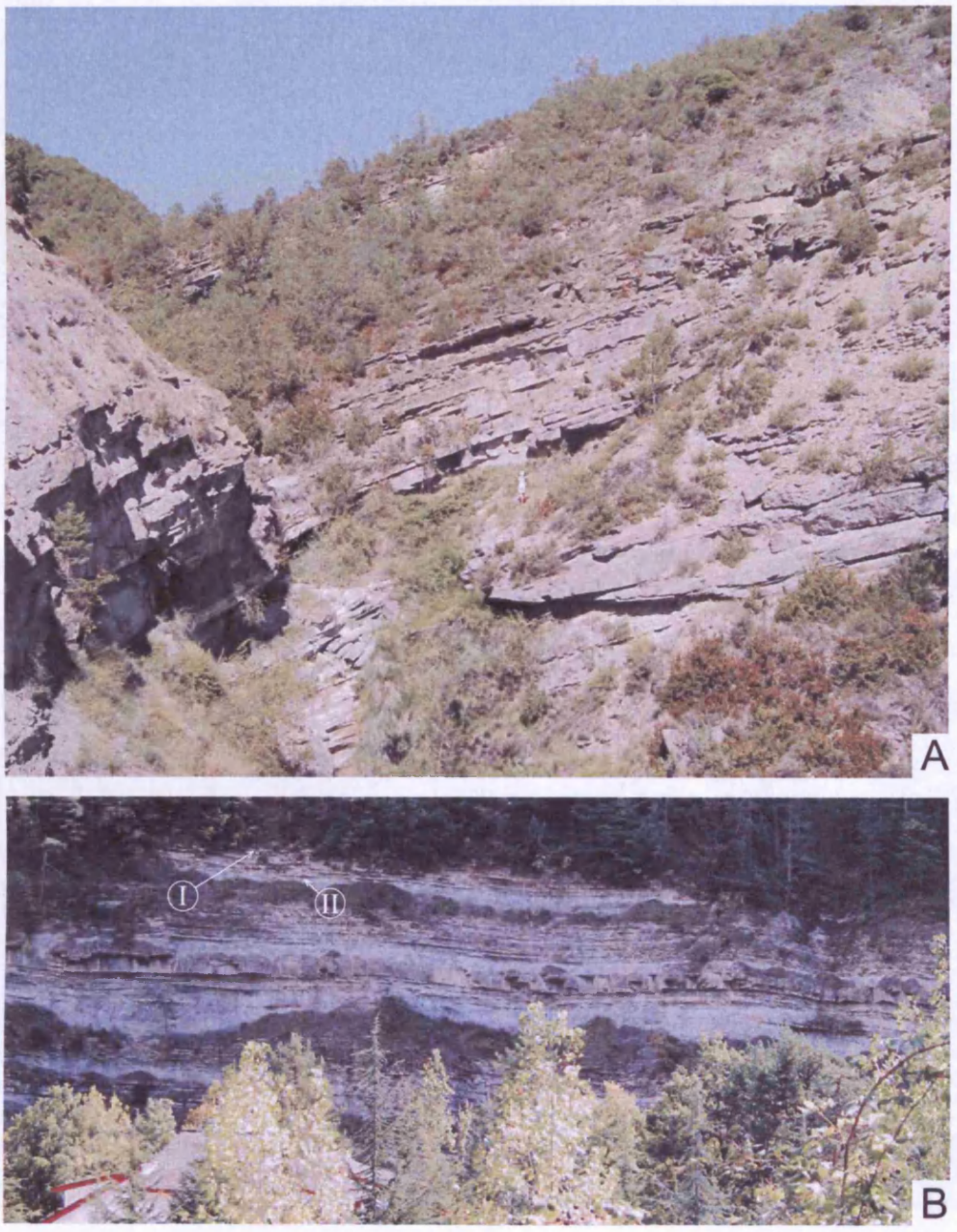

Appendix 4.13. A) FA3e, Morillo I, locality 22; B) FA3f (I) and FA5f (II), Broto system, locality 29.

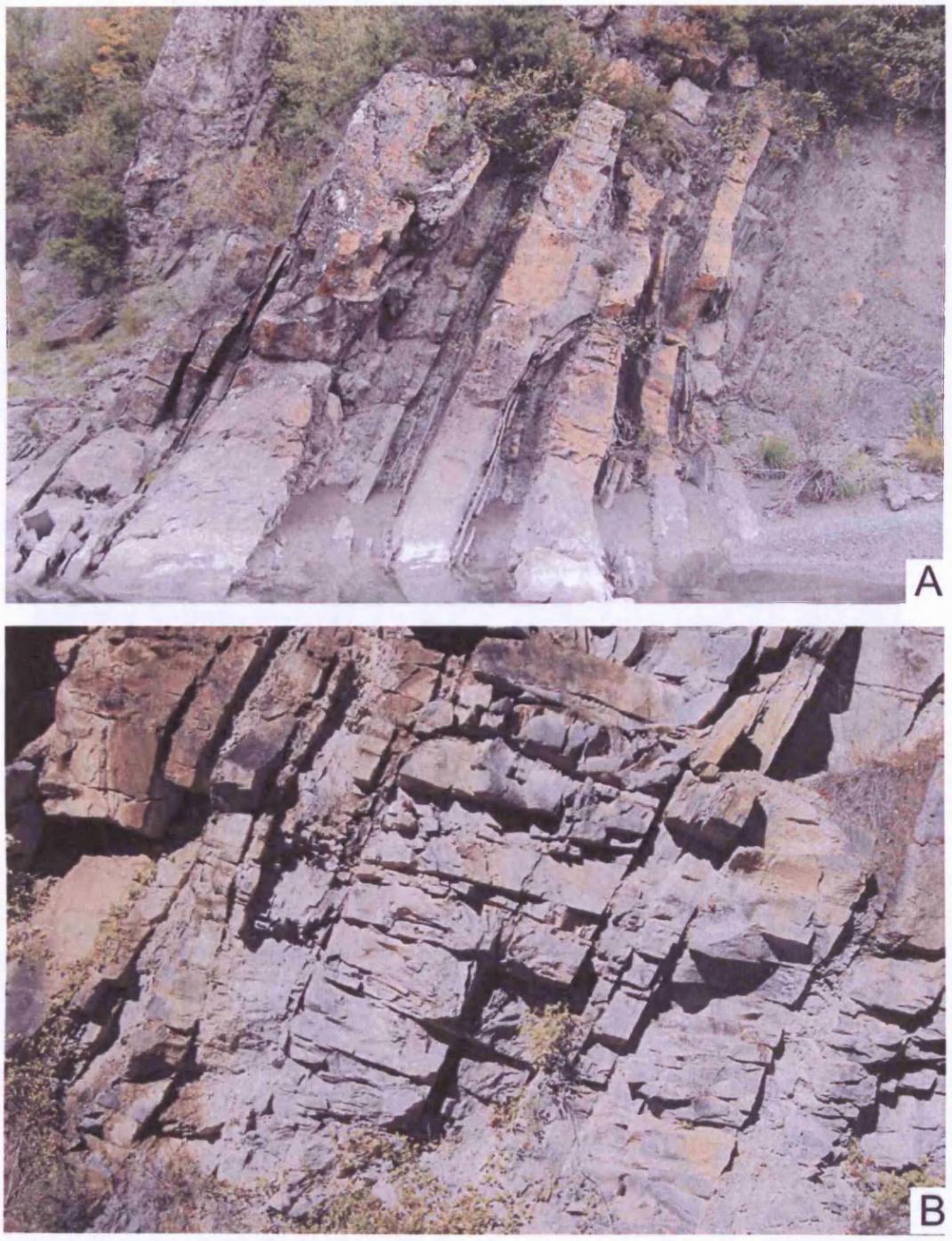

Appendix 4.14. A) FA3g Arro system, locality 7 (height of section ~ 5 m); B) FA3h, Broto system, locality 28 (height of section ~ 4 m).

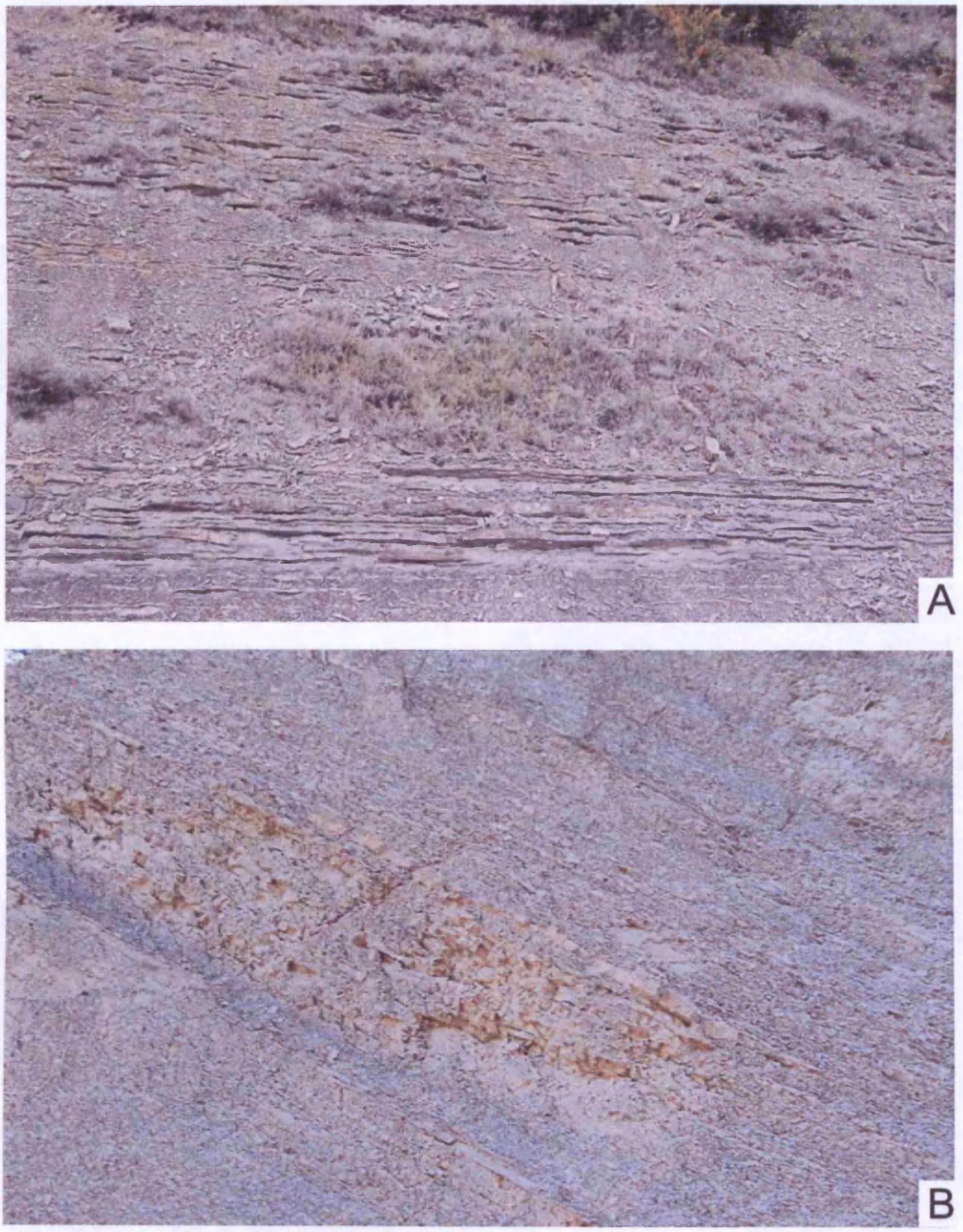

Appendix 4.15. A) FA4a, Ainsa I, locality 18 (height of section ~ 7m); B) FA4b, Ainsa system, locality 21 (height of section ~ 4 m).

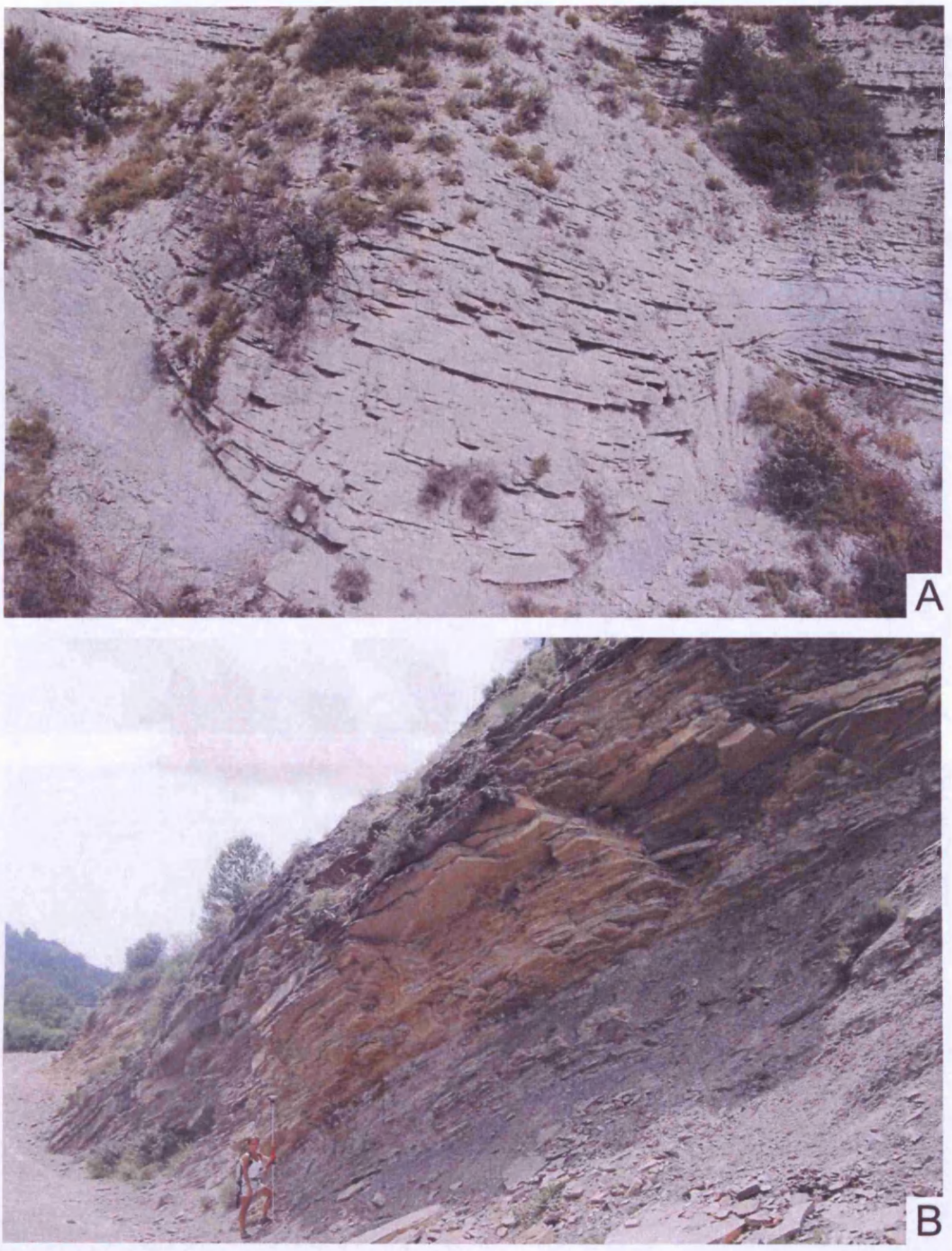

Appendix 4.16. A) FA5a, Guaso system, locality 26 (height of section ~ 12 m); B) FA5b, Ainsa II, locality 20.

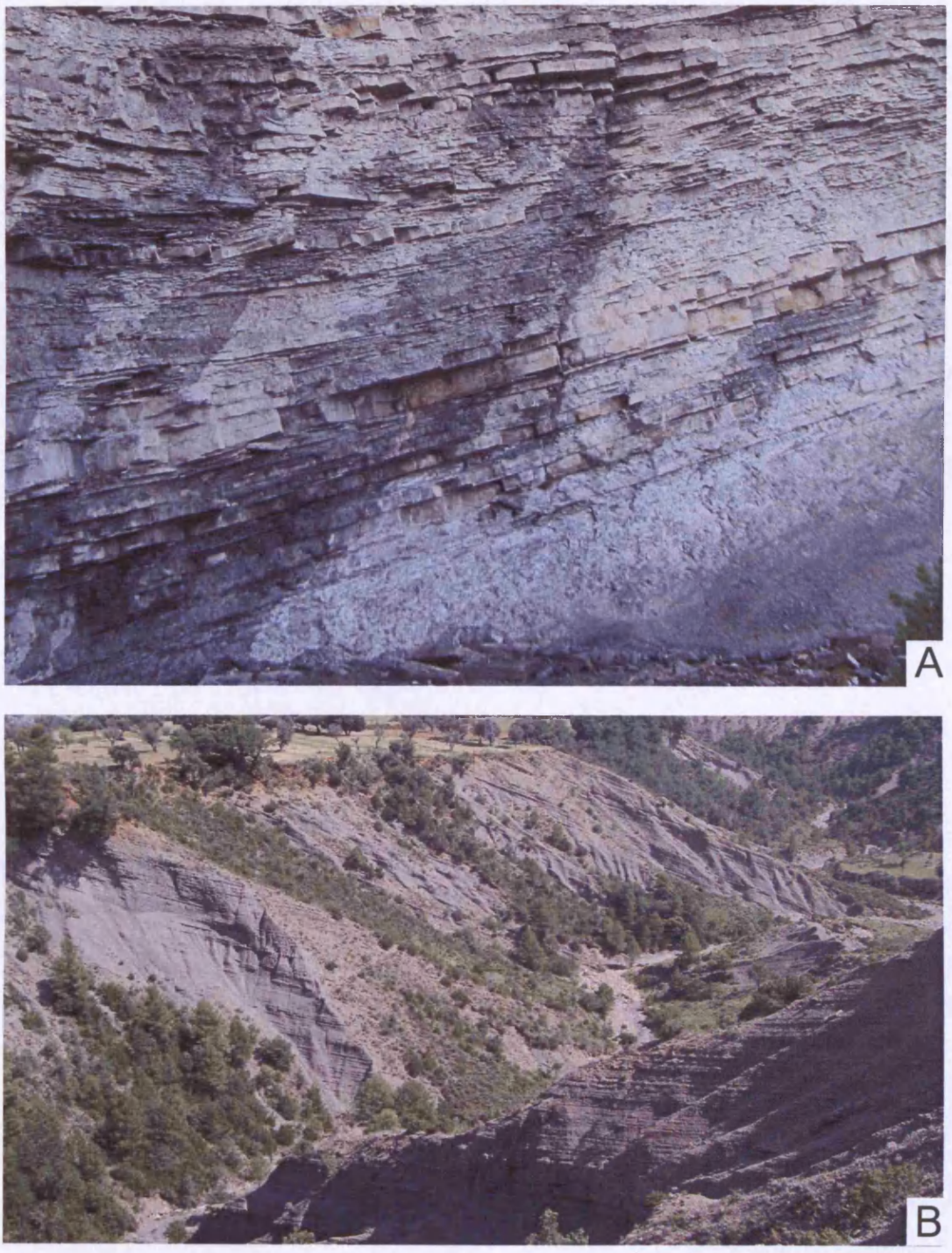

Appendix 4.17. A) FA5b, Arro system, locality 5 (height of section ~ 20 m); B) FA5d, Banaston system, San Vicente.

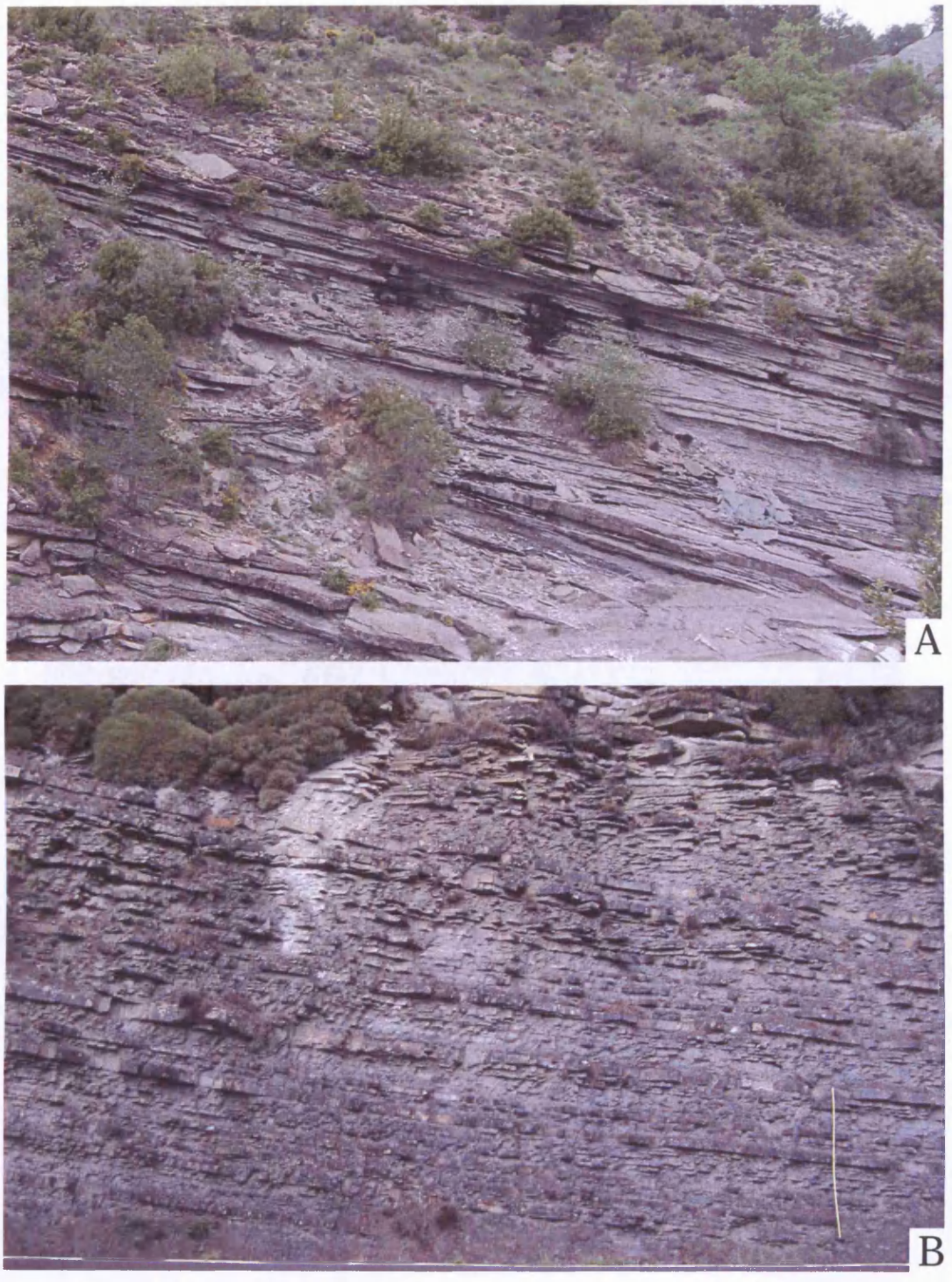

Appendix 4.18. A) FA5e, Guaso system, locality 25 (height of section ~ 12 m); B) FA5g and FA6f, Cotefablo system, locality 31 (2 m scale).

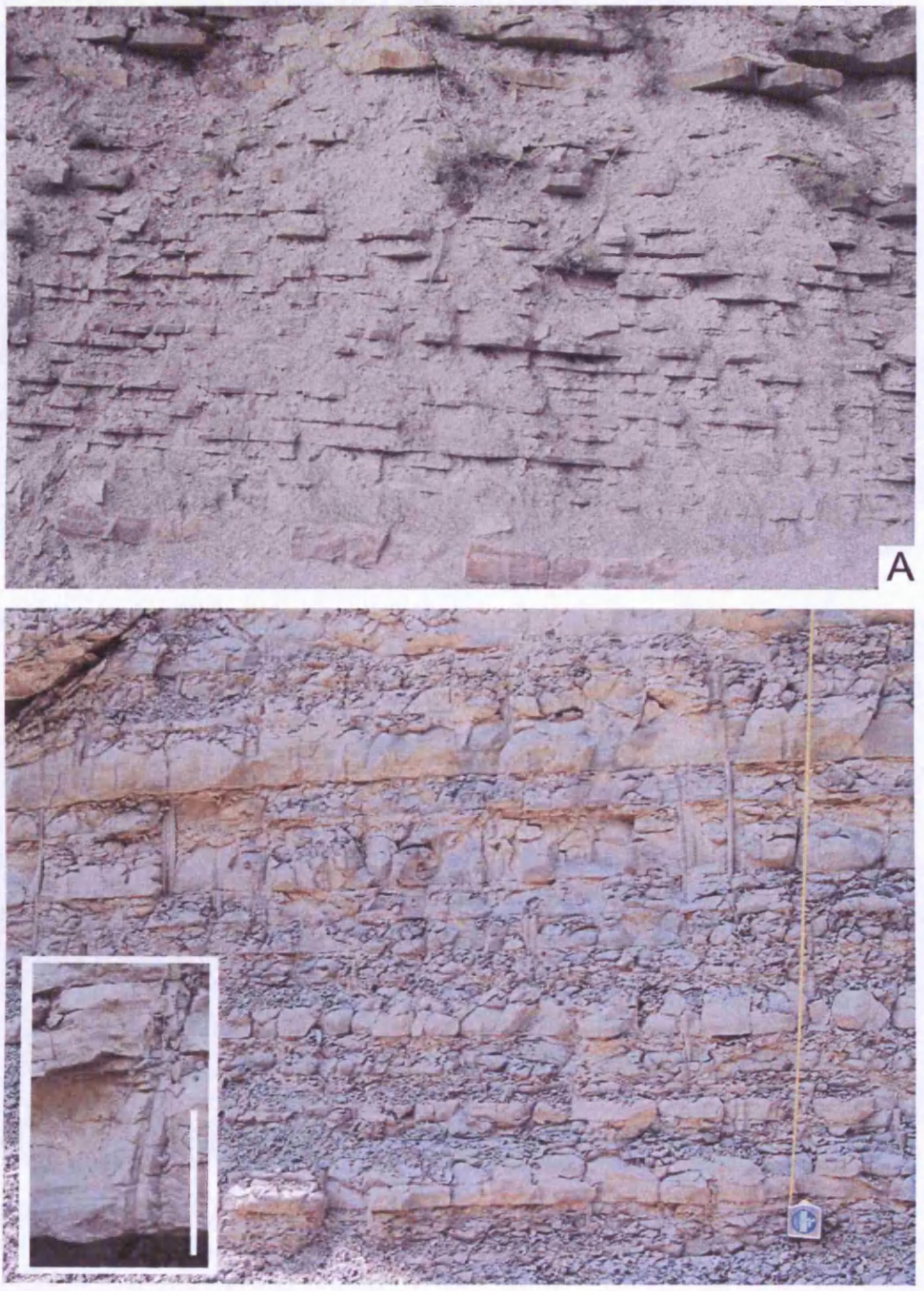

Appendix 4.19. A) FA5h, Cotefablo system, locality 32 (height of section ~ 7 m); B) FA6c, Banaston system, locality 13 (1.5 m scale), and close-up (scale 10 cm).

Appendix 4.20. A) FA6d, Ainsa system and close-up view of mudstones (10 cm scale), locality 21. B) FA6e, Broto system, locality 30 (height of section ~ 3 m).

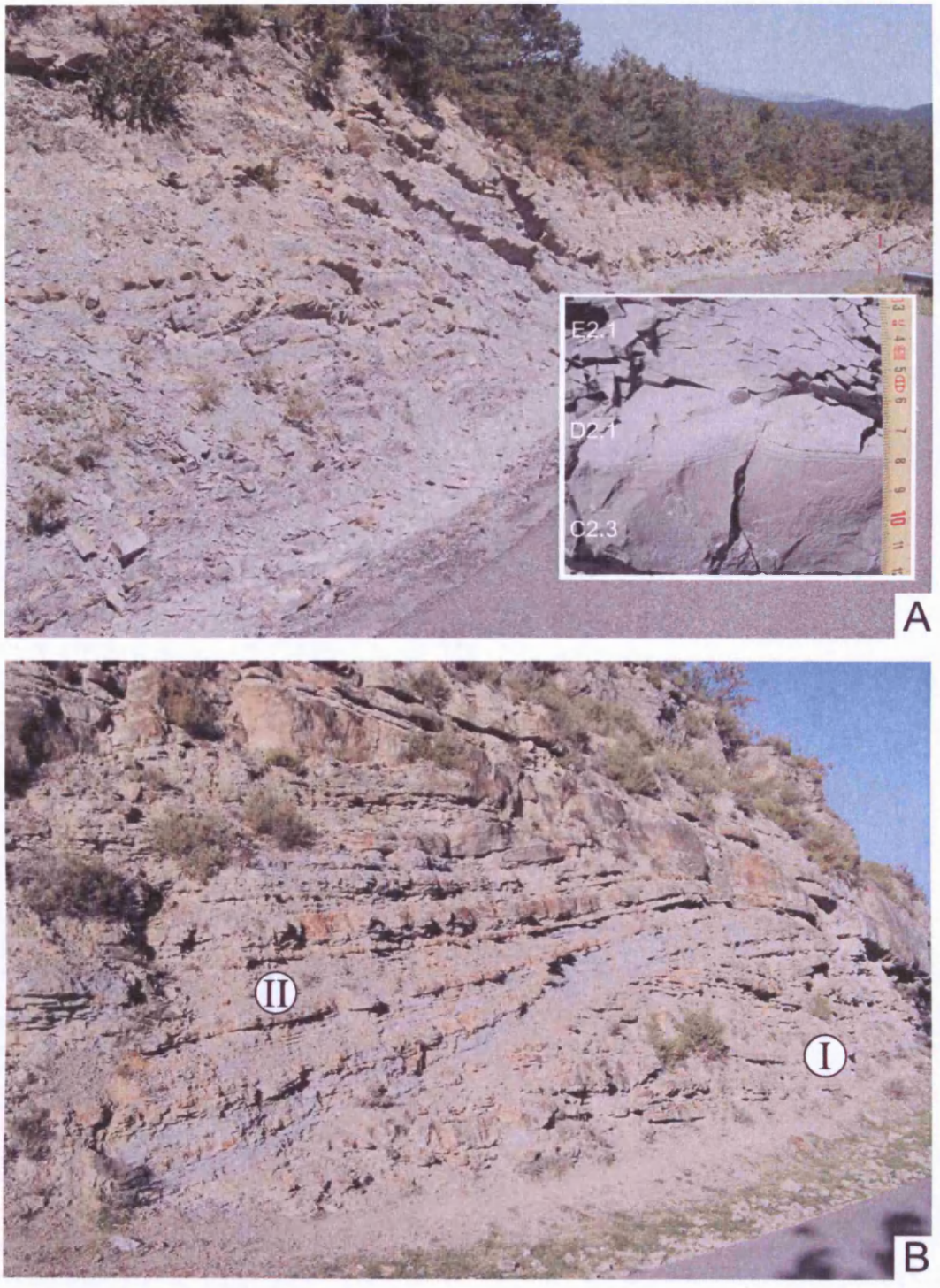

Appendix 4.21. A) FA6g, Cotefablo system, locality 37, with close-up of the facies; B) FA7a (I) and FA7b (II), Formigales, locality 12.

Chapter 5

AINSA BASIN:
Proximal turbidite systems of the Castisent Group

Appendix 5.1. Key for symbols used in sedimentary logs

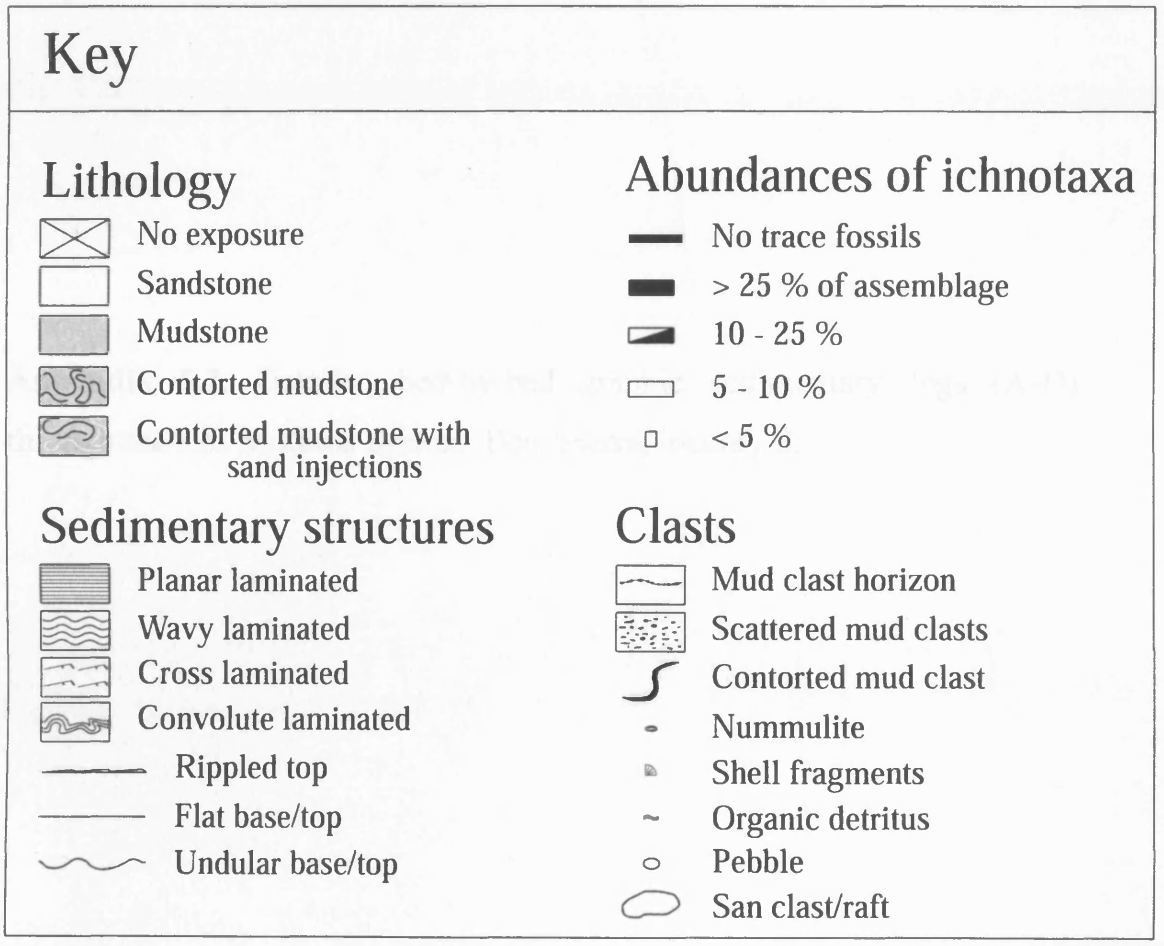

Appendix 5.2. Detailed bed-by-bed graphic sedimentary logs (A-D) through the Los Molinos System, Bco. Sierra, locality 2.

Log A

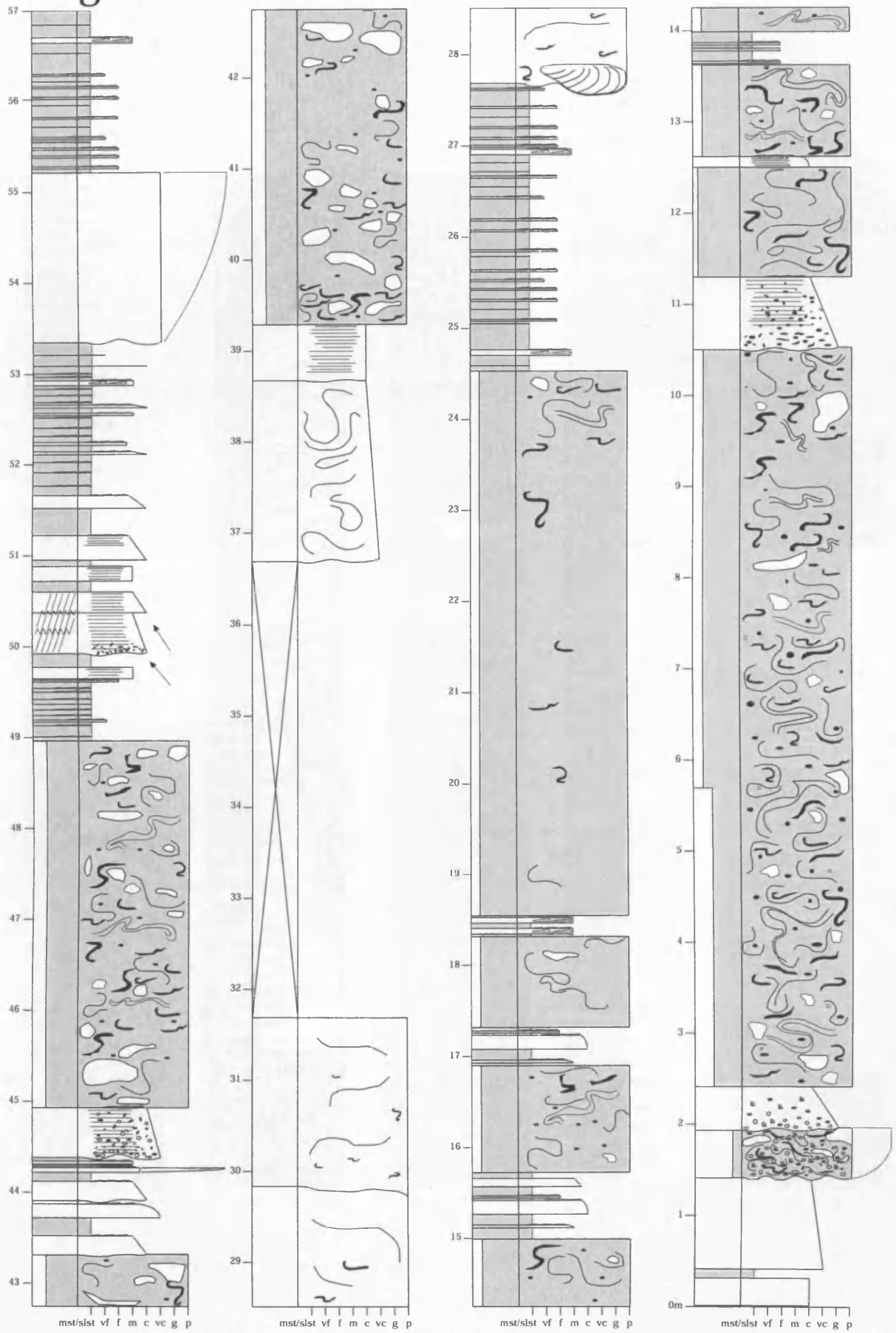
57
56
55
54
53
52
51
50
49
48
47
46
45
44
43
42
41
40
39
38
37
36
35
34
33
32
31
30
29
28
27
26
25
24
23
22
21
20
19
18
17
16
15
14
13
12
11
10
9
8
7
6
5
4
3
2
1
0m
mst/slst vf f m c vc g p

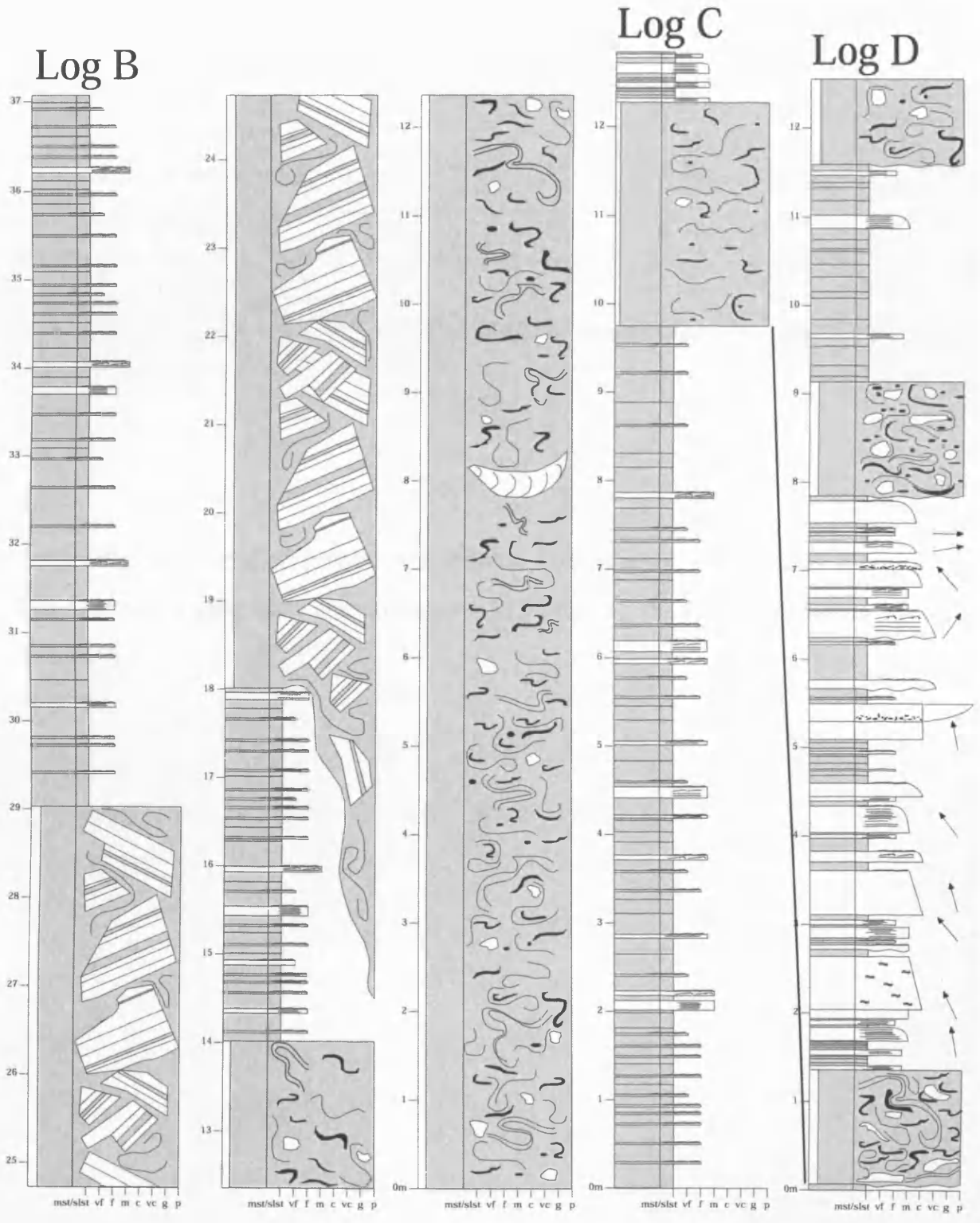
Log B
Log C
Log D
mst/slst vf f m c vc g p
0m

Appendix 5.3. Detailed bed-by-bed graphic sedimentary log through the Los Molinos II sand body and underlying MTCs (~ 82 m), Barranco Sierra, locality 4.

Appendix 5.4. Detailed bed-by-bed graphic sedimentary log through the Los Molinos II sand body (~ 40 m thick), Barranco Caixigosa, locality 3.

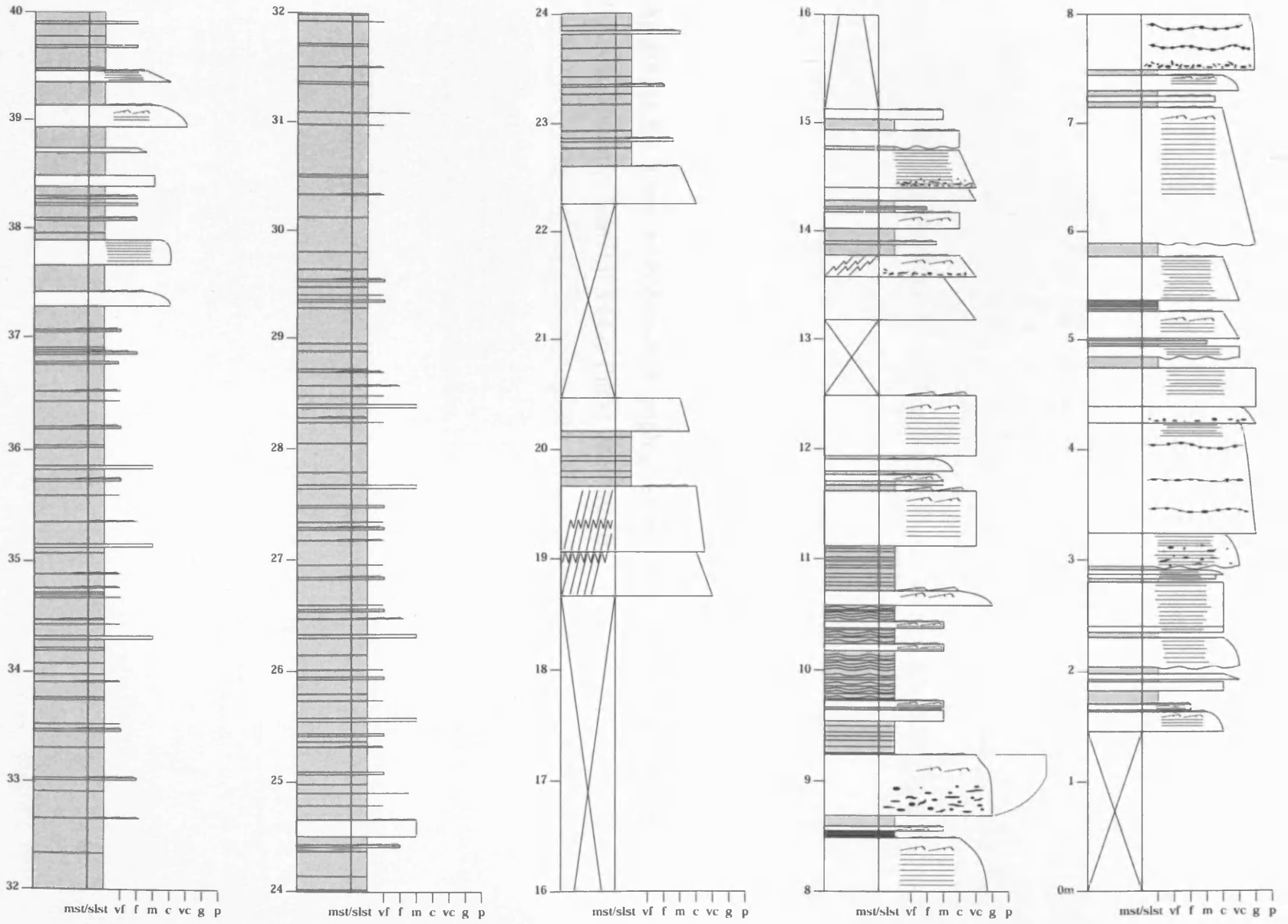
40
39
38
37
36
35
34
33
32
mst/slst vf f m c vc g p
32
31
30
29
28
27
26
25
24
mst/slst vf f m c vc g p
24
23
22
21
20
19
18
17
16
mst/slst vf f m c vc g p
16
15
14
13
12
11
10
9
8
mst/slst vf f m c vc g p
8
7
6
5
4
3
2
1
0m
mst/slst vf f m c vc g p

Appendix 5.5. Detailed bed-by-bed graphic sedimentary log through sands of the Arro system, Charo hill (44 m thick), locality 10.

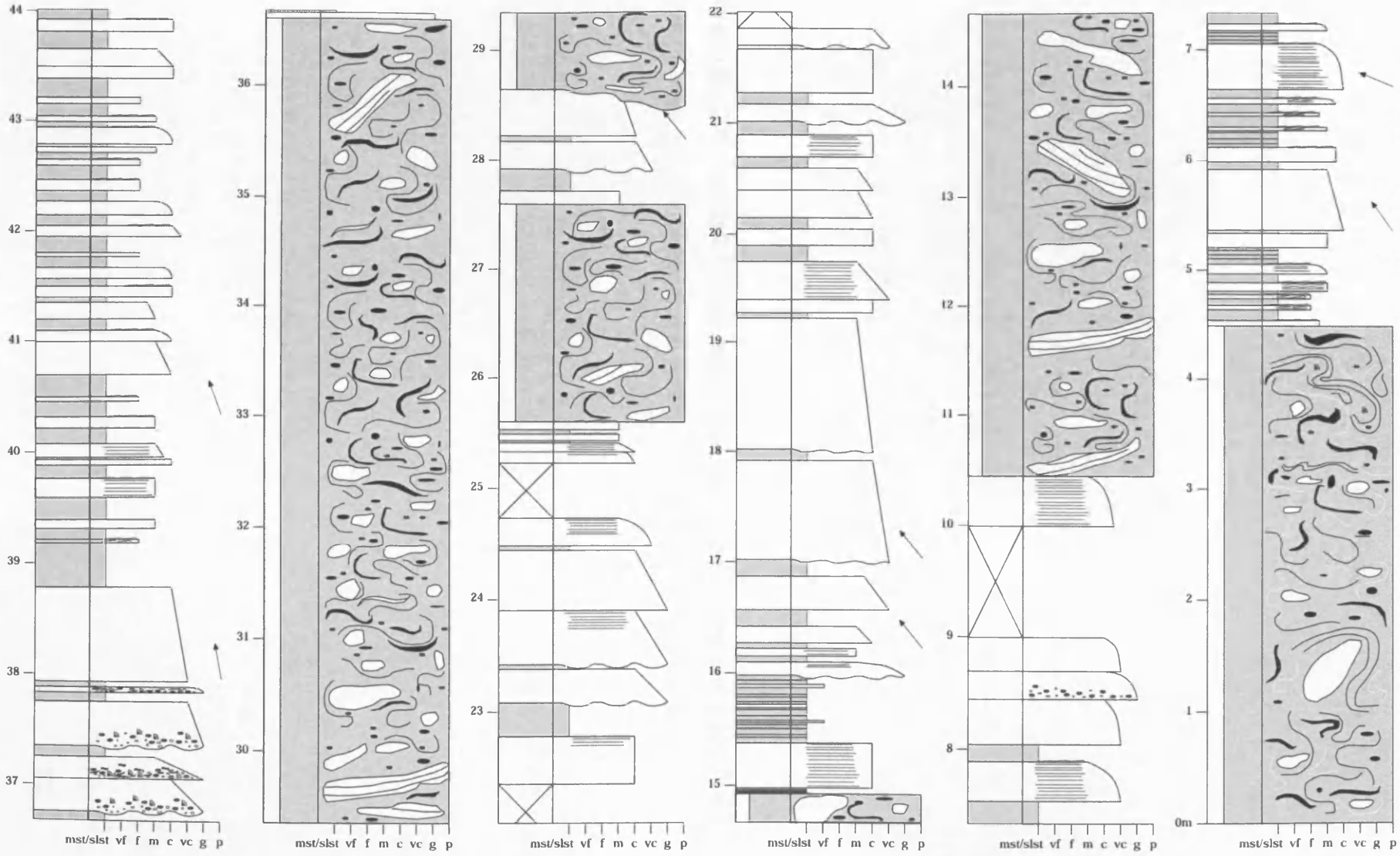
44
43
42
41
40
39
38
37
36
35
34
33
32
31
30
29
28
27
26
25
24
23
22
21
20
19
18
17
16
15
14
13
12
11
10
9
8
7
6
5
4
3
2
1
0m
mst/slst vf f m c vc g p

Appendix 5.6. Detailed bed-by-bed graphic sedimentary log and trace fossil data through the Arro System, Rio Nata (~ 138 m thick).

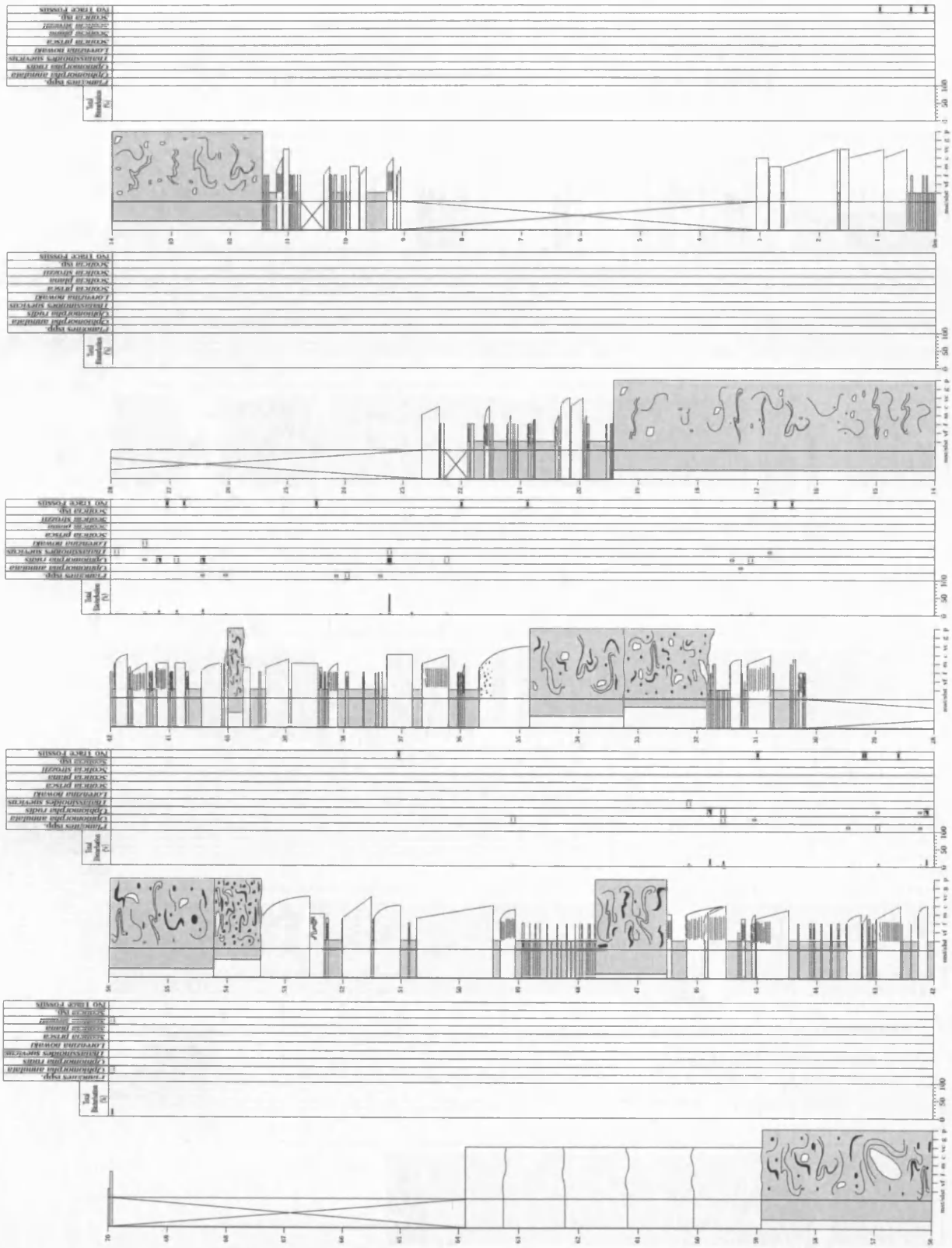

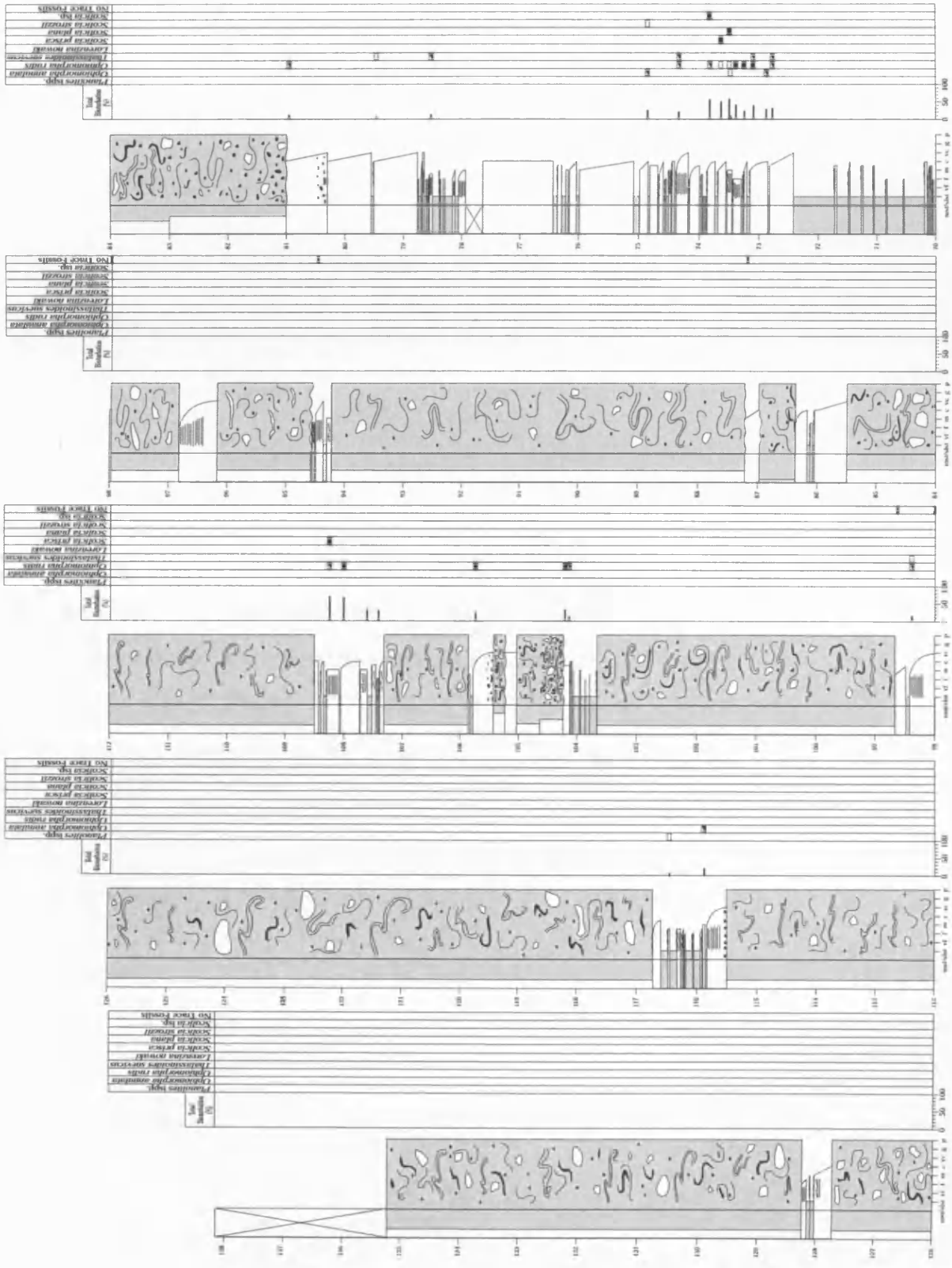
Total Bioturbation (%)
Trunkites hapl.
Cylindrichnus annulata
Cylindrichnus isp.
Thalassinoides suevicus
Lorenzinia bowsei
Scolicia prisca
Scolicia plana
Scolicia strozzi
Scolicia isp.
Two Trace Fossils

Appendix 5.7. Detailed bed-by-bed graphic sedimentary log through the Arro System, Bco. Sierra (~ 179 m thick).

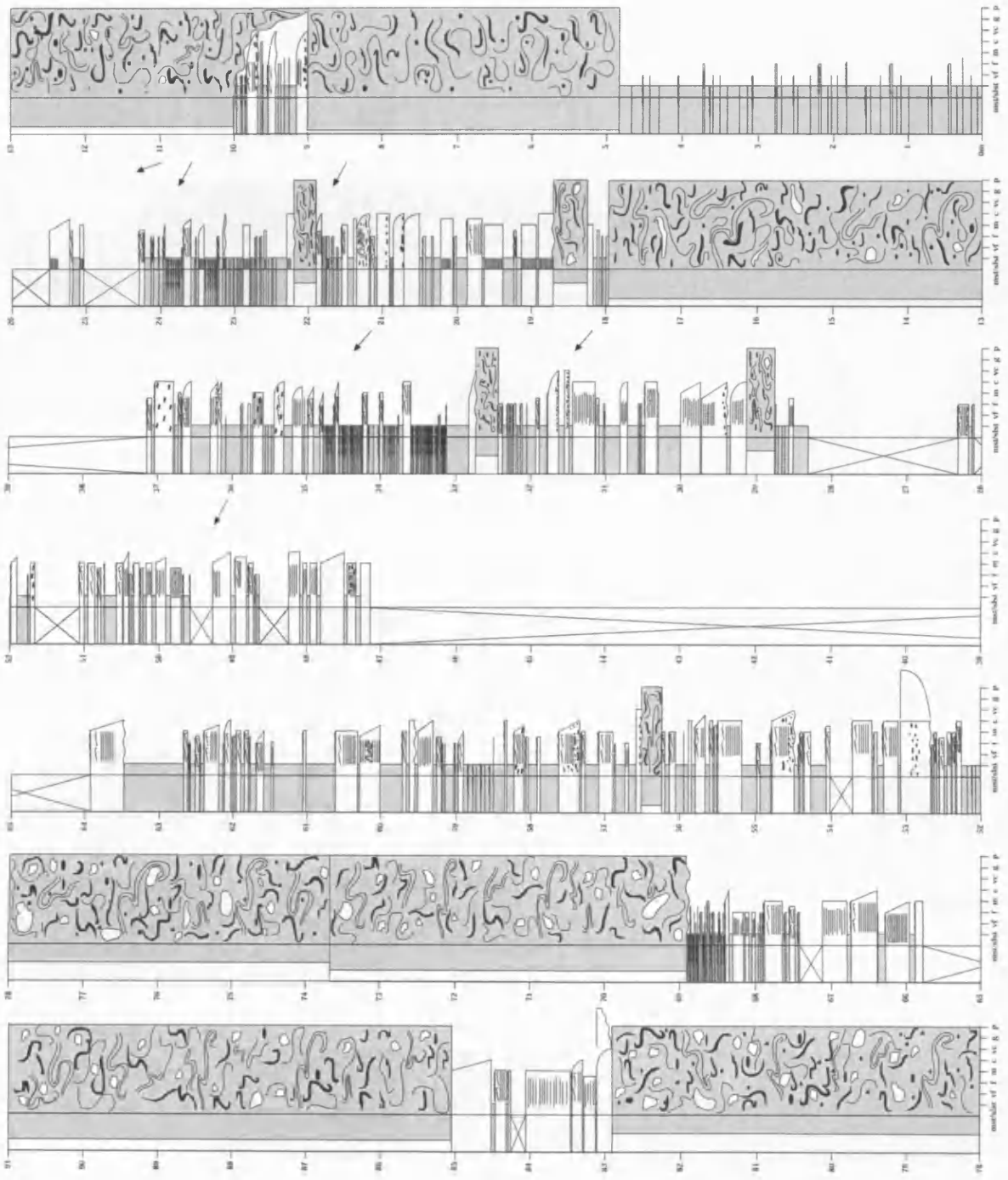

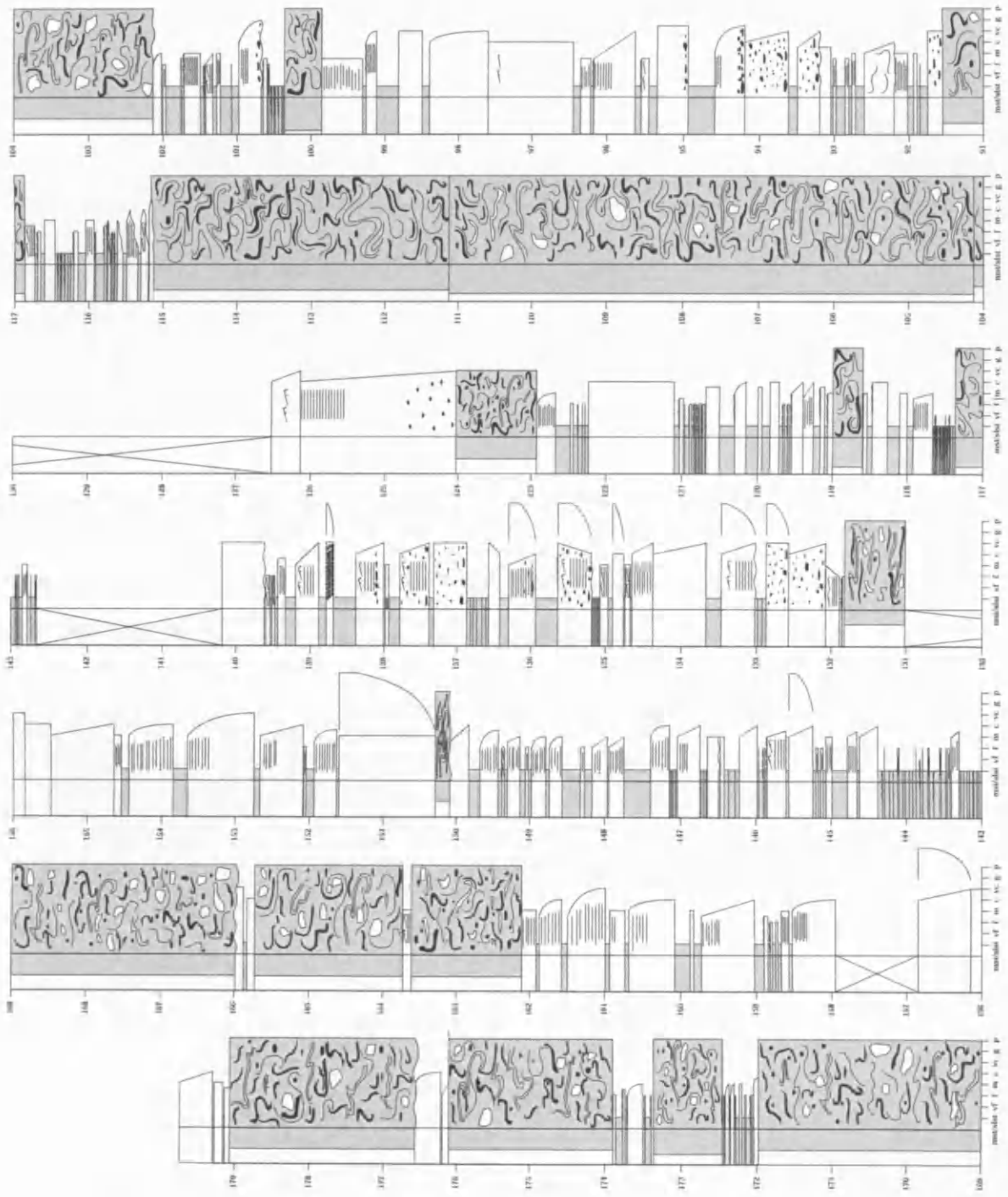

Appendix 5.8. Detailed bed-by-bed graphic sedimentary log and trace fossil data through the Arro System, Bco. Sierra road section (~ 136 m thick).

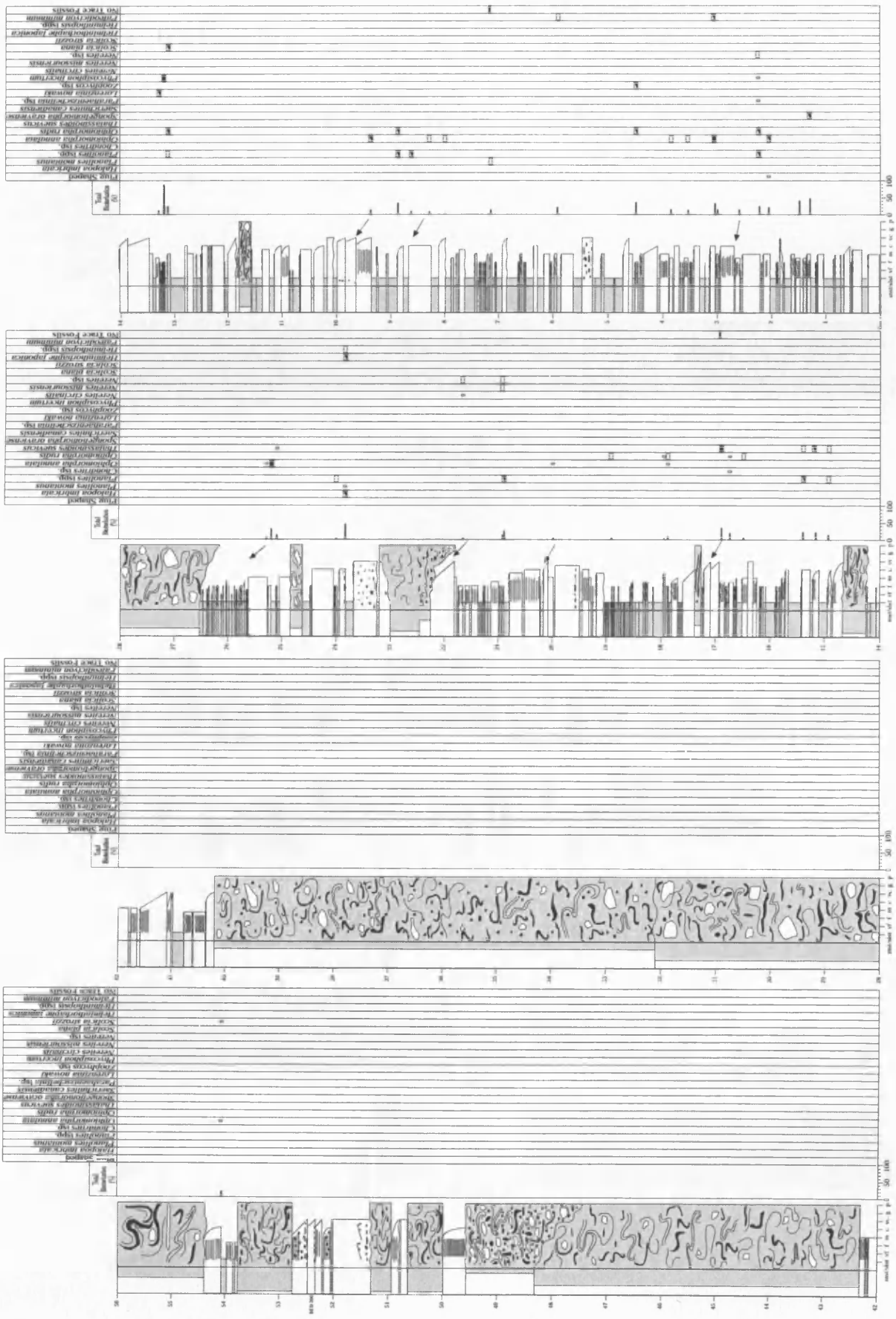

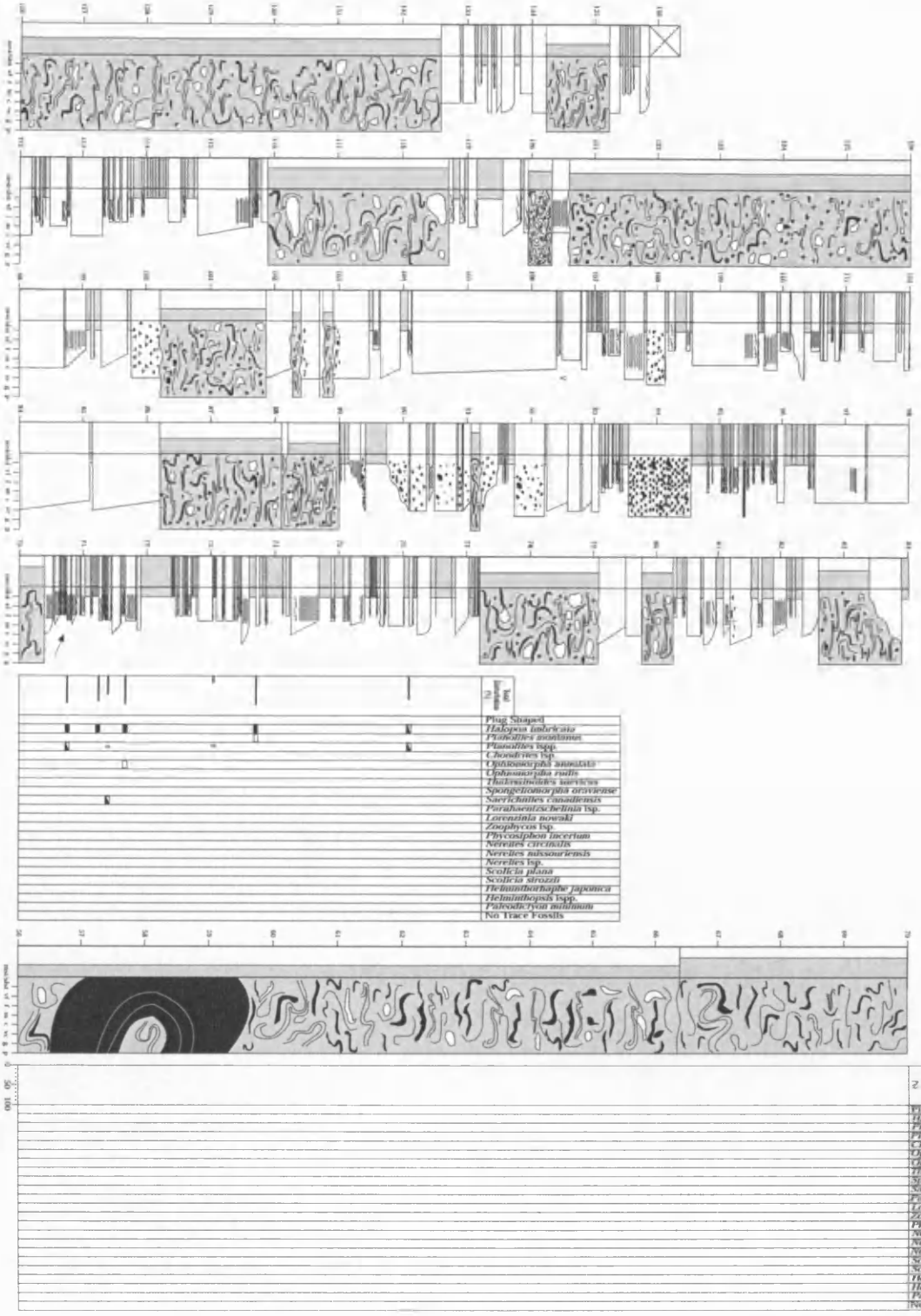
Plug Shaped
Halopoa imbricata
Phalcides bonianus
Planolites isp.
Chondrites isp.
Ophiomorpha annulata
Ophiomorpha rudis
Thalassinoides suevicus
Spongeliomorpha oravense
Saerichnites canadiensis
Parahaentzschellnia isp.
Lorenzinia noviki
Zoophycos isp.
Phycosiphon incertum
Nereites circinatis
Nereites missouriensis
Nereites isp.
Scolicia plana
Scolicia strozzi
Helminthoraphe japonica
Helminthopsis isp.
Paleodictyon minimum
No Trace Fossils

Appendix 5.9. Detailed bed-by-bed graphic sedimentary log and trace fossil data through the Arro System, Santa Catalina (~ 42 m thick).

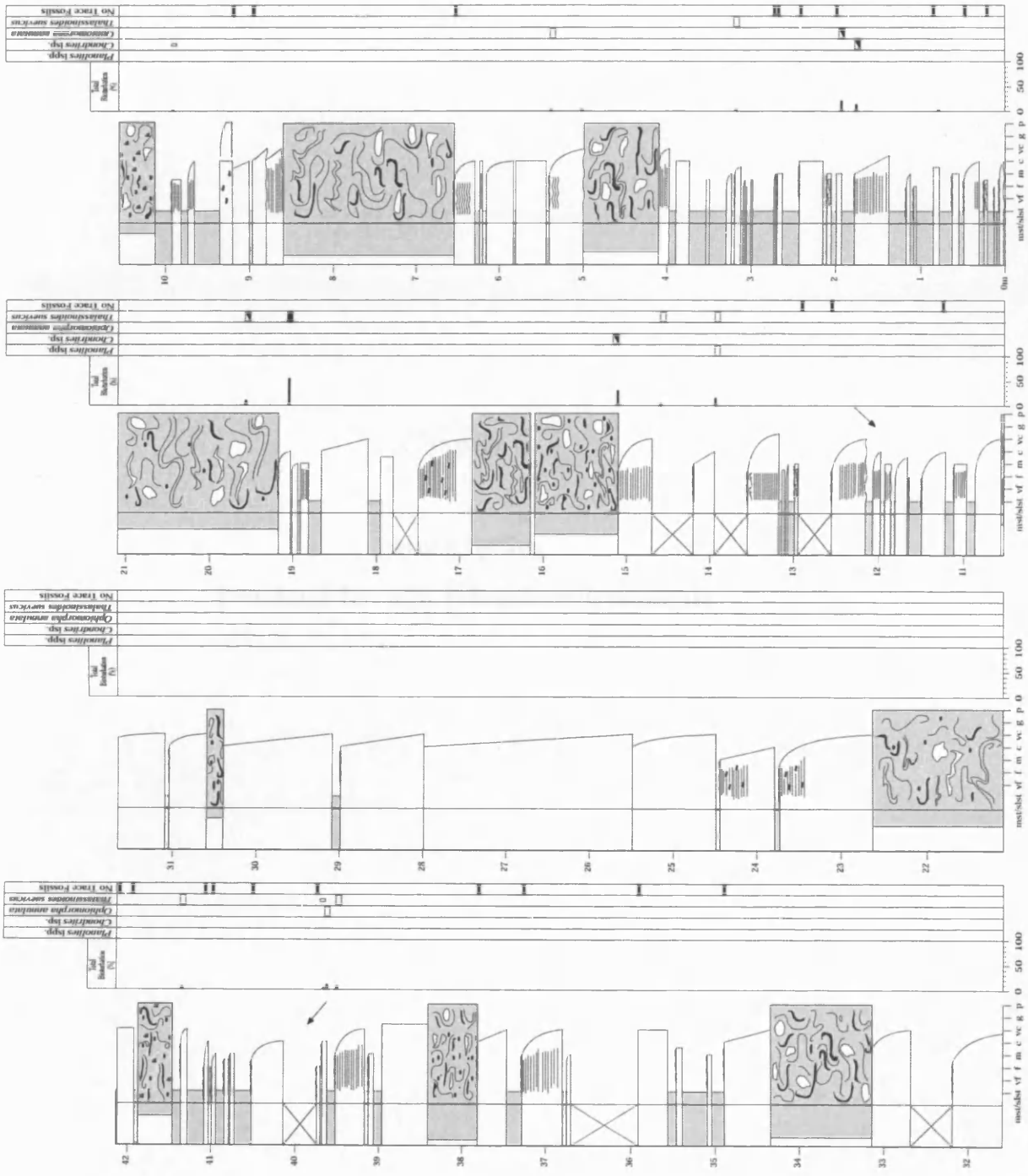
No Trace Fossils
Thalassinoides suevicus
Ophiomorpha annulata
Chondrites isp.
Planolites isp.
Total Bioturbation (%)
0
50
100
msl/shi vf f m c vc g p
0m
1
2
3
4
5
6
7
8
9
10
11
12
13
14
15
16
17
18
19
20
21
22
23
24
25
26
27
28
29
30
31
32
33
34
35
36
37
38
39
40
41
42

Chapter 6

Ainsa basin:
Proximal fan and related environments

Appendix 6.1 Detailed bed-by-bed graphic sedimentary log (~ 110 m thick) and trace fossil data through canyon deposits, Gerbe system, Charo, locality 10.

mud/silt vf f m c vc g p 0 50 100
Bathyalis (m)
Ophiomorpha annulata
Ophiomorpha nodosa
Thalassinoides suevicus
Thalassinoides isp. indet
No Traces

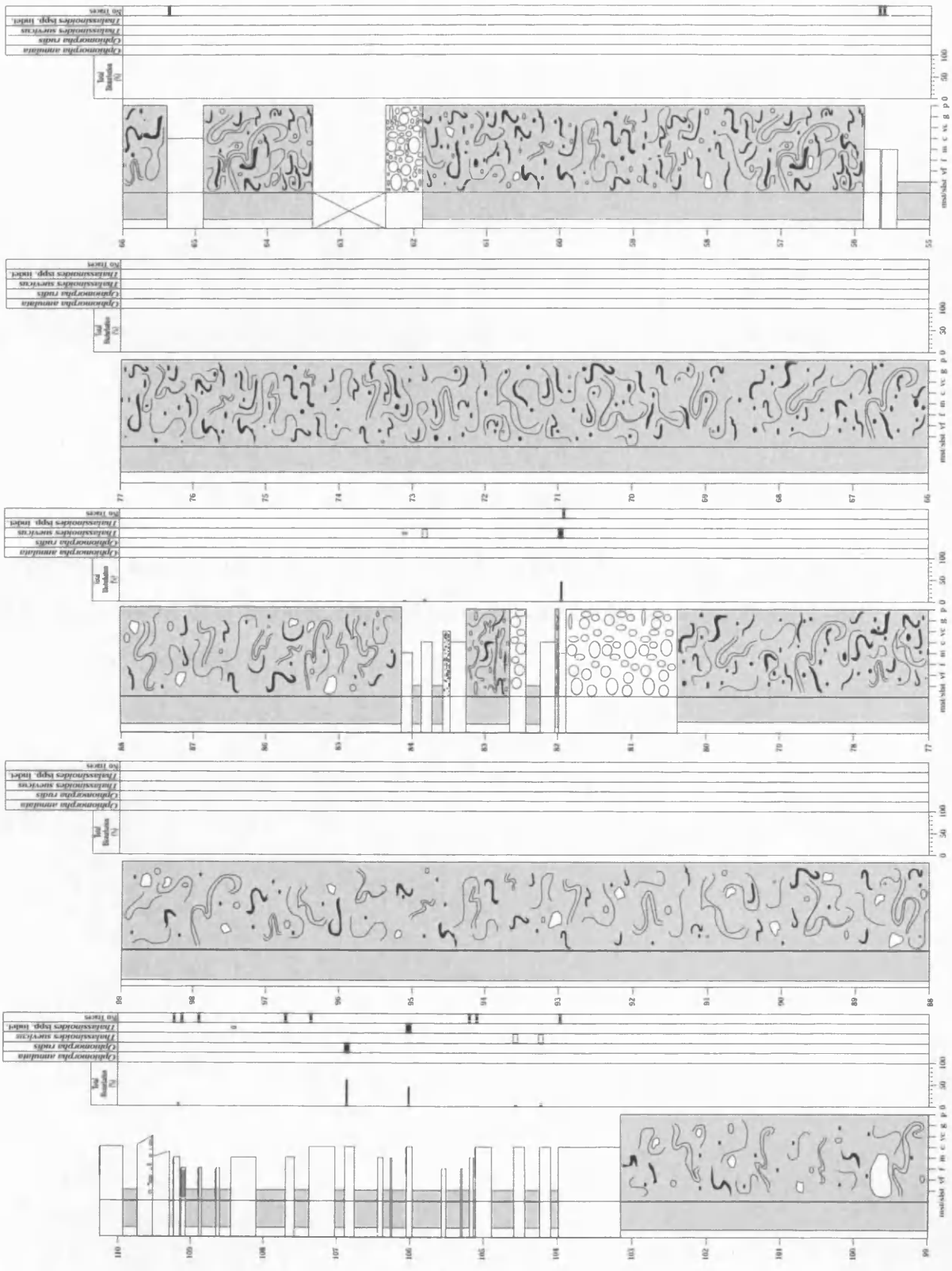

Appendix 6.2. Detailed bed-by-bed graphic sedimentary log (~ 17 m thick) and trace fossil data through channel axis deposits, Gerbe I sandbody (log I), Rio Nata, locality 11.

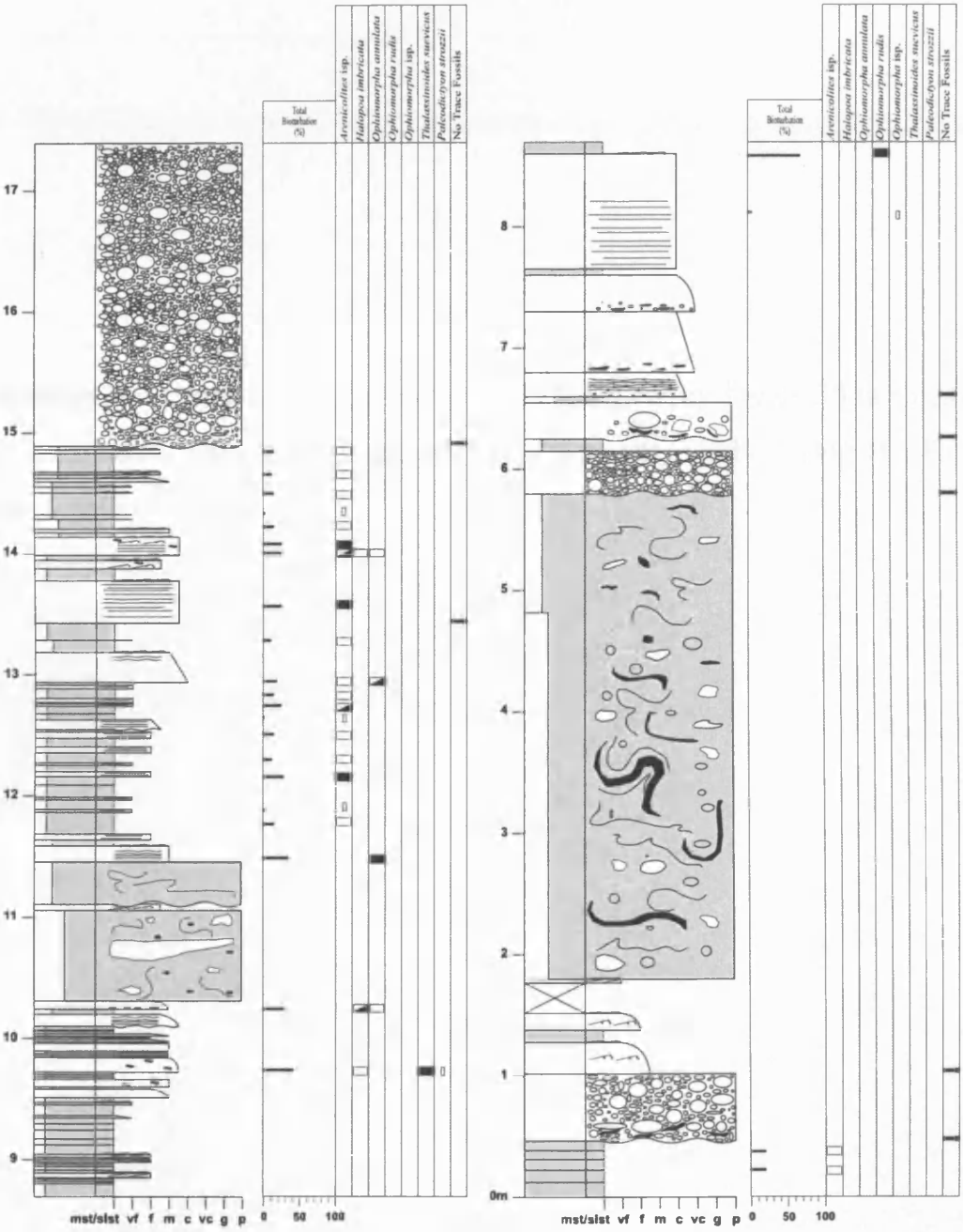
17
16
15
14
13
12
11
10
9
mst/slst vf f m c vc g p
Total Bioturbation (%)
0 50 100
Arenicolites isp.
Halopoa imbricata
Ophiomorpha annulata
Ophiomorpha rudis
Ophiomorpha isp.
Thalassinoides suevicus
Paleodictyon strozzii
No Trace Fossils
8
7
6
5
4
3
2
1
0m
mst/slst vf f m c vc g p
Total Bioturbation (%)
0 50 100
Arenicolites isp.
Halopoa imbricata
Ophiomorpha annulata
Ophiomorpha rudis
Ophiomorpha isp.
Thalassinoides suevicus
Paleodictyon strozzii
No Trace Fossils

Appendix 6.3 Detailed bed-by-bed graphic sedimentary log (~ 30 m thick) and trace fossil data through channel axis deposits, Gerbe I (log II), Rio Nata, locality 11.

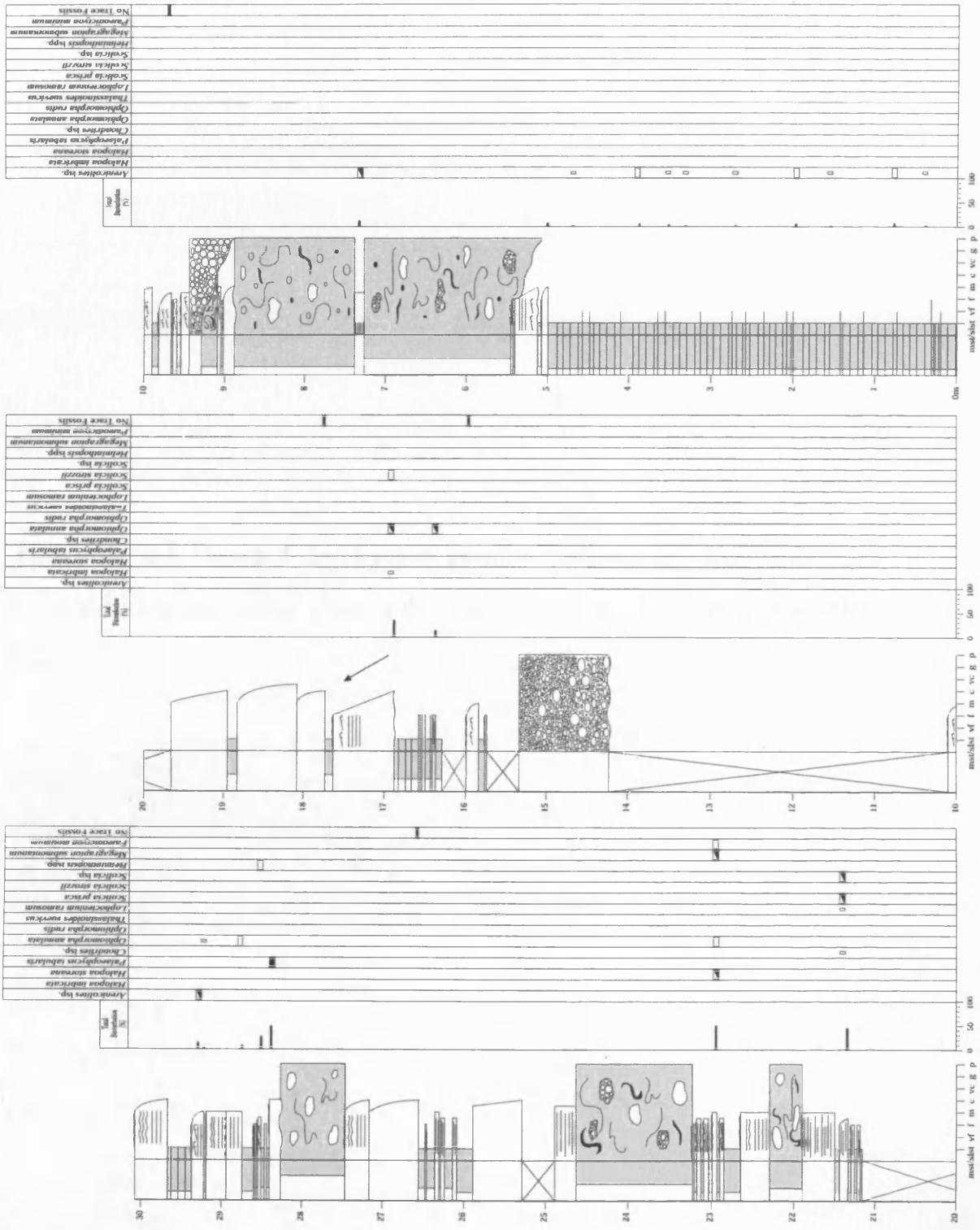
No Trace Fossils
Paraconcyne maximum
Megagraphon submontanum
Helminthopsis hipp.
Scolicia isp.
Scolicia astorzii
Scolicia prisca
Thalassinoides suevicus
Lophoctenium ramosum
Cylindrichnus isp.
Cylindrichnus annulata
Cylindrichnus tadis
Chondrites isp.
Palaeophycus tubularis
Halopoa sinuosa
Halopoa imbricata
Arenicolites isp.
Total Bioturbation (%)
0 50 100
mud/silt vf f m c vc g p
10 9 8 7 6 5 4 3 2 1 0m
No Trace Fossils
Paraconcyne maximum
Megagraphon submontanum
Helminthopsis hipp.
Scolicia isp.
Scolicia astorzii
Scolicia prisca
Thalassinoides suevicus
Lophoctenium ramosum
Cylindrichnus annulata
Cylindrichnus tadis
Chondrites isp.
Palaeophycus tubularis
Halopoa sinuosa
Halopoa imbricata
Arenicolites isp.
Total Bioturbation (%)
0 50 100
mud/silt vf f m c vc g p
20 19 18 17 16 15 14 13 12 11 10
No Trace Fossils
Paraconcyne maximum
Megagraphon submontanum
Helminthopsis hipp.
Scolicia isp.
Scolicia astorzii
Scolicia prisca
Thalassinoides suevicus
Lophoctenium ramosum
Cylindrichnus annulata
Cylindrichnus tadis
Chondrites isp.
Palaeophycus tubularis
Halopoa sinuosa
Halopoa imbricata
Arenicolites isp.
Total Bioturbation (%)
0 50 100
mud/silt vf f m c vc g p
30 29 28 27 26 25 24 23 22 21 20

Appendix 6.4 Detailed bed-by-bed graphic sedimentary logs and trace fossil data through upper slope gully and delta front deposits, Formigales, locality 12.

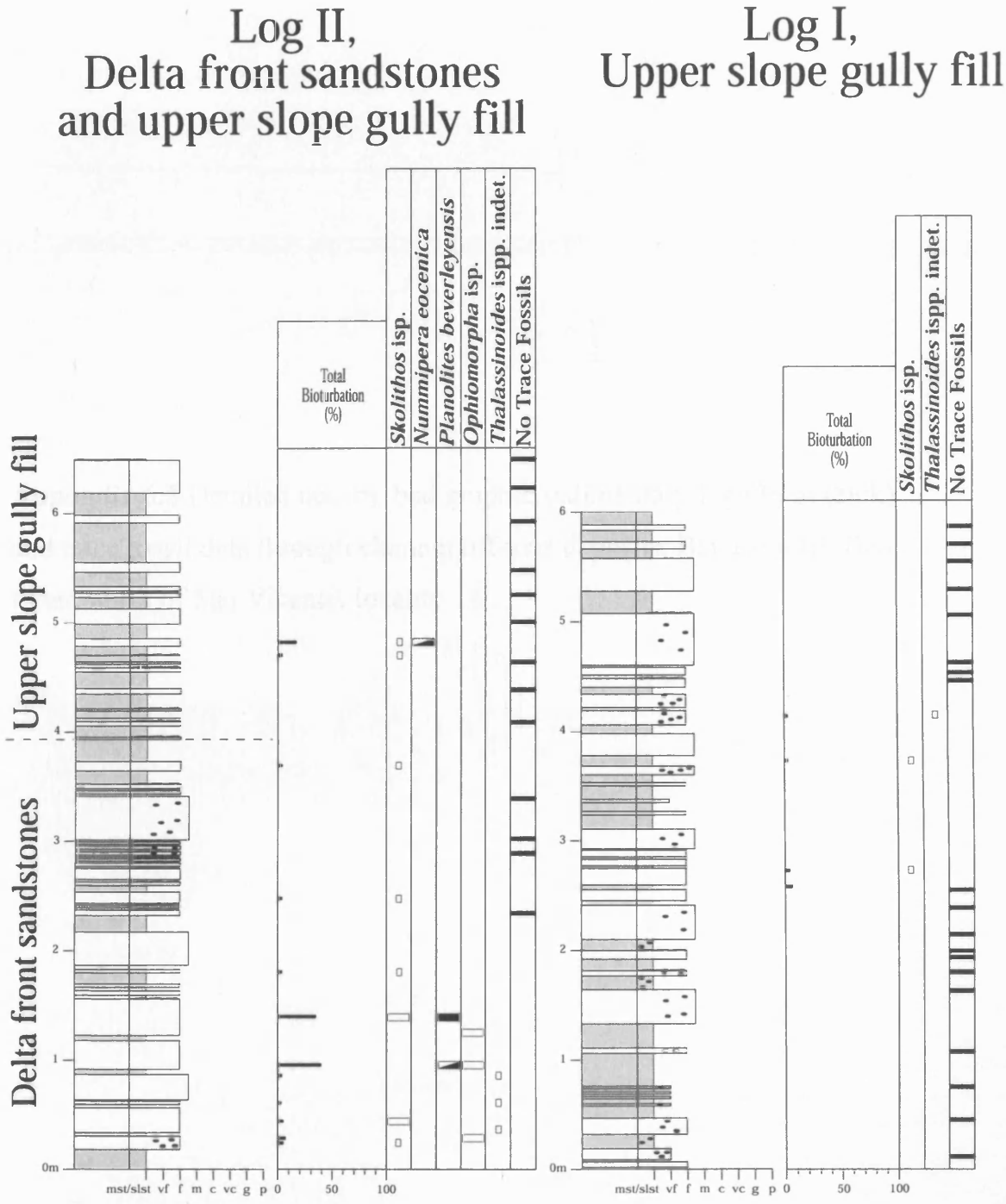
Log II,
Delta front sandstones
and upper slope gully fill
Log I,
Upper slope gully fill
Upper slope gully fill
Delta front sandstones
Total Bioturbation (%)
Skolithos isp.
Nummipera eocenica
Planolites beverleyensis
Ophiomorpha isp.
Thalassinoides ispp. indet.
No Trace Fossils
0m
1
2
3
4
5
6
mst/slst vf f m c vc g p
0
50
100

Appendix 6.5 Detailed bed-by-bed graphic sedimentary log (36 m thick) and trace fossil data through channel off-axis deposits, Banaston III, Bco. Pinar, north of San Vicente, locality 14.

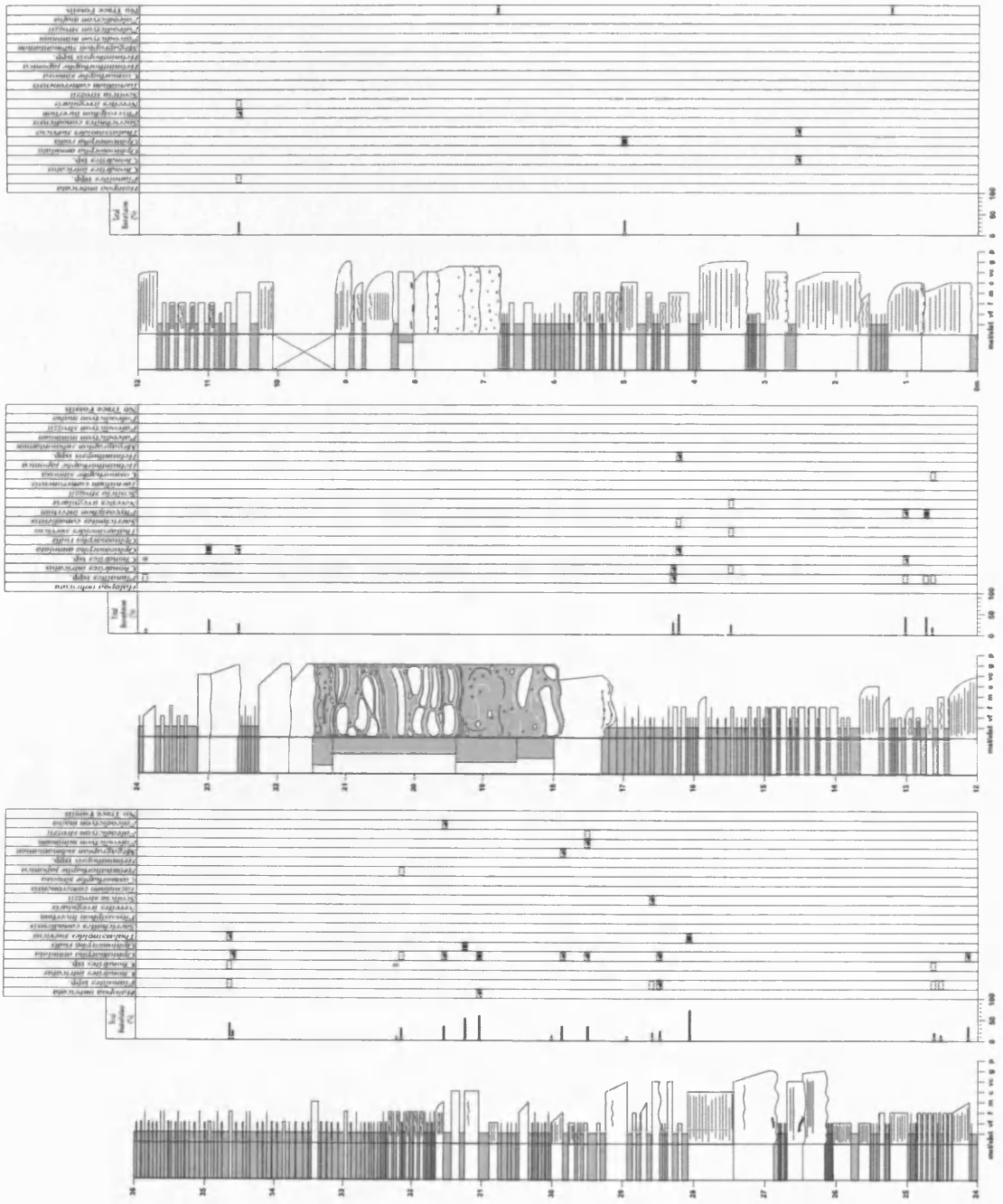

Appendix 6.6 Detailed bed-by-bed graphic sedimentary log (~ 18 m thick) and trace fossil data through channel axis deposits, Ainsa I, Bco. Royo, locality 19.

10
11
12
13
14
15
16
17
18
mst/slst vf f m c vc g p
0
50
100
Total Bioturbation (%)
Ophiomorpha annulata
Ophiomorpha rudis
Ophiomorpha isp.
Thalassinoides suevicus
Scolicia prisca
Scolicia isp.
No Trace Fossils
0m
1
2
3
4
5
6
7
8
9
mst/slst vf f m c vc g p
0
50
100
Total Bioturbation (%)
Ophiomorpha annulata
Ophiomorpha rudis
Ophiomorpha isp.
Thalassinoides suevicus
Scolicia prisca
Scolicia isp.
No Trace Fossils

Appendix 6.7 Detailed bed-by-bed graphic sedimentary log (~ 31 m thick) and trace fossil data through channel axis deposits, Ainsa I, Bco. Buchosa, Ainsa quarry, locality 15.

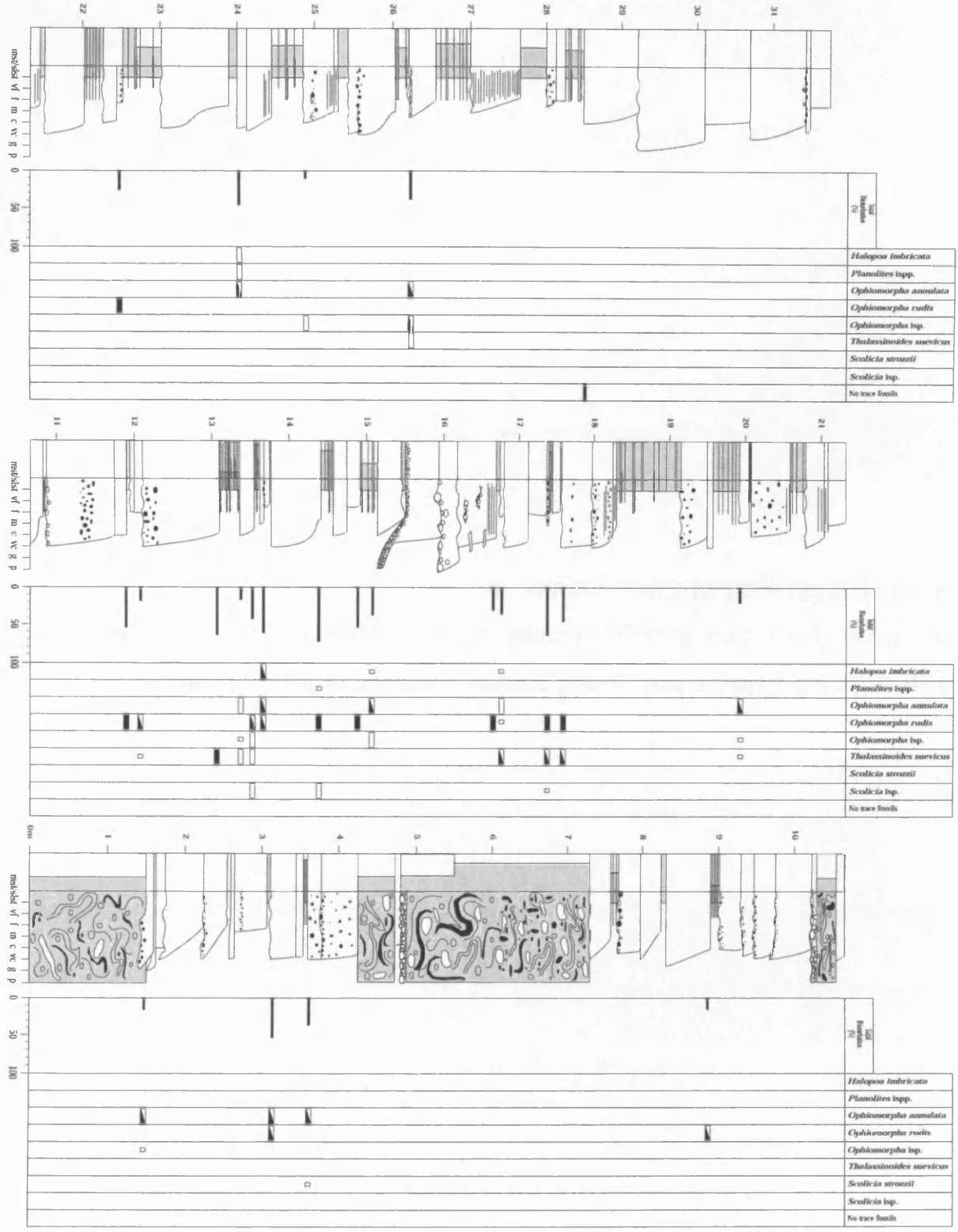
Halopoa imbricata
Planolites isp.
Ophiomorpha annulata
Ophiomorpha rudis
Ophiomorpha isp.
Thalassinoides suevicus
Scolicia strozzii
Scolicia isp.
No trace fossils

Appendix 6.8 Detailed bed-by-bed graphic sedimentary log (~ 10 m thick) and trace fossil data through channel off-axis deposits, Ainsa I. Road section (A138) south of Ainsa, locality 16.

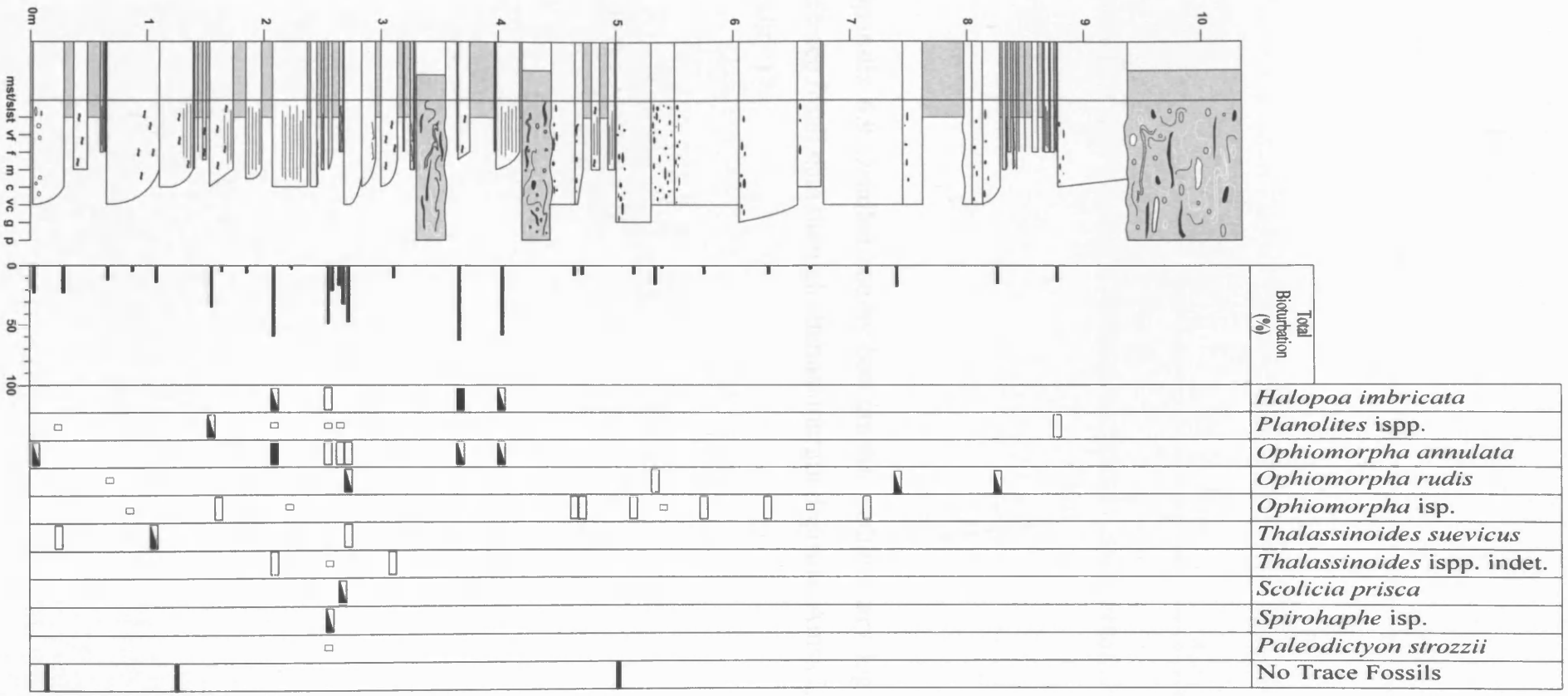
0m
1
2
3
4
5
6
7
8
9
10
mst/slst vf f m c vc g p
0
50
100
Total Bioturbation (%)
Halopoa imbricata
Planolites ispp.
Ophiomorpha annulata
Ophiomorpha rudis
Ophiomorpha isp.
Thalassinoides suevicus
Thalassinoides ispp. indet.
Scolicia prisca
Spirohaphe isp.
Paleodictyon strozzii
No Trace Fossils

Appendix 6.9 Detailed bed-by-bed graphic sedimentary log (13 m thick) and trace fossil data through channel margin deposits, Ainsa I, Bco. Forcaz, locality 17.

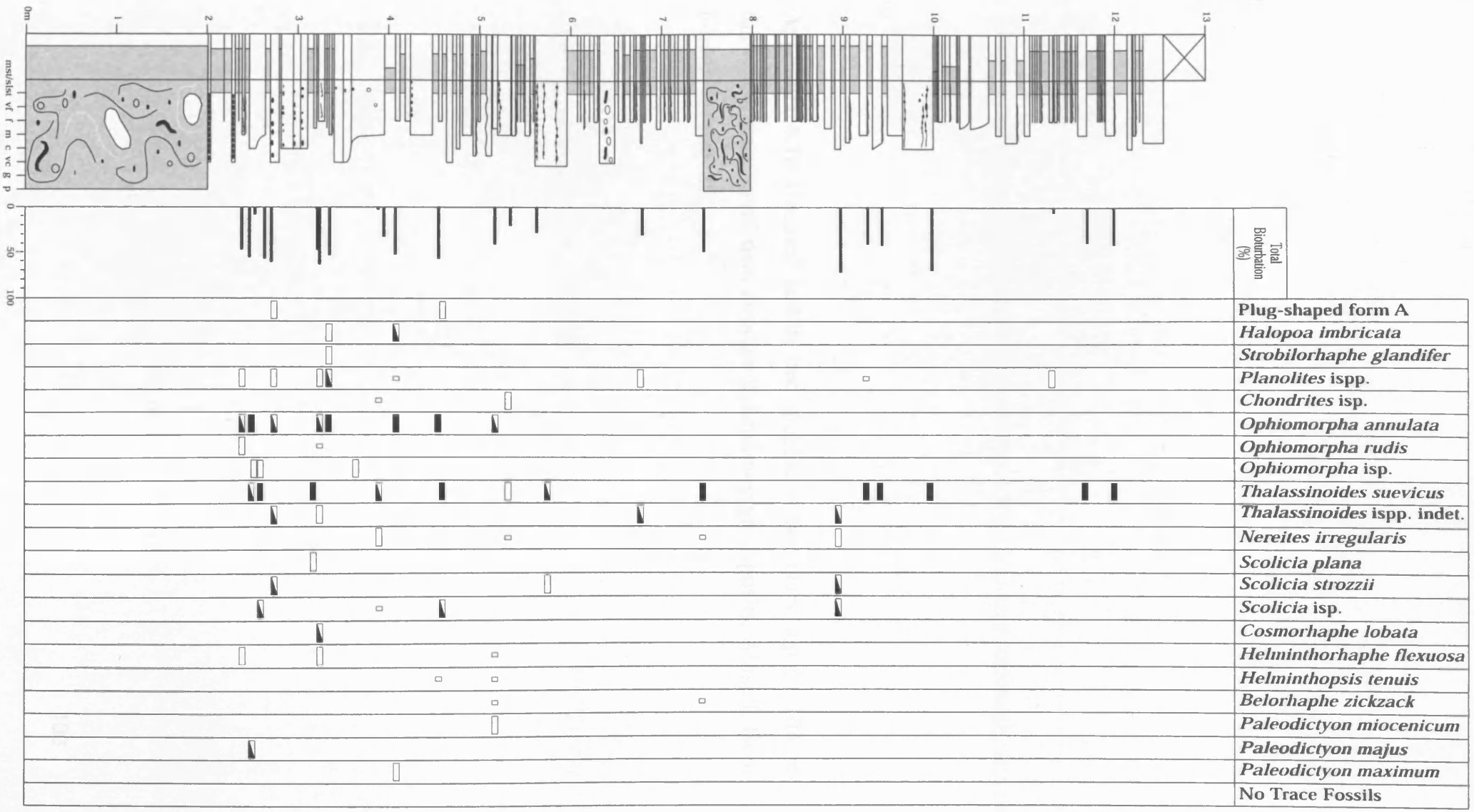
0m
1
2
3
4
5
6
7
8
9
10
11
12
13
mst/slst vf f m c vc g p
0
50
100
Total Bioturbation (%)
Plug-shaped form A
Halopoa imbricata
Strobilorhaphe glandifer
Planolites ispp.
Chondrites isp.
Ophiomorpha annulata
Ophiomorpha rudis
Ophiomorpha isp.
Thalassinoides suevicus
Thalassinoides ispp. indet.
Nereites irregularis
Scolicia plana
Scolicia strozzii
Scolicia isp.
Cosmorhaphe lobata
Helminthorhaphe flexuosa
Helminthopsis tenuis
Belorhaphe zickzack
Paleodictyon miocenicum
Paleodictyon majus
Paleodictyon maximum
No Trace Fossils

Appendix 6.10 Detailed bed-by-bed graphic sedimentary log (~ 103 m thick) and trace fossil data through channel margin deposits, Ainsa I, Bco. Forcaz, locality 20.

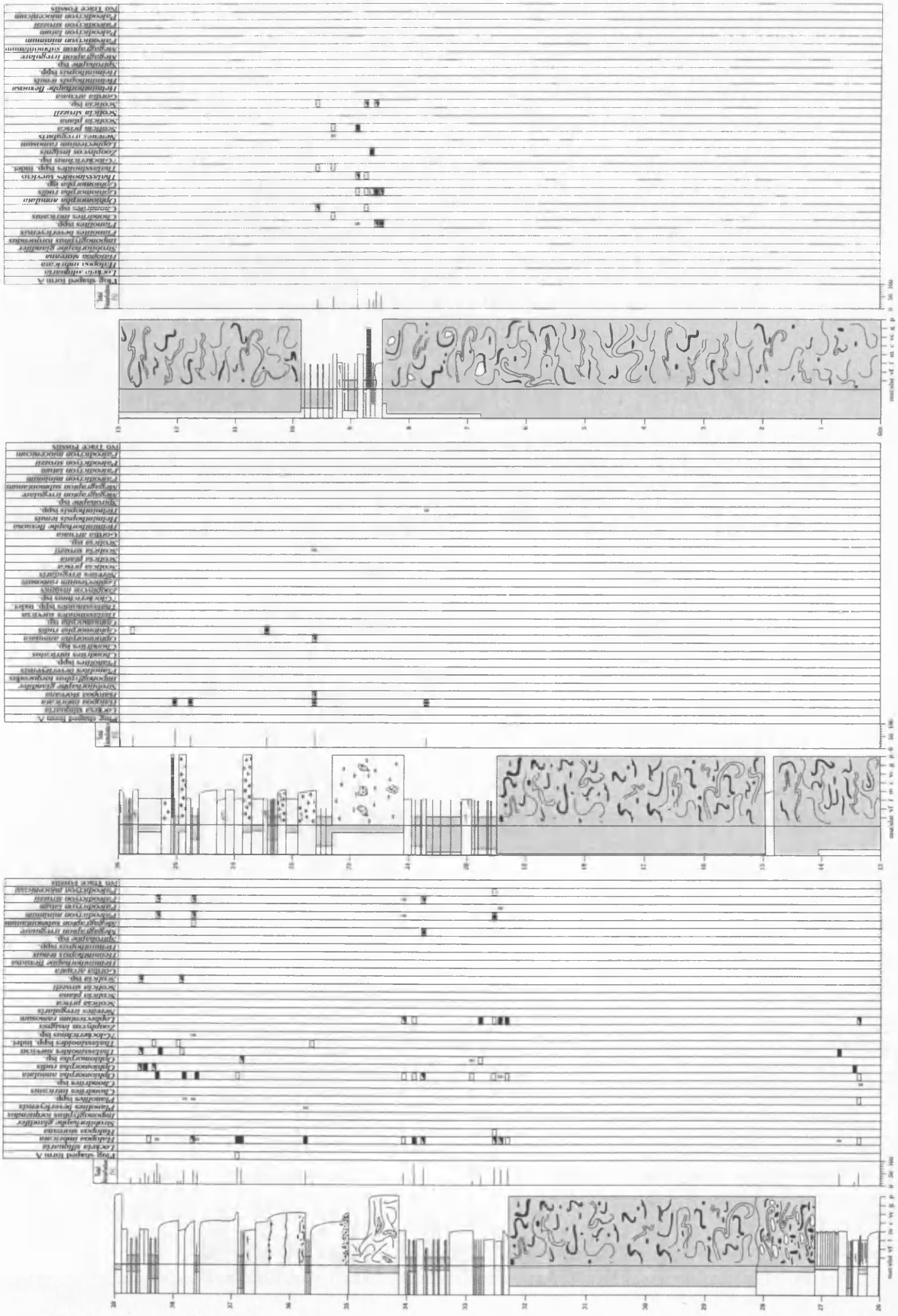

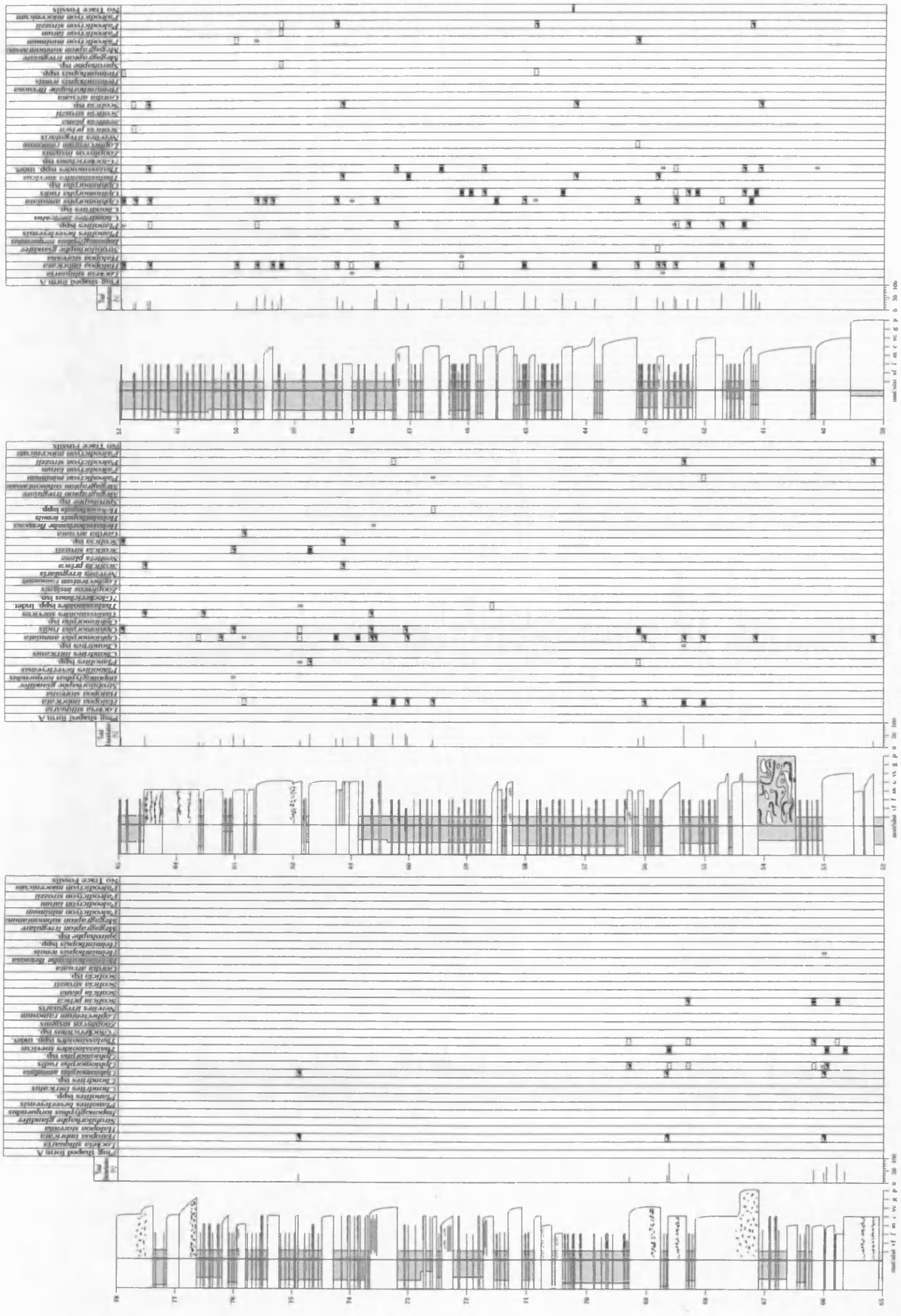

Plug shaped form A
Lockeia siliquaria
Halopoa imbricata
Halopoa sioreana
Strobilorhaphe glandifer
Impossibilophus torquendus
Planolites beverleyensis
Planolites ispp.
Chondrites intricatus
Chondrites isp.
Ophiomorpha annulata
Ophiomorpha rudis
Ophiomorpha isp.
Thalassinoides suevicus
Thalassinoides ispp. indet.
?Glockeriichnus isp.
Zoophycos insignis
Lophoctenium ramosum
Nereites irregularis
Scolicia prisca
Scolicia plana
Scolicia smithi
Scolicia isp.
Gordia arcuata
Helminthorhaphe flexuosa
Helminthopsis tenuis
Helminthopsis ispp.
Sparohaphe isp.
Megagrapton irregulare
Megagrapton submontanum
Paleodictyon minimum
Paleodictyon latum
Paleodictyon smithi
Paleodictyon miocenicum
No Trace Fossils

Appendix 6.11 Detailed bed-by-bed graphic sedimentary log (~ 10 m thick) and trace fossil data through outer channel-to-levee-overbank deposits, Ainsa I, Pena Montenesa hotel, locality 18.

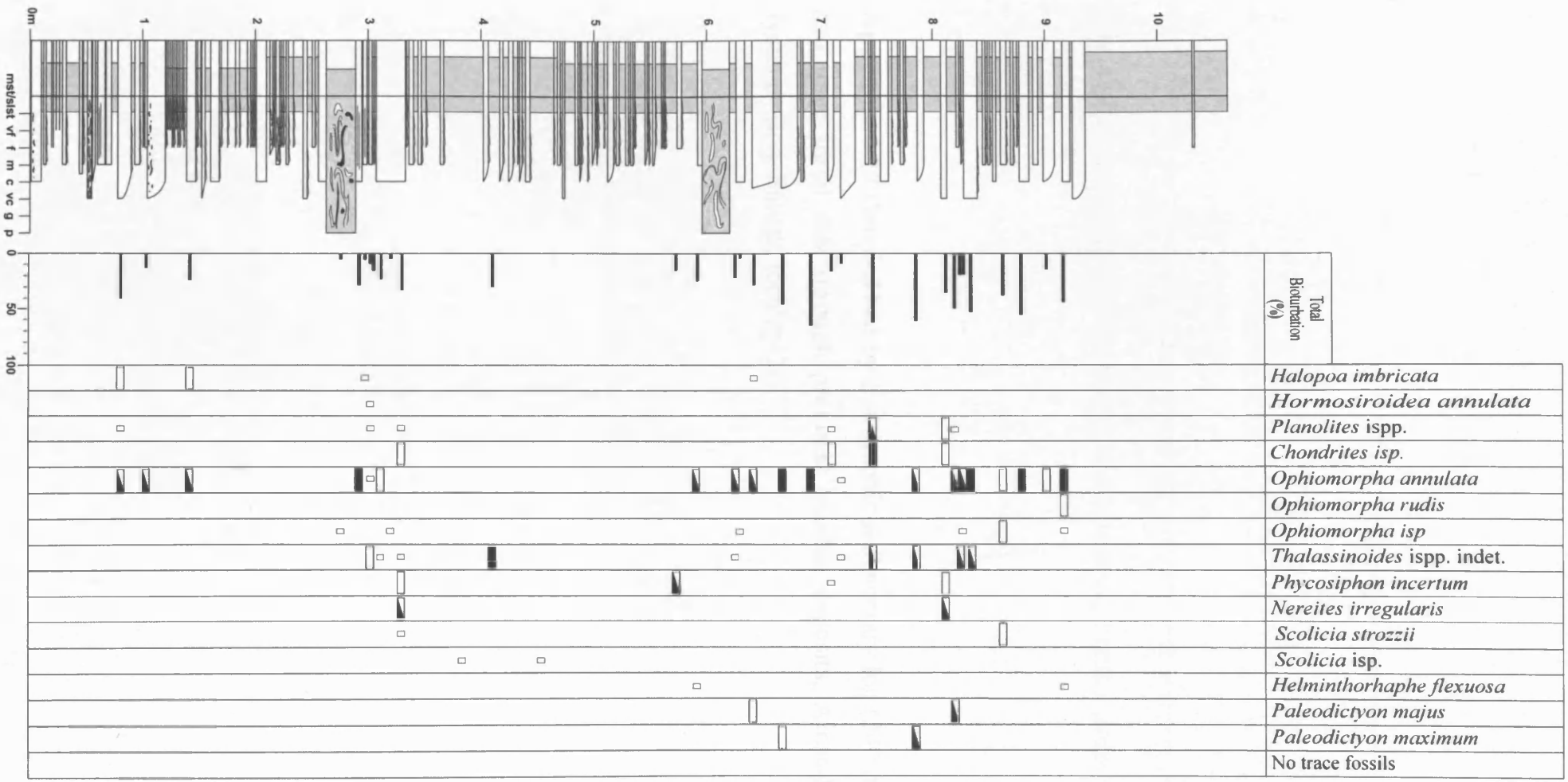
0m
1
2
3
4
5
6
7
8
9
10
ms/slst vf f m c vc g p
0
50
100
Total Bioturbation (%)
Halopoa imbricata
Hormosiroidea annulata
Planolites ispp.
Chondrites isp.
Ophiomorpha annulata
Ophiomorpha rudis
Ophiomorpha isp
Thalassinoides ispp. indet.
Phycosiphon incertum
Nereites irregularis
Scolicia strozzii
Scolicia isp.
Helminthorhaphe flexuosa
Paleodictyon majus
Paleodictyon maximum
No trace fossils

Appendix 6.12 Detailed bed-by-bed graphic sedimentary log (240 m thick) and trace fossil data through proximal interfan deposits, Ainsa-Morillo systems, Bco. Forcaz, locality 21.

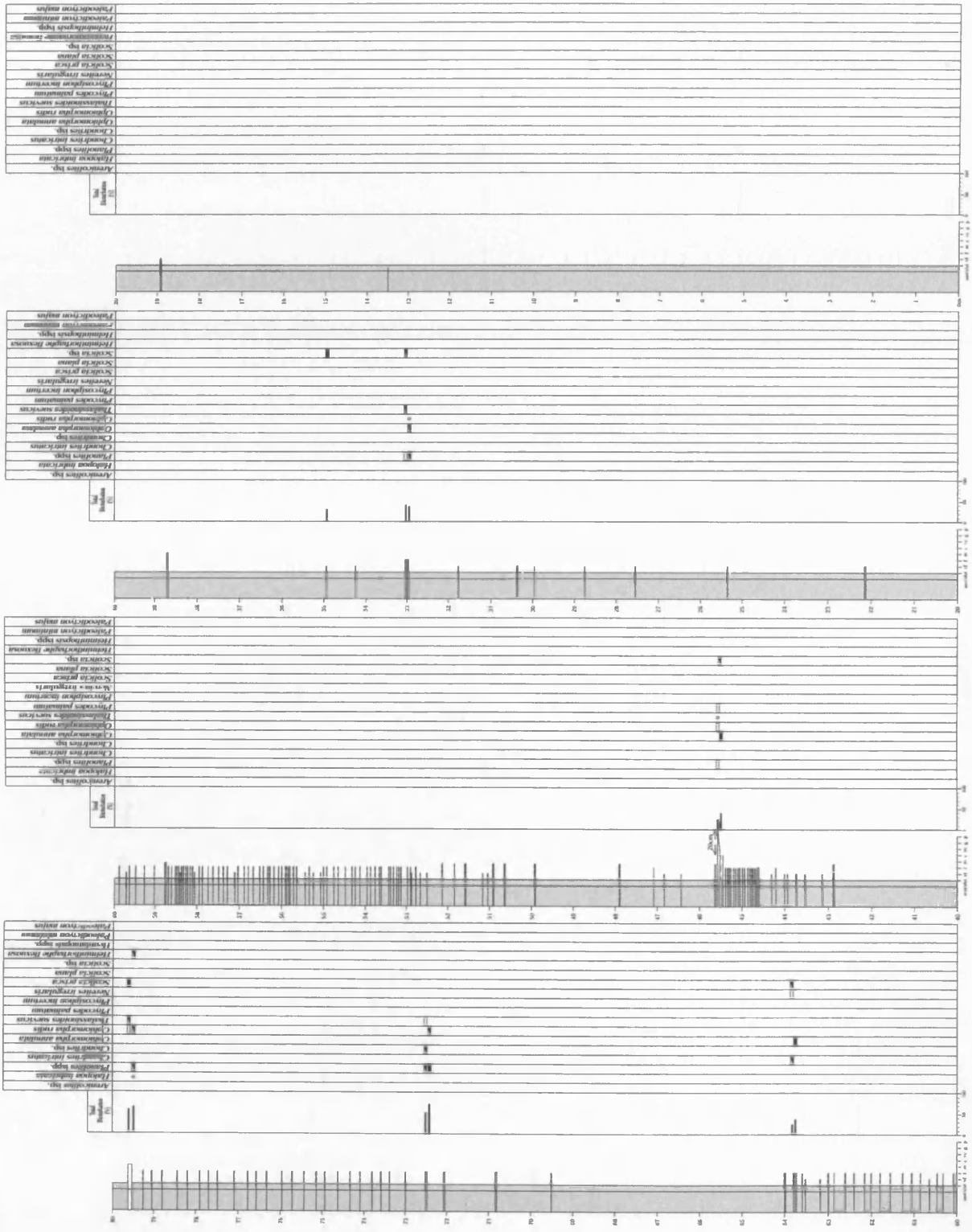

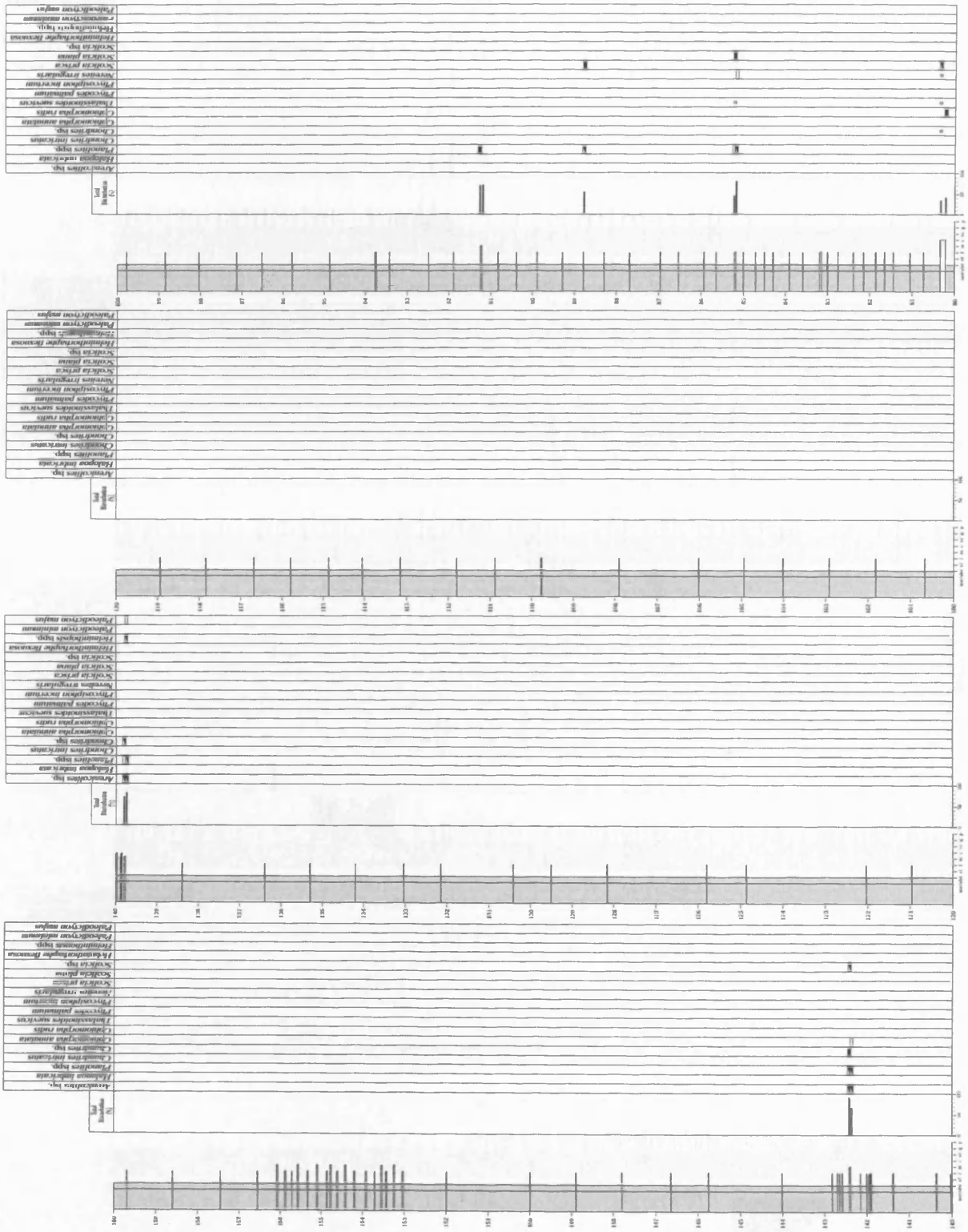

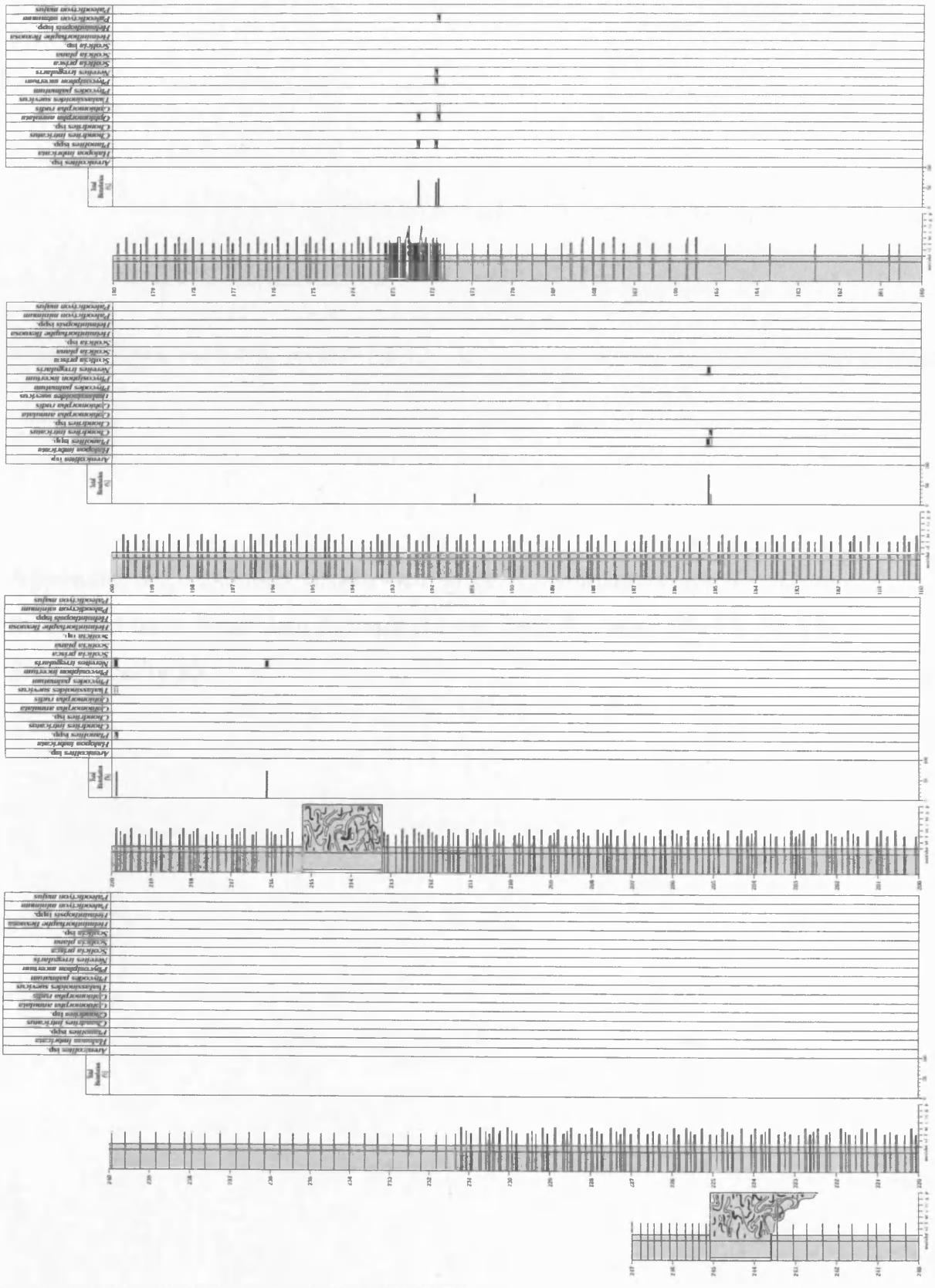

Appendix 6.13 Detailed bed-by-bed graphic sedimentary log (~ 47 m thick) and trace fossil data through channel axis deposits, Morillo II, Rio Sieste, locality 23.

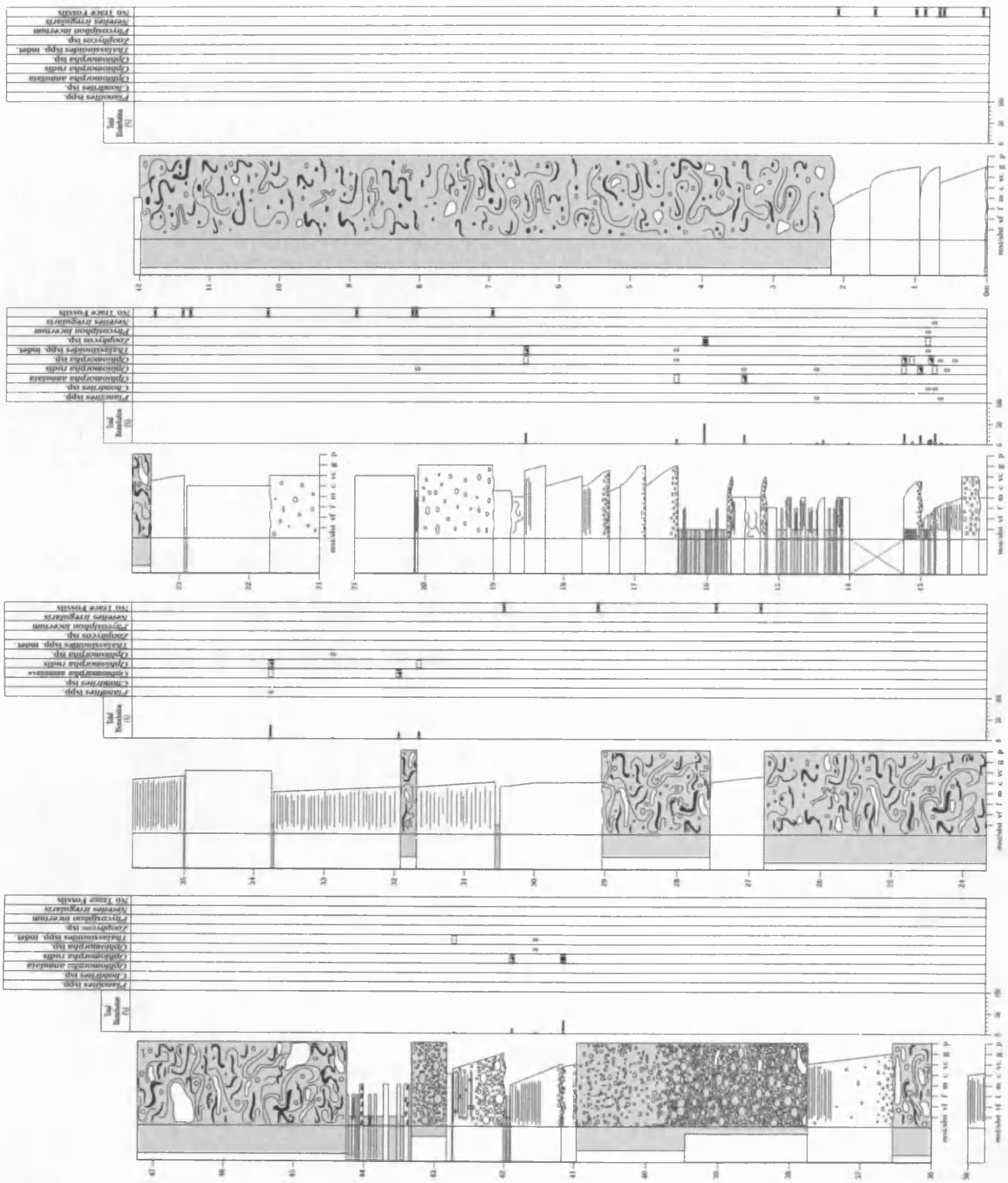

Appendix 6.14 Detailed bed-by-bed graphic sedimentary log (81 m thick) and trace fossil data through channel margin deposits, Morillo I, Bco. Cotón, north of Morillo de tou, locality 22.

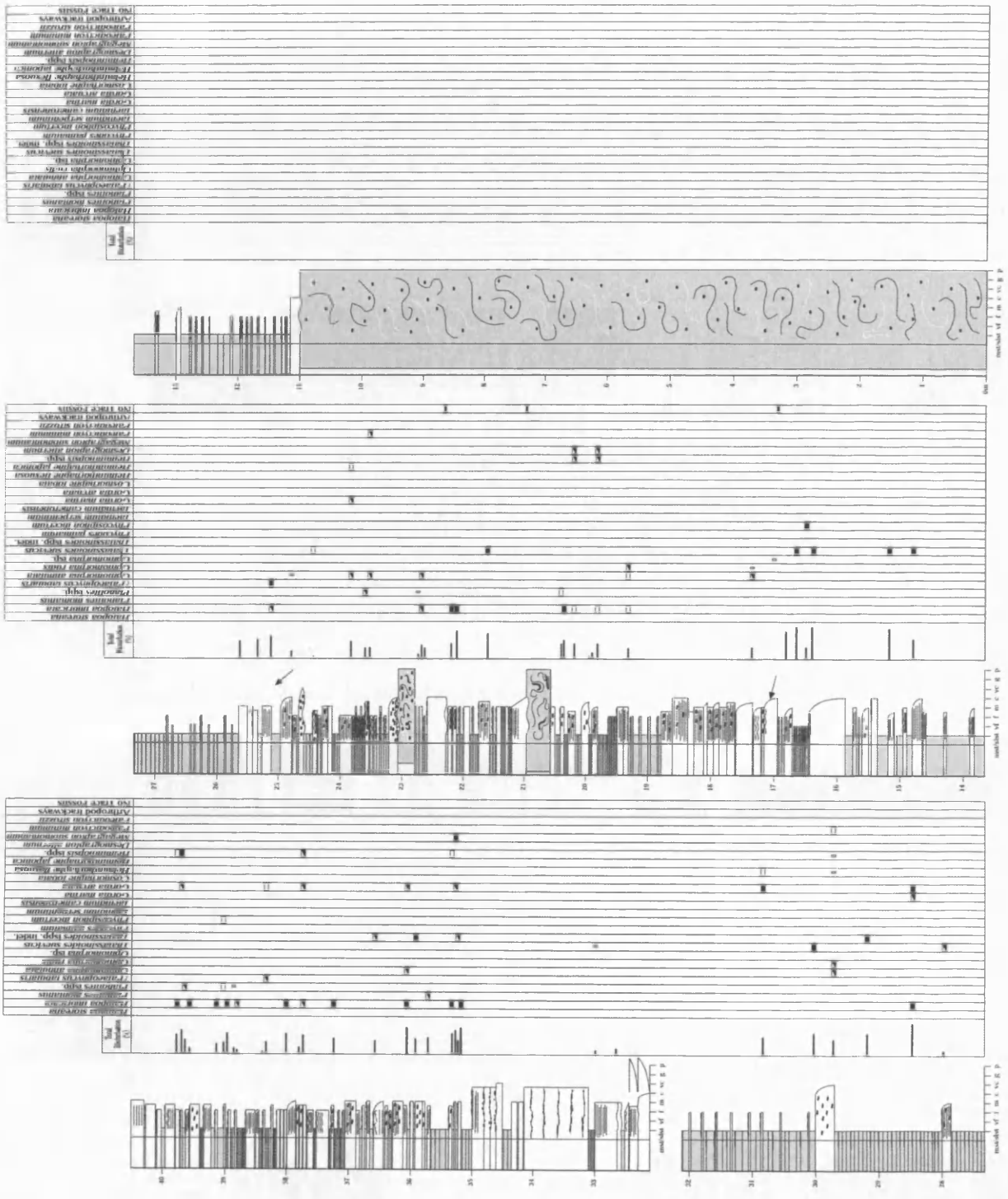

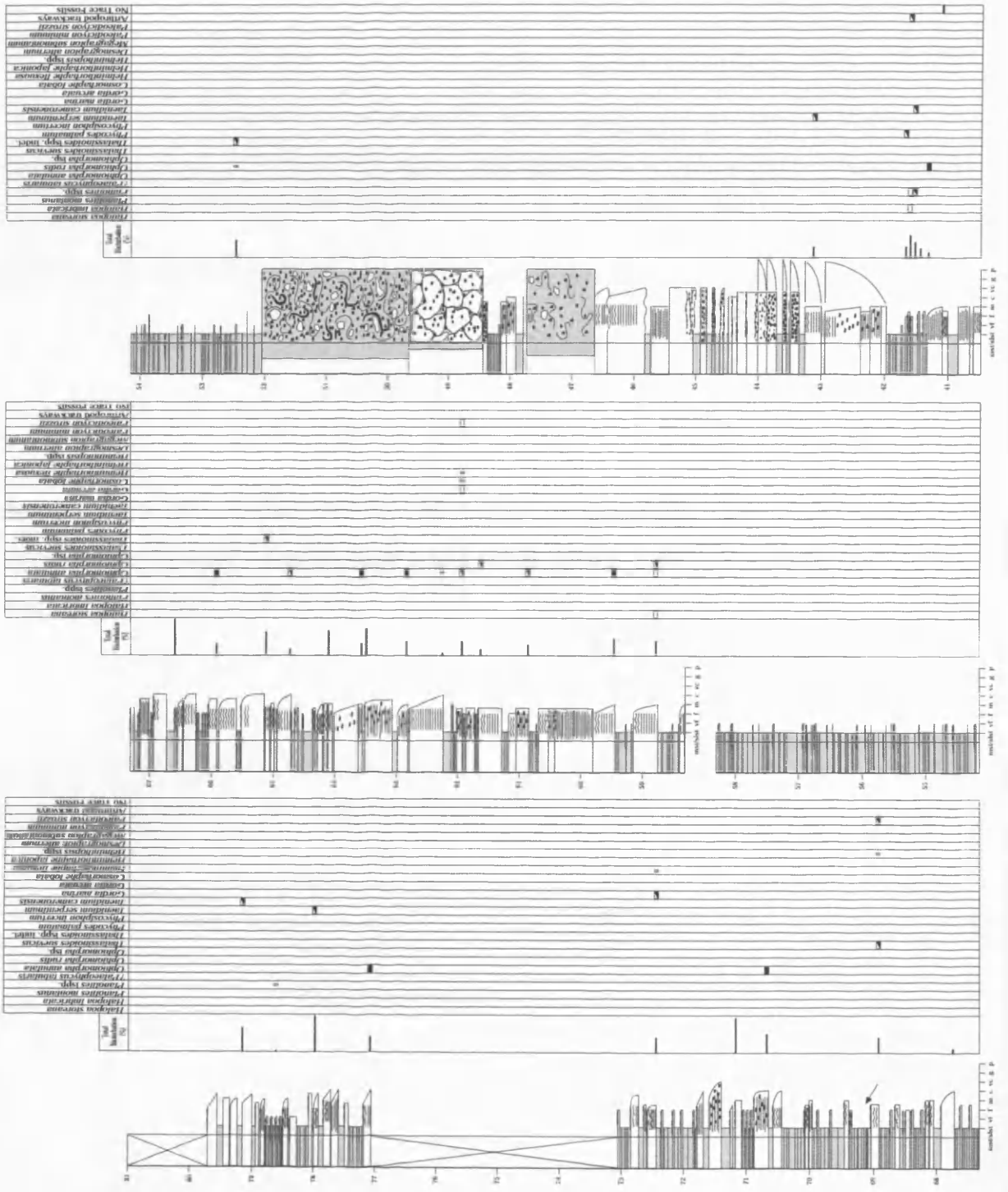

Appendix 6.15 Detailed bed-by-bed graphic sedimentary log (~ 10 m thick) and trace fossil data through basin slope deposits, Guaso system, Rio Ena, locality 27.

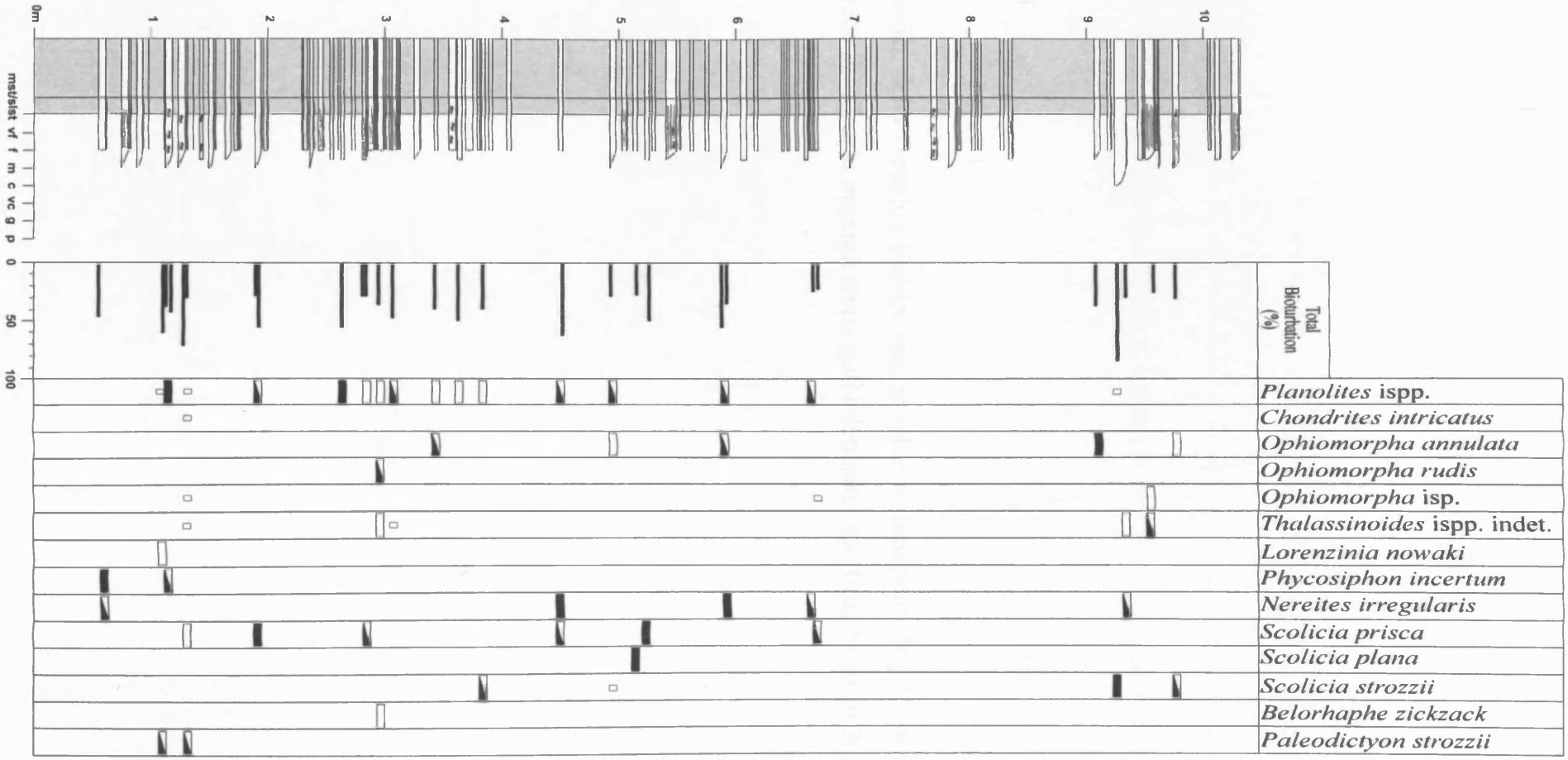
0m
1
2
3
4
5
6
7
8
9
10
mst/slst vf f m c vc g p
0
50
100
Total Bioturbation (%)
Planolites ispp.
Chondrites intricatus
Ophiomorpha annulata
Ophiomorpha rudis
Ophiomorpha isp.
Thalassinoides ispp. indet.
Lorenzinia nowaki
Phycosiphon incertum
Nereites irregularis
Scolicia prisca
Scolicia plana
Scolicia strozzii
Belorhaphe zickzack
Paleodictyon strozzii

Appendix 6.16 Detailed bed-by-bed graphic sedimentary log (6 m thick) and trace fossil data through slope gully deposits, Rio Ena, locality 26.

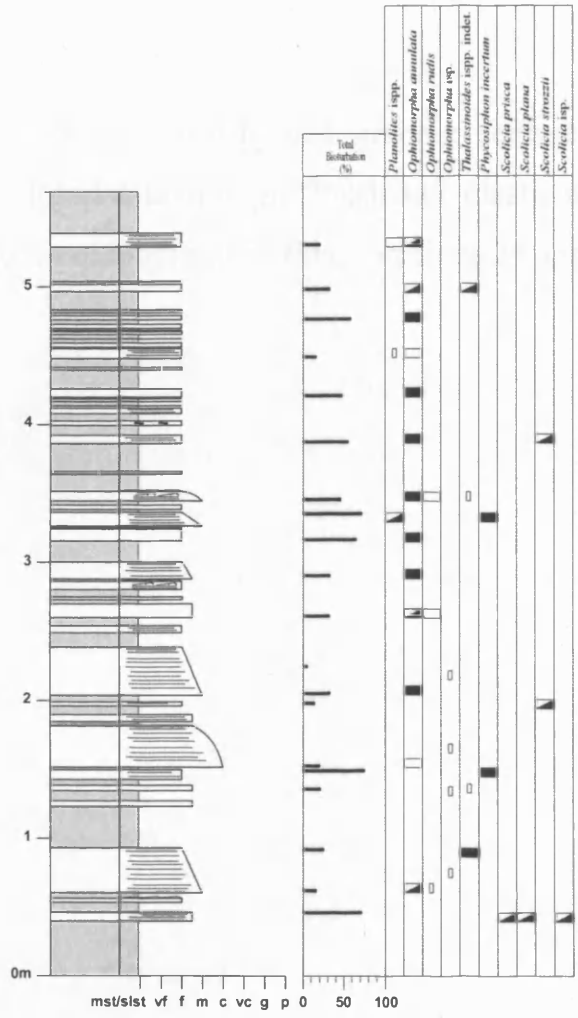
Total Bioturbation (%)
Planolites ispp.
Ophiomorpha annulata
Ophiomorpha rudis
Ophiomorpha isp.
Thalassinoides ispp. indet.
Physosiphon incertum
Scolicia prisca
Scolicia plana
Scolicia strozzii
Scolicia isp.
5
4
3
2
1
0m
mst/slst vf f m c vc g p
0 50 100

Appendix 6.17 Detailed bed-by-bed graphic sedimentary log (~ 77 m thick) and trace fossil data through "Prodeltaic clastic ramp" high net:gross and low net:gross sandbodies, Rio Ena, localities 24 and 25.

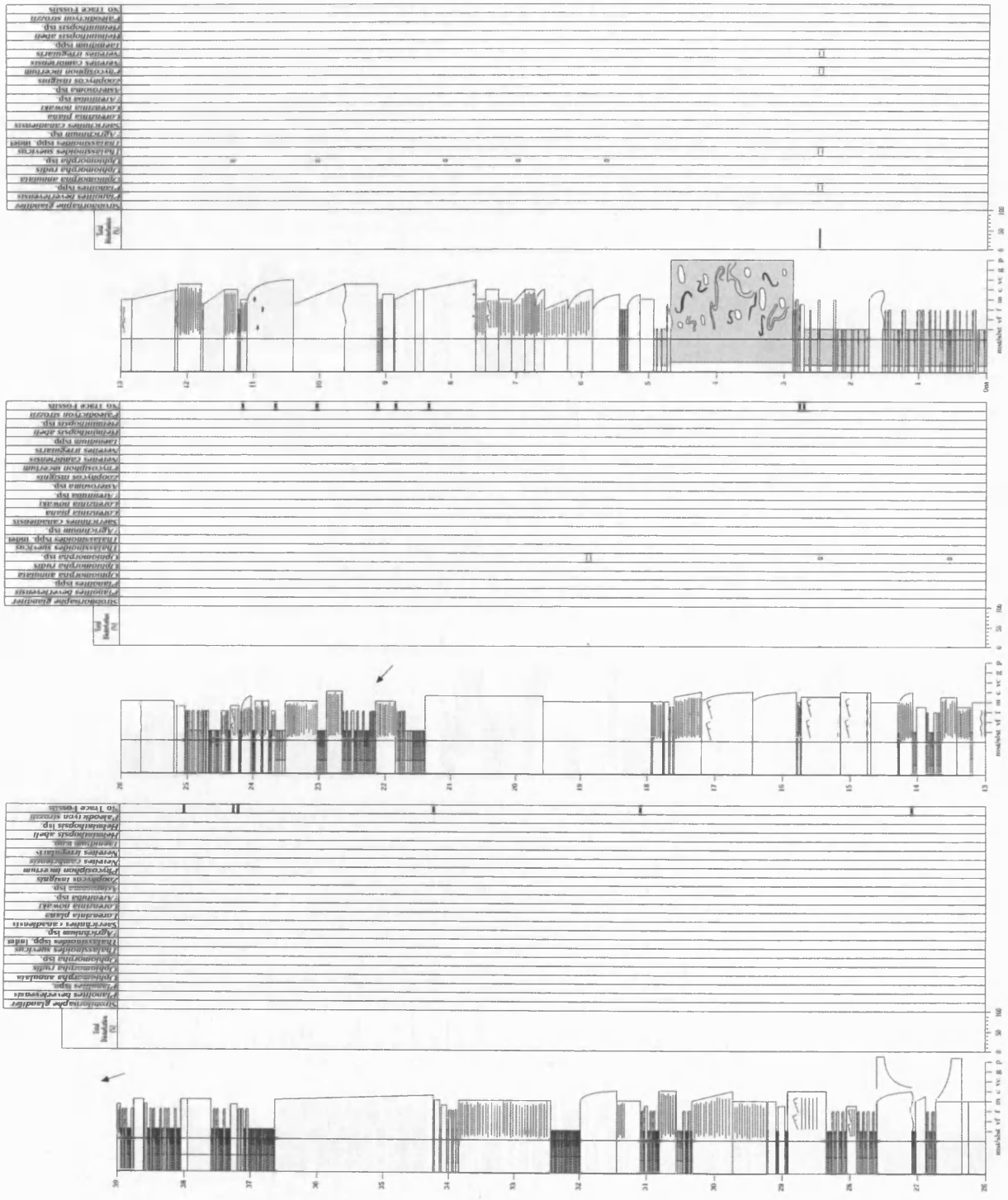

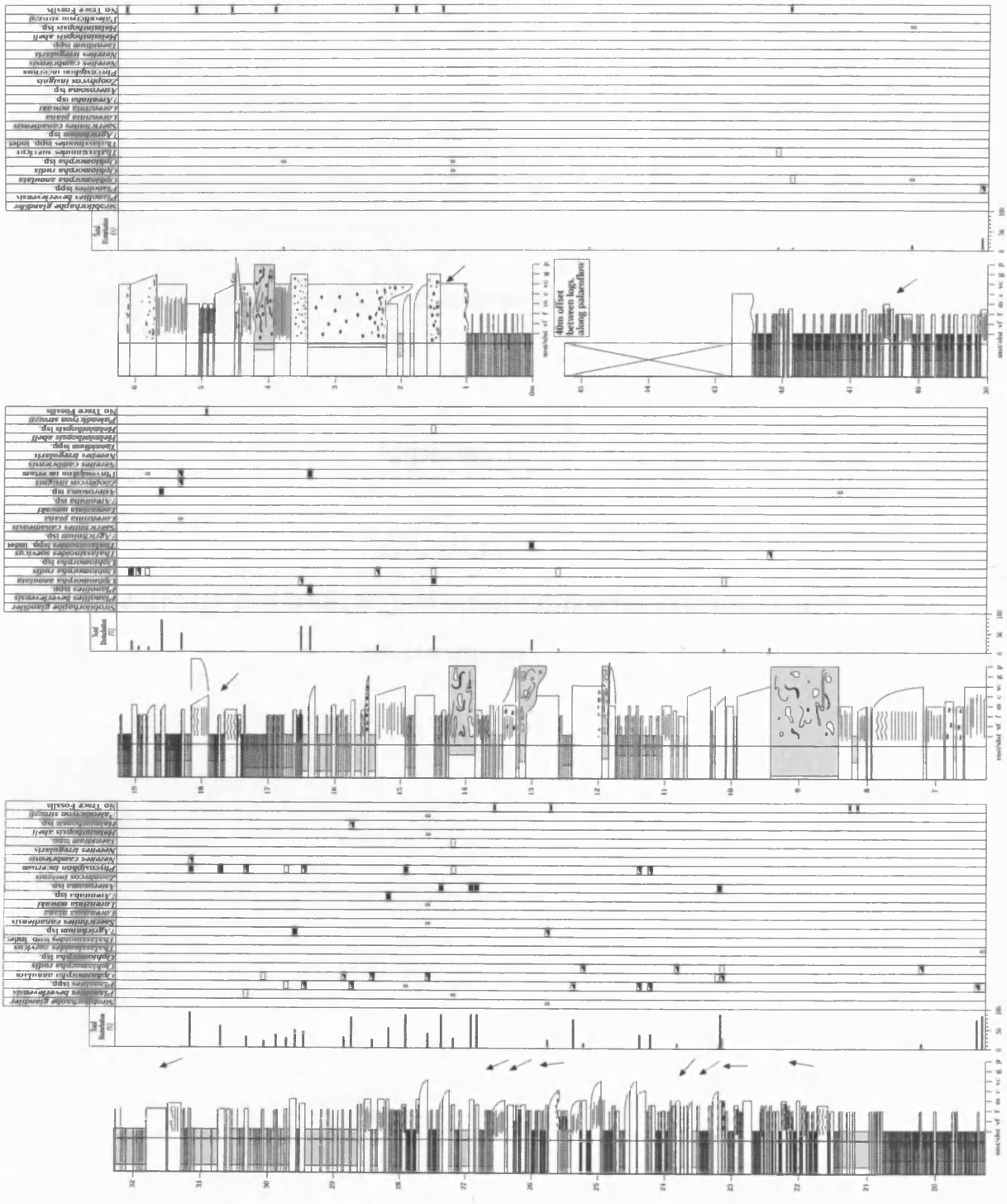
40km offset between legs, along palaeoflow

Appendix 7

Jaca basin:
Sedimentology and ichnology of distal submarine fan and related environments

Appendix 7.1 Detailed bed-by-bed graphic sedimentary log (72 m thick) and trace fossil data through channel-lobe transition deposits, Broto system, Fanlo, locality 28.

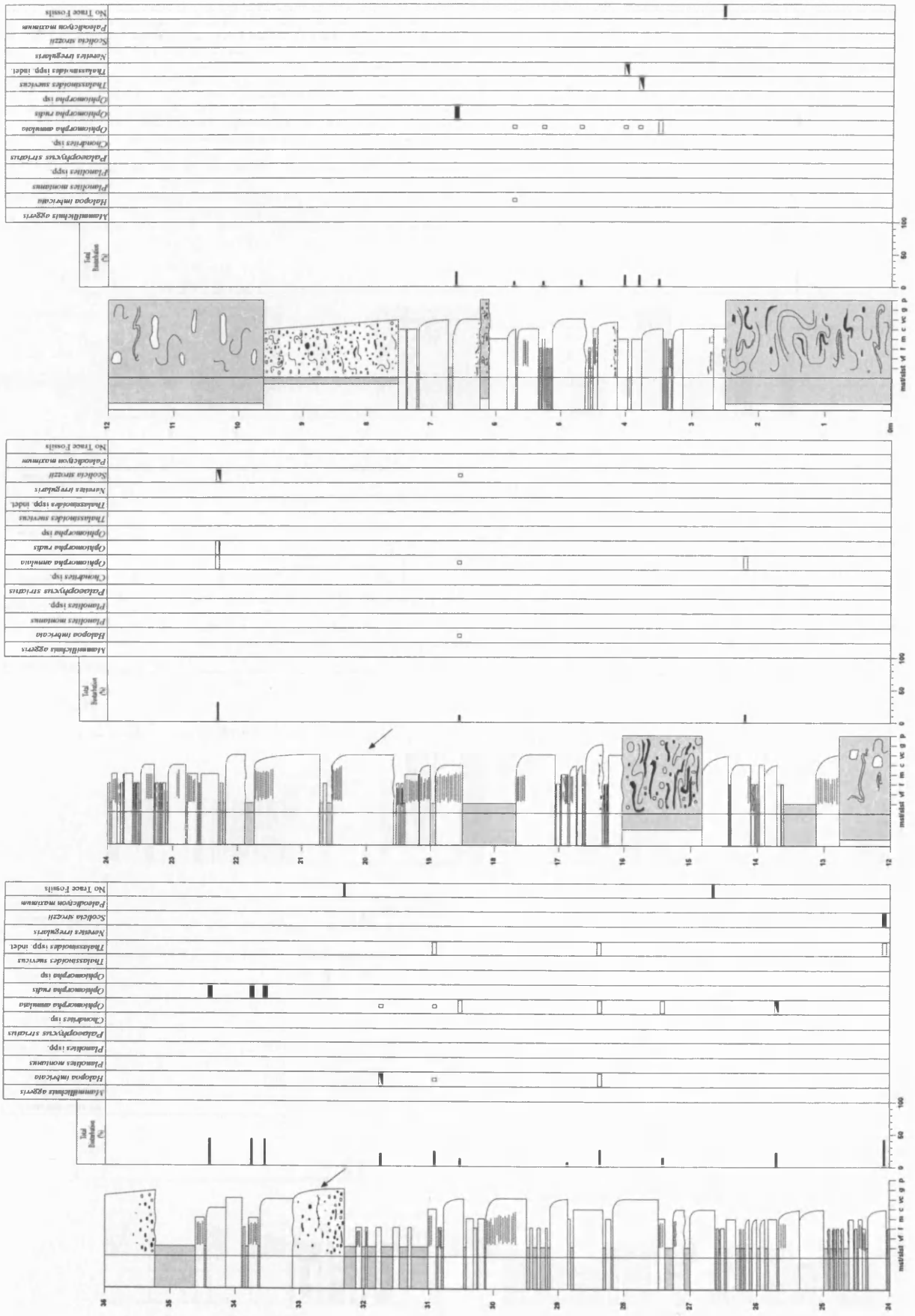
Total Bioturbation (%)
Adamantkhella agger is
Halicopa imbricata
Planolites montanus
Planolites spp.
Palaeophycus striatus
Chondrites isp.
Ophiomorpha annulata
Ophiomorpha rudis
Ophiomorpha isp
Thalassinoides suevicus
Thalassinoides spp. indet.
Nereites irregularis
Scolicia strozzi
Paleodictyon maximum
No Trace Fossils
matrix f m c vc g p
12 11 10 9 8 7 6 5 4 3 2 1 0m
24 23 22 21 20 19 18 17 16 15 14 13 12
36 35 34 33 32 31 30 29 28 27 26 25 24

60
61
62
63
64
65
66
67
68
69
70
71
72
mud/slst vf f m c vc g p
0
50
100
Total Bioturbation (%)
Mammillichnis aggeris
Halopoa imbricata
Planolites montanus
Planolites ispp.
Palaeophycus striatus
Chondrites isp.
Ophiomorpha annulata
Ophiomorpha rudis
Ophiomorpha isp
Thalassinoides suevicus
Thalassinoides ispp. indet.
Nereites irregularis
Scolicia strozzii
Paleodictyon maximum
No Trace Fossils
48
49
50
51
52
53
54
55
56
57
58
59
60
mud/slst vf f m c vc g p
0
50
100
Total Bioturbation (%)
Mammillichnis aggeris
Halopoa imbricata
Planolites montanus
Planolites ispp.
Palaeophycus striatus
Chondrites isp.
Ophiomorpha annulata
Ophiomorpha rudis
Ophiomorpha isp
Thalassinoides suevicus
Thalassinoides ispp. indet.
Nereites irregularis
Scolicia strozzii
Paleodictyon maximum
No Trace Fossils
36
37
38
39
40
41
42
43
44
45
46
47
48
mud/slst vf f m c vc g p
0
50
100
Total Bioturbation (%)
Mammillichnis aggeris
Halopoa imbricata
Planolites montanus
Planolites ispp.
Palaeophycus striatus
Chondrites isp.
Ophiomorpha annulata
Ophiomorpha rudis
Ophiomorpha isp
Thalassinoides suevicus
Thalassinoides ispp. indet.
Nereites irregularis
Scolicia strozzii
Paleodictyon maximum
No Trace Fossils

Appendix 7.2 Detailed bed-by-bed graphic sedimentary log (~ 76 m thick) and trace fossil data through lobe and interlobe deposits, Broto system, Fanlo-Sarvise, locality 29.

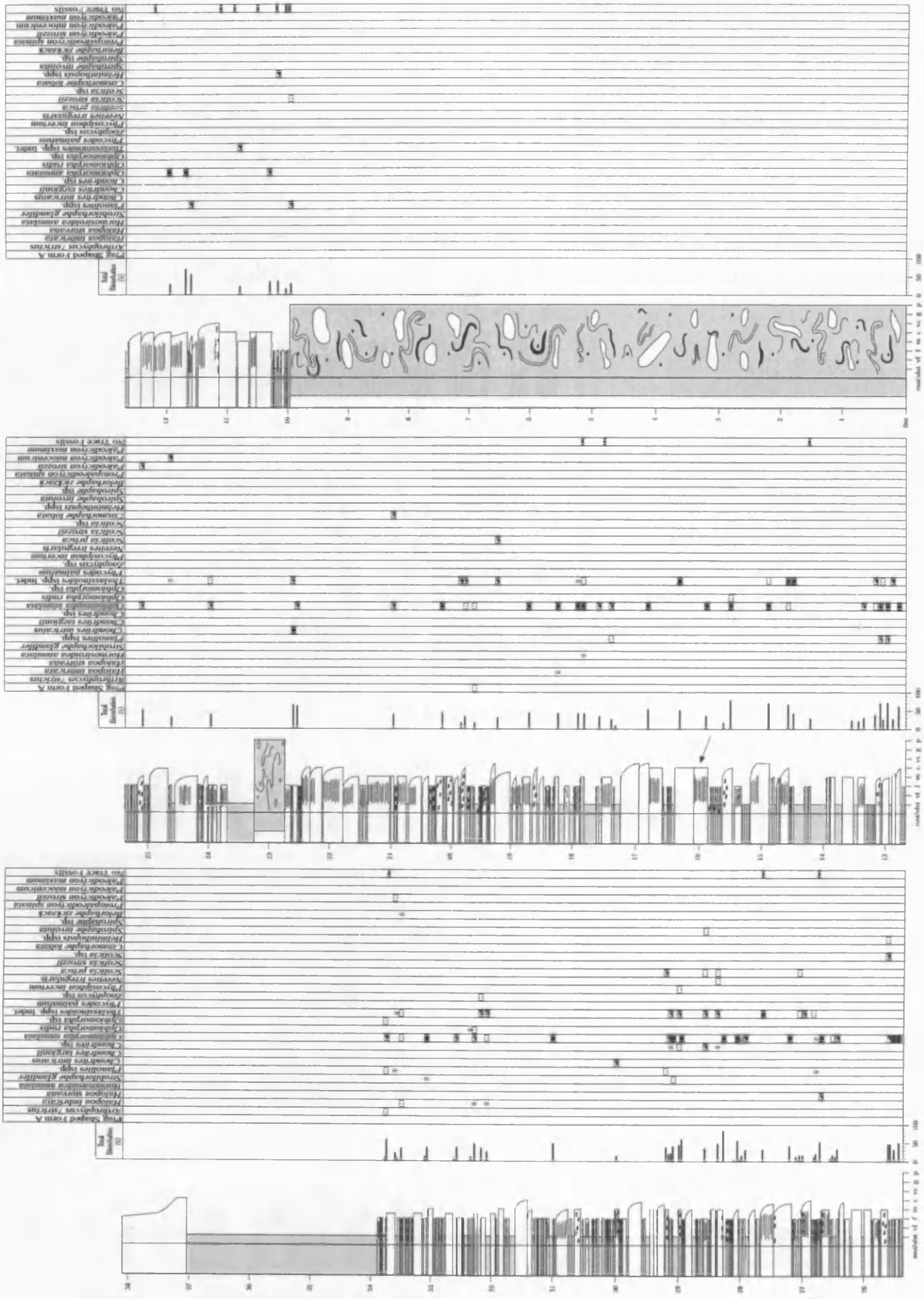

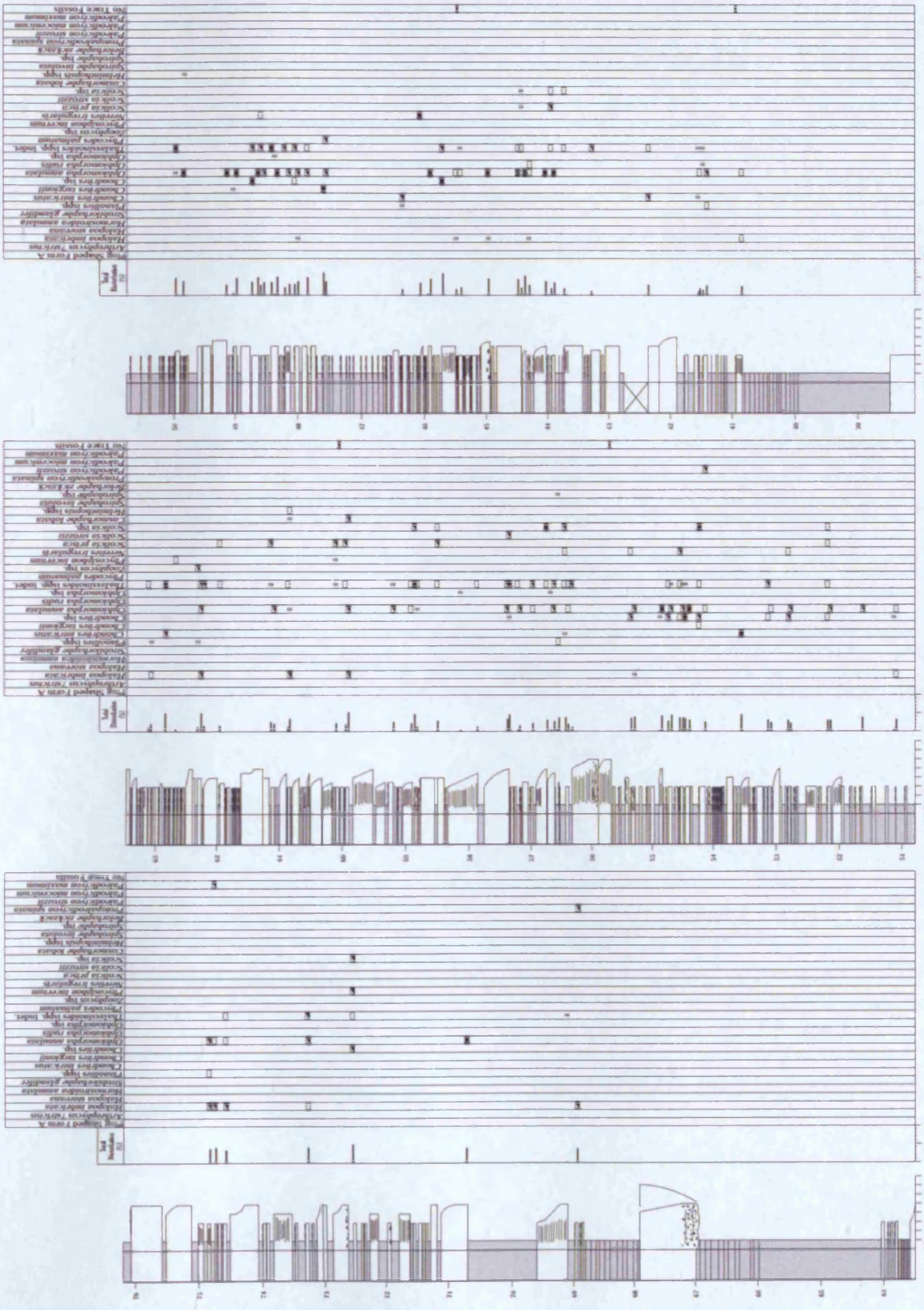

Appendix 7.3 Detailed bed-by-bed graphic sedimentary log (60 m thick) and trace fossil data through lobe and interlobe deposits, Broto system, Aragues del Puerto, locality 30.

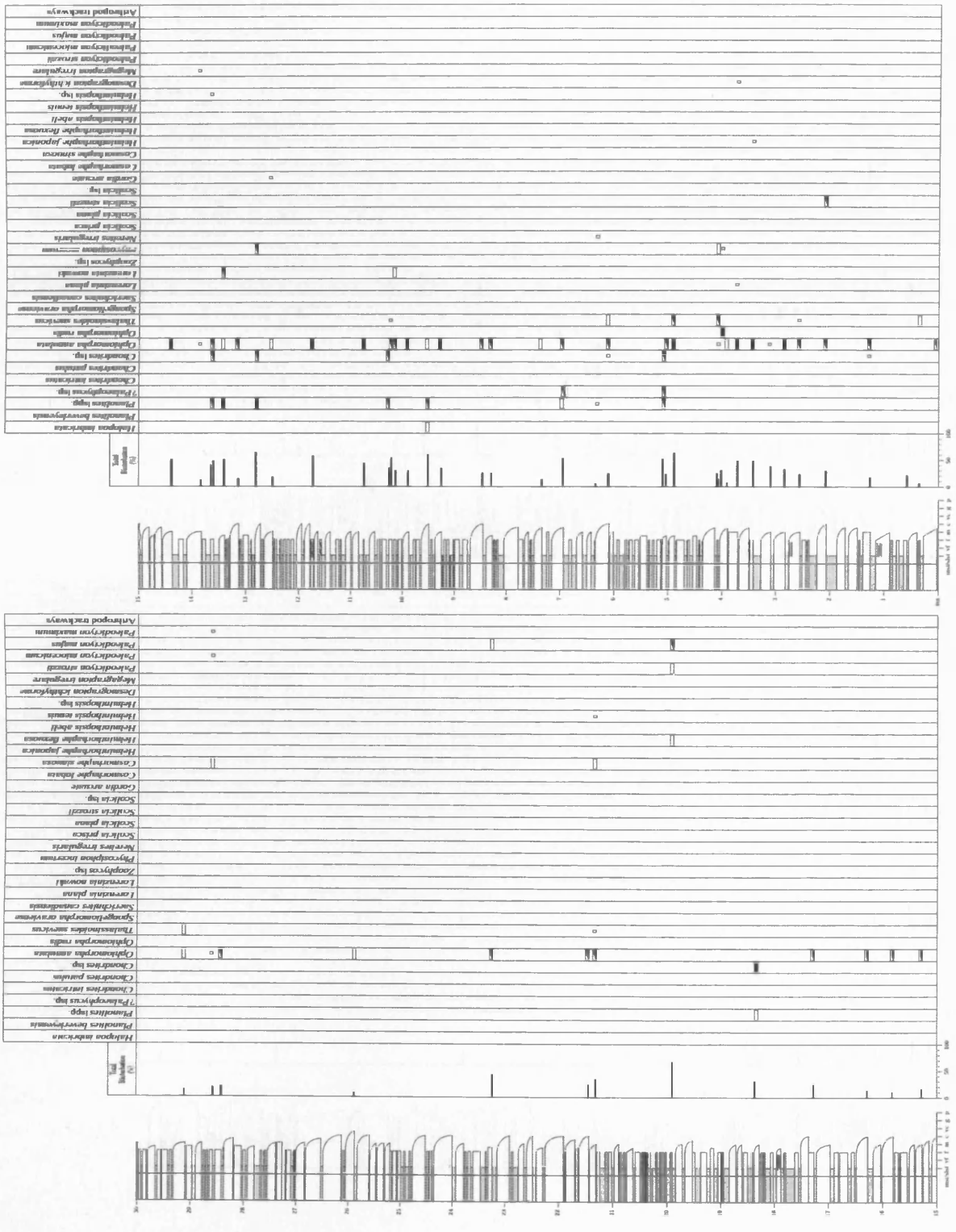
Total Resolution (%)
Haliotrema tokyoense
Haliotrema menezesi
Haliotrema manubriense
Haliotrema longipenis
Haliotrema kabatai
Haliotrema japonica
Haliotrema hirasakai
Haliotrema epinepheli
Haliotrema clarkei
Haliotrema aburatsubo
Haliotrema abbotti
Haliotrema
Gyrodactylus sp.
Gyrodactylus salaris
Gyrodactylus rarus
Gyrodactylus pleuronectis
Gyrodactylus markewitschi
Gyrodactylus longipenis
Gyrodactylus kobayashii
Gyrodactylus katharineri
Gyrodactylus jalensis
Gyrodactylus gasterostei
Gyrodactylus derjavini
Gyrodactylus colemanensis
Gyrodactylus cichlidarum
Gyrodactylus branchialis
Gyrodactylus bullatarudis
Gyrodactylus
Dactylogyrus sp.
Dactylogyrus vastator
Dactylogyrus tincae
Dactylogyrus suecicus
Dactylogyrus nanus
Dactylogyrus minutus
Dactylogyrus lamellatus
Dactylogyrus hemiamphisi
Dactylogyrus extensus
Dactylogyrus dulkeiti
Dactylogyrus cornoides
Dactylogyrus cichlidarum
Dactylogyrus
Cichlidogyrus thurstonae
Cichlidogyrus sclerosus
Cichlidogyrus sp.
Cichlidogyrus halli
Cichlidogyrus dossoui
Cichlidogyrus digitatus
Cichlidogyrus cirratus
Cichlidogyrus casuarinus
Cichlidogyrus bilongus
Cichlidogyrus arthracanthus
Cichlidogyrus
Anacanthorus spathulatus
Anacanthorus penilabiatus
Anacanthorus
Acanthocotyle verrucosa
Acanthocotyle lobianchi
Acanthocotyle elongata
Acanthocotyle
Acanthocotylidae
Monogenea
Arthropod trackways

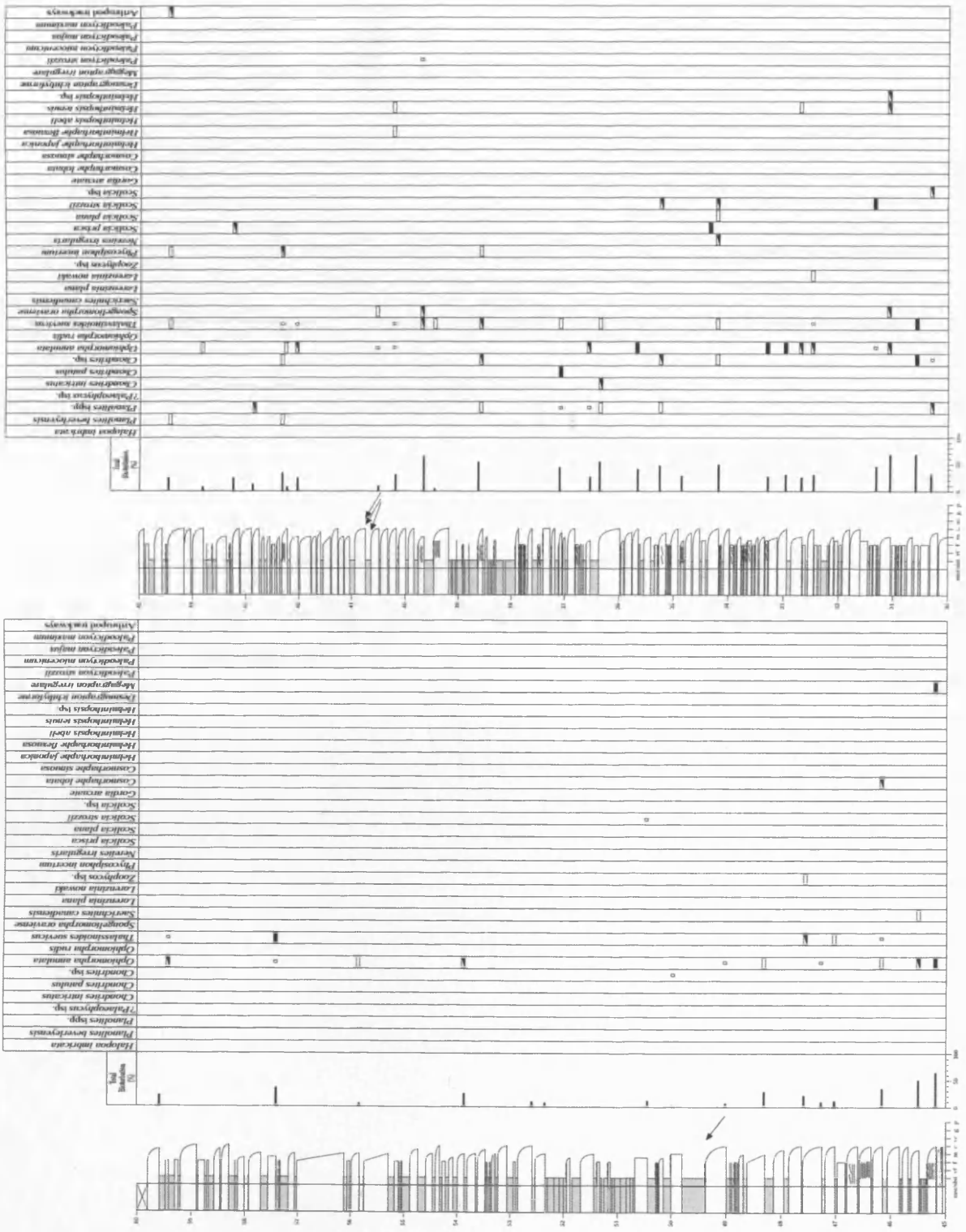
Halopoa imbricata
Planolites beverleyensis
Planolites ispp.
Chaetites ispp.
?Palaeophycus sp.
Chaetites intricatus
Chondrites patulus
Chondrites sp.
Cylindrorhiza annulata
Cylindrorhiza radix
Taphrhelminthopsis ludwigi
Sporidesmotopa cervinae
Sarcichnites candelabrus
Laevinella plana
Laevinella bowdi
Zoophycos sp.
Phycosiphon incertum
Nereites irregularis
Scolicia prisca
Scolicia plana
Scolicia strozzi
Scolicia sp.
Cavetta arcuata
Conostichnus stenosa
Conostichnus lobata
Helminthoidichnites tenuis
Helminthoidichnites fenestrata
Helminthoidichnites isp.
Helminthopsis hieroglyphica
Megagyrolithes irregularis
Phycodes curvicrus
Phycodes palmatum
Phycodes pedum
Planolites montanus
Arthropod trackways

Appendix 7.4 Detailed bed-by-bed graphic sedimentary log (88 m thick) and trace fossil data through lobe fringe deposits, Cotefablo system, Cotefablo tunnel, locality 31.

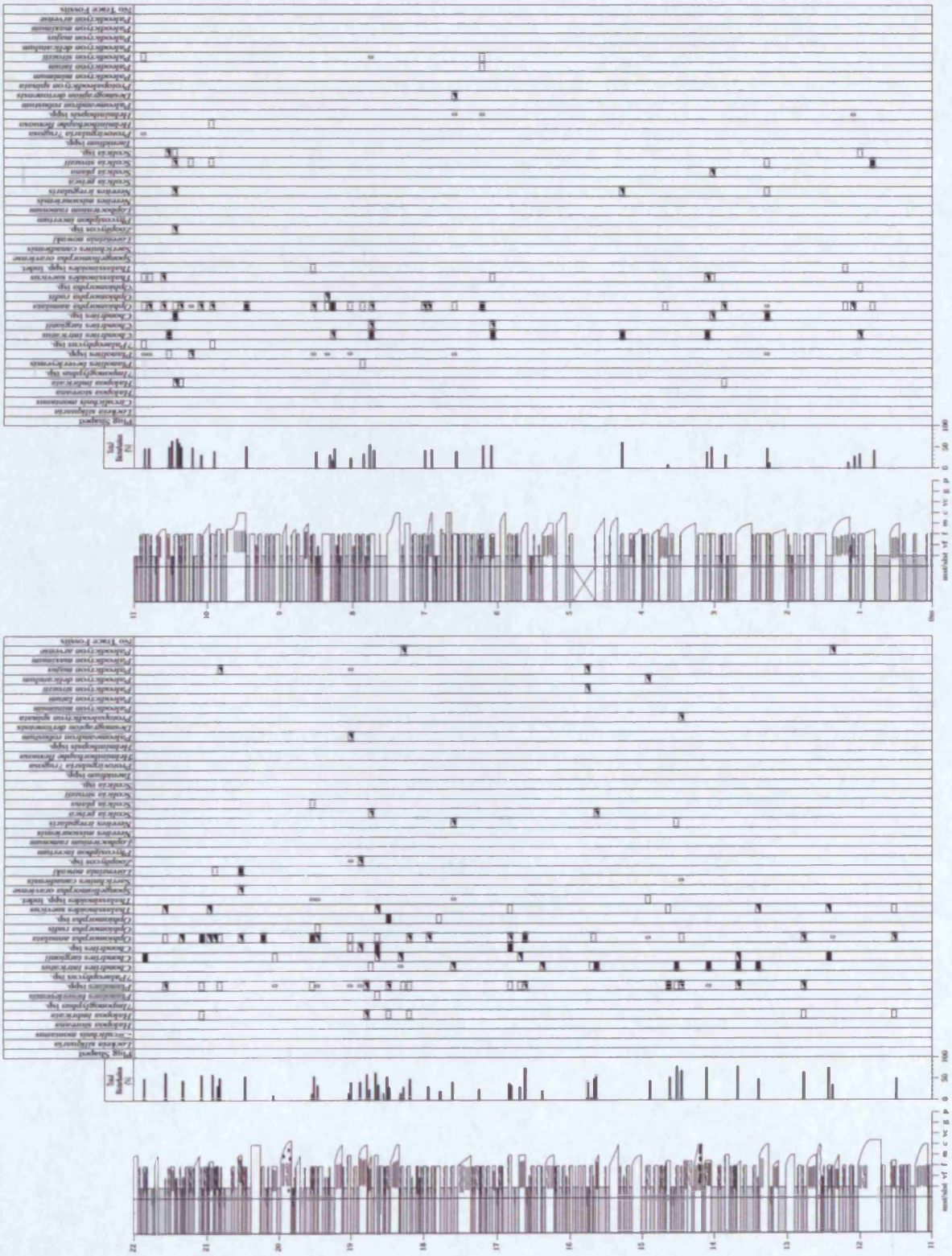

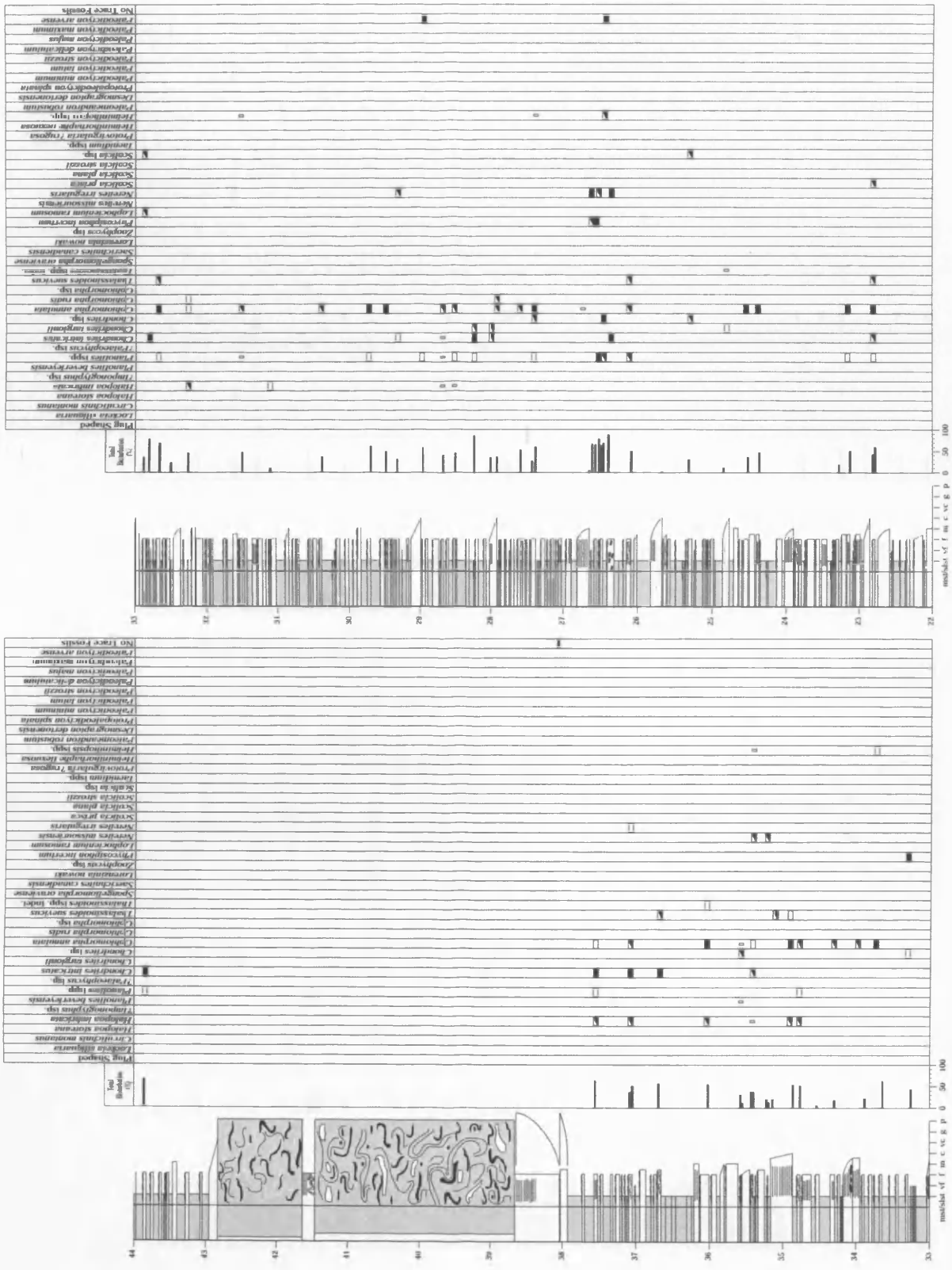
Trait Shaped
Lacuna vitrea
C. trabeata
Littorina littorea
Littorina obtusata
Littorina saxatilis
Littorina sp.
Littorina spp.
Littorina tenebrosa
Littorina sp.
Littorina spp.
Littorina littorea
Littorina obtusata
Littorina saxatilis
Littorina spp.
Littorina tenebrosa
Littorina sp.
Littorina spp.
Littorina littorea
Littorina obtusata
Littorina saxatilis
Littorina spp.
Littorina tenebrosa
Littorina sp.
Littorina spp.
Littorina littorea
Littorina obtusata
Littorina saxatilis
Littorina spp.
Littorina tenebrosa
Littorina sp.
Littorina spp.
No Trace Fossils

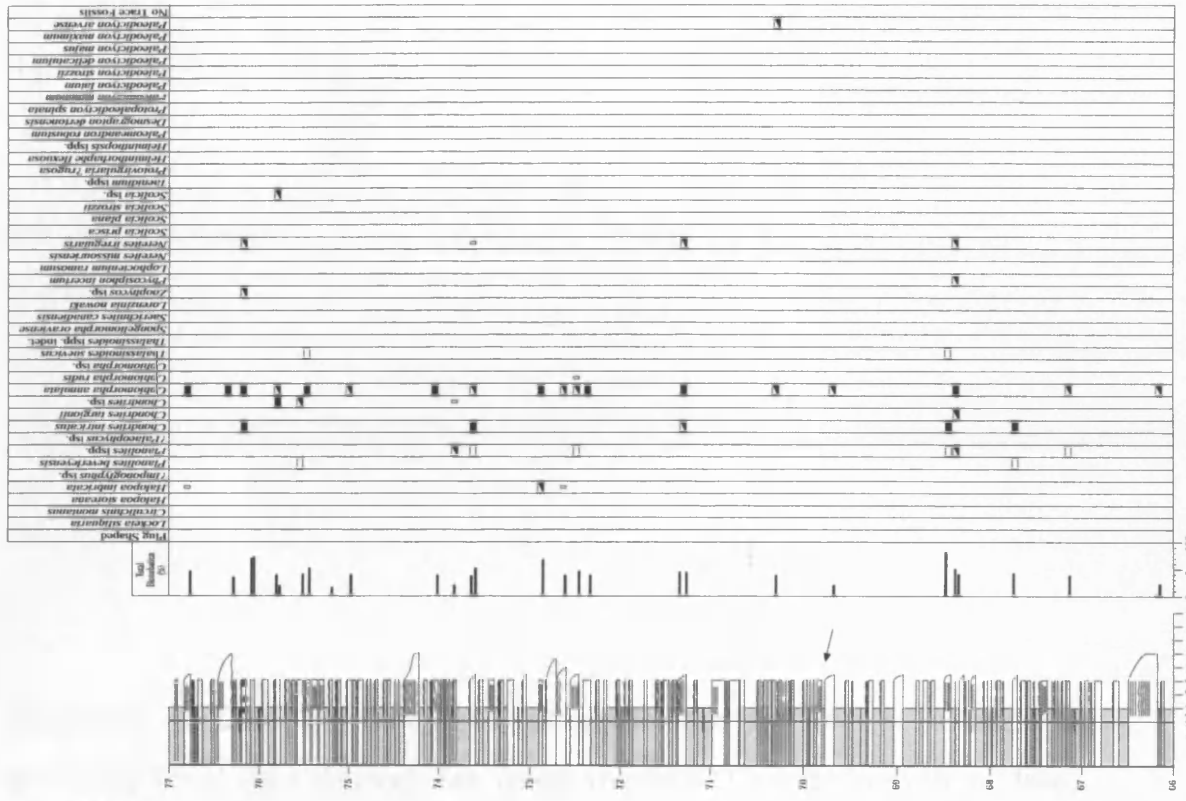
Total Biomass (G)
100
50
0
Time (Ma)
77
76
75
74
73
72
71
70
69
68
67
66

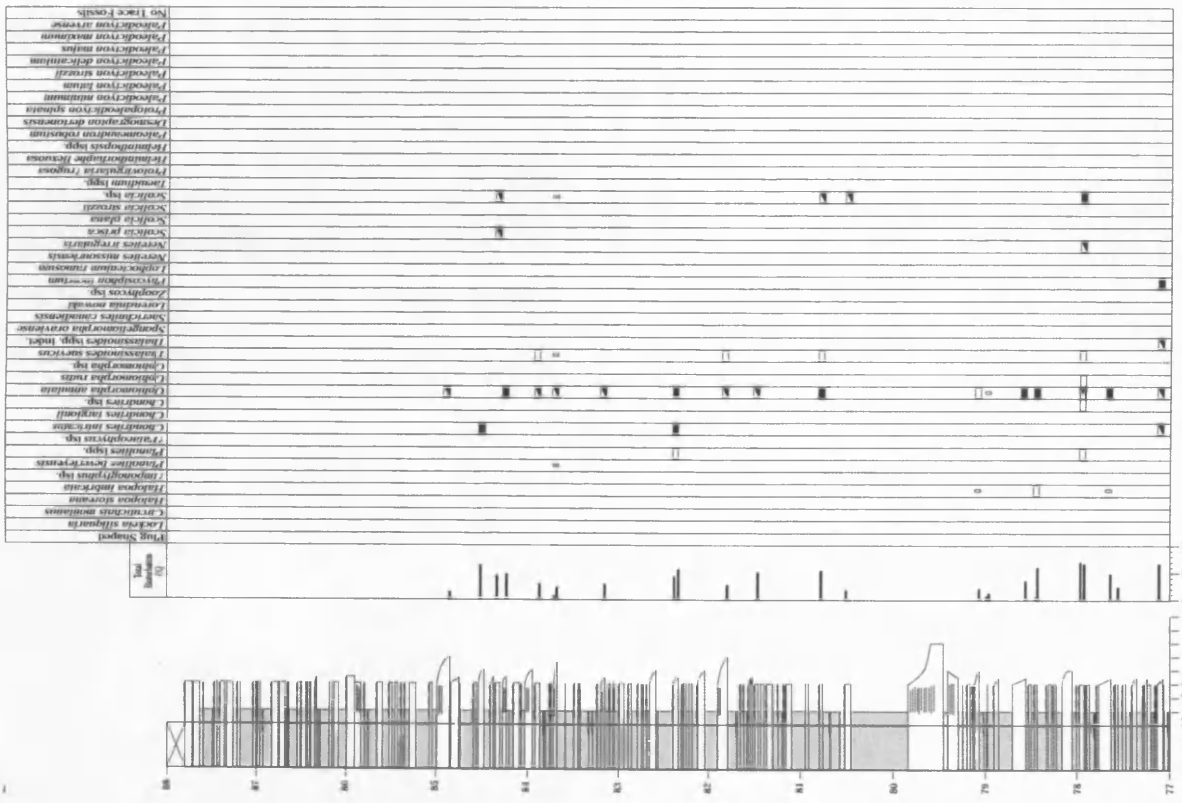
Total Biomass (G)
100
50
0
Time (Ma)
88
87
86
85
84
83
82
81
80
79
78
77

Appendix 7.5 Detailed bed-by-bed graphic sedimentary log (~ 70 m thick) and trace fossil data through fan fringe deposits, Cotefablo system, Jasa, locality 32.

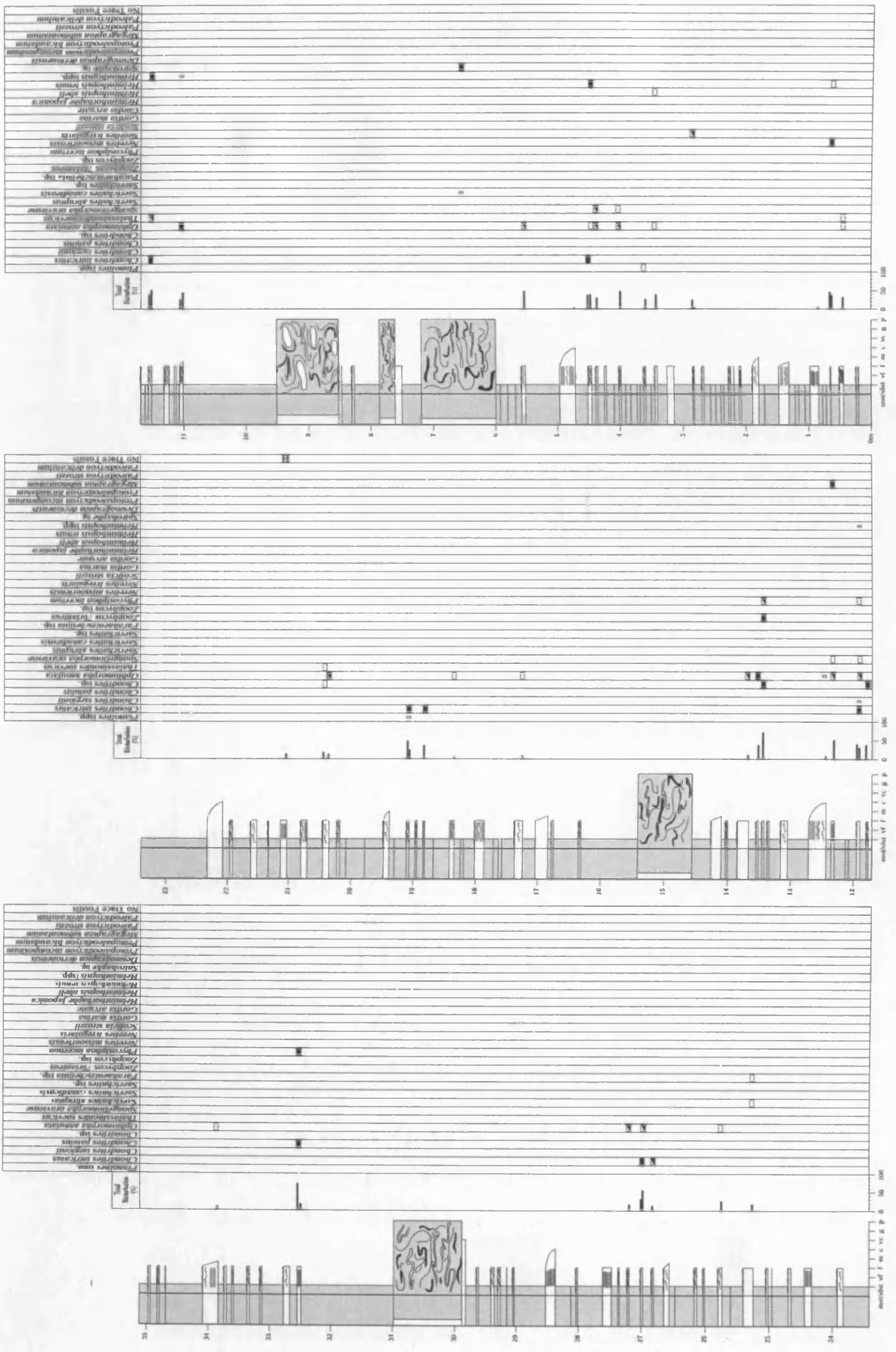

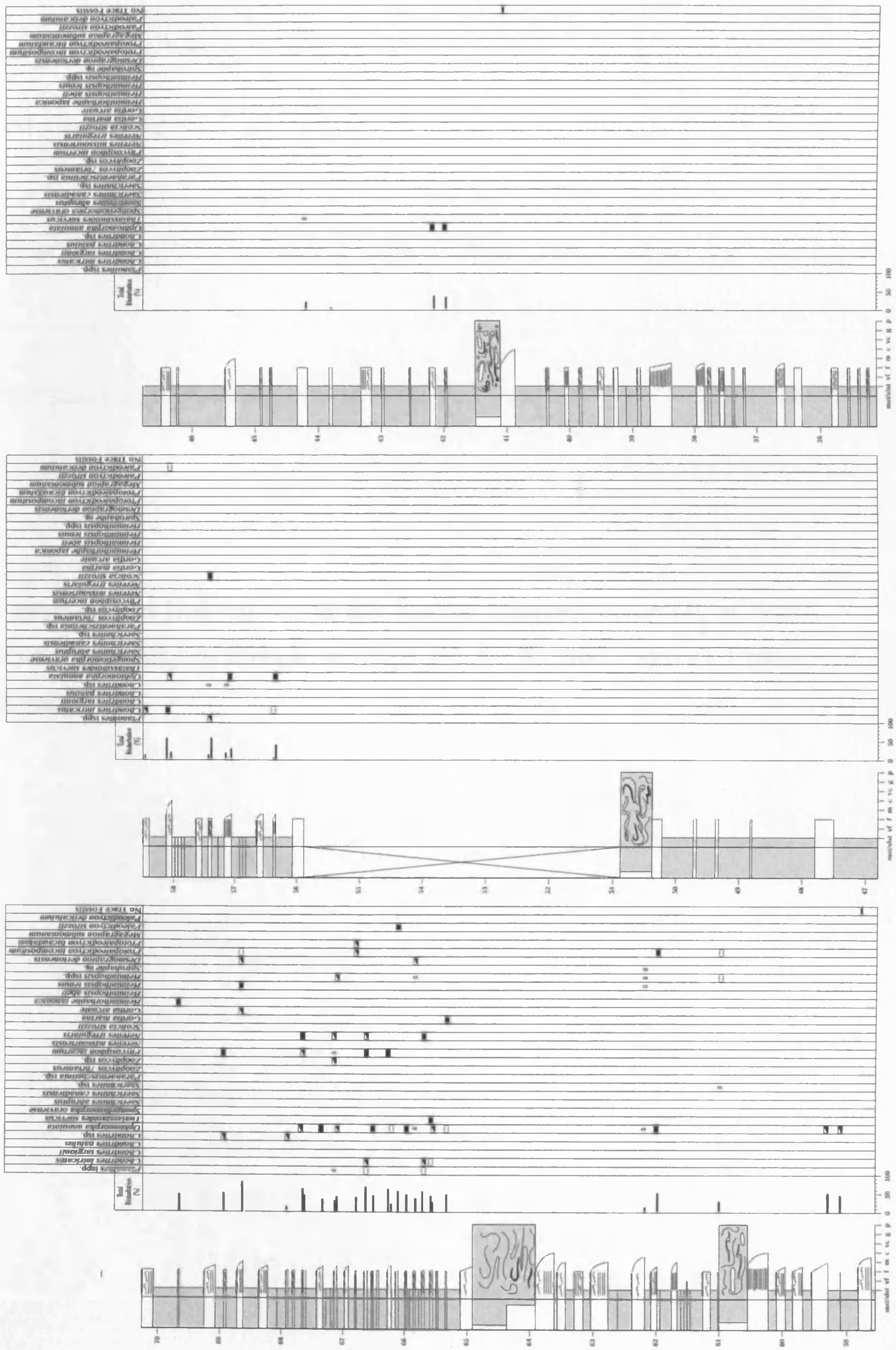

Appendix 7.6 Detailed bed-by-bed graphic sedimentary log (49 m thick) and trace fossil data through fan fringe deposits, Cotefablo system, Urdues, locality 33.

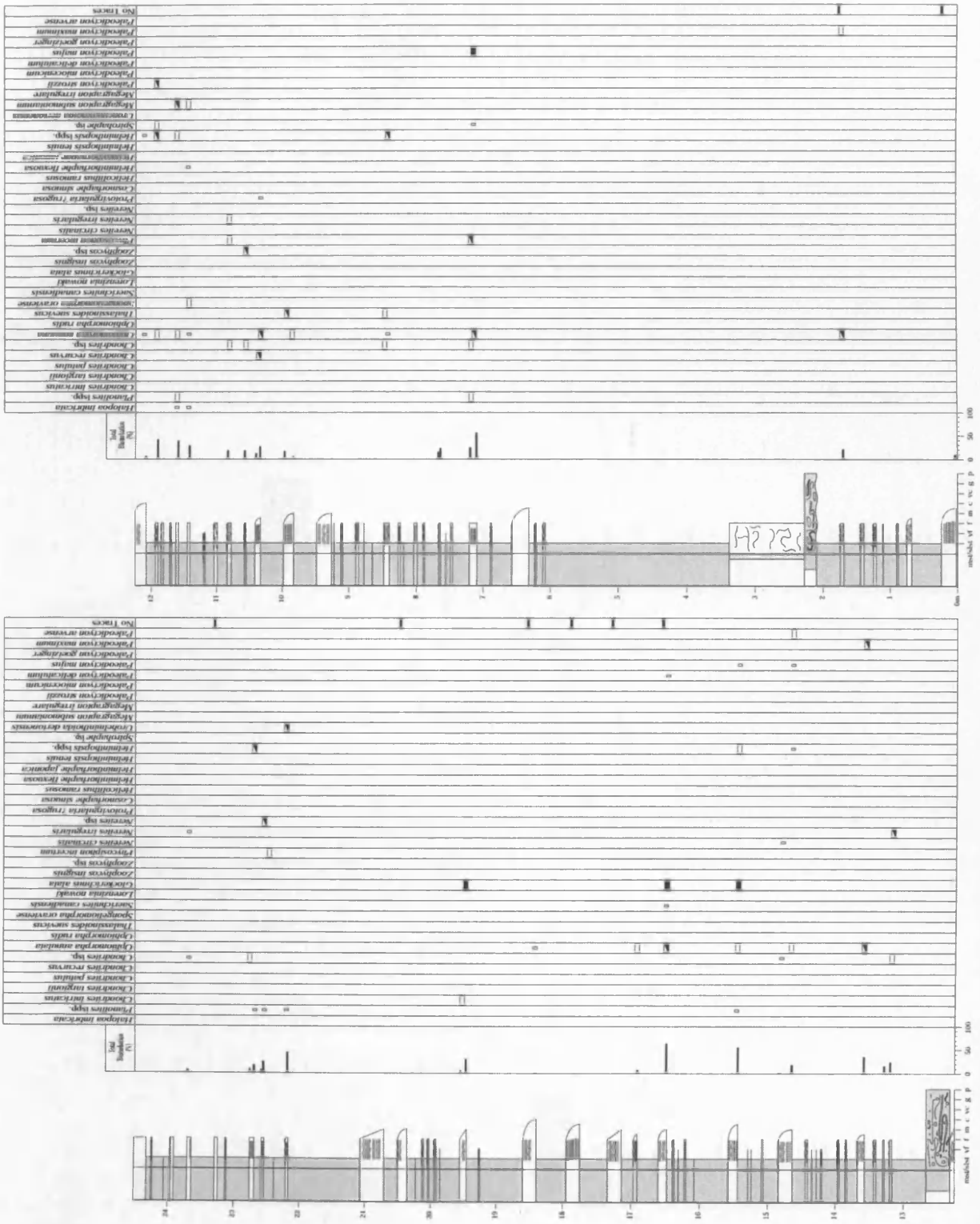

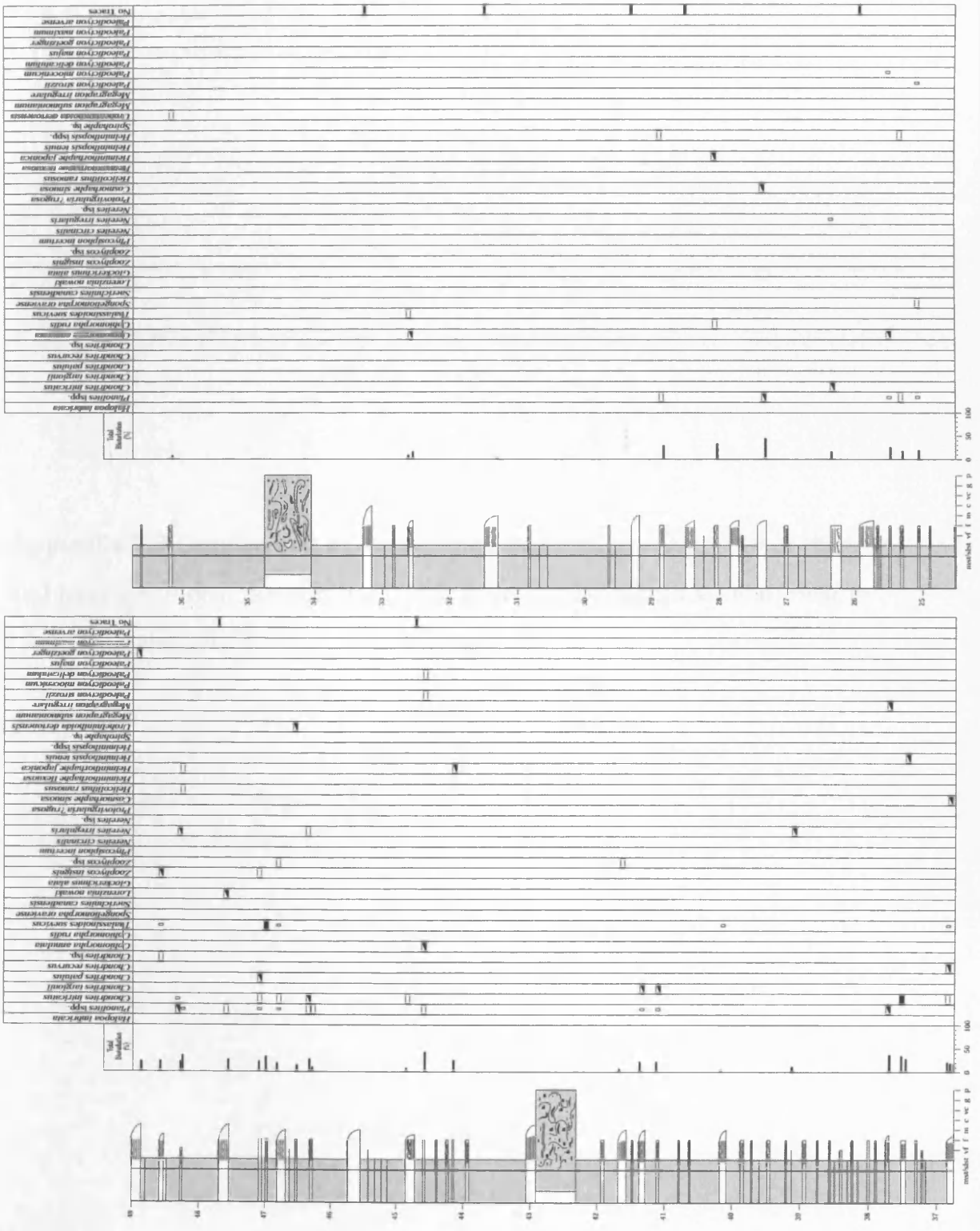

Appendix 7.7 Detailed bed-by-bed graphic sedimentary log (~ 19 m thick) and trace fossil data through fan fringe deposits, Cotefablo system, road to Urdues, locality 34.

Circulichnis montanus
Hormosiroidea annulata
Planolites montanus
Planolites ispp.
Chondrites intricatus
Chondrites isp.
Ophiomorpha annulata
Ophiomorpha rudis
Ophiomorpha isp.
Thalassinoides suevicus
Saerichnites abruptus
Saerichnites canadiensis
Paralhaentzschelinia isp.
Phycosiphon incertum
Nereites irregularis
Scolicia strozzii
Helminthopsis tenuis
Helminthopsis ispp.
Belorhaphe zickzack
Desmograpton altermum
Desmograpton ichthyforme
Urohelminthoida dertonensis
Urohelminthoida appendiculata
Paleodictyon strozzii
Paleodictyon goetzinger
No Trace Fossils

Circulichnis montanus
Hormosiroidea annulata
Planolites montanus
Planolites ispp.
Chondrites intricatus
Chondrites isp.
Ophiomorpha annulata
Ophiomorpha rudis
Ophiomorpha isp.
Thalassinoides suevicus
Saerichnites abruptus
Saerichnites canadiensis
Paralhaentzschelinia isp.
Phycosiphon incertum
Nereites irregularis
Scolicia strozzii
Helminthopsis tenuis
Helminthopsis ispp.
Belorhaphe zickzack
Desmograpton altermum
Desmograpton ichthyforme
Urohelminthoida dertonensis
Urohelminthoida appendiculata
Paleodictyon strozzii
Paleodictyon goetzinger
No Trace Fossils

Appendix 7.8 Detailed bed-by-bed graphic sedimentary log (~ 28 m thick) and trace fossil data through fan fringe deposits, Cotefablo system, Puerto d'Anso, locality 35.

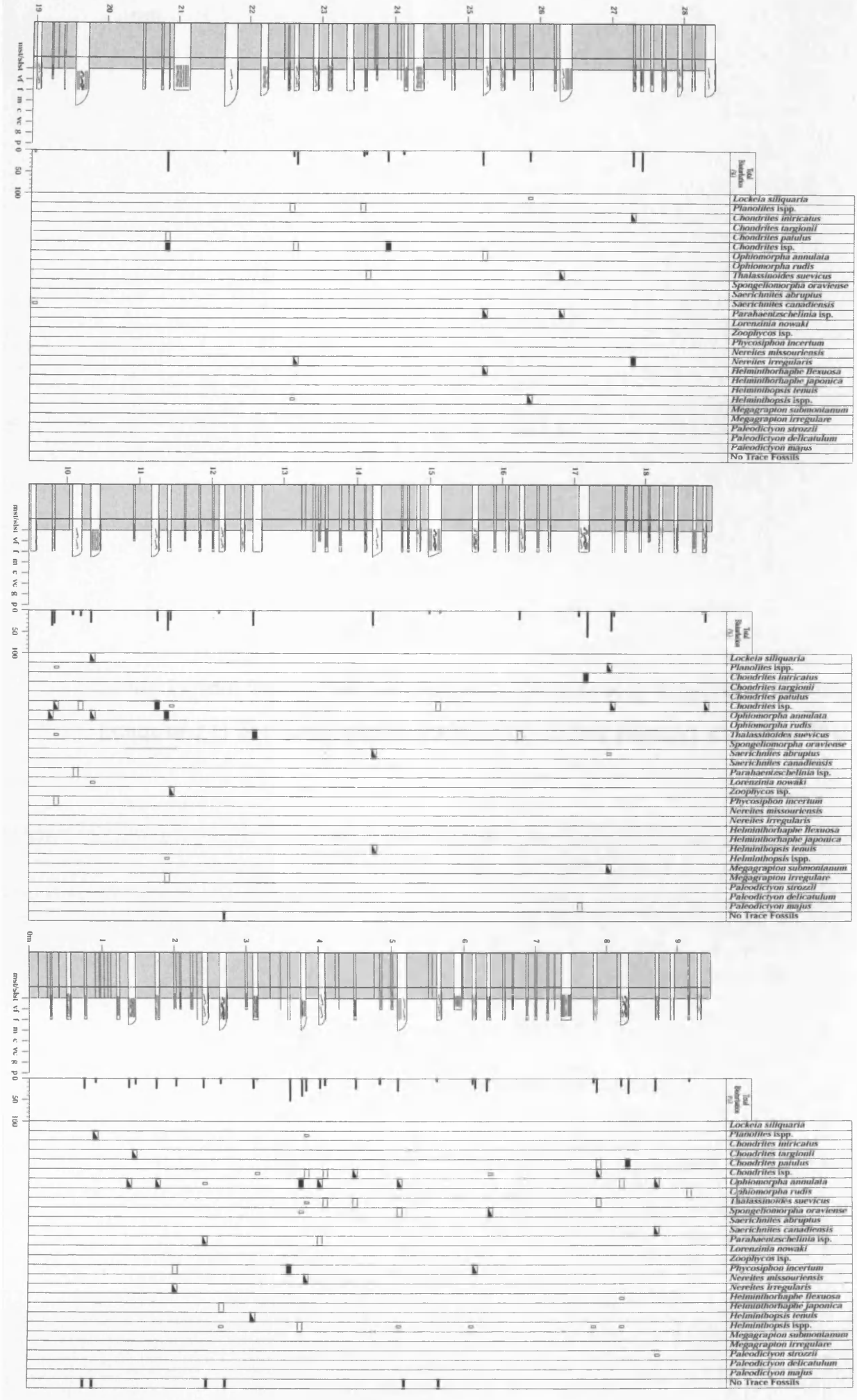
Lockeia siliquaria
Planolites ispp.
Chondrites intricatus
Chondrites targionii
Chondrites patulus
Chondrites isp.
Ophiomorpha annulata
Ophiomorpha rudis
Thalassinoides suevicus
Spongeliomorpha oravicense
Saerichnites abruptus
Saerichnites canadiensis
Parahaentzschelinia isp.
Lorenzinia nowaki
Zoophycos isp.
Phycosiphon incertum
Nereites missouriensis
Nereites irregularis
Helminthorhaphe flexuosa
Helminthorhaphe japonica
Helminthopsis tenuis
Helminthopsis ispp.
Megagrapton submontanum
Megagrapton irregulare
Paleodictyon strozzii
Paleodictyon delicatulum
Paleodictyon majus
No Trace Fossils

Appendix 7.9 Detailed bed-by-bed graphic sedimentary log (12 m thick) through distal basin floor deposits, Cotefablo system, Hecho, locality 36.

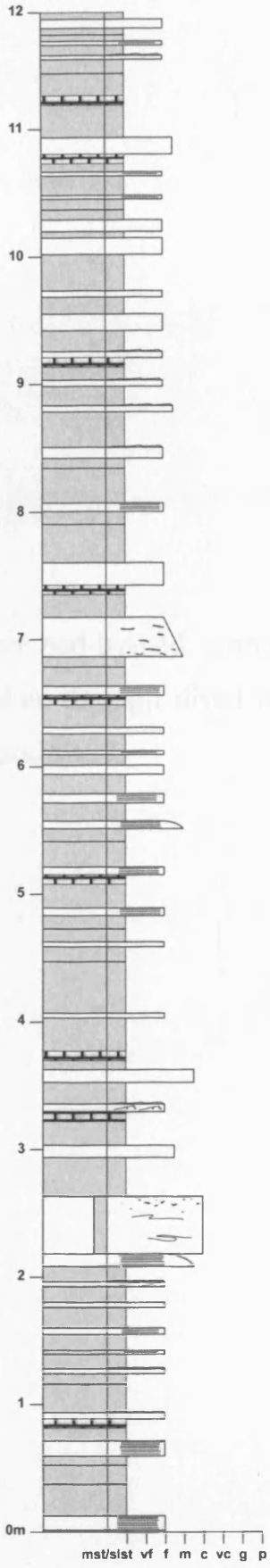
12
11
10
9
8
7
6
5
4
3
2
1
0m
mst/sist vf f m c vc g p

Appendix 7.10 Detailed bed-by-bed graphic sedimentary log (~ 22 m thick) and trace fossil data through distal basin floor deposits, Cotefablo system, Anso-Roncal, locality 37.

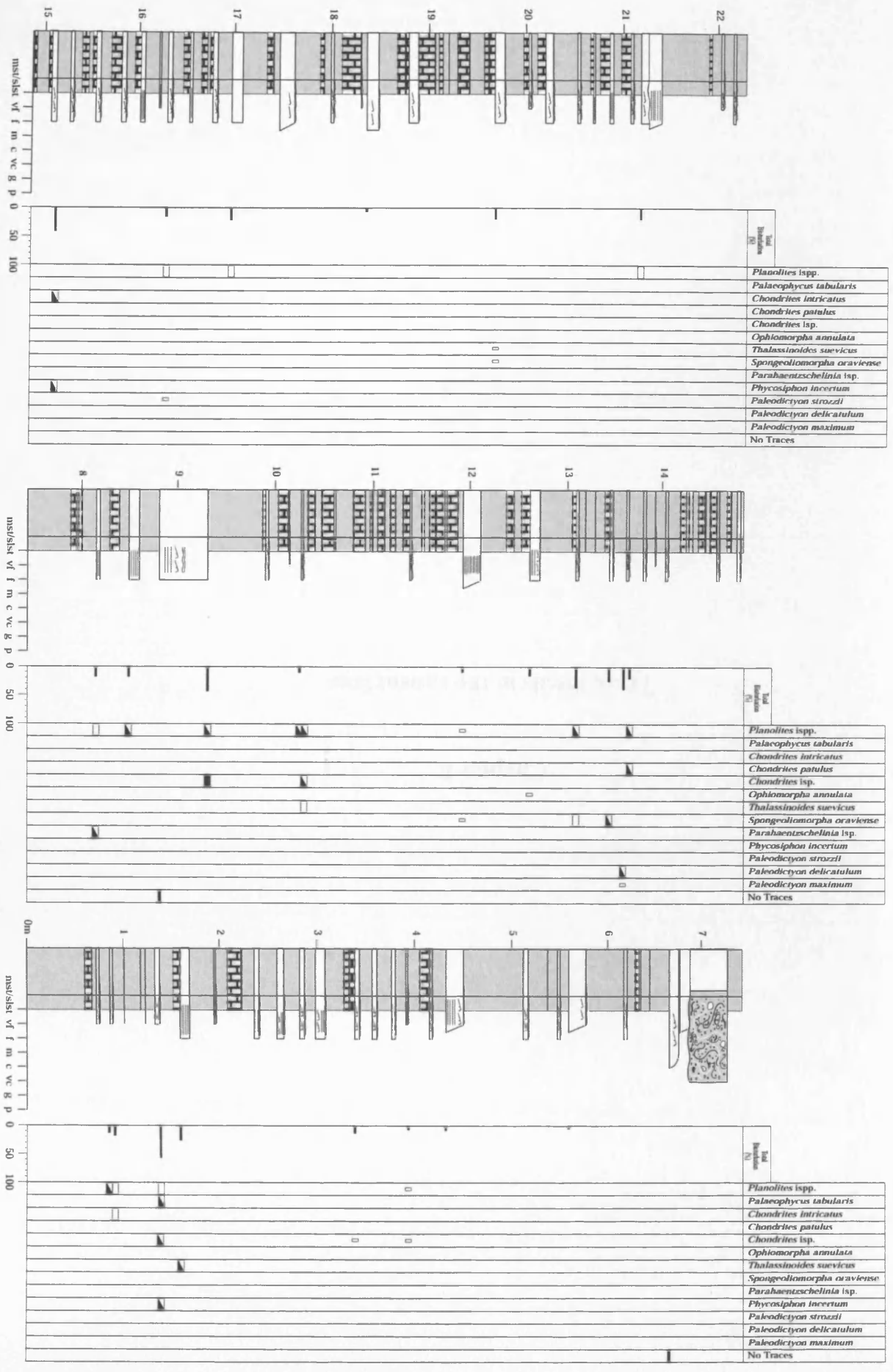
15
16
17
18
19
20
21
22
mst/slst vf f m c vc g p
0
50
100
Total Ichnofabric (%)
Planolites ispp.
Palaeophycus tabularis
Chondrites intricatus
Chondrites patulus
Chondrites isp.
Ophiomorpha annulata
Thalassinoides suevicus
Spongeliomorpha oraviense
Parahaentzschelinia isp.
Phycosiphon incertum
Paleodictyon strozzii
Paleodictyon delicatulum
Paleodictyon maximum
No Traces
8
9
10
11
12
13
14
mst/slst vf f m c vc g p
0
50
100
Total Ichnofabric (%)
Planolites ispp.
Palaeophycus tabularis
Chondrites intricatus
Chondrites patulus
Chondrites isp.
Ophiomorpha annulata
Thalassinoides suevicus
Spongeliomorpha oraviense
Parahaentzschelinia isp.
Phycosiphon incertum
Paleodictyon strozzii
Paleodictyon delicatulum
Paleodictyon maximum
No Traces
0m
1
2
3
4
5
6
7
mst/slst vf f m c vc g p
0
50
100
Total Ichnofabric (%)
Planolites ispp.
Palaeophycus tabularis
Chondrites intricatus
Chondrites patulus
Chondrites isp.
Ophiomorpha annulata
Thalassinoides suevicus
Spongeliomorpha oraviense
Parahaentzschelinia isp.
Phycosiphon incertum
Paleodictyon strozzii
Paleodictyon delicatulum
Paleodictyon maximum
No Traces

Chapter 8

Trace fossils in the subsurface

Appendix 8.1 Downhole date from Well A4 including; graphic sedimentary log, natural gamma (API), ichnofabric indices (ii), total bioturbation (%), biodeformational structures (%) and bioturbation intensities of trace fossils.

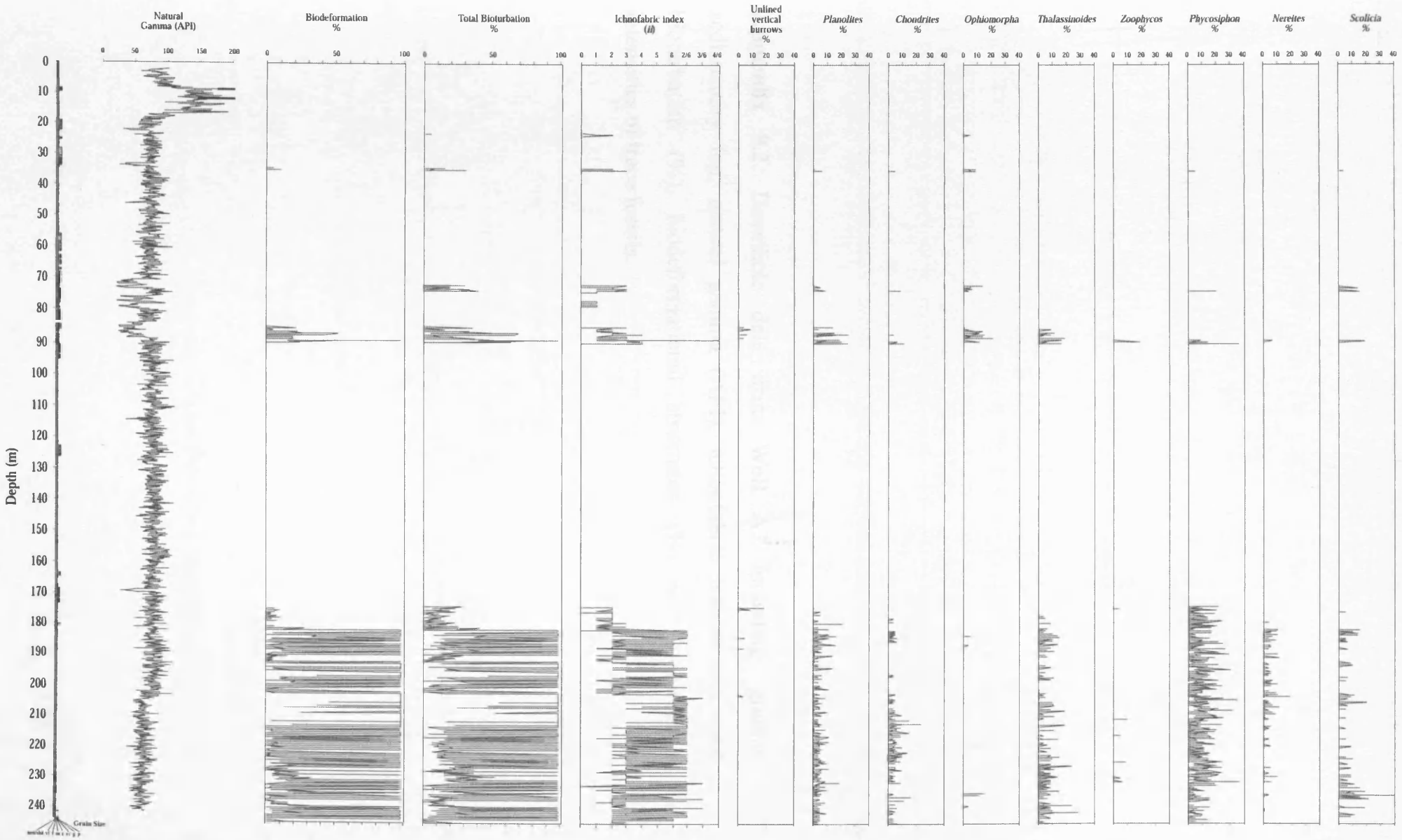
Natural Gamma (API)
Biodeformation %
Total Bioturbation %
Ichnofabric index (ii)
Unlined vertical burrows %
Planolites %
Chondrites %
Ophiomorpha %
Thalassinoides %
Zoophycos %
Phycosiphon %
Nereites %
Scolicia %
Depth (m)
Grain Size

Appendix 8.2. Downhole date from Well A3 including; graphic sedimentary log, natural gamma (API), ichnofabric indices (ii), total bioturbation (%), biodeformational structures (%) and bioturbation intensities of trace fossils.

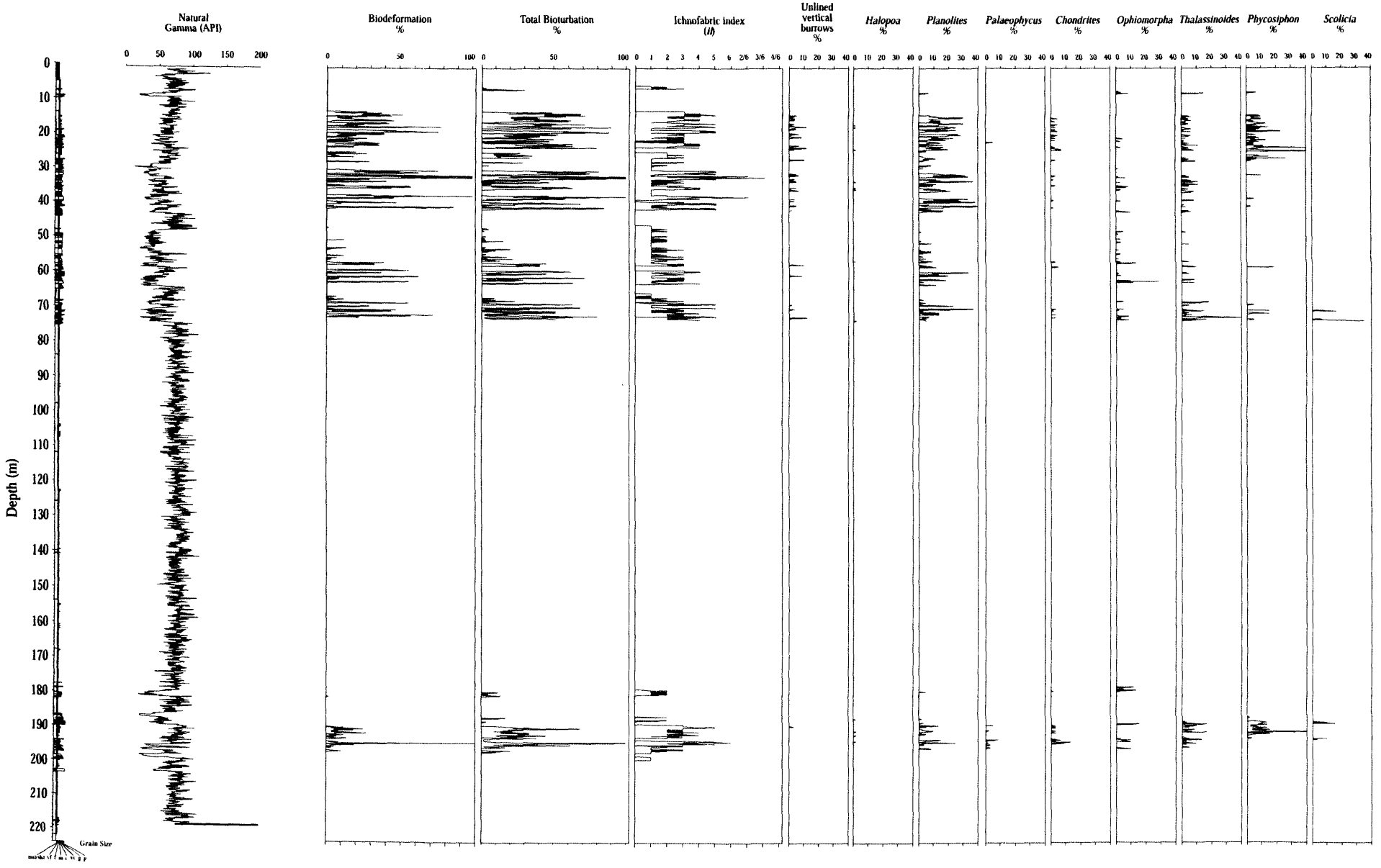
Natural Gamma (API)
0 50 100 150 200
Biodeformation %
0 50 100
Total Bioturbation %
0 50 100
Ichnofabric Index (ii)
0 1 2 3 4 5 6 2/6 3/6 4/6
Unlined vertical burrows %
0 10 20 30 40
Halopoa %
0 10 20 30 40
Planolites %
0 10 20 30 40
Palaeophycus %
0 10 20 30 40
Chondrites %
0 10 20 30 40
Ophiomorpha %
0 10 20 30 40
Thalassinoides %
0 10 20 30 40
Phycosiphon %
0 10 20 30 40
Scolicia %
0 10 20 30 40
Depth (m)
0 10 20 30 40 50 60 70 80 90 100 110 120 130 140 150 160 170 180 190 200 210 220
Grain Size

Appendix 8.3. Downhole date from Well A5 including; graphic sedimentary log, natural gamma (API), ichnofabric indices (ii), total bioturbation (%), biodeformational structures (%) and bioturbation intensities of trace fossils.

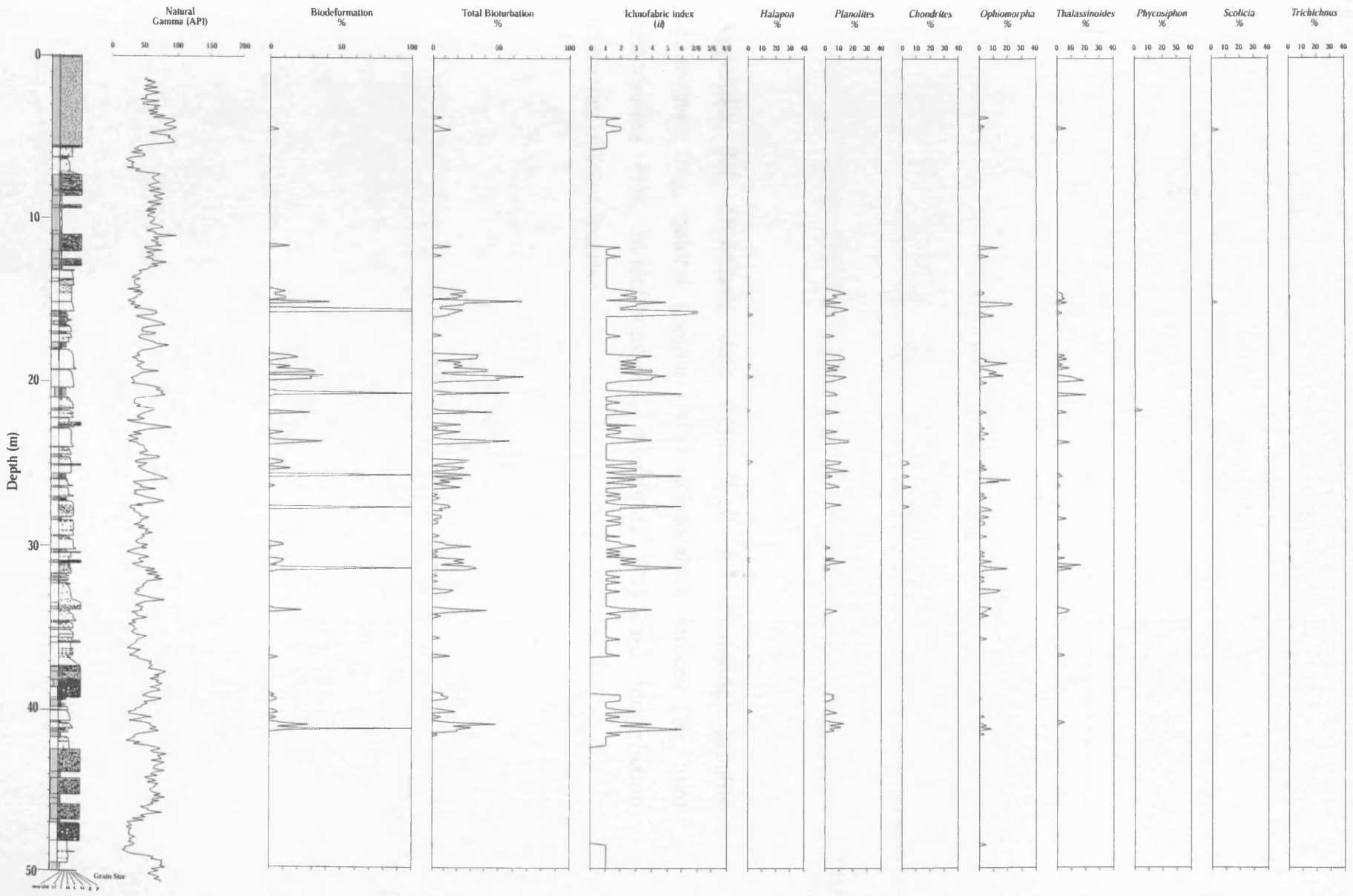
Natural Gamma (API)
0 50 100 150 200
Biodeformation %
0 50 100
Total Bioturbation %
0 50 100
Ichnofabric index (ii)
0 1 2 3 4 5 6 2/6 3/6 4/6
Halapoa %
Planolites %
Chondrites %
Ophiomorpha %
Thalassinoides %
Phycosiphon %
Scolicia %
Trichichnus %
0 10 20 30 40
Depth (m)
0
10
20
30
40
50
Grain Size

Appendix 8.4. Downhole date from Well A2 including; graphic sedimentary log, natural gamma (API), ichnofabric indices (ii), total bioturbation (%), biodeformational structures (%) and bioturbation intensities of trace fossils.

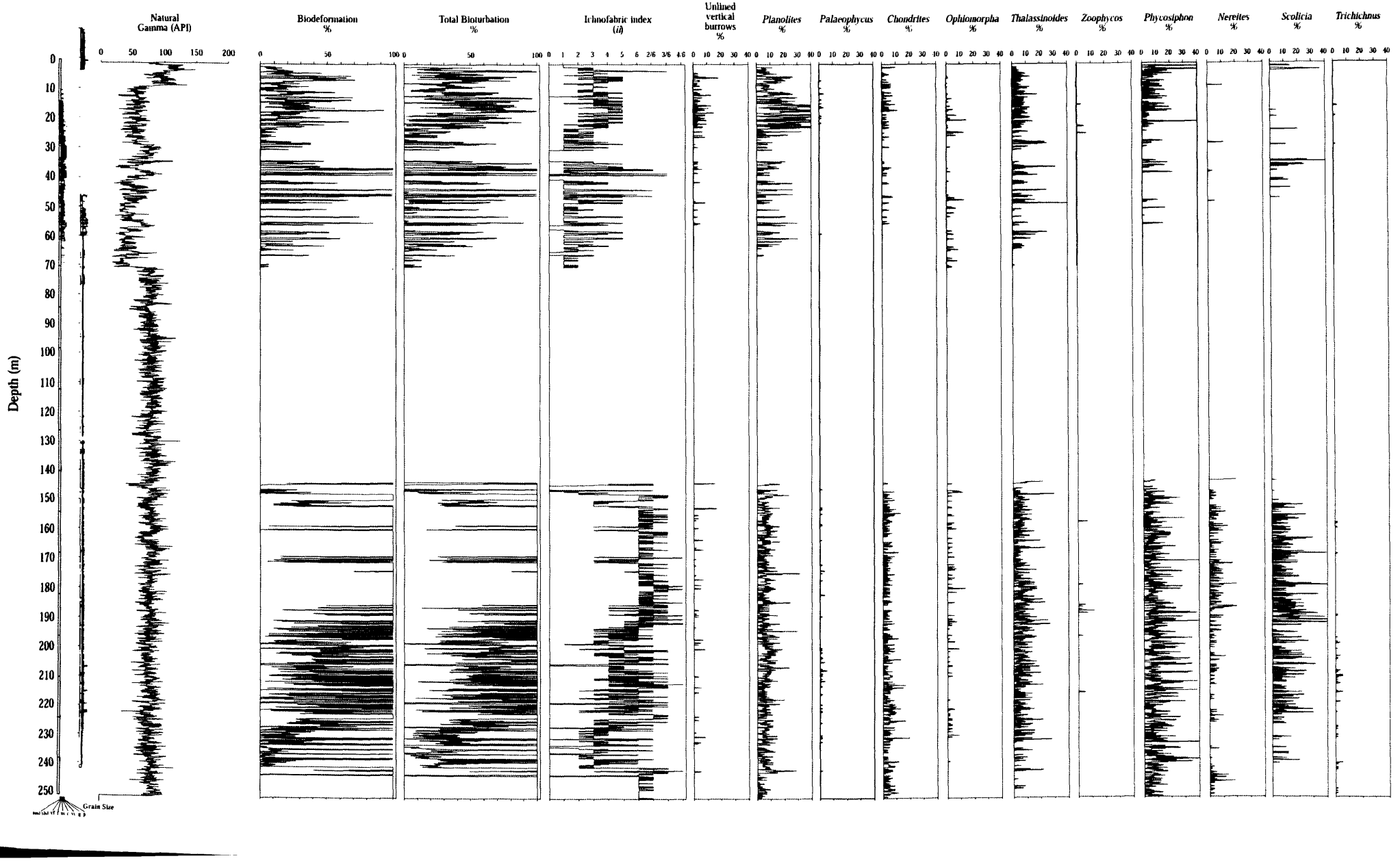
Natural Gamma (API)
Biodeformation %
Total Bioturbation %
Ichnofabric index (ii)
Unlined vertical burrows %
Planolites %
Palaeophycus %
Chondrites %
Ophiomorpha %
Thalassinoides %
Zoophycos %
Phycosiphon %
Nereites %
Scolicia %
Trichichnus %
Depth (m)
Grain Size

Appendix 8.5. Downhole date from Well A1 including; graphic sedimentary log, natural gamma (API), ichnofabric indices (ii), total bioturbation (%), biodeformational structures (%) and bioturbation intensities of trace fossils.

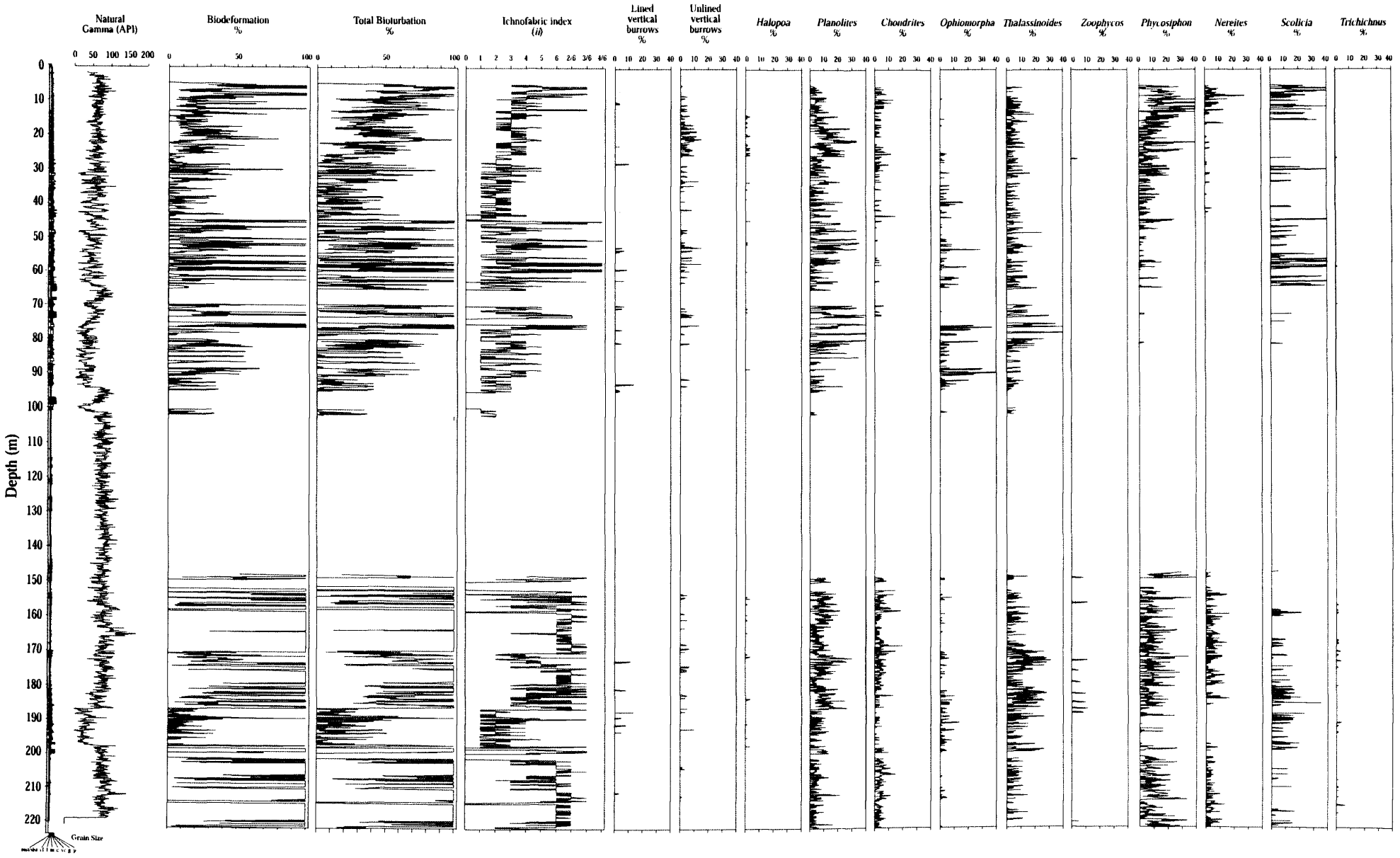
Natural Gamma (API)
0 50 100 150 200
Biodeformation %
0 50 100
Total Bioturbation %
0 50 100
Ichnofabric index (ii)
0 1 2 3 4 5 6 2/6 3/6 4/6
Lined vertical burrows %
0 10 20 30 40
Unlined vertical burrows %
0 10 20 30 40
Halopoa %
0 10 20 30 40
Planolites %
0 10 20 30 40
Chondrites %
0 10 20 30 40
Ophiomorpha %
0 10 20 30 40
Thalassinoides %
0 10 20 30 40
Zoophycos %
0 10 20 30 40
Phycosiphon %
0 10 20 30 40
Nereites %
0 10 20 30 40
Scolicia %
0 10 20 30 40
Trichichnus %
0 10 20 30 40
Depth (m)
0 10 20 30 40 50 60 70 80 90 100 110 120 130 140 150 160 170 180 190 200 210 220
Grain Size

Appendix 8.6. Downhole date from Well L1 including; graphic sedimentary log, natural gamma (API), ichnofabric indices (ii), total bioturbation (%), biodeformational structures (%) and bioturbation intensities of trace fossils.

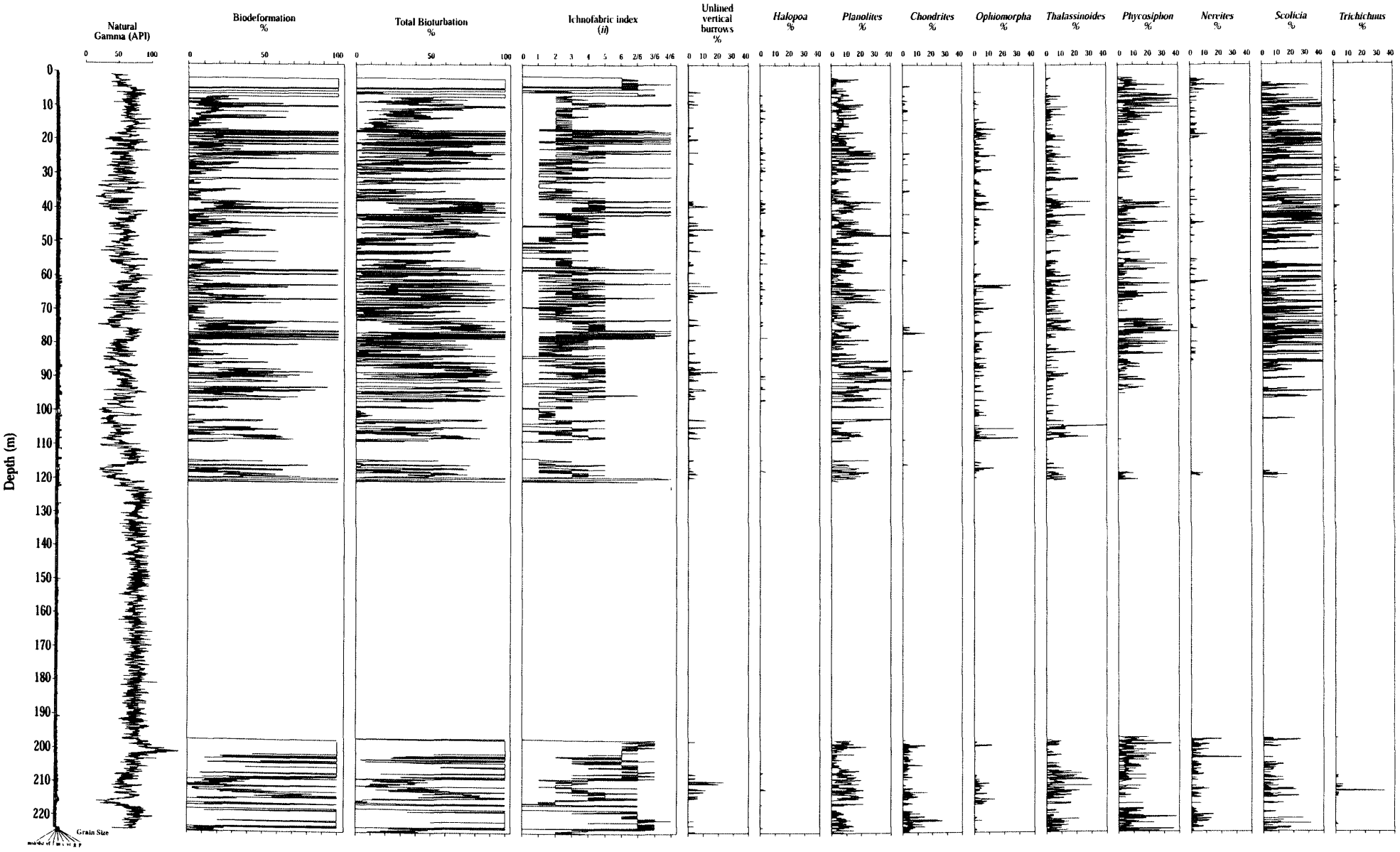
Natural Gamma (API)
Biodeformation %
Total Bioturbation %
Ichnofabric index (ii)
Unlined vertical burrows %
Halopoa %
Planolites %
Chondrites %
Ophiomorpha %
Thalassinoides %
Phycosiphon %
Nereites %
Scolicia %
Trichichnus %
Depth (m)
Grain Size